

6333

FTD-TT-62-942

402909

CATALOGED BY ASTIA

AS AD NO.

TRANSLATION

VIBRATIONAL COMBUSTION

By

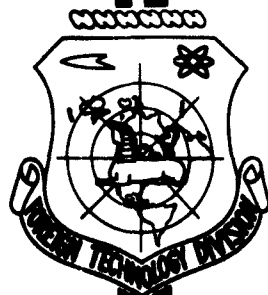
B. V. Raushenbakh

FOREIGN TECHNOLOGY DIVISION

AIR FORCE SYSTEMS COMMAND

WRIGHT-PATTERSON AIR FORCE BASE

OHIO



ASTIA
RECEIVED
MAY 8 1963
JISIA

UNEDITED ROUGH DRAFT TRANSLATION

VIBRATIONAL COMBUSTION

BY: B. V. Raushenbakh

English Pages: 519

S/5827

THIS TRANSLATION IS A RENDITION OF THE ORIGINAL FOREIGN TEXT WITHOUT ANY ANALYTICAL OR EDITORIAL COMMENT. STATEMENTS OR THEORIES ADVOCATED OR IMPLIED ARE THOSE OF THE SOURCE AND DO NOT NECESSARILY REFLECT THE POSITION OR OPINION OF THE FOREIGN TECHNOLOGY DIVISION.

PREPARED BY:

TRANSLATION DIVISION
FOREIGN TECHNOLOGY DIVISION
WP-AFB, OHIO.

B. V. Raushenbakh

VIBRATSIONNOYE GORENIYE

Gosudarstvennoye Izdatel'stvo
Fiziko-Matematicheskoy Literatury
Moskva - 1961

Pages: 1-500

FTD-TT-62-942/1+2

TABLE OF CONTENTS

Foreword	1
Introduction	4
Chapter 1. General Description of Oscillations Excited by Heat Supply	8
§ 1. Certain Experimental Facts	8
§ 2. Scheme for Idealization of the Process of Self- Excitation of Longitudinal Acoustic Oscillations by Combustion	14
Chapter 2. Propagation of Perturbations in a Moving Gas. . .	24
§ 3. Linearization of the Equations of Hydromechanics . .	24
§ 4. Acoustic Waves in a Moving Nonisentropic Gas. . .	30
§ 5. Example of Simplest Boundary Problem	37
§ 6. Standing Wave of \bar{p} and \bar{v}	43
§ 7. Traveling Waves of \bar{u} , \bar{w} , and \bar{s}	55
§ 8. Stability of Gas Stream	57
§ 9. Longitudinal Self-Oscillations in a Gas Stream. . .	68
Chapter 3. Sources of Self-Oscillation Energy	72
§ 10. Two Sources of Energy in Thermal Excitation of Sound	72
§ 11. Flux of Acoustic Energy	79
§ 12. Energy Imparted to the Oscillating System Dur- ing the Realization of the Elementary Processes in the Heat-Supply Zone	89
§ 13. Energy Imparted to the Oscillating System in the General Case	99
§ 14. Excitation of Oscillating System by Entropy Waves	105
Chapter 4. Theoretical Idealization of the Processes in the Combustion Zone	111
§ 15. Change in Perturbation on Crossing the Combustion Region	111
§ 16. Properties of the Heat-Supply Plane Σ	124
§ 17. Reduction of Equations for the Discontinuity Plane Σ to Canonical Form	140
§ 18. Sources of Self-Oscillation Energy for Arbitrari- ly Complicated Processes in the Heat-Supply Zone.	143
§ 19. Excitation of Oscillating System in the General Case	147
§ 20. Diagrams of the Stability Limits for Typical Cases	159

§ 21. Comparison of the Relative Significance of Thermal and Mechanical Energy Sources in the Excitation of Oscillations	164
Chapter 5. Excitation of Oscillations by Heat Supply in the Absence of Losses	172
§ 22. Introductory Remarks	172
§ 23. Formulation and Solution of the Characteristic Equation	180
§ 24. Construction of the Stability Limits	187
§ 25. Analysis of the Excitation Conditions	206
§ 26. Influence of the Delay of the Heat Release on the Excitation of Acoustic Oscillations	213
§ 27. Oscillation Frequencies	220
§ 28. Stepwise Variation of the Oscillation Frequency with Change in the Combustion-Zone Position	224
§ 29. Experiments on the Influence of the Position of the Combustion Zone on the Oscillation Process	233
Chapter 6. Excitation of Oscillations by Heat Supply in the Presence of Losses at the Ends of the Tube	257
§ 30. Losses to Radiation	257
§ 31. Characteristic Equation of the Problem with Account of Losses at the Ends of the Tube	262
§ 32. Numerical Analysis of Some Particular Cases	265
§ 33. Complete Absorption of Energy at One End of the Tube	273
Chapter 7. Feedback Mechanisms in the Excitation of Acoustic Oscillations by Combustion	284
§ 34. Classification of Feedback Mechanism	284
§ 35. Feedback Mechanisms Based on Mixture Formation	293
§ 36. Feedback Mechanisms Based on Hydromechanical Phenomena	305
§ 37. Feedback Mechanisms Based on the Laws of Combustion Proper	323
§ 38. Stability of Plane Flame Front	333
Chapter 8. Calculation of Self-Oscillations Taking into Account the Nonlinear Properties of the Heat-Supply Zone	357
§ 39. General Characteristic of Self-Oscillations	357
§ 40. Essential Nonlinearities in the Combustion Zone	361
§ 41. Oscillations in the Absence of Losses at the Ends of the Tube	371
§ 42. Self-Oscillations in the Presence of Losses at the Ends of the Tube	382
§ 43. Applicability of the Methods Developed to Other Cases	386
Chapter 9. Vibration Combustion	391
§ 44. Stages of Development of the Vibration Combustion Process	391
§ 45. Hypothesis Concerning the Maximum Acoustic Energy Radiated by the Heat-Supply Region	397

§ 46. Experimental Verification of the Hypothesis Concerning the Maximum Acoustic Energy	409
§ 47. Excitation and Suppression of Vibration Combustion	417
Chapter 10. Certain Particular Cases of Self-Excitation of Acoustic Oscillations	436
§ 48. Excitation of Sound in a Rijke Tube	436
§ 49. Vibrational Combustion in Propagation of Flame in Stationary Gas	
§ 50. Occurrence of Oscillations in Pulverized Coal Furnaces	476
§ 51. Vibration Combustion in Ram-Jet Engines	484
§ 52. Longitudinal Oscillations in Liquid Fuel Jet Engines	489

NOTE

The book is devoted to the problem of combustion-process instability encountered in the design of liquid-fuel rocket engines, air-breathing jet engines, highly forced fireboxes in chemical electric-power plants, and in conducting various types of physical tests and experiments in combustion theory.

The book gives a systematic exposition of contemporary theory of the excitation of longitudinal acoustic vibrations by application of heat. The qualitative laws inherent to this type of vibration are given detailed consideration, with information from hydromechanics, acoustics and combustion theory drawn upon extensively for their analysis, with application of the mathematical apparatus of control theory and vibration theory.

The volume is intended for scientific workers, engineers, graduate students and students in advanced courses at the universities and higher technical schools who are concerned with the problems of combustion theory and the theory of vibration of continuous media, as well as for persons working in the field of contemporary engine design and thermal power engineering.

FOREWORD

In recent years the problem of excitation of acoustic oscillations in a gas column in which combustion takes place has become most urgent. The reason for it is that many problems of practical importance, connected with the creation of highly forced combustion chambers, cannot be solved without a thorough analysis of a phenomenon which is sometimes called vibration combustion. This circumstance finds its reflection in the large number of articles published in the foreign publications.

Unfortunately, the papers of the foreign authors are devoted principally to questions of the excitation of instability in rocket engines, and consequently have a relatively narrow sphere of application. At the same time it is known that analogous phenomena are observed also in commercial furnaces, experimental installations for the study of combustion processes, in many physical experiments (the Rijke tube), etc. Therefore the need for a more general examination of the problem of excitation of acoustic oscillations by means of a supply of heat (and particularly by combustion) had arisen long ago. One of the tasks undertaken in writing this book was to develop the principles of a systematic theory of vibration combustion, by which it would be possible to analyze all the variety of particular cases from a unified point of view. However, an analysis of specific engineering problems within the framework of this book would not be advantageous. This would greatly increase the volume of the book and, most important, would make it difficult to investigate the nature of the phenomenon and to

develop general methods, since the reader's attention would unavoidably be distracted by a detailed analysis of various particular problems.

In addition, one must not forget that the engineering problems that are urgent today may become uninteresting after a few years, and those which are of no significance at present may become central problems.

We therefore considered it more correct to present an outline of the general theory, leaving the development of specific problems to those who engage in them directly. Only as a conclusion of the general theory do we give in Chapter 10 examples of application of this theory to a few practical problems.

The undertaken goal determines to a considerable degree both the content of the book and the method of exposition. The main content of the book is the analysis of a certain idealized scheme (combustion in a cylindrical tube), and the experimental material pertains for the most part also to experiments of academic nature (combustion of a mixture in a small tube, behind a simple stabilizer or without a stabilizer, but not combustion in real furnaces, engines, etc.). In order to make the material understandable to a large group of engineers, the exposition is carried out by simplest methods and in sufficient detail; consequently, the usual training in mathematics and mechanics as given by our higher technical institutions of learning is sufficient for an understanding of the problems considered here. Striving for simplicity and brevity, the author has frequently sacrificed rigor of exposition, but attempted, wherever possible, to explain the physical nature of the phenomenon under consideration.

The book presented for the reader's attention is not a complete summary of the present-day status of the question. It contains an exposition of principally the results obtained by the author and partially published at intervals in various journals. This has unavoidably

left its imprint not only on the formulation of the problems and on the method used to analyze them, but also on the content of the book. In those cases when works by other authors are used, the corresponding references are made throughout; the absence of references means that the results (both theoretical and experimental) belong to the author. In addition to several previously published papers, the book was based also on lectures delivered by the author during the last few years at the Moscow Physical-Technical Institute.

The content of the book is aimed at students in the upper classes of higher institutions of learning, graduate students, and engineering-technical workers engaged in problems of oscillation theory, combustion theory, and gas dynamics. The book can also serve as a text for suitable courses.

The author considers it his pleasant duty to express his gratitude to Engineer L.D. Shitova, who participated most actively in the setting up of the experiments the results of which are reflected in the present book, to Engineer T.M. Kuvardina, who contributed to a successful performance of the laborious numerical calculations, and also to N.S. Natanzon, who made several valuable remarks upon becoming acquainted with the manuscript.

INTRODUCTION

As is well known, the construction of highly forced furnaces entails several difficulties. One of them is the struggle against high-frequency oscillations which arise in the combustion chamber. These oscillations can greatly disturb the combustion process and lead to destruction of the structural elements of the furnace or of the engine. There are known examples of excitation of oscillations in furnaces of thermal electric stations on changing over to forced combustion modes. These phenomena are observed, for example, in the case of the adjustment of precombustion chambers using pulverized coal, where the pulsations have brought some of the furnace elements out of order. In addition, analogous phenomena are known also in the practice of final adjustment of liquid fuel rocket engines, as can be seen from the numerous articles published in the journals.

On the other hand, it is known that many experiments set up on commercial furnaces have shown that great promise is offered by the creation of furnaces in which vibration combustion is the normal combustion mode. The realization of such modes yields greater advantages when it comes to increasing the thermal load of the furnace. In addition, in recently published articles it is indicated that great possibilities are being uncovered by the changeover to vibration combustion in metallurgy, the chemical industry, etc.

In all these cases the oscillations (regardless of whether they are harmful or useful) are connected with an interaction between the combustion and the acoustic oscillations of the gas column contained

In the engine, furnace, or some other device. This phenomenon is quite complicated and has not yet been thoroughly studied. This brings about a situation wherein both the struggle against this combustion and its realization in suitable installations are carried out blindly.

In spite of the fact that vibration combustion has been known a long time and has been the subject of relatively many papers, far from all problems in the theory of this phenomenon have been worked out. As a result, the main theoretical conclusions reduce to a statement that the oscillation frequencies are determined by the acoustic properties of the medium, the excitation condition is reduced to the Rayleigh criterion (the inaccuracy of which will be demonstrated in Chapter 3), and from among the large number of possible feedback mechanisms only the so-called Crocco mechanism was considered in any detail until recently (as applied to liquid fuel jet engines).

In attempting to develop the principles of the theory of the vibration combustion process, the necessity arose for a systematic examination of the investigated phenomenon, an examination which was made from a most general point of view. Such generality is useful because it makes it possible to analyze a great variety of cases by using a single procedure.

In addition, the unity and generality of the procedure made it possible to make justified assumptions when turning to some particular problems, and frequently eliminates the fatiguing need for attempting to explain each new experimental fact by means of a new hypothesis, the doubtful advantage of which is the fact that it explains only the fact that brings it to life.

In order to carry out a sufficiently general analysis of the problem, it is necessary to do the following:

- 1) consider the character of propagation of acoustic perturbations

in one-dimensional nonisentropic flow (although this problem was considered also by other authors, it was deemed advantageous to present a solution which differs somewhat from the usual one);

2) present a general method which makes it possible to "join together" the one-dimensional processes to the left and to the right of the combustion zone, without losing the essential properties of the complicated three-dimensional combustion process;

3) estimate the influence of energy losses in the end sections of the stream on the tendency of the system toward self-excitation of acoustic oscillations;

4) investigate the energy aspect of the investigated phenomenon; in particular, solve the problem of the source from which the energy is drawn for the maintenance of the self-oscillations;

5) present a classification of the possible feedback mechanisms and designate the paths toward the solution of the problem of how the oscillating system "chooses" a certain specific feedback mechanism from among the set of possible ones;

6) present an example of the solution of the nonlinear problem, i.e., determine the amplitudes and frequencies of the steady-state oscillations for a certain particular case; this particular case should simultaneously yield a clear notion of a solution method suitable for a large class of analogous problems.

Knowing the laws governing the propagation of acoustic perturbations in one-dimensional gas flow, and being able to reduce an arbitrarily complicated process in the combustion zone to a certain fictitious process in the cross section that separates the "cold" and "hot" parts of the stream, we can use a relatively simple mathematical apparatus for the investigation of the oscillation excitation process. The understanding of the energy aspect of the considered phenomenon is use-

not only because it clarifies this confusing problem, but also because it permits the development of an energy method for solving many problems, a method which in most cases is distinguished for its clarity and simplicity. As regards the study of the feedback mechanisms, it is essential in order to indicate the simplest practical methods of acting on the oscillating system, and also for a complete theoretical description of this action.

In order to complete the analysis of the excitation of an oscillating system, it is necessary to find its limit cycle. The corresponding nonlinear problems are exceedingly complicated. Consequently, in the case considered below the problem is posed in its simplest form: it is assumed that the nonlinearities are concentrated, i.e., they can appear only in individual cross sections of the gas stream.

Since the solution of the aggregate of the mentioned problems calls for the use of results pertaining to different fields of knowledge (hydromechanics and acoustics, combustion theory, the mathematical apparatus of control and oscillation theory), it becomes necessary to develop for the description of the process of thermal excitation of oscillations in a moving gas a special research apparatus, capable of being of theoretical interest also on a larger scale.

Chapter 1
GENERAL DESCRIPTION OF OSCILLATIONS
EXCITED BY HEAT SUPPLY

§1. Certain Experimental Facts

Although careful attention to self-excitation of acoustic oscillations by means of combustion (or by some other form of heat supply) originated only in recent years, principally in connection with the development of rocket technology and the forcing of commercial furnaces, the very fact of self-excitation of oscillations by means of heat supply has been known for more than a hundred years.

A great variety of experiments set up by the physicists of the 19th century indicated the possibility of exciting acoustic oscillations by combustion or by some other form of heat supply. It is sufficient to mention only the phenomenon of "singing flames" and the Rijke tube,* in which the heat is supplied to air with the aid of a hot grid. Let us stop to describe in somewhat greater detail Rijke's experiments. In 1859 Rijke observed that if a sufficiently long tube, open on both ends, is placed vertically and if a dense metallic grid heated to bright red incandescence is placed about $1/4$ of the length of the tube away from the lower end, then almost immediately following the removal of the gas flame used to heat the grid a sound of appreciable force could be heard for several seconds (i.e., during the entire time that the grid remains hot). Rijke observed also that the sound is produced only if a through draft is produced in the tube (the tube is placed vertically precisely in order to create the draft), and that the ex-

Used sound corresponds to the fundamental tone of the tube. Rijke's experiments were modified later in the respect that the grid was heated from a source of electricity, and the sound was continued for an unlimited time.

An entirely different result is obtained if the grid is placed in the upper half of the tube. In this case it is impossible to produce the sound at the fundamental frequency with the aid of the heated grid. However, a modification of the experiment, proposed by Bosscha and Riess, uncovers this possibility. For this purpose the grid placed in the upper tube must be not heated but cooled. At the same time, in the lower part of the tube one must place a gas burner which heats the air and produces a draft, while the grid no longer supplies heat, but carries it away from the air flowing past it.

It follows from the brief description given here, that excitation of acoustic oscillations is connected with the motion of gas along a tube, in one of the cross sections of which the gas stream interacts with a certain positive (heating) or negative (cooling) heat source.

The described phenomenon can be regarded as the simplest process of thermal excitation of sound. This process is at the same time sufficiently close to the vibration combustion, which is of principal interest. It is therefore not surprising that in analyzing many of the problems in the following chapters, reference will be made to Rijke's experiments, and one of the sections of Chapter 10 will be devoted to an exposition of the theory of this phenomenon.

Somewhat later, likewise in the second half of the 19th century, Mallard and LeChatelier observed, in combustion produced in tubes, a changeover from smooth motion of the flame along the tube to vibration combustion. Analogous phenomena were observed later by other authors. The first thoroughly formulated experiments, in which vibration combus-

tion was investigated in sufficient detail, were those of Coward, Hartwell, and Georgson,* published in 1937. The bulk of the experiments were performed in horizontal tubes 100 and 200 mm in diameter and 5 m long, filled with a mixture of methane and air. These tubes had one end closed and the other open. After filling the tube with the combustible mixture, the open end was covered for the time necessary for a complete quieting of the gas in the tube, after which this end of the tube was carefully opened and the mixture ignited at the open end.

At first the flame moved along the tube quietly, but after reaching a certain distance from the open end, strong vibrations began. These vibrations were registered at the closed end in the form of pressure oscillations. In addition, the flame was simultaneously photographed and the results indicated strong oscillations of the flame front, occurring at the same frequency as the pressure oscillations at the closed end.

An interesting circumstance was that the pressure oscillation frequency (and the frequency of the flame) changed jumpwise as the flame front moved along the tube. The observed oscillation frequencies were of the same order as the natural frequencies of the gas column in the tube.

The authors investigated also the influence of obstacles of various types placed at the open end of the tube on the character of the vibration combustion. They gradually brought a plate closer to the open end of the tube and verified that once the plate approached the tube with 100 mm diameter to a distance of 15 mm and less, the oscillations were strongly damped. Vibration combustion was practically completely stopped when glass wool was placed at the open end of the tube.

Figure 1 shows oscillograms of the pressure at the closed end. The oscillograms are plotted as a function of the time which is reckoned

at the instant of ignition of the mixture. The vertical strokes in the right ends of the oscillograms denote the instant when the flame reached the closed end. The numbers above the pressure oscillation curves represent the frequencies of the recorded oscillations in cycles per second.

If we compare Rijke's experiments with the just described experiments of Coward, Hartwell, and Georgson it becomes obvious that they have many attributes in common. The fundamental fact here is that in both cases natural harmonics of the long tubes are excited, and that this excitation is the result of heat supply.

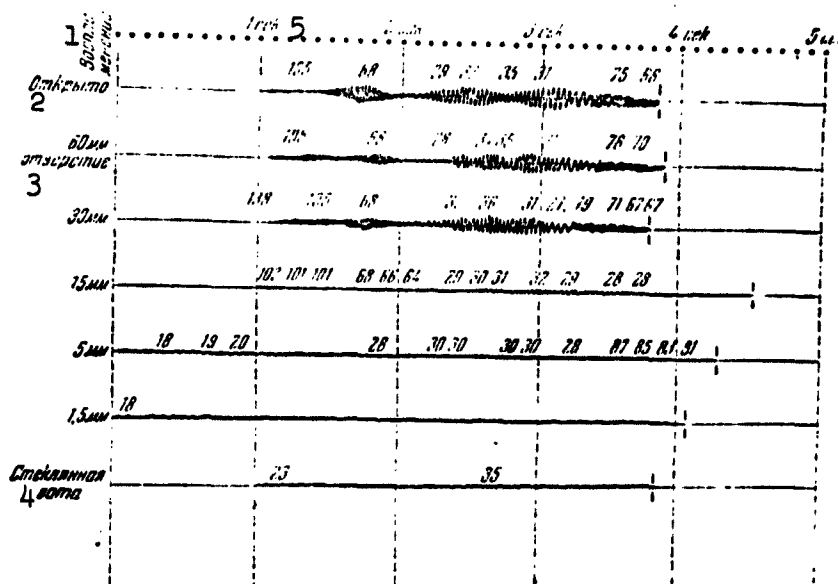


Fig. 1. Oscillograms of the pressure at the closed end of a tube, obtained in the experiments of Coward, Hartwell, and Georgson. 1) Ignition; 2) open; 3) aperture; 4) glass wool; 5) sec.

During the last 10 or 15 years, vibration combustion studies were extended from experiments of academic type such as described above also to engines and furnaces. It turned out that in such devices acoustic oscillations of various types can arise. Let us illustrate this with liquid fuel jet engines as an example.

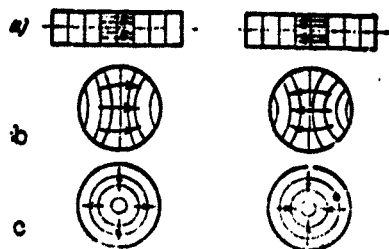


Fig. 2. Possible types of acoustic oscillations of gas masses in a liquid fuel jet engine.

The periodic literature contains many reports of self-excitation of acoustic oscillations observed in liquid fuel jet engines. It turned out that, depending on the specific conditions, two types of oscillations can be excited, longitudinal and transverse. The transverse oscillations can in turn be sub-

divided into tangential and radial. These three types of acoustic oscillations differ in the form of standing waves that are produced during the course of their realization in the combustion chamber.

Figure 2 shows the corresponding patterns. In pattern a are shown longitudinal acoustic oscillations. The lines without the arrows correspond to equal values of the instantaneous pressures, while the arrows show the direction of the gas masses, from the left at the instant when these masses move to the right and from the right a half cycle later (the pattern shows only the oscillating component of the velocity). During these oscillations the air masses move along the symmetry axis of the combustion chamber, so that the pulsating velocity component is superimposed on the average flow velocity of the gas masses along the chamber. In pattern b are shown the tangential oscillations. They are similar to the longitudinal ones in many respects, but are in the transverse direction of the combustion chamber. With this, by virtue of the fact that the transverse cross section of the chamber is a circle, the lines of equal pressures are no longer straight. Pattern c shows the radial oscillations. This type of oscillation has axial symmetry, where the symmetry axis is the axis of the combustion chamber.

If we recall that the frequency of the acoustic oscillations is

connected with the distance that the acoustic momentum must overcome and, furthermore, recognize that the length of the combustion chamber is usually much larger than its diameter, it is easy to visualize that the longitudinal oscillations will have the lowest frequency, the tangential oscillations will occupy an intermediate place, and the radial oscillations will have the highest frequency.

Comparing the three types of acoustic oscillations described here with the experiments of Coward, Hartwell, and Georgson and the sound produced in the Rijke tube, one can easily see that only the longitudinal oscillations in the combustion chamber of the liquid fuel jet engine have much in common with these experiments. In precisely the same manner, the pulsations of pressure observed in pulverized coal furnaces, ramjet engines, and many experimental setups in academic investigations of the combustion processes, etc., turn out to be longitudinal acoustic oscillations. Thus, longitudinal acoustic oscillations are of considerable interest, outside the scope of any one particular narrow problem.

The present book is devoted to an investigation of longitudinal acoustic oscillations only, preference being given to questions not connected with the operating process in liquid fuel jet engines. This was done principally because problems of oscillations (including longitudinal) in combustion chambers of liquid fuel jet engines are the subject of the book by L. Crocco and Cheng Sin-I which was recently published in the Russian language.*

As regards transverse acoustic oscillations, they have not been studied sufficiently completely until now. To become acquainted with them it is best to read the journal articles. Many premises discussed in the present book may turn out to be useful also in the development of a theory of transverse oscillations, for in either case the gist of

the phenomenon reduces to self-excitation of acoustic oscillations by the heat supply.

§2. Scheme for Idealization of the Process of Self-Excitation of Longitudinal Acoustic Oscillations by Combustion

For a theoretical investigation of longitudinal acoustic oscillations in experimental setups, engines, or furnaces it is necessary to specify a certain idealized scheme. In the theoretical analysis of this phenomenon we shall assume that all the devices listed above can be reduced to an equivalent long cylindrical tube, which can be broken up into several portions, separated by short zones, inside of which the heat supply process takes place. The gas moving through these portions (air or combustion products) does not experience any changes in the absence of oscillations. It is usually sufficient to consider two such portions, one corresponding to the supply pipe and the other to the combustion chamber. In the first of these portions we disregard any possible change in the transverse cross sections, the presence of hydraulic losses, changes in the composition of the gas due to the introduction of the fuel into the stream, etc. In the second section we neglect afterburning and mixing of the gases in the part of the combustion chamber adjacent to the exhaust nozzle, and also hydraulic losses, heat losses connected with heat transfer through the combustion-chamber walls, etc.

The combustion process in the representation adopted here is realized in one or several short regions. The smallest of these combustion regions must be understood as relative to the wavelengths of the longitudinal oscillations, and consequently, also in comparison with the total length of the tube (installation). In order to simplify the formulation of the problem, we shall neglect the length of the combustion zones, and replace these regions with strong-discontinuity surfaces.

Thus, the theoretical computation scheme corresponds to a one-dimensional gas flow in a cylindrical tube, separated in the general case by one or several surfaces of strong discontinuities. The properties of the discontinuity surface Σ depend essentially on the combustion process in the region represented by this surface. These essential properties can be formulated by foregoing the simplified one-dimensional analysis of the processes occurring in the combustion zone.

Consequently, in considering the process of the propagation of perturbations between the discontinuity surfaces we shall use a one-dimensional scheme, while in formulating the properties of the discontinuity surface we adopt a three-dimensional scheme for the phenomenon. In describing the properties of the heat supply zone we shall neglect as a rule the hydraulic resistance and the change in the aggregate state of the fuel during the combustion. (Examples of processes when this cannot be done are given in the last, tenth chapter.) The discontinuity surfaces can be introduced not only to describe the combustion process, but also in other cases when the parameters of the flow experience a strong change over a short portion.

In addition to the properties of the surface Σ , which divides the stream into two portions, it is also necessary to determine the properties of the flow at the ends of the tube. Depending on the type of problem that must be investigated, the boundary conditions assume one form or another. In one case these are the ordinary acoustic conditions, and in the other they are the conditions that characterize the nonidealized properties of the Laval nozzle or similar devices.

Inasmuch as the main content of the following chapters is an investigation of oscillatory processes that have an acoustic nature, we shall employ the method of small perturbations below. The main problem in the investigation is as a rule the study of the stability of the

gas flow in a tube of the type described with respect to small perturbations. If the process turns out to be oscillatory-unstable in the idealized scheme, then the natural assumption will be made that such instability leads to self-oscillations.

As is well known, for a complete solution of the self-oscillation problem it is necessary to take into account essentially nonlinear relationships. A problem of this type is considered in Chapter 8. The main simplifying assumption is that all the essentially nonlinear relationships are contained in the properties of the discontinuity surface Σ . As regards the process whereby the perturbations propagate between the discontinuity surface and the ends of the tube, it will be assumed that these processes are sufficiently well described by linear equations even in the stationary self-oscillation mode.

The acoustic type self-oscillations considered below can be characterized as being due to the presence of feedback. In the case when the self-oscillations are excited by the combustion process (vibration combustion) the feedback leads to an influence of the acoustic oscillations on the combustion process. We shall therefore consider in a special chapter a whole series of physical phenomena that lead to the closing of such a feedback loop. In most theoretical calculations, however, the form of feedback will not be made concrete, and will be introduced purely formally, as a dependence of the essential parameter in the combustion zone (on the discontinuity surface Σ) on the magnitude of the oscillatory component of the velocity or of the pressure.

Before we proceed to a systematic exposition of the subject, it is useful to make several preliminary remarks that have a bearing on the exposition method employed in the following chapters.

We shall distinguish in what follows between oscillation modes that are characterized by an increase δ in the amplitude of the cer-

main quantity with the time t , by a constant amplitude, and finally, by a decrease in amplitude. These three cases are shown in Fig. 3 (a, b, and c). The first case is an example of an unstable process, the last is stable, and the middle one is neutral.

When a change takes place in some essential parameter, the oscillating system may change from stable to unstable or vice versa. We shall assume everywhere that in such transitions (if they are completed in a continuous manner) the oscillating system must go through a neutral-oscillation mode. This mode is frequently called the stability boundary.

The task of the theoretical analysis is usually to find the stability boundary. Knowing this boundary, we can formulate the condition

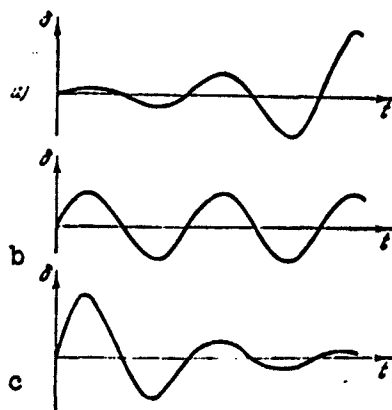


Fig. 3. Unstable, neutral, and damped oscillations.

for system stability in the form of a certain inequality, which is quite convenient in practice. An investigation of the neutral-oscillation mode turns out to be usually simpler than an investigation of modes with variable amplitudes. The reason for it is that in the case of neutral oscillations the variations of the variables are sinusoidal.

It must be pointed out here that not every mode with constant oscillation amplitudes is neutral and corresponds to a stability limit. The same property is possessed also by the stationary self-oscillation mode, although it does correspond to the instability region. However, unlike neutral oscillations, self-oscillations are described by nonlinear systems of equations and the very analysis of a nonlinear system will be specially stipulated in the exposition that follows.

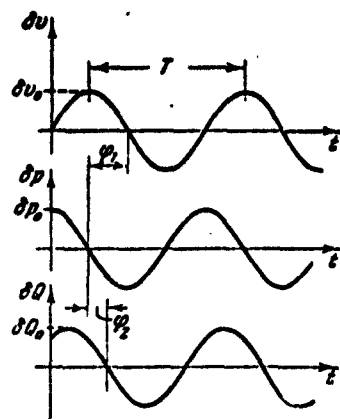


Fig. 4. Dependences of the oscillatory components of the flow parameters on the time.

A certain difficulty arises when the experimental data are compared with the theoretical calculations. The point is that if a certain frequency and amplitude of oscillations is established in an experiment, this means practically always that self-oscillations have arisen in the system, i.e., a phenomenon described by nonlinear relations. At the same time, the frequencies measured in these experiments and even the relative oscillation amplitudes will be

frequently compared with theoretical relations that are valid only for linear processes. Such a simplification is possible because the type of self-oscillations considered below is close in character to the small oscillations that are described by linear systems of equations.

A sufficiently complete representation of the oscillation process can be obtained if curves are available showing the variation of all the parameters as functions of the time. Figure 4 shows a suitable example. Here δv , δp , and δQ are perturbations of the velocity, pressure, and heat supply, respectively. If a given diagram is available, it is possible to estimate the oscillation period T , the oscillation amplitudes δv_0 , δp_0 , and δQ_0 , and the phase shift between the given variables. Thus, if we compare the phases of other oscillations with the phases of the pressure oscillations δp , then the phase of δv will differ from the phase of δp by φ_1 , while the phase of δQ will differ by φ_2 .

In the cases when the oscillation frequency (or the oscillation period which is uniquely related with it) is of no special interest, and the relative amplitudes of the oscillation of the individual vari-

ables and their mutual phase shifts are of importance (in other words, we need only the amplitude-phase relations), it is possible to employ a more illustrative method of representing the oscillation mode. It is shown in Fig. 5, which represents the same process as in Fig. 4. As can be seen from Fig. 5, this method reduces to a construction of a vector diagram. Each variable is represented in the form of a vector, the length of which is equal to the oscillation amplitude, and the angles between vectors are equal to the phase shifts between variables. If we imagine these vectors to be rigidly connected to each other and cause them to rotate together about the center O with frequency ω , then by observing the projections of the vectors on a certain direction, say the x axis, we can obtain a sinusoidal variation of the variables with time, with specified amplitudes and phase shifts. The position of the vectors on Fig. 5 corresponds to the instant of time $t = 0$ on Fig. 4; by rotating the set of vectors shown clockwise we can obtain the values of δv , δp , and δQ in all the succeeding instants of time.

Closely connected with the last method of representing the oscillation process is the question of the method used for analytically

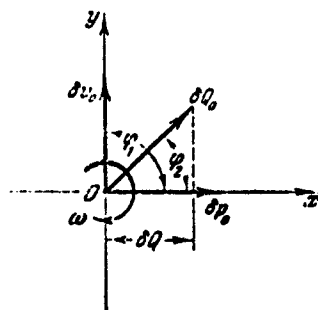


Fig. 5. Vector diagram of the process shown in Fig. 4.

writing down the corresponding expressions. A variable quantity having an amplitude and a phase can be represented in the form of a vector. Analytically a vector can be expressed by using the methods of vector analysis or the complex variable plane. In the exposition that follows we shall use both these methods for writing down the variables. It must be

borne in mind throughout that whereas the sum or difference of two complex numbers can be completely replaced by the

sum or difference of the corresponding vectors, the same cannot be said, as is well known, concerning their product. Consequently, special caution must be exercised when it becomes necessary to consider the product of the variables or the product of a variable and a certain coefficient, if the latter changes not only the magnitude but also the phase.

We shall use below three methods for expressing variables, which are best illustrated by means of an example. Assume that we are considering the variation of two variables \underline{x} and \underline{y} :

$$\left. \begin{aligned} x &= x_0 e^{i\omega\tau} \cos(\omega\tau + \varphi), \\ y &= y_0 e^{i\omega\tau} \cos(\omega\tau + \psi). \end{aligned} \right\} \quad (2.1)$$

From the foregoing expressions it is seen that we are considering two variables that vary in identical fashion in time, but have different initial amplitudes (x_0 and y_0) and different initial phases (φ and ψ).

The notation is changed in the following manner if complex numbers are used:

$$\left. \begin{aligned} x &= x_0 e^{(i\omega + \nu)\tau}, \\ y &= y_0 e^{(i\omega + \nu)\tau}. \end{aligned} \right\} \quad (2.2)$$

Now \underline{x} and \underline{y} are complex numbers, and in order to obtain the same change in variables as in Formulas (2.1), we must agree to assume that only the real parts of \underline{x} and \underline{y} have a physical meaning. This does not mean, of course, that the imaginary components of \underline{x} and \underline{y} are introduced "for nothing." Indeed, let

$$\begin{aligned} x_0 &= a_x + ib_x, \\ y_0 &= a_y + ib_y. \end{aligned}$$

Then the initial amplitudes are $|x_0| = \sqrt{a_x^2 + b_x^2}$ and $|y_0| = \sqrt{a_y^2 + b_y^2}$, and the initial phases are $\varphi = \arctan b_x/a_x$; $\psi = \arctan b_y/a_y$.

Consequently, the complex initial amplitudes x_0 and y_0 determine also the initial amplitudes and the initial phases of the variables.

this lies their essential difference from x_0 and y_0 in Eqs. (2.1). The advantage of writing down the variables in the form (2.2) is that the time dependence is segregated in a separate factor $\exp(\nu + i\omega)\tau$, which is the same for both variables, whereas in the notation of (2.1) these dependences were different by virtue of the fact that they included the initial phases φ and ψ . In addition, the factor $\exp(\nu + i\omega)\tau$ never vanishes. The considerations presented here make a notation of the form of (2.2) preferable, and this method of expressing the variables will be used essentially below.

In those cases when the dependence of the variables on the time is of no interest, and the relation between the amplitudes and phases of the variables \underline{x} and \underline{y} is of principal value, we can use the complex amplitudes x_0 and y_0 in order to describe these relations.

Indeed, multiplication of x_0 and y_0 by the time-dependent factor $\exp(\nu + i\omega)\tau$, although it does change the amplitudes and phases of \underline{x} and \underline{y} , does not change the ratio $|x|/|y|$ and the phase difference, which continues to remain equal to $\varphi - \psi$.

Thus, in the cases indicated we can use the complex amplitudes x_0 and y_0 in place of \underline{x} and \underline{y} , and the time origin $\tau = 0$ can be designated to suit the convenience of the nature of the problem. Let us explain this by means of an example. Assume, for example, that it is required that the initial amplitude x'_0 be a real quantity. This corresponds to an instant of time $\tau = \tau_0$, defined by the equation

$$a_0 e^{\nu \tau_0} \sin \omega \tau_0 + b_0 e^{\nu \tau_0} \cos \omega \tau_0 = 0.$$

If we now introduce a new time scale τ' such as to satisfy the equality $\tau = \tau' + \tau_0$, as well as new initial amplitudes, then we can write in place of (2.2)

$$\left. \begin{aligned} x &= x'_0 e^{(\nu + i\omega)\tau'} \\ y &= y'_0 e^{(\nu + i\omega)\tau'} \end{aligned} \right\} \quad (2.3)$$

where

$$\left. \begin{aligned} x'_0 &= x_0 e^{(v + i\omega)\tau_0} \\ y'_0 &= y_0 e^{(v + i\omega)\tau_0} \end{aligned} \right\} \quad (2.4)$$

The notations (2.2) and (2.3) are perfectly equivalent in essence and identical in form, but the time origins in them differ by τ_0 , and furthermore in the notation of (2.3) the condition that \underline{x} be a real quantity at the instant $\tau' = 0$ is satisfied. Thus, by suitable choice of the time origin it is possible to fulfill certain requirements concerning the initial position of the vector \underline{x} in the complex plane.

In those cases when the time variation of the variables is of no interest, we can use for an estimate of the relative amplitudes and phase differences not only the complex amplitude x_0 and y_0 , but also the vectors \vec{x}_0 and \vec{y}_0 .

This method of writing down the variables has certain advantages. Assume, for example, that the nature of the problem under consideration calls for writing down that the phase shifts between x_0 and y_0 are equal to $\pi/2$. The simplest way of obtaining this notation is to introduce in place of x_0 and y_0 the vectors \vec{x}_0 and \vec{y}_0 and equating their scalar product to zero:

$$x_0 y_0 = 0.$$

Second example: it is required to calculate the quantity

$$\frac{\omega}{2\pi} \int_0^{\frac{2\pi}{\omega}} xy \, d\tau, \quad (2.5)$$

where \underline{x} and \underline{y} are assumed to be written down in the form (2.1) for $v = 0$. It is easy to verify that this quantity is equal to

$$\frac{1}{2} x_0 y_0 \cos(\varphi - \psi).$$

Consequently,

$$\frac{\omega}{2\pi} \int_0^{\frac{2\pi}{\omega}} xy \, d\tau = \frac{1}{2} x_0 y_0.$$

i.e., the vector notation of the variables can be quite useful in this case, too.

We shall use in the present book all three forms of writing down the variables, namely (2.1), (2.2), and the vector form. The choice of any particular method depends entirely on the gist of the problem under consideration and is usually not specially stipulated. It must be emphasized only that in those cases when nonlinear relations are considered [the self-oscillation problem, setting up of expressions of the form (2.5), etc.], complex variables corresponding to the notation of type (2.2) cannot be employed. The reason for it is that the real part of the product xy [where x and y are complex quantities written in the form (2.2)] and the product xy calculated for (2.1) are not equal to each other. In this connection, the complex form of writing down the variables will be used only in linear problems.

Manu-
script
Page
No.

[Footnotes]

- | | |
|----|--|
| 8 | Strutt, J.W. (Lord Rayleigh), Teoriya zvuka [The Theory of Sound], Vol. II, Gostekhizdat [State Publishing House for Theoretical and Technical Literature], 1955, p. 221 et seq. |
| 10 | Coward, H.F., Hartwell, F.J., Georgson, E.H.M., Journ. of the Chemical Society, 1482, 1937. |
| 13 | Crocco, Luigi and Cheng Sin-I, Teoriya neustoychivosti gorennya v zhidkostnykh reaktivnykh dvigatelyakh [Theory of Combustion Instability in Liquid-Fuel Jet Engines], IL [Publishing House for Foreign Literature], Moscow, 1958. |

Chapter 2

PROPAGATION OF PERTURBATIONS IN A MOVING GAS

§3. Linearization of the Equations of Hydromechanics

In the study of processes connected with the excitation of acoustic oscillations by the supply of heat to a moving gas, the ordinary equations of acoustics cannot be used. The reason for it is that the equations of acoustics are obtained by assuming, first, that the medium (air) is subject to no motion whatever except to the motion directly connected with the propagation of the sound waves, and second, by assuming the medium to be isentropic. The initial equations necessary for the investigation are obtained by linearizing the equations of hydromechanics of compressible fluids and of thermodynamics. This method is quite natural, since sound oscillations can be defined as oscillatory motion in a compressible fluid,* characterized by small amplitudes.

As already mentioned, we shall consider henceforth only longitudinal oscillations in sufficiently long cylindrical tubes. (We shall regard tubes as long if their diameter is small compared with the length.) This condition enables us to leave out a detailed analysis of the complex phenomena that occur at the ends of the tube, and replace them by a certain integral effect in the form that it manifests itself at a certain distance from the end. If, in addition, we agree to consider only low frequencies of acoustic oscillations (such that the wavelength is large compared with the tube diameter), then we can assume that all quantities (velocities, pressures, etc.) are constant

Along each transverse cross section of the tube, and the direction of propagation of the perturbation waves coincides with the direction of the tube axis. Of course, the concepts of sufficiently long tube and sufficiently low oscillation frequency are quite indeterminate and the degree to which these conditions are satisfied must be estimated in each specific case by starting from the physical nature of the phenomenon considered and from the requirements imposed on the theoretical analysis. Depending on whether the theory must yield exact quantitative results or merely indicate the qualitative aspect of the phenomenon, this limitation can vary over a wide range. What is essential here is only that in the case when the assumptions made are valid it is possible to confine oneself to a consideration of the problem in a one-dimensional formulation.

Let us make the natural assumption that the main flow in a long cylindrical tube, on which small perturbations are superimposed, can also be regarded as one-dimensional. We shall assume the gas to be ideal (not viscous and not heat conducting). We write down the fundamental equations of one-dimensional hydromechanics, aligning the x axis with the tube axis:

$$\left. \begin{aligned} \frac{\partial v}{\partial t} + v \frac{\partial v}{\partial x} + \frac{1}{\rho} \frac{\partial p}{\partial x} &= 0, \\ \frac{\partial \rho}{\partial t} + v \frac{\partial \rho}{\partial x} + \rho \frac{\partial v}{\partial x} &= 0, \\ \frac{\partial s}{\partial t} + v \frac{\partial s}{\partial x} &= 0. \end{aligned} \right\} \quad (3.1)$$

Here t is the time, v the stream velocity, p the pressure, ρ the density of the flowing medium, and s the entropy.

The first of these equations is, as is well known, the equation of the motion of the fluid (the Euler equation), while the second is the continuity equation and the third the condition for the conservation of the entropy of a particle.

By virtue of the assumption that the gas is ideal, the entropy of any elementary particle of the gas cannot change as it moves along the tube within the limits of those portions of the tube in which there is no heat supply. This follows from the fact that an ideal gas is one without viscosity or heat conduction. The absence of heat conduction means that the temperatures of neighboring volumes, heated to an unequal degree, cannot gradually become equalized. On the other hand, the lack of viscosity does not permit the mechanical energy of flow to change over into heat and thereby change the entropy.

Thus, the entropy s of each element of the gas moving along the tube will remain constant, although the neighboring elements may have different entropy. This is valid, of course, when the gas moves through portions of the tube in which the gas is not subjected to external action (heat supply, etc.). A mathematical expression of this fact is the third equation in (3.1).

The validity of assuming the gas to be ideal in order to obtain the initial system of equations (3.1) is not self-evident. Strictly speaking, it would be necessary to show that the neglect of the viscosity and heat conduction does not introduce an essential error in the results of the analysis. We shall not consider this question in greater detail here. We must point out only that a more thorough analysis, made by Merk* essentially confirms the correctness of such an assumption. He showed that an account of the viscosity and heat conduction merely distorts slightly the pattern of the small oscillations in the nearest vicinity of the heat supply zone and does not manifest itself in any essential manner at the ends of the tube, i.e., in sections for which the boundary conditions are written. The influence of viscosity and heat conduction on the change in the entropy should be more significant. However, in the exposition that follows, the entropy

flux and its perturbations will not play any practical role in the analysis of the process of excitation of acoustic oscillations.

The three equations (3.1) contain four variables: v , p , ρ , and s . It is easy to note that these variables are not independent. The connection between the last three is given by the thermodynamic equation

$$s = c_v \ln p - c_p \ln \rho, \quad (3.2)$$

where c_v is the specific heat at constant volume and c_p is the specific heat at constant pressure.

Eliminating with the aid of (3.2) one of the variables from the system of equations (3.1) we can reduce the number of variables to three. This, however, is best done after the equations are linearized.

We shall consider a certain steady-state gas flow through the cylindrical tube. We eliminate from consideration the portions where heat is supplied. Then, by virtue of the assumptions made above, the gas velocity, its density, pressure, and entropy will be the same in all the sections between the heat-supply portions and at each point. We denote them by v_0 , ρ_0 , p_0 , and s_0 . Assume that weak perturbations of the flow parameters δv , δp , $\delta \rho$, and δs are superimposed on the stationary flow. These perturbations will, of course, be the same for all points of the section under consideration, but can be different for neighboring sections. In this lies their essential difference from v_0 , ρ_0 , p_0 , and s_0 , which are constant for all sections. Thus, for the perturbed flow we can write

$$\left. \begin{aligned} v &= v_0 + \delta v, & p &= p_0 + \delta p, \\ \rho &= \rho_0 + \delta \rho, & s &= s_0 + \delta s. \end{aligned} \right\} \quad (3.3)$$

Substituting the expressions (3.3) in Eqs. (3.1) and (3.2), we discard quantities of higher order of smallness and take into account the properties of the stationary flow. This enables us to obtain equations that are linear in δv , $\delta \rho$, δp , and δs . Let us illustrate this

process by using the first equation of (3.1) as an example. Substituting the values of \underline{v} , ρ , and p from (3.3) into the equation of motion, we obtain

$$\frac{\partial (v_0 + \delta v)}{\partial t} + (v_0 + \delta v) \frac{\partial (v_0 + \delta v)}{\partial x} + \frac{1}{\rho_0 + \delta \rho} \frac{\partial (\rho_0 + \delta \rho)}{\partial x} = 0.$$

If we recognize that by virtue of the above-indicated properties of stationary flow we have $\partial v_0 / \partial t \equiv 0$, $\partial v_0 / \partial x \equiv 0$, $\partial \rho_0 / \partial x \equiv 0$, the equation written down can be reduced to the form

$$\frac{\partial \delta v}{\partial t} + v_0 \frac{\partial \delta v}{\partial x} + \delta v \frac{\partial \delta v}{\partial x} + \frac{1}{\rho_0} \frac{\partial \delta \rho}{\partial x} - \frac{\delta \rho}{\rho_0^2} \frac{\partial \delta \rho}{\partial x} + \varepsilon \frac{\partial \delta p}{\partial x} = 0.$$

In writing down this equation we used the well-known formula, which is valid if $z \ll 1$,

$$\frac{1}{1+z} = 1 - z + \varepsilon,$$

where ε is a quantity of higher order of smallness relative to \underline{z} . Applied to the case under consideration $\delta \rho \ll \rho_0$, this yields

$$\frac{1}{\rho_0 + \delta \rho} = \frac{1}{\rho_0} - \frac{\delta \rho}{\rho_0^2} + \varepsilon.$$

Returning to the preceding equation, we note that the terms $\delta v (\partial \delta v / \partial x)$, $\delta \rho / \rho_0^2 (\partial \delta \rho / \partial x)$, and $\varepsilon (\partial \delta p / \partial x)$ are of higher order of smallness compared with the three other terms of the resultant equation (it is assumed here that the derivatives of the perturbations have the same order of smallness as the perturbations themselves). Discarding these terms, we write down the Euler equation in the form

$$\frac{\partial \delta v}{\partial t} + v_0 \frac{\partial \delta v}{\partial x} + \frac{1}{\rho_0} \frac{\partial \delta \rho}{\partial x} = 0.$$

Inasmuch as v_0 and ρ_0 are constants, this equation is linear in the variables. In this sense it is essentially simpler than the initial equation of motion (3.1). However, this simplicity has been attained at the expense of a strong narrowing down of the region of applicability of the new equation. Whereas the equation in the initial form (3.1)

applicable to all one-dimensional flows of an ideal fluid, in the new form it is valid only for flows that differ little from stationary. The use of the linearized equations in the present book in lieu of the exact equations is fully justified, since acoustic oscillations are characterized by small amplitudes.

Linearizing the second and third equations of the system (3.1), and also Eq. (3.2), we obtain the following initial system of equations for the perturbed flow of a gas stream:

$$\left. \begin{aligned} \frac{\partial \delta v}{\partial t} + v_0 \frac{\partial \delta v}{\partial x} + \frac{1}{\rho_0} \frac{\partial \delta p}{\partial x} &= 0, \\ \frac{\partial \delta \rho}{\partial t} + v_0 \frac{\partial \delta \rho}{\partial x} + \rho_0 \frac{\partial \delta v}{\partial x} &= 0, \\ \frac{\partial \delta s}{\partial t} + v_0 \frac{\partial \delta s}{\partial x} &= 0, \\ \delta s + c_p \frac{\delta \rho}{\rho_0} - c_v \frac{\delta p}{p_0} &= 0. \end{aligned} \right\} \quad (3.4)$$

One remark should be made with respect to this system. As a result of linearization of Eqs. (3.1) and (3.2), the variables v , ρ , p , and s were replaced by the variations of these variables δv , $\delta \rho$, δp , and δs . The manipulations carried out during the linearization were essentially based on the assumption that δv , $\delta \rho$, δp , and δs are small. But if one speaks of the smallness of some quantity, it is always necessary to indicate the other quantity in comparison with which this quantity is small. Looking at Eqs. (3.3) one might think that the smallness referred to is compared with v_0 , ρ_0 , p_0 , and s_0 . This is not at all so, however. Actually, in a stationary medium $v_0 = 0$ and in this particular case any δv , no matter how small, can be regarded as small compared with v_0 . Analogous considerations can be advanced also with respect to δs . As is well known from thermodynamics, the reference point from which entropy is measured can be arbitrarily assigned. Taking it to be s_0 , we immediately obtain $s_0 = 0$ and consequently the deviations of the entropy δs cannot be regarded as small compared with s_0 . Only with

respect to δp and δp can we say that they are small compared with p_0 and p_0 , inasmuch as the transition from the equation (3.2) to the linearized form in the last line of the system (3.4) is possible only for finite values of p_0 and p_0 .

When we spoke of the smallness of the variations of the variables δv , δp , δp , and δs , we had in mind only the fact that the squares and the products of these variations and of their derivatives can be neglected compared with the linear terms. (This does not mean, of course, that in these variables there are no natural scales of smallness; such scales will be given in the next section.)

§4. Acoustic Waves in a Moving Nonisentropic Gas

The system of equations (3.4) can be simplified by eliminating one of the variables with the aid of the finite relation given in the last line. Expressing δp from the fourth equation and substituting it into the second, we obtain the equation

$$\frac{c_p}{c_p} \frac{q_s}{p_s} \left(\frac{\partial \delta p}{\partial t} + v_s \frac{\partial \delta p}{\partial x} \right) - \frac{q_s}{c_p} \left(\frac{\partial \delta s}{\partial t} + v_s \frac{\partial \delta s}{\partial x} \right) + q_s \frac{\partial \delta v}{\partial x} = 0,$$

the second term in the left half of which is equal to zero by virtue of the third equation of the system (3.4). The factor in the first term is equal to $c_v p_0 / c_p p_0 = 1/a^2$, where a is the velocity of sound in the unperturbed flow. This follows from the well-known thermodynamic relations

$$p = qRT, \quad (4.1)$$

$$a = \sqrt{\kappa RT}, \quad (4.2)$$

$$\kappa = \frac{c_p}{c_v} \quad (4.3)$$

(the gas constant R is referred here to unit mass and not weight).

Thus, after eliminating δp , the system (3.4) can be rewritten in the form

$$\left. \begin{aligned} \frac{\partial \delta v}{\partial t} + v_0 \frac{\partial \delta v}{\partial x} + \frac{1}{\rho_0} \frac{\partial \delta p}{\partial x} &= 0, \\ \frac{\partial \delta p}{\partial t} + v_0 \frac{\partial \delta p}{\partial x} + a^2 \rho_0 \frac{\partial \delta v}{\partial x} &= 0, \\ \frac{\partial \delta s}{\partial t} + v_0 \frac{\partial \delta s}{\partial x} &= 0. \end{aligned} \right\} \quad (4.4)$$

A feature of the resultant system is that by choosing as the dependent variables the quantities δv , δp , and δs the first three equations can be integrated apart from the third. This circumstance noticeably simplifies the calculations. The physical meaning of this separation of the third equation from the first two reduces to stating that the acoustic pressure and velocity waves propagate independently of the "thermal" entropy waves. It might seem that one could on this basis confine oneself in general to an examination of the system consisting of the first two equations. In the general case, however, this is not so. The point is that in writing down the boundary conditions or in formulating the laws governing the heat supply process, the quantities δp and δv may turn out to be related with δs , and then the third equation of the system assumes an important role.

The system (4.4) is not, however, the simplest one possible. Indeed, if we introduce the variables

$$\left. \begin{aligned} u &= a \rho_0 \delta v + \delta p, \\ w &= a \rho_0 \delta v - \delta p \end{aligned} \right\} \quad (4.5)$$

and after expressing δv and δp from these equations substitute them in the first two equations of (4.4), and then take a term-by-term sum and difference of the resultant equations, the system (4.4) assumes the form

$$\left. \begin{aligned} \frac{\partial u}{\partial t} + (v_0 + a) \frac{\partial u}{\partial x} &= 0, \\ \frac{\partial w}{\partial t} + (v_0 - a) \frac{\partial w}{\partial x} &= 0, \\ \frac{\partial \delta s}{\partial t} + v_0 \frac{\partial \delta s}{\partial x} &= 0. \end{aligned} \right\} \quad (4.6)$$

Now each of the three equations can already be integrated separately

from the others. In this case all three equations are of exactly the same type and it is therefore enough to integrate any of them. Let us consider for the sake of being definite the third equation. Its general solution, as is well known, is the expression

$$\delta s = F(x - v_0 t), \quad (4.7)$$

where F is an arbitrary differentiable function.

Let us explain the meaning of the obtained solution. It is seen from the expression written down that δs changes, generally speaking, both when x changes and when t changes. However, for the instants of time t and coordinates x satisfying the condition

$$x - v_0 t = \text{const},$$

the quantity δs will remain constant. Assume that δs is a certain specified function of x at the instant of time $t = 0$. This dependence can be clearly visualized in the form of a snapshot of a certain "wave" of δs . We consider the motion of the "crest" of this wave (the sections where δs has a maximum value), assuming that this "crest" exists. If the crest has a coordinate x_1 at the instant of time $t = 0$, the section corresponding to it (i.e., the section in which F reaches a maximum) will move, based on the statement made above, in accordance with the law

$$x = x_1 + v_0 t.$$

We can make exactly the same statement concerning the other points of the "wave." Consequently, the solution (4.7) describes the motion of a wave of δs without a change in its shape in a positive x direction with velocity v_0 .

The formal derivations presented here correspond to a perfectly obvious physical phenomenon — inasmuch as the entropy of an elementary volume of gas cannot change (we recall that we are considering an ideal compressible fluid), the entropy will move along the flow axis together with the volume that carries it, i.e., with the stream velocity.

Perfectly analogous arguments can be applied also to the first two equations of the system (4.6), the only difference being that the waves \underline{u} and \underline{w} propagate with velocities $v_0 + a$ and $v_0 - a$, respectively. Thus, the \underline{u} waves move only to the right and the \underline{w} waves only to the left. These waves can be interpreted as waves of acoustic pulses moving with the stream (with the velocity of the stream plus the velocity of sound) and against the stream (with the velocity of the stream minus the velocity of sound).*

The variables \underline{u} and \underline{w} , which were introduced in purely formal fashion, have consequently a deep physical meaning. To be sure, in a certain sense these variables are less illustrative than δp and δv , and they cannot be directly measured in the experiment, but they turn out to be quite useful in the solution of many problems. We shall use below both forms of writing down the initial equations [(4.4) and (4.6)].

Let us introduce a system of dimensionless variables with the aid of the following equations:

$$\left. \begin{aligned} \bar{v} &= \frac{\delta v}{a}; \quad \bar{p} = \frac{\delta p}{\kappa p_0}; \quad \bar{q} = \frac{\delta q}{q_0}; \quad \bar{s} = \frac{\delta s}{c_p}; \\ \bar{u} &= \frac{u}{a^2 q_0}; \quad \bar{w} = \frac{w}{a^2 q_0}; \quad \tau = t \frac{a}{L}; \quad \xi = \frac{x}{L}. \end{aligned} \right\} \quad (4.8)$$

Here κ is the adiabatic exponent and L a certain characteristic linear dimension, for example the tube length.

The connection between the variables \bar{p} , \bar{v} and \bar{u} , \bar{w} , as well as \bar{s} , \bar{p} , and \bar{q} is expressed by the simple formulas

$$\left. \begin{aligned} \bar{u} &= \bar{v} + \bar{p}, \quad \bar{w} = \bar{v} - \bar{p}, \quad \bar{p} = \frac{\bar{u} - \bar{w}}{2}, \quad \bar{v} = \frac{\bar{u} + \bar{w}}{2}, \\ \bar{s} &= \bar{p} - \bar{q}. \end{aligned} \right\} \quad (4.9)$$

The last formula is given here for the sake of completeness and is a consequence of the fourth equation of the system (3.4).

After introducing the dimensionless variables, the systems of Eqs. (4.4) and (4.6) assume the following form:

$$\left. \begin{aligned} \frac{\partial \bar{v}}{\partial \tau} + M \frac{\partial \bar{v}}{\partial \xi} + \frac{\partial \bar{p}}{\partial \xi} &= 0, \\ \frac{\partial \bar{p}}{\partial \tau} + M \frac{\partial \bar{p}}{\partial \xi} + \frac{\partial \bar{v}}{\partial \xi} &= 0, \\ \frac{\partial \bar{s}}{\partial \tau} + M \frac{\partial \bar{s}}{\partial \xi} &= 0 \end{aligned} \right\} \quad (4.10)$$

and

$$\left. \begin{aligned} \frac{\partial \bar{u}}{\partial \tau} + (M+1) \frac{\partial \bar{u}}{\partial \xi} &= 0, \\ \frac{\partial \bar{w}}{\partial \tau} + (M-1) \frac{\partial \bar{w}}{\partial \xi} &= 0, \\ \frac{\partial \bar{s}}{\partial \tau} + M \frac{\partial \bar{s}}{\partial \xi} &= 0. \end{aligned} \right\} \quad (4.11)$$

Here M is the ratio of the velocity of the unperturbed flow to the velocity of sound in it.

The coefficients of both systems depend only on the number M. This indicates that this parameter plays a major role in our problem.

We seek a solution of the system (4.11). Repeating verbatim everything said concerning the solution of the system (4.6), we can state that the three equations (4.11) correspond to three arbitrary waves \bar{u} , \bar{w} , and \bar{s} , which move with dimensionless velocities $(M+1)$, $(M-1)$, and M.

We shall seek a particular solution of Eqs. (4.11), assuming that the arbitrary function F is exponential.

Then

$$\left. \begin{aligned} \bar{u} &= F_u[\xi - (M+1)\tau] = A_u \exp \left[\beta \left(\tau - \frac{1}{M+1} \xi \right) \right], \\ \bar{w} &= F_w[\xi - (M-1)\tau] = A_w \exp \left[\beta \left(\tau - \frac{1}{M-1} \xi \right) \right], \\ \bar{s} &= F_s[\xi - M\tau] = A_s \exp \left[\beta \left(\tau - \frac{1}{M} \xi \right) \right]. \end{aligned} \right\} \quad (4.12)$$

For convenience in the derivations that follow, we have modified somewhat the notation of the arguments in the right halves of (4.12).

The numbers A_u , A_w , A_s , and β in the right halves of the equations remain indeterminate for the time being. A remark is in order

with respect to β . Generally speaking, the values of β can be different for each of the three variables, inasmuch as the integrated system (4.11) actually broke up into three independent equations. However, we shall consider from now on only cases in which the boundary conditions relating these three variables call for identical values of β in all three exponential functions.

Let us illustrate this by means of an example. Assume that there are no pressure oscillations at the end of the tube (this corresponds to the ordinary boundary condition for the open end, if we neglect the radiation of sound from the tube). By aligning the origin with this end section, we obtain the boundary condition $\bar{p} = 0$ when $\xi = 0$. Converting to the functions \bar{u} , \bar{w} (4.9), we write this condition in the form $\bar{u} = \bar{w}$ when $\xi = 0$. We now have on the basis of Formula (4.12)

$$A_u e^{\beta \tau} = A_w e^{\beta \tau}.$$

Satisfaction of this condition for all values of τ is possible only when $A_u = A_w$ and when the values of β are the same in the right and left halves of the equation.

Let us explain the physical meaning of the quantity β . Let β be an imaginary quantity, $\beta = i\omega$. Then we can write, say for the variable \bar{u} :

$$\begin{aligned} \bar{u} &= A_u \exp \left[i\omega \left(\tau - \frac{1}{M+1} \xi \right) \right] = \\ &= A_u \left[\cos \omega \left(\tau - \frac{1}{M+1} \xi \right) + i \sin \omega \left(\tau - \frac{1}{M+1} \xi \right) \right]. \end{aligned}$$

Let us consider the behavior of \bar{u} in a certain specified section $\xi = \text{const}$, using the real part of the last expression. It is easy to see that under these conditions the variable \bar{u} will execute harmonic oscillations in time, with frequency ω .

Thus, the number β can have the meaning of an oscillation frequency, a frequency which is the same for all ξ . The oscillations of

the gas in the tube, which occur at all cross sections (at all ξ) with identical frequency, should cause all parameters of the gas flow, namely pressure, velocity, density, etc., to oscillate at the same frequency. The latter circumstance is the consequence of the formal deduction made somewhat earlier concerning the identity of β for all three exponential functions (4.12), with the aid of which we expressed the variation of the different parameters of a single gas flow.

The meaning of the quantity β was explained for the case when β was a pure imaginary number. In our case, where β is a complex quantity, one must speak by analogy of a complex frequency β . We shall consider this case in greater detail later on.

The numbers A_u , A_w , and A_s are the coefficients of the exponential functions in Expressions (4.12), and are formally defined as follows. By putting $\tau = 0$ and $\xi = 0$ we obtain $\bar{u} = A_u$, $\bar{w} = A_w$, and $\bar{s} = A_s$. Consequently, the numbers A_u , A_w , and A_s must be defined as the values of \bar{u} , \bar{w} , and \bar{s} at the origin at the instant of time $\tau = 0$.

The solution of the system (4.10), which is equivalent to the just considered system (4.11), can be obtained directly. It is simpler, however, to use the solutions (4.12) and Formulas (4.9), which relate the variables \bar{p} and \bar{v} with the variables \bar{u} and \bar{w} .

Introducing the symbols A_v and A_p for \bar{v} and \bar{p} at the section $\xi = 0$ at the instant of time $\tau = 0$, we obtain

$$\begin{aligned} \bar{v} = \frac{\bar{u} + \bar{w}}{2} = \frac{1}{2} \left[A_u \exp\left(-\frac{1}{M+1}\beta\xi\right) + \right. \\ \left. + A_w \exp\left(-\frac{1}{M-1}\beta\xi\right) \right] e^{\beta\tau} = \\ = \frac{1}{2} \left[(A_u + A_p) \exp\left(-\frac{1}{M+1}\beta\xi\right) + \right. \\ \left. + (A_u - A_p) \exp\left(-\frac{1}{M-1}\beta\xi\right) \right] e^{\beta\tau}. \end{aligned}$$

Let us carry out analogous transformations for the determination of \bar{p} and let us write down finally the particular solution of the sys-

from (4.10) in the following form:

$$\left. \begin{aligned} \bar{v} &= [A_1 \varphi_1(\xi) + A_2 \varphi_2(\xi)] e^{\beta \tau}, \\ \bar{p} &= [A_1 \varphi_2(\xi) + A_2 \varphi_1(\xi)] e^{\beta \tau}, \\ \bar{s} &= A_3 \varphi_3(\xi) e^{\beta \tau}, \end{aligned} \right\} \quad (4.13)$$

where

$$\left. \begin{aligned} \varphi_1(\xi) &= \frac{1}{2} \left[\exp\left(-\frac{1}{M+1} \beta \xi\right) + \exp\left(-\frac{1}{M-1} \beta \xi\right) \right], \\ \varphi_2(\xi) &= \frac{1}{2} \left[\exp\left(-\frac{1}{M+1} \beta \xi\right) - \exp\left(-\frac{1}{M-1} \beta \xi\right) \right], \\ \varphi_3(\xi) &= \exp\left(-\frac{1}{M} \beta \xi\right). \end{aligned} \right\} \quad (4.14)$$

The solution obtained has a somewhat more cumbersome form than (4.12). In many cases, however, it is preferable to the solution (4.12), since it yields direct expressions for the perturbations of the main physical parameters of the stream.

§5. Example of Simplest Boundary Problem

In the preceding section we derived the general solutions of the equations of the acoustics of a moving nonisentropic gas. However, for a unique definition of the investigated process it is necessary to formulate the boundary and initial conditions. These conditions have different forms, depending on the specific content of the problem.

In the simplest case, the boundary conditions can be reduced to linear homogeneous relations between the variables, which must be satisfied at the ends of the tube. Let us align the origin $\xi = 0$ with the left end of the tube and, assuming the characteristic linear dimension L to be the length of the tube, we obtain for the right end the coordinate $\xi = 1$.

We can then write down these conditions, for example, in the form:

$$\left. \begin{aligned} a_{11} \bar{v} + a_{12} \bar{p} + a_{13} \bar{s} &= 0, \\ a_{21} \bar{v} + a_{22} \bar{p} + a_{23} \bar{s} &= 0 \end{aligned} \right\} \text{ for } \xi = 0 \text{ (for all } \tau \geq 0),$$

$$a_{11}\bar{v} + a_{12}\bar{p} + a_{13}\bar{s} = 0 \text{ for } \xi = 1$$

where a_{ik} are numerical coefficients.

Specification of these relations does not define, however, the complete problem, and it is necessary to supplement them with the initial conditions

$$\begin{aligned}\bar{v} &= f_1(\xi) \text{ for } \tau=0, \quad 0 < \xi < 1, \\ \bar{p} &= f_2(\xi) \text{ for } \tau=0, \quad 0 < \xi < 1, \\ \bar{s} &= f_3(\xi) \text{ for } \tau=0, \quad 0 < \xi < 1,\end{aligned}$$

where f_1 , f_2 , and f_3 are specified functions.

Particular interest is attached to those among the described problems in which two out of the three boundary conditions do not contain \bar{s} , as was the case in the preceding example in which $a_{13} = a_{23} = 0$. Then the presence of two boundary conditions containing only \bar{p} and \bar{v} makes it possible to solve the boundary problem for the first two equations of the system (4.10) apart from the last equation of this system. In many cases this is sufficient, since usually the greatest interest is attached to the oscillations of the pressure and of the velocity of the gas stream. Only in those cases when it is necessary to know also the entropy oscillations (or the oscillations of other quantities associated with it) must one turn to the third equation of the system (4.10).

Let us consider the simplest example, that of longitudinal oscillations in a gas flowing along a tube that is open on both ends. If we assume that the open ends communicate with an unbounded space, then in first approximation we can use as the boundary conditions the customary requirement in acoustics, that the pressure be constant on the ends of the tube, a requirement which is natural for a tube in unbounded space. In our problem this condition assumes the form

$$\left. \begin{aligned}\bar{p} &= 0 \text{ for } \xi=0 \quad (\tau > 0), \\ \bar{p} &= 0 \text{ for } \xi=1 \quad (\tau > 0).\end{aligned} \right\} \quad (5.1)$$

These boundary conditions do not contain the variable \bar{s} , so that we shall solve the boundary condition for the first two equations of the system (4.10). Let us specify also the initial conditions

$$\left. \begin{aligned} \bar{v} &= f_1(\xi) \text{ for } \tau=0 \quad (0 \leq \xi \leq 1), \\ \bar{p} &= f_2(\xi) \text{ for } \tau=0 \quad (0 \leq \xi \leq 1). \end{aligned} \right\} \quad (5.2)$$

The specification of the functions f_1 and f_2 means that the perturbation of motion of the gas in the tube is known at the initial instant.

Let us turn to the solution (4.13). We see from Formulas (4.14) that $\varphi_1(0) = 1$, $\varphi_2(0) = 0$ when $\xi = 0$.

Consequently, the second equation in (4.13) yields $p = A_p e^{\beta \tau}$ when $\xi = 0$. According to the first condition of (5.1), this quantity is equal to zero for all values of τ , something possible only if $A_p = 0$. On the other end of the tube, where $\xi = 1$, the condition $\bar{p} = 0$ should be satisfied. It follows from (4.13) and (4.14) that this is possible only for

$$A_1 \varphi_2(1) = 0.$$

The second formula of (4.14) shows that if we discard the trivial case $A_v = 0$, the latter is satisfied only if

$$\exp \left[-\frac{2}{1-M^2} \beta \right] = 1. \quad (5.3)$$

Let β be a complex quantity

$$\beta = v + i\omega.$$

Then (5.3) can be reduced to two equations which themselves define only real quantities

$$\begin{aligned} \cos \frac{2}{1-M^2} \omega \exp \left(-\frac{2}{1-M^2} v \right) &= 1, \\ \sin \frac{2}{1-M^2} \omega \exp \left(-\frac{2}{1-M^2} v \right) &= 0. \end{aligned}$$

Inasmuch as the exponential function of a real variable is always positive, these two equations can be satisfied simultaneously only when

$$\left. \begin{aligned} v &= 0, \\ \omega &= (1 - M^2) k\pi \quad (k = 0, 1, 2, \dots) \end{aligned} \right\} \quad (5.4)$$

Thus, the specified boundary conditions are satisfied by harmonic oscillations with fully defined frequencies ω (we shall not consider the case $k = 0$, since it corresponds to the uninteresting case of the changeover of a stream to a new stationary flow velocity at the same pressure: $\bar{p} = 0$, $\bar{v} = A_v = \text{const}$ for all τ and ξ). It must be noted here that these are precisely the frequencies that would be obtained for boundary conditions $\bar{v} = 0$ on both ends of the tube.

The lowest permissible frequency, corresponding to $k = 1$, namely $\omega_1 = (1 - M^2)\pi$, is called the fundamental tone of the oscillations. The higher frequencies $\omega_2 = (1 - M^2)2\pi$, $\omega_3 = (1 - M^2)3\pi$, ..., etc. are frequently called overtones. In the present book we shall use a different designation for the permissible oscillation frequencies. We shall agree to call them the characteristic values of the frequency or the harmonics. In this case the fundamental tone (the lowest frequency) will be called the first harmonic, the frequency corresponding to $k = 2$ the second harmonic, etc.

Each value of ω obtained from Formula (5.4), i.e., each harmonic, defines a particular solution of the system comprising the first two equations of (4.10) and satisfying the formulated boundary conditions. By virtue of the linearity of these equations, the sum of the particular solution also satisfies these equations and boundary conditions (5.1).

Thus, the solution of the system will be not only the functions (4.13) but also their sums. Taking the sums for all values of k , we obtain

$$\left. \begin{aligned} \bar{v} &= \frac{1}{2} \sum_{k=1}^{\infty} A_{vk} [e^{-i(1-M)k\pi\tau} + e^{i(1+M)k\pi\tau}] e^{i(1-M^2)k\pi\tau}, \\ \bar{p} &= \frac{1}{2} \sum_{k=1}^{\infty} A_{vk} [e^{-i(1-M)k\pi\tau} - e^{i(1+M)k\pi\tau}] e^{i(1-M^2)k\pi\tau}, \end{aligned} \right\} \quad (5.5)$$

The letters A_{vk} denote here numbers, for the time being undetermined, which can be so manipulated as to satisfy the initial conditions.

Strictly speaking, before proceeding further, it would be necessary to prove the convergence of the series (5.5). In courses dealing with the equations of mathematical physics suitable theorems are presented, which enable us to judge what limitations must be imposed on the functions $f_1(\xi)$ and $f_2(\xi)$ (5.2) in order that they be expandable in terms of the functions contained in the right brackets in Expression (5.5). We shall not consider this question as well as mathematical questions related with it, principally because we shall not consider from now on any problems with initial conditions. Those interested in this topic will find the corresponding information in the special books.

For the sake of completeness, however, let us carry through to its conclusion the solution of the problem formulated in the present section, making the simplifying assumption that the gas in the tube is stationary ($M = 0$).

Then the solutions (5.5) assume for $\tau = 0$ the following form:

$$\begin{aligned} \bar{v} &= \sum_{k=1}^{\infty} A_{vk} \cos k\pi\xi, \\ \bar{p} &= \sum_{k=1}^{\infty} -iA_{vk} \sin k\pi\xi. \end{aligned}$$

Putting $A_{vk} = a_k + ib_k$, we obtain from the last equations

$$\left. \begin{aligned} \bar{v} &= \sum_{k=1}^{\infty} a_k \cos k\pi\xi + ib_k \cos k\pi\xi, \\ \bar{p} &= \sum_{k=1}^{\infty} -ia_k \sin k\pi\xi + b_k \sin k\pi\xi \end{aligned} \right\} \quad \text{for } \tau = 0.$$

If we recall that only the real parts of the complex expressions cor-

respond to the actual instantaneous values of \bar{v} and \bar{p} , which can be observed experimentally, then, by comparing the resultant expressions with the initial conditions (5.2), we immediately obtain the equations

$$\left. \begin{aligned} f_1(\xi) &= \sum_{k=1}^{\infty} a_k \cos k\pi\xi, \\ f_2(\xi) &= \sum_{k=1}^{\infty} b_k \sin k\pi\xi. \end{aligned} \right\} \quad (5.6)$$

From the theory of Fourier series it is known that any function $f(x)$ which satisfies the conditions under which it can be expanded in a Fourier series, can be represented in the form

$$f(x) = \frac{c_0}{2} + \sum_{k=1}^{\infty} c_k \cos k\pi x,$$

where

$$c_k = 2 \int_0^1 f(x) \cos k\pi x dx,$$

if $f(x)$ is an even function in the interval from $x = -1$ to $x = 1$, or in the form

$$f(x) = \sum_{k=1}^{\infty} b_k \sin k\pi x,$$

where

$$b_k = 2 \int_0^1 f(x) \sin k\pi x dx,$$

if $f(x)$ is odd in this interval.

The functions $f_1(\xi)$ and $f_2(\xi)$ are specified not in the interval $(-1, 1)$, but only in the interval $(0, 1)$. However, both functions can be continued also into the interval $(-1, 0)$. In this case it is natural to continue the function $f_2(\xi)$ in odd fashion, inasmuch as according to the boundary condition (5.1) we have $f_2(0) = 0$. The function $f_1(\xi)$, which represents the velocity perturbation, is generally speaking not equal to zero when $\xi = 0$, and must be continued in even fashion. Thus,

Without loss of generality, we can assume its mean value to be equal to zero, for if this mean value differs from zero, it can be added to the velocity of the unperturbed flow.

Thus, the undetermined coefficients a_k and b_k of Formulas (5.6) can be readily found to be the coefficients of the corresponding Fourier series

$$a_k = 2 \int_0^1 f_1(x) \cos k\pi x dx,$$

$$b_k = 2 \int_0^1 f_2(x) \sin k\pi x dx,$$

and the problem is solved.

§6. Standing Wave of \bar{p} and \bar{v}

The solution (4.13) shows that the pressure and velocity oscillate at each point of the tube in identical manner in time. The amplitudes of the oscillations can be different in this case, and depend on the coordinate ξ . A motion of this type is customarily called a standing wave. The cross sections at which the variables \bar{p} and \bar{v} are equal to zero at all instants of time are called the nodes of the standing waves, while the sections in which \bar{p} and \bar{v} reach their maximum value are the antinodes.

The representation of arbitrary perturbations in the form of sums (5.5), given in the preceding section, can now be interpreted as the synthesis of an arbitrary form of perturbation by means of a superposition of standing waves.

It is seen from the foregoing that the standing waves of the oscillations are of considerable interest and a further analysis of their properties is essential.

To each harmonic (to each value of ω) there corresponds its own standing wave. If we plot the variation of the oscillation amplitudes

as a function of the coordinates ξ , we obtain a wavy curve, which reaches the ξ axis at the nodes and which reaches the maxima at the antinodes. It is seen from Formulas (5.5) that each standing wave (each term under the summation sign, corresponding to a certain K) is made up of two periodic functions of the variable ξ .

For a certain standing wave corresponding to a specified value of k , we have

$$\left. \begin{aligned} \bar{v}_k &= \frac{1}{2} A_{ck} [e^{-i(1-M)k\pi\xi} + e^{i(1+M)k\pi\xi}] e^{i(1-M^2)k\pi\tau}, \\ \bar{p}_k &= \frac{1}{2} A_{ck} [e^{-i(1-M)k\pi\xi} - e^{i(1+M)k\pi\xi}] e^{i(1-M^2)k\pi\tau}. \end{aligned} \right\} \quad (6.1)$$

Let us find the amplitudes of \bar{v}_k and \bar{p}_k , taking these to mean the absolute values of the complex variables \bar{v}_k and \bar{p}_k . If we recall that the absolute value of a product of complex numbers is equal to the product of the absolute values of the factors, and the absolute value of an exponential function with imaginary exponent is always equal to unity, then

$$\left. \begin{aligned} |\bar{v}_k| &= \frac{1}{2} |A_{ck}| |e^{iMk\pi\xi} (e^{-ik\pi\xi} + e^{ik\pi\xi})| = \\ &= |A_{ck}| |\cos k\pi\xi|, \\ |\bar{p}_k| &= \frac{1}{2} |A_{ck}| |e^{iMk\pi\xi} (e^{-ik\pi\xi} - e^{ik\pi\xi})| = \\ &= |A_{ck}| |\sin k\pi\xi|. \end{aligned} \right\} \quad (6.2)$$

The expressions obtained point to two important properties of standing waves of \bar{v} and \bar{p} . First, the antinodes of \bar{p} correspond to nodes of \bar{v} and vice versa, the nodes being located at equal distances from the neighboring antinodes, while the antinodes are located at equal distances from the neighboring nodes. Second, the amplitudes $|\bar{v}_k|$ and $|\bar{p}_k|$ are periodic functions of the coordinate ξ .

Inasmuch as the amplitudes of the standing waves turned out to be coordinate functions of the coordinate ξ , we can introduce the concept of the wavelength of the perturbation. We define the length of a standing wave as twice the distance between the pressure nodes or velocity

nodes. The wavelength is defined as twice the distance between nodes so that the new definition coincides when $M = 0$ with the customary definition used in the acoustics of a stationary medium. It follows also from this definition that the distance between pressure nodes and the neighboring velocity nodes is equal to one quarter of the wavelength.

As can be seen from the foregoing, many properties of standing waves in a moving medium coincide with the corresponding properties of standing waves in tubes filled with an immobile gas (or the properties of standing waves on a string). However, there are also differences between them. Whereas in a stationary medium the standing wave is characterized by the fact that the phases of the oscillation are the same at all cross sections, for standing waves in a moving medium this property does not hold.

Formulas (6.1) can be written in the form:

$$\left. \begin{aligned} \bar{v}_k &= A_{vk} \cos k\pi\xi e^{ik\pi(M\xi + (1-M^2)\tau)}, \\ \bar{p}_k &= -iA_{vk} \sin k\pi\xi e^{ik\pi(M\xi + (1-M^2)\tau)}. \end{aligned} \right\} \quad (6.3)$$

We recall that if we represent an oscillatory process by using complex variables, then the equality of the phases is expressed in the form of the equality of the arguments of the complex numbers. It is obvious that the constant factors A_{vk} and i influence in equal fashion the arguments of \bar{v}_k and \bar{p}_k for all ξ and τ . In addition, the expressions $\cos k\pi\xi$ and $\sin k\pi\xi$ are real and consequently their arguments are independent of ξ or τ . Consequently, the variation of the arguments resulting from variation of ξ and τ can occur only in connection with the change of the argument of the expression

$$e^{ik\pi(M\xi + (1-M^2)\tau)}.$$

When $M = 0$ (immobile medium) the argument of this expression depends only on τ . Consequently, for specified $\tau = \tau_1$ the arguments of \bar{v}_k and

accordingly \bar{p}_k are the same for all ξ . Consequently, the oscillation phases coincide for all values of ξ in an immobile gas.

When $M \neq 0$ (moving medium) the argument of the expression under consideration depends not only on τ , but also on ξ , the dependence being the stronger the larger M . For specified $\tau = \tau_1$ the argument of \bar{v}_k (and \bar{p}_k) is a linear function of ξ . The difference in the phases of the oscillations in two sections $\xi = \xi_1$ and $\xi = \xi_2$ is equal to

$$k\pi M(\xi_2 - \xi_1)$$

and is independent of the time.

An analysis of this formal deduction shows it to be quite natural. Indeed, a standing wave in an immobile medium is characterized by the equality of the oscillation phases in all the cross sections. If such oscillations occur in a moving gas, they will be standing with respect to the medium, and consequently the nodes and antinodes will move with the same velocity as the medium. In the problem considered here, in accordance with the boundary conditions (5.1) the nodes must be stationary with respect to the walls of the tube and therefore the wave must "travel" against the stream with the same velocity that the stream moves relative to the tube walls. Consequently, we cannot expect a complete agreement between the properties of standing waves in tubes when the medium is at rest and when the medium moves. As shown by the foregoing analysis, when the nodes move relative to the medium, a phase shift arises between the oscillations that pass through different sections.

Formulas (6.2) shows that the patterns of the amplitudes (absolute values) of the standing waves of \bar{v} and of \bar{p} are represented by segments of the trigonometric sine and cosine functions. These patterns are shown in Fig. 6, where the first four harmonics are given. It is clear that in oscillations at the fundamental tone (first har-

ic), half of the wavelength fits in the tube, the second harmonic corresponds to a complete wavelength, the third to one and a half times the wavelength, etc. The larger the number of the harmonic, i.e., the higher the oscillation frequency, the larger the number of half waves that fit on the length of the tube.

In plotting the patterns it was assumed that $|A_{vk}| = 1$ for all harmonics. As was already shown above, actually the values of A_{vk} are determined from the initial conditions.

When looking at the curves shown in Fig. 6, it must not be forgotten that they yield only the absolute values of the amplitude, whereas the actual oscillations of \bar{v} and \bar{p} are shifted in phase. Formulas (6.3) show that this phase shift has an absolute value $\pi/2$ (the factor 1 in the second formula). In order to present a more illustrative idea of the character of the velocity and pressure oscillations, Fig. 7 shows curves of \bar{v} and \bar{p} for the first harmonic at different instants of the time τ . The curves have been plotted for small stream velocities ($M \ll 1$) so that the phase shift between the oscillations in the different cross sections, referred to above, does not manifest itself in these curves.

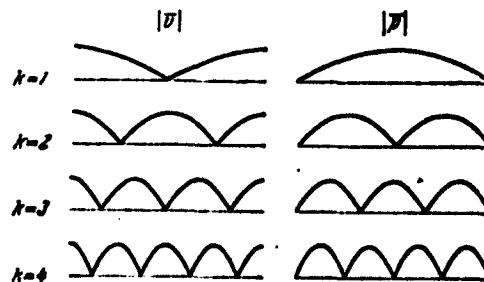


Fig. 6. Pattern of the standing waves of $|\bar{v}|$ and $|\bar{p}|$ for the first four harmonics (tube open on both ends).

As can be seen from the foregoing plots, the instants of maximum

velocity perturbation correspond to instants of practically complete lack of pressure perturbations, and vice versa. This phenomenon can be interpreted physically in the following manner. At the instant $\tau = 0$ the velocity perturbations are positive in the left part of the tube and negative in the right part. Consequently (the positive direction of the ξ axis is to the right), the mass of air acquires in the left part of the tube an additional motion to the right, while in the right half of the tube it acquires additional motion to the left. Thus, the air masses tend so to speak toward the center, which causes an increase in the pressure at the central part of the tube at the instant $\tau = 1/2$, after the masses "collide" and the velocity perturbations are quenched. The air compressed at the center then tends to move toward the region of lower pressure (toward the ends of the tube), the perturbation of pressure disappears at the instant $\tau = 1$, but the gas which moves by inertia (to the left in the left part of the tube and to the right in the right part) leads at the instant $\tau = 3/2$ to the appearance of a maximum rarefaction in the central part of the tube. The air again tends toward the region of decreased pressure (this time toward the center of the tube), and the entire cycle repeats.

The patterns shown in Fig. 7 have been plotted for very small values of the average flow velocity. In order to illustrate the influence of this velocity on the character of the oscillations, and in particular to show the phase shift occurring between oscillations in different sections, Fig. 8 shows the variation of \bar{p} at an instant of time close to $\tau = 0.5$ for $M = 0$ and $M = 0.2$.

Everything said up to now concerned oscillations in a tube that is open on both ends (boundary conditions $\bar{p} = 0$ for $\xi = 0$ and $\xi = 1$). Another classical case, usually considered in acoustics, is the excitation of oscillations in a tube with one end closed. In this case the

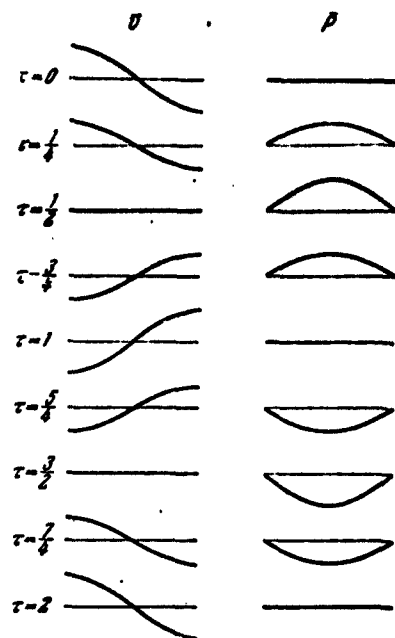


Fig. 7. Patterns of instantaneous values of \bar{v} and \bar{p} for the first harmonic (tube open on both ends).

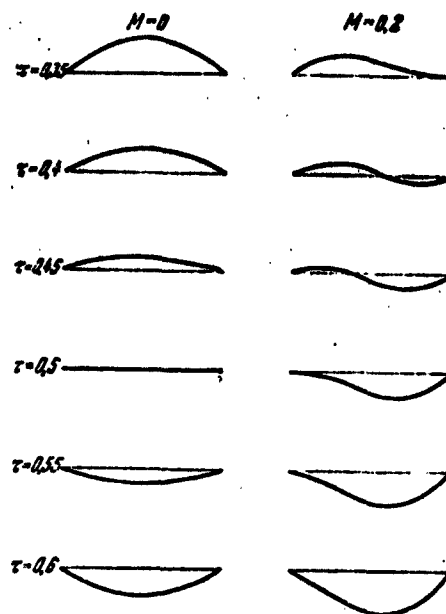


Fig. 8. Patterns of instantaneous values of \bar{p} for the first harmonic (tube open on both ends) for $M = 0$ and $M = 0.2$.

boundary conditions can be written (placing the closed end of the tube on the left) in the following form:

$$\bar{v} = 0 \text{ for } \xi = 0; \quad \bar{p} = 0 \text{ for } \xi = 1.$$

The first boundary condition then yields, in accordance with Formulas (4.13) and (4.14), $A_v = 0$, while the second condition yields

$$A_p \varphi_1(1) = 0.$$

Discarding the trivial solution $A_p = 0$, we obtain the condition under which $\varphi_1(1) = 0$, using the first equation of (4.14):

$$\exp\left(-\frac{2}{1-M^2}\beta\right) = -1.$$

Let us put, as was done above, $\beta = v + i\omega$ and obtain after several simple transformations:

$$\left. \begin{aligned} v &= 0, \\ \omega &= (1-M^2) \frac{k\pi}{2} \quad (k=1, 3, 5, \dots). \end{aligned} \right\} \quad (6.4)$$

Comparing these expressions with the analogous formulas of (5.4)

obtained above, we see that the oscillations remained harmonic in the case considered here, too, but their frequencies changed.

The first harmonic (the fundamental tone of the oscillations) is characterized by a frequency that is half as small, while the higher harmonics are connected with the fundamental tone not by a frequency ratio proportional to the series of natural numbers 1:2:3:..., but by a frequency ratio proportional to the series of odd numbers 1:3:5,.... Thus, for a tube open on both ends, the frequency of the second harmonic is twice the frequency of the fundamental tone, while for a tube closed on one end the second harmonic has three times the frequency of the fundamental tone.

If we consider the standing waves in a tube with one end closed, then most of the deductions obtained in the present section can be readily extended to this case, too. The only difference is that the frequency for $k = 1$ must be taken to be everywhere half as large, k assumes only odd values, and the amplitudes A_{vk} are replaced by A_{pk} with the associated interchange in the roles of the functions $\varphi_1(\xi)$ and $\varphi_2(\xi)$.

In particular, in place of the formulas (6.2) we obtain

$$\left. \begin{aligned} |\bar{u}_k| &= |A_{pk}| \left| \sin \frac{k\pi\xi}{2} \right|, \\ |\bar{p}_k| &= |A_{pk}| \left| \cos \frac{k\pi\xi}{2} \right|, \end{aligned} \right\} \quad (6.5)$$

and in place of the formulas (6.3) we get the following expressions:

$$\left. \begin{aligned} \bar{u}_k &= -iA_{pk} \sin \frac{k\pi\xi}{2} \exp \frac{ik\pi [M_k^2 + (1-M_k^2)\tau]}{2}, \\ \bar{p}_k &= A_{pk} \cos \frac{k\pi\xi}{2} \exp \frac{ik\pi [M_k^2 + (1-M_k^2)\tau]}{2}. \end{aligned} \right\} \quad (6.6)$$

Using these expressions and putting $A_{pk} = 1$, we can readily plot the amplitudes of the oscillations (6.5) for different harmonics, similar to what was done in Fig. 6. Such a construction of the first three harmonics is shown in Fig. 9. These patterns show that in oscil-

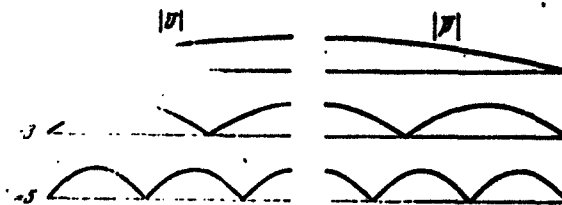


Fig. 9. Standing wave patterns of $|\bar{v}|$ and $|\bar{p}|$ for the three first harmonics (tube open on one end).

lations at the fundamental tone (first harmonic) the length of the tube is equal to one quarter of the wavelength, in the case of the second harmonic it is equal to three quarters of the wavelength, in the case of the third harmonic it corresponds to one and one quarter wavelengths, etc.

If we speak not of absolute values of the perturbation amplitudes but of instantaneous values of the pressure and velocity perturbations, then we must use Formulas (6.6), plotting only the real parts of the resultant quantities. We then obtain for the fundamental tone, taken by way of an example, an oscillation pattern at $M = 0$ as shown in Fig. 10. As in the case of acoustic oscillations, the velocity and pressure oscillations in a tube open on both ends are shifted in phase by $\pi/2$, and the instants of maximum velocity perturbation correspond to instants of zero pressure perturbations, and vice versa. It is easy to draw also for this case plots analogous to those of Fig. 8, i.e., to take account of the phase shift when $M \neq 0$.

The phase shift mentioned here, which is relatively small under ordinary conditions, is connected with the presence of a flow in the tube with nonzero average velocity. The existence of such flow may seem strange for a tube with one closed end. It must be borne in mind that a tube end that is closed from the acoustical point of view may not be closed at all from other points of view. An example of this

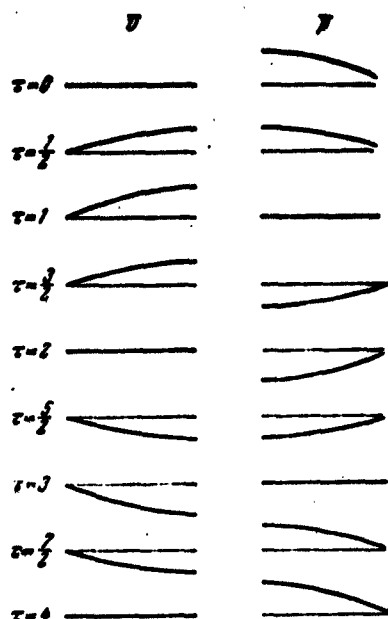


Fig. 10. Patterns of instantaneous values of \bar{v} and \bar{p} for the first harmonic (tube open on one end).

type is the furnace precombustion chamber described in Chapter 10, which operates with pulverized coal fuel. Here we can present another example, which is more illustrative. Let us imagine that nozzles, which supply liquid fuel and a liquid oxidant through very small apertures, are located at the closed end of the tube. These fuel components, upon entering into the combustion reaction, produce a flow of gaseous combustion products, moving through the tube toward its open end. Thus, in a tube of this type, which is the simplest idealization of a liquid-fuel jet engine, one observes

a continuous flow of gas and yet the end of the tube is closed (to the gases).

In conclusion let us turn to consider the periods of the acoustic oscillations. The numerical value of the oscillation period for both types of tube under consideration can be readily obtained if one knows the dimensionless oscillation frequencies given in Formulas (5.4) and (6.4), inasmuch as the connection between the period of the oscillations T and the frequency ω is given by the well-known formula

$$T = 2\pi/\omega, \quad (6.7)$$

which is equally suitable for dimensional and for dimensionless variables.

It is possible, however, to present here an even clearer method of obtaining the necessary formulas. The period of the oscillations is connected with the wavelength and with the propagation velocity of the

perturbations by a known simple relation. For a stationary gas the perturbation velocity is equal to the velocity of sound a and therefore

$$T = \lambda/a, \quad (6.8)$$

where λ is the wavelength.

If we recall that for tubes with open ends the wavelength is equal to twice the tube length, while for tubes with one end closed it is equal to four times the tube length, we immediately obtain the simple formulas

$$T = 2L/a \quad \text{and} \quad T = 4L/a. \quad (6.9)$$

It is sometimes stated in this connection that the oscillation period is equal in the former case to the time necessary for the sound wave to move along the tube and back, and in the latter case one speaks of double motion of the sound wave in the two directions.

The formulations presented above must not be regarded as simple mnemonic rules; they reflect the physical nature of the process, which can be readily explained by turning to the solution written with the aid of the variables u and w.

An analysis of the system (4.6), given on page 33, has shown that the acoustic impulses u and w move in the tube in opposite directions with velocity $v_0 + a$ and $v_0 - a$, respectively. Consequently, the distance equal to twice the length of the tube L will be covered by the impulse u in a positive direction within a time $L/(a + v_0)$, and by the impulse w in a negative direction within a time $L/(a - v_0)$. The boundary condition corresponding to the open end (pressure node) $\delta p = 0$, expressed with the aid of the variables u and w, will have the following form (4.5):

$$u = w, \quad (6.10)$$

while the boundary condition corresponding to the closed end (velocity

node) $\delta v = 0$ will have the form

$$u = -w. \quad (6.11)$$

Assume that some unit acoustic impulse u_I moved in a positive direction along a tube with open ends. On reaching the first end of the tube, it "was reflected" from it in accordance with Boundary Condition (6.10) and an impulse w_I of the same intensity moves to the left. On reaching the left end of the tube and becoming reflected from it, in accordance with the same boundary condition (6.10), the impulse w_I again returns to its initial value u_I , after which the indicated cycle will repeat for an unlimited number of times.

In a tube with one closed end (for example, on the left), the process will not differ in its initial stage at all from that described. However, when the impulse w_I from the open end of the tube reaches the left (closed) end, it will now be reflected in accordance with Boundary Condition (6.11), and the impulse moving to the right is $-u_I$. This is followed by reflection from the open end, an impulse $-w_I$ will travel to the left, and only after the second reflection from the closed end will the initial impulse u_I move to the right.

Thus, the entire cycle, after which the system goes back to the initial state, reduces in a tube with two open ends (or two closed ends) to a single motion of the acoustic impulse in both directions of the tube, while in a tube with one end open and one end closed it reduces to a double motion in both directions.

In connection with the foregoing, the oscillation period for a tube with two open ends or two closed ends is determined by the equation

$$T = \frac{L}{s+v_0} + \frac{L}{s-v_0} = \frac{1}{1-M^2} \frac{2L}{s}, \quad (6.12)$$

while for a tube with one end open and one end closed

$$T = \frac{L}{s+v_0} + \frac{L}{s-v_0} + \frac{L}{s+v_0} + \frac{L}{s-v_0} = \frac{1}{1-M^2} \frac{4L}{s}. \quad (6.13)$$

Comparing Formulas (6.12) and (6.13) with Formulas (6.9) previously obtained for a medium at rest, we see that when the medium moves the periods of the oscillations differ by a factor $1/(1 - M^2)$, which is close to unity at sufficiently small stream velocities ($M^2 \ll 1$).

Thus, the periods of oscillations for acoustic systems with moving gas can in the simplest case considered above be regarded in first approximation, without taking into consideration the average stream velocity.

This result, of course, could have been obtained immediately by using Formulas (5.4) and (6.4) for the oscillation frequencies, from which it is seen that the frequencies for $M = 0$ and $M \neq 0$ differ only in the fact that in the latter case a factor $(1 - M^2)$ appears in the formulas for ω .

§7. Traveling Waves of \bar{u} , \bar{w} , and \bar{s}

At the end of the preceding section we already used the variables \bar{u} and \bar{w} . They turn out to be quite useful in other cases, too. It is therefore advantageous to carry out an analysis of the properties of the \bar{u} and \bar{w} waves, similar to what was just done for the \bar{p} and \bar{v} waves. The latter is all the more useful, since the system of equations (4.10), like the system (4.11), contains also the perturbation of the entropy \bar{s} , the properties of which coincide almost completely with the properties of the perturbations of \bar{u} and \bar{w} .

Let us examine the solutions (4.12). In the case of harmonic oscillations corresponding to $\beta = i\omega$, the amplitudes of the oscillations of \bar{u} , \bar{w} , and \bar{s} will be constant in all sections and equal to $|A_u|$, $|A_w|$, and $|A_s|$, respectively.

In order to emphasize how the waves \bar{u} , \bar{w} , and \bar{s} differ from the waves \bar{p} and \bar{v} , we shall refer to them as traveling waves, taking the latter to mean waves that have a fully defined propagation velocity

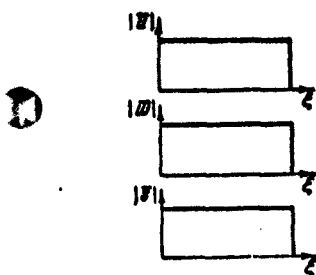


Fig. 11. Patterns of the $|\bar{u}|$, $|\bar{w}|$, and $|\bar{s}|$ waves.

(it is conveniently visualized as the velocity of displacement of the crest of the wave relative to the walls of the tube) and differing in the fact that their amplitudes (height of the crest) remain constant as they move along the ξ axis.

It is obvious from the foregoing that the patterns of the absolute values (amplitudes) of the \bar{u} , \bar{w} , and \bar{s} waves will have the same form for all harmonics (Fig. 11). The fact that the patterns of the amplitudes $|\bar{u}|$, $|\bar{w}|$, and $|\bar{s}|$ have the same form for all harmonics, with the oscillation amplitudes independent of ξ , offers appreciable conveniences for the solution of the problems. It is sufficient to compare the plots shown in Figs. 6 and 9 with the rectangular patterns of Fig. 11 to become convinced of this.

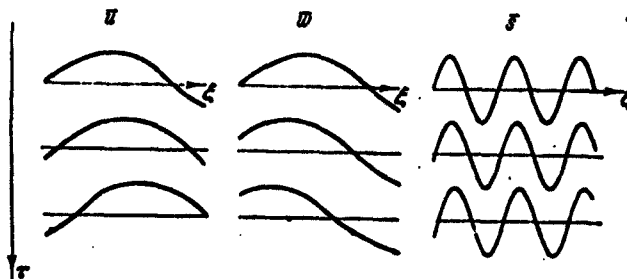


Fig. 12. Patterns of the instantaneous values of \bar{u} , \bar{w} , and \bar{s} .

For the sake of completeness, Fig. 12 shows the variations of the variables \bar{u} , \bar{w} , and \bar{s} as functions of the time τ . In this figure the lower plots pertain to the later instants of time. Comparing the behavior of \bar{u} , \bar{w} , and \bar{s} it is easy to see that the \bar{u} waves move to the right and the \bar{w} waves to the left. As regards the \bar{s} waves, they move, like the \bar{u} waves, to the right, but the distance between the crests of the \bar{s} waves is much smaller than in the case of the \bar{u} and \bar{w} waves.

This is connected with the fact that the acoustic impulses \bar{u} and \bar{w} propagate with the velocity of sound and their displacement is relatively little affected by the much slower motion of the medium, with velocity v_0 . In contrast to this, the entropy waves \bar{s} are transported by the medium and therefore the rate of displacement of the \bar{s} waves is much smaller than that of \bar{u} and \bar{w} .

As was already mentioned, the forms of the amplitude patterns of the waves \bar{u} , \bar{w} , and \bar{s} are independent of the number of the excited harmonic. The same cannot be said concerning the patterns of the instantaneous values of \bar{u} , \bar{w} , and \bar{s} shown in Fig. 12. The higher the number of the harmonic, the larger the number of \bar{u} , \bar{w} , and \bar{s} waves that are equal to the length of the tube.

§8. Stability of Gas Stream

In the two preceding sections we considered certain general properties of perturbation waves, and we can now turn to an examination of the problem concerning the propagation of perturbations, which was started in §5 for the simplest case.

It turns out that the solutions of the problem, with account of the initial and boundary conditions, in the form shown in §5, can usually be avoided. In a tremendous majority of cases of practical interest involving the excitation of acoustic oscillations by heat supply, the solution of the problem with account of the initial conditions is of no interest.

This is connected principally with the fact that usually the oscillations arise as the result of the development of some very small and indeterminate initial perturbations, which are always present in the form of unavoidable fluctuations of the flow parameters. Regardless of the character of these initial fluctuations, the acoustic oscillations in the stream reach during the course of their development

(under conditions favoring this development) noticeable amplitudes, the growth of which is ultimately stopped. As a result, the oscillating system enters into a mode of stationary acoustic oscillations, the character of which is as a rule independent of the specific form of the initial perturbations. An example of such a process will be given in Chapter 6.

The foregoing circumstance simplifies the investigation of the problem, since it enables us to dispense with formulating the initial conditions, a task which is almost impossible because of the extreme indeterminacy of the small initial perturbations of the stream.

In oscillation theory the described course of the phenomenon is known as the case of soft self-excitation.

In order for the system to become excited in the indicated manner, it must be unstable with respect to small stream perturbations. The self-excitation process can be visualized in the following manner. At the initial instant of time there exists some small perturbation of the stream, satisfying the boundary conditions. This perturbation can be represented as a superposition of harmonics of the system,* and the numerical value of the amplitude of each harmonic [for example, the numbers A_{vk} in the sums (5.5)] is determined by the form of the initial perturbation. Inasmuch as the initial perturbations can have a great variety of forms, it must be assumed that the amplitudes of all the harmonics differ from zero. If at least one among the system harmonics is unstable, then its amplitude will increase with time, the stream perturbation will cease to be small, and the unstable harmonic, overtaking in its development all the others, will leave on the entire oscillation process its own characteristic imprint, independently of the form of the initial perturbation.

It thus turns out that it is not only difficult to formulate the

initial conditions, but useless. However, if we disregard the initial conditions, then a certain uncertainty should appear in the mathematical solution of the problem. This uncertainty is manifest in the fact that the initial amplitudes of the standing waves (the numbers A_{vk} and A_{pk}) remain unknown. It is easy to visualize that in a tremendous majority of cases this does not interfere with finding the result, which is of real interest, since it was pointed out above that the main problem is whether there exist among the system harmonics any unstable ones, whose amplitudes tend to increase without limit with time (this increase is limited by the nonlinear properties of the system, which are not at all dependent on the initial conditions). In this case the question of the initial value of the amplitude that tends to increase without limit is quite secondary.

Based on the foregoing, we can formulate the problem to be investigated in the following fashion.

It is required to obtain for the system of equations of the perturbed motion a solution that satisfies specified boundary conditions and to obtain a quantitative estimate of the stability (or instability) of each harmonic of the solution, assuming that at the initial instant of time $\tau = 0$ all the harmonics have certain nonzero initial values of the perturbation amplitudes.

The solution of problems involving oscillations in a stream of gas moving through a tube with two open ends or through a tube with one closed end, given above, yielded for all harmonics sinusoidal oscillations whose amplitudes do not increase or decrease with time. If a more general result is desired, it is necessary to use boundary conditions of more general form, without confining ourselves to cases of pressure or velocity nodes.

In order not to complicate the derivations, let us consider the

relatively simple problem of the excitation of oscillations in the case when a pressure node is present at the exit from the tube and on the inlet to the tube the following homogeneous condition is satisfied:

$$\bar{p} = B\bar{v}.$$

Thus

$$\left. \begin{aligned} \bar{p} &= B\bar{v} \quad \text{for } \xi=0, \\ \bar{p} &= 0 \quad \text{for } \xi=1. \end{aligned} \right\} \quad (8.1)$$

Inasmuch as the conditions (8.1) do not contain perturbations of the entropy \bar{s} , the problem can be solved for the first two equations of the system (4.10), independently of the third. We carry out the solution of the problem in accordance with the same scheme as in the preceding sections. When $\xi = 0$ we have $\varphi_1(\xi) = 1$, $\varphi_2(\xi) = 0$. Then Formulas (4.13) together with the first of the boundary conditions (8.1) yield

$$A_p = BA_v.$$

When $\xi = 1$ the condition $\bar{p} = 0$ together with the first equation in (4.13) and with account of the just obtained connection between A_p and A_v yields the relation

$$\varphi_2(1) + B\varphi_1(1) = 0,$$

if we discard the trivial case $A_p = A_v = 0$.

Turning to Formulas (4.14), we obtain immediately an equation for β :

$$\exp \frac{2}{1-M^2} \beta = \frac{1+B}{1-B}. \quad (8.2)$$

Let the number B be real. This assumption does not distort the over-all picture of the investigated phenomenon, but greatly simplifies the derivations.

After substituting $\beta = \nu + i\omega$ in (8.2) we can easily arrive at the following system, which relates only the real variables:

$$\left. \begin{aligned} \exp \frac{2v}{1-M^2} \cos \frac{2u}{1-M^2} &= \frac{1+B}{1-B}, \\ \exp \frac{2v}{1-M^2} \sin \frac{2u}{1-M^2} &= 0. \end{aligned} \right\} \quad (8.3)$$

The second equation immediately determines the series of frequencies, from among which one can choose frequencies satisfying also the first equation. This series is given by the equation

$$\omega = (1-M^2) \frac{k\pi}{2} \quad (k=0, 1, 2, 3, \dots).$$

It is easy to see that all the frequencies satisfy the system. Indeed, the exponential function $\exp 2v/(1-M^2)$ can assume only positive values and consequently the sign of the cosine and the sign of the fraction $(1+B)/(1-B)$ should be the same. On the other hand, the sign of the cosine depends on whether the values of k are chosen even or odd.

Thus, the final expression for the frequencies of the system ω can be written in the form

$$\omega = (1-M^2) \frac{k\pi}{2} \begin{cases} k=0, 2, 4, \dots, & \text{if } \frac{1+B}{1-B} > 0, \\ k=1, 3, 5, \dots, & \text{if } \frac{1+B}{1-B} < 0. \end{cases} \quad (8.4)$$

Inasmuch as the signs of the fraction $(1+B)/(1-B)$ and of the quantity $\cos 2\omega(1-M^2)$ always coincide, while the absolute value of $\cos 2\omega/(1-M^2)$ is equal to unity, we can obtain v from the first equation of the system (8.3)

$$v = \frac{1-M^2}{2} \ln \left| \frac{1+B}{1-B} \right|. \quad (8.5)$$

Before we analyze the result obtained, we must discuss the physical meaning of the quantity v . For this purpose it is convenient to turn to the solution (4.13). If we consider the oscillations occurring in a certain arbitrary section of the tube $\xi = \xi_1$, then the expressions in the square brackets assume constant values, and \bar{v} and \bar{p} can be written in the form

$$\bar{v} = A_1 e^{i\omega t}, \quad \bar{p} = A_2 e^{i\omega t},$$

where A_1 and A_2 are certain quantities that are constant for the chosen cross section.

Inasmuch as both quantities vary in like fashion with the time, let us consider in greater detail the behavior of only one of them, for example \bar{v} . Setting $\beta = \nu + i\omega$, we obtain

$$\bar{v} = A_1 e^{\nu t} (\cos \omega t + i \sin \omega t).$$

The expression in the parentheses indicates that the quantity \bar{v} oscillates about the value $\bar{v} = 0$. The exponential time function which is a factor of the quantity A_1 , characterizes the variation of the oscillation amplitude with time.

If $\nu > 0$, then the exponential function will increase without limit with time and this will indicate that the process is unstable, for the amplitudes of the perturbations \bar{v} , \bar{p} and of the other parameters of the stream will have a tendency to increase without limit; in this case the quantity ν is frequently called the growth increment of the oscillation.

If $\nu < 0$, then the exponential function will increase with time and approach zero. Consequently, the stream is stable and it is always possible to indicate a time interval τ_1 , during which the amplitudes of the perturbation will assume an absolute value smaller than any specified positive quantity, as small as desired. In this case the number ν is called the damping decrement of the oscillations.

The case $\nu = 0$ is intermediate. When $\nu = 0$ the oscillation amplitudes do not increase and do not decrease with time. This is a state of stationary or neutral oscillations and is of particular interest because it can be regarded as a mode corresponding to the stability limit. Indeed, if the stability of the system varies continuously under continuous variation of some system parameter, then the transition from stability to instability or vice versa is connected with a transi-

through the mode $v = 0$.

Thus, we can henceforth use the following symptoms of stability:

$$\begin{aligned} v > 0 & - \text{unstable flow,} \\ v < 0 & - \text{stable flow,} \\ v = 0 & - \text{steady-state oscillations,} \end{aligned} \quad (8.6)$$

stability limit.

After this brief diversion, let us turn to analyze the expression obtained for v .

It follows from (8.5) that when $B = 0$ the process is neutral, since it corresponds to $v = 0$. This result coincides with the previously obtained deduction, inasmuch as the equality $B = 0$ denotes, as

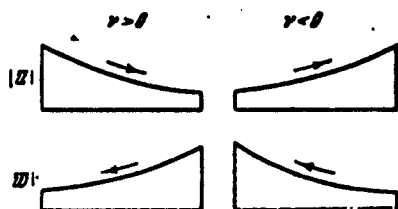


Fig. 13. Patterns of the $|u|$ and $|w|$ waves for unstable ($v > 0$) and stable ($v < 0$) flow.

follows from the boundary conditions (8.1), that a pressure node $\bar{p} = 0$ exists not only at the outlet but also at the inlet. The same result ($v = 0$) is obtained also by making the substitution $B = \infty$ (such a condition denotes the existence of a velocity node at the inlet to the tube).

Unlike the foregoing cases, v assumes values different from zero for all other B . When $B > 0$ we have $v > 0$ and the flow is unstable. When $B < 0$ the flow is stable ($v < 0$).

Thus, the introduction of a somewhat more complicated boundary condition than the velocity or pressure nodes used in the preceding sections immediately leads to a qualitatively different picture. Depending on the number B , the flow can be either stable or unstable.

When $v \neq 0$ the patterns of the perturbation amplitudes are found to be different from those given in the two preceding sections. In order not to clutter up the text, we give only the patterns of $|u|$ and $|w|$, using Formulas (4.12). For each specified τ one obtains the curves

shown in Fig. 13. The arrows near the curves indicate the direction of motion of the \bar{u} and \bar{w} waves.

For unstable flow ($\nu > 0$) the amplitudes $|\bar{u}|$ and $|\bar{w}|$ decrease in the directions of the arrows; this can be interpreted as meaning that the acoustic impulses produced later have a larger amplitude, i.e., the system increases the amplitudes with time. For stable flow ($\nu < 0$) the opposite is observed. It must also be noted that the patterns in Fig. 13 have been constructed for a certain fixed instant of time. For each succeeding instant of time the patterns will have larger ordinates if $\nu > 0$ and smaller ordinates if $\nu < 0$.

Usually one considers in acoustics systems that are characterized either by oscillations with constant amplitude ($\nu = 0$), or with amplitudes that decrease in time ($\nu < 0$). The first case corresponds to an idealized scheme of the phenomenon, in which the unavoidable losses are disregarded, while the second corresponds to real processes connected with energy dissipation. In the example considered here we obtained for $B > 0$ a value $\nu > 0$, which is perhaps unexpected for the customary acoustic phenomena. What we get here is not dissipation of acoustic energy in the medium, which is unavoidable in any real system, but so to speak a generation of more and more new amounts of acoustic energy, which is consumed in a more and more intense swinging of the medium. The question of the source of this energy will be considered in detail in the next chapter. We wish to emphasize here only that in principle this leads to the possibility of self-excitation of acoustic systems of the type under consideration. It is useful to pay attention here to the fact that the cause of the system self-excitation is localized in the example considered here in the inlet section of the tubes. Of course, a real physical process, which would formally be expressed in the form of a boundary condition $\bar{p} = B\bar{v}$, occurs within a certain

volume in the region adjacent to the inlet section, but what is important is that if we are able by suitable idealization to reduce this process to a certain relation that holds true for one section of the stream (in this case the inlet), then this uncovers a way toward a relatively simple mathematical description of the phenomenon as a whole. This circumstance will be extensively utilized in the present book.

Using the variables \bar{u} and \bar{w} we can interpret more illustratively the results obtained in the present section. If we write down the boundary conditions (8.1), using Formulas (4.9), with the aid of the variables \bar{u} and \bar{w} , they will assume the following form:

$$\left. \begin{aligned} \bar{u} &= \frac{1+B}{1-B} \bar{w} & \text{for } \xi=0, \\ \bar{u} &= \bar{w} & \text{for } \xi=1. \end{aligned} \right\} \quad (8.7)$$

Thus, the impulse \bar{u}_I moving from the left end ($\xi = 0$) to the right end ($\xi = 1$) is reflected from the latter without changing its magnitude, and will move to the left in the form of the impulse $\bar{w}_I = \bar{u}_I$. At the left end of the tube the arriving impulse \bar{w}_I will reflect it in the form of an impulse \bar{u}_{II} , where $\bar{u}_{II} \neq \bar{w}_I$. Depending on the value of B , the reflected impulse \bar{u}_{II} will be either larger or smaller in absolute magnitude than the arriving one. If $B > 0$, then $|\bar{u}_{II}| > |\bar{w}_I|$, and since this process of reflection of impulses from both ends of the tube will continue, the amplitudes of the perturbations will have a tendency to increase without limit. Upon each reflection from the left end the arriving impulses will experience, as it were, an additional external jolt. In the case $B < 0$ the process of reflection from the left end of the tube has the opposite character, and the impulses reduce in intensity.

This conclusion confirms the results obtained in the form of Formula (8.5). In addition, the foregoing argument confirms the localiza-

tion of the cause of excitation of the system or the quenching of the oscillations in the inlet section at $\xi = 0$.

In order to illustrate the arguments presented above, let us consider a real case of flow, in which the boundary condition at the inlet assumes the form (8.1) or (8.7).

In test stands intended for the investigation of combustion processes or other purposes one frequently employs the following flow scheme (Fig. 14). Air at the required pressure is propelled through tube AB by means of a suitable blower. The portion of the tube BC is intended for the performance of various experiments, for example those connected with the organization of the combustion process at the end portion of the tube BC. In order for the combustion process, which may be accompanied by clapping when the ignition system is turned on, may be unstable, etc., not to influence the operation of the blower, a constriction is made at the section BB, which is so strong as to form on the right of BB a small region in which the flow has supersonic velocity. Then, as is well known from hydromechanics, no perturbations (provided they do not damage the region of supersonic flow) can be transmitted from the tube portion BC upstream into the portion AB. This causes the blower to operate in a specified steady state independently of what nonstationary processes occur in the portion BC.

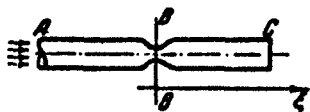


Fig. 14. Pipe with critical constriction.

Thus, the formation of a supersonic flow zone in the vicinity of the section BB contributes to quiet operation of the air blower.

Let us now raise the question of how the presence of such a constriction will influence the

processes occurring in the right portion of the experimental setup, and in particular how this will affect the character of the acoustic oscillation in this portion. At the end C the boundary condition can

written directly: $\bar{p} = 0$, since the open end of the tube communicates with the outside space. This approximate boundary condition is valid in those cases, when no sonic stream velocity (crisis) is produced at the section C, connected with the large supply of heat in the portion BC. As regards the boundary condition at the inlet to the tube BC, it is not obvious.

Beyond the constriction BB, as already mentioned, supersonic flow is produced. This supersonic flow is then decelerated via a certain rather complicated system of shocks, the character of which is practically impossible to predict. Therefore an attempt to write down the boundary condition by analyzing the gas-dynamic flow pattern is not advantageous. We can use here the fact that ahead of the section BB the stream is always unperturbed and therefore the parameters of the flow are constant and are independent of the acoustic oscillations that occur to the right of BB. In particular, the per-second flow of air through the section BB is constant. If the volume of the region in which the supersonic flow is slowed down is small and the instantaneous value of the air mass contained in it does not change, then it can be assumed that in a section lying somewhat to the right of BB, where the stream velocity is again subsonic, the flow of air per second is constant, in spite of the presence of pressure and velocity oscillations. Consequently, at the inlet to the tube BC the following condition will be satisfied:

$$\rho v = \text{const.}$$

We shall assume that the process at the inlet to the tube BC is isentropic. Then, after linearizing this relation and changing over to the adopted system of dimensionless variables, we can readily obtain the boundary condition at the inlet:

$$\bar{p} + \frac{1}{N} \bar{v} = 0. \quad (8.8)$$

Comparing it with the first boundary condition (8.1) we obtain directly $B = -1/M$.

Thus, in the case under consideration the inequality $B < 0$ is obtained and consequently the flow is always stable. In this respect the type of flow under consideration greatly differs from flow in a tube that is open on both ends or is closed on one end, where the oscillations turn out to be neutral ($\nu = 0$). In designing stands in accordance with the scheme shown in Fig. 14, the oscillations in the region BB will be damped, and this will contribute to a more stable course of the process in tube BC (say, combustion).

Thus, if the flow in a tube is characterized by a constant consumption of gas at the inlet, it is subject to damping of the acoustic oscillations. From the point of view of obtaining quiet combustion, less prone to vibrations, this property is useful. Therefore the construction of stands in accordance with the scheme of Fig. 14 for purposes of investigating the laws governing stationary combustion is correct. However, in those cases when the aim of the experiments is the study of processes of oscillation excitation, the construction of stands with constant gas consumption at the inlet may prove to be not advantageous.

If we raise the question of physical processes occurring at the inlet to the tube and leading to the dissipation of energy, then each specific case may have its own separate mechanism for the dissipation of energy.

§9. Longitudinal Self-Oscillations in a Gas Stream

At the end of the preceding section we gave an example of a stationary flow, in which the acoustic oscillations were damped. We shall not present here specific examples of flows which are stable with respect to small perturbations of acoustic nature, since the following

chapters are devoted to this subject. However, it is useful to present even now the general pattern of further development of the instability process.

If the flow turns out to be unstable ($\nu > 0$), then the amplitudes of all the unstable harmonics will increase with time in proportion to the factor $e^{\nu\tau}$. Depending on the value of ν (the oscillation growth increment ν can be different for different harmonics), the amplitudes of the unstable harmonics can increase at different rates, but all will be characterized by an increase without limit as $\tau \rightarrow \infty$. From physical considerations it is clear that such a development of the oscillation process is impossible, and the result obtained is connected with shortcomings in the mathematical idealization of the phenomenon.

As is well known, the problem was solved for linearized hydro-mechanics equations, obtained under the assumption that all the perturbations are small. As soon as the perturbations cease to be small as a result of the increase in the factor $e^{\nu\tau}$, the systems of equations (4.10) and (4.11), and with them also the solutions obtained, are no longer correct. Thus, the solutions obtained here are suitable only for a description of the initial stages of the development of the process.

To obtain a more complete picture of the phenomenon it is necessary to use more exact mathematical relations. It is known that they must be nonlinear. One could attempt to solve the system of nonlinearized exact equations of hydromechanics (3.1) and (3.2). Suitable methods exist and are the subject of the theory of unsteady motions of gas.* In our case, however, special interest attaches to that class of problems, in which the linear relations become invalid at first for individual sections of the stream (for example, the terminal sections), and only then do they become invalid for the entire stream as a whole.

As applied to the example considered, this means that the systems of equations (4.10) and (4.11) along with their solutions still remain valid even when the boundary conditions (8.1) must be replaced by more accurate nonlinear relations.

Assume, for example, that in place of the boundary conditions (8.1) the following conditions apply

$$\left. \begin{aligned} \bar{p} &= (B_1 - |\bar{v}|) \bar{v} & \text{for } \xi = 0, \\ \bar{p} &= 0 & \text{for } \xi = 1, \end{aligned} \right\} \quad (9.1)$$

where B_1 is a sufficiently small positive quantity. We can then expect the following course of the process. At very small initial perturbations ($|\bar{v}| \ll B_1$) the boundary conditions (9.1) will practically coincide with Boundary Conditions (8.1), and by virtue of the inequality $B_1 > 0$ the flow will be unstable. The smallness of B_1 causes the instability process to develop slowly and therefore, during the course of one period of the oscillations, the quantity $B_1 - |\bar{v}|$ can be regarded as constant. As the oscillation amplitudes increase, the value of $|\bar{v}|$ will increase, the difference $B_1 - |\bar{v}|$ decreases, and consequently, the degree of instability will decrease. When $B_1 = |\bar{v}|$ the oscillation process becomes stationary, \bar{v} becomes equal to zero, and the oscillation amplitudes cease to increase. Thus the acoustic system of the type considered will execute self-oscillations with an amplitude close to $|\bar{v}| = B_1$ and $\bar{p} = 0$ in the initial cross section.

If any accidental cause decreases the amplitude of the velocity oscillations, the flow becomes unstable and the amplitude \bar{v} will again increase with time. On the other hand, if some cause increases the amplitude of the velocity oscillations, then the difference $B_1 - |\bar{v}|$ becomes negative, and this is the analog of boundary condition $\bar{p} = B\bar{v}$ when $B < 0$. Such a flow is characterized by stability ($\nu < 0$), its amplitudes will decrease with time, and the system will again return to

oscillations with amplitude $|\bar{v}| = B_1$ in the inlet cross section. Consequently, the occurrence of self-oscillation will be stable, and the small deviations from the steady-state mode in either direction will be constantly smoothed in time.

The analysis presented here is quite approximate and is far from being mathematically rigorous. Its only purpose was to illustrate the fact that oscillatory instability of flow is capable of giving rise to self-oscillations, and to point out a type of self-oscillations in which the cessation in the growth of the amplitudes occurs long before the acoustic laws, derived on the basis of the linearization of the hydromechanics equations, cease to be valid.

Manu-
script
Page
No.

[Footnotes]

- 24 We shall not distinguish in what follows between the terms fluid, compressible fluid, and gas.
- 26 Merk H.J., Analysis of Heat-Driven Oscillations of Gas Flows, Appl. Scient. Res., 1957, A6, No. 4.
- 33 If we consider the character of variation of δp and δv in the cases $u \neq 0$; $w = 0$ or $u = 0$; $w \neq 0$, i.e., if only the u wave or only the w wave exists, then it is easy to obtain the relation $\delta p = +\rho a \delta v$, which is well known in acoustics for a plane traveling wave.
- 58 Here and below we shall not distinguish between the concepts harmonic and its corresponding standing wave, in those cases where no confusion can arise.
- 69 See, for example, K.P. Stanyukovich, Nonsteady Motion of a Continuous Medium, Gostekhnizdat, 1955.

Chapter 3

SOURCES OF SELF-OSCILLATION ENERGY

§10. Two Sources of Energy in Thermal Excitation of Sound

In any self-oscillating system it is possible to separate the oscillating system proper (in our case this system is the gas contained in the tube), the energy source, and a certain mechanism* which supplies energy to the oscillating system.

In the preceding chapter we have explained the most essential properties of the oscillating system. The question of the mechanism that supplies energy to the oscillating system will be partially elucidated in the present chapter, but it will be considered in greater detail in subsequent chapters. The principal content of the present chapter is the disclosure of the energy sources that maintain longitudinal acoustic self-oscillations of the gas in a tube during combustion, and the analysis of the process that makes it possible to replenish periodically the loss of acoustic energy from the oscillating system, due to the losses that are unavoidable in any real phenomenon.

From the point of view of the physics of the process, the disclosure of the energy source that feeds the oscillatory system is one of the principal ones. Unfortunately, this problem, as applied to the excitation of acoustic oscillations by heat supply, has been undeservedly paid little attention, which has led to many erroneous statements in the literature.

Apparently the first researcher to raise this question (to be sure, not in explicit form), was Rayleigh. In connection with the de-

description of the experiments of Rijke, Bosscha, Riess, and other researchers, he said the following concerning the maintenance of oscillations by means of heat:

"If the heat is periodically transferred to a mass of air, which oscillates for example in a cylinder with a piston, and is taken away from it, then the effect obtained depends on the phase of the oscillation at which the heat transfer takes place. If the heat is transferred to the air at the instant of maximum compression or is taken away from it at the instant of maximum rarefaction, then this intensifies the oscillation. To the contrary, if the heat is transferred at the instant of maximum rarefaction, then the oscillation is attenuated thereby."*

In this statement Rayleigh speaks of the possibility of exciting acoustic oscillations at the expense of the supplied heat energy. The process described by him is the method well known from thermodynamics of obtaining mechanical energy from the supplied heat by subjecting the working body to some thermodynamic cycle. Similar processes are the basis of all the piston internal combustion engines. It is quite obvious that the heat can go over into acoustic energy only in such a way, since the acoustic energy is a modification of mechanical energy and not of heat energy. Rayleigh emphasizes this, stating somewhat before that: "In almost all cases when heat is transferred to a body, expansion takes place, and this expansion can be caused to perform mechanical work."**

We wish to emphasize here that the foregoing detailed citation refers to the excitation of acoustic oscillations in a stationary gas (by stationary is meant a gas which has no other motion except that connected with the acoustic oscillations). This is seen at least from the fact that he is speaking of a gas contained in a cylinder with

piston. Changing over to a somewhat more detailed explanation of the experiments of Rijke, Rayleigh suggests the same idea also for a gas that has a certain average velocity of motion through the tube. Giving a purely qualitative description of the phenomenon, Rayleigh emphasizes that alternating transfer of heat from a heated grid to the gas is connected with the motion of the medium, which is made up of a uniform component on which an oscillatory component is superimposed, "while the effect of transfer* depends on the variation of the pressure."**

Thus, Rayleigh believed the energy source to be the heat supply, which, having an oscillatory component, suitably shifted in phase relative to the pressure oscillation, makes possible the realization of a thermodynamic cycle which yields mechanical work. The mechanical energy obtained, fed to the oscillating system in the same rhythm as the thermodynamic cycle, maintains the acoustic oscillations.

The foregoing trend of thought constitutes the contents of the so-called Rayleigh hypothesis, which is frequently used as the basis for theoretical research devoted to the interaction between heat supply (in particular, combustion) and acoustic oscillations. Recently Putnam and Dennis made an attempt to prove this hypothesis and to cast it in mathematical form.*** It later became customary to speak not of a hypothesis but of the Rayleigh criterion, which is usually formulated as follows: if the absolute value of the phase shift between the oscillatory component of the heat supply and the oscillatory component of the pressure is less than $\pi/2$, acoustic oscillations are excited in the system; if this phase shift lies between $\pi/2$ and π , the acoustic oscillations are quenched.

This raises the natural question: does the scheme, proposed by Rayleigh, whereby the acoustic oscillations are maintained by the heat

apply, exhaust all the possible cases? In other words, is the heat supply the only energy source capable of maintaining the acoustic oscillations in the system?

In order to answer this question, it is necessary to ascertain what energy sources, other than the heat supply, are possessed by the oscillating system. Inasmuch as the system under consideration has a nonzero average flow velocity, it is necessary to ascertain first whether the kinetic energy of the flow is capable of serving as the reservoir from which the oscillating system will draw the energy for the maintenance of the oscillations.

Assume that a resistance is placed at some section of the gas stream. Then, if this resistance is variable, it is possible in principle for oscillations to become excited. Indeed, if velocity oscillations take place in the region where the resistance is located, and if at the instant when the stream velocity builds up the resistance decreases, while at the instant when the velocity decreases the resistance increases, such an interaction between the stream and the resistance will cause the system to sway. This can be visualized in simplest fashion as follows. Let us break up the entire resistance into two components, the average value and the component that alternates periodically in time. From the point of view of the effect on the stream, the alternating component of the resistance will alternately retard it and accelerate it. If at the instant when the velocity increases as a result of the acoustic oscillations the alternating component of the resistance accelerates the stream further, while at the instant when the velocity decreases the resistance slows it down further, then the amplitude of the acoustic oscillations will increase. The resistance, as it were, sways the oscillating system in this case.

Devices of this kind are extensively used in all kinds of elec-

tronic circuits. The best known example is the vacuum tube oscillator, in which the grid of the tube plays the role of the alternating resistance of the type described.

Returning to the problem of thermal excitation of sound, we must first point to a resistance capable of producing the effect described above. In the idealized scheme of the process, a scheme that serves as the basis for the study of the type of acoustic oscillations under consideration, no presence of any hydraulic losses in the tube is assumed. Therefore the only type of resistance that must be taken into account is the so-called thermal resistance, which arises even in an ideal fluid.

We shall not develop here the complete theory of this interesting phenomenon; we give only a general idea of thermal resistance, follow-

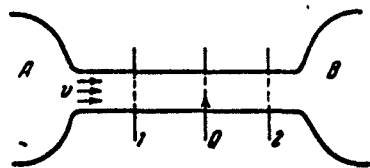


Fig. 15. Theoretical scheme for the calculation of thermal resistance.

ing G.N. Abramovich.* Let the stream velocity in the cylindrical tube be so small, that the effect of the compressibility of the medium can be disregarded. We connect to the inlet of the tube and to its outlet section two reservoirs A and B, of infin-

itely large volume, which are not connected with each other (Fig. 15). Section 1 is the inlet and section 2 the outlet; somewhere between the two, heat Q is supplied to the stream. The fluid is regarded as ideal, so that no hydraulic losses will be considered. The flow parameters in sections 1 and 2 will be designated by the corresponding subscripts, and we introduce for the reservoirs A and B the subscripts 01 and 02, respectively, for the decelerated flow. Then, in accordance with the Bernoulli equation, we have

$$p_{01} = p_1 + \frac{\rho_1 v_1^2}{2},$$

$$p_{02} = p_2 + \frac{\rho_2 v_2^2}{2},$$

from which we get for the change in the total pressure

$$p_{01} - p_{02} = p_1 - p_2 + \frac{\rho_1 v_1^2}{2} \left(1 - \frac{\rho_1}{\rho_2} \right). \quad (10.1)$$

In writing down the last equation we took into account the continuity equation

$$\rho_1 v_1 = \rho_2 v_2.$$

Inasmuch as we are considering an incompressible fluid, the change in density can occur only as a result of heating, so that it is natural to put

$$\frac{\rho_1}{\rho_2} = \frac{T_2}{T_1}.$$

Then Eq. (10.1) can be written in the form

$$p_{01} - p_{02} = p_1 - p_2 + \frac{\rho_1 v_1^2}{2} \left(1 - \frac{T_2}{T_1} \right). \quad (10.2)$$

From the momentum equation we can determine the pressure drop in section 1-2

$$p_1 - p_2 = \rho_1 v_1 (v_2 - v_1).$$

Substituting this difference into (10.2) and using the continuity equation and the connection between the density and the temperature, we obtain the final formula

$$p_{01} - p_{02} = \frac{\rho_1 v_1^2}{2} \left(\frac{T_2}{T_1} - 1 \right). \quad (10.3)$$

Equation (10.3) shows that the presence of heat supply Q , which brings about $T_2 \neq T_1$, is unavoidably connected with the appearance of a difference between the total pressure head in the inlet and outlet sections of the cylindrical tubes. This is the effect that we call thermal resistance.

Let us attempt to present the qualitative picture of the excitation of acoustic oscillations by means of heat supply at the expense of the kinetic energy of the stream. It is seen from Formula (10.3) that when $T_2 > T_1$ (heating) the resistance is positive (the over-all

mechanical energy of the stream ahead of the heat supply zone P_{01} is larger than the analogous quantity behind the heat supply zone). When $T_2 < T_1$ (cooling) the resistance is negative. Thus, if the heat supply fluctuates about zero, then the stream will be alternately acted upon by positive and negative resistance. If at the same time an increase to the stream velocity corresponds to a reduction in the resistance then, as already stated, the system will be swayed.

The presence of a constant time-averaged heat supply cannot change this qualitative excitation picture, just as the presence of an average nonvanishing heat supply does not influence the nature of the effect indicated by Rayleigh.

The excitation mechanism described here escaped Rayleigh's attention. The principal difference between the two types of excitation of acoustic oscillations by means of heat supply is seen, in particular, from the fact that in one case the result of the effect is connected with a phase shift between the heat supply and the pressure, and in the other the phase shift is between the heat supply and the velocity.

The qualitative considerations, which we owe to Rayleigh, and the considerations concerning the possibility of exciting sound by means of oscillations of the thermal resistance, call for a rigorous proof. The last sections of the present chapter will be devoted to this proof. It is appropriate, however, to estimate here the proof of the criterion given by Putnam and Dennis, for the excitation of acoustic oscillations. These authors attempted to obtain a general analytic criterion for the excitation of acoustic oscillations by means of heat supply (reference to this paper was already made previously in connection with the exposition of the Rayleigh hypothesis). As a result of the analysis of the relations they obtained, Putnam and Dennis reached the conclusion that the only and completely general criterion for the

excitation is that proposed by Rayleigh.

Inasmuch as Rayleigh himself does not give a proof of his hypothesis, the conviction arose, following the publication of the paper by Putnam and Dennis, that Rayleigh's hypothesis has been proved for the most general case. However, the proof of Putnam and Dennis contains a principal error in the initial premises. To simplify the equations, Putnam and Dennis neglected the stream velocity compared with the velocity of sound and did not note that by the same token they have excluded from consideration a source of energy which has independent significance, namely the kinetic energy of the stream. When it comes to stationary gas, then the only possible excitation mechanism is that indicated by Rayleigh; Rayleigh himself, as emphasized above, also advanced his hypothesis in connection with a stationary gas contained in a cylinder with a piston. Thus, it is necessary in the exposition that follows to generalize the Rayleigh criterion so as to include the case of a moving medium, to present other possible criteria, and to derive all these results on the basis of the fundamental laws of the mechanics of continuous media. In this case, in addition to clarifying the principally important question of the energy sources of self-oscillations, we shall present energy methods, which have greater simplicity and clarity, for the solution of certain problems.

§11. Flux of Acoustic Energy

We consider the following idealized scheme of the process. A cylindrical tube AB is divided by a region σ into two parts (Fig. 16). To the left of the region σ is located the inlet part of the tube; cold gases pass along this section of the tube, moving toward the right. The region σ is the heat supply region. We shall not make more precise here the process, physical or chemical, which causes the gas to be heated, but agree merely that the heat is transferred simultaneously



Fig. 16. Theoretical scheme for the calculation of acoustic energy fluxes.

and in identical batches to all the moles of the gas, crossing a given stationary section situated inside σ . This assumption allows us to regard the flow as being one dimensional also inside σ . Since the heat can be supplied at each cross section inside

the region σ , we shall assume that the gas is heated gradually, as it moves inside this region. The part of the tube situated to the right of the region σ is filled with the heated gas which moves toward the outlet end B. Certain boundary conditions, which will not be made precise for the time being, are satisfied on the ends A and B of the tube under consideration.

Let us determine under what conditions and at the expense of what sources is the generation of acoustic energy by the region σ effected. Before we answer this question, however, we must establish what is meant precisely by flux of acoustic energy.

As is well known, the energy flux in a one-dimensional gas stream is equal to*

$$s = qv \left(\frac{v^2}{2} + c_p T \right) + pv. \quad (11.1)$$

The first term, which has pv as a factor, describes the transport of energy by the mass stream. The expression in the parentheses indicates that the mass stream carries two types of energy, kinetic and internal. The first is, as is well known, one of the forms of mechanical energy, while the other is thermal. The last term in Formula (11.1) describes the transfer of energy by the pressure; this is also an energy in mechanical form.

The excitation of acoustic oscillations is connected with the transfer of impulses by pressure, so that of the three terms of s [3]

the last term, $p v$, is of primary interest.

Assume that harmonic oscillations were established in the gas stream

$$\left. \begin{aligned} p &= p_0 + \delta p, & \delta p &= |\delta p| \sin \omega t, \\ v &= v_0 + \delta v, & \delta v &= |\delta v| \sin (\omega t + \psi), \end{aligned} \right\} \quad (11.2)$$

where ψ is the phase shift between the pressure and velocity oscillations.

Then the term $p v$ in the formula for the energy flux (11.1) can be represented in the form

$$p v = p_0 v_0 + p_0 \delta v + v_0 \delta p + \delta v \delta p.$$

Integrating this equation with respect to time over the oscillation period $T = 2\pi/\omega$ and referring the resultant quantities to the period, we obtain the average value of the flux $p v$ over the period

$$(p v)_{cp} = p_0 v_0 + \frac{1}{T} \int_0^T \delta v \delta p dt. \quad (11.3)$$

From the formula obtained it is clear that in the case of steady-state harmonic oscillations the flux $p v$ averaged over the period is equal to the sum of two energy fluxes. The flux $p_0 v_0$ is not connected at all with the oscillations, whereas the second term of the right half of (11.3) depends only on the oscillatory components of p and v . It is natural to call this term the flux of acoustic energy A

$$A = \frac{1}{T} \int_0^T \delta v \delta p dt. \quad (11.4)$$

Let us consider some nearly obvious properties of the flux of acoustic energy. Using Expressions (11.2) for δp and δv , we can write

$$A = \frac{1}{2} |\delta p| |\delta v| \cos \psi. \quad (11.5)$$

It follows from the formula that at the pressure nodes, $\delta p = 0$, or at the velocity nodes, $\delta v = 0$, the flux of acoustic energy is equal to zero. This means that when averaged over the period no acoustic en-

energy flows through the section in which the node of δp or of δv is located. From this point of view it is understandable why in the presence of pressure or velocity nodes at the ends of the tube one can state that the boundary conditions permit no radiation of the acoustic energy into the surrounding space.

An equation of the type (11.5) is conveniently written in the form of a scalar product of the vectors $\vec{\delta p}$ and $\vec{\delta v}$. As already indicated in the second section, it is frequently convenient to consider the variations of the variables, which are customarily regarded as complex quantities, in the form of vectors. Consequently, we can write Formula (11.5) in the form

$$A = \frac{1}{2} \vec{\delta p} \vec{\delta v}. \quad (11.6)$$

Using this form of notation, we can readily verify that for steady-state oscillations the quantity A remains constant on going from section to section. Indeed, let us turn to the variables u and w . If we assume δp and δv to be vectors, then u and w must also be regarded not as complex quantities, but as vectors, connected with $\vec{\delta p}$ and $\vec{\delta v}$ by the relations (4.5). But then

$$A = \frac{1}{8\rho_0 c^2} (u^2 - w^2). \quad (11.7)$$

Since the scalar squares of vectors coincide with the squares of the absolute values, and the absolute values $|u|$ and $|w|$ do not change from section to section in the case of harmonic oscillations (see §7), the quantity A cannot vary with variation of the coordinate of the cross section.

This result can be interpreted as the property of conservation of the flux of acoustic energy for steady-state oscillations in the case of motion along the flow axis.

We can draw directly several important conclusions from the fore-

going. If the flux of acoustic energy through a section containing a velocity or pressure node is equal to zero, then the condition $A = 0$ must remain valid for other sections too. But the scalar product can be equal to zero only if the factors are orthogonal (if neither of them vanishes). Consequently, in the presence of a node of δp or δv in a certain section and under steady-state oscillations the phase shift between δp and δv is equal to $\pi/2$ at all other sections. This result was already obtained earlier in the form of Formulas (6.3) and (6.6), from which it is seen that the variables \bar{p}_k and \bar{v}_k differ by an imaginary factor. However, in the present section the deduction that $\vec{\delta p}$ and $\vec{\delta v}$ are orthogonal acquires a physical clarity and can be generalized in the sense that this condition will be valid not only in the presence of nodes of δp or δv , but in all cases when no transfer of acoustic energy occurs (averaged over the period).

In those cases when the flux of acoustic energy A differs from zero in the case of steady-state oscillations (for example, when dissipation of acoustic energy occurs on the ends of the tube), the conservation property $A = \text{const}$ remains valid along the tube axis. From this property it follows, in particular, that if the absolute values of δp and δv vary as functions of the coordinate ξ (standing waves), then this is possible only upon suitable change in the phase shift ψ between them [Formula (11.5)]. In addition to this, it is clear that in such a process no nodes of δp or δv can be formed anywhere, as this would yield $A = 0$.

We see from (11.5) that A can be either positive or negative, and that its sign depends on the angle ψ . The sign of A indicates the direction of motion of the acoustic energy flux. If the acoustic energy moves in a positive direction, to the right, then $A > 0$, if it moves to the left $A < 0$.

Let us turn now to Fig. 16. Comparing the acoustic energy fluxes at the stationary planes 1 and 2, which bound the region σ , we raise the question of the amount of acoustic energy "radiated" by the region σ . We denote the flux of acoustic energy crossing the plane 1 by A' , and the flux crossing plane 2 by A'' . Then the total amount of acoustic energy A_Σ radiated by the region σ will equal

$$A_\Sigma = A'' - A'. \quad (11.8)$$

If we recall the sign rule, then $A_\Sigma > 0$ denotes that the energy moves from the region σ and if $A_\Sigma < 0$ it moves toward σ . In the former case the region σ generates acoustical energy, in the latter it absorbs it, and when $A_\Sigma = 0$ the region σ is neutral.

Assume that the losses of acoustic energy on the ends A and B of the tube are equal to $-R_A$ and $+R_B$, respectively. The signs preceding R_A and R_B are chosen such as to connect the acoustic-energy losses with its motion from the tube AB to the outer medium. The summary losses will obviously be $R = R_B - R_A$. It is then clear from energy considerations that in the case of steady-state oscillations

$$A_\Sigma = R. \quad (11.9)$$

If

$$\left. \begin{array}{l} A_\Sigma > R \\ A_\Sigma < R, \end{array} \right\}$$

or

$$(11.10)$$

then the oscillations cannot have a steady-state character.

In the first case one can speak of excitation of the system and in the second one can speak of the quenching of the oscillations. Indeed, in the first case the zone σ radiates more acoustic energy than is dissipated by the losses at the ends A and B. Consequently, part of the oscillatory energy accumulates in the tube, which should lead to an increase in the oscillation amplitudes, i.e., to excitation of the oscillating system. In the second case the character of the process is

reversed. From this point of view, Eq. (11.9) corresponds to the stability limit.

We must stipulate here that inasmuch as we have considered above the case of steady-state oscillations and the distribution of the acoustic-energy flux was elucidated only for this case, it is only Formula (11.9) that has an exact meaning. As regards the inequalities in (11.10), they must be regarded as useful qualitative criteria.

From the value of A_{Σ} we can judge the behavior of the oscillating system as a whole. From the quantities A' and A'' which are the components of A_{Σ} we can judge the processes occurring to the left and to the right of σ , for example on the ends of the tube. In the case of steady-state oscillations, the quantities A' and A'' are constant for sections lying to the left and to the right of σ , respectively. A deviation of A' and A'' from zero indicates that acoustic energy flows constantly toward the end of the tube from the region σ or from the ends of the tube into the region σ . If the acoustic energy flows from the region σ toward the ends of the tube (i.e., if $A' < 0$; $A'' > 0$), this means that absorbers are situated on the ends of the tube. If the acoustic energy moves from the ends of the tube to the region σ (i.e., if $A' > 0$; $A'' < 0$), this means that acoustic energy is continuously generated on the ends of the tube and is absorbed by the region σ .

Let us describe now in somewhat greater detail the processes occurring inside the heat-supply region σ . A thorough study of this question will be made below, and it is sufficient to note here only certain general properties of this zone. As was already mentioned, heat supply occurs inside the region σ . The region is bounded by the stationary planes 1 and 2. In connection with the processes occurring inside σ , a change takes place, generally speaking, in all the flow parameters between the planes 1 and 2. If we confine ourselves to con-

consideration of only the perturbations of the flow parameters, we can say that δp , δv , and δs change along the region σ not only owing to the presence of acoustic oscillations, but also as a result of the heat-supply process which occurs inside σ . If we assume the distance between the planes bounding σ to be small compared with the wavelengths of the perturbations, so that the waves of the perturbations connected with the acoustic oscillations cannot change noticeably their amplitudes and phases over a distance σ , then the entire change in δp , δv , and δs between planes 1 and 2 will be connected only with the heat-supply process.

We designate by the subscript 1 all the quantities corresponding to the left-hand boundary of the zone σ , and with the subscript 2 quantities corresponding to the right-hand boundary of the zone σ . We can then introduce the following notation, whereby the average value of the pressure in the left (cold) part of the tube is assumed equal to p_1 and the average velocity of sound assumed equal to a_1

$$\left. \begin{aligned} \delta v_2 - \delta v_1 &= a_1 \delta E, \\ \delta p_2 - \delta p_1 &= \kappa p_1 \delta X, \\ \delta s_2 - \delta s_1 &= c_{p_1} \delta S. \end{aligned} \right\} \quad (11.11)$$

We assume that the region σ is compared with the length of the perturbation waves. Then the dimensionless quantities δE , δX , and δS are connected only with the heat-supply process and can be regarded as three parameters describing certain summary properties of the perturbed heat-supply process.

The question of whether these parameters are sufficient for an unambiguous description of the necessary properties of the zone σ , and the question of the actual determination of these quantities, will be considered in the next chapter. It is sufficient to point out here that the introduced quantities described in reasonable fashion physical

phenomena that occur in the heat-supply zone. The quantity δE denotes the expansion of a certain volume as a result of its heating, δX denotes the occurrence of thermal resistance, and δS denotes the accompanying unavoidable change in the entropy.

Let us turn now to the question of the energy sources in thermal excitation of sound. We shall assume as before that the length of the zone σ is small and consequently the steady-state hypothesis can be applied to the processes occurring in it, i.e., we can assume that all the phenomena inside σ are described by equations that hold true for stationary flows. This can be explained as follows. The smallness of σ compared with the wavelengths of the perturbations denotes slowness of the acoustic oscillations compared with the rate at which the processes take place in the short region σ . Therefore the time necessary in order for changes to occur in the region σ and for the process to become established is not sufficient for any noticeable change in the flow parameters outside the region, a change connected with the acoustic oscillations. The processes inside σ immediately "attune" themselves, as it were, to the relatively slow acoustic oscillations.

Let us consider the crossing of the regions σ by an element of the stream. If we write down the energy conservation law separately for the stream element in a reference frame that moves together with the element, and write it separately for the center of gravity of this element, then, using the continuity equation, we readily obtain the following inequalities:

$$Q = qv_0(T_2 - T_1) + \int_0^1 p dv, \quad (11.12)$$

$$P = qv \left(\frac{v_1^2}{2} - \frac{v_2^2}{2} \right) + \int_0^1 v dp. \quad (11.13)$$

Here Q is the heat and P is the mechanical energy supplied to the gas in the region σ . Although in the case under consideration $P = 0$,

we retain this quantity in the formulas in order to make the results obtained more general.

It is obvious that the difference between the total energy fluxes (11.1) between planes 1 and 2 is

$$s_2 - s_1 = Q + P,$$

and

$$p_2 v_2 - p_1 v_1 = \int_{\sigma} p dv + \int_{\sigma} v dp. \quad (11.14)$$

Thus, the component of the energy flux "radiated" by the region σ and equal to $p_2 v_2 - p_1 v_1$, consists of two terms. The first is connected with the heat supply and with the change of the internal energy (11.12), and the second is connected with the mechanical energy supplied and with the change in the flux of the kinetic energy (11.13).

Assume that the quantities p and v have components δp and δv (11.2), which vary harmonically with the time, and let the period of the oscillations be T . Then the average acoustic energy radiated by the region σ is written in the form

$$A_z = \frac{1}{T} \int_0^T (\delta p_2 \delta v_2 - \delta p_1 \delta v_1) dt. \quad (11.15)$$

On the basis of (11.14) we can write

$$A_z = \frac{1}{T} \int_0^T \left[\int_{\sigma} \delta p d\delta v + \int_{\sigma} \delta v d\delta p \right] dt. \quad (11.16)$$

The quantities contained in the brackets in (11.15) and (11.16) are no longer harmonic functions of the time.

Denoting by the symbol Δ periodic but not harmonic components which have an order of δ^2 , we write down, using (11.12) and (11.13)

$$\int_0^T \left[\int_{\sigma} \delta p d\delta v \right] dt = \int_0^T \Delta [Q - qvc_0(T_2 - T_1)] dt, \quad (11.17)$$

$$\int_0^T \left[\int_{\sigma} \delta v d\delta p \right] dt = \int_0^T \Delta \left[P - qv \left(\frac{v_1^2}{2} - \frac{v_2^2}{2} \right) \right] dt. \quad (11.18)$$

We have already mentioned that in thermal excitation of sound no mechanical energy is supplied to the stream and therefore $P = 0$.

Using Eqs. (11.16)-(11.18) and putting $P = 0$, we obtain the following expression for the flux of acoustic energy radiated by the region σ :

$$A_z = \frac{1}{T} \int_0^T \left[\Delta Q - \Delta Q_{uc}, (T_s - T_i) - \Delta Q_v \left(\frac{v_1^2}{2} - \frac{v_2^2}{2} \right) \right] dt. \quad (11.19)$$

The expression for A_z shows that the acoustic oscillations can be maintained at the expense of three sources of energy — external heat supply, the flux of internal energy, and the flux of kinetic energy. However, Formula (11.12) expresses the fact that the first two sources are related to each other. We shall therefore consider only two sources of energy. We shall say that the energy of the acoustic oscillations can be borrowed from the thermal terms (heat supply and internal energy) and from the flux of kinetic energy.

§12. Energy Imparted to the Oscillating System During the Realization of the Elementary Processes in the Heat-Supply Zone

Let us consider a process characterized by the condition $\delta v_1 = \delta v = \delta v_2$. Then $d\delta v = 0$ and in accordance with Formula (11.17) the first two terms in (11.19) make a zero contribution. This means that the entire energy of the acoustic oscillations is borrowed from the kinetic energy of the flow. To the contrary, during a process characterized by the condition $\delta p_1 = \delta p = \delta p_2$, the entire energy of the acoustic oscillations will be borrowed from the thermal term — the heat supplied externally and the internal energy carried by the stream. In each of these two cases the oscillating system will use some single source of energy, and from this point of view the processes in the heat-supply zone, characterized by the conditions $\delta v_1 = \delta v = \delta v_2$ and $\delta p_1 = \delta p = \delta p_2$ can be called elementary. It is easy to show, however,

that it is necessary to include among the elementary processes a broader class of processes in the heat-supply zone.

From the point of view of drawing energy from the available sources, the processes given above in the heat-supply zone, characterized by the conditions $\delta v_1 = \delta v = \delta v_2$ and $\delta p_1 = \delta p = \delta p_2$, are equivalent to the more general processes, characterized by the equations $\delta v_1 = \delta v_2$ and $\delta p_1 = \delta p_2$. Actually, let us compare, for example, the processes with $\delta v_1 = \delta v_2$ and those with $\delta v_1 = \delta v = \delta v_2$.

If we assume that on the boundaries of the region σ all the quantities vary in both cases in identical fashion and the values of $\frac{1}{T} \int_0^T \Delta P dt$ and $\frac{1}{T} \int_0^T \Delta Q dt$ coincide, then the right halves of Eqs. (11.17) and (11.18) will coincide numerically. Consequently, the integrals on the left side will also be identical. Thus, the process of maintaining oscillations by drawing energy from the available energy sources is not connected with the character of variation of δp and δv along the region σ , and is uniquely determined by the values of the variables on the boundaries of the region σ subject to the condition that the variation of the mean value of the heat supply $\frac{1}{T} \int_0^T \Delta Q dt = \Delta Q_{cp}$ is specified (it is assumed that $P = 0$). It is obvious from (11.11) that the conditions $\delta p_1 = \delta p_2$ and $\delta v_1 = \delta v_2$ coincide with the conditions $\delta X = 0$ and $\delta E = 0$.

We shall assume, on the basis of the foregoing, the following elementary processes.

The first elementary process is characterized by the condition $\delta p_1 = \delta p_2$ or $\delta X = 0$. The drawing of the energy is from the external heat supply and from the flux of internal energy.

The second elementary process is characterized by the condition $\delta v_1 = \delta v_2$ or $\delta E = 0$. The drawing of the energy is from the flux of kinetic energy.

Let us consider in greater detail the first elementary process, in which the entire energy necessary to maintain the self-oscillations is drawn from the thermal terms (heat supply and internal energy). The condition $\delta p_1 = \delta p_2$ with the quantity ΔQ_{gr} maintained constant singles out the entire class of processes with identical radiation of acoustic energy from the region σ . For the actual calculation of the flux of acoustic energy $A_\Sigma = A_1$ it is immaterial which of the specific processes of this class are being considered. Therefore we shall make specific the variations of δp within σ in the following fashion: $\delta p_1 = \delta p = \delta p_2$. Then, according to (11.18) (with $P = 0$), the last term of the right half of (11.19) yields zero upon integration and therefore the total flux of acoustic energy is represented for the first elementary process in the form

$$A_1 = \frac{1}{T} \int_0^T [\Delta Q + \Delta (c_1 v_1 c_1 T_1 - c_2 v_2 c_2 T_2)] dt =$$

$$= \frac{1}{T} \int_0^T \left[\int_\sigma \delta p d\delta v \right] dt.$$

Inasmuch as we have $\delta p = \text{const}$ along the region σ , we obtain

$$\int_\sigma \delta p d\delta v = \delta p (\delta v_2 - \delta v_1),$$

which leads to the equality

$$A_1 = \frac{1}{T} \int_0^T (\delta v_2 - \delta v_1) \delta p dt = \frac{a_1}{T} \int_0^T \delta E \delta p dt. \quad (12.1)$$

The last expression is written out with the aid of Conditions (11.11).

The physical meaning of the relation obtained is quite simple. The quantity $\delta E = (\delta v_2 - \delta v_1)/a_1$ characterizes the oscillatory component of the process whereby a certain volume crossing σ is expanded, while δp is the oscillatory component of the pressure in the small

vicinity of σ . Therefore the quantity A_1 is the average work of expansion which is imparted to the system during the process of the oscillations. It will be positive if the phase shift between δE and δp does not exceed $\pi/2$ in absolute magnitude. The latter deduction follows from the formula

$$A_1 = \frac{a_1}{2} |\delta E| |\delta p| \cos \psi_1, \quad (12.2)$$

where ψ_1 is the phase shift between δE and δp . Equation (12.2) is derived in exactly the same way as (11.5).

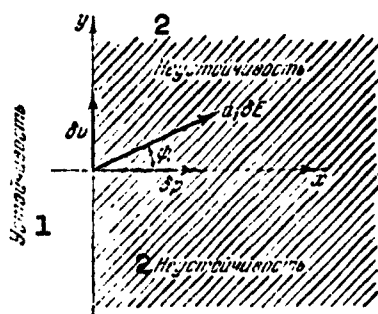


Fig. 17. Diagram showing the stability limits for the first elementary process (there are no losses). 1) Stability; 2) instability.

As was already mentioned, equations of this type are best written in the form of scalar products of the vectors contained in them. In particular,

$$A_1 = \frac{a_1}{2} \delta p \delta E. \quad (12.3)$$

In order to construct the diagram of the stability regions using Eqs. (12.2) or (12.3) we proceed in the following manner. Assume that there is no acoustic energy radiated from the open ends of the tube.

As was shown in the preceding section, the vector $\delta \vec{v}$ is in this case perpendicular to the vector $\delta \vec{p}$. We direct the vector $\delta \vec{p}$ along the x axis and the vector $\delta \vec{v}$ along the y axis. Inasmuch as $\delta \vec{v}_1$ cannot coincide with $\delta \vec{v}_2$, we agree to draw on the diagram $\delta \vec{v}_1$. The position of $\delta \vec{E}$ on this diagram is determined by the angle ψ_1 . As regards the absolute values of $\delta \vec{p}$, $\delta \vec{v}$, and $\delta \vec{E}$, they can be indeterminate in a certain sense. Indeed, if the problem is solved without formulating the initial conditions, then, as was indicated in §8, the solution does not yield the values of the amplitudes. This situation can be made more precise in the sense that the solution for each harmonic is obtained

accurate to within an indeterminate factor; the amplitude of the oscillations of each harmonic remains indeterminate, although the relations between the amplitudes of δp , δv , and the other variables are determined uniquely. Let us illustrate this circumstance, which is known from the theory of differential equations, by means of a simple example. Assume that when $\xi = \xi_1$ a pressure node $\bar{p} = 0$ is situated in the stream. For a specified frequency β , the functions $\varphi_1(\xi_1)$ and $\varphi_2(\xi_1)$ (4.14) are uniquely defined. The second equation of (4.13) yields in this case $A_p/A_v = -\varphi_2(\xi_1)/\varphi_1(\xi_1)$. Consequently, although the amplitudes of A_p and A_v remain indeterminate, their ratio is fully different.

Thus, the diagram shown in Fig. 17 can be constructed accurate to within a scale factor. One of the quantities can be chosen arbitrarily, while the others are determined uniquely. Let, for example, $\delta p = 1$ and let $\delta \vec{p}$ be directed along the x axis. Then each of the vectors $\delta \vec{v}$ and $\delta \vec{E}$ will have not only a definite direction but also a definite magnitude. Such a diagram is convenient because it yields a clear-cut representation of the relative magnitudes and phase shifts of the perturbed parameters of the process.

Let us draw on the diagram of Fig. 17 the stability boundary. We shall define the stability boundary as the hodograph of those values of the vector $\delta \vec{E}$ in which the oscillations take place with constant amplitude. In the case under consideration (absence of losses) the conditions (11.9) and (11.10) assume the following form:

$$\begin{aligned} A_1 &= 0 - \text{stability limit,} \\ A_1 &> 0 - \text{instability,} \\ A_1 &< 0 - \text{stability.} \end{aligned} \quad (12.4)$$

It follows from (12.2) that the stability limit is the y axis; the right half plane of the diagram will correspond to values of $\delta \vec{E}$ which excite the system, while the left half plane corresponds to those

$\delta \vec{E}$ at which the resultant oscillations are quenched. It must be recalled that the vectors $\delta \vec{p}$ and $\delta \vec{v}$ will be perpendicular only when $A_1 = 0$. Therefore when the end of the vector $\delta \vec{E}$ is positioned at points on the (xy) plane which do not lie on the stability limit, the vector $\delta \vec{v}_1$ will no longer coincide with the y axis.

Relations (12.4), Formula (12.2), and the diagram presented enable us to formulate the conditions for the excitation in the first elementary process as follows.

$\delta X = 0$ ($\delta p_1 = \delta p_2$) and there are no losses of acoustic energy, the system becomes excited if the phase shift between δE and the oscillatory component of the pressure δp has an absolute value less than $\pi/2$; if the absolute value of this shift lies between $\pi/2$ and π , the oscillations soon become quenched.

The results obtained are a generalization of the Rayleigh criterion to include the case of a moving medium. The point is that the phase δE and the phase of the oscillatory component of the heat supply δQ coincide only for a stationary medium. In a stationary medium, the expansion of the heated volume, which is characterized by the quantity δE , follows exactly the process of external heat supply δQ . This fact is so obvious that it needs no special proof. Therefore for a stationary medium we can take in place of δE the value of δQ (if we are dealing with phase shifts) and then the excitation condition given above coincides with the Rayleigh criterion. For a moving medium, the phases of δE and δQ may differ. This will be shown in the next chapter. Thus, the excitation conditions formulated here enclose a more general case than the Rayleigh criterion.

Let us find the excitation conditions in the first elementary process for the case when the losses of the acoustic energy R are different from zero, and consequently the region σ radiates constantly

acoustic energy in order to compensate for these losses. In such a case we must write in place of the relations (12.4):

$$\begin{aligned} A_1 &= R - \text{stability limit,} \\ A_1 &> R - \text{instability,} \\ A_1 &< R - \text{stability.} \end{aligned} \quad (12.5)$$

Taking A_1 in accordance with Formula (12.2) and putting $|\delta p| = 1$, we obtain for the stability limit

$$R = \frac{a_1}{2} |\delta E| \cos \psi_1.$$

i.e., the projection of the vector $a_1 \delta E$ on the x axis remains constant at $2R$. This gives the diagram shown in Fig. 18. The stability limit is a line perpendicular to the x axis located a distance $2R$ away from the origin.

An important difference between the stability diagram obtained here and the stability diagram shown in Fig. 17 is that now we cannot

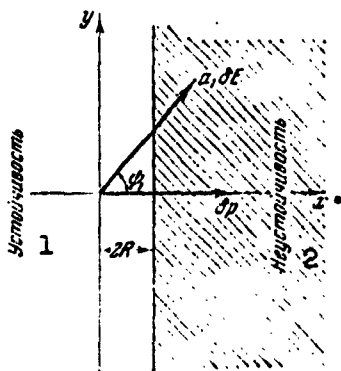


Fig. 18. Diagram of the stability limits for the first elementary process in the presence of losses. 1) Stability; 2) instability.

formulate the excitation conditions by using only the phase shifts between $\delta \vec{E}$ and $\delta \vec{p}$. When $a_1 |\delta E| < 2R$ the excitation is generally impossible, regardless of the phase shift ψ_1 (it must be recalled that we are speaking here of the relative quantities $a_1 \delta E$ and R , for when constructing the diagram we assumed $|\delta p| = 1$).

The excitation conditions are not so easy to formulate simply in this case as in the case when $R = 0$. We therefore pre-

sent them in the form of analytic relations, using Formula (12.3).

When $\delta X = 0$ and the acoustic-energy losses are equal to R the system is excited if $(a_1/2) \delta \vec{p} \delta \vec{E} > R$; the oscillations are quenched if $(a_1/2) \delta \vec{p} \delta \vec{E} < R$.

This formulation is the most general for the first elementary process.

In conclusion attention should be called to one feature of excitation in the first elementary process. Assume that the oscillatory component of the heat supply δQ is exactly sinusoidal, and the average level of the summary heat supply Q_0 does not change after the start of the acoustic oscillations. Then $\Delta Q_{sr} = 0$ and the entire energy needed to maintain the acoustic oscillations will be drawn from the internal energy flux. What is interesting in this case is that one can conceive of a process whereby acoustic oscillations are excited by the heat supply and the external heat supplied is not used as an energy source for the maintenance of the oscillations. Such a process, of course, is impossible in a stationary gas.

Let us turn now to a consideration of the second elementary process. Inasmuch as a study of this type of excitation of acoustic oscillations by means of heat supply is in many respects analogous to that made above, let us report the corresponding results more briefly.

As was already mentioned, the second elementary process is characterized by the condition $\delta E = 0$ or $\delta v_1 = \delta v_2$. For an actual calculation of the flux of acoustic energy in this case (we shall denote this flux by A_2) let us specify the concrete change of δv along σ in the following manner: $\delta v_1 = \delta v = \delta v_2$. Then, in accordance with Formula (11.7), the first two terms in the right half of (11.19) yield a zero contribution after integration, so that the total acoustic-energy flux $A_\Sigma = A_2$ will be

$$A_2 = \frac{1}{T} \int_0^T \left[-\Delta Q v \left(\frac{v_1}{2} - \frac{v_2}{2} \right) \right] dt = \frac{1}{T} \int_0^T \left[\int \delta v d\delta p \right] dt.$$

By definition, $\delta v = \text{const.}$ Consequently,

$$A_2 = \frac{1}{T} \int_0^T (\delta p_1 - \delta p_2) \delta v dt = \frac{\pi p_1}{T} \int_0^T \delta X \delta v dt. \quad (12.6)$$

The last expression is written with the aid of Conditions (11.11).

The physical meaning of the relation obtained is also quite simple. The quantity $\delta X = (\delta p_2 - \delta p_1)/\kappa p_1$ characterizes the oscillatory component of the resistance acting on the flow in the region σ , while δv is the oscillatory component of the velocity in the small vicinity of σ . Therefore the work A_2 is the work of the resistance. The excitation of the system depends in this case on whether the alternating resistance can produce the positive work necessary for the maintenance of the oscillations.

To calculate the flux of acoustic energy A_2 we can write down formulas analogous to (12.2) and (12.3):

$$A_2 = \frac{\kappa p_1}{2} |\delta X| |\delta v| \cos \psi_2, \quad (12.7)$$

$$A_2 = \frac{\kappa p_1}{2} \delta X \delta v. \quad (12.8)$$

(Here ψ_2 is the phase shift between δX and δv .)

Let us construct for the second elementary process the diagrams of the stability regions similar to the diagrams considered above.

In the absence of radiation of acoustic energy from the ends of the tube, the vectors $\delta \vec{p}$ and $\delta \vec{v}$ are mutually perpendicular; assigning to them the same directions as in Fig. 17, we obtain the diagram of Fig. 19. To maintain uniformity, we can construct this diagram to the scale $\delta p_1 = 1$. The stability region is separated from the instability region on the basis of the following obvious criteria:

$$\begin{aligned} A_2 &= 0 - \text{stability limit,} \\ A_2 &> 0 - \text{instability,} \\ A_2 &< 0 - \text{stability.} \end{aligned} \quad (12.9)$$

The first of the conditions written out here, together with Formula (12.7) or (12.8), shows that the stability limit is the x axis, while the second condition of (12.9) indicates that the position of the end of the vector $\delta \vec{X}$ in the upper half plane corresponds to an unstable

process.

Thus, the conditions for the excitation of an oscillating system in the case when the second elementary process is realized in the heat supply zone can be formulated in the following manner.

If $\delta E = 0$ ($\delta v_1 = \delta v_2$) and there are no losses of acoustic energy, the system will be excited if the phase shift between δX and the oscillatory component of the velocity δv is less than $\pi/2$ in absolute value; if the absolute value of this shift lies between $\pi/2$ and π , the oscillations are quenched.

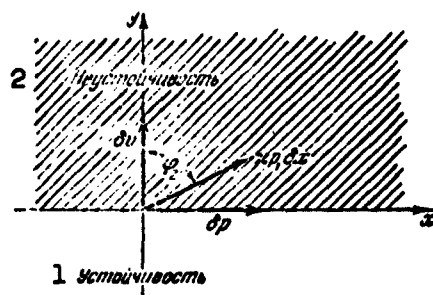


Fig. 19. Diagram of the stability limits for the second elementary process (no losses). 1) Stability; 2) instability.

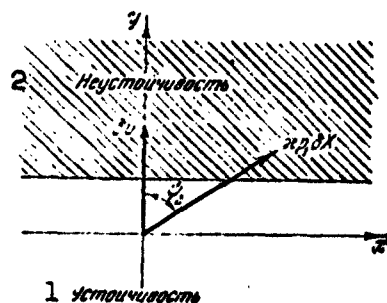


Fig. 20. Diagram of stability limits for the second elementary process in the presence of losses. 1) Stability; 2) instability.

In the case when the summary losses of acoustic energy R differ from zero it is necessary to write down in place of Relations (12.9) criteria that are analogous to (12.5). They yield the following excitation conditions for the second elementary process: when $\delta E = 0$ and the acoustic-energy losses are equal to R , the system becomes excited if $(\kappa p_1/2)\delta X\delta v > R$; the oscillations are quenched if $(\kappa p_1/2)\delta X\delta v < R$. In this case the diagram of the stability regions assumes the form shown in Fig. 20. The stability limit is parallel to the x axis at a certain distance from the origin.

§13. Energy Imparted to the Oscillating System in the General Case

The elementary processes in the heat supply zone yield rather simple conditions for the excitation of the oscillating system. The actual realization of the elementary processes is usually of low probability; these processes are essentially of interest from the principal point of view, inasmuch as they make it possible to separate the case of excitation of oscillations by energy in heat form from the case of excitation of oscillations by energy in mechanical form.

Let us consider the excitation of an oscillating system without imposing any special conditions on the process within the heat supply zone. In the general case, both the velocity oscillations δv_1 and δv_2 on opposite sides of the zone σ , and the pressure oscillations δp_1 and δp_2 , will be different. The summary radiation of acoustic energy from the zone σ can be written, on the basis of (11.6) and (11.8), in the form

$$A_1 = \frac{1}{2} (\delta p_2 \delta v_2 + \delta p_1 \delta v_1). \quad (13.1)$$

The formula obtained enables us to find the flux of acoustic energy radiated by the region σ from the parameters specified on the boundaries of this region. Knowledge of the processes that proceed inside σ is in this case not essential. This form of notation is convenient, in particular, for experimental research, where it is frequently much simpler to measure the oscillations of velocity and pressure on both sides of the heat-supply zone than it is to analyze the phenomena that occur in the heat-supply zone itself.

Formula (13.1) can be rewritten also in a different form, which is convenient for use if it is required to determine A_Σ from the parameters of the flow ahead of the heat-supply zone and from the characteristics of the heat-supply zone. By substituting the values of δp_2 and

δv_2 obtained from the first equations of (11.11) into (13.1) we can obtain the following expression for A_Σ :

$$A_\Sigma = \frac{1}{2} (\alpha_1 \delta p_1 \delta E + \kappa p_1 \delta v_1 \delta X + \kappa \alpha_1 p_1 \delta E \delta X). \quad (13.2)$$

However, neither Formula (13.1) nor the resultant expression (13.2) enable us to establish what fraction of the flux A_Σ comes from the energy present in thermal form and what comes from energy in mechanical form. To answer this question, it is natural to attempt to replace the real process by a succession of two elementary processes with acoustic energy fluxes A_1 and A_2 such that $A_1 + A_2 = A_\Sigma$. It is easy to perceive that if the quantity δp in the portion where the first elementary process takes place is maintained constant at a value δp_2 , and if δv varies from δv_1 to δv_2 , while at the same time in the next section the quantity $\delta v = \delta v_1$ is conserved while δp varies from δp_1 to δp_2 , then, as can be seen from (13.1), A_Σ assumes the required value. However, a more attentive analysis of the question shows that the problem is not uniquely solved. Indeed, it is possible to obtain one and the same summary effect (a value of acoustic energy flux equal to A_Σ) by taking two different sequences of elementary processes: the one described above or its inverse (i.e., first change the variation of pressure δp , and then the variation of velocity δv). Although the summary acoustic energy flux A_Σ radiated by the region will be the same in both cases, its components A_1 and A_2 will change.

A way out of this situation is possible by approximating the fictitious schemes to the real ones. Actually, during the course of heat supply the changes in velocity and pressure occur simultaneously. It is therefore natural to break down the entire process into a set of alternating elementary processes.

In the case under consideration one can apply to the flow inside

the region of heat supply σ the usual laws of hydraulics, and therefore the continuity equation and the momentum equation can be written in the form

$$\begin{aligned} Qv &= Q_1 v_1, \\ p &= (p_1 + Q_1 v_1^2) - Q_1 v_1 v. \end{aligned}$$

The quantities without subscripts characterize the flow parameter at a certain section inside σ . On the right-hand boundary of the region σ they reach the values p_2 , v_2 , and p_2 . From the last equation it is seen that the pressure p and the velocity v are linearly related and consequently if p changes from p_1 to p_2 and v changes from v_1 to v_2 , then equal fractions in the change of p correspond to equal fractions in the change of v . In other words, when the pressure p at a certain section inside σ reaches a value

$$p = p_1 + \theta(p_2 - p_1) \quad (0 < \theta < 1),$$

then the velocity v reaches at the same section the value

$$v = v_1 + \theta(v_2 - v_1).$$

The last two relations are linear with respect to p and v , so that they hold true also for the variations of the pressure δp and the velocity δv at a certain cross section inside σ : if

$$\text{then } \left. \begin{aligned} \delta p &= \delta p_1 + \theta(\delta p_2 - \delta p_1), \\ \delta v &= \delta v_1 + \theta(\delta v_2 - \delta v_1) \end{aligned} \right\} \quad (0 < \theta < 1). \quad (13.3)$$

If we compare these formulas with (11.11) we readily see that equal fractions of the variation in δE correspond to equal fractions of the variation in δX . This enables us to construct that sequence of the two elementary processes which coincides in the limit with the actual process that occurs in the heat-supply region σ .

Figure 21 shows a scheme of such a process. Let us break down the entire zone σ into a set of successive sections. The boundaries of the region σ will be the sections 1 and $2n$. (It is more convenient to des-

ignate the right-hand boundary section of the region σ not by 2, but by $2n$.) Assume that on going over from section 1 to section $2n$ the variations of the pressure and velocity, δp and δv , change by the following amounts:

$$\begin{aligned}\Delta \delta p &= \delta p_{2n+1} - \delta p_1, \\ \Delta \delta v &= \delta v_{2n+1} - \delta v_1.\end{aligned}$$

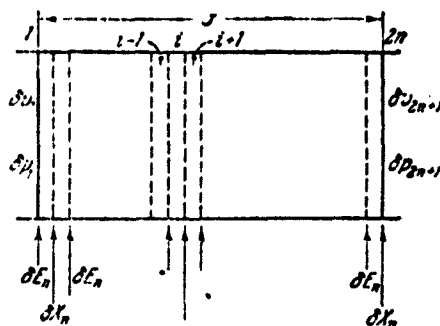


Fig. 21. Scheme showing the alternation of the elementary processes in the zone σ .

Let us break up the process between sections 1 and $2n$ into $2n$ alternating elementary processes, of which n constitutes identical velocity variations only, and the other n pressure variations only.

For the first type of elementary processes we can write

$$\delta v_i - \delta v_{i-1} = \frac{\Delta \delta v}{n} = \frac{\epsilon_1 \delta E}{n} = \delta E_n \quad (i = 2, 4, 6, \dots), \quad (13.4)$$

and for the second type

$$\delta p_{i+1} - \delta p_i = \frac{\Delta \delta p}{n} = \frac{\kappa p \delta X}{n} = \delta X_n \quad (i = 2, 4, 6, \dots). \quad (13.5)$$

It is seen from the presented formulas that in each passage through the introduced fictitious surfaces a change takes place in δv or in δp by a fraction amounting to $1/n$ of the total change.

Consequently, the requirement that equal fractions of the change in δp correspond to equal fractions of the change in δv [see Conditions (13.3)] will be satisfied here for any arbitrary section with an error not exceeding $1/n$ parts of the total change in δv and δp . As

$n \rightarrow \infty$ this error will tend to zero, and the fictitious process will approach in the limit to the real one.

Let us find the values of the components of the total acoustic energy flux, A_1 and A_2 [see Formulas (12.1) and (12.6)]:

$$A_1 = \frac{1}{T} \left[\int_0^T \delta E_n \delta p_1 dt + \int_0^T \delta E_n \delta p_2 dt + \dots + \int_0^T \delta E_n \delta p_{n-1} dt \right],$$

$$A_2 = \frac{1}{T} \left[\int_0^T \delta X_n \delta v_1 dt + \int_0^T \delta X_n \delta v_2 dt + \dots + \int_0^T \delta X_n \delta v_{n-1} dt \right].$$

If we recognize that

$$\begin{aligned} \delta p_1 &= \delta p_2, & \delta v_2 &= \delta v_3, \\ \delta p_2 &= \delta p_3, & \delta v_3 &= \delta v_4, \\ &\dots & \dots \end{aligned}$$

and in addition

$$\begin{aligned} \delta p_2 &= \delta p_2 + \delta X_n, & \delta v_2 &= \delta v_1 + \delta E_n, \\ \delta p_3 &= \delta p_3 + \delta X_n, & \delta v_3 &= \delta v_2 + \delta E_n, \\ &\dots & \dots \end{aligned}$$

then the expressions for A_1 and A_2 are written in the form

$$A_1 = \frac{1}{T} \left[\int_0^T \delta E_n \delta p_1 dt + \int_0^T \delta E_n (\delta p_1 + \delta X_n) dt + \dots + \int_0^T \delta E_n [\delta p_1 + (n-1) \delta X_n] dt \right],$$

$$A_2 = \frac{1}{T} \left[\int_0^T \delta X_n (\delta v_1 + \delta E_n) dt + \int_0^T \delta X_n (\delta v_1 + 2\delta E_n) dt + \dots + \int_0^T \delta X_n (\delta v_1 + n\delta E_n) dt \right].$$

By grouping the terms in suitable manner we obtain

$$A_1 = \frac{1}{T} \int_0^T (n\delta E_n \delta p_1 + [1+2+3+\dots+(n-1)] \delta E_n \delta X_n) dt,$$

$$A_2 = \frac{1}{T} \int_0^T (n\delta X_n \delta v_1 + [1+2+3+\dots+n] \delta E_n \delta X_n) dt.$$

Recalling the well-known formula

$$1 + 2 + 3 + \dots + n = \frac{n(n+1)}{2},$$

we obtain the limit as $n \rightarrow \infty$, taking (13.4) and (13.5) into account, the following final expressions for A_1 and A_2 :

$$\left. \begin{aligned} A_1 &= \frac{1}{T} \int_0^T \left(a_1 \delta E \delta p_1 + \frac{\kappa a_1 p_1}{2} \delta E \delta X \right) dt, \\ A_2 &= \frac{1}{T} \int_0^T \left(\kappa p_1 \delta X \delta v_1 + \frac{\kappa a_1 p_1}{2} \delta E \delta X \right) dt. \end{aligned} \right\} \quad (13.6)$$

In analogy with the manner whereby (11.4) was reduced to the form (11.6), the expressions obtained can be written also in the form of scalar products

$$\left. \begin{aligned} A_1 &= \frac{1}{2} \left[a_1 \delta E \delta p_1 + \frac{\kappa a_1 p_1}{2} \delta E \delta X \right], \\ A_2 &= \frac{1}{2} \left[\kappa p_1 \delta X \delta v_1 + \frac{\kappa a_1 p_1}{2} \delta E \delta X \right]. \end{aligned} \right\} \quad (13.7)$$

As expected the sum $A_1 + A_2$ yields an expression coinciding with that obtained for A_Σ directly [Expression (13.2)].

Formulas (13.6) and (13.7) enable us to determine not only the total amount of acoustic energy A_Σ radiated by the heat-supply region, but also to separate the fractions A_1 and A_2 connected with two independent energy sources which feed the oscillating system.

Comparing Formulas (13.7) with Expressions (12.3) and (12.8) which were derived previously and which are valid for the elementary processes, it must be emphasized that in the general case the value of A_1 depends not only on the absolute values of $\delta \vec{E}$, $\delta \vec{p}_1$ and on the phase shift between them. Even if $A_2 = 0$ and the energy of the acoustic oscillations is thus drawn only from the thermal source, its value depends also on δX , i.e., on the variation of the resistance. The reason for it is that when $\delta X \neq 0$ the value of δp , which is essential for the drawing of energy from the thermal source, varies along σ . Therefore

the phase shift between δE and the value of δp in the left boundary section of the region σ can no longer determine the character of the entire process. But in this case the various excitation criteria, such as the Rayleigh criterion, which state that a certain phase shift is essential between the pressure and the heat supply etc., lose their meaning, since the value of δp (including also the phase of δp) varies over the length of the zone σ , and the very concept of the phase of δp as a certain general characteristic of the zone σ as a whole becomes meaningless. Perfectly similar arguments can be advanced also for the case $A_2 \neq 0$, $A_1 = 0$.

To conclude the analysis of the question of the energy imparted to the oscillating system in the general case, it would be necessary to plot stability diagrams similar to those given in the preceding section. In addition, it is useful to estimate the relative significance of each of the two energy sources feeding the oscillating system. However, these two questions are best considered after a method is presented for the actual determination of the quantities δE , δX , and δS and after considering the question of in which cases the rather complicated physical and chemical processes occurring inside the heat-supply zone can be described with the aid of these three dimensionless parameters.

§14. Excitation of Oscillating System by Entropy Waves

In addition to perturbations of velocity and pressure, which are unified by the concept of acoustic perturbations, the stream can also transport entropy waves. In the cases when the oscillations in the system have a harmonic character, the entropy perturbations carried by the stream have the form of sinusoidal waves, as was shown in the second chapter.

Entropy perturbations in themselves cannot act in any manner on

the acoustic oscillations. They can, however, cause the occurrence of acoustic oscillations in those cases when the entropy waves interact on certain surfaces with the pressure or velocity perturbations.* Let us explain the foregoing by means of an example. Assume that in some region the tube through which the gas flows ceases to be cylindrical and experiences a rather steep constriction, which furthermore is such that the stream flows in the minimal cross section with the velocity of sound. Let us adopt the steady-state hypothesis. We shall assume that during the time that an element of the fluid crosses the constriction region neither the pressure nor the velocity change prior to entering the indicated region, and the stream can be regarded as isentropic in the vicinity of this region during the same time interval. The foregoing means that the period of the acoustic oscillations is large compared with the time of motion of the elementary volume of the liquid along the constriction region, and the length of the entropy wave carried by the stream is large compared with the length of the constriction region. If we assume this hypothesis, then, in accordance with the known laws of gasdynamics, the ratio of the stream velocity to the local velocity of sound in the initial cross section of the constriction region will remain constant during the entire time of the oscillations. This condition can be assumed, in particular, as the boundary condition for the cylindrical portion of the tube, if the tube has a strong constriction in the region of the outlet end.

Thus, assume that in a certain section (say, the end section) of the tube the following condition is satisfied

$$M = \frac{v}{c} = \text{const.} \quad (14.1)$$

From this we obtain immediately the equation

$$\delta\left(\frac{v}{c}\right) = \bar{v} - M \frac{\delta s}{c} = 0.$$

Using Formulas (4.1), (4.2), and (4.9), we can easily write down the relation obtained in the following form:

$$2\bar{v} - M\bar{s} - M(\kappa - 1)\bar{p} = 0. \quad (14.2)$$

Condition (14.2) can almost always be replaced by the approximate condition

$$2\bar{v} - M\bar{s} = 0, \quad (14.3)$$

inasmuch as the coefficient of \bar{p} is small for ordinary flows.

Let us find the flux of acoustic energy A'' in the end section

$$A'' = \frac{1}{T} \int_0^T \delta p \delta v dt. \quad (14.4)$$

In accordance with Condition (14.3) and taking into account Formulas (14.1) and (4.8) we have here

$$\delta v = \frac{v}{2c_p} \delta s. \quad (14.5)$$

Let

$$\begin{aligned} \delta p &= A_p \sin \omega t, \quad A_p > 0, \\ \delta s &= A_s \sin(\omega t + \psi), \quad A_s > 0. \end{aligned}$$

Then

$$A'' = -\frac{v}{2Tc_p} \int_0^T \delta p \delta s dt = -\frac{v}{4c_p} A_p A_s \cos \psi. \quad (14.6)$$

Thus, the sign of A'' depends on ψ , i.e., on the phase shift between the pressure and entropy oscillations in the vicinity of the critical constriction of the stream. When $|\psi| < \pi/2$ we have $A'' > 0$, in other words the acoustic energy moves toward the outlet section and consequently acoustic energy is absorbed in the vicinity of the constriction. When $\pi/2 < \psi < \pi$ we have $A'' < 0$, and the acoustic energy moves from the end section toward the center of the tube, i.e., energy is generated in the vicinity of the outlet end.

The physical process of generation of acoustic waves is the consequence of the periodic "blocking" of the nozzle by a gas stream that

has a wave-like temperature (entropy) distribution along the flow axis.

Other conditions being equal, the magnitude of the average flux of acoustic energy A'' increases in proportion to A_s , i.e., it increases with increasing amplitude of entropy oscillation. Entropy oscillations of any appreciable value are conceivable only as the result of oscillating heat supply in the combustion zone. Consequently, in the absence of heat supply, the excitation conditions should depend very little on the conditions at the outlet end.

In the example considered here, the excitation of the acoustic oscillations by entropy waves took place only because there existed a certain cross-section of the tube, in which the maintenance of a constant value of the ratio v/a required an oscillating variation of v , inasmuch as the local velocity of sound a (uniquely related with the local value of the temperature) had a harmonic component. The entropy waves passing through this cross section brought into being, as it were, perturbations in the stream velocity, i.e., acoustic oscillations. In other cases the processes that lead to a similar connection between the \bar{s} waves and the \bar{p} and \bar{v} waves can be different, but this will always be some physical phenomenon in which the change in the entropy is connected with a change in the velocity or pressure or both. Inasmuch as in the linear formulation of the problem in the one-dimensional flow itself there occurs no interaction whatever between the acoustic oscillations and the entropy waves [this is seen, in particular, from Eq. (4.4)], the realization of such interaction is possible only in the heat-supply zone or at the ends of the tube (or in other cross sections where the gas stream experiences some external action).

Thus, the entropy waves are capable of exciting acoustic oscillations not directly but only indirectly.

One of the methods of constricting the flow, such as was consid-

ered above, is to install a Laval nozzle at the outlet of the tube. The deduction obtained above shows that if gas with periodically varying temperature enters into the nozzle, this may excite acoustic oscillations. It doesn't follow at all from the foregoing that the Laval nozzle always contributes to the occurrence of instability. To the contrary, under ordinary conditions (in isentropic flow) it serves as a weak damper for the acoustic oscillations. Indeed, let us put $\bar{s} = 0$. It then follows from (14.2) that

$$\delta v = \frac{\kappa - 1}{2\kappa} \frac{v}{p} \delta p.$$

According to Formula (14.4) this yields

$$A'' = \frac{(\kappa - 1)^2 v}{4\kappa p} (\delta p)^2.$$

The expression obtained is always positive. This indicates that the flux of acoustic energy A'' always flows toward the nozzle, i.e., from the tube into the outer space, this indicating that the Laval nozzle has damping properties.

In conclusion we must point out that the generation of acoustic energy in the outlet section at the expense of the entropy waves which were produced, for example, in the heat-supply zone and were then carried by the stream to the outlet end presupposes that the produced entropy waves do not vanish and do not become smooth during the time that they move from the heat-supply region to the outlet end of the tube. This corresponds fully to the properties of one-dimensional flow of an ideal gas. Actually, however, in the flow of a viscous and heat-conducting gas, the entropy waves will become smoothed out and vanish as they move through the tube. It is important to note here that while taking account of viscosity and thermal conductivity influences very little the acoustic properties of the flow, the influence of viscosity and thermal conductivity on the propagation of the entropy waves is

much more appreciable. It is therefore not excluded that if the heat-supply zone is located very far away from the outlet end of the tube, the effect described above, whereby acoustic oscillations are excited by interaction between the entropy waves and the end section, will not be observed at all.

Manu-
script
Page
No.

[Footnotes]

- 72 The term mechanism is used very broadly both here and below. It is usually used to refer to a number of physical processes which are linked by a causal relationship.
- 73 *Rayleigh, Teoriya zvuka [The Theory of Sound], Gostekhizdat [State Publishing House for Theoretical and Technical Literature], 1955, page 220.
- 73 **Ibid, page 219.
- 74 *I.e., excitation of acoustical oscillations (B.R.).
- 74 **Ibid, page 227.
- 74 ***Putnam, A.A., Dennis, W.R., Trans. ASME 75, No. 1, 15 (1953). Russian translation: Putnem, A., Dennis U., Issledovaniye vibratsionnogo gorenija v gorelках [Investigation of Vibrational Heating in Jets], Voprosy raketnoy tekhniki [Problems of Rocket Technology], No. 5 (23), 1954.
- 76 Abramovich, G.N., Prikladnaya gazovaya dinamika [Applied Gasdynamics], Gosudarstvennoye izdatel'stvo tekhnikoteoreticheskoy literatury [State Publishing House for Technical and Theoretical Literature], 1953.
- 80 Here and below, thermal quantities are expressed in mechanical units, so that it becomes unnecessary to use dimensional constants in the formulas.
- 106 This section is somewhat beyond the scope of the chapter. It is included here because the problem of which it treats is solved by the energy method.

Manu-
script
Page
No.

[List of Transliterated Symbols]

80 э = e = energiya = energy flux
81 cp = sr = sredniy = average

Chapter 4
THEORETICAL IDEALIZATION OF THE PROCESSES
IN THE COMBUSTION ZONE

§15. Change in Perturbations on Crossing the Combustion Region

In considering the excitation of acoustic oscillations by means of heat supply in the preceding chapter, three assumptions were made: it was assumed that the stationary heat-supply zone has a small length compared with the wavelength of the excited oscillations, that the heat supply process is one-dimensional, and that the steady-state hypothesis is applicable to the processes inside the heat supply region.

These assumptions cannot appear to be too artificial for phenomena such as, for example, the excitation of sound in a Rijke tube with the aid of a heated grid. However, when we consider the excitation of acoustic oscillations by means of a flame, all these assumptions cease to be obvious.

The last two assumptions, namely one-dimensionality of the heat supply process and the steady-state hypothesis, become in the majority of cases simply erroneous. As regards the first assumption, namely that the length of the heat-supply zone is small, it must be used with certain caution. In view of the foregoing, the derivations obtained in the preceding chapter are valid only for a relatively narrow class of phenomena.

The task of the present chapter is to develop a scheme for the theoretical idealization of the processes in the combustion zone, a scheme free of the limiting assumptions of the preceding chapter, and

the extension of the previously obtained deductions to include this general case.

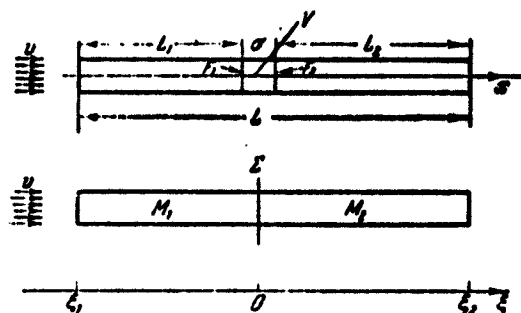


Fig. 22. Theoretical idealization of the flow in a tube in the presence of heating in the region σ .

Of all the assumptions made above, we retain only one, namely we assume that the length of the combustion zone σ is small compared with the length of the tube L (Fig. 22). We shall make this assumption more precise in the sense that when we speak of the smallness of σ we have in mind not the entire combustion zone, but only that part in which noticeable fluctuations in the heat supply occur. Usually this zone corresponds to the initial portion of the combustion region. It is possible for a small amount of heat to be released in the initial portion when averaged over the period, yet the oscillatory component of the heat release may be appreciable. This is natural, since the initial portions of the combustion region, where the combustion has not yet fully developed, are particularly sensitive to fluctuations in the parameters of the fuel mixture that is fed to the combustion region. In addition, in the initial portions of the combustion region is located the flame front, which can vary in position, etc. As regards the portions located at a certain distance from the flame front, deep inside the combustion region, the oscillations in the heat supply are much less intense, although a noticeable release of heat may occur there.

Consequently, when speaking of the combustion zone σ , we shall always bear in mind that we are referring only to that part of the heat-supply region which is characterized by considerable oscillations of the heat supply. The remaining part of this region will be called the afterburn zone, which will be defined in a sense different from the ordinary. In the cases under consideration, a noticeable fraction of the total amount of heat supplied to the gas in the combustion chamber may be released in the afterburn zone.

We shall thus assume the length of the zone σ to be small compared with the total length of the tube L , but we shall not neglect the nonstationary and volume (three-dimensional) character of the processes that occur in it. As regards the portions L_1 and L_2 to the left and to the right of σ , we shall continue to assume that the propagation in them occurs in one-dimensional fashion and is described by the expressions obtained in the second chapter. We add merely that along the portion L_2 (hot gas) the afterburn may actually cause a change in the temperature and in the average stream velocity.

In order to use the simple formulas of the second chapter, we shall average the temperature and the stream velocity over the portion L_2 . An estimate has shown that this cannot greatly influence the results of the calculations.

The scheme adopted for the phenomenon raises great difficulties in the analytical investigation of the acoustic oscillations in the tube. The basis of these difficulties is that the process in portions L_1 and L_2 is one-dimensional and is described by the acoustic equations, whereas inside the short zone σ it becomes necessary to take into account the three-dimensionality of the combustion process and a whole series of complicated physical and chemical laws that are typical of combustion. The zone σ not only divides the entire stream into two

portions, but appreciably changes the character of the acoustic perturbations in the regions to the left and to the right of this zone.

A clear-cut idea of this role of the zone σ can be obtained by considering the motion of some single acoustic impulse along the tube L. Let such an impulse move over the portion L_1 to the right. After reaching the zone σ and entering into interaction with the combustion process, this impulse is partially reflected and moves to the left through portion L_1 , and partially passes through the zone σ . However, the impulse entering into the portion L_2 will differ in phase and in amplitude from the impulse that gave rise to it.

As can be seen from the statements made here, the zone σ is a region in which the acoustic perturbations become transformed. If the character of this transformation is known beforehand for some reason, then the calculation can be carried out by directly relating the acoustic perturbations on the boundary planes F_1 and F_2 (see Fig. 22), without being concerned with the details of the phenomena that occur within σ . In order not to introduce thereby any distortions in the acoustic properties of the system, which depend on the total length of the tube L, we considerably lengthen the portions L_1 and L_2 . This argument leads to the theoretical scheme shown in the lower part of Fig. 22. The entire tube is divided into two parts not by the short zone σ , but by the plane Σ . The perturbations of flow on the left side of the plane Σ coincide with the perturbations on F_1 , while the perturbations on the right side of the plane Σ correspond with the corresponding quantities on F_2 . Inasmuch as the amplitudes and phases of like perturbations on F_1 and F_2 do not generally speaking coincide, the fictitious plane Σ must be attributed the properties of a surface with strong discontinuities in the gasdynamic flow parameters. With such an idealization of the processes in the tube, these parameters will be one-dimensional

throughout and will obey the acoustic laws. On the other hand, the properties of the plane Σ must still be determined. One must not think that the introduction of the plane Σ in lieu of the zone σ greatly distorts the entire pattern of the phenomenon, inasmuch as the rather complicated combustion process which occurs within a certain volume is replaced by an instantaneous heat supply on the plane Σ . It would be more correct to use a different representation. The zone σ is "extracted" as it were from the stream and is investigated in detail separately. Once its properties become clear, i.e., once the connection between the parameters on F_1 and F_2 become clear, these properties are formally assigned to the left and right sides of the plane Σ .

In introducing in place of the real combustion zone σ a strong-discontinuity surface Σ , we must, of course, attribute to this surface all the essential properties of the heat-supply zone σ . The introduction of a discontinuity surface in place of an extended heat-supply zone is a measure which is used by almost all authors engaged in the study of the process of thermal excitation of sound. As regards the properties of the introduced surface Σ , they are usually formulated incorrectly, something that has led to distortions in the results of the investigation. We shall therefore present a rigorous derivation of the properties that must be ascribed to the surface Σ , and for this purpose we obtain the connection between the flow parameters on the planes F_1 and F_2 .

We determine first of all the boundaries of the region σ . We define the combustion zone as a certain volume V , contained between two stationary planes normal to the tube axis, inside which the combustion process takes place. The length of the combustion zone σ must be taken here with allowance not only for the possible curvature of the flame front, but also with account of the oscillations of the front with

time, namely, the flame surface must not cross the boundaries of the volume V in any of their positions.

Inasmuch as the process outside the combustion zone V is assumed to be one-dimensional, such an assumption must be made also with respect to the character of flow in the sections bounding the volume V . Consequently, the combustion zone can have a somewhat greater length than the distance between the extreme positions of the surface of the flame, attained as the result of the oscillations.

As was shown in the second chapter, the process of propagation of the perturbations is described by three variables which depend on the coordinates and on the time. Therefore, in order to "join together" the perturbations that propagate to the left and to the right of the combustion zone it is necessary to find three independent connections between the perturbations on the left and on the right of V . To formulate these connections it is advantageous to use the conservation laws. Let us use the equations for the mass, momentum, and energy fluxes in the form presented in the textbook of L. Landau and Ye. Lifshits,* supplementing these equations with several new terms.

First, the energy flux equation must be written with account of the chemical energy q per unit mass of combustible mixture. A change in the value of q upon crossing the zone σ indicates that part of this energy has been converted into thermal form as the result of the combustion process.

Second, in the heat-supply zone σ there can be located sources of mass, momentum, or energy. Sources of mass can exist, for example, in the form of a system of nozzles which supply the fuel, if these nozzles are located not ahead of the combustion zone but within it. Usually, however, the combustible mixture is prepared ahead of the combustion zone, so that there is no real source of mass in the zone σ .

Even in those cases when a source mass of this type is located in the combustion zone, it can usually be neglected. Therefore, writing down for the sake of generality the corresponding term M' in the equation for the mass flux, we shall henceforth set $M' = 0$ almost everywhere in this book. In order for this statement not to cause misunderstanding, we point out that the condition $M' = 0$ reflects sufficiently accurately the processes involved when fuel is consumed in air. In the analysis of the operation of liquid-fuel jet engines it would be incorrect to set $M' = 0$. In the theory of liquid-fuel jet engines it is customary to neglect the volume occupied by the fuel in the liquid phase. Consequently, the most natural idealization of the combustion process in such engines is the following scheme. The drops of liquid move through the gas medium up to a certain cross section of the combustion chamber, where they are instantaneously converted into gas (are consumed). Consequently, in this cross section there is a powerful source of gases (mass source). This is analogous to the case when nozzles feeding fuel to the air are situated in the combustion zone, but unlike this case, what is fed through the nozzles in liquid-fuel jet engines is not a small fraction of the mass entering the combustion zone, but the entire mass. Inasmuch as a detailed analysis of the work of liquid-fuel jet engines is not the purpose of the present research, we shall assume everywhere (except in the corresponding section of Chapter 10) that $M' = 0$.

With respect to the source of momentum located inside the zone σ , the following remarks can be made. The presence of such a source is perfectly probable. It can be imagined in the form of a certain resistance \bar{P}' , which various structural elements (for example, stabilizers), situated in the combustion chamber, present to the stream. Since the aerodynamic forces that are applied to these construction

elements do not perform external work, it can be stated that such a momentum source is not a source of energy (the resistances merely change the ratio of the amounts of mechanical and thermal energy transported by the stream, but do not change their sum). As regards the source of thermal energy Q' , which is taken into account when writing down the equation for the energy flux, we shall agree to take it to mean the heat supply not connected with combustion, for example, the heat supply delivered by heated grids in a Rijke tube, etc., or else the heat supply from fuel introduced directly into the volume V , by-passing its boundaries.

We shall agree also not to distinguish henceforth between the concepts "source" and "sink" (the latter will be regarded as a negative source).

Taking into account the remarks made above, the conservation laws for the mass, momentum, and energy can be written in the following form:

$$\left. \begin{aligned} \oint q_v df &= -\frac{\partial}{\partial t} \int q dV + M', \\ \oint \Pi_{ik} df_k &= -\frac{\partial}{\partial t} \int q v_i dV + P'_i, \\ \oint q_v \left(\frac{v^2}{2} + c_p T + q \right) df &= -\frac{\partial}{\partial t} \int q \left(\frac{v^2}{2} + c_p T + q \right) dV + Q'. \end{aligned} \right\} \quad (15.1)$$

Here the vector $d\vec{r}$ corresponding to the elementary area df of the surface bounding the volume V is directed along the outward normal to the surface, while the momentum flux density tensor is defined by the expression

$$\Pi_{ik} = p\delta_{ik} + \rho v_i v_k,$$

where δ_{ik} is a unit tensor. The integrals in the left halves of (15.1) are taken over the stationary surface bounding the combustion zone V .

Usually these surface integrals are easy to calculate. Let the stream axis coincide with the \underline{x} axis, and let the combustion zone be cylindrical, cut out of the over-all volume by the stationary planes

F_1 and F_2 (see Fig. 22). According to the condition agreed upon above, the flow in the sections F_1 and F_2 is one-dimensional. Consequently, on the surfaces bounding the volume V (the planes F_1 and F_2 and the lateral surface of the cylinder), the only velocity component that differs from zero is v_x . But then the integrals over the surface bounding the region V reduce to a difference between the integrals over the planes F_1 and F_2 .

Introducing the indices "unity" for the stream parameters on F_1 (cold stream) and the indices "two" for the stream parameters on F_2 (hot stream), we obtain with allowance for the fact that by virtue of the assumed cylindrical form of the combustion zone the areas of sections F_1 and F_2 are equal to each other:

$$\left. \begin{aligned} q_2 v_2 &= q_1 v_1 - \frac{1}{F} \frac{\partial}{\partial t} \int_V q dV + M^*, \\ q_2 v_2^2 + p_2 &= q_1 v_1^2 + p_1 - \frac{1}{F} \frac{\partial}{\partial t} \int_V q v_x dV + P_2^*, \\ q_2 v_2 \left(\frac{v_2^2}{2} + c_{p2} T_2 + q_2 \right) &= q_1 v_1 \left(\frac{v_1^2}{2} + c_{p1} T_1 + q_1 \right) - \\ &\quad - \frac{1}{F} \frac{\partial}{\partial t} \int_V q \left(\frac{v^2}{2} + c_p T + q \right) dV + Q^*, \end{aligned} \right\} \quad (15.2)$$

where

$$\begin{aligned} M^* &= \frac{M'}{F}; \\ P_2^* &= \frac{P_2'}{F}; \\ Q^* &= \frac{Q'}{F}. \end{aligned}$$

F is the area of the cross section of the chamber.

In the general case, by virtue of the incompleteness of the combustion process, $q_2 \neq 0$. Let us introduce the concept of instantaneous effective completeness of combustion

$$\eta_{\text{eff}} = \frac{q_1 - q_2}{q_1}. \quad (15.3)$$

It is easy to see that in the case of a stationary process or when $V = 0$ the introduced definition of η_{sg} coincides with the custom-

any definition of completeness of combustion.

In nonstationary combustion, Expression (15.3) does not have such a simple physical meaning, since the consumed portion of the fuel mixture crossing the plane F_2 could have a different calorific value prior to combustion (in view of the fluctuations in q) from the mixture crossing the plane F_1 during the same instant.

Using Formula (15.3) and the first equation of (15.2), we can rewrite the last equation of the system (15.2) in the form

$$\begin{aligned} q_2 v_2 \left(\frac{v_1^2}{2} + c_{p_1} T_1 \right) = q_1 v_1 \left(\frac{v_1^2}{2} + c_{p_1} T_1 + \eta_{cr} q_1 \right) + \\ + q_1 (1 - \eta_{cr}) \frac{1}{F} \frac{\partial}{\partial t} \int_V q dV - \frac{1}{F} \frac{\partial}{\partial t} \int_V q \left(\frac{v_2^2}{2} + c_p T + q \right) dV + Q^* \end{aligned} \quad (15.4)$$

(here $M^* = 0$).

Following the customary method, we linearize the obtained system of equations. As a result we have

$$\left. \begin{aligned} q_2 \delta v_2 + v_2 \delta q_2 = q_1 \delta v_1 + v_1 \delta q_1 - \frac{1}{F} \frac{\partial}{\partial t} \int_V q dV + \delta M^*, \\ 2q_2 v_2 \delta v_2 + v_2^2 \delta q_2 + \delta p_2 = 2q_1 v_1 \delta v_1 + v_1^2 \delta q_1 + \delta p_1 - \\ - \frac{1}{F} \frac{\partial}{\partial t} \int_V q v_x dV + \delta P_x^*, \\ \left(\frac{3}{2} q_2 v_2^2 + q_2 c_{p_2} T_2 + q_2 q_2 \right) \delta v_2 + \\ + \left(\frac{v_2^2}{2} + v_2 c_{p_2} T_2 + v_2 q_2 \right) \delta q_2 + c_{p_2} q_2 v_2 \delta T_2 + \\ + q_2 v_2 \delta q_2 = \left(\frac{3}{2} q_1 v_1^2 + q_1 c_{p_1} T_1 + q_1 q_1 \right) \delta v_1 + \\ + \left(\frac{v_1^2}{2} + v_1 c_{p_1} T_1 + v_1 q_1 \right) \delta q_1 + c_{p_1} q_1 v_1 \delta T_1 + \\ + q_1 v_1 \delta q_1 - \frac{1}{F} \frac{\partial}{\partial t} \int_V q \left(\frac{v_2^2}{2} + c_p T + q \right) dV + \delta Q^*. \end{aligned} \right\} \quad (15.5)$$

If we write the last equation of the system (15.2) in the form (15.4), then the corresponding equation of the system (15.5) assumes the form

$$\begin{aligned} \left(\frac{3}{2} q_2 v_2^2 + q_2 c_{p_2} T_2 \right) \delta v_2 + \left(\frac{v_2^2}{2} + v_2 c_{p_2} T_2 \right) \delta q_2 + c_{p_2} q_2 v_2 \delta T_2 = \\ = \left(\frac{3}{2} q_1 v_1^2 + q_1 c_{p_1} T_1 + q_1 \eta_{cr} q_1 \right) \delta v_1 + \\ + \left(\frac{v_1^2}{2} + v_1 c_{p_1} T_1 + v_1 \eta_{cr} q_1 \right) \delta q_1 + \\ + c_{p_1} q_1 v_1 \delta T_1 + q_1 v_1 \eta_{cr} \delta q_1 + q_1 v_1 q_1 \delta \eta_{cr} + \end{aligned}$$

$$+ q_1(1-\eta_{cr}) \frac{1}{F} \frac{\partial}{\partial t} \int_V q dV - \frac{1}{F} \frac{\partial}{\partial t} \int_V q \left(\frac{v^2}{2} + c_p T + q \right) dV + \delta Q^*. \quad (15.6)$$

Using Relations (4.8), we reduce the system of equations (15.5) to a dimensionless form, and we set in the first equation $\delta M^* = 0$, while the last equation of this system is written in the form (15.6). Taking into account the fact that according to (4.9) we have $\bar{s} = \bar{p} - \bar{p}$ and that for the unperturbed flow the partial derivatives with respect to the time of the integrals in the right halves of (15.2) vanish, we obtain the following system*:

$$\left. \begin{aligned} \frac{1}{M_1} \bar{v}_2 + \bar{p}_2 - \bar{s}_2 &= \frac{1}{M_1} \bar{v}_1 + \bar{p}_1 - \bar{s}_1 + \bar{J}_1, \\ 2\bar{v}_2 + \left(M_2 + \frac{1}{M_1} \right) \bar{p}_2 - M_2 \bar{s}_2 &= \\ = \frac{1}{n} \left[2\bar{v}_1 + \left(M_1 + \frac{1}{M_1} \right) \bar{p}_1 - M_1 \bar{s}_1 + M_1 \bar{J}_1 + M_1 \bar{P}_x^* \right], \\ \left(3M_2 + \frac{2}{(n-1)M_1} \right) \bar{v}_2 + \left(M_2^2 + \frac{2n}{n-1} \right) \bar{p}_2 - M_2^2 \bar{s}_2 &= \\ = \frac{1}{n^2} \left[\left(3M_1 + \frac{2}{(n-1)M_1} + \frac{1}{M_1} Q_1 \right) \bar{v}_1 + \right. \\ \left. + \left(M_1^2 + \frac{2n}{n-1} + Q_1 \right) \bar{p}_1 - (M_1^2 + Q_1) \bar{s}_1 + \right. \\ \left. + Q_1 (\bar{\eta}_{cr} + \bar{q}_1) + 2M_1 \bar{J}_1 + 2M_1 \bar{Q}^* \right]. \end{aligned} \right\} \quad (15.7)$$

Here

$$\left. \begin{aligned} Q_1 &= \frac{2\eta_{cr} q_1}{a_1^2}, \quad \bar{\eta}_{cr} = \frac{\delta \eta_{cr}}{\eta_{cr}}, \quad \bar{q}_1 = \frac{\delta q_1}{q_1}, \\ \bar{P}_x^* &= \frac{\delta P_x^*}{c_1 v_1^2}, \quad \bar{Q}^* = \frac{\delta Q^*}{c_1 v_1^2}, \quad n = \frac{a_2}{a_1}, \\ \bar{J}_1 &= -\frac{1}{c_1 v_1^2} \frac{\partial}{\partial t} \int_V q dV, \\ \bar{J}_2 &= -\frac{1}{c_1 v_1^2} \frac{\partial}{\partial t} \int_V q v_2 dV, \\ \bar{J}_3 &= -\frac{1}{c_1 v_1^2} \left[\frac{\partial}{\partial t} \int_V q \left(\frac{v^2}{2} + c_p T + q \right) dV - \right. \\ &\quad \left. - q_1(1-\eta_{cr}) \frac{\partial}{\partial t} \int_V q dV \right]. \end{aligned} \right\} \quad (15.8)$$

In these formulas ρ_1 , v_1 , η_{sg} , and q_1 correspond to the unperturbed process; no additional subscripts are used to denote the parameters of the stationary flow.

The terms \bar{P}_x^* and \bar{Q}^* in the system (15.7) will as a rule be left out, since the former does not play a noticeable role in the vibration-

combustion process, while the latter (which corresponds to heat supply not connected with the crossing of the boundaries of the region V by the fuel) appears only in special cases (excitation of oscillations by means of heated grids, introduction of fuel directly into the combustion zone).

The quantity $Q_1 = 2\eta_{sg}q_1/a_1^2$ which enters into the third equation of the system (15.7) is not independent. It is determined completely by specifying the flow parameters to the left and to the right of σ . For steady-state flow we can write the third equation of the system (15.2) with $Q^* = 0$ in the form

$$Q_1 \frac{v_1^2}{2} + \frac{\kappa}{\kappa-1} p_1 v_1 + Q_1 v_1 (q_1 - q_2) = Q_2 \frac{v_2^2}{2} + \frac{\kappa}{\kappa-1} p_2 v_2.$$

After dividing both halves of the equation by $\rho_1 v_1^3/2$ and taking into account the fact that $p/\rho v^2 = 1/\kappa M^2$, we obtain immediately

$$Q_1 = \frac{2(q_1 - q_2)}{a_1^2} = n^2 \left(M_2^2 + \frac{2}{\kappa-1} \right) - \left(M_1^2 + \frac{2}{\kappa-1} \right). \quad (15.9)$$

The quantity $n = a_2/a_1$ can be determined (for $P_x^* = 0$ and $M^* = 0$) from the first equations of (15.2) for a steady-state stream:

$$n = \frac{\frac{1}{\kappa M_1} + M_1}{\frac{1}{\kappa M_2} + M_2}. \quad (15.10)$$

Thus, using Formulas (15.9) and (15.10), we can represent all the coefficients of the system (15.7) as functions of M_1 and M_2 , which are the Mach numbers of the stationary flow to the left and to the right of σ .

The system of equations (15.7), like the initial system (15.1), is valid not only for a combustion zone of short range, but for any portion of the flow, as large as desired. The assumption introduced above that the combustion zone is small in extent is essential because of the following considerations. As was already mentioned, in the un-

perturbed flow $\bar{J}_1 = \bar{J}_2 = \bar{J}_3 = 0$. In a perturbed flow these quantities are generally speaking different from zero and depend on the distribution of the perturbations of ρ , y , and T over the volume V under consideration. The perturbations of these parameters can be connected both with acoustic processes and with the combustion process. If the share of the former is negligibly small, then the quantities \bar{J}_1 , \bar{J}_2 , and \bar{J}_3 in Eqs. (15.7) depend only on the combustion process. This circumstance is exceedingly important, for only in the latter case can we carry out the hypothetical operation of "extracting" the zone σ from the tube L , an operation necessary in order to interrelate the flow parameters on the boundaries of σ . After all, this connection must be the same for all types of acoustic perturbations and for all frequencies, which are determined (depending on the properties of the portions L_1 and L_2) only after the properties of the zone σ have already been formulated.

Consequently, the short length of the zone σ must be understood as short compared with the wavelengths of the acoustic perturbations. The idealization measure adopted here ceases to be valid for very short waves corresponding to the higher harmonics. However, this circumstance does not limit essentially the applicability of the developed method, since the higher harmonics are usually not excited.

In those cases when the heat-supply zone in which considerable oscillations occur in the heat release is large compared with the wavelength of the perturbation, we can introduce several discontinuity surfaces Σ , corresponding to fractions of the zone σ and suitably spaced relative to one another. Such a measure is applicable in the case when the oscillations of the heat release occur not within one short zone, but in two or three zones, which are separated a considerable distance apart.

15. Properties of the Heat-Supply Plane Σ

It is obvious that the properties essential for the excitation of acoustic oscillations should be the same in the plane Σ and in the zone σ . These properties have been written out above in the form of the system (15.7), which relates the flow parameters \bar{v} , \bar{p} , and \bar{s} on the two sides of the strong-discontinuity surface Σ . Glancing at the system of equations (15.7) we can easily verify that the fictitious strong-discontinuity surface Σ , which was introduced in lieu of the zone σ , has special qualities.

A distinguishing feature of this discontinuity surface is that in all three equations describing its properties there are contained along with the variables \bar{p} , \bar{v} , and \bar{s} the quantities \bar{J}_1 , \bar{J}_2 and \bar{J}_3 , \bar{Q}_1 , $\bar{\eta}_{sg}$, and \bar{q}_1 . If we recall that the first equation of (15.7) expresses the law of mass conservation, the second the law of momentum conservation, and the third the law of energy conservation, we must assume that on the discontinuity surface Σ there are located sources of mass, momentum, and energy even when $M^* = P^*_x = Q^* = 0$.

Indeed, inasmuch as the zone σ is reduced to the plane Σ , the quantities \bar{J}_1 , \bar{J}_2 , and \bar{J}_3 can no longer be treated as derivatives of integrals over the volume V , since this volume is equal to zero; they must be regarded as intensities of sources situated on Σ .

This becomes most readily understandable if we turn to the initial system of equations, written in the form (15.2). We put

$$J_1 = -\frac{1}{\rho} \frac{\partial}{\partial t} \int \rho dV.$$

Then the continuity equation assumes the form

$$\rho_1 v_1 = \rho_1 v_1 + J_1.$$

If we recognize that in a flow scheme with a discontinuity surface Σ the quantities ρ_1 and v_1 pertain to the left side of the sur-

face while ρ_2 and v_2 pertain to the right side, then J_1 can be regarded only as the intensity of a mass source located on Σ . Perfectly analogous reasoning can be applied also to the other two equations.

Consequently, although there may actually be no sources of mass and momentum inside the combustion zone, they must be introduced for the fictitious discontinuity surface Σ , in order to retain the essential properties of this zone. The character of these fictitious sources J_1 , J_2 , and J_3 are determined uniquely by Formulas (15.8), i.e., by the real process inside the combustion-zone volume V .

Thus, a combustion zone of short length, with a process that is as complicated as desired occurring within it, can always be replaced by a stationary strong-discontinuity surface Σ provided that one locates on this surface fictitious sources of mass, momentum, and energy of the necessary intensity. It is easy to see that this will include all possible types of oscillations in the tube. Indeed, by specifying in arbitrary fashion the values of \bar{v} , \bar{p} , and \bar{s} on both sides of Σ we can, as can be seen from the system (15.7), relate them without violating the three principal conservation laws, by choosing the corresponding values of the dimensionless intensities of the mass, momentum, and energy sources.

The following remarks must be made. The components of all the sources are divided into fictitious ones and real ones. As already mentioned, a real mass source can be fuel introduced in the combustion zone into the air stream, and a real momentum source can be the resistance of the stabilizers, the prechambers, and other devices which can be located in the combustion zone. However, usually these components can be neglected. Therefore in many cases it is stated in this book that there are no real mass and momentum sources in the heat-supply zone.

With respect to the energy sources, this cannot be said, for the combustion zone yields a powerful real source of heat. Let us consider therefore the flux of thermal energy generated by sources located inside the region σ in greater detail. It can be broken up into a real component and a fictitious one. If we confine ourselves only to perturbations of the energy flux, then the real component should be $2M_1^2\bar{Q}^*$, which is the perturbation of the heat supply which is not connected with the crossing of the combustion-region boundaries by the fuel, the sum $Q_1[(1/M_1)\bar{v}_1 + \bar{p}_1 - \bar{s}_1]$, which is the heat-supply perturbation due to the change in the mass of the combustible mixture fed into the combustion zone through its boundaries, and $Q_1(\bar{\eta}_{sg} + \bar{q}_1)$, which is the heat-supply perturbation due to fluctuations in the completeness of combustion and the calorific value of the combustible mixture. All these components can be combined, writing

$$\bar{Q} = 2M_1^2\bar{Q}^* + Q_1\left(\frac{1}{M_1}\bar{v}_1 + \bar{p}_1 - \bar{s}_1\right) + Q_1(\bar{\eta}_{cr} + \bar{q}_1). \quad (16.1)$$

The term $2M_1^2\bar{J}_3$ in (15.7) yields a fictitious energy source (just like \bar{J}_1 and \bar{J}_2 are fictitious sources of mass and momentum), which is introduced only in order to retain the essential properties of the extended combustion zone after it is reduced to a discontinuity surface Σ . It must be kept in mind here that unlike \bar{Q} , the energy connected with the fictitious component \bar{J}_3 can have not only thermal form, but also mechanical or chemical, which follows, in particular, from the expression (15.8) for \bar{J}_3 .

Let us make one more almost self-evident remark. The concept "energy source" is given here a different meaning than in the preceding chapter, in which we investigated energy sources feeding a self-oscillating system. Here we are speaking of the supply of energy to the heat-supply zone independently of whether this energy is expended

on the excitation of acoustic oscillations, on heating, or in some other manner. In addition, as can be seen from the formulas for \bar{Q} and \bar{J}_3 , we are speaking only of the time-varying component of the energy source. The latter must always be kept in mind, inasmuch as a considerable time-invariant component of the heat supply exists in the combustion zone.

Thus, by replacing the real combustion zone σ with a strong-discontinuity surface Σ , we must assign the latter the same value of the dimensionless perturbation in the external heat supply \bar{Q} that characterizes the zone σ (\bar{P}_x^* is assumed negligibly small), and in addition it is necessary to assume that fictitious mass, momentum, and energy sources with dimensionless intensities \bar{J}_1 , \bar{J}_2 , and \bar{J}_3 are situated on the surface Σ .

The physical meaning of the quantities \bar{J}_1 , \bar{J}_2 , and \bar{J}_3 is sufficiently evident. Let us consider, for example, \bar{J}_1 . Inasmuch as the combustion zone actually has a definite length, and inasmuch as the position of the flame front in this zone can vary, the amounts of hot and cold gases in this zone will not be invariant. Consequently, the instantaneous values of the mass flows at the inlet to the combustion zone and at the outlet from it may not coincide, although when averaged over the cycle they do coincide in the case of steady-state oscillations. This is equivalent to the existence of fictitious mass sources on the plane Σ with oscillating flow, which is equal to zero when averaged (over the cycle). Perfectly analogous arguments can be advanced also for \bar{J}_2 and \bar{J}_3 . The values of the momentum and energy contained in the volume V can also fluctuate here, and when the volume V is reduced to the plane Σ this makes it necessary to assume the existence on Σ of fictitious sources of momentum and energy with zero average (over the cycle) flow.

The quantities \bar{Q} , P^*_x , J_1 , J_2 , J_3 which enter into the system of equations (15.7) and which characterize the process of nonstationary heat supply can be determined only after the pattern of the process inside the combustion zone is specified. This is usually the main difficulty and calls for the setting up of a whole series of precise experiments, for example, high-speed motion-picture photography of the combustion zone with simultaneous inertialess recording of the oscillations of the gas-flow parameters. Sometimes a particular theoretical scheme is assumed for the vibration-combustion process, and this scheme must be investigated; in this case the determination of all the necessary quantities by means of Formulas (15.8) is simpler.

Let us consider several very simple cases, which enable us to illustrate the use of the formulas derived in the preceding section, and in addition enable us to disclose some interesting properties of the heat-supply zone. We turn first to two limiting cases which enable us to pay attention to one circumstance of principal importance. We investigate, on the one hand, the supply of heat when the stream crosses a stationary plane normal to the flow axis, and on the other hand the supply of heat when an infinitesimally thin flame front, also normal to the flow axis but vibrating freely together with the stream, crosses the plane.

Heat supply at stationary plane. This case corresponds to the excitation of oscillations in a Rijke tube, inasmuch as in the idealized scheme we can represent the heated grid as a plane which is stationary relative to the tube walls, and which heats the air stream passing through it. For combustion chambers, this case corresponds to some degree to a dense arrangement of the igniting sources in one normal cross-section plane of the chamber, although here the degree of approximation of the real process by the idealized scheme is already smaller.

A distinguishing feature of the process considered here is that the volume of the combustion zone (or, in the more general case, the heat-supply zone) is equal to zero. At the same time, obviously, $\bar{J}_1 = \bar{J}_2 = \bar{J}_3 = 0$, and all that is located on the surface Σ which is introduced into the calculations is an energy source, which yields a perturbed component of the external heat supply \bar{Q} . In combustion, oscillations can be excited due to variation of the completeness of combustion η_{sg} and the calorific value of the mixture q_1 .* This case will be considered in greater detail in the next chapter.

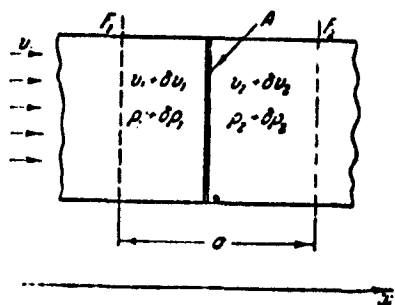


Fig. 23. Theoretical scheme for the zone σ .

For a Rijke tube, the energy equation will contain the quantity \bar{Q}^* , which depends on the heat transfer from the grid to the air.

Heat supply in planar flame front.

Let the flame front, as already indicated, be normal to the tube axis and not fixed relative to its walls. In the steady state the flame surface is stationary relative to the walls because the stream velocity of the mixture in the tube is numerically equal to the flame-propagation velocity. Let us assume that the combustible mixture is homogeneous and has the same composition everywhere, and that the combustion process occurs instantaneously in the infinitesimally thin flame front and always has the same completeness, for example $\eta_{sg} = 1$. It is obvious that in this case $\bar{\eta}_{sg} = \bar{q}_1 = 0$ and the excitation of the system will be connected with the quantities \bar{J}_1 , \bar{J}_2 , and \bar{J}_3 which generally speaking are different from zero because of the mobility of the flame front.

To calculate the quantities \bar{J}_1 , \bar{J}_2 , and \bar{J}_3 we turn to Fig. 23, which shows the combustion scheme for our case. The planar flame front

A oscillates between the stationary sections F_1 and F_2 , and the velocity, density, and other parameters in the front and rear of the combustion zone are equal, respectively, to $v_1 + \delta v_1$, $\rho_1 + \delta \rho_1$, etc.; $v_2 + \delta v_2$, $\rho_2 + \delta \rho_2$, etc. Therefore

$$J_1 = -\frac{1}{\rho_1 v_1} \frac{\partial}{\partial t} \left[\int_{V_k} (\rho_1 + \delta \rho_1) dV + \int_{V_g} (\rho_1 + \delta \rho_1) dV \right],$$

where V_{kh} is the instantaneous value of the "cold" volume of the combustion zone (from F_1 to A) and V_g is the instantaneous value of the "hot" volume of the combustion zone (from A to F_2).

Since we are considering small oscillations, the order of magnitude of σ is that of perturbations. The volumes V_{kh} and V_g connected with it will have the same order of magnitude. It is obvious that the terms $\delta \rho_1$ and $\delta \rho_2$ under the integral signs can be neglected. From geometrical considerations it is clear that the changes in V_{kh} and V_g are equal and of opposite sign:

$$\frac{\partial}{\partial t} \int_{V_k} dV = -\frac{\partial}{\partial t} \int_{V_g} dV.$$

Consequently,

$$J_1 = \frac{\rho_1 - \rho_2}{\rho_1 v_1} \frac{\partial}{\partial t} V_g(t). \quad (16.2)$$

The same arguments should be repeated verbatim for the calculation of J_2 and J_3 . By virtue of the fact that the continuity equation for a stationary flow of this type has the form $\rho_1 v_1 = \rho_2 v_2$, the value of J_2 turns out to be zero.

$$J_3 = \frac{\rho_1 - \rho_2}{\rho_1 v_1} \frac{\partial}{\partial t} V_g(t). \quad (16.3)$$

$$J_3 = \frac{\rho_1 \left(\frac{v_1^2}{2} + c_p T_1 + q_1 \right) - \rho_2 \left(\frac{v_2^2}{2} + c_p T_2 + q_2 \right) - \rho_1 (1 - \eta_{ad})(q_1 - q_2)}{\rho_1 v_1} \times \frac{\partial}{\partial t} V_g(t). \quad (16.4)$$

The quantity $(1/F)(\partial/\partial t)V_g(t)$ which is contained in all three re-

sultant equations is, as can be readily seen, the instantaneous velocity N of flame propagation relative to the tube walls. Inasmuch as the positive direction of the x axis coincides with the direction of the steady-state flow velocity, we can write

$$N = -\frac{1}{\rho} \frac{\partial}{\partial t} V_r(t). \quad (16.5)$$

Let us denote the flame propagation velocity relative to the gas particles by U . We note here that the introduced velocity U coincides numerically with the flame front propagation velocity U_{sgor} , which is customarily employed in combustion theory, but has the opposite sign. Indeed, at the direction used here for the x axis positive values of U correspond to motion to the right, toward the hot gases. Thus, the flame propagation velocity U_{sgor} , which is directed toward the cold gases, should correspond in the notation employed here to $U < 0$. We shall use henceforth almost everywhere the velocity U , but all the deductions can be readily formulated also for U_{sgor} .

We now write down the obvious kinematic relation

$$v + U = N. \quad (16.6)$$

Then $\delta v + \delta U = \delta N$, but since $N = 0$ in the steady state, δN will coincide with N . This enables us to rewrite (16.6) in the form

$$\delta v + \delta U = N. \quad (16.7)$$

Reducing the last relation to dimensionless form by dividing by the velocity of sound a_1 in the cold stream, we can write on the basis of Formulas (16.2)-(16.5) and (16.7) the following expression for J_1 , J_2 , and J_3 :

$$\left. \begin{aligned} J_1 &= A_1(\bar{v}_1 + \bar{U}_1), \\ J_2 &= 0, \\ J_3 &= A_3(\bar{v}_1 + \bar{U}_1). \end{aligned} \right\} \quad (16.8)$$

Here $\bar{U}_1 = \delta U/a_1$ is the dimensionless perturbation of the flame propagation velocity relative to the cold gas, while the numerical coeffi-

icients A_1 and A_3 are determined from the formulas

$$\left. \begin{aligned} A_1 &= \frac{1}{nM_0} - \frac{1}{M_1}, \\ A_3 &= \frac{nM_1}{M_1^2} \left(\frac{1}{2} + \frac{1}{n(n-1)M_1} \right) - \\ &\quad - \frac{1}{M_1} \left(\frac{1}{2} + \frac{1}{n(n-1)M_1} + \frac{q_1 - q_2}{M_1^2} \right). \end{aligned} \right\} \quad (16.9)$$

Let us compare now the two cases considered. It is easy to see that they differ in principle. In the first case the oscillations can be excited by the perturbations of the external heat supply \bar{Q} , while in the second case they are due to perturbation in the flame propagation velocity \bar{U}_1 . This raises the natural question whether any effect whereby the flame propagation velocity perturbation \bar{U}_1 can be reduced to an equivalent perturbation of the external heat supply \bar{Q} exists. This question can be answered only in the negative: while oscillating heat release occurring on a stationary heat-supply plane gives a non-zero component only in the third (energy) equation of the system (15.7), the mobility of the flame leads to the appearance of nonzero terms in the other equations also [in our case $\bar{J}_1 \neq 0$ and $\bar{J}_3 \neq 0$]. It is therefore impossible in principle to replace the effect of an oscillating flame by some equivalent oscillating heat released on a stationary heat-supply plane. We can advance here a simple argument to illustrate that attempts to find equivalent heat-release perturbations for an arbitrary process in the combustion zone are fruitless. Assume that we have specified the perturbations \bar{p} , \bar{v} , and \bar{s} on both sides of the combustion zone. In order to relate them without violating the three conservation laws, we need three free independent parameters, for example \bar{J}_1 , \bar{J}_2 , and $\bar{Q} + 2M_1^2 \bar{J}_3$. At the same time, such a connection can generally speaking not be established if only one parameter \bar{Q} is available. This question is almost self-evident and is emphasized here only because there are many known attempts to reduce all the nonstationary

combustion processes to a certain effective heat-release oscillation, something always involving the violation of the mass and momentum conservation laws.

Heat supply in flame front of arbitrary configuration. By way of a third case, we consider the supply of heat in a flame front A of ar-

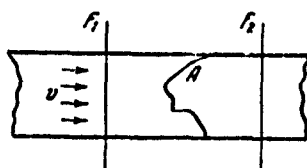


Fig. 24. Illustrating the determination of the effective flame propagation velocity for arbitrary flame-front configuration.

bitrary configuration, characterized by the fact that it is a continuous infinitesimally thin surface which separates the hot gas from the cold one in a homogeneous combustible mixture (Fig. 24). Let the flame front A execute oscillations between the sections F_1 and F_2 , continuously varying its configuration. If it is assumed that the existence of a curved

front A does not influence the flow ahead of it, that the completeness of combustion is always the same, and that the density, pressure, and velocity behind the front are always equal to the corresponding stream parameters at the section F_2 ,* then all the conclusions made in the foregoing item remain in force. The only difference is that the quantity $-(1/F)(\partial/\partial t)V_g(t)$ will no longer be the instantaneous flame propagation velocity relative to the tube walls. However, in analogy with the foregoing we can denote this expression by N_{eff} and call it the effective flame front velocity relative to the walls. Accordingly, the quantity \bar{U} can be replaced by $\bar{U}_{1\ eff} = \bar{N}_{eff} - \bar{v}_1$ (where $\bar{N}_{eff} = N_{eff}/a_1$) and called the effective flame propagation velocity relative to the cold gas. Once these concepts are introduced, the problem reduces immediately to Formulas (16.8) in which \bar{U}_1 is replaced by $\bar{U}_{1\ eff}$. All other properties of the case analyzed above, that of the oscillations of a planar flame front, are likewise retained. It is obvious that in the latter case $\bar{U}_{1\ eff} = \bar{U}_1$.

Let us present for the last two cases a system of equations analogous to the system (15.7). This can be done by substituting the obtained values \bar{J}_1 , \bar{J}_2 , and \bar{J}_3 (16.8) into (15.7). We shall proceed somewhat differently, however. If we use the values of \bar{J}_1 , \bar{J}_2 , and \bar{J}_3 , written in the form of Formulas (16.2), (16.3), and (16.4) and take into account the definition (16.5) and the kinematic condition (16.6), then, by using (15.8), we can readily determine the values of

$$\frac{1}{F} \frac{\partial}{\partial t} \int_V q dV, \quad \frac{1}{F} \frac{\partial}{\partial t} \int_V q v_x dV$$

and

$$\frac{1}{F} \frac{\partial}{\partial t} \int_V p \left(\frac{v^2}{2} + c_p T + q \right) dV.$$

Substituting them directly into the system of equations (15.2) we obtain the condition on Σ in the form

$$\left. \begin{aligned} q_1 U_1 &= q_2 U_2, \\ q_1 v_1 U_1 - p_1 &= q_2 v_2 U_2 - p_2, \\ q_1 U_1 \frac{v_1^2}{2} + p_1 \left(\frac{U_1^2}{x-1} - v_1 \right) - q_1 U_1 (q_2 - q_1) &= \\ &= q_2 U_2 \frac{v_2^2}{2} + p_2 \left(\frac{U_2^2}{x-1} - v_2 \right). \end{aligned} \right\} \quad (16.10)$$

In writing down this system, the effective flame propagation velocity U_{eff} is not designated by any particular index. This system of equations is obtained from the general equations (15.2). It is easy to see that it coincides with the ordinary conditions imposed in gasdynamics on the plane surfaces of strong discontinuities, and differs from them only in the term corresponding to the heat release.

Let us supplement this system with the kinematic condition

$$v_1 + U_1 = v_2 + U_2, \quad (16.11)$$

which shows that the left and right sides of the flame front move with equal velocity relative to the observer.

Let us linearize the equations (16.10) and (16.11), changing over

simultaneously to dimensionless variables. We take into account at the same time the fact that in a steady-state flow we have $v_1 + U_1 = v_2 + U_2 = 0$ and we assume that as a result of the homogeneity of the mixture and the constancy of the completeness of combustion the quantity $q_1 - q_2$ is constant. After several simple transformations, which are left out here, we obtain the following system of equations, describing the properties of the discontinuity plane Σ in terms of the dimensionless variation of the flame propagation velocity relative to the cold mixture:

$$\left. \begin{aligned} \frac{1}{M_1} \bar{v}_2 + \bar{p}_2 - \bar{s}_2 &= \frac{1}{n M_1} \bar{v}_1 + \bar{p}_1 - \bar{s}_1 + \left(\frac{1}{n M_1} - \frac{1}{M_1} \right) \bar{U}_1, \\ 2\bar{v}_1 + \left(M_1 + \frac{1}{M_1} \right) \bar{p}_1 - M_1 \bar{s}_1 &= \\ &= \frac{1}{n} \left[2\bar{v}_1 + \left(M_1 + \frac{1}{M_1} \right) \bar{p}_1 - M_1 \bar{s}_1 \right], \\ \left(3M_1 + \frac{2}{(n-1)M_1} \right) \bar{v}_2 + \left(M_1^2 + \frac{2n}{n-1} \right) \bar{p}_2 - M_1^2 \bar{s}_2 &= \\ &= \frac{1}{n^2} \left\{ \left[2M_1 + \frac{2}{n M_1} + n \left(M_2 + \frac{2}{n(n-1)M_2} \right) \right] \bar{v}_1 + \right. \\ &\quad + \left(M_1^2 + \frac{2n}{n-1} + 2 \frac{q_1 - q_2}{a_1^2} \right) \bar{p}_1 - \\ &\quad - \left(M_1^2 + 2 \frac{q_1 - q_2}{a_1^2} \right) \bar{s}_1 - \left[M_1 + \frac{2}{n(n-1)M_1} + \right. \\ &\quad \left. \left. + \frac{2}{M_1} \frac{q_1 - q_2}{a_1^2} - n \left(M_2 + \frac{2}{n(n-1)M_2} \right) \right] \bar{U}_1 \right\}. \end{aligned} \right\} \quad (16.12)$$

It is easy to see that if we put $\bar{U}_1 = -\bar{v}_1$, i.e., if we stop somehow the flame front, then the resultant system coincides, as expected, with the system (15.7) provided that we equate in the latter the quantities \bar{P}_x^* , \bar{Q}^* , \bar{J}_1 , \bar{J}_2 , \bar{J}_3 , and $\bar{\eta}_{sg} + \bar{q}_1$ to zero. The quantities $2(q_1 - q_2)/a_1^2$ and n which enter into the system (16.12) can be determined from Formulas (15.9) and (15.10).

The system (16.12) is convenient in those cases when we specify in the combustion zone not an oscillating heat supply, but the spatial oscillations of the flame front. Usually the latter are specified in terms of the oscillation of some effective flame propagation velocity.

We recall once more that when using the system (16.12) it is necessary to bear in mind that a positive value of \bar{U}_1 corresponds to a

reduction in the absolute value of the flame propagation velocity relative to the gas particles (the gas flows from left to right while the flame travels opposite to the flow). Taking into account the adopted rule for the signs, an intensification of the combustion process will correspond to negative \bar{U}_1 .

Idealized scheme of vibration combustion. At the start of the present section we have shown that in place of a complicated combustion process inside a zone σ it is possible to introduce into the theoretical scheme a certain heat-supply plane Σ , subject, however, to the condition that this plane contain certain sources of mass, momentum, and energy. Although such a representation of the vibration-combustion process cannot be subjected to essential objections, it lacks in clarity.

Let us consider the question of how it is possible to replace in rational manner the real combustion process inside σ by another simple and clear process in such a way that no properties of the real combustion process which are essential for the excitation of the acoustic oscillations are lost on going over to this new process. The examples given somewhat earlier make it possible to suggest as the effective idealized perturbed-combustion process one consisting of two essential processes, namely the perturbations of the heat supply and the perturbations of the position of the planar flame front. We have already stated earlier that these processes cannot be reduced to each other and therefore of the three independent quantities which we need to connect (without violating the three conservation equations) the perturbations \bar{p} , \bar{v} , and \bar{s} , which are arbitrarily specified on the left and on the right sides of σ , two are already available. As the third quantity we can take, for example, the variation of P^*_x , which is easiest to visualize as the variation of the hydraulic resistance of the combus-

tion chamber under fluctuations in the parameters of the cold stream incident on the chamber.

The first equation of the system (15.7) contains \bar{J}_1 as a parameter characterizing the perturbation of the combustion process, the second contains $M_1(\bar{J}_2 + \bar{P}_x^*)$, and the third contains $Q_1(\bar{\eta}_{sg} + \bar{q}_1) + 2M_1^2(\bar{J}_3 + \bar{Q}^*)$.

If we replace a certain real process, defined by means of these quantities, by a simple equivalent process of the type proposed here, it is necessary to stipulate that the corresponding terms in all three equations (15.7) be equal to the same terms in the analogous equations of the equivalent process. This leads to the following three equations [written down with allowance for Formulas (16.8)]:

$$\left. \begin{aligned} \bar{J}_1 &= A_1(\bar{v}_1 + \bar{U}_{1s}), \\ \bar{J}_2 + \bar{P}_x^* &= \bar{P}_{x0}^*, \\ Q_1(\bar{\eta}_{cr} + \bar{q}_1) + 2M_1^2(\bar{J}_3 + \bar{Q}^*) &= \\ &= 2M_1^2[A_2(\bar{v}_1 + \bar{U}_{1s}) + \bar{Q}_0^*]. \end{aligned} \right\} \quad (16.13)$$

The quantities \bar{Q}_0^* , \bar{U}_{1e} , and \bar{P}_{xe}^* are the equivalent perturbations of the heat supply, the rate of displacement of the planar flame front relative to the gas particles, and the hydraulic resistance of the combustion zone. They can be readily determined from Eq. (16.13)

$$\left. \begin{aligned} \bar{U}_{1s} &= \frac{\bar{J}_1}{A_1} - \bar{v}_1, \\ \bar{P}_{x0}^* &= \bar{P}_x^* + \bar{J}_2, \\ \bar{Q}_0^* &= \bar{Q}^* + \bar{J}_3 + \frac{Q_1}{2M_1^2}(\bar{\eta}_{cr} + \bar{q}_1) - \frac{A_2}{A_1} \bar{J}_1. \end{aligned} \right\} \quad (16.14)$$

Thus, no matter how complicated the real process inside σ may be, it can always be replaced by a certain equivalent process, which is made up of an effective perturbation in the heat supply \bar{Q}_0^* , a perturbation in the propagation velocity of a certain effective planar flame front \bar{U}_{1e} , and an effective perturbation of the hydraulic resistance of the combustion chamber \bar{P}_{xe}^* . Such a substitution is possible

only when all the refinements of the processes occurring inside σ are known, so that it is possible to calculate \bar{J}_1 , \bar{J}_2 , \bar{J}_3 , $\bar{\eta}_{sg}$, etc. It is sufficient to know (from experiment or in some other way) \bar{p} , \bar{v} , and \bar{s} , on both sides of σ , in order to obtain directly the equivalent process in the combustion zone. Indeed, using Eqs. (16.13) it is possible to exclude from (15.7) all the quantities that describe the actual course of the complicated combustion process inside σ and replace them by the corresponding quantities of the equivalent simple process. Then knowledge of \bar{p}_1 , \bar{v}_1 , \bar{s}_1 , \bar{p}_2 , \bar{v}_2 , and \bar{s}_2 immediately enables us to find \bar{U}_{1e} , \bar{P}^*_{xe} , and \bar{Q}^*_e from the transformed equations (15.7). Very frequently, particularly in theoretical research, one neglects the sum $\bar{P}^*_x + \bar{J}_2$ in the second equation of (15.7). Then, obviously, $\bar{P}^*_{xe} = 0$ and the process of nonstationary combustion is completely characterized by effective values of the perturbation of the heat supply and the rate of propagation of the planar flame front.

The possibility observed here of introducing into the theoretical scheme a simple equivalent process in lieu of the complicated process in the combustion zone σ enables us to confine ourselves in the exposition that follows to perturbations of the heat supply and to perturbations of the velocity of flame propagation. The reader can easily find out for himself when we refer in those cases to "effective" and not to real quantities. To simplify notation, we shall henceforth leave out the subscript "e" [э] of \bar{Q}^* , \bar{U}_1 , and \bar{P}^*_x from now on.

The system of equations (15.7) assumes in the case when one describes the vibration-combustion process with the aid of the quantities \bar{Q}^* , \bar{U}_1 , and \bar{P}^*_x the following form:

$$\left. \begin{aligned}
& \frac{1}{M_1} \bar{v}_1 + \bar{p}_1 + \bar{s}_1 + \left(A_1 + \frac{1}{M_1} \right) \bar{v}_1 + \bar{p}_1 + \bar{s}_1 + A_1 U_1, \\
& 2\bar{v}_2 + \left(M_2 + \frac{1}{M_2} \right) \bar{p}_2 + M_2 \bar{s}_2, \\
& = \frac{1}{\kappa} \left[2\bar{v}_1 + \left(M_1 + \frac{1}{M_1} \right) \bar{p}_1 - M_1 \bar{s}_1 + M_1 \bar{p}_2 \right], \\
& \left(3M_2 + \frac{2}{(\kappa-1)M_2} \right) \bar{v}_2 + \left(M_2^2 + 2\frac{\kappa}{\kappa-1} \right) \bar{p}_2 - M_2^2 \bar{s}_2 = \\
& = \frac{1}{\kappa^2} \left[\left(3M_1 + \frac{2}{(\kappa-1)M_1} + \frac{1}{M_1} Q_1 + 2M_1^2 A_2 \right) \bar{v}_1 + \right. \\
& \quad \left. + \left(M_1^2 + 2\frac{\kappa}{\kappa-1} + Q_1 \right) \bar{p}_1 - (M_1^2 + Q_1) \bar{s}_1 + \right. \\
& \quad \left. + 2M_1^2 (A_2 \bar{U}_1 + \bar{Q}^*) \right].
\end{aligned} \right\} \quad (16.15)$$

The quantities A_1 and A_3 are calculated here from Formulas (16.9). If air is admitted into the combustion zone, and not a previously prepared combustible mixture (i.e., if the mixture is prepared inside the zone σ , which is subsequently reduced to the plane Σ), then Q_1 vanishes, for in this case $q_1 = 0$.

In conclusion it is necessary to clarify one property which the effective hydraulic resistance \bar{P}_x^* must possess. Inasmuch as it is introduced in order to relate, without violating the momentum conservation law, the perturbations of the parameters of the flow to the left and to the right of σ which, generally speaking, are arbitrarily specified, the phase of \bar{P}_x^* may not coincide with the phase of the perturbation of the velocity head of the stream ahead of the zone σ . This should not worry the reader, for the actual hydraulic resistance of a real combustion chamber in the case of a nonstationary combustion process does not follow at all the variations of the velocity head of the incoming stream. The complicated character of the flow in the region of intense combustion, connected with the periodic vortex formation and with the fact that the devices contained in the combustion zone (stabilizers, etc.) have cold and hot jets of gas flowing around them either wholly or in part, prevent the resistance from following the velocity head of the incoming stream the way it customarily does in

the case of stationary flow.

§17. Reduction of Equations for the Discontinuity Plane Σ to Canonical Form

The system of equations (15.7) [or (16.15)] obtained above can be used directly to relate the perturbed flow parameters on both sides of the strong-discontinuity plane Σ . Of particular interest in this case is that formulation of these relations by which it would be convenient to analyze the influence of the combustion process on the excitation of the oscillations. More accurately speaking, it is desirable to recast (15.7) in a form such that, on the one hand, it becomes sufficiently simple, and on the other hand it represents most completely the physical aspect of the investigated processes. The point is that the very quantities J_1 , J_2 , J_3 , and \bar{Q} [and likewise \bar{Q}^* , \bar{U}_1 , and \bar{P}_x^* in Eqs. (16.15)] are not primary, and therefore the most rational way of writing down the system (15.7) or (16.15) is still not obvious.

It may be quite helpful in this case to apply the energy point of view to the excitation of the acoustic oscillations by the heat supply, a point of view developed in the preceding chapter. It was shown there that the elementary processes whereby an oscillating system is excited at the expense of one of two energy sources is connected with the non-vanishing of the differences $\delta p_1 - \delta p_2$ and $\delta v_1 - \delta v_2$. It therefore turned out to be advantageous to write down the connection between the perturbations of the flow parameters to the left and to the right of the heat-supply region with the aid of the system (11.11).

We shall call the notation (11.11) canonical and embark on a reduction of the relations for the discontinuity plane Σ to canonical form. We first reduce (11.11) to dimensionless form

$$n\bar{v}_1 - \bar{v}_1 = \delta E, \quad m\bar{p}_1 - \bar{p}_1 = \delta X, \quad g\bar{s}_1 - \bar{s}_1 = \delta S. \quad (17.1)$$

Here $n = a_2/a_1$, $m = \kappa_2 p_2 / \kappa_1 p_1$, $g = c_{p2}/c_{p1}$. In those cases when it is possible to disregard the change in the specific heat of the gas as

the latter is heated, we have $g = 1$ and $m = p_2/p_1$.

The system (15.7) reduces to canonical form by means of simple algebraic transformations. Putting $\bar{P}_x^* = 0$ we recast the left halves of the equations in the same form as the left halves of (17.1); in the right halves we obtain linear functions of the variables contained in the system (15.7). As a result we have

$$\left. \begin{aligned} n\bar{v}_2 - \bar{v}_1 &= a_{11}\bar{v}_1 + a_{12}\bar{p}_1 + a_{13}\bar{s}_1 + b_{11}\bar{J}_1 + b_{12}\bar{J}_2 + \\ &\quad + b_{13}(2M_1^2\bar{J}_3 + \bar{Q}), \\ m\bar{p}_2 - \bar{p}_1 &= a_{21}\bar{v}_1 + a_{22}\bar{p}_1 + a_{23}\bar{s}_1 + b_{21}\bar{J}_1 + b_{22}\bar{J}_2 + \\ &\quad + b_{23}(2M_1^2\bar{J}_3 + \bar{Q}), \\ g\bar{s}_2 - \bar{s}_1 &= a_{31}\bar{v}_1 + a_{32}\bar{p}_1 + a_{33}\bar{s}_1 + b_{31}\bar{J}_1 + b_{32}\bar{J}_2 + \\ &\quad + b_{33}(2M_1^2\bar{J}_3 + \bar{Q}). \end{aligned} \right\} \quad (17.2)$$

The values of the coefficients a_{ik} and b_{ik} are best determined numerically, during the process of reducing the system (15.7) to the form (17.2). Comparing (17.1) with (17.2) we readily obtain expressions for δE , δX , and δS . In this case we are immediately struck with the fact that the quantities δE , δX , and δS are made up of two groups of terms: one dependent on the perturbations \bar{v}_1 , \bar{p}_1 and \bar{s}_1 of the flow parameters ahead of the plane Σ (before the combustion zone), and another dependent on the perturbations of the combustion process itself (\bar{J}_1 , \bar{J}_2 , \bar{J}_3 , \bar{Q}).

It is therefore natural to write

$$\left. \begin{aligned} \delta E &= \delta E_0 + \delta E', \\ \delta X &= \delta X_0 + \delta X', \\ \delta S &= \delta S_0 + \delta S', \end{aligned} \right\} \quad (17.3)$$

where

$$\left. \begin{aligned} \delta E_0 &= a_{11}\bar{v}_1 + a_{12}\bar{p}_1 + a_{13}\bar{s}_1, \\ \delta E' &= b_{11}\bar{J}_1 + b_{12}\bar{J}_2 + b_{13}(2M_1^2\bar{J}_3 + \bar{Q}), \\ \delta X_0 &= a_{21}\bar{v}_1 + a_{22}\bar{p}_1 + a_{23}\bar{s}_1, \\ \delta X' &= b_{21}\bar{J}_1 + b_{22}\bar{J}_2 + b_{23}(2M_1^2\bar{J}_3 + \bar{Q}), \\ \delta S_0 &= a_{31}\bar{v}_1 + a_{32}\bar{p}_1 + a_{33}\bar{s}_1, \\ \delta S' &= b_{31}\bar{J}_1 + b_{32}\bar{J}_2 + b_{33}(2M_1^2\bar{J}_3 + \bar{Q}). \end{aligned} \right\} \quad (17.4)$$

The quantities $\delta E'$, $\delta X'$, and $\delta S'$ characterize nonstationary proc-

esses occurring in the combustion zone, and in this sense they can completely replace the quantities J_1 , J_2 , $2M_1^2 J_3 + \bar{Q}$. As regards the terms δE_0 , δX_0 , and δS_0 , they can be regarded as the coordinates of the origin of the reference frame for the quantities $\delta E'$, $\delta X'$, and $\delta S'$.

When the conditions on the surface Σ are written in this manner, the following misunderstanding can arise. In the canonical notation (17.1) the right halves (the quantities δE , δX , and δS) depend not only on the processes that occur in the combustion zone ($\delta E'$, $\delta X'$, and $\delta S'$), but also on the character of the oscillations in the nearest vicinity of the combustion zone (δE_0 , δX_0 , and δS_0). At the same time, it was shown in the preceding chapter that the quantities δE , δX , and δS determine the stability of the process. It turns out that the excitation of acoustic oscillations is connected not only with processes occurring inside the heat-supply zone.

The point is that the same processes in the combustion zone actually yield different effects, being under different conditions in the sense of the character of the oscillations of the surrounding medium. For example, as was already shown earlier, periodic heat release in stationary gas produces oscillations that are the larger, the closer the heat-supply plane is to the pressure antinode; when located in a section containing a pressure node, the heat-supply surface will not excite the system at all (for simplicity we do not stipulate here the excitation phase conditions).

Consequently, the notation adopted here takes into account both factors, the processes in the heat-supply zone as well as the character of the oscillations in its vicinity.

It is necessary, of course, to distinguish which factor contributes to the development of the oscillations in each given specific case, and to what extent — whether these are the processes in the com-

bustion zone or the singularity in the position of this zone relative to the standing waves produced in the system.

The writing down of the conditions on Σ in the form of the canonical relations (11.11) or (17.1) is attractive because of its simplicity. Its advantage is also the fact that it is directly related with the energy nature of the processes that occur during the excitation of acoustic oscillations. This form of notation, however, is of course not the only sensible one. There is no doubt that cases can be encountered in which the perturbations of the parameters behind the heat-supply zone, namely \bar{v}_2 , \bar{p}_2 , and \bar{s}_2 , turn out to be preferably expressed directly in terms of \bar{v}_1 , \bar{p}_1 , and \bar{s}_1 as well as the characteristics of the combustion zone. A system of this type is readily obtained from (17.2). Using the notation of (17.4), it can be readily written in the form

$$\left. \begin{aligned} \bar{v}_2 &= \frac{1}{n} [(1 + a_{11}) \bar{v}_1 + a_{12} \bar{p}_1 + a_{13} \bar{s}_1 + \delta h''], \\ \bar{p}_2 &= \frac{1}{m} [a_{21} \bar{v}_1 + (1 + a_{22}) \bar{p}_1 + a_{23} \bar{s}_1 + \delta X'], \\ \bar{s}_2 &= \frac{1}{l} [a_{31} \bar{v}_1 + a_{32} \bar{p}_1 + (1 + a_{33}) \bar{s}_1 + \delta S']. \end{aligned} \right\} \quad (17.5)$$

§18. Sources of Self-Oscillation Energy for Arbitrarily Complicated Processes in the Heat-Supply Zone

It was shown in §11 that when the flow inside the heat-supply zone has a one-dimensional character, there exist two sources of energy capable of maintaining the acoustic oscillations, external heat supply and the flux of internal energy (thermal terms), on the one hand, and the flux of kinetic energy on the other.

Inasmuch as in a real combustion zone the process is not one-dimensional, it remains unclear to what extent this deduction is valid also for the more general case of an arbitrarily complicated process in the heat-supply zone. Consequently, before we proceed further, we must determine more accurately the extent to which it is valid to re-

that the conditions on Σ to the form (17.1) for an arbitrary process in the heat-supply zone.

In the observed general case, any process in the combustion zone can be reduced, as was already shown above, to a process whereby energy, momentum, and mass are supplied to the stream at the plane Σ . In order to be able to look, as it were, at the processes occurring "inside" Σ , we shall consider in the present section not the plane Σ , but an arbitrarily small (but finite) region σ , along which the mass, momentum, and energy sources will be located. The flow inside σ will be assumed one-dimensional, and because of the smallness of σ we shall assume the steady-state hypothesis to be satisfied. This measure enables us to make the analysis of the stream crossing the plane Σ similar to the analysis already given in §11. The essential difference between these two cases will be the presence of mass and momentum sources inside σ .

Let us write, as before, the energy conservation law for an element of the stream in a reference frame moving together with the stream, and separately for the center of gravity of this element.

In the reference frame that moves together with the fluid element inside the region σ we can write the following obvious equation:

$$dMc_p T + p dV = dQ^* + dE'. \quad (18.1)$$

Here M is the mass of the element, V its volume, Q^* the amount of heat supplied, and E' [E'] is the energy introduced by the mass source.

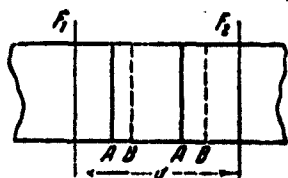


Fig. 25. Displacement of stream element inside the zone σ .

Unlike the ordinary thermodynamic relations, the differentiation symbol in (18.1) applies to the mass of the element (since it is variable), and account is taken of the energy supplied not only from the heat source, but also introduced by the mass source.

The quantities under the differentiation sign in the left half of (18.1) can be determined in the following manner.

Let the liquid element change within a short time Δt from the position AA to the position BB (Fig. 25). Then the change in the internal energy of the element $dMc_v T$ can be expressed by the formula

$$dMc_v T = F \Delta t (qv dc_v T + c_v T dqv). \quad (18.2)$$

The change in the volume will be

$$dV = F \Delta t dv.$$

Substituting these expressions into (18.1) we obtain immediately the following relation:

$$dqvc_v T + p dv = dQ + d\mathcal{E}', \quad (18.3)$$

where Q and \mathcal{E}' [\mathcal{E}'] are the intensities of the sources of thermal energy and of the energy introduced by the mass

$$dQ = \frac{dQ^*}{F \Delta t}; \quad d\mathcal{E}' = \frac{d\mathcal{E}'}{F \Delta t}.$$

Physically these two quantities represent the amount of energy introduced per unit cross section area and per unit time.

Let us consider now the displacement of the center of gravity of the isolated element of fluid. On the basis of the momentum equation we write

$$dI = -F \Delta t dp + dH, \quad (18.4)$$

where I [\mathcal{I}] is the momentum supplied to the fluid element from the corresponding source (including the mass source).

Using the same procedures as in the derivation of (18.3), we can write

$$qv dv + v dqv = -dp + d\mathcal{H}.$$

where

$$d\mathcal{H} = \frac{dH}{F \Delta t}.$$

Multiplying the left and right halves of this equation by y we

obtain after some simple transformations

$$dqv \frac{v^2}{2} + v dp = v d\mathcal{H} - \frac{v^2}{2} dqv.$$

The terms in the right half have the following meaning: the first term represents the summary intensity of the energy source, connected with the direct supply of momentum and the supply of momentum by the mass, while the second indicates what part of this energy has been consumed in imparting the necessary kinetic energy to the mass introduced into the corresponding fluid element in order for the introduced mass to move with the same velocity as the element. It is obvious that the difference between these two quantities gives the effective intensity of the energy source connected with the direct momentum supply. Denoting this difference by de'' [$d\varepsilon''$], we finally obtain the sought-for relation in the form

$$dqv \frac{v^2}{2} + v dp = d\varepsilon''. \quad (18.5)$$

Integration of (18.3) and (18.5) yields

$$\left. \begin{aligned} (qvc, T)_2 - (qvc, T)_1 + \int_1^2 p dv &= Q + \varepsilon', \\ \left(qv \frac{v^2}{2} \right)_2 - \left(qv \frac{v^2}{2} \right)_1 + \int_1^2 v dp &= \varepsilon''. \end{aligned} \right\} \quad (18.6)$$

Comparing the results obtained with (11.12) and (11.13) we see immediately that they are quite similar. Repeating verbatim all the arguments given in §11, we can readily verify the correctness of the conclusion that there exist two independent (thermal and mechanical) energy sources, which maintain the acoustic oscillations. All the subsequent considerations of the elementary processes in the heat supply etc. remain likewise valid.

In deriving formulas of the type (11.17), (11.18), and (11.19) from (18.6), it must be remembered that the formally introduced mass and momentum sources are fictitious. The flow from these fictitious

sources, averaged over the cycle, is equal to zero in the case of steady-state oscillations, as was already indicated above, so that, of course, these sources cannot supply energy from the outside. This is expressed analytically by the conditions:

$$\int_0^T j' dt = 0, \quad \int_0^T j'' dt = 0.$$

§19. Excitation of Oscillating System in the General Case

In the preceding chapter we have considered the excitation of an oscillating system during the course of realization of elementary processes inside the heat-supply zone.

In the present section we consider a method of constructing the stability limits, similar to those constructed in §12, but now for a process in the heat-supply zone which is no longer elementary. First, however, we derive some consequences from the expressions obtained in the present chapter.

It is first necessary to verify that the previously introduced elementary processes in the heat supply zone can actually be realized, so that the arguments advanced before cannot be regarded as abstract theoretical schemes.

As follows from Formulas (17.3) and (17.4), the conditions $\delta E = 0$ and $\delta X = 0$ can actually be realized. Let, for example, there be specified the perturbations \bar{v}_1 , \bar{p}_1 , and \bar{s}_1 of the variables ahead of the heat-supply zone. These three quantities determine δX_0 , and in order for δX to vanish it is necessary to satisfy the condition $\delta X' = -\delta X_0$. Thus, the first elementary process will be realized in the heat-supply zone if $\delta X'$ has a fully defined modulus and argument. This can be realized in a variety of ways, for in order to obtain the necessary value of $\delta X'$ it is possible to make use of the four independent parameters J_1 , J_2 , J_3 , and Q . If we consider, for the sake of being definite, the

simplest case of the excitation of acoustic oscillations in a Rijke tube, then in place of the four free parameters only one remains, namely \bar{Q}^* , the dimensionless perturbation of the external heat supply. Equations (16.1) and (17.4) show that the first elementary process will be realized in the Rijke tube when

$$\bar{Q}^* = -\frac{\delta X_0}{2M_1^2 \bar{E}_0},$$

which is a perfectly defined oscillating component of the heat supply. A precisely similar argument can be advanced also to justify the reality of the second elementary process ($\delta E = 0$).

The second circumstance that must be noted is that in a moving medium the phases of δE and of the oscillating component of the heat supply \bar{Q} do not coincide. Indeed, if we consider for example the simplest case of oscillations in a Rijke tube, we can write on the basis of Formulas (16.1), (17.3), and (17.4)

$$\delta E = \delta E_0 + 2b_{12} M_1^2 \bar{Q}^*.$$

Inasmuch as the phase of δE_0 does not generally speaking coincide with the phase of \bar{Q}^* , the foregoing statement is proved. This circumstance enabled us to consider the excitation conditions obtained in §12 for the first elementary process as a generalization of the Rayleigh criterion (the latter is valid only if the phases of δE and \bar{Q}^* are the same).

Let us consider now certain properties which can be possessed by processes in the heat-supply zone and which make it possible to obtain in many cases quite illustrative diagrams of the stability regions.

As was already indicated above, the stability limit is determined by the equation (11.9) $A_2 = R$. In the general case, introducing the dimensionless flux of acoustic energy by means of the formulas

$$\bar{\lambda} = \frac{A}{\pi a_1^2 \rho_1}; \quad \bar{R} = \frac{R}{\pi a_1^2 \rho_1}, \quad (19.1)$$

we obtain from (13.2)

$$\bar{A}_2 = \frac{1}{2} (\bar{p}_1 \delta E + \bar{r}_1 \delta X + \delta E \delta X). \quad (19.2)$$

The condition for the existence of a stability limit is written in the form

$$\bar{A}_2 = \bar{R}. \quad (19.3)$$

Equations (19.2) and (19.3) show that for specified \vec{p}_1 and \vec{v}_1 there exists a complicated aggregate of values of $\delta \vec{E}$ and $\delta \vec{X}$ satisfying the condition that defines the stability limit. It is difficult to present this aggregate in clear form, since the connection between the sought-for quantity and the two vectors reduces, as is well known, to a connection between this quantity and four scalar variables. In addition, one must not forget that the quantities \vec{p}_1 and \vec{v}_1 can themselves vary (when the discontinuity surface Σ moves along the standing wave produced in the system).

The analysis of the excitation conditions is usually greatly simplified in those cases when the quantities δE and δX turn out to be functions of one and the same complex variable if we disregard their dependence on \vec{v}_1 , \vec{p}_1 , and \vec{s}_1 . Let us cite a few examples of such processes in the heat-supply zone.

By way of the first example let us consider all the cases when the process in the heat-supply zone can be represented as a heat-supply process in a certain region that is stationary with respect to the tube walls and has a negligibly small extent in the direction of the tube axis (Rijke tube, etc.). The small extent of the heat-supply region, if this region is stationary, leads to $J_1 = J_2 = J_3 = 0$ and consequently, as shown by Formulas (16.1) and (17.4),

$$\left. \begin{aligned} \delta E' &= 2b_{12} M_1' \bar{Q}^* \\ \delta X' &= 2b_{13} M_1' \bar{Q}^* \end{aligned} \right\} \quad (19.4)$$

In the case of combustion $2M_1^2\bar{Q}^*$ may be replaced by the quantity \bar{Q} .

Another example will be the case of constant heat supply on a stationary flame surface. As can be seen from Formulas (16.2), (16.3), and (16.4), \bar{J}_1 , \bar{J}_2 , and \bar{J}_3 will be functions of the quantity $-(1/F)(\partial/\partial t)V_g(t)$, which can be represented as a sum of \bar{v}_1 with \bar{U}_1 or $\bar{U}_1 \text{ eff}$. Thus, the quantities $\delta E'$ and $\delta X'$ turn out to be functions of \bar{v}_1 and of the perturbation of the effective flame front propagation velocity relative to the cold mixture:

$$\left. \begin{aligned} \delta E' &= a_E \bar{v}_1 + b_E \bar{U}_1 \text{ eff} \\ \delta X' &= a_X \bar{v}_1 + b_X \bar{U}_1 \text{ eff} \end{aligned} \right\} \quad (19.5)$$

where a_E , a_X , b_E , b_X are certain numerical coefficients.

The quantity \bar{v}_1 , which is contained in Formulas (19.5), does not prevent us from regarding $\delta E'$ and $\delta X'$ as functions of the single variable $\bar{U}_1 \text{ eff}$. The point is that \bar{v}_1 (like p_1) is usually specified, and furthermore v_1 is contained in Formula (19.2) directly and enters also in the terms δX_0 and δE_0 . Thus, the free parameters which can be varied arbitrarily and whose influence on the stability it is advisable to study are the complex variable $\bar{U}_1 \text{ eff}$.

By way of a third example let us consider a process in which \bar{J}_1 , \bar{J}_2 , and \bar{J}_3 , as well as $\bar{\eta}_{sg}$ and \bar{q}_1 are different from zero. Let, for example, a mixture with variable excess-air coefficient α enter into the combustion zone. Such a mixture will be characterized by a value of \bar{q}_1 different from zero. If we assume that the completeness of the combustion η_{sg} is determined uniquely by α , \bar{v}_1 , and \bar{p}_1 , and that the position of the flame front, and consequently also \bar{J}_1 , \bar{J}_2 , and \bar{J}_3 are also functions of α , \bar{v}_1 , and \bar{p}_1 , then the quantities δE and δX will depend only on α , in the sense referred to above with respect to the dependence of δE and δX only on $\bar{U}_1 \text{ eff}$.

The number of such examples can be increased. For all the cases

cited, the analysis of the excitation conditions becomes simpler because the dependence of \bar{A}_2 on one complex parameter can be well represented on a plane. This makes it possible to construct illustrative diagrams of the stability limits. In order not to be tied down to any single concrete example, we shall consider the problem in a more general formulation — we shall assume that the quantities δE and δX depend on a certain complex parameter \bar{Y} (the dimensionless perturbation of some essential quantity Y), and also on \bar{p}_1 and \bar{v}_1 . Formulas (17.4) show that it is possible to expect the quantities δE and δX to depend also on \bar{s}_1 , but usually the flow in the cold part of the tube, prior to the crossing of the heat-supply zone by the air stream, is isentropic and therefore $\bar{s}_1 = 0$.

Consequently, in the case under consideration the first two equations of (17.5) can be written in the form

$$\left. \begin{aligned} \bar{v}_2 &= a_{11}\bar{v}_1 + a_{12}\bar{p}_1 + a_{13}\bar{Y}, \\ \bar{p}_2 &= a_{21}\bar{v}_1 + a_{22}\bar{p}_1 + a_{23}\bar{Y}. \end{aligned} \right\} \quad (19.6)$$

where a_{ik} are certain numerical coefficients [different from the coefficients of Eqs. (17.5), which are designated in the same manner].

The calculation of \bar{A}_2 by Formula (19.2) is meaningless in this case, since Relations (19.6) do not contain δE and δX , expressed directly in terms of \bar{Y} . We therefore use Formula (13.1) which assumes on changing to dimensionless variables the form

$$\bar{A}_2 = \frac{1}{2} (nm\bar{p}_2\bar{v}_2 - \bar{p}_1\bar{v}_1). \quad (19.7)$$

Here, as before, $n = a_2/a_1$, $m = \kappa_2 p_2 / \kappa_1 p_1$.

Regarding the variables \bar{v} , \bar{p} , and \bar{Y} which enter into (19.6) as vector quantities, we take the scalar products of these equations with each other:

$$\bar{p}_1\bar{v}_2 = a_{11}a_{21}\bar{v}_1^2 + a_{11}a_{22}\bar{p}_1^2 + a_{11}a_{23}\bar{Y}^2 +$$

$$+ (a_{11}a_{22} + a_{12}a_{21}) \vec{p}_1 \vec{v}_1 + \\ + (a_{11}a_{22} + a_{12}a_{21}) \vec{v}_1 \vec{p}_1 + (a_{11}a_{22} + a_{12}a_{21}) \vec{p}_1 \vec{p}_1.$$

Using (19.7) and the last equation we obtain from Eq. (19.3) the following relation, which is equivalent to the stability condition,

$$A \vec{Y}^2 + B \vec{p}_1 \vec{Y} + C \vec{v}_1 \vec{Y} + D \vec{p}_1^2 + E \vec{v}_1^2 + F \vec{p}_1 \vec{v}_1 - R = 0, \quad (19.8)$$

where A, B, C, D, E, and F are numerical coefficients,

$$A = \frac{1}{2} nm a_{12} a_{22}, \quad D = \frac{1}{2} nm a_{12} a_{22}, \\ B = \frac{1}{2} nm (a_{12} a_{22} + a_{13} a_{22}), \quad E = \frac{1}{2} nm a_{11} a_{21}, \\ C = \frac{1}{2} nm (a_{11} a_{23} + a_{13} a_{21}), \quad F = \frac{1}{2} [nm (a_{11} a_{22} + a_{12} a_{21}) - 1].$$

Let us use Condition (19.8) to construct the stability-limit diagram. We begin the construction with the simplest case, characterized by the absence of acoustic-energy losses.

Assume that to the left and to the right of the heat-supply zone the acoustic-energy losses are equal to zero (for example, velocity or pressure nodes are located to the left and to the right of the indicated zone). Then, as was shown in §11 in the discussion of Formula (11.7), the vectors \vec{p} and \vec{v} should be orthogonal and therefore $\vec{p}_1 \vec{v}_1 = \vec{p}_2 \vec{v}_2 = 0$. We therefore obtain in lieu of (19.8)

$$A \vec{Y}^2 + B \vec{p}_1 \vec{Y} + C \vec{v}_1 \vec{Y} + D \vec{p}_1^2 + E \vec{v}_1^2 = 0. \quad (19.9)$$

We shall plot the stability limit in a rectangular coordinate system (x, y). Let the vectors \vec{p}_1 , \vec{v}_1 , and \vec{Y} both start at the origin and both rotate about the origin with frequency ω (see §2). We choose an instant of time such that the vector \vec{p}_1 is directed along the x axis, while the y axis is directed along the vector \vec{v}_1 . The vector \vec{Y} has a certain arbitrary position relative to the coordinate frame. The stability limit in the (x, y) plane will be defined as the geometric locus of the ends of the vectors \vec{Y} satisfying (19.9). We introduce a notation for the vectors \vec{p}_1 , \vec{v}_1 , and \vec{Y} in terms of their x and y projections. They will be expressed in the following manner: $(\vec{p}_1, 0)$; $(0, \vec{v}_1)$;

(\bar{Y}_x, \bar{Y}_y) . We now write down the sum of the scalar products (19.9) in terms of the projections of the factors:

$$A(\bar{Y}_x^2 + \bar{Y}_y^2) + B\bar{p}_1\bar{Y}_x + C\bar{v}_1\bar{Y}_y + D\bar{p}_1^2 + E\bar{v}_1^2 = 0. \quad (19.10)$$

It is easy to see that when \bar{p}_1 and \bar{v}_1 are specified, Eq. (19.10) indicates that the end of the vector \vec{Y} moves along a circle, the position and radius of which depend on \bar{p}_1 and \bar{v}_1 . Consequently, the set of vectors \vec{Y} which excite the oscillations is segregated from all the remaining vectors on the (x, y) plane by a hodograph that has a circular form. Inasmuch as the dimensions and the position of this circle change with variation of \bar{p}_1 and \bar{v}_1 , different positions of the heat-supply plane Σ along the length of the tube — closer to or farther away from the pressure node — or different oscillation frequencies, i.e., different \bar{p}_1 and \bar{v}_1 , may correspond to different stability limits. Thus, the conditions for the excitation of the system may change as the position of Σ or the oscillation frequency change. Figure 26 shows the stability limit for certain specified values of \bar{p}_1 and \bar{v}_1 .

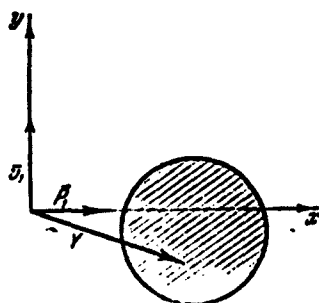


Fig. 26. Stability diagram for specified \bar{p}_1 and \bar{v}_1 .

On the basis of the foregoing arguments we can state only that when the end of the vector \vec{Y} lies on the drawn circle the oscillations will be neutral. The question of which side of the circle is the stability limit and which the instability limit calls for an additional investigation. In the majority of practical cases there is no need to

carry out such an investigation, for an answer is usually clear from the physical nature of the problem.

However, an analysis of this problem does not entail great difficulties even in those cases when the physical considerations do not yield immediately an obvious solution.

We can follow, for example, the following qualitative reasoning. Let the quantity \vec{Y} be such that the process is neutral. We maintain \vec{p}_1 and \vec{v}_1 constant and change \vec{Y} somewhat (in such a way that the end of this vector moves away from the stability limit). Then Eq. (19.10) is violated and, on the basis of the arguments presented in the derivation of (19.8), we can write

$$A(Y_x^2 + Y_y^2) + B\vec{p}_1\vec{Y}_x + C\vec{v}_1\vec{Y}_y + D\vec{p}_1^2 + E\vec{v}_1^2 = \bar{A}_\Sigma.$$

In the absence of losses in the system, the stability limit corresponds to $\bar{A}_\Sigma = 0$, when $\bar{A}_\Sigma > 0$ we have instability, and $\bar{A}_\Sigma < 0$ yields stability of the process. At the origin we have $\vec{Y}_x = \vec{Y}_y = 0$ and $\bar{A}_\Sigma = D\vec{p}_1^2 + E\vec{v}_1^2$. Consequently, if

$$D\vec{p}_1^2 + E\vec{v}_1^2 < 0, \quad (19.11)$$

then the process is stable in the vicinity of the origin, meaning that it is unstable inside the circle.

Let us agree to cross-hatch the instability region. Then, if Inequality (19.11) is satisfied, the inside of the circle on Fig. 26 will be cross-hatched. This is precisely the pattern observed, for example, in those cases when the acoustic oscillations are excited by heat supply concentrated in one plane which is stationary with respect to the tube walls (Rijke tube, etc.).

The reason why the qualitative arguments presented here are not rigorous is that when $\bar{A}_\Sigma \neq 0$ the oscillations cease to be harmonic, the formulas given above for the fluxes of the acoustic energy become incorrect, and the angle between the vectors \vec{p}_1 and \vec{v}_1 begins to differ from $\pi/2$.

If we strive for a more exact analysis, the simplest procedure is to actually calculate the damping decrement of the oscillations for some point of the diagram, say the origin. The suitable methods will be developed in the following chapters.

Comparing the result obtained here and shown in Fig. 26 with the excitation conditions in the two elementary processes, considered in the preceding chapter, we readily note that the excitation conditions have become more complicated. This complication is manifest in the fact that, first, the phase relations between \vec{Y} and \vec{p}_1 or \vec{v}_1 cannot be formulated as simply as for the elementary processes; second, in addition to the phase relations, it becomes necessary to take into account also the amplitude relations, i.e., the magnitude of $|\vec{Y}|$; thirdly, the excitation conditions depend on the position of the discontinuity plane Σ along the length of the tube (on \vec{p}_1 and \vec{v}_1). It must be noted that such a complication of the excitation conditions is not connected with the transition to the parameter \vec{Y} in place of δX and δE . An analysis of the stability limits for specified \vec{p}_1 , \vec{v}_1 , $\delta \vec{X} \neq 0$ and variable $\delta \vec{E}$ (or for specified $\delta \vec{E} \neq 0$ and variable $\delta \vec{X}$) shows that in such an approach the phase relations become more complicated, the absolute value of the variable parameter ($\delta \vec{E}$ or $\delta \vec{X}$) begins to assume an important role, and the excitation conditions become functions of the position of the plane Σ along the length of the tube (functions of \vec{p}_1 and \vec{v}_1). Thus, unlike the elementary processes (when δE or δX are equal to zero), all the remaining processes yield, by virtue of their physical nature, complicated excitation conditions. The reason lies in the fact that in those cases the energy is drawn from two sources simultaneously, which leads to a complicated interaction pattern between them. This problem will be discussed in somewhat greater detail below.

The stability limit shown in Fig. 26 was obtained under the assumption that the values of \vec{p}_1 and \vec{v}_1 are specified. However, it was emphasized already many times here that the values of \vec{p}_1 and \vec{v}_1 can change, depending on the position of the heat-supply zone along the length of the tube (more accurately, depending on its position relative

to the perturbation standing wave), and consequently the circle on Fig. 26 will shift and change in size. Therefore it is natural to raise the question of finding a family of such circles, corresponding to all the values of \bar{p}_1 and \bar{v}_1 conceivable for the given tube.

We are dealing here, of course, not only with the absolute values of \bar{p}_1 and \bar{v}_1 , but with their ratio. As already mentioned, the method employed gives all the quantities accurate to a scale factor.

The solution of the oscillation problem in the variables \bar{u} , \bar{w} shows that in the case of neutral oscillations both these quantities remain constant in absolute magnitude for all cross sections of the tube, provided there are no discontinuity surfaces between these sections. This condition is satisfied, in particular, in the section of the tube through which the cold gas flows. We can therefore write that on this section

$$|\bar{u}_1| = \text{const.}, \quad |\bar{w}_1| = \text{const.}$$

or

$$\bar{u}_1^2 = \text{const.}, \quad \bar{w}_1^2 = \text{const.}$$

Relations (4.9), which relate the variables \bar{u} , \bar{w} with p , \bar{v} , make it possible to write on this basis

$$\begin{aligned} \bar{v}_1^2 + 2\bar{v}_1\bar{p}_1 + \bar{p}_1^2 &= \text{const.}, \\ \bar{v}_1^2 - 2\bar{v}_1\bar{p}_1 + \bar{p}_1^2 &= \text{const.} \end{aligned}$$

From this we get the connection between \bar{p} and \bar{v} in the case of neutral oscillations

$$\bar{v}_1^2 + \bar{p}_1^2 = \text{const.}$$

Writing down the scalar squares in terms of the vector projections, we obtain

$$\bar{v}_1^2 + \bar{p}_1^2 = \text{const.} \quad (19.12)$$

Equation (19.10) indicates that the position of the center of the circle shown in Fig. 26 is determined by the coordinates

$$\left. \begin{aligned} x_0 &= -\frac{1}{2} \frac{B}{A} \bar{p}_1 \\ y_0 &= -\frac{1}{2} \frac{C}{A} \bar{v}_1 \end{aligned} \right\} \quad (19.13)$$

Comparing (19.12) with (19.13) we can see that the centers of the circles (x_0, y_0) will move along an elliptical arc. We need merely add that the centers (x_0, y_0) will lie not along the entire ellipse, but only on one of its quadrants. Indeed, in the chosen coordinate system \bar{p}_1 and \bar{v}_1 are always positive. The position of the sought quadrant of the ellipse depends on the signs of the numerical coefficients B/A and C/A . Calculations show, for example, that for the excitation of oscillations by means of an alternating heat supply ($\bar{Y} = \bar{Q}$) this will always be the fourth quadrant.

The analysis performed enables us to state that the family of all the stability boundaries is made up of a set of circles, whose centers

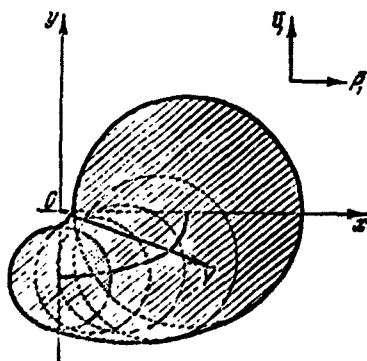


Fig. 27. Stability diagram for arbitrary \bar{p}_1 and \bar{v}_1 .

move along one quadrant of an ellipse. The envelope of this family delineates the region shown in Fig. 27 (this region is plotted, for the sake of being definite, as applied to the case $\bar{Y} = \bar{Q}$). When the end of the vector \bar{Y} enters into the shaded region, excitation of the system becomes possible.

Realization of this possibility depends on whether the end of the vector \bar{Y}

is located inside that circle of the family corresponding to the actual position of the discontinuity surface Σ (the actual values of \bar{p}_1 and \bar{v}_1). Inside the cross-hatched region there can exist a subregion which belongs to all the circles of the family. In Fig. 27 this region is doubly hatched. When the end of the vector \bar{Y} falls into this sub-

region, the excitation becomes possible independently of the position of the surface Σ along the tube axis. In this sense one can speak of values of the vector \vec{Y} for which excitation is particularly probable. The position of the end of the vector \vec{Y} outside the shaded regions always corresponds to system stability.

In order to understand correctly the meaning of the constructed diagrams, let us point out one important circumstance. Each circle or stability limit was plotted for specified invariant values of \bar{p}_1 and \bar{v}_1 . But this does not mean that all the modes corresponding to the points of such a circle can actually be realized in one and the same tube. Indeed, let the oscillating mode corresponding to one of the points of a certain stability limit be realized in a tube with a heat-supply region located at a distance L_1 from the inlet end and L_2 from the outlet. Assume that pressure nodes are located on the ends of the tube. We now move mentally to the neighboring point on the same circle — the stability limit. Then \bar{p}_1 and \bar{v}_1 do not change, and the frequency ω cannot change, for otherwise the boundary condition at the inlet is violated. (This is seen, for example, from Formulas (4.13) and (4.14).) Thus, on going over to the neighboring point of the stability limit, the process of oscillation does not change at the inlet section. Motion along the circle that represents the stability limit denotes in this case only in the change in the vector \vec{Y} .

As can be seen from Eqs. (19.6), a change in \vec{Y} with invariant \bar{p}_1 and \bar{v}_1 unavoidably leads to changes in \bar{p}_2 and \bar{v}_2 . Inasmuch as the dimensional oscillation frequency is the same for both parts of the tube, the oscillation frequency in the hot part of the tube cannot change. But then the functions φ_1 and φ_2 for the hot part also remain invariant and the boundary condition at the outlet end is violated by virtue of the change in the values of \bar{p}_2 and \bar{v}_2 in the heat-supply plane [the

values of A_v and A_p in Eqs. (4.13)]. In order to retain the boundary condition at the outlet, it is necessary to change the length L_2 . Thus, on moving along the stability-limit circle, it becomes necessary to change mentally some characteristic of the tube, for example, the length L_2 .

This result, which is at first glance strange, is perfectly natural, for in the construction of the stability limits we used only energy considerations and the boundary conditions were not stipulated at all.

If the boundary conditions are specified, then as \bar{Y} varies changes will take place not only in \bar{p}_2 and \bar{v}_2 but also in \bar{p}_1 , \bar{v}_1 , and in the oscillation frequency, while the stability limit for such a tube with fixed dimensions will be made up of points belonging to different circles of the family already determined in the present section. In this case the instability region will turn out to be inside the shaded portion of the diagram of Fig. 27.

In conclusion, attention should be called to the form of the stability limits of this type in those cases when the plane Σ is located exactly in velocity or pressure nodes. To be sure, it is necessary to stipulate that the term "exactly" is meaningful only for elementary processes, for in the general case the perturbation of the pressure or velocity does not remain invariant on crossing the heat-supply region σ . If we agree to define a nodal position of the plane Σ as coinciding with the section where $\bar{p}_1 = 0$ or $\bar{v}_1 = 0$, then the corresponding stability limits will occupy, in accordance with (19.13), the positions indicated in Fig. 28. On the left is shown the position for Σ in a velocity node, and on the right — for a pressure node.

§20. Diagrams of the Stability Limits for Typical Cases

The present section is devoted to an analysis of the stability

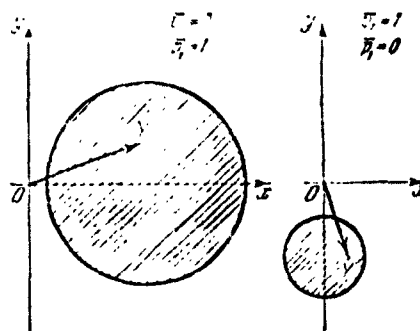


Fig. 28. Stability diagrams when the heat-supply plane Σ is located in a velocity node and in a pressure node.

diagrams for certain typical cases. The main problem will be an analysis of the change in the configuration of the stability limits as a function of the singularities of the heat-supply process in the zone σ . However, before we proceed with such an analysis, we make one remark.

The diagram shown in Fig. 27 is typical of the case when oscillations are excited by the heat supply ($\bar{\gamma} = \bar{Q}$). Notice should be taken of an interesting feature of such a case — the origin does not fall in the shaded region. This means that to excite the system it is necessary to have a finite value of the vector \bar{Q} ; when \bar{Q} has an absolute value which is less than a certain amount, the system will not be excited at all at any time. It must be emphasized that a finite \bar{Q} does not mean that a finite perturbation of the heat supply at the initial instant of time is necessary. The point is that in constructing diagrams of the type shown in Figs. 26 and 27, the value of the sum $\bar{v}_1^2 + \bar{p}_1^2$ is arbitrarily assumed equal to unity, similar to what was done in constructing the stability diagrams for the elementary processes. Consequently, in the general case, when speaking of the quantity $\bar{\gamma}$, it must be understood that what is referred to is the ratio of the quantity $\bar{\gamma}$ to the quantity which is assumed as unity. In the initial instant of time, when the true amplitude of the pressure perturbation

(the arbitrary unity) is small, obviously \bar{Q} also has the same order of smallness.

Let us consider now some particular cases of stability diagrams. The diagram constructed in Fig. 27 corresponds to excitation of oscillations when $\bar{J}_1 = \bar{J}_2 = \bar{J}_3 = 0$, i.e., due to the perturbation of the heat supply \bar{Q} alone. It is constructed for the most general case. Let us assume that in the steady-state motion the heating of the gas as it crosses the surface Σ is negligibly small, so that we can set in Eqs. (15.7) $M_1 = M_2 = M$ and $a_1 = a_2$; this corresponds, in first approximation, to the excitation of sound in a Rijke tube. Then the system (15.7) can be written in the form

$$\left. \begin{aligned} \bar{v}_2 + M\bar{p}_2 - M\bar{s}_2 &= \bar{v}_1 + M\bar{p}_1 - M\bar{s}_1, \\ 2M\bar{v}_2 + (1 + M^2)\bar{p}_2 - M^2\bar{s}_2 &= \\ &= 2M\bar{v}_1 + (1 + M^2)\bar{p}_1 - M^2\bar{s}_1 + M^2\bar{p}_x^*, \\ \left(3M^2 + \frac{2}{\kappa - 1}\right)\bar{v}_2 + M\left(M^2 + 2\frac{\kappa}{\kappa - 1}\right)\bar{p}_2 - M^2\bar{s}_2 &= \\ &= \left(3M^2 + \frac{2}{\kappa - 1}\right)\bar{v}_1 + \\ &+ M\left(M^2 + 2\frac{\kappa}{\kappa - 1}\right)\bar{p}_1 - M^2\bar{s}_1 + \bar{Q}, \end{aligned} \right\} \quad (20.1)$$

where for a Rijke tube we have

$$\bar{Q} = 2M^2\bar{Q}^*. \quad (20.2)$$

The complete symmetry of the left and right halves of (20.1) (accurate to the term \bar{Q} and for $\bar{p}_x^* = 0$) makes the elimination of the variables exceedingly simple. Simple algebraic manipulations yield

$$\left. \begin{aligned} \bar{v}_2 &= \bar{v}_1 + \frac{\kappa - 1}{2(1 - M^2)}\bar{Q}, \\ \bar{p}_2 &= \bar{p}_1 - M\frac{\kappa - 1}{2(1 - M^2)}\bar{Q}. \end{aligned} \right\} \quad (20.3)$$

Comparing the obtained equations with (19.6) we see that $a_{12} = -a_{21} = 0$, and this leads in Eq. (19.8) to $D = E = 0$. But the vanishing of D and E indicates that the circle defined by Eq. (19.10) always goes through the origin. Thus, when the amount of heating is small in the region σ all the circles which are stability limits cross at a

single point, and this point is the origin. The corresponding construction is shown in Fig. 29b, and to complete the picture we show alongside (Fig. 29a) a similar construction for the case of finite heating ($M_1 < M_2$), analogous to the diagram of Fig. 27. A comparison of diagrams a and b shows that in the case of small heating the system becomes less stable in the sense that its excitation is possible by means of as small relative perturbations of the heat supply \bar{Q}^* as are desired.

Let us consider, finally, the third case of this series. Let $M_1 = M_2 = 0$, i.e., let there be no over-all motion of the gas. Then Eqs. (20.3) yield

$$\left. \begin{aligned} \bar{v}_2 &= \bar{v}_1 + \frac{\pi-1}{2} \bar{Q}, \\ \bar{p}_2 &= \bar{p}_1. \end{aligned} \right\} \quad (20.4)$$

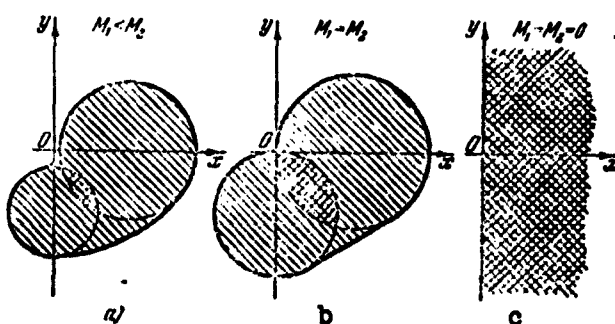


Fig. 29. Influence of the stream velocity on the configuration of the stability limits.

Now A, C, D, and E in Eq. (19.8) will vanish, and the equation of the circle (19.10) degenerates into a straight line $Y_x = 0$, i.e., the stability limit becomes the y axis, independently of \bar{p}_1 and \bar{v}_1 . This form of the stability-limit diagram is shown in Fig. 29c. It is obvious that the last case is the Rayleigh case, inasmuch as the system is excited if the phase shift between the perturbed component of the heat supply \bar{Q} and the periodic component of the pressure \bar{p}_1 is smaller than $\pi/2$. This result could be predicted, inasmuch as the second equation

of (20.4) indicates that the first elementary process is realized in this case.

If we compare the three types of stability diagrams shown in Fig. 29, then by examining them in reverse order we see how the conditions for the excitation become more complicated first as flow sets in, then following strong stationary heating. In this case the region which is doubly cross-hatched decreases more and more, i.e., along with the properties of the heat-supply process, a more important role is assumed also by the position of the plane Σ relative to the standing wave produced in the tube.

By constructing analogous stability diagrams for this type of heat supply in which the flame front oscillates freely together with the stream, it can be shown that when the heat-supply front moves the oscillating system is in a certain sense more prone to excitation. Let us turn for this purpose to the system of equations (16.12). Eliminating \bar{s}_2 from the left halves of this system and recognizing that $\bar{s}_1 = 0$ in the cold stream, we arrive at a system of two equations, containing \bar{v}_2 , \bar{p}_2 , \bar{v}_1 , \bar{p}_1 , and \bar{U}_1 . If we eliminate from them \bar{v}_2 and at the same time take account of Formulas (15.9) and (15.10), then we readily verify that the coefficient of \bar{v}_1 in the equation that defines \bar{p}_2 vanishes. In the notation of (19.6) this means that $a_{21} = 0$, which leads in Eqs. (19.8) and (19.9) to $E = 0$. But then when $\bar{p}_1 = 0$ the stability limit passes through the origin. Comparing this case when that considered above (Fig. 30) we see that the excitation of the acoustic oscillations due to the mobility of the flame front (\bar{U}_1) is more probable than excitation due to oscillating heat supply (\bar{Q}). It is necessary to note, to be sure, that this difference is more of academic than of practical interest.

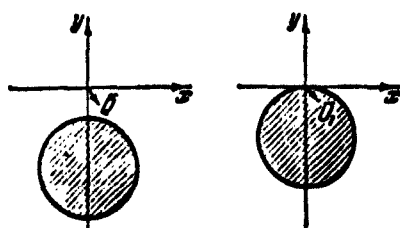


Fig. 30. Stability diagrams for the excitation of a system by means of heat supply and a moving flame ($P_1 = 0$).

§21. Comparison of the Relative Significance of Thermal and Mechanical Energy Sources in the Excitation of Oscillations

To conclude the present chapter let us turn once more to the question of the sources of the energy necessary for the excitation of acoustic oscillations. In the preceding chapter it was shown that under certain assumptions concerning the

character of the heat supply one can point to two principally different energy sources for acoustic oscillations, and in §18 this deduction was extended to include also the more general case of an arbitrary combustion of a mixture entering into the heat-supply zone.

The formulas obtained in the present chapter, which characterize the processes that occur inside the combustion zone σ , enable us to raise the question of a numerical estimate of the relative significance of each of the two obtained energy sources.

However, before we decide whether the oscillating system is fed principally at the expense of the kinetic energy of the flow or at the expense of the energy which is in thermal form, we must make one remark. In the preceding chapter we derived Formulas (13.7), which upon changing to the dimensionless notation (19.1) for the acoustic-energy flux assume the form

$$\left. \begin{aligned} \bar{A}_1 &= \frac{1}{2} \left(\bar{p}_1 \delta E + \frac{1}{2} \delta E \delta X \right), \\ \bar{A}_2 &= \frac{1}{2} \left(\bar{v}_1 \delta X + \frac{1}{2} \delta E \delta X \right). \end{aligned} \right\} \quad (21.1)$$

From these formulas it is possible to estimate the components of the total flux of acoustic energy, radiated by the region σ , corresponding to the two independent energy sources. In the derivation of these formulas we made use of the circumstance that equal fractions of

change in δp inside σ corresponded to equal fractions of change in δv . Analytically this condition was expressed by Formulas (13.3).

In the general case, for an arbitrary complicated combustion process inside σ , the arguments that lead to Formulas (13.3) turn out to be incorrect. This would follow at least from the fact that Formulas (13.3) have been obtained by assuming the flow inside σ to be one-dimensional, whereas in the general case this flow can be essentially not one-dimensional.

Nonetheless, we shall use in the present section the formulas presented here for \bar{A}_1 and \bar{A}_2 . The point is that these formulas are valid for all those cases when the change in δp and in δv along the region σ occurs simultaneously and equal fractions of the change in δp correspond to equal fractions in the change of δv . For one-dimensional flow in the region σ this can be readily proved. In the general case, however, this is a most natural assumption, since it is difficult to imagine a real combustion process which would be characterized, for example, by the fact that in the first part of the region σ there is only a pressure perturbation and in the second only a velocity perturbation, or vice versa. Qualitative arguments of this kind enable us to use the formulas previously obtained, with the expressions for \bar{A}_1 and \bar{A}_2 , for the analysis of the general case, too.

Inasmuch as we are dealing in the present section only with the limited problem of estimating the relation between \bar{A}_1 and \bar{A}_2 , we shall consider only several very simple cases.

When $\bar{R} = 0$ (no losses at the ends of the tube), Formula (11.9) yields the following equation, which is valid for an oscillating system at the stability limit:

$$\bar{A}_1 + \bar{A}_2 = 0, \quad (21.2)$$

from which it follows directly that $|\bar{A}_1| = |\bar{A}_2|$. Thus, the absolute

values of both fluxes of acoustic energy, of which one is due to the kinetic energy of flow and the other to the energy in thermal form, are equal to each other at the stability limit. From this point of view, both sources of self-oscillation energy are perfectly equivalent.

According to (21.2), the fluxes \bar{A}_1 and \bar{A}_2 have opposite signs, and cancel each other at the stability limit. In this case one of them tends to excite the system and the other to quench the oscillations. Further development of the process depends on whether the same equilibrium is maintained or whether one of the "fighting" fluxes \bar{A}_1 and \bar{A}_2 prevails. It is necessary to bear in mind here that depending on the specific conditions, both the excitation and the quenching of the oscillations can be connected with the drawing of energy from any of the two existing energy sources. From this point of view \bar{A}_1 and \bar{A}_2 are also perfectly equivalent.

The condition $\bar{A}_1 = -\bar{A}_2$, which is satisfied at the stability limit in the absence of losses to the external medium, is interesting in that respect that it gives an illustrative idea of the role of the two energy reservoirs which the oscillating system possesses. Each of these reservoirs can serve as a source for acoustic energy or, to the contrary, absorb it. For example, if $\bar{A}_1 > 0$ and consequently $\bar{A}_2 < 0$, then in the case of oscillations in the combustion zone mechanical energy is produced at the expense of the thermal terms in the energy flux, but this mechanical energy does not go to reinforce the acoustic oscillation, but is consumed entirely in an increase of the average flux of the stream kinetic energy. Were the system to have some single energy reservoir, then the energy drawn from it could be used only to excite the acoustic oscillations or only to compensate losses in the external medium. The presence of a second energy reservoir uncovers as it were the possibility of damping the oscillations even in the absence

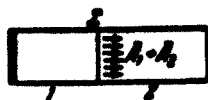


Fig. 31. Scheme showing the flow of acoustic energy in a tube with one end closed.

of any external losses.

In order to present a quantitative estimate of the energy processes that are inherent in the phenomenon under consideration in the steady-state self-oscillation process, we turn to a particular case (Fig. 31). We consider a tube closed on the left end. In this case the flux of summary acoustic energy to the left will equal zero, since it is impossible to radiate energy into the outside space through the closed end. But then in the left part of the tube the phase shift between \bar{p}_1 and \bar{v}_1 is $\pi/2$ and Eq. (19.12) will hold true. Assume that the losses of acoustic energy are always equal to the summary acoustic energy $\bar{A}_1 + \bar{A}_2$ moving toward the open end of the tube. Under these conditions the oscillations have a steady-state character and it is legitimate to use Formulas (21.1).

In order to obtain a simple picture of the process, let us consider the case when the excitation occurs at the expense of heat-supply oscillations, and the heating in the plane Σ is weak ($M_1 = M_2 = M$, $n = 1$, and $m = 1$). Under these assumptions we can obtain from (20.3) and (17.1)

$$\begin{aligned}\delta E = \bar{v}_2 - \bar{v}_1 &= \frac{n-1}{2(1-M^2)} \bar{Q}, \\ \delta X = \bar{p}_2 - \bar{p}_1 &= -M \frac{n-1}{2(1-M^2)} \bar{Q},\end{aligned}$$

and from Formulas (21.1) we get

$$\left. \begin{aligned}\bar{A}_1 &= \frac{1}{2} \left(\alpha \bar{Q} \bar{p}_1 - \frac{1}{2} M \alpha^2 \bar{Q}^2 \right), \\ \bar{A}_2 &= \frac{1}{2} \left(-M \alpha \bar{Q} \bar{v}_1 - \frac{1}{2} M \alpha^2 \bar{Q}^2 \right),\end{aligned} \right\} \quad (21.3)$$

where

$$\alpha = \frac{n-1}{2(1-M^2)}.$$

Here the perturbation of the heat supply \bar{Q} is written in vector form. From Formulas (21.3) it is seen that for the oscillating process under

consideration the second terms in \bar{A}_1 and \bar{A}_2 always yield negative components, i.e., they always quench the oscillations. Consequently, the excitation of the system can be produced only by the first terms, and in \bar{A}_1 the angle between \vec{p}_1 and \vec{Q} should not exceed $\pi/2$, while in \bar{A}_2 the angle between \vec{v}_1 and \vec{Q} should be larger than $\pi/2$. Inasmuch as \vec{p}_1 and \vec{v}_1 in the left part of the tube adjacent to the closed end are related by the condition (19.12)

$$\vec{v}_1 + \vec{p}_1 = \text{const.},$$

the possible largest absolute values of \vec{p}_1 and \vec{v}_1 coincide. A comparison of the first terms of Expressions (21.3) shows that the acoustic-energy flux going into excitation of the system at the expense of the kinetic energy of the stream increases in direct proportion to the number M . When $M \rightarrow 1$ both energy sources (thermal and mechanical) are equalized in this sense.

This does not mean that at small (but finite) M it is merely possible to neglect the energy flux \bar{A}_2 . This can be seen most simply from the following argument. Let the first term of \bar{A}_2 be equal to zero (for example, owing to the phase shift between \vec{Q} and \vec{v}_1). Then the excitation will be due to only the first term of \bar{A}_1 . Let us start to increase the absolute value of \vec{Q} . In this case the second terms, in which \vec{Q} is of the second degree, will increase more rapidly than the first, and at a certain $\vec{Q} = Q_{\max}$ the total flux $\bar{A}_1 + \bar{A}_2$ will vanish. Consequently, the exciting action of the first term of \bar{A}_1 will be completely offset by the second terms of \bar{A}_1 and \bar{A}_2 , and to a perfectly equal degree.

These qualitative deductions were confirmed by the exact calculations of the particular cases of some specific flows. To illustrate the foregoing, Fig. 32 shows a diagram showing how the flux of acoustic energy $\bar{A}_1 + \bar{A}_2$ changes when the modulus of \vec{Q} varies, for the particular case $M_1 = 0.1$, $M_2 = 0.25$, $|\vec{v}_1| = |\vec{p}_1|$. As can be seen from the figures

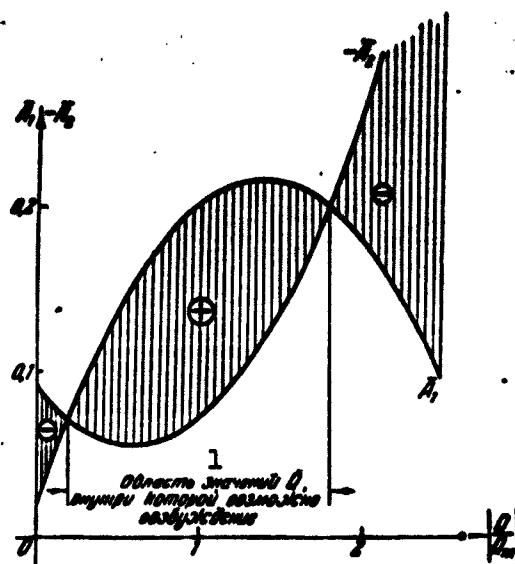


Fig. 32. Diagram showing the variation of the flux of acoustic energy with varying modulus of \bar{Q} . 1) Region of values of \bar{Q} inside of which excitation is possible.

presented, we are dealing with a relatively slow stream: the condition $|\bar{v}_1| = |\bar{p}_1|$ has been chosen in order to have ahead of the heat-supply plane noticeable oscillations in both the velocity and in the pressure. In the calculations the phase of \bar{Q} was chosen constant and such that for specified \bar{p}_1 and \bar{v}_1 a certain modulus $\bar{Q} = \bar{Q}_{\max}$ must cause a maximum of $\bar{A}_1 + \bar{A}_2$ (the vector \bar{Q} passes through the center of the circle which is the stability limit for the chosen \bar{p}_1 and \bar{v}_1). In constructing the diagrams the ordinates were the quantities \bar{A}_1 and $-\bar{A}_2$, and consequently the distance between the two curves in a vertical direction is equal to the flux $\bar{A}_1 + \bar{A}_2$, and in those portions where the curve of \bar{A}_1 lies above that of $-\bar{A}_2$ the summary flux is positive, and where $-\bar{A}_2$ passes above \bar{A}_1 it is negative.

It is seen from the diagram that when $\bar{Q} = 0$ we have $\bar{A}_1 + \bar{A}_2 < 0$, i.e., in the absence of oscillations in the heat supply the system is stable. This circumstance was already emphasized above in the construc-

tion of the stability limits (§20).

The diagram shown in Fig. 32 fully confirms the results obtained in the present section. In addition, it is seen from it that at such a relatively slow flow, the oscillating system is excited at the expense of the heat supply and the internal-energy flux, and the interaction between the system and the flux of kinetic energy leads to a strong damping of the oscillations.

This result is generally characteristic of slow streams ($M \ll 1$), which are excited by heat supply. Such streams are excited at the expense of the kinetic-energy flux only in exceptional cases, when \bar{p}_1 is close to zero, and in these cases the absolute value of $\bar{A}_1 + \bar{A}_2$ is small.

It does not follow from the foregoing, however, that the flux \bar{A}_2 never plays a noticeable role as an active factor in the excitation of oscillations. First, with increasing M the fraction of A_2 as part of the total flux of acoustic energy increases proportionally, and second, the picture may change radically if the process in the heat-supply zone ceases to be regarded as a function of one complex parameter (in the present case, \bar{Q}). If we assume, for example, that both heat-supply oscillations and oscillations in the position of the flame front can occur simultaneously in the heat-supply zone, and the phase shift between them can be arbitrary, then it is easy to construct examples of systems in which the principal source of energy for the excitation of the oscillations will be the kinetic energy of the flow.

In addition, if we turn to Fig. 28, which shows the stability limits for the cases $\bar{v}_1 = 0$ and $\bar{p}_1 = 0$ and recognize that these limits have been constructed so as to maintain the scale for the slow flow considered in the present section, it is easy to verify that \bar{A}_2 can be an active factor in the excitation also in such exceptionally unfavor-

able conditions as $M_1 = 0.1$. Indeed, the diameter of the instability region in the right half of the figure (corresponding to $\bar{p}_1 = 0$) is only 2.5 times smaller than the diameter of the instability region shown to the left. At the same time, it is seen from the example (21.3) that when $\bar{p}_1 = 0$ the only acoustic-energy flux exciting the system is \bar{A}_2 , and when $\bar{v}_1 = 0$ this role is assumed by \bar{A}_1 . Consequently, the neglect of such a reservoir of energy for the maintenance of self-oscillations as the kinetic energy of the stream may not only distort the picture in those cases when the excitation is due to the energy which is in thermal form, but also lead to incorrect conclusions concerning the possibility of self-excitation of the system in such regions of the parameter plane, for which the excitation of the oscillations at the expense of the energy in thermal form is generally impossible.

Manu-
script
Page
No.

[Footnotes]

- 116 L. Landau and Ye. Lifshits, Mekhanika sploshnykh sred [The Mechanics of Continuous Media], Gostekhizdat, 1953.
- 121 In order to simplify the notation of the system, we do not distinguish henceforth between κ_1 and κ_2 , which are the adiabatic exponents in the cold and hot gas. If desired this can always readily be taken into account.
- 129 The term $Q_1[(1/M_1)\bar{v}_1 + \bar{p}_1 - \bar{s}_1]$ which is contained in \bar{Q} is of no interest, since it is uniquely connected with \bar{v}_1 , \bar{p}_1 , and \bar{s}_1 and cannot be freely varied as, for example, $\bar{\eta}_{sg}$ and \bar{q}_1 .
- 133 These assumptions must be regarded as rather crude. They are justified by the fact that the terms $v^2/2$ play a relatively insignificant role compared with $c_v T$ and g .

Manu-
script
Page
No.

[List of Transliterated Symbols]

119	cr = sg = sgoraniye = combustion
130	x = kh = kholodnyy = cold
130	r = g = goryachiy = hot
131	crop = sgor = sgoraniye = combustion
133	эфф = eff = effektivnyy = effective
137	э = e = ekvivalentnyy = equivalent
144	Э = E = energiya = energy
145	э = e = energiya = energy
145	I = I = impul's = momentum

Chapter 5
EXCITATION OF OSCILLATIONS BY HEAT SUPPLY
IN THE ABSENCE OF LOSSES

§22. Introductory Remarks

The present chapter is devoted to the solution of the problem of the stability of the flow of a heated gas under the assumption that the acoustic energy is not radiated from the ends of the tube and consequently it is not dissipated in the surrounding space. In the theoretical analysis of thermal excitation of sound, such an assumption is made almost always, since it is valid with a certain degree of approximation for the case of excitation of the low frequencies, which are of principal interest. An approximate formulation of the problem makes it possible to obtain in many cases sensible analytical results, which are essentially valid even under more general assumptions concerning the dissipation of the acoustic energy. We shall not estimate here the extent of the validity of the assumption made, for we consider in the next chapter an analogous problem with account of the energy losses at the ends of the tube.

Unlike the preceding chapters, where we considered essentially the elements of the excitation of acoustic oscillations by heat supply (propagation of longitudinal acoustic perturbations along the tube, questions concerning the variation of these perturbations as they cross the heat-supply region), we shall present here an analysis of the problem as a whole, using the results previously obtained. However, before we proceed to a solution of our problem, we must make one remark.

In all the preceding arguments, where the stability limits were constructed on the basis of energy considerations, we left out continuously one logical link. All the results obtained above reduced in final analysis to the statement that if the relations between the phases and the amplitudes of the oscillating system and the heat-supply process satisfy certain conditions, then the system becomes excited. Speaking more accurately, we proved that if the processes in the heat-supply zone have a definite oscillatory character, then acoustic oscillations are excited in the system. However, in order for the process to be closed, it is necessary to demonstrate also that the acoustic oscillations of the medium do in turn lead to oscillatory processes in the heat-supply zone. The presence of this feedback would make self-oscillation of the system possible. This can be demonstrated by using the following qualitative argumentation: assume that a weak acoustic perturbation has arisen in the system and has led to a perturbation in the combustion zone, the result of which was a new acoustic perturbation, which combined with the preceding one and intensified it, the intensified acoustic perturbation has led to a more intense perturbation of the process in the combustion zone, the latter has again produced an intensifying acoustic perturbation, etc.

Consequently, it is necessary to add to the already-demonstrated premises that the oscillating combustion process is capable of giving rise to acoustic oscillations also the proof that the acoustic oscillations are in turn capable of producing an oscillating combustion process. The existence of this feedback is a very important aspect in our sequence of reasoning. If we turn to an analysis of the physical processes that serve as the basis for the occurrence of feedback, we find that they are quite numerous, complicated, and sufficiently varied. This makes it necessary to devote a special chapter of the book

known trigonometric identity

$$\frac{\sin \alpha}{1 - \cos \alpha} = \operatorname{ctg} \frac{\alpha}{2}.$$

We then obtain

$$n \operatorname{ctg} \frac{\omega l_2}{\pi(1-M_1)} - m \operatorname{ctg} \frac{\omega l_1}{1-M_1} = 0. \quad (22.7)$$

Equation (22.7) enables us to obtain a discrete series of frequencies ω , satisfying the characteristic equation.

Assume now that the process in the heat-supply zone is characterized by the condition $\delta X = 0$. This corresponds to the first elementary process considered in the preceding chapters. Then the conditions (17.1) on Σ assume the form

$$\left. \begin{aligned} \bar{v}_1 &= n\bar{v}_2 - \delta E, \\ \bar{p}_1 &= m\bar{p}_2. \end{aligned} \right\} \quad (22.8)$$

In order to relate in explicit manner the quantity δE with the phase of the oscillation, we assume that

$$\delta E = y\bar{p}_1, \quad (22.9)$$

where y is a certain complex number.

The complex coefficient y , which is introduced here in purely formal fashion, has a deep physical meaning. Writing down Eq. (22.9) is a formal introduction of the feedback referred to at the beginning of the present section. Let the physical process in the combustion zone remain indeterminate, but Eq. (22.9) indicates that the pressure oscillations \bar{p}_1 give rise to a corresponding oscillatory process in the heat-supply zone.

Indeed, inasmuch as $\delta X = 0$ by definition, δE completely characterizes the perturbations of the heat-supply process to the extent needed for the solution of the problem. Equation (22.9) shows that these perturbations are connected with the perturbations of \bar{p}_1 and consequently, if \bar{p}_1 oscillates, then δE will also oscillate, and furthermore with

(Chapter 7) to the feedback mechanisms. In order to clarify these arguments here, it is necessary to present a certain example of a phenomenon of this type. For this purpose we point out the almost obvious fact that the acoustic oscillations are connected with the oscillations in the stream velocity, and the stream velocity influences, as is well known, the combustion process (it changes the configuration of the flame front, it changes the rate of combustion, etc.). Thus, oscillations in the stream velocity, brought about by acoustic phenomena, generate in turn oscillatory combustion.

It will be shown below that this example does not exhaust the large number of possible mechanisms of feedback, but it must be mentioned here in order to show that the feedback mechanisms actually exist and therefore all the preceding arguments were not without purpose. In addition, by pointing out the importance of this link in the oscillation excitation process we induce the reader to follow more attentively the premises that will be advanced during the course of further exposition and which will contain every time, in explicit or implicit form, some assumption which is equivalent to introducing feedback.

It is advantageous to start the analysis of the excitation of oscillations in a tube without losses at the ends with the already-known simplest cases, which are characterized by the realization of elementary processes in the heat-supply zone, so as to apply to them the new solution method.

We assume, for the sake of being definite, that pressure nodes are located at the ends of the tube. Let the heat-supply plane Σ , which is equivalent to the heat-supply region σ , be located at distances ξ_1 and ξ_2 from the end of the tube. We place the origin in a section coinciding with Σ , so that the left end of the tube will have a coordinate $\xi_1 < 0$, and the right end has a coordinate $\xi_2 > 0$.

The boundary conditions are written in the form

$$\bar{p}_1(\xi_1) = 0; \quad \bar{p}_2(\xi_2) = 0.$$

We then obtain from the solution of (4.13)

$$\left. \begin{aligned} \bar{v}_1 \varphi_1(\xi_1) + \bar{p}_1 \varphi_1(\xi_1) &= 0, \\ \bar{v}_2 \varphi_2(\xi_2) + \bar{p}_2 \varphi_2(\xi_2) &= 0. \end{aligned} \right\} \quad (22.1)$$

Here \bar{v}_1 , \bar{p}_1 , \bar{v}_2 , and \bar{p}_2 are the values of the perturbations \bar{v} and \bar{p} at the section $\xi = 0$, to the left and to the right of the surface Σ , respectively.

We start the consideration of the problem with the case when the process in the heat-supply zone is characterized by the condition $\delta E = \delta X = 0$.

From the canonical form (17.1) of the conditions on Σ it follows that when $\delta E = \delta X = 0$ we have $\bar{v}_1 = n\bar{v}_2$, $p_1 = m\bar{p}_2$. But then the system (22.1) becomes linear and homogeneous with respect to \bar{p}_2 and \bar{v}_2 . It will have nontrivial solutions if the following condition is satisfied

$$\begin{vmatrix} n\varphi_1(\xi_1) & m\varphi_1(\xi_1) \\ \varphi_2(\xi_2) & \varphi_1(\xi_2) \end{vmatrix} = 0.$$

When $\varphi_2 \neq 0$ we can write the resultant characteristic equation of the system in the form

$$n \frac{\varphi_1(\xi_1)}{\varphi_2(\xi_2)} - m \frac{\varphi_1(\xi_1)}{\varphi_2(\xi_2)} = 0. \quad (22.2)$$

Using Formulas (4.14), we obtain, setting $\beta = \nu + i\omega$

$$\frac{\varphi_1(\xi)}{\varphi_2(\xi)} = \frac{1 - \exp \frac{4\nu\xi}{1-M^2} + 2i \exp \frac{2\nu\xi}{1-M^2} \sin \frac{2\omega\xi}{1-M^2}}{1 + \exp \frac{4\nu\xi}{1-M^2} - 2 \exp \frac{2\nu\xi}{1-M^2} \cos \frac{2\omega\xi}{1-M^2}}. \quad (22.3)$$

The denominator of the resultant expression is always larger than zero (since the case $\varphi_2 = 0$ is excluded from consideration). If we recognize that \underline{n} and \underline{m} in (22.2) are positive numbers by definition, then, confining ourselves for the time being to a consideration of the real part of Eq. (22.2) only, we obtain immediately

$$C\left(1 - \exp \frac{4v_1 \xi_1}{1 - M_1^2}\right) - D\left(1 - \exp \frac{4v_2 \xi_2}{1 - M_2^2}\right) = 0, \quad (22.4)$$

where C and D are certain positive numbers.

Before we proceed to an analysis of the relation obtained, we call attention to one important circumstance. The quantities v_1 and v_2 in the exponentials, or, in the more general case, the complex frequencies β_1 and β_2 contained in the functions φ_1 , φ_2 , and φ_3 , are different for the "cold" and "hot" portions of the tube. This is connected with the fact that for the system of dimensionless variables (4.8) used in the present book the time scales L/a are different on the different sides of Σ , owing to the change in the velocity of sound a when the gas becomes heated. At the same time it is physically obvious that the dimensional frequency of oscillations should be the same for the entire tube. On this basis, we can readily establish a connection between β_1 and β_2 :

$$\beta_1 = \frac{a_2}{a_1} \beta_2 = n \beta_2. \quad (22.5)$$

Consequently, analogous relations will exist between v_1 and v_2 :

$$v_2 = \frac{1}{n} v_1.$$

We can now rewrite (22.4) in a more convenient form

$$C\left(1 - \exp \frac{4v_1 \xi_1}{n(1 - M_1^2)}\right) + D\left(\exp \frac{4v_1 \xi_2}{1 - M_2^2} - 1\right) = 0. \quad (22.6)$$

Let us consider Relation (22.6) in greater detail. The quantities C, D, $4/n(1 - M_2^2)$, and $4/(1 - M_1^2)$ in this equation are positive. The coordinates of the pressure nodes ξ_1 and ξ_2 have opposite signs: $\xi_1 < 0$ and $\xi_2 > 0$. Consequently, both terms in the left part of Eq. (22.6) have the same signs, independently of the value of v . The vanishing of this sum is possible only if each term is equal to zero separately.

From this we obtain immediately

$$v_1 = 0.$$

Thus, we have obtained here the same result as above, in the energy analysis of the problem: if $\delta E = \delta X = 0$, then neutral oscillations are produced. It must be noted that in the present section this derivation is obtained only for a particular form of boundary conditions, namely pressure nodes at the ends of the tube. However, it can be readily extended to include also a more general case. Assume that on the left and on the right of Σ there are located in a certain section (not necessarily the ends) ξ_1 and ξ_2 not pressure nodes but velocity nodes or a velocity node on one end and a pressure node on the other. The change in the boundary conditions effected in this manner leads to characteristic equations of the type (22.2). The difference reduces to the fact that in place of the ratio of the functions φ_1/φ_2 the equation will contain the ratios φ_2/φ_1 or simultaneously φ_1/φ_2 and φ_2/φ_1 . However, it is known from the theory of complex numbers that the signs of the real parts of the complex numbers z and $1/z$ are the same. Inasmuch as the deduction given above is based precisely on an examination of the signs of the real parts of the function φ_1/φ_2 , it will be valid also for the characteristic equations containing φ_2/φ_1 or φ_1/φ_2 and φ_2/φ_1 simultaneously.

The results obtained here, as was already indicated, are not new. However, comparing the method used in the present section to solve the problem of the stability of flow of a heated gas with the previously developed energy method, we can point to certain advantages of the solution method considered here. Unlike the energy method, the direct solution of the characteristic equation enables us to obtain, in particular, the frequencies of the oscillations.

Indeed, let us turn to Eq. (22.2). Using Formula (22.3), we now write the second consequence of Eq. (22.2), equating its imaginary part to zero. We take account here of the fact that $v = 0$ and use the

known trigonometric identity

$$\frac{\sin a}{1 - \cos a} = \operatorname{ctg} \frac{a}{2}.$$

We then obtain

$$n \operatorname{ctg} \frac{\omega_1 k_2}{n(1-M)} - m \operatorname{ctg} \frac{\omega_1 k_1}{1-M} = 0. \quad (22.7)$$

Equation (22.7) enables us to obtain a discrete series of frequencies ω , satisfying the characteristic equation.

Assume now that the process in the heat-supply zone is characterized by the condition $\delta X = 0$. This corresponds to the first elementary process considered in the preceding chapters. Then the conditions (17.1) on Σ assume the form

$$\left. \begin{aligned} \bar{v}_1 &= n\bar{v}_2 - \delta E, \\ \bar{p}_1 &= m\bar{p}_2. \end{aligned} \right\} \quad (22.8)$$

In order to relate in explicit manner the quantity δE with the phase of the oscillation, we assume that

$$\delta E = y\bar{p}_1, \quad (22.9)$$

where y is a certain complex number.

The complex coefficient y , which is introduced here in purely formal fashion, has a deep physical meaning. Writing down Eq. (22.9) is a formal introduction of the feedback referred to at the beginning of the present section. Let the physical process in the combustion zone remain indeterminate, but Eq. (22.9) indicates that the pressure oscillations \bar{p}_1 give rise to a corresponding oscillatory process in the heat-supply zone.

Indeed, inasmuch as $\delta X = 0$ by definition, δE completely characterizes the perturbations of the heat-supply process to the extent needed for the solution of the problem. Equation (22.9) shows that these perturbations are connected with the perturbations of \bar{p}_1 and consequently, if \bar{p}_1 oscillates, then δE will also oscillate, and furthermore with

the same frequency. The quantity y determines uniquely the relationship between the amplitudes of δE and \bar{p}_1 (the modulus of the number y) and the phase shift between them (the argument of the number y).

Using Eqs. (22.8) and (22.9), let us turn to Eqs. (22.1). In the case under consideration the characteristic equation of our system will differ from Eq. (22.2) only in the right half:

$$\pi \frac{v_1(\xi_2)}{v_1(\xi_1)} - \pi \frac{v_1(\xi_1)}{v_1(\xi_2)} = -my. \quad (22.10)$$

Confining ourselves, as before, to an examination of the real part of the equation (22.10) and using the same arguments as in the derivation of (22.6), we write down an equation that determines the real part of the number y :

$$\operatorname{Re}(y) = \frac{1}{\pi} \left[C \left(\exp \frac{4v_1 \xi_2}{\pi(1-M)} - 1 \right) + D \left(1 - \exp \frac{4v_1 \xi_1}{\pi(1-M)} \right) \right]. \quad (22.11)$$

An analysis of this equation, based on the fact that $4/n(1 - M_2^2)$ and $4/(1 - M \pm \frac{2}{1})$ are positive, whereas $\xi_1 < 0$ and $\xi_2 > 0$, shows that the quantities in the parentheses have the same sign as v_1 . But then, recognizing that m , C , and D are also positive quantities, we can state that the real part of the number y has the same sign as v_1 .

If we turn to Eq. (22.9), it becomes obvious that the sign of the real part of y determines the phase shift between δE and \bar{p}_1 . In particular, a positive sign of $\operatorname{Re}(y)$ indicates that the phase shift between δE and \bar{p}_1 has a smaller absolute magnitude than $\pi/2$, whereas a negative value of $\operatorname{Re}(y)$ corresponds to a phase shift between $\pi/2$ and π .

Comparing this result with the excitation condition obtained in §12 for the first elementary process, we see that the two agree completely: the system becomes excited ($v > 0$) if the phase shift between δE and \bar{p}_1 has an absolute value smaller than $\pi/2$.

In exactly the same manner as in the foregoing case, we can extend this result to include the more general case by virtue of the

equality of the signs of $\text{Re}(\varphi_1/\varphi_2)$ and $\text{Re}(\varphi_2/\varphi_1)$.

The properties of the second elementary process could be obtained in exactly analogous fashion.

As can be seen from the material presented in the present section, the deductions obtained earlier in the analysis of the energy relations can be obtained also directly, by solving the characteristic equation. Comparing these two methods we must say that whereas the energy methods are somewhat simpler and possess great clarity, the solution of the characteristic equation yields not only the excitation conditions, but makes it possible to determine numerically the oscillation frequencies and the decrements (increments) of the attenuation (or growth) of the oscillations.

In particular, equating the real and imaginary parts of (22.10) to zero separately, we could write two equations that relate only real variables:

$$\begin{aligned} F_1(v_1; \omega_1) &= 0, \\ F_2(v_1; \omega_1) &= 0. \end{aligned}$$

Simultaneous solution of these two equations would make it possible to obtain pairs of values of v_1 and ω_1 satisfying the characteristic equation (22.10). This is not done here, since an analogous problem will be solved for the more general case somewhat later.

§23. Formulation and Solution of the Characteristic Equation

In order to illustrate the method for solving the problem of the stability of a gas stream of the type considered, we develop here the calculation scheme for one of the possible cases of excitation of acoustic oscillations by heat supply. In the example presented to the reader's attention, the fundamental factor is indeed the methodological aspect of the solution of the problem. As regards deductions of technical or physical character, which can be made from the analysis of

the solution obtained, they are more particular in character.

We consider the flow of gas in a tube, and assume that the zone of time-varying heat supply satisfies the necessary requirement and has already been reduced to a certain fictitious strong-discontinuity surface Σ . We use the same notation as in the preceding section, and let the boundary conditions again correspond to pressure nodes at the open ends of the tube:

$$\bar{p}_1(\xi_1) = 0; \quad \bar{p}_2(\xi_2) = 0.$$

Then, using the solution (4.13), we can write

$$\left. \begin{aligned} \bar{v}_1 \varphi_1(\xi_1) + \bar{p}_1 \varphi_1(\xi_1) &= 0, \\ \bar{v}_2 \varphi_2(\xi_2) + \bar{p}_2 \varphi_2(\xi_2) &= 0. \end{aligned} \right\} \quad (23.1)$$

Let the conditions on Σ be specified in the form

$$\left. \begin{aligned} \bar{v}_2 &= a_{11} \bar{v}_1 + a_{12} \bar{p}_1, \\ \bar{p}_2 &= a_{21} \bar{v}_1 + a_{22} \bar{p}_1. \end{aligned} \right\} \quad (23.2)$$

This form of notation differs from the canonical one. It can be obtained from Formulas (17.5) by assuming that the "cold" part of the stream is isentropic ($\bar{s}_1 = 0$) and that the quantities $\delta E'$ and $\delta X'$ which characterize the nonstationary combustion process can be represented in the form

$$\left. \begin{aligned} \delta E' &= b_{11} \bar{v}_1 + b_{12} \bar{p}_1, \\ \delta X' &= b_{21} \bar{v}_1 + b_{22} \bar{p}_1. \end{aligned} \right\} \quad (23.3)$$

The equations written out here must again be treated as a formal introduction of a certain feedback. The physical meaning of Formulas (23.3) reduces to the fact that the combustion process follows the changes in the pressure and velocity ahead of the combustion zone and, in particular, if \bar{p}_1 and \bar{v}_1 are subject to oscillation (if acoustic waves are produced) the combustion process acquires an oscillatory character. This formal notation will be made more specific later on.

Eliminating v_2 and \bar{p}_2 from the system (23.1) with the aid of

(23.2), we arrive at a characteristic equation in the form

$$\begin{vmatrix} \varphi_1(\xi_1) & \varphi_1(\xi_2) \\ a_{11}\varphi_1(\xi_1) + a_{21}\varphi_1(\xi_2) & a_{12}\varphi_1(\xi_1) + a_{22}\varphi_1(\xi_2) \end{vmatrix} = 0. \quad (23.4)$$

The functions φ_1 and φ_2 will be replaced by their expressions in accordance with Formulas (4.14), taking Relation (22.5) into account and introducing $\underline{l}_1 = -\xi_1$ and $\underline{l}_2 = \xi_2$ (in order to deal with positive quantities, namely the dimensionless lengths \underline{l}_1 and \underline{l}_2 of the cold and hot parts of the tube). After several transformations, which are left out here, we obtain the characteristic equation of the system in the following form*:

$$C_1 \exp\left(\frac{2l_1}{1-M_1} + \frac{2l_2}{n(1-M_1)}\right) \beta + C_2 \exp \frac{2l_1 \beta}{1-M_1} + C_3 \exp \frac{2l_2 \beta}{n(1-M_1)} + C_4 = 0, \quad (23.5)$$

where

$$\left. \begin{aligned} C_1 &= a_{11} - a_{12} - a_{21} + a_{22}, \\ C_2 &= -a_{11} + a_{12} - a_{21} + a_{22}, \\ C_3 &= a_{11} + a_{12} - a_{21} - a_{22}, \\ C_4 &= -a_{11} - a_{12} - a_{21} - a_{22}. \end{aligned} \right\} \quad (23.6)$$

It must be emphasized that the coefficients a_{11} , a_{12} , a_{21} , a_{22} entering into the expressions (23.2), and characterizing the processes in the combustion zone and their dependence on the acoustic oscillations, are assumed to be real. Then the numbers C_1 , C_2 , C_3 , and C_4 will also be real and will depend only on the properties of the heat-supply zone.

If we recognize that $\beta = \nu + i\omega$ then, by substituting the expression for β in (23.5) and separating the real and imaginary parts, we obtain a system of two equations for the determination of ν and ω :

$$\left. \begin{aligned} C_1 e^{(h_1+h_2)\nu} \cos(h_1+h_2)\omega + C_2 e^{h_1\nu} \cos h_1\omega + \\ + C_3 e^{h_2\nu} \cos h_2\omega + C_4 = 0, \\ C_1 e^{(h_1+h_2)\nu} \sin(h_1+h_2)\omega + C_2 e^{h_1\nu} \sin h_1\omega + \\ + C_3 e^{h_2\nu} \sin h_2\omega = 0. \end{aligned} \right\} \quad (23.7)$$

Here

$$h_1 = \frac{2l_1}{1-M_1}; \quad h_2 = \frac{2l_2}{n(1-M_1)}. \quad (23.8)$$

It is easy to verify that the solution of the system of transcendental equations (23.7) is practically impossible in general form. We present here a graphic analytic method of solving such a system.

We write down the system (23.7) in the form

$$\left. \begin{aligned} C_2 e^{h_1 v} \cos h_1 \omega + C_3 e^{h_2 v} \cos h_2 \omega &= \\ &= -C_4 - C_1 e^{(h_1+h_2)v} \cos (h_1+h_2) \omega, \\ C_2 e^{h_1 v} \sin h_1 \omega + C_3 e^{h_2 v} \sin h_2 \omega &= \\ &= -C_1 e^{(h_1+h_2)v} \sin (h_1+h_2) \omega. \end{aligned} \right\} \quad (23.9)$$

Squaring the left and right halves of these equations and adding them, we obtain

$$\begin{aligned} C_2^2 e^{2h_1 v} + 2C_2 C_3 e^{(h_1+h_2)v} \cos (h_1-h_2) \omega + C_3^2 e^{2h_2 v} = \\ = C_1^2 + 2C_1 C_4 e^{(h_1+h_2)v} \cos (h_1+h_2) \omega + C_1^2 e^{2(h_1+h_2)v}. \end{aligned}$$

Elementary transformations convert this relation into

$$\begin{aligned} [C_2^2 e^{(h_1-h_2)v} + C_3^2 e^{-(h_1-h_2)v}] - [C_1^2 e^{(h_1+h_2)v} + C_4^2 e^{-(h_1+h_2)v}] = \\ = 2[C_1 C_4 \cos (h_1+h_2) \omega - C_2 C_3 \cos (h_1-h_2) \omega]. \end{aligned} \quad (23.10)$$

The sought-for quantities v and ω are located here on opposite sides of the equal sign. Using this circumstance, we can readily plot in coordinates v and ω the curve defined by Eq. (23.10). For this purpose it is sufficient to plot the left half as a function of v , the right half as a function of ω , and transfer the points corresponding to Eq. (23.10) to the coordinate plane v, ω .

If we regard (23.9) as a system of linear inhomogeneous equations for the determination of the quantities $C_2 e^{h_1 v}$ and $C_3 e^{h_2 v}$, we can write

$$\begin{aligned} C_2 e^{h_1 v} &= \frac{1}{\Delta} \begin{vmatrix} -C_4 - C_1 e^{(h_1+h_2)v} \cos (h_1+h_2) \omega & \cos h_2 \omega \\ -C_1 e^{(h_1+h_2)v} \sin (h_1+h_2) \omega & \sin h_2 \omega \end{vmatrix}, \\ C_3 e^{h_2 v} &= \frac{1}{\Delta} \begin{vmatrix} \cos h_1 \omega & -C_4 - C_1 e^{(h_1+h_2)v} \cos (h_1+h_2) \omega \\ \sin h_1 \omega & -C_1 e^{(h_1+h_2)v} \sin (h_1+h_2) \omega \end{vmatrix}, \end{aligned}$$

where the determinant of the system is

$$\Delta = \begin{vmatrix} \cos h_1 \omega & \cos h_2 \omega \\ \sin h_1 \omega & \sin h_2 \omega \end{vmatrix} = \sin (h_2 - h_1) \omega.$$

After simple transformations we arrive at the following equations:

$$\left. \begin{aligned} C_2 e^{h_1 v} &= \frac{-C_4 \sin h_2 \omega + C_1 e^{(h_1+h_2)v} \sin h_2 \omega}{\sin (h_2 - h_1) \omega}, \\ C_3 e^{h_2 v} &= \frac{C_4 \sin h_1 \omega - C_1 e^{(h_1+h_2)v} \sin h_1 \omega}{\sin (h_2 - h_1) \omega}. \end{aligned} \right\} \quad (23.11)$$

These equations are valid, of course, only if

$$\Delta = \sin(h_2 - h_1)\omega \neq 0.$$

Multiplying the left and right halves of (23.11), respectively, we obtain after certain simplifications

$$C_1^2 e^{2(h_1 + h_2)v} + e^{(h_1 + h_2)v} \times \frac{C_2 C_3 \sin^2(h_2 - h_1)\omega - C_1 C_4 (\sin^2 h_1 \omega + \sin^2 h_2 \omega)}{\sin h_1 \omega \sin h_2 \omega} + C_1^2 = 0.$$

The last equation is quadratic in $e^{(h_1 + h_2)v}$, and consequently

$$e^{(h_1 + h_2)v} = \frac{f(\omega) \pm \sqrt{f^2(\omega) - 4C_1^2}}{2C_1}, \quad (23.12)$$

where

$$f(\omega) = \frac{C_2 C_3 \sin^2(h_2 - h_1)\omega - C_1 C_4 (\sin^2 h_1 \omega + \sin^2 h_2 \omega)}{\sin h_1 \omega \sin h_2 \omega}.$$

In the coordinates v, ω the equation (23.12) defines a certain curve, the plotting of which is an elementary operation.

The sought values of ω and v , satisfying the system (23.9), will be the coordinates of the points of intersection of the curves (23.10) and (23.12). We must point out here, however, a certain additional difficulty. In deriving Eqs. (23.10) and (23.12) it was necessary to carry out such operations as squaring and term-by-term multiplication of two equations. As a result the system of equations (23.10) and (23.12) yields not only the roots of the system (23.9), but also several superfluous roots which must be separated. The separation of the roots is best carried out by direct verification, substitution of the obtained graphical values of v and ω into the second equation of the system (23.7).

Let us give an example of such a calculation. Let $\underline{l}_1 = \underline{l}_2 = 0.5$, the air temperature prior to heating 288°K , after heating 1500°K , and the velocity of the cold stream 50 m/sec. The processes in the heat-supply are assumed such that $\underline{T}_1 = \underline{T}_2 = \underline{T}_3 = 0$ and the system can be excited only because of perturbations in the heat supply \underline{Q} . Then at

certain fixed properties of \bar{Q} , which will be indicated below, it is possible to make the calculations in accordance with the procedure described above.

Without carrying out any numerical calculations and intermediate constructions, we present immediately the plot from which the values of v and ω are determined. As was just demonstrated, these quantities can be determined as the points of intersection of curves in the v, ω plane, defined by Eqs. (23.10) and (23.12). We denote the former by $F(v, \omega) = 0$ and the latter by $f(v, \omega) = 0$.

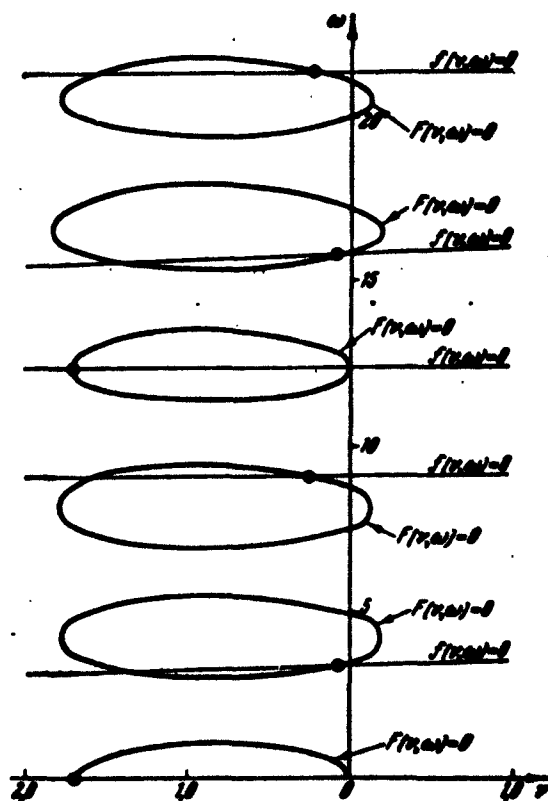


Fig. 33. Graphic method of determining the roots of the characteristic equation.

In Fig. 33 this construction has been given for the specific case under consideration. It must only be borne in mind that the branches $f(v, \omega) = 0$, which yielded superfluous roots, are omitted in Fig. 33.

In addition, inasmuch as reversal of the sign of ω does not change the system of initial equations (23.7), the construction was made for positive ω only. The points on the v, ω plane which represent solutions are designated by circles. The construction presented is of interest (and is typical) from two points of view. What is striking first of all is the fact that the oscillation frequencies that the system can maintain differ from the frequencies determined by the usual acoustic procedure. Indeed, in a cylindrical tube with two open ends the oscillations might appear to have the following periods: the maximum equal to the time necessary for the sound wave to move from the inlet to the outlet of the tube and back, and a series of periods amounting to $1/2$, $1/3$, $1/4$..., etc. of the maximum period (see §§5 and 6). If such a calculation is made for the case under consideration, it appears that the system should support the following series of frequencies:

$$\omega = 0; 4,11; 8,22; 12,33; 16,44; 20,55; \dots$$

The actual frequencies are

$$\omega = 0; 3,38; 9,1; 12,33; 15,7; 21,4; \dots$$

This singularity of the case under consideration is explained in the following way.

When a sound wave passes through the discontinuity surface Σ , some part of the wave is reflected and travels in the opposite direction. Consequently, the elementary considerations which lead to the customary acoustic rule are not applicable here. The complicated interference between the refracted and reflected waves, considering their reflections from both ends of the tube, yields the results in the second set of frequencies ω . Comparison of the two sets shows that the simple acoustic rule can be employed only in those cases when a rough estimate of the frequency is required.

Another singularity disclosed by this calculation is that the

different harmonics attenuate with different decrements. In the considered numerical example the closest to the stability limit ($\nu = 0$) were the first and fourth harmonics. As regards the aperiodic term ($\omega = 0$) and the third harmonic, these are the stablest. Therefore when a relatively small change takes place in the parameters of the surface Σ (small change in Q) the most probable is the occurrence of an oscillating instability with frequencies of the first and fourth harmonics.

Inasmuch as in real processes the higher harmonics are characterized, other conditions being equal, by an increased energy dissipation, in the case when instability sets in this system is most likely to oscillate with the frequency of the first harmonic (fundamental tone). Thus, the calculation presented allows us to understand how the oscillating system "chooses" the oscillation frequency.

§24. Construction of the Stability Limits

The solution presented in the preceding section for the characteristic equation of the problem under consideration was based on the fact that the processes in the heat-supply zone can be described by Eqs. (23.3). Let us consider the question of the properties of the heat-supply zone in greater detail. In order to simplify greatly the analysis of the excitation conditions, we assume that the quantities $\delta E'$ and $\delta X'$ depend on a single complex parameter; we have already introduced such a parameter, \bar{Y} , earlier. In specific cases this parameter can be, for example, the perturbation of the effective linear combustion velocity \bar{U}_1 , the perturbation of the heat-supply \bar{Q} , or the perturbation of some other quantity characterizing the nonstationary combustion. Let us settle on some specific assumption. Let, for example, this essential parameter be the perturbation of the heat supply \bar{Q} . Then Eqs. (17.4) allow us to write

$$\left. \begin{aligned} \delta E &= \delta_{11} \bar{Q} \\ \delta X &= \delta_{12} \bar{Q} \end{aligned} \right\} \quad (24.1)$$

Comparing these expressions with (23.3) we see that the dimensionless perturbation of the heat supply \bar{Q} can depend in explicit form on \bar{p}_1 and \bar{v}_1 :

$$\bar{Q} = Q_v \bar{v}_1 + Q_p \bar{p}_1. \quad (24.2)$$

But then Formulas (23.2), which are the consequence of Eqs. (17.5), can be rewritten in the form

$$\left. \begin{aligned} \bar{v}_1 &= (a'_{11} + a'_{11} Q_v) \bar{v}_1 + (a'_{12} + a'_{12} Q_p) \bar{p}_1 \\ \bar{p}_1 &= (a'_{21} + a'_{21} Q_v) \bar{v}_1 + (a'_{22} + a'_{22} Q_p) \bar{p}_1 \end{aligned} \right\} \quad (24.3)$$

Here $a'_{11} + a'_{11} Q_v = a_{11}$; ..., etc. It is seen from Formula (24.2) that Q is determined completely (for specified \bar{p}_1 and \bar{v}_1) by the coefficients Q_v and Q_p . We have previously chosen to determine the perturbation \bar{Q} in terms of its amplitude and its phase, but now we use the projections of the vector \vec{Q} on \vec{p}_1 and \vec{v}_1 . Both methods of writing down \bar{Q} can be employed with equal success. The previously employed method of specifying \bar{Q} (or \bar{Y} , etc.) in terms of the amplitude and the phase has the advantage of being more general. In some cases, however, when the dependence of the heat released on the state of the oscillating system is known, it is convenient to express this dependence in explicit form. Let, for example, the heat release \bar{Q} be a known function of the pressure and velocity

$$Q = Q(v_1; p_1)$$

and let it be independent of other parameters. Then, taking the variation of this expression and changing over to the adopted system of dimensionless variables, we can write

$$\bar{Q} = C_1 \frac{\partial Q}{\partial v_1} \bar{v}_1 + C_2 \frac{\partial Q}{\partial p_1} \bar{p}_1, \quad (24.4)$$

where C_1 and C_2 are certain constants.

Comparing Expressions (24.2) and (24.4), we see that the coefficients Q_v and Q_p are proportional to $\partial Q/\partial v_1$ and $\partial Q/\partial p_1$, i.e., they express a certain really existing dependence of the heat release on the stream velocity and on the pressure.

Let us consider the question of the stability limits when the properties of the discontinuity plane Σ are represented by Eqs. (24.3). We use for this purpose the measure employed in §19, namely we regard $\bar{v}_1, \bar{p}_1, \bar{v}_2, \bar{p}_2$ as vectors and take the scalar products of Eqs. (24.3) with each other. By virtue of the orthogonality of \bar{p} and \bar{v} , the products $\bar{p}\bar{v}$ vanish when $v = 0$, yielding the following connection between the coefficients Q_p and Q_v on the stability limit:

$$\bar{v}_1^2 (c_{11}' + c_{11}' Q_v) (c_{11}' + c_{11}' Q_v) + \bar{p}_1^2 (c_{11}' + c_{11}' Q_v) (c_{11}' + c_{11}' Q_v) = 0. \quad (24.5)$$

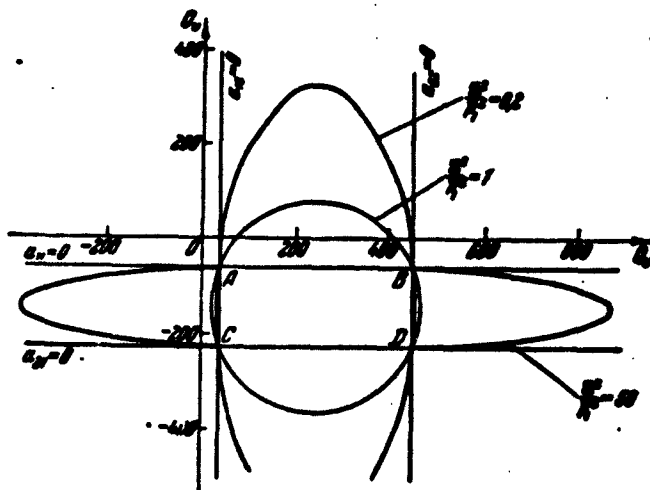


Fig. 34. Stability diagram in the plane of the variables Q_p and Q_v .

For each specified ratio \bar{v}_1^2/\bar{p}_1^2 , Eq. (24.5) corresponds to a second-order curve in the plane $(Q_p; Q_v)$. All these curves pass through the four points A, B, C, and D (Fig. 34), the coordinates of which are obtained by equating to zero the first and third, the second and fourth, etc., terms in parentheses in Eqs. (24.5), and the curves themselves lie inside the bands delineated by the lines parallel to the

coordinate axis and passing through these points. A more detailed numerical analysis shows that the family of curves is a family of ellipses, three of which are shown in Fig. 34, constructed for flows characterized by $M_1 = 0.1$; $M_2 = 0.25$.

The ellipses as shown in Fig. 34 must not be regarded under any circumstance as the stability limits. These ellipses, which are derived from energy considerations for constant \vec{p}_1^2/\vec{v}_1^2 and consequently with no account of boundary conditions, have only one important property: the point corresponding to the stability limit can lie only on the ellipses, and consequently, only on the boundaries of the vertical and horizontal strips delineated by the lines $a'_{11} + a''_{11}Q_v = 0$, ..., etc. (or, using the shorter notation, the lines $a_{11} = 0$, $a_{12} = 0$, $a_{21} = 0$, and $a_{22} = 0$).

Stability diagrams for the simplest cases. Being situated inside or on the boundaries of the obtained strips, the stability limits, constructed with account of the boundary conditions, can yield different configurations for the stability regions. Let us show this for the limiting cases. Let the length l_1 be negligibly small, i.e., let the entire tube be full of hot gases, and let the combustion occur at the inlet section. Then the boundary condition adopted above, $\vec{p}_1 = 0$, should be satisfied ahead of the combustion zone. This immediately leads to the vanishing of the second term of Eq. (24.5), and the only stability limits (regardless of the value of \vec{v}_1) will be the lines $a_{11} = 0$ and $a_{21} = 0$. The corresponding stability diagram is shown in Fig. 35a. Inasmuch as it is known that the origin corresponds to the stable mode, the instability region (the shaded part of the diagram) is determined immediately. The same figure (diagram b) shows for the sake of completeness the case when the boundary condition for $l_1 = 0$ has the form $\vec{v}_1 = 0$ (closed end). Then we obtain in precisely the same

manner the boundaries in the form of the equations $a_{12} = 0$ and $a_{22} = 0$ for all \bar{p}_1 .

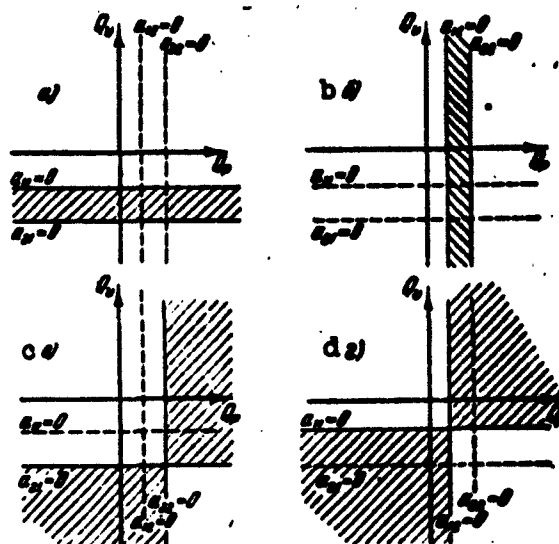


Fig. 35. Stability diagrams for the limiting cases.

Another limiting case will be a tube with negligibly small length of the hot portion of the stream: $\underline{l}_2 = 0$. Let us find the stability limits for the boundary condition $\bar{p}_2 = 0$. To this end we rewrite Eqs. (23.2) in the form

$$\left. \begin{aligned} \bar{v}_1 &= \frac{1}{\Delta} (a_{22}\bar{v}_2 - a_{12}\bar{p}_2), \\ \bar{p}_1 &= \frac{1}{\Delta} (-a_{11}\bar{v}_2 + a_{21}\bar{p}_2), \end{aligned} \right\} \quad (24.6)$$

where

$$\Delta = \begin{vmatrix} a_{11} & a_{12} \\ a_{21} & a_{22} \end{vmatrix}$$

and it is assumed that $\Delta \neq 0$. Taking, as before, the scalar product of Eqs. (24.6) by each other (we regard \bar{v} and \bar{p} as vectors), we obtain in lieu of (24.5):

$$\bar{v}_1 a_{11} \bar{v}_1 + \bar{p}_1 a_{11} \bar{p}_1 = 0, \quad (24.7)$$

from which we get immediately for $\bar{p}_2 = 0$ the stability limits for arbitrary \bar{v}_2 , namely $a_{21} = 0$ and $a_{22} = 0$. The corresponding type of sta-

bility diagram is shown in Fig. 35c. Unlike the diagrams of the type a and b, the instability region is located in this case not inside the strips, but encompasses completely two quadrants of the entire infinite plane of parameters Q_p and Q_v . As in the preceding case, we give for the sake of completeness the stability diagram corresponding to the boundary condition $\bar{v}_2 = 0$. Then for all \bar{p}_2 the boundaries of the stability region become the lines $a_{11} = 0$ and $a_{12} = 0$, which yields diagram d of Fig. 35.

We see from the foregoing example that the configuration of the stability regions can change in our case quite radically, depending on what the values of \bar{p}_1 , \bar{v}_1 , \bar{p}_2 , and \bar{v}_2 are in the heat-supply plane. Such a variety of configurations is connected, in particular, with the fact that the stability boundaries can go to infinity. If we construct analogous boundaries in the coordinate system employed in §19, then the cases $\bar{p}_1 = 0$ and $\bar{v}_1 = 0$ would give perfectly identical configurations of the instability region, namely circles. These circles are shown, for example, in Fig. 28. As regards the cases $\bar{p}_2 = 0$ and $\bar{v}_2 = 0$, in the coordinate system of §19 the instability regions would not have such simple boundaries. The point is that this system presupposes that the vectors $\vec{\bar{p}}_1$ and $\vec{\bar{v}}_1$ are oriented in the positive directions of the coordinate axis, whereas the position of the vectors $\vec{\bar{p}}_2$ and $\vec{\bar{v}}_2$ remains arbitrary. This and a few additional difficulties do not make it advantageous to analyze in detail the boundaries of this type.

The use of the variables Q_p and Q_v , while it does complicate the configuration of the stability boundaries, permits on the other hand a simplification of the analysis of the excitation conditions, as will be shown from the content of the next section.

Before we proceed to discussing the configuration of the stability boundaries in the plane of the parameters Q_p and Q_v with $\underline{1}_1$ and $\underline{1}_2$

simultaneously different from zero, let us point out one other property of the stability diagrams shown in Fig. 35.

When $Q_p \rightarrow \pm\infty$ or $Q_v \rightarrow \pm\infty$, the damping decrement (or growth increment) of the oscillations tends to zero. Thus, there exists, as it were, still another stability boundary at infinity. This can be demonstrated in various ways. We shall present here a proof of this statement by analysis of the characteristic equation of the system (23.7), which enables us to cast light in passing on still another question. We take, for example, the stability diagram shown in Fig. 35c. Putting $\underline{1}_2 = 0$ we obtain $h_2 = 0$ and Eqs. (23.7) assume the extremely simple form

$$\left. \begin{aligned} (C_1 + C_2) e^{h_1 v} \cos h_1 \omega + C_3 + C_4 &= 0, \\ (C_1 + C_2) e^{h_1 v} \sin h_1 \omega &= 0. \end{aligned} \right\} \quad (24.8)$$

It is obvious that the natural frequencies will be determined by the equation $\sin h_1 \omega = 0$. Without refining them further, we note only that in this case $\cos h_1 \omega = \pm 1$. Inasmuch as $e^{h_1 v}$ can be only positive, the sign of $\cos h_1 \omega$ will coincide with the sign of the ratio $-(C_3 + C_4)/(C_1 + C_2)$, making it possible to write

$$v = \frac{1}{h_1} \ln \left| \frac{C_3 + C_4}{C_1 + C_2} \right|.$$

Let us use the connection (23.6) between C_1 , C_2 , C_3 , and C_4 , on the one hand, and a_{11} , a_{12} , a_{21} , and a_{22} on the other, and also Formulas (24.3), so as to rewrite the last equation in the form

$$v = \frac{1}{h_1} \ln \left| \frac{(a_{11} + a_{12}) + a_{12} Q_v + a_{11} Q_p}{(a_{11} - a_{12}) - a_{12} Q_v + a_{11} Q_p} \right|. \quad (24.9)$$

Putting $v = 0$ (the condition for the existence of the stability limit) in (24.9), we readily obtain with allowance for (23.2) and (24.3) the already known stability limits $a_{21} = 0$ and $a_{22} = 0$, and in addition we have $Q_p = \pm\infty$ and $Q_v = \pm\infty$. This statement can be proved in exactly the same way for the other types of diagrams shown in Fig. 35.

Formula (24.9) enables us to point out a circumstance which is not always borne in mind. At certain combinations of Q_p and Q_v the numerator or denominator of the fraction under the absolute-value sign can vanish. This will correspond to $v \rightarrow +\infty$ or $v \rightarrow -\infty$. Thus, arguing formally, we can state that somewhere in the plane of the parameters Q_p and Q_v are located two lines which correspond to infinitely large stability or infinitely large instability of the stream. Actually, this is connected with the fact that the problem of the stream stability is regarded here, as everywhere in this book, without account of the initial conditions. But such an approach is valid only for those oscillation modes, for which one can assume that the instant of time under consideration is sufficiently removed from the initial instant of time, and as a result of the energy dissipation which is unavoidable in a real system, the influence of the initial conditions has been attenuated sufficiently. These assumptions can correspond only to modes of neutral and nearly neutral oscillations. On the other hand, if the solution of the problem yields values $v = \pm\infty$, then this merely indicates that it is necessary to take into account the initial conditions and the nonlinear properties of the system. If values $v = \pm\infty$ are obtained, it is possible to state, apparently, that the system becomes especially stable or especially unstable in the vicinity of the corresponding values of Q_p and Q_v .

If we take this stipulation into consideration and construct the lines $v = 0$ and $v = \pm\infty$ in the plane of the parameters Q_p and Q_v , then we obtain a perfectly symmetrical picture, as shown in Fig. 36. The lines $v = +\infty$ and $v = -\infty$ make angles of 45° to the coordinate axes, inasmuch as $a_{21}'' = a_{22}'' = b_{23}$. Precisely the same arguments can be carried out also for the diagrams a, b, and d of Fig. 35, drawing on them the lines $v = +\infty$ and $v = -\infty$. These lines make it possible to obtain a

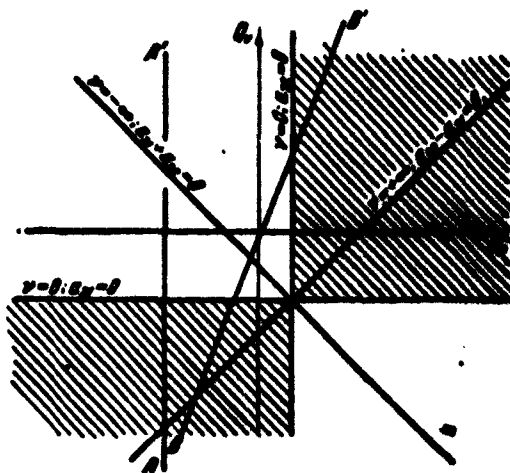


Fig. 36. Characteristic lines on the stability diagram.

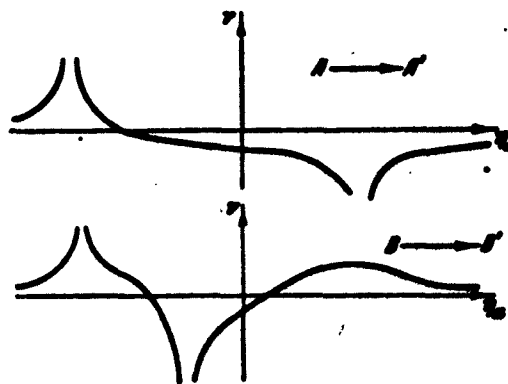


Fig. 37. Variation of the quantity ν during the course of motion along the lines AA' and BB' on Fig. 36.

qualitatively correct picture of the variation of ν on the entire parameter plane. If, for example, we assume that Q_p remains constant and Q_v changes (line AA' on Fig. 36), then the curve showing the variation of ν will have the form shown in the upper part of Fig. 37, and if we move along a certain line BB' , then the variation of ν as a function of the position of the representative point on the line BB' will have the form shown in the lower part of Fig. 37.

Stability limits for the general case. To construct the stability

limit in the general case it is advantageous to proceed in the following manner.

The coefficients C_1 , C_2 , C_3 , and C_4 contained in the system (23.7) are linear functions of Q_p and Q_v . In fact, these coefficients are made up of linear combinations of a_{11} , a_{12} , a_{21} , and a_{22} , which, as already indicated, are equal to

$$\left. \begin{aligned} a_{11} &= a'_{11} + a''_{11} Q_p, & a_{12} &= a'_{12} + a''_{12} Q_p, \\ a_{21} &= a'_{21} + a''_{21} Q_p, & a_{22} &= a'_{22} + a''_{22} Q_p. \end{aligned} \right\} \quad (24.10)$$

Therefore the system (23.7) can be represented as linear with respect to Q_p and Q_v , with coefficients that depend on v and on ω , which are regarded as the parameters of the system. Simple algebraic transformations enable us to write in place of (23.7) the following system:

$$\left. \begin{aligned} Q_p F_{11}(v, \omega) + Q_v F_{12}(v, \omega) &= F_{13}(v, \omega), \\ Q_p F_{21}(v, \omega) + Q_v F_{22}(v, \omega) &= F_{23}(v, \omega). \end{aligned} \right\} \quad (24.11)$$

Here the functions F_{ik} are sums of the form

$$a_1 e^{(h_1+h_2)v} \cos(h_1+h_2)\omega + a_2 e^{h_1 v} \cos h_1 \omega + a_3 e^{h_2 v} \cos h_2 \omega + a_4,$$

for the first equation of this system, and sums of the form

$$b_1 e^{(h_1+h_2)v} \sin(h_1+h_2)\omega + b_2 e^{h_1 v} \sin h_1 \omega + b_3 e^{h_2 v} \sin h_2 \omega$$

for the second equation (a_1 and b_1 are certain constant coefficients).

Fixing the values of v and ω , we can, generally speaking, obtain the values of Q_p and Q_v corresponding to them:

$$Q_p = \frac{\Delta_p}{\Delta}; \quad Q_v = \frac{\Delta_v}{\Delta}, \quad (24.12)$$

where

$$\begin{aligned} \Delta &= \begin{vmatrix} F_{11}(v, \omega) & F_{12}(v, \omega) \\ F_{21}(v, \omega) & F_{22}(v, \omega) \end{vmatrix}, \\ \Delta_p &= \begin{vmatrix} F_{13}(v, \omega) & F_{12}(v, \omega) \\ F_{23}(v, \omega) & F_{22}(v, \omega) \end{vmatrix}, \\ \Delta_v &= \begin{vmatrix} F_{11}(v, \omega) & F_{13}(v, \omega) \\ F_{21}(v, \omega) & F_{23}(v, \omega) \end{vmatrix}. \end{aligned}$$

When $\Delta = 0$ the system must be investigated further. If it turns out simultaneously that $\Delta_p = 0$ (or $\Delta_v = 0$) then, as is well known, Eqs.

(24.11) are linearly dependent and their aggregate determines not a point in the plane of the parameters (Q_p , Q_v), but a line. We shall consider this case in greater detail below.

If we disregard combinations of values of (v , ω) for which $\Delta = 0$, then each point in the plane (v , ω) will correspond to a point in the plane of the parameters (Q_p , Q_v). On moving along an arbitrary curve in the plane (v , ω), it is possible to obtain the corresponding curve in the plane of the parameters (Q_p , Q_v) with the aid of Eqs. (24.12).

In practice it is necessary to consider most frequently motion in the (v , ω) plane along lines parallel to the ω axis. These lines correspond to oscillation modes with constant values of v . It is possible to consider here, in particular, a mode with $v = v_1$ ($v_1 < 0$), i.e., with a constant damping decrement, the mode $v = v_2$ ($v_2 > 0$), i.e., with a constant growth increment, and finally, the mode $v = 0$, which is the stability limit. The last mode is usually of greatest interest. Inasmuch as $v = \text{const}$ in all these cases, the coefficients F_{1k} of the system (24.11) become for each of the corresponding curves in the (Q_p , Q_v) plane functions of only one parameter, the frequency ω .

By plotting a series of such curves for different $v = \text{const}$ and for all values of the frequencies $0 < \omega < \infty$ on each curve,* it is possible to obtain a complete and quite illustrative picture of the behavior of the oscillating system for arbitrary Q_p and Q_v .

The construction of these diagrams is simple, but rather tiresome. Recognizing that with increasing ω the losses in real systems increase appreciably, it is necessary to confine oneself in the calculations to some sensible value of ω . Usually, for some roughly specified upper limit of ω , the order of the expected frequencies can be estimated with sufficient accuracy.

In order to present a clear-cut notion of diagrams of this type,

let us consider one example of the construction. The example presented below is sufficiently typical, and is at the same time chosen such that the construction of the lines $v = \text{const}$ is possible without the tiring calculation of the coordinates of the points of these curves.

Let the heat-supply plane Σ be located in a section of the tube defined by the equation

$$h_1 = h_2 = h.$$

Then the system of equations (23.7) simplifies appreciably and assumes the form

$$\left. \begin{aligned} C_1 e^{2hv} \cos 2hw + (C_2 + C_3) e^{hv} \cos hw + C_4 &= 0, \\ \sin hw [2C_1 e^{2hv} \cos hw + e^{hv} (C_2 + C_3)] &= 0. \end{aligned} \right\} \quad (24.13)$$

Let us find the stability limit. For this purpose we investigate the system (24.13) with $v = 0$.

We consider first the special case $\sin hw = 0$. The value $\sin hw = 0$ corresponds to two possible values of $\cos hw$. When $\cos hw = 1$ we have from the first equation of (24.13)

$$C_1 + C_2 + C_3 + C_4 = 0, \quad (24.14)$$

or, in accordance with Formulas (23.6), $a_{21} = 0$, which gives on the basis of (24.10) the line

$$Q_1 = -\frac{a_{11}^2}{a_{21}^2}. \quad (24.15)$$

For $\cos hw = -1$ we have

$$C_1 - (C_2 + C_3) + C_4 = 0, \quad (24.16)$$

which leads after analogous transformations to $a_{12} = 0$, i.e.,

$$Q_2 = -\frac{a_{11}^2}{a_{12}^2}. \quad (24.17)$$

Let now $\sin hw \neq 0$. Then, dividing the second equation of (24.13) by this factor, we obtain by eliminating $\cos hw$ from the system (24.13) the following condition for the existence of the stability limit:

$$-C_1 + C_4 = 0, \quad (24.18)$$

or

$$a_{11} + a_{22} = 0. \quad (24.19)$$

Using Formulas (24.10), we write the equation of this line in the (Q_p, Q_v) plane

$$c_1 Q_p + c_2 Q_v + c_3 = 0. \quad (24.20)$$

It must be noted here that whereas the lines (24.15) and (24.17) are in their entirety stability limits, the same cannot be stated with respect to the line (24.20). The latter is connected with the fact that $\cos h\omega$ in Eqs. (24.13) cannot have an absolute value exceeding unity. Let us find the ends of the segment lying on the line (24.20) and belonging to the stability boundary of the system. The second equation of (24.13) assumes after dividing by $\sin h\omega$ and using (24.15) the following form

$$(C_1 + C_2) \cos h\omega + (C_3 + C_4) = 0.$$

As ω varies from zero to infinity the quantity $\cos h\omega$ will vary periodically from 1 to -1. At the extreme points, the values of $\cos h\omega$ equal to +1 or -1 will correspond to the equations

$$\begin{aligned} C_1 + C_2 + C_3 + C_4 &= 0, \\ C_1 + C_2 - (C_3 + C_4) &= 0. \end{aligned}$$

Comparing these equations with (24.14) and (24.16) we can readily see that the ends of the sought segment lie on the lines (24.15) and (24.17).

Consequently, the stability limits in the case under consideration will be the two straight lines parallel to the coordinate axes and an inclined segment lying between these lines.

It is useful to supplement the construction of the stability boundaries with construction of the lines of constant ν , analogous to the one given above.

It is only necessary to consider that when $\nu \neq 0$ we replace C_1 in all the formulas by $C_1 e^{2h\nu}$, and replace $C_2 + C_3$ by $(C_2 + C_3) e^{2h\nu}$.

performance of these calculations is quite elementary and will not be presented here. It is easy to visualize that in this case the lines of constant v in this example will be straight.

The diagram of the stability limits and of the lines of equal v for $e^{hv} = 1.1$ ($v > 0$) and $e^{hv} = 1/1.1$ ($v < 0$), constructed in accordance with the procedure indicated here, is shown in Fig. 38. The construction was carried out for $M_1 = 0.1$, $M_2 = 0.25$.

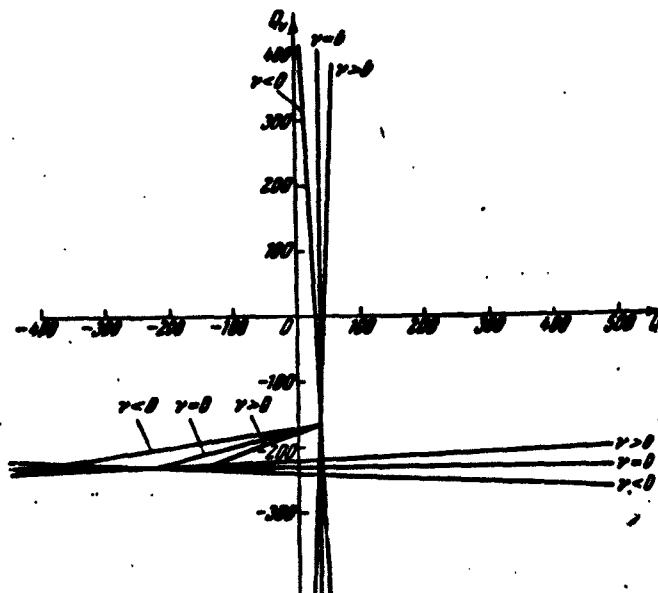


Fig. 38. Lines of equal v near the stability limit.

As can be seen from the presented diagram, the distribution of the regions of stability ($v < 0$) and instability ($v > 0$) recalls their distribution in Figs. 35c and d. Diagram 38 indicates one essential fact which must always be kept in mind. The lines of equal v (the three groups in Fig. 38 arbitrarily designated $v < 0$, $v = 0$, and $v > 0$) cross in the plane of the parameters of the oscillating system (Q_p , Q_v). Consequently, at the point of intersection of the lines $v > 0$ and $v < 0$ the system should be simultaneously unstable and stable, while at the point of intersection of the lines $v = 0$ and $v > 0$ it should be

simultaneously neutral and unstable, etc. This conclusion does not contain an unresolvable contradiction, as might appear at first glance. The point is that the intersecting lines correspond to different frequencies, and the fact that one harmonic can be more stable for specified Q_p and Q_v while the other can be less stable is almost obvious. An example of this is shown, in particular, in Fig. 38. Were we to plot in lieu of Fig. 38 a three-dimensional diagram with the frequency ω plotted along the third axis, then the lines of equal ν would not intersect but would pass over one another at different heights (at different ω). To be able to judge which frequencies correspond to the points on the equal-decrement lines, it is useful to mark the frequencies along these lines. No such marking is done on Fig. 38, but the reader can fill this gap without difficulty, if he recognizes that the line drawn along the Q_v axis was obtained for $\sin h\omega = 0$ and $\cos h\omega = -1$; the line along the Q_p axis was obtained for $\sin h\omega = 0$ and $\cos h\omega = 1$, while the group of the inclined lines was obtained for all other ω .

One must not think that in order to separate the stability regions from the instability regions it is necessary to plot in addition to the $\nu = 0$ lines also the $\nu > 0$ and $\nu < 0$ lines. Such a more limited result can be obtained also in simpler fashion, by using the so-called shading rule. This rule is frequently used in the theory of automatic control, where it is sometimes called the method of D-decomposition of the parameter space of the system. Although this method is used in control theory for a characteristic equation in the form of a polynomial, it remains valid also for transcendental equations. Those who wish to become better acquainted with this method had best go to the special literature.* We shall give only a brief idea of this method and indicate the practical ways of employing it.

The mathematical foundation of the shading rule described below can be developed as follows. Equations (24.11), which may be briefly written as

$$\left. \begin{aligned} R(Q_p, Q_v, v, \omega) &= 0, \\ I(Q_p, Q_v, v, \omega) &= 0, \end{aligned} \right\} \quad (24.21)$$

can be regarded as the equations for the transformation of a certain region in the (v, ω) plane into a region in the (Q_p, Q_v) plane, and vice versa. The (v, ω) plane is shown on the left of Fig. 39. To each point of this plane corresponds a completely defined state of the oscillating system (more accurately, a defined frequency and a rate of buildup or attenuation of the oscillations). On the right is shown the plane of the system parameters (Q_p, Q_v) , each point of which determines a certain process in the heat-supply zone.

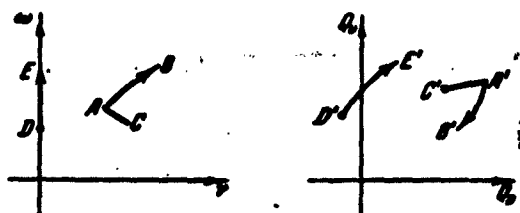


Fig. 39. Mapping of the plane (v, ω) on the parameter plane (Q_p, Q_v) .

Assume that the system (24.21) has a certain solution, for example, that when $Q_p = Q_p^A$ and $Q_v = Q_v^A$ oscillations occur with $v = v_A$ and $\omega = \omega_A$. Corresponding to the first pair of points is the point A' in the plane (Q_p, Q_v) , while the second pair corresponds to the point A on the plane (v, ω) . We can therefore say that the point A' corresponds to the point A and vice versa. If we vary v and ω continuously, moving for example along the curve AB on the (v, ω) plane, then the corresponding point in the (Q_p, Q_v) plane will also be displaced and move along a certain curve $A'B'$. This enables us to state that the curve $A'B'$ is the mapping of the curve AB . In courses of mathematical

analysis one proves a theorem according to which a unique expression of Q_p and Q_v as functions of v and ω is possible only if the functional determinant

$$\Delta = \begin{vmatrix} \frac{\partial R}{\partial Q_p} & \frac{\partial R}{\partial Q_v} \\ \frac{\partial N}{\partial Q_p} & \frac{\partial N}{\partial Q_v} \end{vmatrix}. \quad (24.22)$$

differs from zero. It turns out here that the sign of the determinant (24.22) plays an important role. Assume that in addition to the curve AB, there is given in a small vicinity of the point A in the (v, ω) plane another segment AC, which lies to the right of the curve AB, if one moves from A to B. Corresponding to the segment AC is the segment A'C' in the (Q_p, Q_v) plane. If $\Delta > 0$, then the transformation (24.21) has that property that the segment A'C' will lie also to the right of A'B' (motion from A' to B'). On the other hand, if $\Delta < 0$, then the transformation (24.21) will change the position of the point C' which will then be oriented in a manner opposite to C: if C lies to the right of AB, then C' will lie to the left of A'B'.

This property of the transformation (24.21) can be used in the following fashion. We choose as the curve whose mapping in the plane (Q_p, Q_v) is desired, the ordinate axis in the (v, ω) plane. On moving from the point D to the point E in the (Q_p, Q_v) plane, we obtain the segment of the curve D'E'. Assume, for the sake of being definite, that $\Delta > 0$ for all the values of ω under consideration. We can then argue as follows. On the line DE the system is neutral ($v = 0$); consequently the line D'E' is the stability limit in the parameter plane (Q_p, Q_v) . To the right of the line DE lies the region $v > 0$ (instability). Consequently, to the right of D'E' there will be a region of the parameters Q_p and Q_v , at which the oscillating system will be unstable. Were we to have $\Delta < 0$, the instability region would lie to the left of

D'E'.

The considerations advanced here enable us to formulate the following shading rule. We shall set $v = 0$ in (24.21) and vary ω from $-\infty$ to $+\infty$ and find for each value of ω the corresponding point in the parameter plane (Q_p, Q_v) . The totality of these points determines a curve on which the direction of motion will be specified (from the points with small ω to the points with large ω). Let us agree to shade the right side of this curve if $\Delta > 0$ and the left side if $\Delta < 0$.** This will lead, in accordance with the statements made above, to a situation whereby the vicinity of the stability limit corresponding to $v > 0$ (instability) will be shaded.

Further consideration of the question of shading the stability boundary and, in particular, the case $\Delta = 0$, is best carried out not on the basis of the rather general equations (24.21), but by writing down these equations for the investigated case (24.11). What is essential in this case is that the quantities Q_p and Q_v enter into these equations linearly. The functional determinant (24.22) will in this case be equal to

$$\Delta = \begin{vmatrix} F_{11}(0, \omega) & F_{12}(0, \omega) \\ F_{21}(0, \omega) & F_{22}(0, \omega) \end{vmatrix}, \quad (24.23)$$

i.e., it will coincide with the determinant of the system (24.11) which is linear (with respect to Q_p and Q_v). In those cases when $\Delta = 0$ and furthermore $\Delta_p = 0$ (or $\Delta_v = 0$), the equations of the system (24.11) become linearly dependent and, as already indicated above, they define not points but straight lines in the (Q_p, Q_v) plane. We shall call these lines the singular lines. If $\Delta = 0$ and Δ_p or Δ_v differ from zero, this means that the stability boundary in the (Q_p, Q_v) plane goes to infinity.

(Inasmuch as the functions F_{1k} contained in (24.23) are continuous

functions of ω , Δ is also a continuous function of ω and consequently we can reverse sign only by going through zero. Therefore the shading of the curve, referred to above, can change only when the line encounters a singular line or when it goes to infinity. The shading of singular lines is in accordance with the shading of the curves.

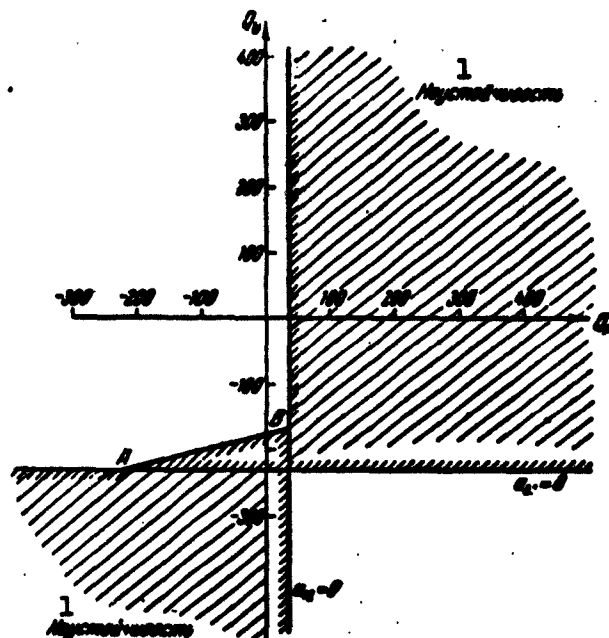


Fig. 40. Stability-limit diagram corresponding to the case shown in Fig. 38.
1) Instability.

Let us illustrate the statements made above by using as an example the diagram of Fig. 38. As can be verified from Formulas (24.13), (23.6), and (24.10), in this case the singular lines are $a_{21} = 0$ and $a_{12} = 0$, while for the remaining values of ω all the points of the stability boundary lie on the straight line AB (Fig. 40). Numerical calculation shows that the value $\omega = 0$ corresponds to the point A on Fig. 40; as ω increases, the representative point moves toward B and when $h\omega = \pi$ it goes over into the point B. Here the determinant Δ , which was positive during the motion from A to B, vanishes, and with further increase of ω it becomes negative. The representative point

moves then from B to A; after the representative point reaches A it again moves toward B, etc. Whenever the point moves from A to B we have $\Delta > 0$ and during the motion from B to A we have $\Delta < 0$. It is obvious that the lower part of the segment AB should be shaded. At the point A the singular line $a_{21} = 0$ has a common point with the line AB and at this point the shadings of AB and of $a_{21} = 0$ are compatible. This compatibility is clear from the figure. The singular line $a_{12} = 0$ is shaded in accordance with the character of the shading of the line AB at the point B.

As a result we obtain the picture shown in Fig. 40. The regions into which the shading is directed correspond to instability. A comparison of the diagrams shown in Figs. 38 and 40 shows that they are in complete agreement. Thus, the shading rule makes it possible to construct the stability-region diagram without finding the lines of equal values of v .

It must be pointed out that such a simple configuration of the diagram was the result of the fact that the necessary position of Σ along the tube, namely $h_1 = h_2$, was specified. In the general case the picture is much more confusing, although the construction and the shading of the stability boundaries is just as simple.

§25. Analysis of the Excitation Conditions

In the preceding section we have considered in detail the question of the configuration of the stability and instability regions in the plane of the parameters Q_p and Q_v of the oscillating system. It is clear, however, that to be able to point out the desirable or, to the contrary, the dangerous combinations of Q_p and Q_v yields relatively little if one does not know how these quantities are expressed in terms of the quantities that are familiar to the designer of the combustion chamber (or of some other device).

We shall present below an example of the analysis of excitation conditions, based on the preceding results, as applied to the excitation of oscillations in a system consisting of combustion chambers of a specific type to which an inlet and an exhaust tube are attached.

Let the combustion region σ , which is then mentally reduced to a discontinuity surface Σ , have the following properties. Ahead of the zone σ pure air flows in the tube, while inside the region σ there are located nozzles which atomize the fuel. The fuel is instantaneously distributed over the zone σ and is instantaneously burned. Inasmuch as the pressure at which the fuel is applied is quite high, and the pressure oscillations in the stream are relatively insignificant, the flow of fuel through the nozzles is constant and is dependent on neither the pressure of the surrounding medium nor the stream velocity. This idealization is admittedly quite crude, if for no other reason than that it does not take into account the time necessary for the mixture formation, evaporation of the fuel, the delay time of the ignition, etc. The influence of such a delay will be investigated later on. As regards the scheme assumed for the process inside σ , its extreme simplicity enables us to carry through the analysis of the case under consideration to conclusion.

Inasmuch as the consumption of fuel is completely independent of the state of the oscillating system, and inasmuch as the influence of the delay is not considered here, a nonzero perturbation of the heat supply \bar{Q} can occur only as a result of the perturbation of the completeness of combustion of the fuel injected into the stream. Experiments have shown that the completeness of combustion depends little on the pressure of the medium, provided this pressure deviates insignificantly from normal. In the combustion of a mixture in an open tube, the pressure actually fluctuates relatively little (by fractions of an

atmosphere), so that we shall neglect henceforth the influence of pressure on the completeness of combustion. The stream velocity is a more significant parameter. Frequently the increase in the stream velocity leads, once a certain value is exceeded, to a noticeable decrease in completeness of combustion. In the limit, upon sufficient increase in the stream velocity, the so-called collapse of the flame can occur and combustion ceases completely. The greatest influence on the completeness of combustion is exerted usually by the excess-air coefficient α (the ratio of the actual amount of air per unit mass of mixture to the amount of air which is theoretically necessary for complete combustion of the fuel contained in it). We thus assume that

$$\eta_{kr} = \eta_{kr}(\bar{v}_1, \alpha)$$

and consequently

$$\delta \eta_{kr} = \frac{\partial \eta_{kr}}{\partial \bar{v}_1} \delta \bar{v}_1 + \frac{\partial \eta_{kr}}{\partial \alpha} \delta \alpha.$$

Going over to the dimensionless system of variables (4.8), we can write

$$\bar{\eta}_{kr} = \frac{\frac{\partial \eta_{kr}}{\partial \bar{v}_1}}{\eta_{kr}} \bar{v}_1 + \alpha \frac{\frac{\partial \eta_{kr}}{\partial \alpha}}{\eta_{kr}} \bar{\alpha} \quad (\bar{\alpha} = \delta \alpha / \alpha, \bar{\eta}_{kr} = \delta \eta_{kr} / \eta_{kr}). \quad (25.1)$$

By definition, α is directly proportional to the mass of the air entering into the combustion zone (since the consumption of fuel remains unchanged)

$$\alpha = k \bar{v}_1 \bar{v}_2,$$

where k is a certain constant. It is obvious that

$$\bar{\alpha} = \bar{v}_2 + \frac{\bar{v}_2}{\bar{M}_1}.$$

As already mentioned earlier, the cold flow can be regarded as isentropic ($\bar{S}_1 = 0$). Then $\bar{P}_1 = \bar{p}_1$ (4.9) and the formula for $\bar{\eta}_{sg}$ can be written in final form

$$\bar{\eta}_{kr} = \left(\eta_M + \frac{\alpha}{\bar{M}_1} \eta_a \right) \bar{v}_1 + \alpha \eta_a \bar{P}_1. \quad (25.2)$$

where

$$\eta_M = \frac{\frac{\partial Q_p}{\partial M}}{\eta_{sg}}, \quad \eta_\alpha = \frac{\frac{\partial Q_p}{\partial \alpha}}{\eta_{sg}}.$$

The fuel fed directly to the combustion zone produces a term \bar{Q}^* in the equations (15.7). If the fuel entering into the zone σ per unit time and per unit stream cross section has a chemical energy Q_{khim} , which burns with an average completeness of combustion η_{sg} , then $Q^* = \eta_{sg} Q_{khim}$. Therefore, taking (15.8) into account, we have

$$\bar{Q}^* = \frac{\partial Q^*}{\partial \sigma} = \frac{\eta_{sg} Q_{khim}}{\sigma^2} \bar{\sigma}.$$

or, in terms of \bar{Q} (16.1),

$$\bar{Q} = B \eta_{sg}, \quad (25.3)$$

where

$$B = \frac{2M \eta_{sg} Q_{khim}}{\sigma^2}.$$

Comparing Formulas (24.2), (25.2), and (25.3), we can state that in the case under consideration

$$\left. \begin{aligned} Q_p &= B \eta_{sg}, \\ Q_v &= B \left(\eta_M + \frac{\sigma}{M} \eta_\alpha \right). \end{aligned} \right\} \quad (25.4)$$

Thus, the quantities Q_p and Q_v turn out to be functions of two partial derivatives, the completeness of combustion relative to the excess-air coefficient α , and the completeness of combustion relative to the M number of the air stream incident on the combustion zone.

In order to consider the influence of these two partial derivatives on the oscillation-excitation process, it is necessary first to have stability diagrams in the plane of the parameters of the oscillating system (Q_p , Q_v). Such diagrams were constructed in the preceding section. At this point it is sufficient to indicate that in most cases they have a form analogous to the diagrams of Fig. 36. Such a form is possessed, for example, by the stability diagram constructed

for frequencies close to the fundamental tone of the oscillating system when the cold and heated portion of the stream have equal lengths.

1) We therefore use the diagram indicated here for further analysis of the process of excitation of acoustic oscillations.

We shall analyze the influence of η_α and η_M on the oscillating system separately. Let first $\eta_\alpha = 0$. Then Eqs. (25.4) yield

$$Q_p = 0; \quad Q_v = B\eta_M.$$

In the diagram of Fig. 36 this corresponds to motion of the representative point along the ordinate axis, wherein Q_v turns out to be directly proportional to η_M . The corresponding plot showing the variation of v is given in the upper part of Fig. 37. As can be seen from the plot (on which a scale for η_M is given), the system becomes unstable at a certain negative value of Q_v , i.e., at a certain $\eta_M < 0$.

Let now $\eta_M = 0$. We then have from (25.4)

$$Q_p = B\eta_\alpha; \quad Q_v = \frac{B\eta_\alpha}{M_1}.$$

Hence

$$Q_v = Q_p / M_1. \quad (25.5)$$

Thus, when η_α changes the representative point moves in the (Q_p, Q_v) plane along the line (25.5). Corresponding to this is motion along the line BB' on the diagram of Fig. 36 and the plot showing the variation of v and given in the lower part of Fig. 37.

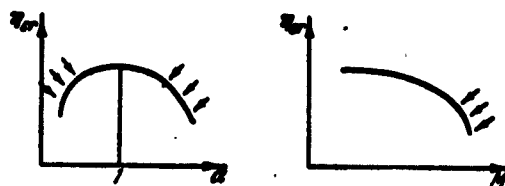


Fig. 41. Regions in which the excitation of the system is most probable (marked with arrows).

The origin on the diagram of Fig. 36 corresponds to $\eta_\alpha = 0$, while

positive η_α correspond to motion in the direction from B to B'. This leads to a connection between η_α and v as shown in Fig. 37, from which we can see that the only time when the system cannot be excited is when η_α is close to zero. When η_α has sufficiently large absolute value (irregardless of the sign), the oscillating system can be excited.

Thus, the oscillating system will be excited at sufficiently large absolute values of $\eta_M < 0$, $\eta_\alpha < 0$, and $\eta_\alpha > 0$.

If we turn to the dependence of the completeness of combustion on M_1 and on α , then the corresponding curves will have the form shown arbitrarily in Fig. 41. The arrows indicate the regions of most probable occurrence of oscillations: $\eta_\alpha > 0$, $\eta_\alpha < 0$, $\eta_M < 0$. It can be seen from these plots that excitation of oscillations is most probable if the mixture is enriched to $\alpha < 1$ or when the mixture is very lean, $\alpha \gg 1$. It must be pointed out that the first of these possibilities is apparently the more essential. This is connected with the fact that when the mixture is enriched the completeness of combustion decreases more steeply than when the mixture is made lean. In addition, in the region of rich mixtures the coefficient B, which is proportional to the fuel energy Q_{khlm} entering into the combustion zone per unit time, assumes likewise a greater significance.

The qualitative results obtained here are on the whole in satisfactory agreement with the experimental data. Insofar as can be judged from several experiments, vibration combustion actually occurs when the combustion zone is over-enriched and in many cases it is possible to observe its connection with the decrease in the completeness of combustion as the mixture becomes richer.

It is easy to analyze, in exactly the same manner as before, the influence exerted on the possibility of excitation of oscillations by the connection between the completeness of combustion and the M number

of the stream entering into the combustion zone. This factor, however, is probably of secondary significance, inasmuch as a noticeable influence of the stream velocity on the completeness of combustion manifests itself as a rule at modes that are remote from those prevailing under operation. In addition, the quantity η_M enters into the expression (25.4) for Q_v with a factor equal to unity, whereas η_α enters with a larger factor (α/M_1).

The analysis presented here was aimed at giving a very simple example of developing the problem until quantities are derived which are customary in the theory of combustion, so that a better idea of the physical nature of the excitation process is afforded. At the same time, it must be kept in mind that the example considered far from covers the entire problem dealing with the conditions under which acoustic oscillations are excited by combustion.

To conclude the present section, two remarks are in order. The first reduces to the following. We have already pointed out many times the role assumed by feedback in the investigated phenomenon. The example considered enables us to indicate a very important feedback mechanism, consisting of the fact that the acoustic oscillations brought about by the oscillating heat delivery lead to oscillations in the flow of air in the region where the nozzles are located. As a result, the excess-air coefficient oscillates, which in turn causes oscillations in the completeness of combustion, i.e., the heat delivery.

The second remark pertains to the validity of the idealized scheme of the process in the combustion zone as assumed in the present section. The partial derivatives η_M and η_α contained in Formulas (25.4) cannot be obtained, strictly speaking, from experiments carried out in the usual fashion. The point is that when the experimenter records the dependence of the completeness of the combustion on α or on M , he goes

through a series of stationary modes with different fixed values of these parameters. It is possible to extend the regularities determined in this manner (of the type plotted in Fig. 41) to a patently nonstationary process such as vibration combustion only under certain stipulations and for purely qualitative considerations. The static characteristics apparently display correctly, in general, the main tendency namely the deterioration of the completeness of combustion upon moving away from $\alpha = 1$.*

If an attempt is made to determine what new information is obtained by taking into account the nonstationary nature of the combustion process, then there arises in first order the natural tendency of taking into account the unavoidable delay of the ignition of the fuel. This delay is due to the time necessary to evaporate and mix the fuel with the air, the ignition delay time, etc. An account of this delay can be carried out relatively simply. In order to demonstrate the procedure of this account, let us consider a simple example.

§26. Influence of the Delay of the Heat Release on the Excitation of Acoustic Oscillations

In the preceding section we analyzed one of the possible cases of excitation of acoustic oscillation by combustion. The analysis was carried out without taking into account the delay in the heat release. It is possible to return to this case and to disclose the new information that is yielded by an account of the delay. It is more advantageous, however, to consider a second example, one in which the role that can be played by the delay of ignition is most clearly pronounced. By way of such an example we consider a system which, unlike the one described above, is not excited at all in the absence of the delay.

Let the heat-supply plane Σ lie in the inlet cross section, i.e., let $l_1 = 0$. Then the combustion products will occupy the entire length

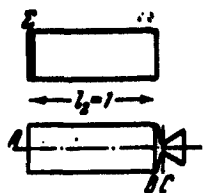


Fig. 42. Idealized scheme of liquid-fuel jet engine.

of the tube, corresponding to $\frac{1}{2} = 1$ (Fig. 42). We formulate the boundary conditions as follows: velocity nodes are located at the inlet and outlet of the tube. Such boundary conditions can be regarded, for example, as a first approximation to the real boundary conditions observed in combustion chambers of liquid-fuel jet engines. The lower part of Fig. 42 shows a diagram of a typical chamber of such an engine. To the left, at the so-called head of the chamber A, are located nozzles which feed the fuel components — the combustible material and the oxidizer, while in the right part of the combustion chamber is located a Laval nozzle. It is obvious that the solid wall A does not permit vibrations of the stream velocity at the left end of the cylindrical portion of the chamber (we assume the rate of flow of the fuel components to be constant). On the right, at the critical section C of the Laval nozzle, the stream velocity is always equal to the velocity of sound. If we disregard the possible fluctuation in the velocity of sound itself, we can assume that a constant stream velocity is maintained at the section C. When the distance from B to C is small, this causes the stream velocity at section B also to be constant. This leads to a formulation for the second boundary, namely that there be no velocity oscillations in the right end section (B) of the cylindrical part of the combustion chamber. We note that the fact that the boundary conditions which we have written out are close to the boundary conditions for a liquid-fuel jet engine combustion chamber does not mean that we are about to present a stability analysis of the working process in such an engine. This will be the subject of a special section in the book later on. It is probably not out of order to mention here that the instability of combustion in a liquid-fuel jet engine is connected primarily with the

perturbation in the mass flow and not in the heat supply.

We shall describe the process of perturbed heat supply in a plane Σ which coincides with the section A on Fig. 42, by means of Eqs. (17.5) with account of the condition $\bar{s}_1 = 0$ and Formulas (24.1) and (24.2), i.e., we assume that in the heat-supply region there are only perturbations in the influx of heat and there are no oscillations of the flame front, etc. We also take it into account that $\bar{v}_1 = 0$ in accordance with the boundary condition. Then the conditions on the plane Σ are written in the form

$$\left. \begin{aligned} \bar{v}_2 &= a_{12}\bar{p}_1 + a_{13}Q_p\bar{p}_1, \\ \bar{p}_2 &= a_{22}\bar{p}_1 + a_{23}Q_p\bar{p}_1, \end{aligned} \right\} \quad (26.1)$$

where a_{12} , a_{13} , a_{22} , and a_{23} are certain constants. We must stipulate immediately that this notation is valid only when the change in the combustion process follows instantaneously the change in the pressure \bar{p}_1 . If the combustion process lags the pressure \bar{p}_1 acting on it by a time $\Delta\tau$, then it is necessary to write in place of the equations (26.1) some other equations. The first terms in the right halves of these equations do not change, but the second terms, which are connected with the perturbation of the heat supply, must be chosen to correspond to an instant separated from the instant under consideration by a time $\Delta\tau$. This can be written as follows:

$$\left. \begin{aligned} \bar{v}_2(\tau) &= a_{12}\bar{p}_1(\tau) + a_{13}Q_p\bar{p}_1(\tau - \Delta\tau), \\ \bar{p}_2(\tau) &= a_{22}\bar{p}_1(\tau) + a_{23}Q_p\bar{p}_1(\tau - \Delta\tau). \end{aligned} \right\} \quad (26.2)$$

(The quantities τ and $\tau - \Delta\tau$ in the parentheses indicate the instant of time for which the variables are taken.)

As is known from the foregoing, in the formulation of the problem as used here all the perturbed quantities vary in proportion to $e^{\beta\tau}$. Therefore Formulas (26.2) can be rewritten in the following form ($\bar{v}_{20} = \bar{v}_2$ when $\tau = 0$, etc.):

$$\left. \begin{aligned} \bar{v}_{20} e^{\beta \tau} &= a_{12} \bar{p}_{10} e^{\beta \tau} + a_{13} Q_p \bar{p}_{10} e^{\beta(\tau - \Delta \tau)}, \\ \bar{p}_{20} e^{\beta \tau} &= a_{22} \bar{p}_{10} e^{\beta \tau} + a_{23} Q_p \bar{p}_{10} e^{\beta(\tau - \Delta \tau)}. \end{aligned} \right\} \quad (26.3)$$

We note that we do not always designate β and τ with the subscripts "one" or "two." The point is that, although the time scales in the cold and hot portions of the stream are different (since they depend on the velocity of the sound) and it is therefore necessary to distinguish between β_1 and β_2 or τ_1 and τ_2 , the product $\beta\tau$ is independent of the chosen time scale, for the time unit is contained in the denominator of one of these factors and in the numerator of the other. Canceling the factor $e^{\beta\tau}$ from both equations in (26.3), we write the conditions on Σ , with allowance for the delay, in the final form:

$$\left. \begin{aligned} \bar{v}_{20} &= a_{12} \bar{p}_{10} + a_{13} Q_p \bar{p}_{10} e^{-\beta \Delta \tau}, \\ \bar{p}_{20} &= a_{22} \bar{p}_{10} + a_{23} Q_p \bar{p}_{10} e^{-\beta \Delta \tau}. \end{aligned} \right\} \quad (26.4)$$

In writing out these equations, we already used the first boundary condition ($\bar{v}_1 = 0$). The second boundary condition, namely $\bar{v}_2 = 0$ when $\xi = \underline{1}_2 = 1$, yields, on the basis of the first formula of (4.13),

$$v_{20} \Phi_1(1) + p_{20} \Phi_2(1) = 0.$$

Substituting into the last equation \bar{v}_{20} and \bar{p}_{20} from (26.4) we obtain after several simplifications

$$\begin{aligned} &(a_{12} + a_{13} Q_p e^{-\beta \Delta \tau}) \left(1 + \exp \frac{2\beta_1}{1-M_1} \right) + \\ &+ (a_{22} + a_{23} Q_p e^{-\beta \Delta \tau}) \left(1 - \exp \frac{2\beta_1}{1-M_1} \right) = 0. \end{aligned} \quad (26.5)$$

(We shall henceforth leave out the subscript "2" for β for the sake of simplicity.)

It must be emphasized that the conditions (26.4) on Σ with account of delay, unlike the conditions on Σ for cases when the time delay is disregarded, become dependent on the complex frequency β . This circumstance makes it difficult to solve the characteristic equation. In par-

ticular, the method developed in §23 turns out to be inapplicable, since the coefficients C_1 , C_2 , C_3 , and C_4 in (23.5) become functions of the complex frequency β . In this case Relations (23.7) are incorrect, since they were obtained under the assumption that C_1 , C_2 , C_3 , and C_4 are real.

Let us rewrite (26.5) in the form

$$Q_p e^{-i\omega\Delta\tau} = - \frac{a_{11} \left(1 + \exp \frac{2\beta}{1-M_1} \right) + a_{22} \left(1 - \exp \frac{2\beta}{1-M_1} \right)}{a_{12} \left(1 + \exp \frac{2\beta}{1-M_1} \right) + a_{21} \left(1 - \exp \frac{2\beta}{1-M_1} \right)} = \\ = A(\beta) + iB(\beta),$$

where $A(\beta)$ and $B(\beta)$ are real quantities. On the stability limit we have $\beta = i\omega$ and then the equation written out breaks up into two which relate only real variables

$$\left. \begin{aligned} Q_p \cos \omega\Delta\tau &= A(\omega), \\ Q_p \sin \omega\Delta\tau &= -B(\omega). \end{aligned} \right\} \quad (26.6)$$

From this we obtain directly

$$\left. \begin{aligned} \omega\Delta\tau &= \arctg \left[-\frac{B(\omega)}{A(\omega)} \right] + k\pi, \\ Q_p &= \frac{A(\omega)}{\cos \omega\Delta\tau}, \end{aligned} \right\} \quad (26.7)$$

where k are integers. Specifying different values of ω , we obtain $\omega\Delta\tau$ from the first formula and Q_p from the second. It thus becomes possible to obtain pairs of values of Q_p and $\Delta\tau$ satisfying the conditions for the existence of a stability limit.

Figure 43 shows the result of such a calculation for $M_1 = 0.1$, $M_2 = 0.25$. As can be seen from the plot ($k = 0$; $k = 1$), instability is possible only for two types of alternating closed regions in the $(Q_p, \omega\Delta\tau)$ plane. These regions are shifted relative to each other (with respect to the $\omega\Delta\tau$ axis) by an angle equal to π , and correspond to values of Q_p with opposite signs. The existence of precisely these types of regions for the case under consideration could be readily predicted on the basis of the diagram shown in the left part of Fig. 28. Indeed,

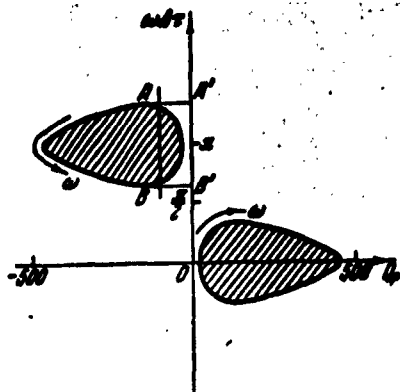


Fig. 43. Stability diagram in the presence of delay $\Delta\tau$.

setting $Q_p e^{i\omega\Delta\tau} = \vec{Q}$ we reduce the case under consideration to that investigated previously. The corresponding stability diagram of the type shown in Fig. 28 is given in Fig. 44, where the argument of the vector \vec{Q} varies in the instability region from $-\theta$ to $+\theta$ (the directions of OB and OA). Taking the last equation into account, we can readily find that the values $Q_p > 0$ of the instability re-

gion correspond to the following limits for $\Delta\tau$:

$$-\theta < \omega\Delta\tau < 0,$$

while values $Q_p < 0$ correspond to

$$\pi - \theta < \omega\Delta\tau < \pi + \theta,$$

which is in full agreement with the results shown in Fig. 43.

Although the result presented in Fig. 43 could be predicted, it was derived here by numerical analysis of Eq. (26.5) principally with an aim to illustrate by means of a simple example the method of solving the problem of excitation of acoustic oscillations by heat supply with account of the delay of the perturbed heat-supply process. In more general cases such a simple analysis of the excitation conditions with the aid of a diagram such as shown in Fig. 44 is difficult. In addition, one must not forget that the result obtained in the present section contains not only information regarding the position of the stability boundaries, but also concerning the frequencies corresponding to individual points on these boundaries.

Let us examine the diagram shown in Fig. 43 in greater detail, imposing on the problem additional limitations. We assume that the physical nature of the heat-supply process is such that Q_p can have

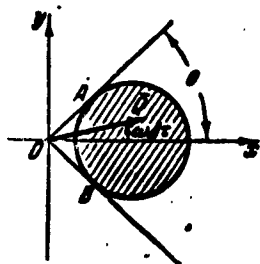


Fig. 44. Effect of the delay $\Delta\tau$ on the position of the vector \vec{Q} on the stability diagram.

only negative values which do not exceed 100 in absolute magnitude. Then the excitation of the system turns out to be possible only in those cases when the representative point on the diagram of Fig. 43 lies in the shaded part of the rectangle AA'BB'. This circumstance imposes specific limitations on the permissible values of $\Delta\tau$. To demonstrate this, let us plot on Fig. 45 the connection between $\Delta\tau$ and ω , picking off Fig. 43 the values of $\omega\Delta\tau$ and ω corresponding to the segment AB on the stability boundary. As is seen from Fig. 45, excitation is possible only at definite frequencies ω and calls at the same time for definite values of $\Delta\tau$. It is important to note here that if we disregard very large ω (which are almost always unrealistic), the system cannot be excited at values of $\Delta\tau$ close to zero. This constitutes a major difference between the problem considered here and the problem of the preceding section, where the system was capable of excitation also at $\Delta\tau = 0$. Thus, an account of the delay may turn out to be essential, and this circumstance must be taken into consideration.

To conclude the analysis of the influence of $\Delta\tau$ on the excitation of oscillations, we make one remark. Figure 45 shows only the minimum values of $\Delta\tau$ necessary for the excitation of the oscillating system. If $\Delta\tau$ is increased such that the new value $\Delta\tau = \Delta\tau'$ is related with the value $\Delta\tau = \Delta\tau_0$ shown in Fig. 45 by the relation $\omega\Delta\tau' = \omega\Delta\tau_0 + 2k\pi$, where k is an integer, then obviously the representative points for these two cases will coincide on the diagram of Fig. 44.

Consequently, when $\Delta\tau$ is varied continuously from zero to infinity, regions of values of $\Delta\tau$ for which the system is stable may periodically alternate with regions of values of $\Delta\tau$ for which the system

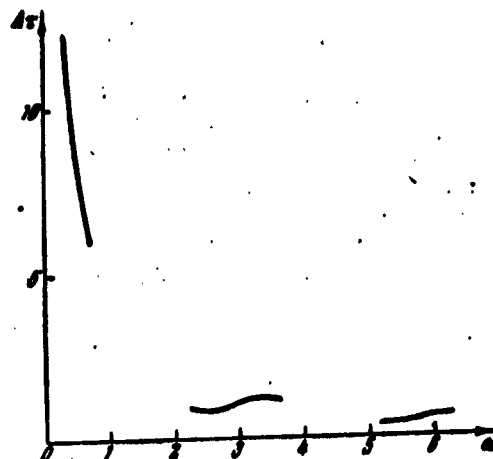


Fig. 45. Connection between the oscillation frequencies ω and the delay $\Delta\tau$.

is unstable.

§27. Oscillation Frequencies

In the analysis of the frequencies of the oscillations excited by the heat supply it is necessary to take into account the fact that in this case the laws governing the excitation of the frequencies are not as simple as in ordinary acoustic systems. This circumstance was already emphasized above in connection with an example wherein the characteristic equation was solved (§23). It was stated there, in particular, that the deviation of the oscillation frequency from the values predicted by the simplest acoustic formulas is connected with the fact that when the acoustic wave crosses the discontinuity surface Σ only part of the wave goes over to the region with the different temperature, while another part is reflected from the discontinuity surface.

The point lies not so much in the fact that gas with different temperatures flows on both sides of Σ . The processes that occur in the combustion zone (i.e., formally, the properties of the surface Σ) influence in most essential fashion the values of the excited frequencies.

Let us examine this phenomenon in greater detail. Let the system

be at the stability limit and let it execute oscillations with constant amplitude ($\nu = 0$). For the sake of being definite we assume that the system has pressure nodes on the left and on the right of the heat-supply plane Σ , at sections with coordinates ξ_1 and ξ_2 . Let \bar{p}_1 , \bar{v}_1 and \bar{p}_2 , \bar{v}_2 be the pressure and velocity perturbations on the left and on the right of the plane $\Sigma(\xi = 0)$, respectively. Then the initial system will have the form

$$\left. \begin{aligned} \bar{v}_1 \varphi_1(\xi_1) + \bar{p}_1 \varphi_2(\xi_1) &= 0, \\ \bar{v}_2 \varphi_1(\xi_2) + \bar{p}_2 \varphi_2(\xi_2) &= 0. \end{aligned} \right\} \quad (27.1)$$

The conditions on Σ are written in canonical form (17.1):

$$\left. \begin{aligned} \bar{v}_1 &= \frac{1}{n}(\bar{v}_1 + \delta E) = \frac{1}{n}(\bar{v}_1 + y_1 \bar{p}_1), \\ \bar{p}_1 &= \frac{1}{m}(\bar{p}_1 + \delta X) = \frac{1}{m}(\bar{p}_1 + y_2 \bar{v}_1), \end{aligned} \right\} \quad (27.2)$$

where the numbers y_1 and y_2 are introduced (as in the analogous cases above) in order to relate in explicit form the quantities δE and δX with the phases and amplitudes of the system oscillations. These numbers represent formal introduction of a certain feedback, the specific form of which is not needed here.

Using (27.2), we transform the characteristic equation of the system (27.1) into the form

$$\frac{m}{n} y_1 - \frac{\varphi_1(\xi_1)}{\varphi_2(\xi_1)} \frac{\varphi_1(\xi_2)}{\varphi_2(\xi_2)} y_2 = \frac{m}{n} \frac{\varphi_1(\xi_1)}{\varphi_2(\xi_1)} - \frac{\varphi_1(\xi_2)}{\varphi_2(\xi_2)}. \quad (27.3)$$

The ratios of the functions $\varphi_1(\xi)/\varphi_2(\xi)$, which are contained in the expression written down here, can be determined on the basis of Formula (22.3). Putting $\beta = i\omega$ (by definition $\nu = 0$) and denoting

$$\frac{2\omega\xi}{1-M^2} = \alpha, \quad (27.4)$$

we readily obtain

$$\frac{\varphi_1(\xi)}{\varphi_2(\xi)} = i \frac{\sin \alpha}{1 - \cos \alpha}. \quad (27.5)$$

Let us analyze, on the basis of Eq. (27.3), the two simplest cases

of oscillation excitation, one characterized by the condition $\delta X = 0$ ($y_2 = 0$) and the other by the condition $\delta E = 0$ ($y_1 = 0$). In both cases, as follows from (27.5), an imaginary quantity will be contained in the right half of (27.3), and the coefficients of y_1 or y_2 in the left half will be real.

Thus, neutral oscillations are realized when y_1 and y_2 are imaginary, thus pointing to the oscillation excitation conditions that are already known from §§12 and 22, according to which the phase shift between δE and \bar{p}_1 (or between δX and \bar{v}_1), which is equal to $\pi/2$, corresponds to the stability limit. This result is of course independent of the oscillation frequency.

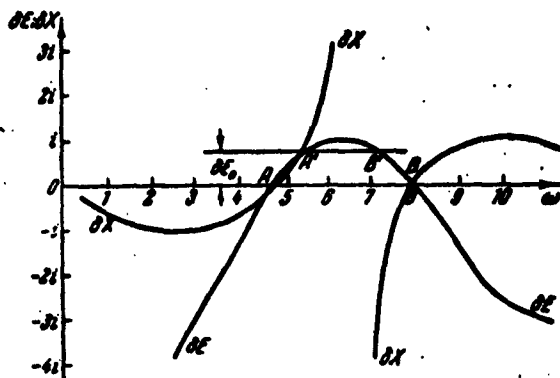


Fig. 46. Determination of the natural frequencies of the oscillating system.

Let us see what frequencies can be excited in the investigated system. A change in the value of ω leads to a change in α (27.4) and consequently also in the functions $\varphi_1(\xi_1)/\varphi_2(\xi_1)$ and $\varphi_1(\xi_2)/\varphi_2(\xi_2)$ (27.5). Thus, to each value of ω there corresponds its own value of y_1 (or y_2), at which neutral oscillations of the system are possible with specified frequency ω ; this value is determined in elementary fashion from Eq. (27.3).

In order to illustrate the foregoing, Fig. 46 shows results of

such a calculation. For greater clarity we use not the values y_1 and y_2 , but $\delta E = y_1 \bar{p}_1$ and $\delta X = y_2 \bar{v}_1$ (with \bar{p}_1 and \bar{v}_1 regarded as real and positive). The calculation was made for the case of a tube with pressure nodes at the end sections and with a plane Σ situated at equal distances from both ends. The stream velocity in the "cold" part is characterized by $M = 0.15$ and the relative heating is $T_{02}/T_{01} = 6.25$ (here T_0 denotes the temperature of the completely stopped gas). In the calculations the value of \bar{v} in the "cold" end section was arbitrarily assumed equal to unity.

The most important deduction that follows from (27.3) is that by proper variation of δE and δX it is possible to obtain any prescribed frequency (this fact was already used in §24 to plot the stability boundaries, where the variation of Q_p and Q_v for continuous variation of ω was determined). Unlike the usual problems in acoustics, the oscillation frequency is determined here not only by the properties of the oscillating gas and by the tube dimensions, but also by the character of the heat-supply process on Σ . Therefore such concepts as the "fundamental tone of the oscillations" or "overtones" must be used with caution. These usual concepts are meaningful for prescribed fixed values of δE and δX . Indeed, for example, when $\delta E = \delta X = 0$ the only frequencies that can be realized among those shown in Fig. 46 are those corresponding to the points A and B. The frequency $\omega = 4.82$ (point A) can be regarded as the first harmonic, the frequency $\omega = 7.95$ (point B) as the second, etc. (no other harmonics are shown in Fig. 46). If the character of the process on Σ is different, for example $\delta E = \delta E_0$, then the same harmonics will correspond to the points A' and B'. By continuously varying δE it is possible to change over smoothly from the first to the second harmonic.

We have considered here elementary cases of the excitation of os-

cillations, in which δE or δX is equal to zero. However, the deductions obtained here remain the same also in the general case, when arbitrary relations exist between δE and δX . This can be readily verified by analyzing Eq. (27.3).

§28. Stepwise Variation of the Oscillation Frequency with Change in the Combustion-Zone Position

Experimenters are well acquainted with the existence of a connection between the position of the combustion zone (length of the "hot" part of the tube) and the oscillation frequencies. It is known, for example, that when flame propagates in a tube filled with a combustible mixture, the frequencies excited by the flame change jumpwise as the flame front moves along the tube. This property can be readily analyzed on the basis of the characteristic equation of the problem under consideration. What is remarkable in this case is that such a jumpwise change in frequencies is not connected at all with the specific form of the combustion process; it becomes unobservable only when the mechanism of excitation is a function of the position of the combustion zone along the tube axis or a function of the oscillation frequency. Let us consider this phenomenon in greater detail.

As boundary conditions we choose pressure or velocity nodes at the sections $\xi = \xi_1$ to the left of the heat-supply surface and $\xi = \xi_2$ to the right of it. Thus,

$$\bar{p} = 0 \text{ or } \bar{v} = 0 \text{ for } \xi = \xi_1 \text{ and } \xi = \xi_2. \quad (28.1)$$

When using boundary conditions of the type (28.1), it is possible to disregard the entropy waves in the solution and, if we agree in addition to set $\bar{s}_1 = 0$ and if the formulas relating \bar{v}_1 , \bar{p}_1 and \bar{v}_2 , \bar{p}_2 on Σ contain neither the complex oscillation frequency β nor the location of the plane Σ relative to the tube axis, then the quantities ξ and β will be contained in the characteristic equation only via the functions

φ_1 and φ_2 .

Under these assumptions, the two boundary conditions (28.1) will yield two equations which relate, for example, \bar{p}_1 and \bar{v}_1 in the Σ plane [similar to what was obtained in §23 in setting up the characteristic equation (23.4)], while the coefficients of \bar{p}_1 and \bar{v}_1 will be linear functions of φ_1 and φ_2 . This yields in final analysis a characteristic equation of the form

$$\begin{vmatrix} a_{11}\varphi_1(\xi_1) + a_{12}\varphi_2(\xi_1) & a_{21}\varphi_1(\xi_1) + a_{22}\varphi_2(\xi_1) \\ a_{31}\varphi_1(\xi_2) + a_{32}\varphi_2(\xi_2) & a_{41}\varphi_1(\xi_2) + a_{42}\varphi_2(\xi_2) \end{vmatrix} = 0, \quad (28.2)$$

where the real coefficients a_{ik} will be functions of the properties of the surface Σ . The fact that the coefficients are real is implied by the formulation of the conditions on Σ in the form given in §23.

If we recognize that the functions φ_1 and φ_2 depend linearly on the two expressions (4.14) which contain ξ and β ,

$$\exp\left(\frac{-\beta\xi}{M+1}\right); \exp\frac{\beta\xi}{1-M},$$

then, by taking outside the determinant sign the quantity $\exp \beta_1 \xi_1 / (M_1 + 1)$ from the first row and $\exp [-\beta_2 \xi_2 / (M_2 + 1)]$ from the second row and dividing by these quantities we obtain a characteristic equation that depends on the expressions

$$\exp \frac{-\beta_1 \xi_1}{1-M_1}; \exp \frac{\beta_2 \xi_2}{1-M_2}.$$

As is well known, the quantities β_1 and β_2 are related by Eq. (22.5), and if the origin of ξ is located on Σ (Fig. 22), then ξ_1 and ξ_2 satisfy the equation

$$\xi_2 - \xi_1 = 1.$$

Taking the foregoing into account, we can rewrite the characteristic equation (28.2) in the form

$$F\left(\exp \frac{\beta_1(1-\xi_1)}{1-M_1}; \exp \frac{\beta_2 \xi_2}{1-M_2}\right) = 0. \quad (28.3)$$

Here F is an integral rational function of the second degree with real

coefficients.

Let us analyze the solution of this equation. It yields the variation of β_1 as a function of the relative length of the "hot" section ξ_2 , which we shall henceforth denote by $\underline{1}_2$, for specified fixed boundary conditions of the form (28.1) and for conditions of the type indicated above on Σ . Assume that as $\underline{1}_2$ increases the damping decrement ν of the oscillations increases and passes through zero. This will correspond to a transition from stability ($\nu < 0$) to instability ($\nu > 0$). On the stability limit we have $\nu = 0$ and $\beta = i\omega$.* We choose a pair of values $\underline{1}_2$ and ω corresponding to the stability limit and denote them $\underline{1}_2^{(1)}$ and $\omega^{(1)}$. Having these two quantities, we can easily determine the entire set of values of the pairs of numbers $\underline{1}_2$ and ω corresponding to all the harmonics of the system at the instant of passage through the stability limit as $\underline{1}_2$ is increased.

Indeed, when $\beta = i\omega$ Eq. (28.3) becomes a relation between trigonometric quantities

$$\left. \begin{aligned} F \left[\cos \frac{2\omega(1-l_2)}{1-M^2} + i \sin \frac{2\omega(1-l_2)}{1-M^2}; \right. \\ \left. \cos \frac{2\omega l_2}{\pi(1-M^2)} + i \sin \frac{2\omega l_2}{\pi(1-M^2)} \right] = 0. \end{aligned} \right\} \quad (28.4)$$

By definition, it is satisfied when $\underline{1}_2 = \underline{1}_2^{(1)}$ and $\omega = \omega^{(1)}$. But then it will also be satisfied for all values of ω and $\underline{1}_2$ which satisfy the equations

$$\left. \begin{aligned} \frac{2\omega(1-l_2)}{1-M^2} = 2K\pi \pm \frac{2\omega^{(1)}(1-l_2^{(1)})}{1-M^2}, \\ \frac{2\omega l_2}{\pi(1-M^2)} = 2N\pi \pm \frac{2\omega^{(1)}l_2^{(1)}}{\pi(1-M^2)}. \end{aligned} \right\} \quad (28.5)$$

Here K and N are arbitrary integers, limited by the natural conditions $\omega > 0$ and $0 \leq \underline{1}_2 \leq 1$.

It must merely be added that the signs of the second terms must be chosen the same, either plus in both cases or minus in both cases. In the former case the same complex number corresponding to $\underline{1}_2^{(1)}$ and

$\omega^{(1)}$ remains in the left half of (28.4), while in the latter case the conjugate complex number appears. Inasmuch as the right half of (28.4) is equal to zero, this means that the real and imaginary parts of the number on the left side must vanish. However, the absolute values of both the real and the imaginary parts of the complex conjugate numbers coincide. (This circumstance enables us to write both signs in (28.5).)

Solving the system (28.5), we obtain

$$\left. \begin{aligned} \omega &= \pi [(1-M_1^2)K + n(1-M_2^2)N] \pm \omega^{(1)}, \\ l_1 &= \frac{\pi n(1-M_1^2)N \pm \omega^{(1)}l_1^{(1)}}{\omega}. \end{aligned} \right\} \quad (28.6)$$

It may turn out that the quantities $\omega^{(1)} \frac{l_1^{(1)}}{l_2^{(1)}}$ and $\omega^{(1)}$ are large, and to find all the possible combinations of $0 \leq \frac{l_1}{l_2} \leq 1$ and $\omega > 0$ corresponding to the stability limits it becomes necessary to take negative values of the integers N and K. In order to avoid this and to employ henceforth only positive or zero values of N and K, the following measure can be adopted. Let us write N and K in the form $K = K' \mp K''$ and $N = N' \mp N''$, where the numbers K' , K'' , N' , N'' are nonnegative integers. Then Formulas (28.6) assume the form

$$\begin{aligned} \omega &= \pi [(1-M_1^2)K' + n(1-M_2^2)N'] \pm \omega^{(1)}, \\ l_1 &= \frac{\pi n(1-M_1^2)N' \pm \omega^{(1)}l_1^{(1)}}{\omega}. \end{aligned}$$

Here

$$\begin{aligned} \omega^{(1)} &= \omega^{(1)} - \pi [(1-M_1^2)K'' + n(1-M_2^2)N''], \\ \omega^{(1)}l_1^{(1)} &= \omega^{(1)}l_1^{(1)} - \pi n(1-M_2^2)N''. \end{aligned}$$

The numbers K'' and N'' must be chosen such that

$$0 < \omega^{(1)} < \pi(1-M_1^2); \quad 0 < \omega^{(1)}l_1^{(1)} < \pi n(1-M_2^2),$$

and then K' and N' cannot be negative, for in the opposite case ω and $\frac{l_1}{l_2}$ would assume negative values, in contradiction to the conditions assumed above.

We shall henceforth assume, unless otherwise stipulated, that the corresponding recalculations in Formulas (28.6) have already been made,

i.e., $\omega^{(1)}$ and $\omega^{(1)}\underline{1}_2^{(1)}$ have the minimum possible values. Then the quantities $\omega^{(1)}$ and $\underline{1}_2^{(1)}$ defined in this formal manner have no physical meaning ($\omega^{(1)}$ is found to be very close to zero, and $\underline{1}_2^{(1)} > 1$). This should not worry us, for such a result merely indicates that actually these modes (which correspond to $K = 0$) will not be observed.

Let us consider first those solutions, which are obtained when the plus signs are used in Formulas (28.6). Then, specifying different values of K and N , we can obtain all the stability limits of the same type as the initial stability limit, corresponding to $\omega^{(1)}$ and $\underline{1}_2^{(1)}$. This must be understood in the sense that if, for example, the process changes from stable to unstable with increasing $\underline{1}_2$, then all the other stability limits $\omega; \underline{1}_2$ obtained on the basis of (28.6) will correspond to a transition from stability to instability with increasing $\underline{1}_2$.

The use of minus signs in (28.6) leads to stability limits that are of the opposite type compared with the initial one. Then, for example, if with increasing $\underline{1}_2$ the transition through $\underline{1}_2^{(1)}$ makes the process change from stable to unstable, then all the limits obtained from (28.6) with minus signs in front of $\omega^{(1)}\underline{1}_2^{(1)}$ and $\omega^{(1)}$ will correspond to transition from instability to stability with increasing $\underline{1}_2$.

The property of the stability limits indicated here can be readily proved. For this purpose it is sufficient to assume that upon continuous variation of $\underline{1}_2$ the complex frequency β also varies continuously for all the harmonics (we discard here the uninteresting case when $\nu = 0$ for all $\underline{1}_2$). This is a perfectly natural assumption, since the properties of the surface Σ were assumed to be invariant. But it is then obvious that as $\underline{1}_2$ varies continuously an observer which traces one and the same harmonic will note generally speaking, multiple transitions through the stability limits at the instants when Eqs. (28.5) are satisfied. It is important to note here that the points $(\underline{1}_2, \omega)$

corresponding to the stability limits and obtained using the "plus" and "minus" signs in Formulas (28.6) will alternate. This is seen, for example, from the second equation of (28.5) if it is noted that by definition the second term of the right half has an absolute value smaller than 2π . Indeed, the second equation of (28.5) yields in the $(\underline{l}_2; \omega)$ plane nonintersecting hyperbolas, which alternately belong to two families of hyperbolas obtained using the "plus" and "minus" signs in the indicated equation. When these hyperbolas cross the curve $\omega = \omega(\underline{l}_2)$ belonging to some harmonic of the system, they define the points corresponding to $v = 0$ which belong alternately to the first and second family of hyperbolas.

It was assumed above that β has a continuous variation as a function of \underline{l}_2 . Then, when \underline{l}_2 changes monotonically, the oscillating system, upon crossing the stability boundaries, will alternately become stable and unstable (we do not consider here the question of the possible realization of such oscillating systems in which two points corresponding to neighboring stability limits contract to a single point). Consequently, on passing through the boundaries corresponding to one family of hyperbolas, the oscillating system will always turn say from stable to unstable, and on crossing the boundaries corresponding to the second family of hyperbolas it will turn from unstable to stable. This was the statement to be proved.

The arguments presented can be made clearer by presenting a graphic interpretation of Formulas (28.6). For this purpose we turn to Fig. 47, which shows for a certain numerical example the lines of equal K and equal N under the assumption that $\omega^{(1)} = 0$. In addition, we show here the dependences of ω on \underline{l}_2 for different harmonics (the numbers of the harmonics are designated alongside with Roman numerals), under the assumption that the simplest acoustic rule for a tube with

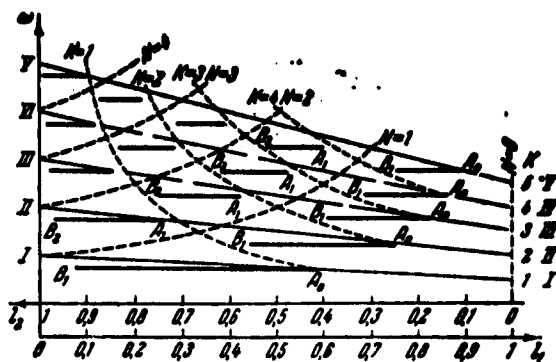


Fig. 47. Illustrating the construction of the diagram showing the dependence of the excited frequencies on the position of Σ along the tube.

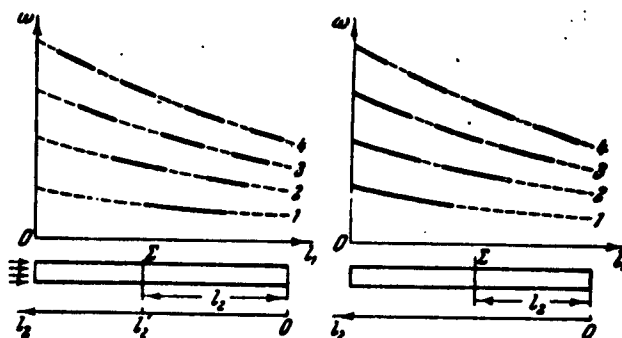


Fig. 48. Connection between the position of Σ along the tube and the excited oscillation frequencies.

open ends hold true, namely that the period of the oscillations is equal to twice the time necessary for an acoustic impulse to traverse the entire tube (without account of interaction with the heat-supply zone), i.e., that the frequency is

$$\omega = \frac{\pi}{\frac{l_1}{1-M_1^2} + \frac{l_2}{1-M_2^2}}.$$

Specifying then certain nonvanishing values of $\omega^{(1)}$ and $\omega^{(1)}_{\underline{1}2(1)}$, we obtain the stability limits for the use of both signs in Formulas (28.6). The points corresponding to the stability limits are arbitrarily joined with straight lines, with which the instability regions are designated. The points A_0 correspond here to the stability limits

obtained for $N = 0$, A_1 and B_1 correspond to $N = 1$, etc. The points A correspond to the use of the minus sign and B correspond to the plus signs in Formulas (28.6). As can be seen from the figure, inside of each curvilinear quadrangle formed by the lines of equal K and N there lies one instability region.

Based on the foregoing, we can readily draw diagrams which give a clear-cut picture of the distribution of the stable and unstable combustion process regions as the combustion zone moves along the stream axis. A similar construction is shown in Fig. 48 for two types of boundary conditions: tubes with open ends and tubes with one end closed. The values of \underline{l}_2 marked on the abscissa axis give the position of the combustion zone, while the ordinates represent the oscillation frequencies ω . The natural frequencies of the system are given by the dotted lines marked with the number of the harmonic. The instability regions are shown by the solid lines. In order to show different possible types of instability-region distributions, the right-hand diagram shows a case when the fundamental tone has only one and not two stability limits. Such a case is quite probable for a tube with one closed end.

The general laws which immediately suggest themselves upon examination of the diagrams shown in Fig. 48, can be reduced to two premises.

First, the higher the number of the harmonic, the larger the number of alternating regions of stability and instability that fit within the length of the tube (in this case the first harmonic has one instability region, the second two, the third three, etc.). Second, it is seen that several harmonics can be unstable simultaneously, and when the flame front position is at the open end all the harmonics are stable (although in the case of the higher harmonics the instability

regions come as close as desired to the open end).

In the discussion of these diagrams it must be remembered that they have been obtained under the assumption that no energy is radiated from the open ends (pressure nodes as boundary conditions). It is known, however, that with increasing oscillation frequency the amount of energy radiated from the tube into the surrounding space increases sharply (this question will be discussed in greater detail in the next chapter). An account of the energy dissipation upon interaction of the acoustic waves with the ends of the tube cause the instability regions to start to become narrower with increasing oscillation frequency, and to disappear completely starting with a certain frequency. Consequently, high harmonics will not be observed in practice, and when the flame front is situated in a certain sufficiently large vicinity of the end of the tube the process will always be stable.

As a net result we can predict the following general character for the course of the process. As the combustion zone moves away from the open end, the process which was initially stable should become unstable and the frequency of the oscillations will decrease jumpwise to the fundamental tone of the system. This leads, it might appear, to a paradoxical behavior of the oscillating system: an increase in the relative length of the portion of the tube filled with the hot gas will lead to a decrease in the oscillation frequency, whereas all the harmonics should increase in their natural frequency. This explanation can be readily found on the diagram of Fig. 48: although the frequencies of each harmonic do increase with increasing l_2 , as this increase proceeds more and more of the lower harmonics become unstable and since they dissipate less energy into the outer space, they will be easier to excite than the higher harmonics and can suppress the latter. Only at very large values of l_2 , when both ends of the tube are open,

does a higher probability of secondary excitation of the higher harmonics appear. The totality of the available experimental data confirms this conclusion.

Relations (28.6) which were obtained in the present section on the basis of a formal analysis of the characteristic equation have a simple physical meaning. If it is assumed that under certain conditions the fundamental tone of the oscillating system becomes unstable, i.e., the instability is brought about by a certain combination of the quantities \bar{p} , \bar{v} , \bar{Q}^* , and \bar{U}_1 , then it is easy to visualize that if we assume the process in the combustion zone to remain unchanged, precisely similar conditions (\bar{p} , \bar{v} , \bar{Q}^* , and \bar{U}_1) are encountered twice in the second harmonic, three times in the third, etc. This is connected with the fact that the second harmonic duplicates as it were the standing wave of the fundamental tone twice, the third duplicates it three times, etc. Similar arguments hold true also for the instant of transition from instability to stability.

§29. Experiments on the Influence of the Position of the Combustion Zone on the Oscillation Process

Many results obtained in the present chapter were confirmed by numerous experiments. Particularly instructive in this sense were the experiments connected with the study of the influence of the position of the combustion zone along the tube on the excitation of the acoustic oscillations. Some of the deductions obtained in this case can have not only theoretical but also practical significance.

In the processing of the experimental data it is advantageous to simplify somewhat Formulas (28.6). Inasmuch as all the experiments described below were carried out at relatively small values of M_1 (on the order of 0.05-0.1), the differences $1 - M^2$ will be assumed equal to unity. In addition, it is advantageous to write down Formulas (28.6)

in terms of dimensional variables (frequencies in cycles per second, lengths in meters) so as to compare them directly with the experimental points. Taking all these remarks into account, the relations between the oscillation frequencies and the lengths of the cold and hot parts of the stream assume the following form:

$$\left. \begin{aligned} \Omega &= (K + nN) \frac{a_1}{2L} \pm \Omega^{(n)}, \\ L_2 &= \frac{\frac{na_1}{2} N \pm \Omega^{(n)} L_2^{(n)}}{\Omega} \end{aligned} \right\} \quad (29.1)$$

Here L and L_2 are the total length and the length of the hot part of the stream, a_1 is the velocity of sound in the cold part of the stream, and Ω is the frequency of the oscillations in cycles per second. $\Omega^{(1)}$ and $L_2^{(1)}$ are the oscillation frequency on the stability limit and the corresponding length of the hot part of the stream.

The formula obtained is exceedingly simple and contains no quantities characterizing the details of the combustion process, a numerical estimate of which is difficult. They are all included in the experimentally determined quantities $\Omega^{(1)}$ and $L_2^{(1)}$. The remaining quantities (n_1 , a_1 , L , L_2 , and Ω) also are quite simple to measure.

In those cases when (as is frequently the case in experiments) only one "staircase" of frequencies is observed, for example only the instability regions $A_0 B_1$ on Fig. 47, Formulas (29.1) can be further simplified. Inasmuch as all the points A_0 on Fig. 47 are obtained for $N = 0$, while the points B_1 are obtained for $N = 1$, i.e., for constant values of N (which are completely defined by specifying at least one point A_0 and B_1), Formulas (29.1) can be rewritten as

$$\left. \begin{aligned} \Omega &= \frac{a_1}{2L} K + \Omega^{(n)}, \\ L_2 &= \frac{L_2^{(n)} \Omega^{(n)}}{\Omega} \end{aligned} \right\} \quad (29.2)$$

where $\Omega^{(1)}$ and accordingly $L_2^{(1)}$ already include the terms that de-

pend on N . The use of these formulas is exceedingly simple. By determining experimentally $\Omega^{(1)}$ and $L_2^{(1)}$ for some point A_0 , we immediately obtain the entire series of like points. To construct the series of points B_1 it is necessary to substitute into Expression (29.2) the values of $\Omega^{(1)}$ and $L_2^{(1)}$ corresponding to some point B_1 , etc. If the lowest observed frequencies $\Omega^{(1)}$ are taken for such calculations, then the numbers K will be positive for all the other harmonics.

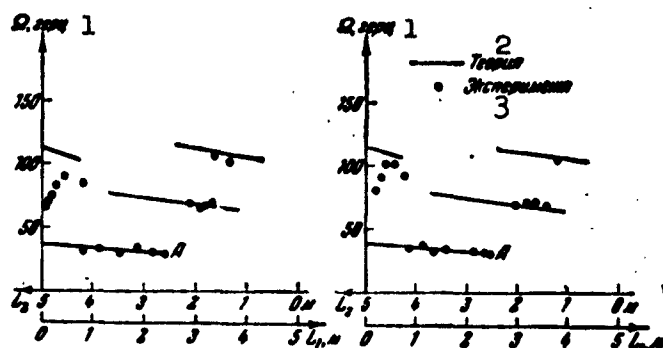


Fig. 49. Connection between the position of the flame front and the excited frequencies in accordance with the experiments of Coward, Hartwell, and Georgson. 1) cps; 2) theory; 3) experiment.

A certain advantage of Formulas (29.2) is, in addition to all others, that they do not contain such quantities as $n = a_2/a_1$, the measurement of which is connected with certain difficulties and data on which are not always cited by the experimenters.

Comparison of the experimental data with theory is best started with an examination of the experiments of Coward, Hartwell, and Georgson, which were already referred to in the introductory chapter. The experiments consisted of a study of vibration combustion occurring in the case of slow propagation of flames in a tube which is open on one end and filled with a combustible mixture, which is ignited at the open end. In these experiments L_2 is equal to the distance from the open end of the tube to the flame front. The diagram of the setup and

the results of the experiment are shown on Figs. 49 and 50. The experiments were performed on two tubes which differed somewhat in length and had different diameters (100 and 200 mm), so that each of the figures shows two diagrams. The difference between Figs. 49 and 50 lies in the procedure used to obtain them. The theoretical instability regions shown in Fig. 49 (the solid lines show the theoretically obtained instability regions while the points show the experimental data) were obtained in the following fashion. The position of one point A in the plane ($L_2; \Omega$) was taken from the experiment, after which Formula (29.1) was used to determine all the other points corresponding to the stability boundaries of both types. These points were joined by straight lines which showed arbitrarily the variation of Ω as a function of L_2 within the instability region. The actual determination of the oscillation frequency for the points lying inside the instability region (i.e., those for which $\nu > 0$) was not carried out, and this is why we speak here of the arbitrary variation of Ω as a function of L_2 inside the instability region. The diagram does not show the instability regions which exist theoretically but were not observed experimentally. All these regions correspond to higher frequencies than those shown in the diagram, and therefore are of no practical interest. We have already mentioned that the excitation of these oscillations has low probability.

In Fig. 50 the instability regions were also constructed by using Formulas (29.1), but this time only with the plus sign. In order to compensate for the loss of half the stability boundary in such a calculation, not one initial point A but two (A and B), belonging to stability limits of opposite types, were taken into consideration. In all other respects the construction of the diagrams on Fig. 50 did not differ at all from the construction described above.

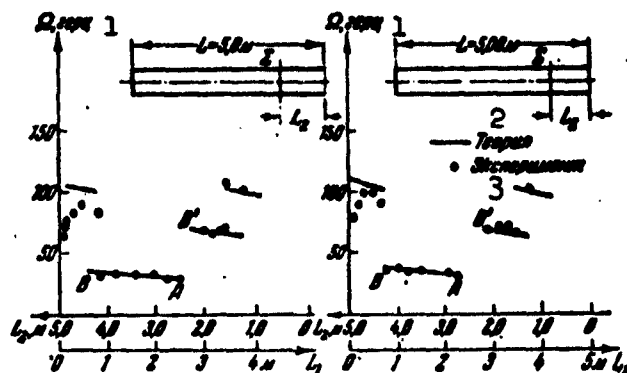


Fig. 50. Connection between the position of the flame front and the excited frequencies according to the experiments of Coward, Hartwell, and Georgson. 1) cps; 2) theory; 3) experiment.

The comparison between the theoretically obtained instability regions and those observed experimentally must be conceded to be quite satisfactory, particularly for those regions which are shown in Fig. 50. The only exceptions are the points corresponding to L_2 close to zero (i.e., flame-front positions in the direct vicinity of the closed end of the tube). This is connected with the peculiarities of the self-excitation mechanism and will be explained in §49.

If we compare the character of agreement between the experimental data and the theoretical instability regions on Figs. 49 and 50, we can draw the following conclusion. The better agreement between theory and experiment on Fig. 50 is connected with the fact that the series of boundaries of the same type was obtained by using the point A, whereas the series of boundaries of the opposite type was obtained by using the point B, while in Fig. 49 the two series of boundaries were obtained with the aid of the point A. Physically this means that the characters of the perturbed combustion process at the instant of the onset of the instability and at the instant of its disappearance are not exactly the same. Were they to coincide, the instability zones

would be distributed as shown by the solid lines in Fig. 49. The reason for this difference will become clear in §49.

More important than the possible difference between the properties of the surface Σ during the transition through the stability boundary upon occurrence and disappearance of the instability is the good agreement between the theoretical and experimental instability regions. This indicates that the same excitation mechanism acts independently of the number of the harmonic and satisfies the conditions advanced at the start of the preceding section. It was assumed there, in particular, that the properties of the heat-supply surface Σ do not depend on the frequency. This assumption includes, of course, the assumption that there is no delay, since the introduction of the delay time in one form or another would lead, as shown above, to a frequency dependence of the properties of the plane Σ [see, for example, Formula (26.4)].

In the experiment considered here the combustion was produced by a previously prepared mixture of gaseous fuel and air, and the mixture was consumed in a tube which had no devices whatever to maintain the combustion process (nozzles, stabilizers, etc.). For such a combustion character it is natural to set in the equations that describe the properties of the surface Σ (16.15) $\bar{Q}^* = 0$ and $\bar{P}^*_x = 0$, i.e., it is natural to assume that the oscillations are excited only because the perturbation in the effective flame propagation velocity \bar{U}_1 differs from zero. But then, in analogy with Formula (24.2), we can write

$$\bar{U}_1 = U_p \bar{a}_1 + U_v \bar{a}_1. \quad (29.3)$$

i.e., we can assume that \bar{U}_1 depends on the pressure and velocity perturbations. The coefficients a_{11} , a_{12} , a_{21} , and a_{22} in Formulas (23.2) become in this case linear functions of U_v and U_p , and consequently the same properties will be possessed by the coefficients C_1 , C_2 , C_3 , and C_4 in Expressions (23.7).

Substituting in (23.7) for $v = 0$ the experimentally obtained value ω (for example for the point A) and the values of h_1 and h_2 which are known for the same point A (inasmuch as they are determined uniquely by specifying the relative length of the hot part of the tube), we can regard the system (23.7) as a linear inhomogeneous system for the determination of U_v and U_p . The actual calculation of U_v and U_p enables us to establish the relative amplitude of the perturbation of the effective velocity of flame propagation and its phase relative to the perturbations \bar{v}_1 and \bar{p}_1 . Calculations of this type can yield useful information regarding the process occurring in the combustion zone at the instant of the onset (or disappearance) of the instability. We do not present these calculations here, since they have no direct bearing on the content of the present section.

The experiments considered here were carried out in a stationary mixture of hot gases, in which the flame front propagated freely. However, when the conditions of the experiment are changed the laws observed also remain in force. We turn for this purpose to experiments in which a previously prepared mixture of gasoline vapor and air moving in a cylindrical tube was ignited. In these experiments an attempt was made to excite as many harmonics as possible, so as to compare most completely the theoretical relationships with experiment. This was attained to a certain degree — whereas in the previously described experiment of Coward, Hartwell, and Georgson three harmonics were excited, in this case seven harmonics were excited.

The experimental setup consisted of a tube open on both ends, 4.57 m long and 100 mm in diameter. A heated stream of gasoline-air mixture was blown freely through this tube; the mixture was prepared continuously in a special receiver, separated from the inlet section of the tube by a free gap. This was done in order to obtain clear-out

boundary conditions on both ends of the tube: both the inlet and the outlet sections of the tube communicated with the surrounding space.

-) By special measurements it was shown that the acoustic oscillations in the tube were not transmitted to the receiver, i.e., the gap between the exhaust nozzle with which the receiver was terminated and the inlet to the tube was sufficiently large. The combustion in the tube was produced behind a group consisting of several flame stabilizers (made in the form of cones), arranged in one and the same plane, which in turn was normal to the tube axis. The total area of the projections of the stabilizers on this plane was small compared with the area of the tube cross section, i.e., the stabilizers did not block the section, and the acoustic waves passed freely through the section without experiencing noticeable reflections from the housings of the stabilizers.

The experiment consisted of gradually moving the group of stabilizers, which could be readily displaced along the tube as a unit, and recording the oscillation frequencies for every 50 mm of displacement.

The results of the experiment are shown in Fig. 51. The theoretical instability regions are constructed in accordance with the very simple formulas (29.2), using the experimentally obtained coordinates of the ends of the instability regions A and B. The relative placement of the theoretical and experimental instability regions again confirms the correctness of the relations obtained in the preceding section. It is necessary to emphasize here especially that both groups of experiments considered here were set up with different boundary conditions (in some experiments one end of the tube was closed and the other open, while in others both ends were open), with a different character of gas motion (gas stationary relative to the walls in the cold part of the tube and a stream of combustible mixture), and with different types of combustion (free flame front and combustion behind poorly stream-

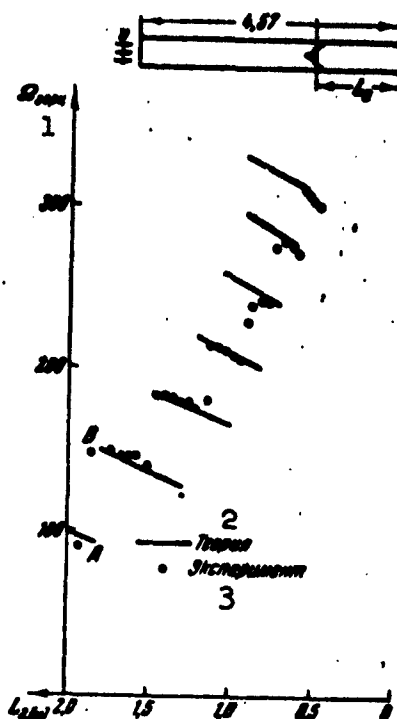


Fig. 51. Connection between the position of the flame stabilizer along the tube and the excited frequencies. 1) cps; 2) theory; 3) experiment.

lined stabilizers). This indicates that the theoretical relations derived are extremely general. It must be stated that this is confirmed also by many other experiments, for example the already-mentioned experimental researches of Putnam and Dennis* and of others.

Let us turn to the diagram of Fig. 51 and examine it from a somewhat different point of view. Along with the good agreement, for so complicated a phenomenon, between the theoretical and experimentally-obtained instability regions, it is easy to note a certain systematic shift of the theoretical values relative to the experimental ones. This indicates that the properties of the heat-supply zone do not coincide completely with those postulated at the start of the preceding section. Apparently in this case the properties of the zone depend

to a certain degree on the oscillation frequency, inasmuch as the disparity between the theoretical instability regions and the experimental points is systematically connected with a change in the oscillation frequency. This result is natural. It will be shown in Chapter 7 that upon ignition of a previously prepared mixture behind poorly streamlined flame stabilizers the mechanism whereby the oscillations are excited and maintained is essentially connected with the process whereby the vortices break away from the stabilizer. It is known from hydro-mechanics that this process can "attune itself" to the frequency of the velocity oscillations of the gas flowing past the stabilizer. It is difficult to assume, however, that this process will not be influenced by other properties of vortex formation.

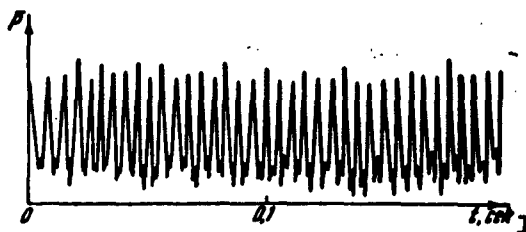


Fig. 52. Oscillogram of pressure oscillations in vibration combustion. Example of simultaneous excitation of two frequencies.
1) sec.

By the same mechanism as was indicated somewhat earlier, it is possible to determine from these experiments the variation of U_v and U_p with the variation of the oscillation frequency, and thus obtain a deeper insight into the properties of the heat-supply zone. Such an analysis, however, is not within the scope of the present section.

We note finally that Fig. 51 shows only those instability regions which correspond to a reduction in the oscillation frequency with increasing length of the hot part. At the same time, the left-hand diagram of Fig. 48 shows that when both ends of the tube are open and the

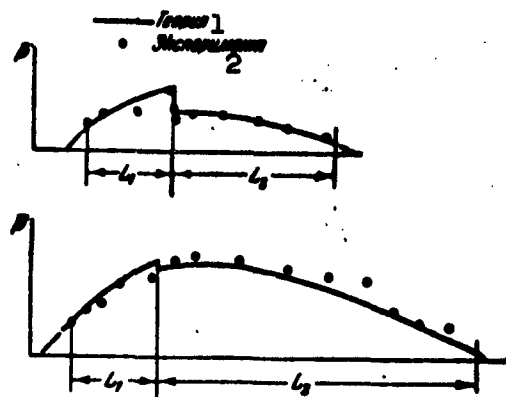


Fig. 53. Comparison of theoretical and experimental pressure standing-wave patterns. 1) Theory; 2) experiment.

length of the hot part is increased the oscillation frequencies should again jump over to the higher harmonics. Although such a phenomenon is observed relatively rarely in the experiment (for in this case it is necessary to have a short cold portion of the stream and a relatively long hot portion), it could be registered in setups similar to that used for the experiments described here.

The instability regions shown in Figs. 48, 49, 50, and 51 are so arranged that at certain relative lengths of the hot part of the stream several harmonics become unstable simultaneously. This causes sometimes the excitation of two or even three harmonics immediately. This phenomenon is observed quite frequently and becomes perfectly understandable from an examination of the diagrams mentioned here. Figure 52 shows an example of an oscillogram of pressure oscillations, taken during the course of vibration combustion; the oscillogram shows clearly the superposition of two harmonics — the fundamental and the one with double its frequency. Sometimes the oscillograms acquire an even more complicated form and special methods must be used to decipher them. However, usually the fundamental frequency can be separated in-

mediately and frequently no attention is paid at all to the frequencies accompanying the fundamental.

At the end of the preceding section it was stated that the physical basis for the observed jumpwise change in the oscillation frequency is the ability of the oscillating system of duplicating, as it were, the form of the standing wave twice during the excitation of the second harmonic, three times during the excitation of the third, etc. From this point of view the agreement between the theoretical pattern of the jumpwise change in the oscillation frequency with experiment is indirect evidence of the fact that the forms of the standing waves are also close to theoretical. This fact can be registered directly by measuring the form of the standing wave with oscillations excited in the system. This is simplest to do for a pressure standing wave. Figure 53 shows two examples of a comparison of the theoretical and experimental patterns for the absolute values of the pressure standing-wave amplitudes. As can be seen from the diagrams, the experimental points follow the theoretical relationships sufficiently well. The jumpwise change in the theoretical pattern in the central part of the diagram corresponds to the strong-discontinuity plane Σ , which represents the combustion zone in idealized form.

Whereas the analysis of the jumpwise change in the oscillation frequency upon variation of the length of the hot part of the tube (with the total length of the tube remaining constant) is more of physical interest, the real practical interest attaches to a related phenomenon, which outwardly manifests itself in a manner that is in a certain sense the opposite. We are referring here to the tendency of the oscillating system to conserve a constant value of the dimensional frequency of oscillations with invariant length of the hot part and with considerable increase in the total length of the tube.

Let the length of the hot part of the tube L_2 remain constant, while the total length L is increased continuously. In this case the relative length of the hot part, L_2/L , will decrease, i.e., if we turn to the preceding diagrams, the motion will be not from right to left, but from left to right. Consequently, the point which corresponded to the vanishing of an instability will now correspond to its occurrence, and vice versa.

In accordance with Formulas (29.1) we can write

$$\left. \begin{aligned} \Omega &= \frac{c_1}{2L} (K + nN) \pm \Omega'' \\ \Omega &= \frac{\frac{m_1}{2} N \pm \Omega'' L_2''}{L} \end{aligned} \right\} \quad (29.4)$$

Let us set in these formulas $N = \text{const}$, i.e., we consider related points (for example, all the left ends or all the right ends of the segments on Fig. 51).

Let now, as already mentioned, the dimensional length of the hot part of the flow remain constant ($L_2 = \text{const}$). Then in the right half of the second equation of (29.4) only constant quantities will appear. Consequently, with change in the total length of the tube L , but with the length of the hot part L_2 remaining constant, the oscillating system will strive to conserve the oscillation frequency Ω invariant upon any new occurrence of instability.

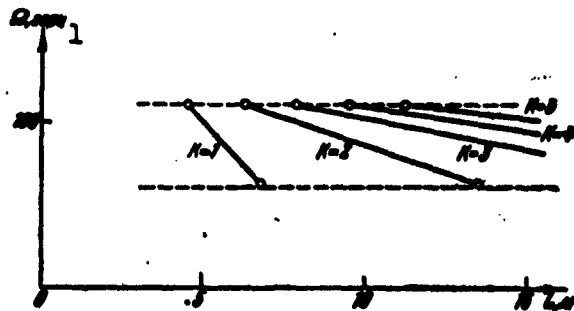


Fig. 54. Connection between the excited frequencies and the length of the tube for a constant length of the hot part of the tube. 1) cps.

If we now turn to the first formula of (29.4) we see immediately that this tendency of the oscillating system can be satisfied only at the expense of K , i.e., by changing over to the excitation of higher harmonics as the total length L of the tube is increased.

In order to make these deductions clearer, let us turn to the calculation example. Let us find, using the formulas (29.4), the instant of occurrence of instability for $N = 1$, and, setting $N = 0$, let us reverse the signs of $\Omega^{(1)}$ and modify the absolute value of $\Omega^{(1)}$ in suitable manner to determine the instants when the instability disappears. We represent the results of the calculation in the form of a plot $\Omega = \Omega(L)$, and join the points designating the start and the end of the instability arbitrarily by means of straight lines, so as to delineate the instability regions. The corresponding construction is shown in Fig. 54, with the instability regions marked by the value of K to which they correspond. The example has been constructed for the same numerical values of the parameters as for the experiment of Fig. 51. The diagram of Fig. 54 shows that one can expect in the system, independently of the length of the tube L , the occurrence of oscillations only with frequencies ranging from 61 to 110 cps. When the total length of the tube L is increased, the oscillation frequency at first begins to decrease, for example for the instability region corresponding to $K = 1$ from 110 cps to 61 cps, which corresponds entirely to the expected behavior of the system, since an increase in L increases the time required for a sound impulse to travel along the tube.

However, subsequently Ω not only fails to continue its decrease, but to the contrary, it rises abruptly again to 110 cps, inasmuch as the next harmonic becomes unstable, corresponding to $K = 2$. In this case there can exist in a certain range of values of L frequencies of the order of 105-110 cps and 61-72 cps simultaneously, for the two re-

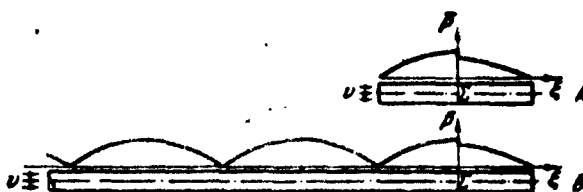


Fig. 55. Standing-wave patterns in tubes having identical length of the hot part of the stream.

gions $K = 2$ and $K = 1$ which lie one on top of the other.

The described phenomenon was observed in a special experiment. A tube with freely flowing air stream had a telescopic device which allowed the length of the inlet portion to be increased continuously, without changing the conditions under which air was blown into the inlet section. In the end portion of the tube was situated the combustion zone. After vibration combustion was excited, the length of the cold part of the tube was gradually increased and the variation of the oscillation frequency continuously observed. The oscillation frequencies first had a tendency to drop, but then rose abruptly to the initial value.

The physical processes on which this phenomenon is based are rather simple. Assume, for example, that there exists a certain tube with approximately equal lengths of the cold and hot parts, and that oscillations at the fundamental tone are excited in it. Figure 55A shows schematically this tube as well as the pattern of the pressure-oscillation amplitudes in it. Let us assume that the excited frequency and the patterns of the oscillations δp and δv related with it produce in the combustion zone the conditions which contribute the most to the excitation of the system. Then, as the total length of the tube is increased, it is possible to maintain invariant the processes in the combustion zone (in particular, maintain also the configurations of the δp and δv oscillation amplitude patterns) only by maintaining con-

stant the dimensional frequency of the oscillations (in the figure - the distances between the nodes on the pattern), i.e., by changing over to higher harmonics. In the lower part of Fig. 55 is shown the corresponding scheme of the tube with lengthened cold part.

Thus, the oscillation frequency excited by the system is determined to a certain extent by the length and properties of the hot part of the tube, i.e., the combustion chamber. This conclusion agrees with all the available experimental data.

It must be noted that this conclusion has great practical significance. The point is that in the investigation of combustion chambers the question arises of the possibility of testing the chambers away from the engine, by joining them to an air pipe, which frequently is very long. It might appear that this destroys any similarity to the acoustic operating conditions and that one can therefore not investigate with such a setup the vibration combustion processes. However, the analysis of the phenomenon which was presented above shows that this simple argument is incorrect and if the combustion chamber has a tendency toward instability (vibration combustion), then this instability will manifest itself (and furthermore in the same form, without change of oscillation frequency, etc.) also in a setup with a long inlet air duct.

The result obtained must not be interpreted in the sense that the oscillating system is in general insensitive to variation of the length of the cold part of the tube. In fact, all that was shown here is that if we take in lieu of a certain length L_1 of the cold part a different length L^*_1 , and if the new length is many times larger than the initial one ($L^*_1 \gg L_1$), then the oscillation process will be characterized by a tendency toward conservation of both the frequency and all other properties. This enables us to test combustion chambers on stands

that are characterized by very long air supply pipes, without an excessive risk of producing in the combustion zone acoustic conditions that differ radically from the natural conditions. It does not follow from this at all, however, that when the length L_1 is changed all the properties of the oscillating system remain the same. To demonstrate this, let us consider the following example. Let the instability region be small and let under normal conditions the system remain unexcited. We start to increase the length of the cold part of the tube L_1 , retaining all the dimensions of the hot part constant. Then the diagram showing the distribution of the instability regions, analogous to that shown in Fig. 54, may have the form shown in Fig. 56. Let the initial total length of the tube be, for example, $L = 2.5$ m (length AA in Fig. 56). This corresponds to the absence of oscillations, inasmuch as the length AA does not cross the instability regions (shown by solid lines on the figure). Let us lengthen now the inlet portion of the tube, retaining constant the dimensions of the combustion zone and of the portion of the tube through which the combustion products flow. When $L > 3.1$ m any length L will correspond to some instability region (line BB in Fig. 56), i.e., when the inlet portion of the tube is made sufficiently long, the initially stable process can become unstable. To be sure, this presupposes that the system as a whole is prone to excitation, i.e., has instability regions. Thus, if the system is capable of becoming excited, this capability is particularly easy to realize by lengthening the inlet portion of the flow.

This result is also of appreciable practical interest. It means that if the combustion chamber is adjusted on a stand with a long pipe and does not give rise on the stand to vibration-combustion modes, then it is little likely that such modes will be produced in it on changing over to shorter inlet sections. And at the same time, if the

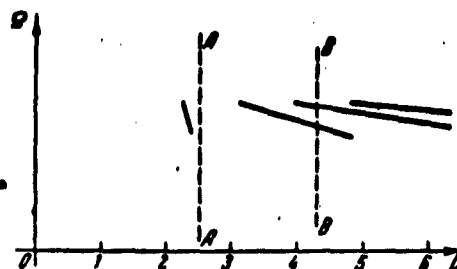


Fig. 56. Influence of the length of the tube on the stability of the flow.

combustion chamber is adjusted with an inlet portion of short length, simply lengthening the inlet is capable of causing vibration combustion.

The foregoing can be confirmed by the following experiment. The experiments were carried out with a combustion chamber with an inlet portion 700 mm long. By varying the fuel feed, excess-air coefficients ranging from $\alpha = 1$ to $\alpha = 3$ were obtained. During the time of the experiment, the pressure oscillation amplitudes δp ahead of the combustion zone were registered. These amplitudes were with respect to the relative pressure (with respect to the outer medium) of the completely stagnant air flow q ahead of the combustion chamber. The relative pressure perturbations $\delta p/q$ were plotted as functions of the excess-air coefficient α . At normal "quiet" combustion modes $\delta p/q$ did not exceed 0.1 or 0.15. Figure 57 shows the experimentally obtained functions $\delta p/q = f(\alpha)$ for three cases: curve a corresponds to the initial version of the setup, with an inlet section $L_1 = 700$ mm long; curve f pertains to a 1400 mm inlet portion; curve d pertains to a 2800 mm inlet portion. As can be seen from the experiment, the initially stable combustion process started to vibrate (with the oscillation amplitudes increasing by a factor 5-10) as a result of merely increasing the length of the cold portion of the stream, L_1 , as would follow from the theory developed here.

It must be added, to be sure, that the arguments on which the foregoing deductions were based started from the assumption that all the instability regions are characterized by perfectly identical mechanisms for the excitation and the quenching of the oscillations. This of course is not always the case, particularly if the oscillating system is capable of becoming excited by various physical processes which realize the feedback (these are discussed in detail in Chapter 7). Nevertheless, the confirmation of many of the consequences of the very simple theory developed here indicates that the theory can be used for first approximation.

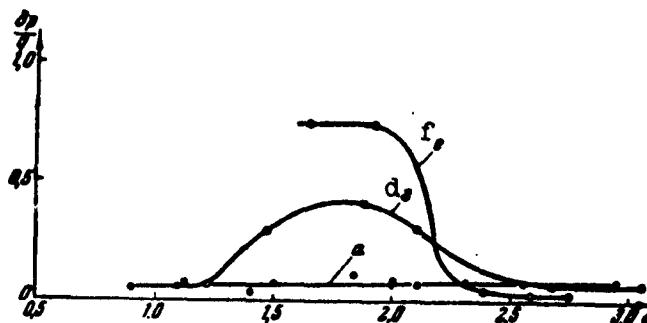


Fig. 57. Effect of length of the inlet portion of the stream on the tendency of the system toward excitation.

To conclude the present section it is useful to present some additional data on the acoustics of stand installations which do not pertain directly to the question of the influence of the relative lengths of the hot and cold portions of the stream on the instability regions.

Although tests of the combustion chamber using a long supply air duct provide a certain guarantee that on changing over to shorter inlet portions the tendency of the oscillating system toward excitation is more likely to decrease than to increase, it may be of interest sometime to test the combustion chamber with a short inlet portion on

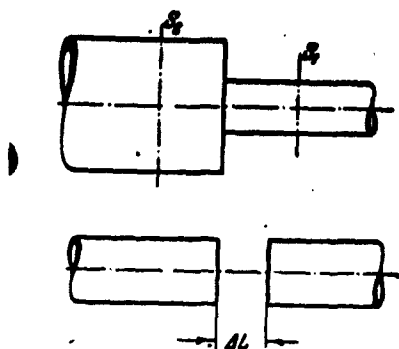


Fig. 58. Two methods of separating the stand air duct from the inlet portion of the combustion chamber.

which the air supply duct does not have any effect. In this case one can conceive of two schemes which separate acoustically the inlet portion of the combustion chamber from the stand air duct (Fig. 58).

The first of these two schemes reduces to the creation of a receiver ahead of the inlet section of the channel that leads to the combustion chamber, while the second reduces to a break in the duct in the required place (it is applicable only for limited pressure inside the duct).

Let us consider the first of these schemes. It is clear intuitively that if the section of the receiver S_2 is much larger than the section of the tube S_1 , then the receiver becomes an "external medium" of a sort, and a pressure node is produced at the junction. The tube with the combustion chamber will be separated, as it were, from all other lines that supply air. Usually the section S_2 cannot be made very large so that it is of interest to obtain a numerical estimate of the influence of the ratio of S_2/S_1 on the degree to which the conditions at the junction between tubes of different diameters approach a pressure node.

In the book by Andreyev and Rusakov* the following expression is given for the ratio of the amplitude of a pressure wave passing through the junction of the tubes to the amplitude of the approaching wave:

$$\eta = \frac{2}{1 + \frac{S_1}{S_2}}.$$

It is obvious that the coefficient η characterizes the degree with which the change in cross section under consideration approaches a

completely open end. In this case $\eta = 0$ indicates the absence of a transmitted wave (complete reflection), while $\eta = 1$ denotes that the wave is completely transmitted. Thus, a reduction in η means an approach to the condition of an open end. In a specially set up experiment, a cylindrical tube 100 mm in diameter, in which vibration combustion took place, was joined to receivers having diameters of 150, 300, 400, and 500 mm. The amplitudes of the pressure oscillations were measured along the receiver and along the tube in the vicinity of the junction. The corresponding patterns and the over-all scheme of the setup are shown in Fig. 59.

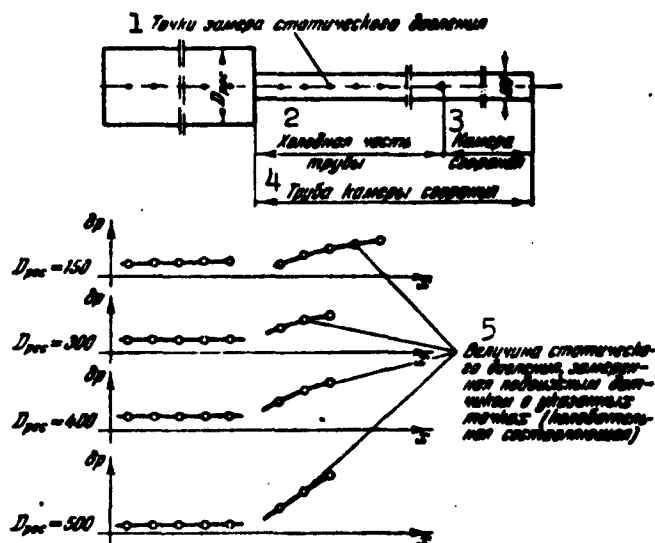


Fig. 59. Patterns of pressure-oscillation amplitudes at the junction between the receiver and the initial portion of the combustion-chamber tube. 1) Points where the acoustic pressure was measured; 2) cold part of the tube; 3) combustion chamber; 4) combustion-chamber tube; 5) value of static pressure measured by a moving transducer at the indicated points (oscillating component).

It is seen from the presented plots that with increasing ratio S_2/S_1 the conditions on the junction of the pipes approach more and more the conditions that are characteristic of an open end. Even suc

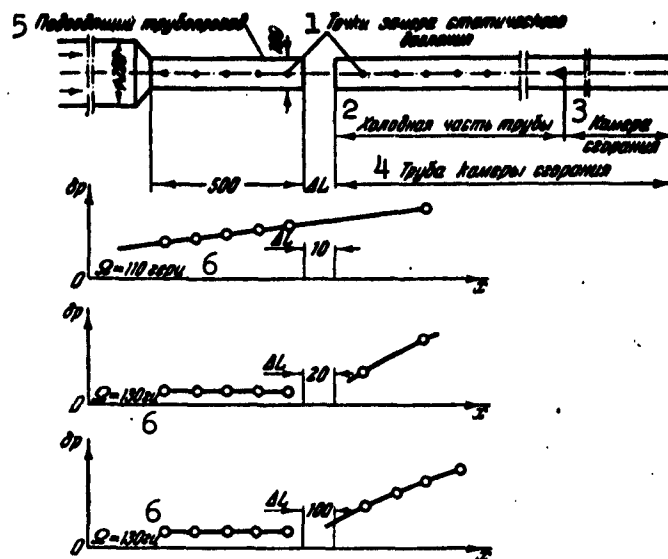


Fig. 60. Patterns of pressure-oscillation amplitudes in the vicinity of a break in the pipe. 1) Points where the acoustic pressure was measured; 2) cold part of the tube; 3) combustion chamber; 4) combustion-chamber tube; 5) supply pipe; 6) cycles per second.

a small increase in diameter in the transition to the receiver as a change from 100 to 150 mm produces a clear-cut standing-wave pattern in the tube. With increasing S_2 , the amplitudes of the oscillations in the receiver decrease, as expected. It is apparently sufficient to have $S_2/S_1 \geq 3$ in order to produce a complete separation of the receiver from the tube.

The second scheme was also investigated experimentally. The break in the pipe had the same purpose, namely to form oscillations with a pressure node at the break. A diagram of the experimental setup and the oscillation-amplitude distribution for vibration combustion, measured in the vicinity of the break, are shown in Fig. 60. As in the preceding experiments, vibration combustion was excited in a tube 100 mm in diameter. With a gap $\Delta L = 10$ mm, the oscillations were transmitted through the break as if it did not exist at all. In this case the

oscillation frequency (110 cps) was in complete agreement with the total length of both parts of the tube separated by the gap. For gap lengths of 20 and 100 mm, the picture changed radically. The pressure-oscillation pattern showed a clear-cut tendency to vanishing at the break, while on the left part of the tube there were observed oscillations of constant but low amplitude. The oscillation frequency increased to 130 cps and started to correspond to the length of the right half of the tube, without the portion lying on the other side of the break. This indicated that to obtain the necessary effect the gap between the tubes should be on the order of 20% of the diameter of the tubes or more.

One can, of course, combine both the indicated schemes, making the supply tube of larger diameter than the tube in which combustion takes place, and simultaneously retaining the gap.

The experimental results obtained are in good agreement with the experiments of Coward, Hartwell, and Georgson, described in §1. Bringing a plate closer to the open end of the tube (the diameter of which was also 100 mm) scarcely influenced the character of the oscillations when the distances between the plate and the tube were equal to 60 and 30 mm. At distances of 15 mm and less, the character of the vibration combustion changed quite radically (see Fig. 1). Thus, removing the plate more than 20% of the diameter away from the end of the tube broke in this case, too, the coupling between the gas oscillations in the tube and the obstacle brought together at the end of the tube.

Manu-
script
Page
No.

[Footnotes]

- 182 The subscripts "one" for β , γ , and ω are omitted here and below.
- 197 It may be seen from Eq. (23.7) that a change in the sign of ω does not violate the equality and it is consequently sufficient to consider the interval $0 < \omega < \infty$ rather than $-\infty < \omega < \infty$.
- 201 For example, see M.A. Ayzerman, Lektsii po teorii avtomaticheskogo regulirovaniya [Lectures on the Theory of Automatic Control], Gostekhnizdat, Moscow, 1958.
- 204 *It has already been stated that, for the equations considered in this chapter, it is sufficient to vary ω from 0 to $+\infty$.
- 204 **In control theory, the left-hand side is generally cross-hatched when $\Delta > 0$ and the right-hand side is generally cross-hatched when $\Delta < 0$. We are here adopting another rule, since the region of instability is cross-hatched in this book.
- 213 In combustion chambers, it is necessary to differentiate the excess-air coefficient calculated for the chamber as a whole from the local value of α in the heating zone. The total α is rarely greater than one because of the air which bypasses the heating zone and mixes with the combustion products below the zone of intensive heating.
- 226 The subscript "one" is henceforth omitted for ω .
- 241 Putnem and Dennis, Issledovaniye vibratsionnogo gorenija v gorelках [Investigation of Vibrational Heating in Jets], Voprosy raketnoj tekhniki [Problems of Rocket Technology], No. 5 (23), 1954.
- 252 Andreyev, N.N. and Rusakov, I.G., Akustiki dvizhushcheysya sredy [The Acoustics of Moving Media], GTII [State Theoretical and Technical Editions], 1934.

Manu-
script
Page
No.

[List of Transliterated Symbols]

- 208 $cr = sg = sgoraniye = combustion$
- 209 $xhm = khim = khimicheskiy = chemical$

Chapter 6

EXCITATION OF OSCILLATIONS BY HEAT SUPPLY IN THE PRESENCE OF LOSSES AT THE ENDS OF THE TUBE

§30. Losses to Radiation

In the present chapter we consider the same problem as in the preceding one, except that we leave out the assumption that there are no losses of acoustic energy. The losses that accompany acoustic oscillations can be arbitrarily broken down into two groups: internal losses, connected with viscosity and heat-conduction forces acting inside the tube, and external losses, connected with the radiation of the oscillatory energy into the outside medium. We shall consider here only the second of these types of losses, and furthermore in simplest form.

Radiation of acoustic energy from the end of a tube is connected with the presence of a nonzero flux of acoustic energy moving from the tube into the outer space. From the expression for the flux of acoustic energy through any section (11.6) we see that the question of the magnitude and the sign of the flux A is connected with the amplitudes of δp and δv and with the phase shift between them. To determine these quantities one introduces in acoustics the concept of impedance. It can be defined formally as a complex factor which relates δp and δv . It is more convenient to introduce here directly the dimensionless impedance \underline{z} , which relates \bar{p} and \bar{v} ,

$$\bar{p} = z\bar{v}. \quad (30.1)$$

Inasmuch as \bar{p} and \bar{v} are different in different sections of the

standing wave, the impedance \underline{z} will also be different, depending on where the section is chosen. Usually the greatest interest is attached to the impedances of the end sections, inasmuch as the radiation of the energy into the outside medium occurs naturally through the end sections.

In order to disclose the physical meaning of the real and imaginary components of the impedance

$$z = r + ix, \quad (30.2)$$

we turn to the variables \vec{u} , \vec{w} .

We introduce in analogy with the acoustic impedance \underline{z} a quantity ζ , which relates \underline{u} and \underline{w} . For this purpose it is convenient to regard \underline{u} and \underline{w} as complex numbers. The quantity ζ is defined by the equation

$$w = \zeta u, \quad (30.3)$$

from which it follows immediately that

$$|\zeta| = \frac{|w|}{|u|}. \quad (30.4)$$

Because the absolute values of \underline{u} and \underline{w} between the discontinuity surfaces Σ do not depend on the coordinate ξ in the case of steady-state oscillations, the quantity $|\zeta|$ will possess the same property. This distinguishes ζ favorably from the impedance \underline{z} , and the property that $|\zeta|$ is independent of ξ will be made use of later on in Chapter 8.

Let us determine ζ . Using (4.9), (30.1), and (30.4) we can readily verify that

$$\zeta = \frac{1-r}{1+r}. \quad (30.5)$$

With account of (30.2) we obtain

$$|\zeta|^2 = \frac{(1-r)^2 + r^2}{(1+r)^2}. \quad (30.6)$$

Equations (11.7) and (30.4) enable us to write the following formula for the flux A of the acoustic energy (we regard \underline{u} and \underline{w} again

as vectors here and below):

$$A = \frac{1}{8\rho_0 c} (1 - |\zeta|^2) \omega^2 \quad (30.7)$$

Since all the quantities contained in this formula are positive, the sign of A will depend entirely on the difference $1 - |\zeta|^2$. Consequently, the sign of the flux of acoustic energy is determined by the modulus of ζ . When $|\zeta| > 1$ the flux of acoustic energy is negative, i.e., it is directed against the stream, while when $|\zeta| < 1$ it is positive (directed with the stream).

The modulus of ζ depends on the real and imaginary parts of the acoustic impedance \underline{z} . It is known from acoustics that the real part \underline{r} of the impedance determines the active resistance of the acoustic system, while the imaginary part \underline{x} determines the reactance. The losses are obviously connected with the active resistance. This is clear, in particular, from Formula (30.6), which shows that the deviation of the modulus ζ from unity is connected with the value of the dimensionless coefficient of active resistance \underline{r} . When $r = 0$ we have $|\zeta| = 1$ and the acoustic radiation of energy from the end of the tube, as follows from Formula (30.7), is nil. When $r > 0$ we have $|\zeta| < 1$ and when $r < 0$ we have $|\zeta| > 1$, i.e., different signs of \underline{r} correspond to opposite directions of motion of the acoustic-energy flux. It must always be remembered that the impedances z_1 and z_2 , corresponding to different ends of the tube, have real parts that are of opposite signs. The impedance z_2 , corresponding to the section through which the hot gases flow, has positive \underline{r} (the radiation is in the positive direction of the ξ axis) while the impedance z_1 has negative \underline{r} . Accordingly, $|\zeta_2| < 1$, i.e., the acoustic-energy flux moves along the stream at the outlet section, from the tube into the surrounding space, while $|\zeta_1| > 1$, i.e., the acoustic-energy flux at the inlet to the tube flows against the stream,

consequently, again from the tube into the surrounding space. This indicates that acoustic energy is being dissipated on both ends of the tube.

When solving the problem with allowance for the loss of acoustic energy into the space surrounding the tube, we shall use both methods of taking these losses into account: with the aid of the impedance \underline{z} and with the aid of the coefficient ζ . The choice of the particular method will be determined by the character of the problem considered.

In conclusion, it is necessary to present formulas with which to carry out the actual determination of the impedances. For the previously chosen system of dimensionless variables, both components of the dimensionless impedances \underline{z} (30.2) coincide with those adopted in acoustics. One can, for example, use the following approximate formulas proposed by Gutin*:

$$r = \frac{k^2 d^2}{16}, \quad z = \frac{k d}{\pi},$$

where \underline{d} is the tube diameter and \underline{k} is the wave number (the ratio of the frequency to the velocity of sound).

For subsequent use, it is convenient to recast these quantities in a somewhat different form. Representing the wave number in the form

$$k = \omega/L,$$

we obtain for \underline{z} the expression

$$z = \left(\frac{d}{4L}\right)^2 \omega^2 + i \frac{d}{\pi L} \omega. \quad (30.8)$$

The values of the impedance \underline{z} obtained from Formula (30.8) can be used only for sufficiently small values of $d\omega/L$. An estimate shows that for the "long" tubes considered in the present book and for the first harmonics the condition that $d\omega/L$ be small is always satisfied.

Closely related with the question of radiation of acoustic energy into the surrounding space is the question of the so-called "effect of

the open end."

Usually the boundary condition at the open end is written either in the form of Eq. (30.1) or, in a less rigorous analysis, in the form $\bar{p} = 0$. In the latter case it is assumed that there are no pressure oscillations in the end section of the open end of the tube. This assumption was used already by Lagrange, Euler, and Bernoulli, but the researches of the acousticians of the 19th century have shown that it can be used only with certain stipulations. The theoretical solution of the problem concerning the reflection of an acoustic impulse from the open end of a tube is made complicated by the fact that a plane wave moving through the tube becomes spherical (more accurately, ceases to be one-dimensional) outside the tube. However, for many specific schemes, theoretical solutions were obtained and in addition, corresponding experiments were set up. A review of these researches was presented, in particular, by Rayleigh.* Without going into details here, we shall indicate only two circumstances which must be taken into account when writing down the boundary conditions for the open ends of the tube.

First, the oscillating process at the open end always causes dissipation of acoustic energy into the surrounding space. In this case the dissipation is connected not with the conversion of acoustic energy into heat, but with the transfer of mechanical (acoustic) energy to surrounding masses which are external with respect to the tube. This phenomenon was essentially taken into account by the formulas presented in the present section.

Second, even if we neglect energy dissipation, then the effect of the inertia of the medium ahead of the outlet of the tube reduces to an apparent elongation of the tube. The frequencies excited in the tube are somewhat lower than those which would be obtained were the

realized scheme ideal. Therefore in order to take this phenomenon into account it is customary to increase the length of the tube somewhat in the calculations, so as to obtain better agreement with experiment. Rayleigh recommends to increase the theoretical dimension of the tube by an amount equal to approximately 0.3 of the tube diameter for the open end.

In carrying out all the calculations below it will be assumed that this correction has already been introduced and the "effect of the open end" will no longer be discussed.

§31. Characteristic Equation of the Problem with Account of Losses at the Ends of the Tube

In the preceding chapter we have found the characteristic equation of the problem in the absence of losses at the ends of the tube. Here we consider a more general case.

Assume that on the plane Σ (Fig. 22) at the section $\xi = 0$ the dimensionless perturbations of the pressure and velocity on the left are \bar{p}_0 and \bar{v}_0 , respectively, while on the right they are \bar{p}'_0 and \bar{v}'_0 . The connection between these perturbations is established by the properties of the surface Σ . We proceed further in exactly the same manner as was done in §23. Assuming a certain specified connection between $\delta E'$, $\delta X'$ and \bar{v}_0 , \bar{p}_0 , and using Eqs. (17.5), we obtain the following form for the conditions on Σ :

$$\left. \begin{aligned} \bar{v}_0 &= a_{11}\bar{v}_0 + a_{12}\bar{p}_0 \\ \bar{p}_0 &= a_{21}\bar{v}_0 + a_{22}\bar{p}_0 \end{aligned} \right\} \quad (31.1)$$

Let us express \bar{p} and \bar{v} at the ends of the tube (at $\xi = \xi_1$ and $\xi = \xi_2$) in terms of \bar{v}_0 , \bar{p}_0 and \bar{v}'_0 , \bar{p}'_0 , with the aid of Formulas (4.13), and let us use the following boundary conditions

$$\left. \begin{aligned} \bar{p} &= z_1\bar{v} \text{ for } \xi = \xi_1, \\ \bar{p} &= z_2\bar{v} \text{ for } \xi = \xi_2. \end{aligned} \right\} \quad (31.2)$$

As a result we obtain

$$\begin{aligned}\bar{v}_0[z_1\varphi_1(\xi_1) - \varphi_1(\xi_1)] + \bar{p}_0[z_1\varphi_1(\xi_1) - \varphi_1(\xi_1)] &= 0, \\ \bar{v}_0[z_2\varphi_2(\xi_2) - \varphi_2(\xi_2)] + \bar{p}_0[z_2\varphi_2(\xi_2) - \varphi_2(\xi_2)] &= 0.\end{aligned}$$

Taking into consideration Relations (31.1), we can readily reduce the number of dependent variables in the last equations to two, for example \bar{v}_0 and \bar{p}_0 .

As a result we obtain the characteristic equation of the problem:

$$\begin{vmatrix} z_1\varphi_1(\xi_1) - \varphi_1(\xi_1) & z_2\varphi_2(\xi_2) - \varphi_2(\xi_2) \\ a_{11}[z_1\varphi_1(\xi_1) - \varphi_1(\xi_1)] + & a_{12}[z_2\varphi_2(\xi_2) - \varphi_2(\xi_2)] + \\ + a_{21}[z_1\varphi_1(\xi_1) - \varphi_1(\xi_1)] & + a_{22}[z_2\varphi_2(\xi_2) - \varphi_2(\xi_2)] \end{vmatrix} = 0. \quad (31.3)$$

Using Relations (4.14) and (22.5) we obtain from (31.3)

$$\begin{aligned}C_1 \exp\left(\frac{2}{1-M_1} \beta_1\right) \exp\left(\frac{2}{1-M_2} \beta_2\right) + C_2 \exp\left(\frac{2}{1-M_1} \beta_1\right) + \\ + C_3 \exp\left(\frac{2}{1-M_2} \beta_2\right) + C_4 = 0,\end{aligned} \quad (31.4)$$

where

$$\left. \begin{aligned}C_1 &= (z_1 - 1)(z_2 + 1)(a_{12} - a_{22} - a_{11} + a_{21}), \\ C_2 &= (z_1 - 1)(z_2 - 1)(a_{12} + a_{22} - a_{11} - a_{21}), \\ C_3 &= (z_1 + 1)(z_2 + 1)(a_{12} - a_{22} + a_{11} - a_{21}), \\ C_4 &= (z_1 + 1)(z_2 - 1)(a_{12} + a_{22} + a_{11} + a_{21}).\end{aligned} \right\} \quad (31.5)$$

Thus, the obtained characteristic equation differs from (23.5) only in the expressions for the coefficients C_1 , C_2 , C_3 , and C_4 .

In the preceding chapter the characteristic equation (23.5) was reduced to a system of two equations (23.7) which related only real variables. If we attempt to do the same in the present case, the equations obtained will be more cumbersome. The point is that it is no longer possible to assume that C_1 , C_2 , C_3 , and C_4 are real, inasmuch as the impedances z_1 and z_2 are generally speaking complex numbers. The separation of Eq. (31.4) into a system of two equations which relate real variables is best carried out after the actual numerical values of z_1 , z_2 , a_{11} , a_{12} , a_{21} , and a_{22} have been substituted in.

It is easy to obtain particular cases from the general equation (31.4). In the preceding chapter we considered the characteristic equation of the same problem, but under the assumption that pressure nodes are located at the ends of the tube. The pressure nodes are described by the condition $\bar{p} = 0$. Comparing this condition with (30.1) we see that the pressure node corresponds to the case $z = 0$. In precisely the same manner we obtain that a velocity node $v = 0$ corresponds to an acoustic impedance $z = \infty$.

If we combine the two types of boundary conditions ($\bar{p} = 0$ and $\bar{v} = 0$) then altogether only four cases are possible:

- 1) $\bar{p}_1 = 0, \bar{p}_2 = 0;$
- 2) $\bar{p}_1 = 0, \bar{v}_2 = 0;$
- 3) $\bar{v}_1 = 0, \bar{p}_2 = 0;$
- 4) $\bar{v}_1 = 0, \bar{v}_2 = 0.$

We introduce for the quantities in (31.5) the following notation:

$$\begin{aligned} c_1 &= a_{12} - a_{22} - a_{11} + a_{21}, \\ c_2 &= a_{12} + a_{22} - a_{11} - a_{21}, \\ c_3 &= a_{12} - a_{22} + a_{11} - a_{21}, \\ c_4 &= a_{12} + a_{22} + a_{11} + a_{21}. \end{aligned}$$

Then the first case corresponds to the equalities

$$C_1 = -c_1, \quad C_2 = c_2, \quad C_3 = c_3, \quad C_4 = -c_4;$$

the second to

$$C_1 = -c_1, \quad C_2 = -c_2, \quad C_3 = c_3, \quad C_4 = c_4;$$

the third to

$$C_1 = c_1, \quad C_2 = -c_2, \quad C_3 = c_3, \quad C_4 = -c_4$$

and the fourth to

$$C_1 = c_1, \quad C_2 = c_2, \quad C_3 = c_3, \quad C_4 = c_4.$$

Assuming the coefficients c_1, c_2, c_3 , and c_4 to be real, we can carry out the analysis of the properties of the oscillating system in all these cases in the same manner as was done for the first case in Chapter 5.

It must be noted that there exists no such simple method for solving and analyzing Eqs. (31.4) in the case of arbitrary values of the boundary impedances. The main difficulty lies in this case in the fact that the frequency ω is contained in the expression for z (30.8). Therefore the solution of (31.4) can be obtained only by cumbersome numerical methods.

§32. Numerical Analysis of Some Particular Cases

An analysis of the character of the perturbed process on the basis of Eq. (31.4) can be carried out in two ways. First, by considering numerical examples and, second, by a theoretical investigation of particular cases which admit of an analytic treatment. In the present section we shall use the first of these possibilities.

In analogy with the calculations given in the preceding chapter, let us determine the stability limit in the presence of losses at the ends of the tubes, i.e., we seek those values of δX and δE , for which the oscillating system is neutral. We shall assume the flow conditions and the position of the heat-supply plane to be specified (i.e., n , M_1 , M_2 , \underline{l}_1 , and \underline{l}_2 are specified), and we choose as the variable parameter the oscillation frequency ω . Since by definition $v = 0$ (we are considering the stability limit), by the same token all the quantities contained in (31.4) are specified (for each value of ω), except for the coefficients C_1 , C_2 , C_3 , and C_4 , which depend (through a_{11} , a_{12} , a_{21} , a_{22}) on the sought values of δX and δE .

Comparing Formulas (17.1) and (31.1), we readily see that when $\delta E = y_1 \bar{p}_0$ and $\delta X = y_2 \bar{v}_0$ (where y_1 and y_2 are complex coefficients which express mathematically the existence of a certain feedback mechanism) we have:

$$\left. \begin{aligned} a_{11} &= \frac{1}{n}, & a_{12} &= -\frac{M_1}{n}, \\ a_{21} &= -\frac{M_2}{m}, & a_{22} &= \frac{1}{m}. \end{aligned} \right\} \quad (32.1)$$

Let us consider, for the sake of being definite, the case of excitation of oscillations with $\delta E = 0$. Under the assumption made $y_1 = 0$ and Eq. (31.4) becomes linear with respect to y_2 , which is readily determined from this equation.

The results of calculations of this type will be presented below. The calculations were made for two cases. In the first analysis was made of the influence of the oscillation frequency on the position of the stability limit, while in the second the influence of the change in the relative length L/d of the tube (more accurately, a quantity reciprocal to L/d) on the same factor was determined. In both cases the calculations were made for $M_1 = 0.15$; $n = 2.5$; $m \approx 1$; $\underline{l}_1 = \underline{l}_2 = 0.5$.

In the first series of calculations, the aim of which was to illustrate the influence of the oscillation frequency on the position of the stability limit, d/L was assumed equal to 0.2, i.e., a relatively short tube was considered, with a 5 caliber length. The results of the calculation are shown in Fig. 61. The abscissas and the ordinates are the real and imaginary parts of y_2 , respectively. The complex coefficient y_2 makes it possible to judge the amplitude-phase relation between δX and \bar{v}_0 . In the preceding chapter and earlier we obtained an exceedingly simple self-excitation condition for the oscillations in the absence of losses, namely that the angle between the phases of \bar{v}_0 and δX must be less than $\pi/2$. Inasmuch as for $\delta X = y_2 \bar{v}_0$ the phases of δX and \bar{v}_0 coincide at positive (real) values of y_2 , the stability boundary in the previously considered example is the imaginary axis, and the instability region is the entire right half plane of Fig. 61. As can be seen from the placement of the y_2 curves on Fig. 61, when the losses are taken into account the instability region decreases, namely the stability boundaries shift to the right away from the imaginary axis, the shift being the greater, the higher the oscillation

frequency (the "unstable" side of the stability boundary is shaded in the diagram). In this case the excitation condition becomes more complicated, and not only the phase of δX but also its amplitude becomes important now.

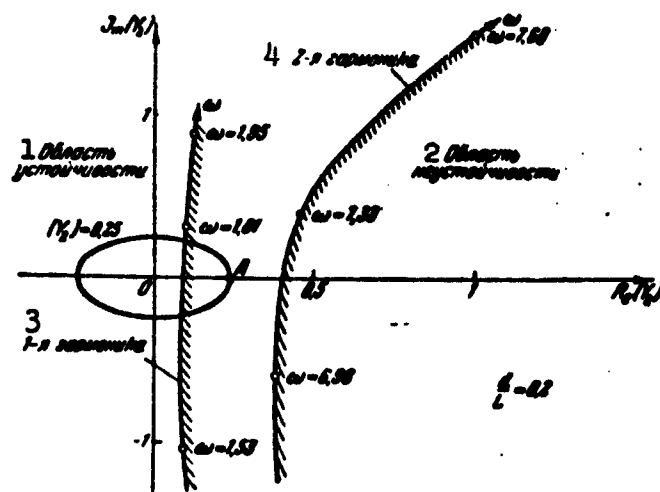


Fig. 61. Influence of oscillation frequency ω on the position of the stability boundary. 1) Stability region; 2) instability region; 3) first harmonic; 4) second harmonic.

The smallest relative amplitude of δX (\bar{v}_0 is arbitrarily assumed as unity) at which excitation is possible is obtained when the phases of δX and \bar{v}_0 coincide (y_2 is a real quantity). Figure 61 shows only two branches of y_2 (corresponding to the first and second harmonics). As can be seen from the diagram, an increase in frequency (changeover from the first to the second harmonic) involves an increase in the absolute values of y_2 , i.e., an increase in the relative amplitudes δX necessary to excite the system.

This result can be readily explained. Let us estimate the influence of the oscillation frequency on the losses of acoustic energy in the space surrounding the tube. For this purpose we use Expression (30.7), which enables us to calculate the flux of acoustic energy mov-

ing through the end section of the tube. We employ here Formula (30.6), which enables us to express $|\zeta|^2$ in terms of the real and imaginary parts of the impedance \underline{z} . Then

$$A = \frac{r}{2\rho_0 c [(1+r)^2 + x^2]} \omega^2.$$

The formula obtained indicates, in particular, that the sign of A (the direction of the flux of acoustic energy) is connected with the sign of the coefficient of active resistance \underline{r} . This formula can be simplified in the following fashion. We note that the expression in the square brackets is close to unity, since \underline{r} and \underline{x} are small compared with unity for the problems under consideration. This is seen, for example, from the approximate formula for \underline{z} (30.8) and was particularly emphasized at the end of §30.

Thus, for sufficiently "long" tubes and for low harmonics we have

$$A \approx \frac{r\omega^2}{2\rho_0 c} \approx \left(\frac{d}{4L}\omega\right)^2 \frac{\omega^2}{2\rho_0 c}. \quad (32.2)$$

The approximate equality (32.2) shows that the flux of acoustic energy through the end section of the tube is proportional to the square of the frequency. Consequently, the reduction in the probability of excitation on going over to higher harmonics is perfectly natural and the course of the curves on Fig. 61 should be regarded as typical. Higher frequencies would yield stability limits which would be shifted even further to the right.

In practice y_2 cannot increase without limit. The really existing feedback mechanisms bring about the existence of an upper limit for this quantity. If, in particular, the upper limit of y_2 exceeds the values necessary for the excitation of the first harmonic but is smaller than the values necessary for the excitation of the second (point A on Fig. 61), then excitation of oscillations at the fundamental tone is possible, while that at all higher harmonics is impossible.

The example considered explains well the fact that in experiments one observed always excitation of oscillations at relatively low frequencies.

Let us estimate the order of y_2 . It is known from experiments that when the vibration-combustion process is fully developed the amplitude of the pressure oscillations δp has the order of the pressure drop between the cold and hot gas, i.e., the order of the hydrostatic head produced by the thermal resistance. This drop can be expressed by the following formula

$$p_1 - p_2 = \rho_1 v_1^2 \left(\frac{v_2}{v_1} - 1 \right).$$

Thus

$$|\delta p| \approx \rho_1 v_1^2 \left(\frac{v_2}{v_1} - 1 \right).$$

Changing over to dimensionless variables and assuming that in first approximation we have $v_2/v_1 = T_2/T_1 = n^2$, we get

$$|\bar{p}_1| \approx M_1^2 (n^2 - 1).$$

When the oscillations are fully developed, the velocity-oscillation amplitude has the order of magnitude of the velocity of the steady-state flow of the cold gas, and consequently

$$|\bar{v}_1| = \left| \frac{\delta v_1}{v_1} \right| \approx \frac{v_1}{v_1} = M_1.$$

The order of magnitude of $\delta X \approx \bar{p}_2 - \bar{p}_1$ can be regarded as coinciding with the order of the quantities \bar{p}_1 and \bar{p}_2 . Then

$$|y_1| < \left| \frac{\bar{p}_1}{n} \right| \approx M_1 (n^2 - 1).$$

A smaller value of y_2 is more probable, since the pressure difference on the left and on the right of the combustion zone usually amounts to not more than 1/2 to 1/3 of the total oscillation amplitude δp .

In the numerical example considered here ($n^2 = 6.25$; $M_1 = 0.15$)

the order of the absolute magnitude of y_2 will thus not exceed $|y_2| = 0.25$. Comparing this value with the abscissas of the points where the y_2 curves cross the real axis (Fig. 61), we can readily conclude that in this case excitation is possible at the first harmonic of the system only, and this only under specially favorable circumstances. This can be seen from the fact that the circle $|y_2| = 0.25$ encloses only a very insignificant part of the instability region (at the scales chosen for Fig. 61, this circle has become an ellipse). Such a result is connected with the fact that the ratio $d/L = 0.2$ assumed in the calculation is too large. What is essentially considered here is too "short" a tube ($L = 5d$), for which the relative losses will be high.

This is seen, for example, from Formula (32.2), according to which the losses increase not only in proportion to the square of the frequency, but also in proportion to the square of the ratio d/L . Consequently, with decreasing d/L the amount of acoustic energy radiated into the surrounding space should decrease and the oscillating system becomes more and more prone to excitation. This explains the well-known experimental fact that vibration combustion can be observed only in sufficiently "long" tubes, i.e., in tubes with small values of the parameter d/L .

In order to clarify these qualitative considerations, Fig. 62 shows the stability limits for the second harmonics of the same oscillating system as considered above, but for three values of the parameter d/L : 0.2, 0.06, and 0. It is clearly seen from this diagram that with decreasing ratio d/L the value of $|y_2|$ required for the excitation decreases and tends to zero together with d/L .

An experimental confirmation of the theoretical deductions obtained here is afforded by the observation made by Kirkby and Wheeler.* These authors write that at a tube diameter of 100 mm it becomes pos-

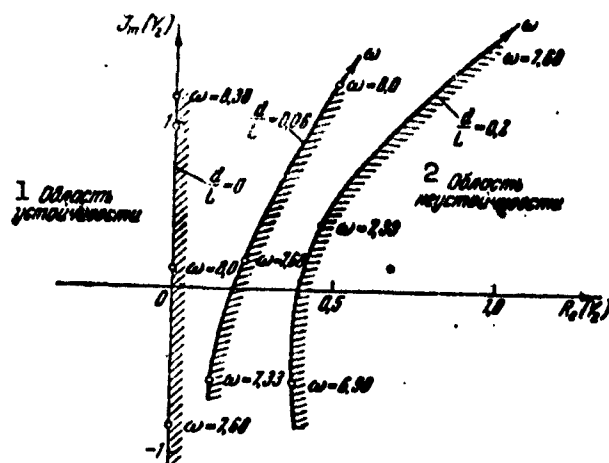


Fig. 62. Influence of the parameter d/L on the position of the stability boundary. 1) Stability region; 2) instability region.

sible to excite vibration combustion in it only when the total length of the tube exceeds 1400 mm.

If we return to the numerical example and continue to assume that the upper limit of $|y_2|$ is 0.25, then it follows from Fig. 62 that when $L \cong 18d$ ($d/L = 0.06$) the second harmonic can be excited, whereas for $d/L = 0.2$ this is impossible.

The example given above of the damping influence of the increase in the oscillation frequency enables us to clarify the arguments advanced at the start of Chapter 2, namely that the initial conditions can be neglected.

Assume that the oscillating system has the same parameters as were used in the numerical example of §23. The only difference will lie in the fact that the losses to radiation of acoustic energy into the outside medium will not be neglected. Figure 33 shows the values of ω and ν obtained for different harmonics without account of radiation losses. If we take these losses into account, then ν and ω could hardly change in noticeable manner for the first harmonic. The second

and third harmonics are damped sufficiently strongly ($\nu \ll 0$) even without the losses to radiation, and an account of these losses merely increases this damping. As regards the fourth harmonic, it is practically neutral, like the first harmonic, without account of the radiation losses. However, an account of the losses alters radically this position, since the frequency of this harmonic is 4.5 times larger than the frequency of the fundamental tone, and the radiation losses increase consequently by 20 times. This consideration enables us to regard all harmonics above the third as damped much more strongly than the first. We shall therefore take into consideration in all the subsequent calculations only the first three harmonics.

Let the character of the process in the combustion zone, on the basis of which we plotted the curves of Fig. 33, change little. Let this small change occur in such a way that the first harmonic becomes neutral ($\nu = 0$). As regards the second and third harmonics, we retain the values of ν corresponding to them, although an account of the losses is more likely to increase the damping decrement.

Let us assume that at the initial instant $\tau = 0$ a complicated oscillatory motion of the air masses takes place in the tube, and this motion consists of standing waves of the first three harmonics, with the amplitudes of the second and third harmonics being twice as large as the amplitudes of the standing wave of the fundamental tone, and the phases of all three harmonics coinciding. Then the pattern for the instantaneous value of the perturbation \bar{p} would have the form shown in the upper part of Fig. 63. The form of the same pattern in succeeding instants of time τ_1 , τ_2 , and τ_3 is shown in the same figure below. We can readily see that after a time $\tau \approx 12$ only the oscillations of the fundamental tone are left. This time corresponds to approximately six or seven oscillations of the fundamental tone. If we recognize that

the longitudinal acoustic oscillations with which we deal in practice range between 20 and 1000 cps, it is obvious that this effect, which is connected with the initial conditions, vanishes within a fraction of a second.

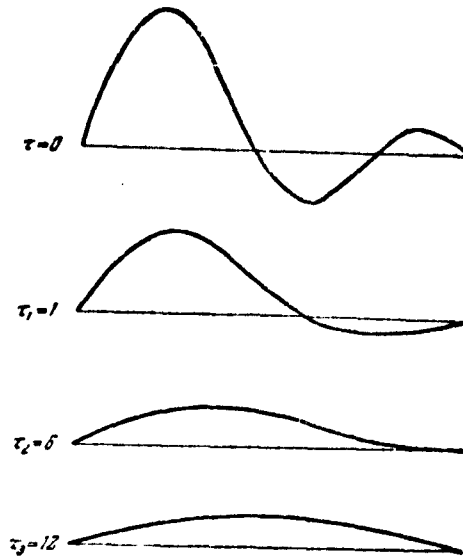


Fig. 63. Gradual vanishing of the influence of the initial conditions.

The crude estimate presented here was aimed at giving a clear-cut representation of the speed with which the influence of the initial conditions is smoothed out in the systems under consideration.

§33. Complete Absorption of Energy at One End of the Tube

It was already indicated above that a numerical analysis of the specific cases is practically the only method of investigating the problems considered in the present chapter. In some cases, however, it is possible to use an analytic approach. Such a problem is, in particular, the investigation of an oscillating system when the energy of the incident acoustic wave is completely absorbed at one end of the tube.

Assume that at the end section of the tube, with coordinate ξ_1

(Fig. 22), the impedance of the aperture is known and is equal to z_1 .

At the other end of the tube, with coordinate ξ_2 , let the total energy of the acoustic waves reaching ξ_2 be absorbed. In such a case the boundary condition for the end with coordinate ξ_2 will be:

$$z_2 = 1.$$

Indeed, if we change over to the variables \underline{u} and \underline{w} , then Formula (30.5) yields $\zeta = 0$ when $z = 1$. But then it follows from (30.3) that $w = 0$ when $u \neq 0$. It was stated in the second chapter that the quantities \underline{w} and \underline{u} are acoustic impulses moving with the stream (u) and against the stream (w). Thus, when $z_2 = 1$ we find that the nonvanishing acoustic impulse \underline{u} that moves with the stream produces upon interaction with the right end ($\xi = \xi_2$) a reflected pulse \underline{w} of zero intensity. This indicates total absorption of the acoustic energy \underline{y} at the end with coordinate $\xi = \xi_2$.

Substituting $z_2 = 1$ in the characteristic equation (31.4) we obtain immediately a particular form of this equation, corresponding to the problem under consideration:

$$\exp\left(\frac{2}{1-M_1^2} \beta l_1\right) = \frac{-(z_1+1)(a_{11}-a_{21}+a_{11}-a_{21})}{(z_1-1)(a_{11}-a_{21}-a_{11}+a_{21})}. \quad (33.1)$$

With the process in the combustion zone specified (δE and δX specified, i.e., in final analysis, when a_{11} , a_{12} , a_{21} , a_{22} are specified) the right half of (33.1) is completely determined. In the general case the calculations yield a certain complex number $A + Bi$. Then we can write in lieu of (33.1)

$$\exp\left(\frac{2}{1-M_1^2} v l_1\right) \left[\cos \frac{2}{1-M_1^2} \omega l_1 + i \sin \frac{2}{1-M_1^2} \omega l_1 \right] = A + Bi. \quad (33.2)$$

Equating real and imaginary parts we immediately obtain

$$\left. \begin{aligned} \omega &= \frac{1-M_1^2}{2l_1} \operatorname{Arctg} \frac{B}{A}, \\ v &= \frac{1-M_1^2}{2l_1} \ln \frac{A}{\cos \left[\operatorname{Arctg} \frac{B}{A} \right]} \end{aligned} \right\} \quad (33.3)$$

Let all the frequencies ω given by the first formula (33.3) represent a solution. Obviously, from among the set of frequencies it is necessary to choose those for which $\cos [\text{Arctan } B/A]$ has the same sign as the number A , inasmuch as $\exp [2v\underline{1}_1/(1 - M_1^2)]$ can only be positive.

It is appropriate to make a few remarks concerning the solution obtained here. The distance $\underline{1}_2$ between the combustion zone and the section at which total absorption of the oscillating energy occurs does not exert any influence at all on the solution. This result is understandable, since at the section ξ_2 all the waves that come from the combustion zone are quenched, and no reflected waves arise. Consequently, there exist on the right of the heat-supply plane Σ only waves that travel in the positive ξ direction. From this point of view, the presence to the right of the plane Σ of a section with impedance $z = 1$ is equivalent to a tube of infinite length in the positive direction. In this connection the existence of natural frequencies, given by the first formula of (33.3), may appear to be unexpected. As is well known, standing waves of the type described by the solution (33.3) arise as the result of a sequence of reflections of acoustic impulses from both ends of the tube. In the case under consideration the boundary condition $z_2 = 1$ is equivalent to a semi-infinite tube, in which there are no waves reflected from the right end. Standing waves nevertheless arise because the second boundary condition comprises essentially the conditions for the interaction between the acoustic waves and the processes in the heat-supply zone. The point is that the waves approaching the heat-supply zone not only pass through it, but are partially also reflected. In addition, the heat-supply process which oscillates under the influence of the incident wave is itself capable of generating acoustic waves propagating in both directions. These reflected and generated waves return to the section ξ_1 , so that between

the left end of the tube and the heat-supply there exist both types of waves, both those traveling in the positive direction and those traveling in the negative direction. Their interaction indeed gives rise to the standing wave. This explains also the fact that the natural frequencies depend only on the distance l_1 , on the value of M_1 , on the impedance z_1 , and on the properties of the heat-supply plane Σ .

This raises a natural question: can such a system become excited, i.e., can there exist conditions on Σ such as to yield $\nu > 0$?

To answer this question let us simplify the problem somewhat by assuming that a pressure or velocity node is located at the section ξ_1 ($z_1 = 0$ or $z_1 = \infty$).

It is seen from the solution (33.1) that these two cases differ only in the sign of the first part of the solution. Turning to Formulas (33.3), we can easily note that this difference leads only to a decrease in the oscillation frequency, but cannot change the value of ν . Consequently, both cases will be considered simultaneously, and for the sake of being specific we shall put $z_1 = \infty$. This choice of the boundary condition on the left end of the tube is also dictated by the fact that there are known experiments, to which reference will be made below, which make it possible to compare the obtained theoretical solution with the experiment. In order to find the number

$$A + Bi = - \frac{a_{11} - a_{22} + a_{11} - a_{22}}{a_{11} - a_{22} - a_{11} + a_{22}},$$

we turn to Formulas (32.1). After substituting the values of the coefficients a_{11} , a_{12} , a_{21} , and a_{22} we obtain

$$A + Bi = - \frac{\frac{m}{n} (y_1 + 1) - (y_1 + 1)}{\frac{m}{n} (y_1 - 1) + (y_1 - 1)}.$$

Let us consider, as was done in the preceding chapter, two elementary processes in the heat-supply zone. One is characterized by the

condition $\delta E = 0$ ($y_1 = 0$) and the other by the condition $\delta X = 0$ ($y_2 = 0$). Let us write out the values of the number $A + Bi$ for both cases:

$$\left. \begin{aligned} A + Bi &= -\frac{\frac{n}{m} - (y_1 + 1)}{\frac{n}{m} - (y_1 - 1)} & (y_2 = 0), \\ A + Bi &= \frac{\frac{m}{n} - (y_2 + 1)}{\frac{m}{n} - (y_2 - 1)} & (y_1 = 0). \end{aligned} \right\} \quad (33.4)$$

Comparison of the two expressions in (33.4) shows that they have a perfectly identical structure. Therefore the results obtained in the investigation of one case can be readily transferred to the other case.

For the sake of being specific, we assume $y_1 = 0$. We put further

$$y_2 = a + bi. \quad (33.5)$$

After simple transformations we obtain

$$A + Bi = \frac{\left[\left(a - \frac{m}{n} \right)^2 - 1 + b^2 \right] - 2M}{\left(a - 1 - \frac{m}{n} \right)^2 + b^2}.$$

To abbreviate the notation we denote

$$\exp\left(\frac{2}{1-M_1^2} \omega l_1\right) = c. \quad (33.6)$$

Then on the basis of (33.2) we can set up the following system of equations, which relates the real variables \underline{a} and \underline{b} :

$$\left. \begin{aligned} \left(a - \frac{m}{n} \right)^2 - 1 + b^2 &= -2b \operatorname{ctg} \frac{2}{1-M_1^2} \omega l_1, \\ c \left[\left(a - 1 - \frac{m}{n} \right)^2 + b^2 \right] &= \frac{-2b}{\sin \frac{2}{1-M_1^2} \omega l_1}. \end{aligned} \right\} \quad (33.7)$$

We shall seek the lines of equal v in the complex plane of the variable y_2 (33.5). For specified values of \underline{l}_1 and M_1 and for a specified constant v the quantity \underline{c} is also a specified number. Using the system (33.7), we can obtain the values of \underline{a} and \underline{b} , which are the real and imaginary parts of y_2 , for a series of specified values of v . Physically this means a determination of the relative values of δX at which oscillations with prescribed increment or decrement v arise. The

frequency ω which enters in the system (33.7) is a parameter that must be eliminated.

) Squaring (33.7) and using the well-known trigonometric relation

$$\operatorname{ctg}^2 \alpha + 1 = \frac{1}{\sin^2 \alpha},$$

we obtain the sought-for relation between \underline{a} and \underline{b} :

$$\begin{aligned} & \left[\left(a - \frac{m}{n} \right)^2 - 1 + b^2 \right]^2 - \\ & - c^2 \left[\left(a - 1 - \frac{m}{n} \right)^2 + b^2 \right]^2 + 4b^2 = 0. \end{aligned} \quad (33.8)$$

Equation (33.8) is of the fourth degree in \underline{a} and \underline{b} . We can therefore expect a complicated form of the curve, determined by these equations in the coordinate plane (a, b) . Careful analysis enables us to establish that Eq. (33.8) can be recast in the form

$$\begin{aligned} & \left[\left(a - 1 - \frac{m}{n} \right)^2 + b^2 \right] \left\{ \left[\left(a + 1 - \frac{m}{n} \right)^2 + b^2 \right] - \right. \\ & \left. - c^2 \left[\left(a - 1 - \frac{m}{n} \right)^2 + b^2 \right] \right\} = 0. \end{aligned}$$

Thus, Eq. (33.8) breaks up into two quadratic equations, and in place of a fourth-degree curve in the (a, b) plane we obtain the circle

$$\left(a + 1 - \frac{m}{n} \right)^2 + b^2 - c^2 \left[\left(a - 1 - \frac{m}{n} \right)^2 + b^2 \right] = 0, \quad (33.9)$$

the position and radius of which depend on the parameter \underline{c} , as well as a circle which shrinks to the point

$$\left(1 + \frac{m}{n}; 0 \right). \quad (33.10)$$

Physical interest attaches to the circle (33.9). By definition we have on the stability limit $v = 0$, which on the basis of (33.6) leads to $c = 1$. But then (33.9) degenerates into the equation of a straight line and yields

$$a = m/n. \quad (33.11)$$

Thus, the stability limit in the case under consideration is a line parallel to the imaginary axis and located a distance m/n from

the origin. In the general case the family of circles (33.9) is characterized by the fact that the centers of the circles always lie on the real axis (the equation for the family does not have terms that depend linearly on \underline{b}). Further analysis of the solution obtained is best carried out with a numerical example.

Let us put, as in the preceding example, $m/n = 0.4$. Specifying values $c = 2.5, 1.67, 1.25, 1.0, 0.83$, and 0.713 ($c > 1$ represents instability and $c < 1$ stability), we obtain the family of lines $v = \text{const}$ shown in Fig. 64. As can be seen from this diagram, as v tends to either $-\infty$ or $+\infty$ ($c \rightarrow 0$ and $c \rightarrow \infty$, respectively), the radii of the circles decrease and tend to zero. In the limit as $c \rightarrow 0$ we obtain from (33.9) a circle of zero radius (a point) with coordinates $(-1 + m/n; 0)$, and as $c \rightarrow \infty$ we get the point $(1 + m/n; 0)$. These points are marked in Fig. 64 by the letters A and B. With respect to the last point it should be noted that it is not only the limiting value of the line of equal increment when $v \rightarrow +\infty$, but satisfies also all other values of v , as can be seen from a comparison of the coordinates of the point B and (33.10).

The location of the stability boundaries on Fig. 64 indicates that when $\delta X = \delta E = 0$ (origin) the system is stable. We recall that in the absence of losses at the end the system was neutral when $\delta X = \delta E = 0$. Thus the presence of losses, as expected, makes an oscillating system more stable and less prone to excitation.

Let us determine the degree of stability of the system in this case. Using Formulas (33.3) and (33.4) and putting $y_1 = y_2 = 0$, we obtain directly

$$\omega = \frac{1 - M_1}{2z_1} k\pi,$$

where $k = 0, 1, 2, 3, \dots$; in this case $z_1 = 0$ corresponds to even

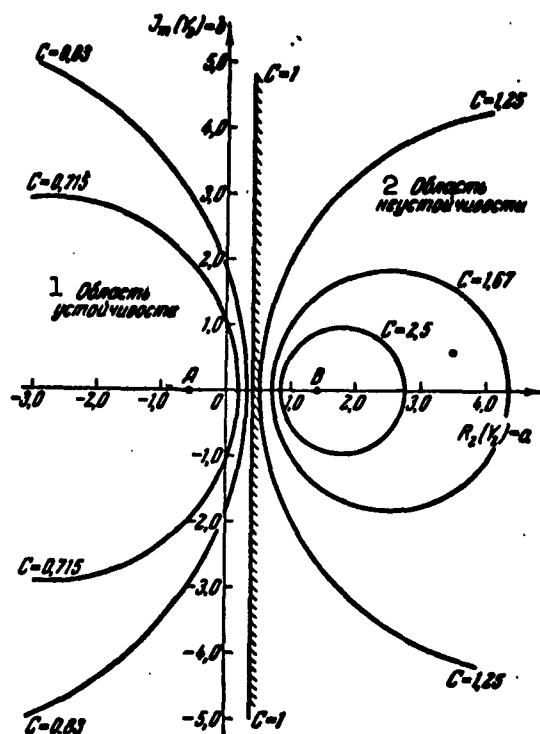


Fig. 64. Stability diagram for the case of total absorption of acoustic energy at one end of the tube. 1) Stability region; 2) instability region.

values of k and $z_1 = \infty$ to odd values. Independently of these values of z_1 , the damping decrement will be

$$\nu = \frac{1-M^2}{2I_1} \ln \frac{1-\frac{m}{n}}{1+\frac{m}{n}}.$$

As can be seen from the formula obtained, the degree of stability of the oscillation process depends principally on m/n , more accurately on \underline{n} , inasmuch as $m \cong 1$. The value of \underline{n} is equal to the ratio of the velocity of sound in hot and cold gas, and consequently, the degree of stability of the process in this system depends primarily on the ratio of the temperatures of the hot and cold gas. The larger this ratio (the larger \underline{n}) the closer the process is to neutral. When the temperatures on both sides of Σ are equal (i.e., when $n = 1$) and when $m = 1$ (as al-

ready mentioned, this quantity is always close to unity) we have $v \rightarrow -\infty$.

Physically this picture is explained by the fact that the higher the temperature to the right of Σ , the greater the fraction of the waves that is reflected from Σ and the greater the fraction of the energy of these waves that remains in the portion l_1 . When $n = 1$ there is no reflection at all and the process is therefore formally infinitely stable.

The solution obtained here shows that in principle a system with total absorption of the oscillatory energy on one end of the tube can become excited. Let us estimate the probability of such an excitation. As follows from (33.11) and (33.5), on the stability boundary we have $|y_2| \geq m/n$. In the numerical example considered this leads to the necessary excitation condition $|y_2| > 0.4$. However, the estimate presented above (see §32) shows that such values of $|y_2|$ are practically improbable. Thus, in the numerical example under consideration the excitation of oscillations is practically impossible. This result is typical of the excitation of acoustic oscillations by a flame.

It is interesting to note that the theoretical conclusion obtained here is confirmed experimentally. In the experiments of Coward, Hartwell, and Georgson, which were already mentioned in the introduction, the following fact was observed along with the others. When the open end of the tube, in which the flame propagated, was not blocked at all, then the experimenters obtained clearly pronounced acoustic oscillations with a jumpwise change in the oscillation frequency, such as were described in detail above. On the other hand, in cases when glass wool was located at the open end of the tube, no oscillations were produced at all.

The glass wool placed in the open end can be regarded as a device which completely quenches the acoustic waves incident on it and does

not prevent the escape of the combustion products. In the theoretical scheme such a boundary condition corresponds to $z_2 = 1$.

Figure 1 shows records of the pressure oscillations obtained in the experiments of Coward, Hartwell, and Georgson. In the upper part of Fig. 1 is shown the record in the absence of glass wool at the open end of the tube, while in the lower part is shown the record obtained under the same condition, but with the acoustic oscillations damped with the aid of the glass wool. The curves presented clearly illustrate the theoretical deductions obtained in the present section.

We have considered theoretically here only one of the possible processes in the combustion zone, namely the process characterized by the condition $\delta E = 0$. All the laws obtained are valid also for the other elementary process ($\delta X = 0$). The corresponding formulas can be obtained by replacing m/n by n/m in the expressions of the present section. More complicated cases ($\delta E \neq 0$; $\delta X \neq 0$) can also be investigated in accordance with the procedure developed here, although they do necessitate a laborious numerical analysis. These cases are not analyzed, since the problem considered is only of limited interest. The estimates presented show that in all these cases the final result does not change, namely the presence of total energy absorption on one of the ends of the tubes makes it extremely difficult to excite the oscillating system. This circumstance makes it possible to compare the results of the experiments of Coward, Hartwell, and Georgson, obtained for unknown values of δE and δX , with the calculations presented in the present section for the elementary processes.

- 260 Furduev, V.V., Elektroakustiki [Electroacoustics], Gostek-
hizdat, 1948, page 111. It must be noted that the formulas
presented were obtained for a stationary medium. The effect
of the stream velocity on the terminal impedances are ne-
glected here and throughout. Consequently, the results ob-
tained below are valid for sufficiently slow streams, and
in all other cases they can be regarded as correct only
qualitatively.
- 261 Strutt, J.W. (Lord Rayleigh), Teoriya zvuka [The Theory of
Sound], Vol. II, Chapter XVI, Gostekhizdat, Moscow, 1955.
- 270 Kirkby, Wheeler, Journ. of the Chem. Soc., 1931, page 847.
- 279 We recall once more that when $|v| \rightarrow \infty$ the solution has only
a formal meaning. In order to obtain the true behavior of
the system at parameters that yield $|v| \rightarrow \infty$ it would be nec-
essary to solve the problem with account of the initial con-
ditions and of the nonlinear properties of the system.

Chapter 7

FEEDBACK MECHANISMS IN THE EXCITATION OF ACOUSTIC OSCILLATIONS BY COMBUSTION

§34. Classification of Feedback Mechanisms

In earlier chapters we solved several problems involving the excitation of acoustic oscillations by heat supply and in each case, implicitly or explicitly, the assumption was introduced concerning the existence of feedback, i.e., the reaction of the acoustic oscillations on the combustion process. The important role that is played in this phenomenon by feedback was already discussed in §22. It was introduced most frequently in purely formal fashion, for example in the form of a certain factor γ , which relates the perturbation of the stream velocity \bar{v} (an acoustic phenomenon) with the quantity δX (a parameter that characterizes the perturbation of the combustion process). In some cases, for example in §25, the feedback mechanism was described in detail, and then there was no need for introducing such a formal connection between the acoustic oscillations and the combustion process.

The present chapter is devoted to a description of various physical phenomena, by means of which the feedback is realized in the oscillating system under consideration. It must be pointed out immediately that as a rule the acoustic oscillations are connected with the oscillations in the combustion process by an entire chain of processes. Thus, for example, oscillations in the stream velocity in the region where the nozzles are located leads to oscillations in the excess-air coefficients and other characteristics of the mixture formation (the

quality of vaporization of the fuel, the trajectories of motion of the fuel drops, etc.), and the periodically varying properties of the combustible mixture lead to periodical perturbations of the combustion process. In the present example the "chain" consists of only two links: the acoustic oscillations perturb the mixture production, and the mixture production transmits its perturbations to the combustion process. In general, on the other hand, the number of such links may also be larger.

In explaining the feedback mechanisms, these cascaded causes and effects will be described in as much detail as possible. However, in the theoretical analysis the entire chain of causes and effects can be regarded as an entity or as a single feedback mechanism.

A detailed description of the feedback mechanism is necessary for two purposes. First, only a clear-cut idea of the physical nature of the phenomenon that plays the role of feedback in any particular case makes it possible to "break open" the resultant feedback loop and thereby suppress the oscillations if they are undesirable or, to the contrary, stimulate the excitation of the oscillations. Second, knowing the physical nature of the feedback mechanism, we can describe it analytically and obtain a theoretical solution of the problem involving the excitation of the oscillating system not as a function of the amplitude-phase relations between \bar{v} , \bar{p} and δE , δX , but as a function of "clearer" parameters which are more convenient for the engineer. In §25 above we gave an example wherein the problem involving the excitation of acoustic oscillations by combustion was carried through to such a form. By specifying a certain concrete feedback mechanism (we do not concern ourselves here with the extent to which this mechanism is probable), concrete deductions are obtained, for example, the deduction that the system will be excited in the case of a sufficiently

steep increase in the completeness of combustion with increasing excess-air coefficient.

) Frequently those engaged in the study of vibration combustion seek some single principal cause of the instability. This is essentially reduced usually to searches for the principal feedback mechanism. Sometimes this can be done for some specific case of vibration combustion, observed under specific conditions in some experimental setup. However, an attempt to find such a principal feedback mechanism suitable for a large group of experimental installations, combustion chambers of engines or furnaces, usually ends in failure.

The point is that in fact there exist many different feedback mechanisms, which in final analysis lead to oscillating heat supply or to oscillations in the flame-front position (or to both simultaneously) and through them, as was shown above, also to excitation and maintenance of acoustic oscillations. It turns out here that the "principal" feedback mechanism may be one or the other, depending on the specific experimental conditions.

We shall present below the characteristics of the main feedback mechanisms. Of course, far from all of the probable causes of maintenance of vibration combustion are covered by the mechanisms listed below. In the present chapter we give a brief summary of only those phenomena, which have up to the present time been sufficiently frequently observed and which apparently play the principal role in the considered type of self-oscillations. Inasmuch as the combustion processes in the combustion chambers of furnaces and engines are connected with the processes of mixture-formation, vortex-formation, and combustion proper, all the feedback mechanisms can be broken up into those connected with mixture production, the hydromechanics of the stream, and combustion proper. Of course, this classification, like other con-

ceivable classifications, is quite arbitrary, and many phenomena can simultaneously gravitate toward two and even all three subdivisions.

We note here that the feedback loop can, generally speaking, be closed also through automatic control systems installed in the furnaces or in the engines. However, if such oscillations, connected with the control system, do become excited, they are usually not acoustical, since the operating speed of automatic control systems is insufficient to respond to acoustic oscillations which frequently are of the order of 100 cycles per second and more. Inasmuch as we are investigating in the present book only acoustic oscillations, the flow-parameter and combustion-process oscillations connected with the operation of the automatic control system will not be considered here. If we do encounter somewhere an interaction between the control system and the acoustic oscillations, an analysis of this process can be carried out by the same methods as are used to analyze the self-excitation of acoustic oscillations by heat supply in the absence of any regulators for the combustion process or for the flow of the air or combustion process through the furnace or the engine.

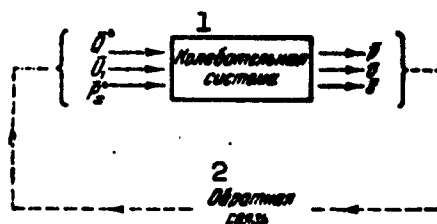


Fig. 65. Schematic representation of the feedback loop. 1) Oscillating system; 2) feedback.

The classification of feedback mechanisms presented somewhat earlier in accordance with the physical nature of the phenomena on which these mechanisms are based can be supplemented with a classification in accordance with the action of the feedback on the oscillating sys-

tem. Although the acoustic system under consideration is a classical example of an oscillating system with distributed parameters, and modern automatic-control systems comprise principally systems with lumped parameters (systems described by ordinary differential equations and not by partial differential equations), it is convenient to use here certain illustrative schemes which are used in the theory of automatic control.

Let us represent the oscillating system in the form of a certain element, the inputs to which are coordinates characterizing the combustion process (\bar{Q}^* , \bar{U}_1 , \bar{P}_x^*), and the output coordinates of which are the parameters of the acoustic oscillations \bar{p} , \bar{v} , and \bar{s} (Fig. 65). Let us explain the circuit presented here in somewhat greater detail. The input in Fig. 65 is the combustion region, in which the process can be completely described, as shown in §16, by the effective perturbations of the heat supply \bar{Q}^* , the rate of displacement of the flame front \bar{U}_1 , and the hydraulic resistance \bar{P}_x^* . Therefore by specifying \bar{Q}^* , \bar{U}_1 , and \bar{P}_x^* we specify the perturbed-combustion process and inasmuch as the acoustic properties of the oscillating system are assumed known, we specify thereby the quantities \bar{p} , \bar{v} , and \bar{s} for all the sections in the tube. The output in Fig. 65 is the entire mass of oscillating gas, with the exception of the combustion zone. Consequently, the circuit shown in Fig. 65 must be understood in the following fashion: if the properties of the oscillating system are specified (M_1 , M_2 , position of the combustion zone, etc.) and in addition we specify also the properties of the perturbed combustion (\bar{Q}^* , \bar{U}_1 , \bar{P}_x^*), then by the same token we determine also the parameters of the acoustic oscillations (\bar{p} , \bar{v} , and \bar{s}).

The presence of feedback causes the acoustic oscillations (output coordinates) to act on the combustion process (input coordinates). In the circuit this is conventionally shown in the form of a dashed line

drawn from the output coordinates to the input coordinates. Although each of the input coordinates depends generally speaking on all three output coordinates, so actually one should draw nine lines joining \bar{p} , \bar{v} , and \bar{s} with each of the input coordinates, this can be avoided. The point is that \bar{p} , \bar{v} , and \bar{s} are not completely independent parameters, but physically they represent some unified process of acoustic oscillations. Therefore, by drawing a single line to represent the feedback, we can say that the acoustic oscillations (as a whole) act through a certain feedback loop on the combustion process (as a whole). With such an approach we need not be interested at all in the three output and the three input coordinates, but represent a single input and a single output coordinate. The single input coordinate will be the perturbation of the combustion process (which has components \bar{Q}^* , \bar{U}_1 , and \bar{P}_x^*), and the output coordinate will be the acoustic perturbation (which has components \bar{p} , \bar{v} , and \bar{s}). For the analysis that follows such an approach is perfectly adequate and therefore all the circuits will be drawn with a single line. This, of course, does not mean that it is in general not advantageous to describe in detail the character of the dependence of the input coordinates on the output coordinates. When a thorough analysis of some concrete feedback loop is necessary, it may turn out to be essential also to make a more detailed study of the singularities of the dependence of each input parameter on all the output parameters. In the present section, however, such a degree of detail would be excessive.

Let us consider the singularities that can be possessed by feedbacks of different types, characteristic of the process of thermal excitation of acoustic oscillations.

The first, simplest type of feedback is shown in Fig. 66a. Here the output coordinate is converted prior to returning to the input of

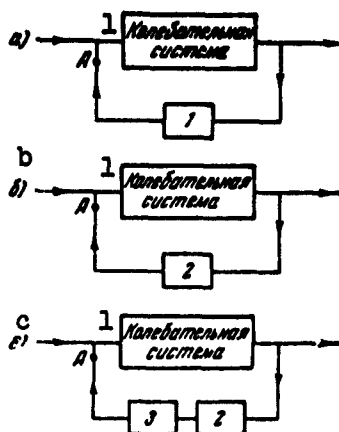


Fig. 66. Principal types of feedback. 1) Oscillating system.

the oscillating system in element 1, which is characterized by the fact that it changes the components of the output coordinate into the components of the input coordinate. In this case element 1 is described by a system of equations of the form

$$\left. \begin{aligned} \bar{Q}^* &= a_{11}\bar{p} + a_{12}\bar{v} + a_{13}\bar{s}, \\ \bar{U}_1 &= a_{21}\bar{p} + a_{22}\bar{v} + a_{23}\bar{s}, \\ \bar{P}_x^* &= a_{31}\bar{p} + a_{32}\bar{v} + a_{33}\bar{s}, \end{aligned} \right\} \quad (34.1)$$

where the coefficients $a_{11}, a_{12}, \dots, a_{33}$ are real constants.

Such a feedback is distinguished by the fact that the components of the input coordinate \bar{Q}^*, \bar{U}_1 , and \bar{P}_x^* follow instantaneously the changes in the components of the output coordinate \bar{p}, \bar{v} , and \bar{s} . The values of the coefficients $a_{11}, a_{13}, \dots, a_{33}$ play in this case a very important role: when all tend simultaneously to zero, the reaction \bar{p}, \bar{v} , and \bar{s} on the combustion process decreases and it becomes natural to speak of weakening of the feedback; if, for example, we reverse the signs of all the coefficients of the linear transformation (34.1), then the phases of \bar{Q}^*, \bar{U}_1 , and \bar{P}_x^* change by π , and the process which was previously stable can become unstable, etc. This type of feedback is the simplest one and was encountered several times in the preceding sections.

The second type of feedback is essentially close to the one just considered, and is shown in Fig. 66b. Element 2 is described by a linear transformation (34.1), just like element 1, but its coefficients are now complex, and can in particular depend on the complex oscillation frequency β . This type of feedback can occur only when the physical processes on which it is based depend not only on \bar{p}, \bar{v} , and \bar{s} ,

but also on other quantities, for example on their derivatives.

We shall describe below a combustion process which depends in essential fashion on the acceleration of the flame front. For this process it would be necessary to introduce into the linear transformation (34.1) terms proportional to $d\bar{v}/d\tau$:

$$\bar{Q}^* = a_{11}\bar{p} + a_{12}\bar{v} + a_{13}\bar{s} + a_{14}\frac{d\bar{v}}{d\tau} \\ \dots\dots\dots$$

etc.

Inasmuch as all the parameters of the oscillating system vary with time in proportion to the factor $e^{\beta\tau}$, we have $d\bar{v}/d\tau = \beta\bar{v}$ and the linear transformation (34.1) assumes the form

$$\bar{Q}^* = a_{11}\bar{p} + (a_{12} + a_{14}\beta)\bar{v} + a_{13}\bar{s} \\ \dots\dots\dots$$

etc.

We see immediately from this equation that the coefficient of \bar{v} has become complex and ceased to be a constant, for it now depends on β .

Physically the second type of feedback is distinguished, like the first one, by the fact that it follows instantaneously the changes in the components of the output coordinate $(\bar{p}, \bar{v}, \bar{s})$, but is subject in this case to additional phase shifts. Indeed, the multiplication of \bar{v} by a complex coefficient $(a_{12} + a_{14}\beta)$ denotes not only a change in scale but also a rotation of the corresponding component in the complex plane.

The third type of feedback is shown in Fig. 66c. In the simplest case it consists of two elements connected in cascade, the first one of which coincides with element 2 just considered (element 1 can be regarded as a particular case of element 2), and element 3 which produces a time delay. This type of feedback is realized when the combustion process follows the variations of \bar{p} , \bar{v} , and \bar{s} not instantaneously,

but with a certain delay. An example of such a feedback was already considered in §26. The simplest case shown in Fig. 66c corresponds to a process in which the time delay $\Delta\tau$ can be assumed to be the same for all the components of the corresponding linear transformation of the type (34.1). Only in this case can the elements 2 and 3 be connected in cascade. It must be noted that one usually considers only processes of this type. Should it become necessary to introduce more than one delay time, for example $\Delta\tau_1$, $\Delta\tau_2$, and $\Delta\tau_3$, connected with \bar{p} , \bar{v} , and \bar{s} , respectively, then this would not lead to the necessity for developing new methods for calculating the oscillating system, but would only increase the computational difficulties. When delay is taken into account in accordance with the circuit shown in Fig. 66c, the coefficients of the linear transformation (34.1) become, generally speaking, complex and they are all multiplied by one and the same complex factor $e^{-\beta\Delta\tau}$ (see §26), which depends on the delay time $\Delta\tau$.

Thus, different types of feedback can be classified in accordance with the form of the coefficients of linear transformation (34.1). If they contain $e^{-\beta\Delta\tau}$ as a factor, then we have on hand a feedback system with delay, if they are complex but do not contain a delay time, then the feedback is characterized by the presence of additional phase shifts; if they are real, then we are dealing with the simplest type of feedback. Of course, this classification, like the preceding one, is arbitrary and incomplete.

To conclude the present section let us make a few general remarks.

In describing different types of feedback it will be assumed below that the oscillation process is close to stationary, i.e., that the system is close to the stability limit. We have already emphasized above that when solving a problem without initial conditions it is necessary to assume that the oscillation process has been going on for

a sufficiently long time and that during that time it has not gone beyond the limits (in amplitude) that are allowed by linear theory. This immediately limits the permissible scales of instability. However, the point lies not only in such formal considerations. Usually the greatest interest is attached to a feedback mechanism which maintains the already produced self-oscillations. A description of such a mechanism is naturally carried out for stationary oscillations. In such an approach, of course, a certain lack of rigor is permitted in the argumentation. Inasmuch as the self-oscillation process has become established, the phenomenon has become essentially nonlinear and the references made above to the properties of the linear oscillating system cannot be deemed sufficiently convincing. However, since our purpose is only a qualitative description, we can make the assumption that the main physical phenomena which lead to the formation of the feedback can be the same both during the slow buildup of the oscillations (linear oscillating system), and when the oscillations have been established (when the nonlinear terms have assumed a dominant role in the oscillating system). Therefore in the analysis of the possible feedback mechanisms we shall assume throughout that the oscillations have already been established, and that we are describing a chain of phenomena leading to the maintenance of these oscillations; no difference is made here between the two cases, namely a linear system at the stability limit and a nonlinear system in the stationary self-oscillation mode.

§35. Feedback Mechanisms Based on Mixture Formation

In most cases, various kinds of furnaces, combustion chambers for engines, etc. contain as one of their basic elements devices for the preparation of the combustible mixture. Frequently these devices are made in the form of nozzles to atomize the fuel ahead of the combus-

tion zone. Sometimes other constructions are used. No matter what the devices for the preparation of the combustible mixture may be, if they exist at all the mixture-formation process can influence in appreciable fashion the combustion and in particular the excitation of vibration combustion. This is simplest to see from the following considerations. Mixture formation can be characterized by a certain nonuniformity. If this nonuniformity has furthermore a periodic character, then the mixture entering the combustion chamber can have periodically varying excess-air coefficients or a periodically varying ratio between the fuel in the liquid and in the vapor phase, etc. This can lead both to the appearance of oscillation in the heat release and to mobility of the flame front, and consequently, to the maintenance of oscillations. Such a case was already considered in §25. However, this case does not exhaust all the possibilities, so that the general considerations presented here are best made somewhat more specific, by describing in greater detail the typical mechanisms for the maintenance of oscillations connected with the mixture-formation process.

a) Nonuniform fuel supply. If for some reason the fuel is not supplied uniformly, but with a certain periodicity, the result is a combustion which also has a periodic character. Nonuniform fuel supply can be due to uneven operation of the pumps or of other devices that supply the fuel. Usually such nonuniformity is not connected with acoustic oscillations of gases inside the furnace or the engine. Therefore, if oscillations in the combustion process do result, they must be regarded as forced oscillations. Unlike self-oscillations, whose frequency is determined by the properties of the oscillating system, the frequency of forced oscillations is determined by the external action, for example by the number of revolutions of the pump supplying the fuel, etc. This circumstance makes it possible to distinguish

readily between forced oscillations and self-oscillations and, if necessary, to adopt measures toward their suppression. It is obvious that to combat forced oscillations of this type it is necessary to take some action on the external devices that supply the fuel (change the construction of the fuel pump, etc.). We shall not consider this simple question further, since it does not pertain to the main subject of the book, which is devoted to self-oscillating phenomena.

If we confine ourselves only to cases when the variable flow of fuel is directly connected with the acoustic oscillations in the gas stream moving through the engine or through the furnace, then one of the main factors bringing about such an interaction is the influence of the oscillations in the pressure of the surrounding medium on the flow of fuel through the nozzle.

Let us denote the flow of the fuel mass per unit cross section area of the tube through which the air flows by m_g . As is well known, the flow of liquid through a nozzle is proportional to the square root of the pressure drop in the nozzle (the difference between the supply pressure and the pressure in the medium in which the nozzle is installed)

$$m_r = k_1 \sqrt{p_r - p},$$

where k_1 is a certain numerical coefficient which depends on the dimensions of the nozzle and on similar factors, p_g is the liquid pressure at the inlet to the nozzle, and p is the air pressure in the tube. Inasmuch as in the case of acoustic oscillations in the tube the value of p has a periodic component, the fuel flow m_g should also oscillate. Let us determine the oscillating component of the fuel flow:

$$\delta m_r = \frac{-k_1}{2\sqrt{p_r - p}} \delta p. \quad (35.1)$$

It is seen from this formula that the oscillating component of

the fuel flow is shifted relative to the oscillating component of the pressure of the surrounding medium by π .

The formula obtained describes the perturbation of the fuel flow in the section of the tube in which the nozzles are installed, and the quantity δp also pertains to this section. Frequently, however, the plane where the collector with the nozzles is located and the plane of the intense heat supply (the combustion zone) are separated by a distance which cannot be neglected. Then the connection between the acoustic oscillations and the oscillations of the amount of fuel, which enters into the combustion zone, can be determined from the following considerations (Fig. 67). Let the heat-supply plane Σ be located in the section $\xi = 0$, and the plane Φ where the nozzles are located correspond to the coordinate $\xi = \xi_f$. Further, let the oscillations be characterized by a frequency ω and by pressure and velocity perturbations δv_0 and δp_0 to the left of the plane Σ . The perturbation $\delta p = \delta p_f$ entering into Formula (35.1) can be readily represented, on the basis of (4.8) and (4.13), in the form

$$\delta p_\Phi = \left[\frac{\kappa p_1}{a_1} \varphi_2(\xi_\Phi; \omega) \delta v_0 + \varphi_1(\xi_\Phi; \omega) \delta p_0 \right] e^{i\omega t}.$$

The pressure oscillations δp_f give rise to fuel-flow oscillations in the section ξ_f , and the combustion process occurs at $\xi = 0$. Consequently, it is also necessary to take into account the time required for the stream to transport the fuel through a distance ξ_f . It is obvious that this time, when reduced to dimensionless form, will be equal to

$$\tau_\Phi = -\frac{\xi_\Phi}{M_1}$$

($\tau_f > 0$ since $\xi_f < 0$). Consequently, the perturbation of the amount of fuel in the stream will reach the plane Σ with a delay equal to τ_f . If we assume that on crossing the plane Σ the fuel is consumed instan-

taneously, with constant completeness of combustion, i.e.,*

$$\bar{Q}^* = k_2 \delta m_r,$$

then

$$\begin{aligned} \bar{Q}^* = -\frac{k}{2\sqrt{p_r - p}} \left[\frac{x p_1}{a_1} \varphi_3(\xi_\phi; \omega) \delta v_0 + \right. \\ \left. + \varphi_1(\xi_\phi; \omega) \delta p_0 \right] e^{i\omega \left(\tau + \frac{L_\phi}{a_1} \right)}, \end{aligned} \quad (35.2)$$

where $k = k_1 k_2$.

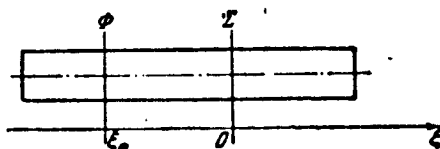


Fig. 67. Position of the sections where the fuel is introduced (ϕ) and combustion takes place (Σ) along the tube.

The formula obtained enables us to make the following remarks. It is seen first of all that feedback is produced in the oscillating system, for the acoustic oscillations in the combustion zone Σ , with amplitudes δv_0 and δp_0 , produce a perturbation equal to \bar{Q}^* in the heat released in the same zone. As is well known from the preceding, if the necessary amplitude-phase relations are satisfied here between \bar{Q}^* on the one hand and δp_0 and δv_0 on the other, then the system can become excited. Formula (35.2) was obtained under the assumption that these amplitude-phase relations are realized and that the system is on the stability limit so that $\beta = i\omega$. The feedback obtained corresponds in its character to the third type of feedback considered in the preceding section, namely feedback with delay.

In order to disclose certain properties of the investigated excitation mechanism it is useful to open mentally the self-oscillating system and to consider it from a somewhat unusual point of view. Assume that stationary acoustic oscillations are present. Let us trace

the values assumed by \bar{Q}^* ; in this case we shall not stipulate for the time being that the obtained values of \bar{Q}^* be precisely those (in amplitude and in phase) that are capable of maintaining acoustic oscillations, the existence of which is assumed. If we turn to Fig. 66, this corresponds to opening the circuits drawn at the point A, applying to the input of the oscillating system in the third circuit a periodically varying \bar{Q}^* (for example, from a certain external source), which maintains the stationary oscillations under consideration, and analyzing the question of what \bar{Q}^* will be obtained as a result of the action of the feedback mechanism on the output of the element 3. If these values of \bar{Q}^* coincide this means that the closed-loop system can maintain oscillations of this type, and if they are different then the system will not execute steady-state oscillations; the oscillations will either be damped, or else will proceed with increasing amplitude.

Considering (35.2) from this point of view, let us specify ω , δv_0 , and δp_0 , i.e., the entire process of acoustic oscillation, and let us analyze the influence of ξ_f on \bar{Q}^* in the open system. The influence of ξ_f on the expression in the square brackets is usually insignificant. When ξ_f is varied within sensible limits, this expression changes somewhat in absolute magnitude and remains practically unchanged in phase. This was already mentioned in §6 in the analysis of the standing wave patterns. The factor $\exp i\omega(\tau + \xi_f/M_1)$ is an entirely different matter. At small values of M_1 (which is precisely the customary case), even an insignificant change in ξ_f will lead to a large phase shift of \bar{Q}^* relative to the specified values of δp_0 and δv_0 . Indeed, elementary calculation shows that a displacement of the collector with the nozzles by 5-10% of the total length of the tube ($\Delta\xi_f = 0.05-0.1$) changes the phase of \bar{Q}^* by $\pi/2$ or more. Consequently, by a small displacement of the collector along the tube it is possible to produce an appreciable

phase shift in \bar{Q}^* . But this might appear to open up a way of combating self-oscillations. In the case when a feedback of the type described here actually is realized, it is sufficient to displace the collector with the nozzles slightly along the tube to change radically the phase of \bar{Q}^* . We have already mentioned earlier (see Chapter 5) that when the phase shift between \bar{Q}^* and δp_0 or δv_0 has the proper value, excitation is generally impossible; therefore, by choosing experimentally the position of the collector relative to the combustion zone it is possible to suppress vibration combustion.

Unfortunately, the matter is not as simple as that. The properties of the acoustic system excited by the combustion are more complicated than the easily visualized circuits described here. They will be considered in detail in Chapter 9.

The influence of pressure oscillations in the combustion chamber on the fuel flow may turn out to be appreciable in the case of liquid-fuel jet engines, since the pressure oscillations can reach rather large values in such engines. The problem is simplified here in the respect that the heat-supply zone is directly adjacent to the head of the combustion chamber, and consequently we can set $\xi_f = 0$. A more detailed analysis shows, however, that the presence of flow oscillations, brought about by the pressure oscillations in the chamber of such an engine, is by itself insufficient for self-excitation of the system. Indeed, when the pressure is increased the flow of fuel decreases. If we assume that the combustion occurs instantaneously, we find that the increase in the heat supply occurs at instants when the pressure is decreased and the system will not become excited. This argument contains the tacit assumption that the system can become unstable only as a result of oscillations in the heat supply. But in our case this is not so. As will be shown in Chapter 10, the principal factor in

this case is the perturbation of the gas production.

In order for the system to become excited, it is necessary to change the phase of the gas production, which coincides with the combustion phase, relative to the phase of \bar{p} . Such a change is possible if the ignition of the mixture is delayed in the system. More details concerning this are found in §37 of the present chapter.

Even more essential apparently are the oscillations in the fuel flow in devices with low-pressure fuel supply systems, for example in pulverized-coal furnaces. The pulverized coal is supplied here by a stream of so-called primary air through a special unit (a vane-wheel burner) into the combustion zone in the precombustion chamber, where the secondary air is supplied. If vibration combustion occurs in such a precombustion chamber, then the cross section in which the devices supplying the pulverized coal are located can be regarded in first approximation as a closed end of the tube. During the oscillations, a pressure antinode is produced in this section, so that the pulverized coal supplied by the primary air will experience a periodic back pressure at the outlet. The oscillating component of the back pressure, which can be realized in the case of vibration combustion, is of the same order of magnitude as the excess pressure (against the precombustion chamber) with which the primary air is supplied, i.e., at the instant when the maximum pressure is attained in the precombustion chamber, the pulverized coal supply may completely stop.

Although such a feedback mechanism should be quite powerful, it is by itself incapable of exciting the oscillating system, for the phase of the maximum fuel supply will correspond to the phase of the minimum pressure in the precombustion chamber. However, the really existing delays (delay in the ignition), which will be referred to in §37, make it possible to realize the necessary phase relationships be-

tween the heat-supply and pressure perturbations.

In conclusion we must also add that sometimes it may be necessary to consider a more complicated oscillating system than in the present case. The oscillations of the back pressure may give rise to acoustic oscillations in the pulverized coal ducts (or in the fuel lines of the engines) and then it becomes necessary to study the joint oscillations of the medium in the main tube (precombustion chamber, engine combustion chamber) and in the fuel supply lines.

b) Oscillating air flow. Let us return to the question of the excitation of vibration combustion in a tube through which air flows and in which is located a collector with nozzles which supply liquid fuel. We have already mentioned that in principle feedback can be produced as a result of the influence of the pressure oscillating in the stream on the fuel consumption. However, a realization of this mechanism is improbable in practice, owing to the weak dependence of the flow through the nozzles, in which the supply pressure is appreciable, on the acoustic oscillations of the medium. In a certain sense, however, an inverse feedback mechanism is possible. Let us assume that the fuel flow is strictly constant. Then the air, flowing about the collector with the nozzles, will carry away with it the same quantity of fuel per unit time, independently of the instantaneous value of the pressure and velocity of the stream in the section where the nozzles are located.

Whereas the amount of fuel carried away is constant, the excess-air coefficient may experience appreciable oscillations, owing to the oscillations in the flow of the air in the section where the nozzles are located. Indeed, the excess-air coefficient is

$$\alpha = \frac{Q_0}{L_{0m}},$$

where L_0 is the ratio of the air mass necessary theoretically for complete combustion of a unit fuel mass to the fuel mass.

As a result of the acoustic oscillations, the flow of air per unit area of the transverse section of the stream, ρv , will also oscillate. This will lead to a perturbation of the coefficient α

$$\delta\alpha = \frac{1}{L_0 m_f} (v\delta\rho + \rho\delta v) = \alpha \left(\bar{v} + \frac{1}{M_1} \bar{v} \right)$$

(the α in the right half of the equation corresponds to the unperturbed value of the excess-air coefficient).

An analysis of the possible values of \bar{p} and \bar{v} shows that the former, being connected with the pressure perturbation, is usually small. In an open tube with subsonic flow the pressure oscillations can reach only small fractions of one atmosphere, so that the quantity $\bar{p} = \delta p / \kappa p$ (the equality corresponds to isentropic gas flow) cannot exceed 0.05-0.15. At the same time \bar{v}/M_1 can reach values of the order of unity. (This occurs when the oscillating component of the velocity is close to the average flow velocity. As will be shown in the following chapters, such an oscillation scale is customary.) We can thus write in first approximation

$$\delta\alpha = \alpha \frac{\bar{v}}{M_1}, \quad (35.3)$$

thereby demonstrating that α fluctuates in phase with \bar{v} . Repeating almost verbatim the deduction presented in the present section in the analysis of the dependence of δm_g on δp , we can write

$$\delta\alpha = \frac{\alpha}{M_1} [\varphi_1(\omega; \xi_\phi) \bar{v}_0 + \varphi_2(\omega; \xi_\phi) \bar{p}_0] e^{i\omega(\tau + \frac{L_0}{M_1})}. \quad (35.4)$$

The necessary connection between the oscillations of α and the oscillations of the heat supply \bar{Q}^* or the flame-propagation velocity \bar{U}_1 can be readily obtained if it is recognized (as was already mentioned in Chapter 5) that the completeness of combustion (just as

the rate of flame propagation) can depend materially on α . Then, confining ourselves for the sake of being specific to the influence of α on the completeness of combustion, we write

$$\bar{Q}^* = \text{const} \frac{\partial \eta_{cr}}{\partial \alpha} \delta \alpha. \quad (35.5)$$

Formulas (35.4) and (35.5) taken together show that in this case we have feedback with a delay that depends essentially on ξ_f . It must be emphasized that unlike the preceding case, the present feedback mechanism can play a noticeable role in the excitation of acoustic oscillations in tubes in which pulverized liquid fuel burns. It might seem then that by slight displacement of the collector it is possible to position it in such a way as to suppress the oscillations. However, in this case, too, for reasons which will be detailed later on, such a method of combating vibration combustion has little effectiveness.

c) Oscillations in the quality of the atomization. Since acoustic oscillations are accompanied by periodic components in the velocity and in the pressure, a periodic change takes place also in the velocity head of the stream $\rho v^2/2$. As is well known, when a nozzle operates in an air stream, the trajectories of the droplets of the atomized fuel (the long range of the nozzle), the fineness of the atomization, and other parameters connected with mixture formation (in particular, evaporation) depend to a great extent on the velocity head of the incoming flow into the nozzle. Therefore the quality of the atomization also varies periodically, following rigorously the acoustic oscillations in the stream. As a result, the mixture of fuel and air which enters into the combustion zone has a periodically varying quality. This causes nonvanishing oscillating components of the effective perturbed heat supply \bar{Q}^* and of the effective perturbed flame propagation velocity \bar{U}_1 to be realized in the combustion process, i.e., self-

oscillations of the system can be supported. This feedback mechanism can play a particularly noticeable role if the periodically varying quality of the mixture interacts with important structural elements of the combustion chamber. One can conceive, for example, of cases in which the oscillating flight trajectories of the fuel drops are directed alternately either direct to the stabilizer, or to an air jet that moves at a certain distance from the stabilizer, or else periodically strike the combustion-chamber walls. In all these and similar cases the fluctuation in the quality of atomization should manifest itself most strongly, since it influences directly the most vital portions of the combustion chamber.

If such a feedback mechanism is realized, it may be useful to change the relative placement of the fuel-collector elements and of the combustion-chamber elements. These changes must be made in purely empirical fashion, since a detailed investigation of the interrelation between the nonstationary mixture formation and the nonstationary combustion is a problem that is still far from solved and calls for a very deep theoretical treatment and highly precise experiments.

If one undertakes the more modest task of presenting an external description of this phenomenon so as to obtain formulas relating \bar{Q}^* and \bar{U}_1 with \bar{p}_0 and \bar{v}_0 , then after introducing some likely hypothesis concerning the connection between the oscillations of the long-range nature of the nozzles or the quality of the atomization and the combustion process it is possible to obtain formulas of the same type as (35.2), (35.4), and (35.5) which were presented above. Here, as in the preceding cases when $\xi_f \neq 0$, a feedback with delay is obtained.

If we summarize the statements made in the present section, we must point out first that even the small number of examples presented here makes it possible to state that the process of mixture formation

can serve as the basis for the occurrence of a whole series of feedback mechanisms. It is quite clear that the individual mechanisms described above, those connected with the variations in the fuel supply, the variations in the excess-air coefficient, and the quality of the fuel atomization, should appear most frequently as an entity, as different aspects of one and the same disturbed mixture-formation process. Of course, this does not mean that some aspect of the process under consideration cannot play a leading role in some specific case; this is indeed the justification for describing various aspects of the unified process of perturbed mixture formation as independent feedback mechanisms. A common property of all these mechanisms is the presence of a delay associated with the time that the stream needs to carry the atomized fuel to the combustion zone. This delay becomes equal to zero only when the fuel is fed directly into the combustion zone.

§36. Feedback Mechanisms Based on Hydromechanical Phenomena

If mixture formation were the only process capable of ensuring the realization of some feedback mechanism, then it would be very easy to combat vibration combustion. It would be sufficient to prepare the combustible mixture in a separate receiver, which is acoustically isolated from the combustion chamber, and then vibration combustion would never arise. However, direct experiments refute this. Experiments were set up, for example, on the excitation of vibration combustion in a tube into which not air, but a previously prepared mixture of gasoline and air was blown. This mixture was prepared in a separate receiver, and the experimental setup was prepared in accordance with a scheme close to that shown in Fig. 60. The gap between the tube in which the combustion zone was placed and the nozzle which fed the gasoline-air mixture exceeded the caliber of the tube. Moreover, the tube supplying the mixture had a larger diameter than the tube in which the combustion

chamber was located. All this prevented the oscillations occurring in the tube with the combustion chamber from being transmitted at all to the receiver in which the nozzles were located and the mixture was prepared. This circumstance was confirmed by direct measurements of the pressure oscillations in the receiver. Thus, the possibility of interaction between the acoustic oscillations in the tube and the mixture formation occurring in the receiver was completely eliminated. Nevertheless vibration combustion did occur. The experimental results shown in Fig. 51 were obtained in precisely this type of installation.

It follows therefore that in addition to mixture formation, there can exist some other processes which make the realization of feedback possible. Many of these processes can be unified in accordance with the attribute that they are all connected with the hydromechanical processes in the gas moving through the tube. This group of mechanisms for feedback is based on the fact that the acoustic oscillations produced during the combustion essentially change the character of the flow and produce in it a periodic component. In order to clarify this general statement to some degree, we present here the results of one experiment.

In the laboratory setup in which certain vibration-combustion problems were investigated, use is made of a thermoanemometer, which makes it possible to record the instantaneous values of the stream velocity. This thermoanemometer was installed ahead of the combustion zone. In the case of stationary vibration combustion (of even low intensity) the amplitude and period of the stream velocity oscillations became strictly constant, and the turbulent velocity pulsations observed prior to this settling "disappeared" as it were against the background of clear-cut oscillations of acoustic nature. Two oscillograms, one corresponding to normal combustion and the other to vibra-

tion combustion, are shown in Fig. 68. It must be added that when the thermoanemometer was displaced along the tube diameter the amplitude of the velocity oscillations did not change in any noticeable fashion, i.e., the air stream vibrated as a unit. Such ordered oscillations of large gas masses are capable, of course, of influencing appreciably the character of the stream and particularly the vortex formation in the stream.

a) Vortex formation ahead of the combustion zone. In the portions of the engine or furnace preceding the combustion zone, there are prac-

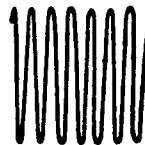


Fig. 68. Oscillograms of velocity oscillations ahead of the combustion zone: normal combustion on the top, and vibration combustion at the bottom.

tically always elements which permit noticeable vortex formation to arise. Such an element may be a sharp bend in the stream axis, an expanding portion of a pipe, a sufficiently sharp change in the area of the pipe, and finally merely the presence of a poorly streamlined structural element inside the tube. In normal operation of the combustion chamber the vortex formation will occur in all these cases in accordance with the usual laws of hydromechanics. But if vibration combustion sets in, then there will be superimposed on the main motion of the stream also an ordered oscillating variation of the stream velocity and then vortex

formation will be the result not of the usual flow of the stream around solid bodies, but of the flow of a stream whose velocity has a noticeable and ordered periodic component.

Vortex formation is connected with the viscosity of the liquid, and the theory of flow of a viscous liquid constitutes one of the very important and far from developed branches of hydromechanics. This pertains all the more to the flow of a stream whose velocity has a peri-

odic component around solid bodies. Although there is essentially no theory of this process, there are known experimental investigations devoted to related problems, particularly problems involving the flow of a viscous liquid around oscillating solid bodies (for example, work devoted to the interaction between vortex formation behind factory smoke stacks in winds and the natural oscillations of these stacks). It was shown in these investigations that when a solid vibrates at a definite frequency, the frequency of the collapse of the vortices can become modified and assume the same value as this "driving" frequency. It is important to note here that the vortex formation itself becomes stronger in this case.

It is therefore natural to assume that if vibration combustion has set in, then the oscillations of the air stream flowing around stationary solid bodies will cause a modification of the vortex formation ahead of the combustion zone and this formation can now occur at the frequency of the acoustic oscillations.

Pressure oscillations can also contribute to this. The pressure standing wave patterns shown in the second chapter indicate that in the portions located away from the pressure antinodes there exists a nonzero pressure gradient along the flow axis. It is known from the theory of the flow of viscous liquids that the presence of a static-pressure gradient of definite sign in a stream may cause detachment of the stream from the walls, owing to the influence of this gradient on the flow of the liquid in the boundary layer. Without going into details connected with this question, we merely point out that during the time of acoustic oscillations the static-pressure gradient will vary periodically and in particular will reverse sign every half cycle. Therefore, roughly speaking, during each oscillation cycle there will exist an instant when the detachment of the boundary layer (i.e., the

formation of a vortex) will be particularly probable.

Thus, not only oscillations of the stream velocity, but also pressure oscillations will contribute to vortex formation, with a period equal to the period of the acoustic oscillations.

We can, finally, present an example of excitation of acoustic oscillations in a wind tunnel, which was investigated in detail by S.P. Strelkov, G.A. Bendrikov, and N.A. Smirnov.* Without presenting a description of this interesting research, we merely indicate that an important role was played in the self-oscillation process by periodic formation of a vortex ring under the influence of the acoustic oscillations.

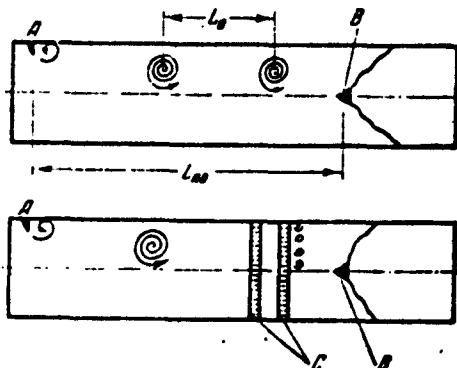


Fig. 69. Diagram showing vortex formation ahead of the combustion zone.

Thus, many indirect experimental data and theoretical arguments of general character point to the fact that in the presence of acoustic oscillations, powerful vortices, with a period equal to the period of the acoustic oscillations, can be produced behind those structural elements of an engine or of a furnace which contribute to noticeable vortex formation.

Let us assume that this possibility is realized and let us trace in what manner this leads to the closing of the feedback loop in vibra-

tion combustion. The upper part of Fig. 69 shows a schematic representation of the discussed phenomenon. In the cold part of the tube, at the point A, is located the place where the stream becomes detached and a vortex forms. In this diagram the cause is a poorly streamlined baffle plate. In fact, as was already indicated above, this may be a place where the stream turns or where the stream passes through an expanding channel, etc. The vortices formed at the point A are carried by the stream toward the combustion zone. Let the period of the acoustic oscillations be T . Then at a stream velocity v_1 the distance between vortices will be $L_B = v_1 T$. If we assume that the rate of flow does not change in the portion between the baffle plate A and the stabilizer B, then the vortices reaching the combustion zone will interact periodically (with period equal to L_B/v_1) with the flame front maintained by the stabilizer. This will close the feedback loop. Indeed, let there exist acoustic oscillations which lead to the formation of a chain of vortices moving toward the combustion zone. On reaching the flame front, each vortex deforms the front and consequently the flame front will experience periodic deformations. It was already shown in Chapter 4 that periodic displacement of the flame front inside the combustion zone is equivalent to the existence of a nonzero amplitude of the oscillations in the effective flame propagation velocity \bar{U}_1 , which is in itself capable of exciting the system (or maintaining the already produced self-oscillations), provided suitable amplitude-phase relations exist. Consequently, if a sufficiently powerful vortex is produced at the point A, is detached, and starts moving together with the stream at an instant of time such that it arrives at the flame front and deforms it with the required phase of the acoustic oscillations, then the oscillating system will become excited.

The vibration combustion produced in accordance with this scheme

can conceivably be combated by two different methods. On the one hand, a favorable effect can be expected if one changes the phase of the detachment of the vortex, and on the other hand, if its dimensions are decreased. As regards the first path, it must be stated immediately that it is very difficult to act on the phase of such a complicated phenomenon as the detachment of a vortex. If we follow the second path, on the other hand, then a simple structural measure, namely the installation of rectifying grids along the path of the vortex, may exert a noticeable influence on the vibration-combustion process. The rectifying grids are used, as is well known, in those cases when it becomes essential to "quiet down" the stream and impart to all its component jets a direction parallel to the walls of the tube. These grids comprise a set of thin plates, which usually cross one another at right angles, installed in some cross section of the tube in such a way as to make the planes of the plates parallel to the stream axis. It is usually sufficient to install two such grids in succession, at a certain distance from each other. These grids can have a small hydraulic resistance and do not change the character of the flow in any significant manner, if we disregard its "quieting down." The effect of these grids reduces essentially to breaking down a large vortex, which passes through such a grid, into many small vortices. As a result there enters into the combustion zone not a single powerful vortex capable of strongly deforming the surface of the flame front, but an assembly of many small vortices, which act on the flame not as a factor deforming its surface, but merely as a stream with somewhat higher turbulence. Although the combustion process does indeed depend on the turbulence of the incoming stream, this dependence cannot compare at all with the powerful distortions in the flame front configuration due to large vortices. In the lower part of Fig. 69 is shown the flow pattern

when rectifying grids C are installed ahead of the combustion zone.

The general considerations advanced here were confirmed by means of special experiments. The scheme of the experimental setup is essentially shown in Fig. 69. The tube in which the combustion chamber was located was subjected to a free stream. The inlet part of this tube permitted powerful vortices to arise. In order to break the resultant coupling between the vortex-formation and combustion processes, two rectifying grids were located in sections close to the combustion zone. The experiments consisted of studying the combustion process (from the point of view of the possibility of exciting vibration combustion) with and without rectifying grids. The supply of fuel is gradually increased (the excess-air coefficient α is gradually decreased) and the variation of the character of the oscillations observed.

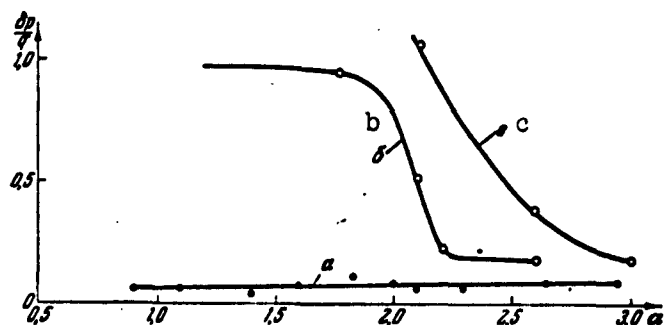


Fig. 70. Influence of vortex formation ahead of the combustion zone on the tendency of the system toward excitation.

First to be determined was the influence of the rectifying grids on the degree of vorticity of the air flow ahead of the combustion zone. This was done in the following manner. Cold air is blown through the setup and the outlet section of the tube was reduced in size until the flow of air through the setup was the same as the flow during combustion. Then the degree of vorticity of the flow was determined in a section located behind the second rectifying grid with the aid of a

thermoanemometer. We must specify here that the term "vorticity" is used in the present book to denote turbulence of large scale, produced as a result of the detachment of large vortices in portions of the duct located ahead of the combustion chamber.

The results of the measurements of the velocity oscillations yielded for the vorticity without the rectifying grids a value of 70%, and with the rectifying grids a value of 20%. The following should be noted with respect to the numerical data presented here. The thermoanemometer used in the experiments was not designed for the measurement of such intense turbulence. Therefore the numerical data presented here should be regarded as a qualitative description of the degree of vorticity of the stream. They leave no doubt that the installation of the grids reduces noticeably the degree of vorticity of the stream.

The results of the experiments are shown in Fig. 70, which gives the amplitudes of the pressure oscillations ahead of the combustion zone δp as a function of the excess-air coefficient. Curve a characterizes the operation of the setup in the presence of rectifying grids, while curve c is without them. As can be seen from the experimentally obtained curves, the installation of rectifying grids eliminates the powerful vibration combustion ($\delta p/q \cong 1$) and reduces the pressure oscillations to a normal level ($\delta p/q < 0.1$). At the same time, the oscillograms have demonstrated that the oscillations themselves have a different character. In the case of vibration combustion (curve c) the oscillations had a clear-cut and regular character, while in normal combustion (curve a) a complicated and indeterminate frequency spectrum is observed.

Thus, in the experiment described (and in many others) the favorable influence of breaking the coupling between the vortex formation ahead of the combustion zone and the combustion process was clearly

demonstrated.

Of course, the insulation of rectifying grids is not the only method of breaking this coupling. If the vortex formation is due to the presence of a poorly streamlined body in the inlet portions, then the same effect can be attained by removing this body or by streamlining it. The importance of such measures is illustrated by curve b of Fig. 70. This curve corresponds to an experimental setup with rectifying grids, but differing in the fact that behind the grids there were located on the tube walls (for structural reasons) lugs in the form of parallelepipeds. When these were streamlined, the vibration combustion stopped and the relative amplitudes of the pressure oscillations dropped to the tolerable level $\delta p/q \cong 0.1$.

It must be stated that there are no general standard means of combating vibration combustion resulting from vortex formation in the cold part of the stream. In each specific case it is necessary to find the source of this vortex formation and to take appropriate measures. Sometimes this may be the installation of grids or the streamlining of the bodies, and in other cases this may be the installation of guiding devices (for example, guiding vanes in the parts where the stream takes a sharp turn), drawing away the boundary layer, or other measures which have been well worked out in experimental aerodynamics.

If it is desired to represent the considered feedback mechanism in the form of analytic relationships, certain difficulties arise. These are connected with the insufficient development of the theory of vortex formation and the lack of quantitative data on the influence of the vortex brought into the combustion zone on the change of the flame-front configuration.

If these data are specified (or if experimental data are obtained by a study of the discussed phenomenon), then the further path is quite

obvious. The motion of a chain of vortices through the flame front leads to a periodic change in the volume of the hot gases in the combustion zone σ , and, in accordance with the results of §16, we can write

$$\bar{U}_1 = \frac{-1}{a_1 F} \frac{\partial}{\partial t} V_g(t) - \bar{v}_1, \quad (36.1)$$

where, as is well known, $V_g(t)$ is the volume of the zone σ occupied by the combustion products and F is the cross-sectional area of the stream.

The distance L_{AB} between the flame front and the location of the vortex formation (Fig. 69) enables us to relate the phase of the vortex detachment with the phase of its contact with the flame front, in analogy with what was done in §35, by introducing the factor $\exp i\omega(\tau - L_{AB}/LM_1)$.

As a result it is easy to obtain formulas of the same type as (35.2), for example

$$\bar{U}_1 = C \left[\varphi_1 \left(\omega; \frac{L_{AB}}{L} \right) \bar{v}_0 + \varphi_2 \left(\omega; \frac{L_{AB}}{L} \right) \bar{p}_0 \right] \exp i\omega \left(\tau - \frac{L_{AB}}{LM_1} \right). \quad (36.2)$$

The last formula is written down under the assumption that the detachment of the vortex is connected with velocity oscillations at the point A, and the constant C includes the numerical characteristic of the detached vortex (its phase and amplitude, which is assumed proportional to the perturbation \bar{v}_1 at the point A). As can be seen from (36.2), feedback with delay is produced in this case.

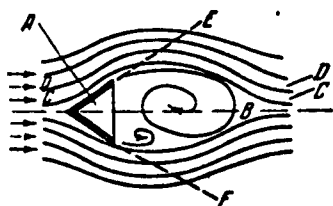


Fig. 71. Flow diagram behind a poorly streamlined flame stabilizer.

b) Vortex formation in the combustion zone. Another phenomenon which is also connected with the hydromechanics of poorly streamlined bodies and may also become a feedback mechanism is the vortex formation behind the flame stabilizers. As is well known, for continuous

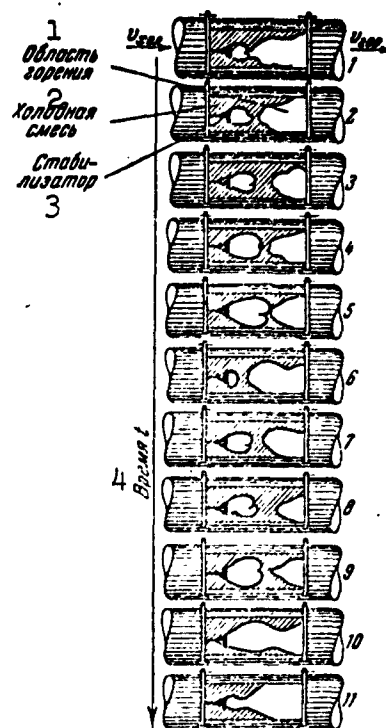


Fig. 72. Vortex formation behind a conical stabilizer in the case of vibration combustion (high speed motion picture photography). 1) Combustion region; 2) cold mixture; 3) stabilizer; 4) time t .

ignition of a combustible mixture moving in a tube one uses various types of igniting devices, the simplest type of which is a poorly streamlined body (for example sheet metal wrapped in the form of a cone and placed with the vertex opposite to the stream), so that the backwash zone serves as a continuously acting source of ignition. Such a stabilizer is shown schematically in Fig. 71. The hot mixture is incident on the stabilizer A, in the aerodynamic "shadow" of which there exists a region AB of stagnant flow; in this region vortices are periodically formed and are carried away further by the stream that flows over the stabilizer. In this backwash zone the velocities are low, so that the combustion process occurs under favorable

conditions. The jet CC closest to the backwash zone stays in the stream for a relatively long time in contact with the hot gases of the zone behind the stabilizer, and has time to become heated and to start burning. The flame then jumps over to the next jet DD, etc.

In normal combustion the vortex-formation process behind the stabilizer obeys the usual laws and in general its character is independent of whether the flow around the stabilizer is produced by cold air or by a hot mixture which ignites behind it. In this case the flame front behind the stabilizer has the character of a somewhat mobile, randomly deforming cone, with the average flame-front position being along

the lines AE and AF.

The combustion process behind the stabilizer assumes an entirely different character in those cases when vibration combustion sets in. The acoustic oscillations, for the same reasons as mentioned somewhat earlier, impose, as it were, their frequency on the vortex formation behind the stabilizer, and the dimensions of the vortices which detach themselves from the region behind the stabilizer become noticeably increased. This process interacts with the combustion in the backwash zone and results in a qualitatively new pattern of the entire phenomenon.

Instead of a more or less stable conical flame front behind the stabilizer, one observes a clear-cut periodic process. The gradual increase in the flame burning behind the stabilizer stops once the flame reaches a certain size and breaks away, then being carried away by the stream. At this instant the combustion behind the stabilizer attenuates, as it were, but soon the initial focus of the flame remaining behind it makes it possible for combustion to resume, the hot volume increases more and more, continuing to "hold on" behind the stabilizer, and after reaching the critical size it again breaks away from the stabilizer and starts moving together with the stream. It is quite clear that this periodic detachment of the hot flames from the stabilizer represents a detachment of vortices in which (as the latter grow) the combustion process envelops larger and larger masses of combustible mixture.

The phenomenon described here was recorded with high-speed motion picture photographs of the combustion behind a single cone stabilizer through a transparent window built into the wall of a cylindrical tube 200 mm in diameter, in which vibration combustion was investigated. The sequence of the most characteristic frames recorded by the camera



Fig. 73. Oscillogram of the pressure oscillations δp_1 and of the illumination of the combustion zone ϕ in the case of vibration combustion.

is shown in Fig. 72. It must be noted that in these experiments small amounts of special substances were placed in the fuel to make the flame glow brightly.

In order to show that the frequency at which the hot regions are detached (the frequency of vortex formation) coincides with the frequency of the acoustic oscillations, two quantities were recorded simultaneously

in these same experiments by means of a loop oscillograph, namely the pressure and the luminosity of the flame in the combustion zone. A phototransducer installed at the required distance from quartz glass made it possible to record the integral luminosity of the combustion zone, which was proportional to the visible area of the hot regions. Consequently, periodic detachments of the hot regions from the stabilizer and their constant replenishment, shown in Fig. 72, should lead to a periodic change in the readings of the phototransducer. The corresponding records obtained on the oscillograph chart are shown in Fig. 73. It is easy to see that the oscillations of the luminosity and of the pressure had exactly the same frequency, confirming the fact that the vortex formation and combustion process adapts itself to the acoustic frequency.

If we turn to a mathematical description of this type of combustion-process perturbation, it is quite obvious that a periodic change of the volume occupied by the hot gases takes place in the zone σ . This leads, as in the preceding case, to the appearance of a nonzero periodic component in the effective propagation velocity of the plane flame front, \bar{U}_1 , and the magnitude of this component can be determined from Formula (36.1). If it is assumed further that the vortex-formation

process behind the stabilizer is connected exclusively with the perturbation in the stream velocity \bar{v}_1 , then the quantity $(1/a_1 F)(\partial/\partial t)v_g(t)$ can be represented (in the linear approximation) in the form

$$\frac{1}{a_1 F} \frac{\partial}{\partial t} V_r(t) = \text{const } \bar{v}_1, \quad (36.3)$$

where const stands, generally speaking, for a complex quantity characterizing the amplitude and the phase of the expression on the left for a certain single value of \bar{v}_1 . Thus, \bar{U}_1 can be represented in the form

$$\bar{U}_1 = \text{const } \bar{v}_1. \quad (36.4)$$

In this expression the constant factor preceding \bar{v}_1 differs by unity from the constant factor in Formula (36.3), as is clearly seen from a comparison of (36.1), (36.3), and (36.4).

Were it to turn out that the detachment of the vortex is connected not only with velocity oscillations, but also with pressure oscillations, then Formulas (36.3) and (36.4) would assume a more complicated form, and in the right halves \bar{v}_1 would be replaced by a linear combination of \bar{p}_1 and \bar{v}_1 . Thus, the type of feedback is characterized in the present case by the lack of delay due to the transport of the factor causing the combustion perturbation, i.e., it corresponds to the schemes shown in Figs. 66a and b.

To conclude the present section let us make a few general remarks. In the two examples of feedback due to the hydromechanics of the flow, we spoke of the influence of vortex formation on the combustion and emphasized the action of the vortex formation on the magnitude of the perturbations in the flame propagation velocity \bar{U}_1 . This does not mean, of course, that vortex formation cannot cause disturbances in \bar{Q}^* , for example, by disturbing the mixture production (when the vortex passes through the zone where the nozzles are located) or directly by changing the completeness of the combustion in the zone σ as the result of dis-

turbances of the combustion process. The same can also be stated with regard to \bar{P}_x . Periodic detachments of the vortices from the stabilizers will undoubtedly lead to a periodic change in the instantaneous values of the coefficient of hydraulic resistance of the devices placed in the combustion zone. If desired it is also possible to take into consideration these two components of the combustion-perturbation process but, principally to save space, we presented here only the most clearly pronounced connection between the vortex formation and the deformation of the flame front.

In the present section we referred everywhere to the ability of the vortex formation to adapt itself to the frequency of the acoustic oscillations. This fact was observed directly also in a study of vibration combustion. High-speed motion picture photography of combustion behind a single conical stabilizer, which was referred to somewhat earlier, has confirmed the existence of this connection between vortex formation and the acoustic oscillations. It is interesting to note that the frequency "staircase" shown in Fig. 51 was obtained in the combustion of a previously prepared mixture behind a conical stabilizer. The observed jumpwise change in the frequencies offers indirect evidence that the ability of the vortex formation to adapt itself to the frequency of the acoustic oscillations is quite appreciable.

It must be stated that both types of vortex formation, ahead of the combustion zone and behind the stabilizer, are perfectly capable of interacting with the combustion process. The following experiment is instructive in this respect. A previously prepared combustible mixture was burned in a tube having a combustion chamber of square cross section in which the "plane" combustion problem was investigated. The flame was maintained by a stabilizer located in the middle of the stream and constructed in the form of a horizontal angular profile the

edge of which met the stream head on. In the direct vicinity of the front of the stabilizer was placed a rectangular shutter covering half the quadratic section of the combustion chamber (the shutter was installed flush against one of the walls). In spite of the closeness to the stabilizer, the shutter did not enter the combustion zone and could be placed either horizontally or vertically. In the former case its edge, over which the stream of mixture flowed, was parallel to the edges of the stabilizer, and in the latter case it was perpendicular to them. In addition, the shutter could be returned in such a way that it was aligned "with the stream" and thus did not disturb the character of the flow at all. The experiments consisted essentially of exciting vibration combustion in such a system, with measurements of the frequencies and amplitudes of the pressure oscillations. The results of the experiments have shown that when the shutter was positioned vertically the frequencies remained the same as when the shutter was turned "with the stream," but the oscillation amplitudes were decreased. A transition to a horizontal placement of the shutter has led to a reduction in the oscillation frequencies by a factor of two and to an increase in the oscillation amplitudes. If vibration combustion is attributed to processes connected with vortex formation, this result is natural: in the former case half the stabilizer was in a shadow, as it were, and thus the intensity of the overall vortex-formation process was decreased; in the latter case the shutter and the stabilizer could interfere and this led to an increase in the vortex-formation intensity, as well as to a change in the frequency with which the vortices were detached. The latter led to the excitation of a second harmonic in the system, which was in better agreement with the new character of the vortex formation.

When it comes to the possibility of describing the action of vor-

tex formation on the combustion process by means of formulas of the type (36.2) and (36.4), the following remarks are in order. In these formulas the connection between the acoustic oscillations and the vortex formation is in the form of a linear relation. Yet the intensity of the vortex is connected with the amplitudes of the acoustic oscillations in a more complicated fashion, since the dimensions of the vortex are determined to a considerable degree by the dimensions of the poorly streamlined body, which, naturally, are independent of the frequency of the acoustic oscillations. Consequently, Formulas (36.2) and (36.4) can have only a limited application. In order to describe the vibration combustion process more completely, it would be necessary to take into account the nonlinear relations that are inherent in the vortex-formation process. This can be done formally by formulating the appropriate properties of vortex formation. An example of the solution of the vibration-combustion problem in which the nonlinear properties of the combustion zone are taken into account will be presented in the next chapter.

Let us conclude with a few words about methods of combating vibration combustion (if such combustion is not desirable) in the case when the feedback loop is closed through the vortex formation. We have already mentioned earlier that if the vortex-formation source is located ahead of the combustion zone, then installation of rectifying grids and analogous measures may be useful. If the oscillations are excited by the vortex formation behind the stabilizer, the situation becomes more complicated. It is impossible to eliminate this vortex formation, inasmuch as the presence of a backwash zone behind the stabilizer is an essential condition for its operation as an ignition source. Something can be done here by empirically choosing the most suitable geometrical stabilizer configurations.

There are indications in the literature that the vibration combustion that occurs sometimes in commercial furnaces is connected not only with perturbations in the fuel supply (which were discussed in the preceding section) but also with the formation of powerful regular vortices in the region where fuel is fed to the combustion zone. In those cases when the vibration combustion is undesirable, it is recommended that the sharp edges be rounded off and that other measures be adopted to streamline the aerodynamic passages of the corresponding portion of the furnace. This practical rule becomes understandable in light of the considerations advanced before.

It is interesting to note that in the descriptions of vortex formation in furnaces, in connection with the pulsating character of the combustion in the furnaces, it is emphasized that the vortex in which the combustion takes place has a tendency to become particularly powerful. Something similar was observed also in the previously described experiments in vortex formation behind the stabilizers in the case of vibration combustion. It must be noted, to be sure, that the question of the influence of the combustion process in the vortex on its properties has not yet been thoroughly investigated.

§37. Feedback Mechanisms Based on the Laws of Combustion Proper

In addition to causes that lead to vibration combustion and that are in a certain sense indirect, namely mixture production and vortex formation, the combustion process itself contains mechanisms that are capable of assuming the role of feedback in this self-oscillating phenomenon.

The existence of such feedback mechanisms, which are based on the laws of the combustion itself, is proved, for example, by the fact that vibration combustion arose in the experiments of Coward, Hartwell, and Georgson, which were already mentioned several times, in a pre-

viously prepared immobile gas mixture, i.e., under conditions in which one must exclude all effects connected with vortex formation or mixture production.

We therefore present a description of certain feedback mechanisms which are directly connected with the combustion process.

a) Normal flame propagation velocity. This velocity depends on the mixture temperature and on its pressure; the turbulent propagation velocity can, in addition, change also as a function of the stream velocity and the degree of its turbulization. When the gas column in an engine oscillates, all the mentioned stream parameters (with the exception perhaps of the degree of turbulization) have periodic components. Consequently, the flame propagation velocity will also vary periodically, and this may serve as the cause of vibration combustion.

Let us show this by means of an example in which a system is excited by a plane flame front, the propagation velocity of which depends on the temperature of the mixture and on its pressure ahead of the combustion zone. Inasmuch as the temperature is not included in the system of chosen variables (p , v , s), we use the equation of state $p = \rho RT$ and the adiabatic condition $s = \text{const}$, with which p and ρ can be related, to represent the flame propagation velocity as a function of only the pressure ahead of the combustion zone. A dependence of this type is usually determined experimentally and is represented in the form of a power function

$$U_1 = U_1^{(0)} \left(\frac{p_1}{p_1^{(0)}} \right)^r,$$

where the index "zero" denotes the initial values of U_1 and p_1 . In considering small deviations of U_1 from $U_1^{(0)}$ we can write

$$\delta U_1 = U_1^{(0)} r \frac{\delta p_1}{p_1^{(0)}}. \quad (37.1)$$

We shall assume that the initial values of U_1 and p_1 , which enter into

Formula (37.1), coincide with U_1 and p_1 in the cold portion of the tube and recognize that by virtue of the steady state of the flame front relative to the observer in the stationary flow we have $v_1 = -U_1$, and then changing to the dimensionless variables used in the present book we obtain from (37.1)

$$\bar{U}_1 = -\kappa M_1 \bar{r} \bar{p}. \quad (37.2)$$

It must be recalled here that, as was already mentioned in §16 in the course of the discussion of the system (16.12), an increase in the absolute flame propagation velocity corresponds, by virtue of the sign rule adopted, to $U_1 < 0$. Thus, when $r > 0$ an increase in pressure corresponds to an increase in the absolute value of the combustion rate.

Formula (37.2) describes one of the possible feedback mechanisms directly related with the combustion process. This feedback is of the simplest type shown in the upper part of Fig. 66.

The main parameters of the gas flow, \bar{p} and \bar{v} , can influence the excitation of the self-oscillations not only via \bar{U}_1 , but also via \bar{Q}^* . This will occur in those cases when the completeness of combustion is a function, say, of the stream velocity v_1 . Oscillations of the stream velocity ahead of the combustion zone will then give rise to oscillations in the completeness of combustion, and consequently also to oscillations in the heat supply. If we cast these arguments in analytic form, we can readily obtain for \bar{Q}^* an expression analogous to (37.2). It is easy to visualize that to excite acoustic oscillations the completeness of combustion must decrease at a sufficient rate with increasing stream velocity.

b) Presence of igniting source. The feedback mechanisms listed above could manifest themselves also in the absence of a special igniting source. The presence of such a source leads to the possibility of periodic disturbance in the ignition of the system. This is con-

ected with the fact that in practice there always exists a certain cold-stream velocity at which combustion is interrupted. This velocity depends on the power of the igniting source; its existence is due to the fact that in order to ignite a combustible mixture this mixture must be in contact with the flame for a certain time and, in addition, the flame itself must be sufficiently powerful not to become extinguished by the stream. This question is discussed in sufficient detail in works on combustion theory and will therefore not be analyzed here.

Assume that the igniting source, behind which the flame is "secured," is characterized by a certain critical stream velocity v^*_1 , at which the combustion of the mixture incident on the igniting source stops. Then at the instants of time when $v_1 + \delta v_1 > v^*_1$ the flame will be detached from the ignition source and carried away by the stream (provided, of course, that the flame existed in the preceding instants). At the instants of time when $v_1 + \delta v_1 < v^*_1$, the ignition of the mixture will resume. The feedback mechanism described here frequently plays an important role. As a rule, this mechanism is observed in the combustion of a mixture behind a stabilizer in a mode of strongly developed oscillations. This case will be considered in greater detail somewhat later. It is advantageous to start at this point the description of such a mechanism with a different case. In order to eliminate the influence of vortex formation, special experiments were set up in which a previously prepared homogeneous mixture was ignited by means of a thin and flat gas burner installed in a tube of square cross section with quartz walls. The gas burner was constructed so as not to disturb noticeably the stream in the cold part of the square tube, and the flame behind the burner (when pure air, without fuel, was fed through the tube) had the form of a thin, short, and flat tongue moving in the center of the quadratic cross section from one quartz wall

of the combustion chamber to the opposite wall. When the combustible mixture was fed to the tube, this strip of continuously present flame, fed with fuel and with oxygen from a separate source, ignited the combustible mixture moving along the combustion chamber. High-speed motion picture photography through the transparent walls of the combustion chamber, which was carried out in such a way that the optical axis of the camera was parallel to the igniting tongue of the burner flame, i.e., perpendicular to the transparent wall of the chamber, made it possible to observe the "planar" combustion picture behind such an ignition source.

In this case all phenomena connected with vortex formation were completely eliminated. No oscillations of the continuous flame front behind the burner were observed. As in the case of combustion behind a poorly streamlined body, the principal role was played in this experiment by the volumes of hot gas which were detached from the igniting source and which grew, moving together with the stream, until they filled the entire section. Figure 7⁴ shows the characteristic frames of the motion pictures obtained in this experiment. It is clearly seen on these frames how a gas burner ignites periodically the combustible mixture, in connection with the oscillations of the mixture velocity. With increasing stream velocity relative to the burner, its power is no longer sufficient to ignite the mixture. The mixture is ignited again as soon as the oscillating component of the stream velocity is directed opposite to the average stream velocity.

Something analogous can be observed also in the combustion of a previously prepared combustible mixture behind stabilizers built in the form of poorly streamlined bodies, in the case of strongly developed oscillations accompanied by a periodic "hurling" of the flame upstream, into the region lying ahead of the stabilizer. This process

will be considered in greater detail (but from a somewhat different point of view) in Chapter 9.

An analytic description of this phenomenon, as a periodic detachment of the hot regions from the ignition source that maintains the

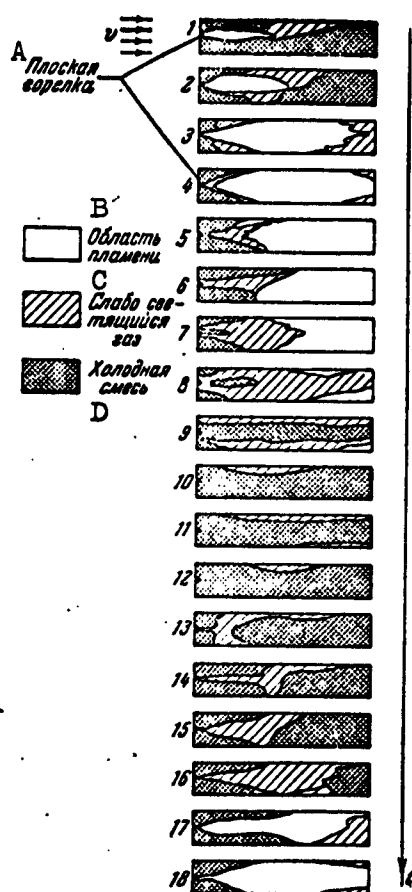


Fig. 74. Character of vibration combustion behind a burner that excludes the possibility of vortex formation, registered by high-speed motion picture photography. A) Flat burner; B) region of flame; C) weakly glowing gas; D) cold mixture.

flame, entails no difficulties. Here, as in §36, it is necessary to consider the periodic variation of the volume $V_g(t)$ of the hot gases in the combustion chamber, then change over to the effective perturbation of the flame propagation velocity U_1 , and obtain finally an expression in the form (36.4). To be sure, it must be added that such a description can be readily obtained for self-oscillations that have already been established. If we attempt to consider this process as a mechanism for the excitation of self-oscillations, starting with infinitesimally small amplitudes, it becomes immediately clear that such an excitation is impossible. After all, the detachment of the flame from the ignition source can occur only after the amplitude of the velocity oscillations has reached the required value. Thus, the described mechanism is capable of appear-

ing in two cases. First, if the initial perturbation was sufficiently large. Such cases are known in oscillation theory as cases of hard self-excitation. Second, it may turn out that initially the oscillating

instability of the stream was the result of realization of a different feedback mechanism, capable of making the system unstable with respect to infinitesimally small perturbations (soft self-excitation), and only after the oscillation amplitudes have noticeably increased does the oscillating system change to the feedback mechanism described above.

c) Delay phenomena in the combustion zone. It is easy to construct examples in which only a delay in the combustion process can produce the amplitude-phase relation between the heat-supply perturbations and pressure perturbations necessary for the excitation of acoustic oscillations. Let us illustrate this by means of an example taken from the theory of excitation of oscillations in liquid-fuel jet engines.*

As will be shown in greater detail in Chapter 10, when longitudinal acoustic oscillations are excited in liquid-fuel jet engines, the most significant is not the perturbation of the heat supply, but the perturbation in the gas production (the combustion of a liquid fuel can be reasonably regarded as a gas-production process). This process can be connected with a certain induction period. Analogous mechanisms of delay in the ignition are conceivable also in those cases when the gas production does not play an important role, since the amount of injected fuel is small compared with the air fed to the combustion zone, but an important role is played by the perturbation in the heat supply connected with the delays in ignition (ordinary furnaces).

In considering the role of the delay of the ignition processes in the excitation of acoustic oscillations we shall speak in the present section only of heat-supply perturbations \bar{Q}^* . It must be borne in mind, however, that everything stated here pertains also to the perturbation of gas production (and perhaps even to a greater degree). Therefore, in Chapter 10 below, the principal relations obtained here will be directly applied to the question of the perturbation in gas production

occurring in liquid-fuel jet engines.

Let us assume that the flow of fuel is constant, and that the combustion occurs instantaneously at the moment that the fuel leaves the nozzle. Then the heat supply is not perturbed and $\dot{Q}^* = 0$, and consequently self-excitation of the system is impossible. The picture will be entirely different if the fuel-combustion process is connected with time delays. Before we consider this, let us present brief data on the possible causes of the existence of such delays.

The conversion of the fuel components from the liquid state into gaseous combustion products calls for a certain time; this time is naturally called the induction period. The induction period is connected with a complicated chain of physical and chemical processes occurring in the combustion chamber. These processes are the atomization of the fuel, its heating, and partial or complete evaporation of the fuel droplets, the development of the chemical reactions which lead in final analysis to the formation of the combustion products. A feature of many of the above-mentioned phenomena is their pressure dependence. With increasing pressure in the combustion chamber, the rate of mixture production increases — the atomization is finer, the evaporation and the heating of the fuel droplets accelerates. In addition, the speed of many chemical reactions (particularly those in the gas phase) increases with increasing pressure. As a result the overall induction period can have a clearly pronounced tendency toward decreasing with increasing pressure in the combustion chamber.

It follows from the foregoing that the induction period can be regarded as a time after the lapse of which the fuel is instantaneously converted into combustion products. (The latter is connected with the fact that after suitable preparation the mixture burns very rapidly, inasmuch as the reaction rate increases unusually rapidly with increas-

ing temperature and, in particular, heating of the mixture, connected with the start of its combustion, makes the subsequent combustion practically instantaneous. Of course, this picture is only a first approximation to the true phenomena.)

The overall induction period can be determined only by experiment. However, on the basis of the statements made above, we can propose the following relation as an analytic first-approximation dependence:

$$t_1 = t_{10} + t_{11}, \quad (37.3)$$

where $t_{10} = \text{const}$ and t_{11} is determined from the equation

$$t_{11} p^r = \text{const}. \quad (37.4)$$

Here, inasmuch as an increase in pressure should correspond to a reduction in the induction period, we have $r > 0$.

According to Formula (37.3), the induction period consists of two components: the first, t_{10} , which is independent of the pressure, and the second, t_{11} , which is related with the pressure by (37.4).

We shall assume below that $t_{10} = 0$ and that the entire induction period can be connected with the pressure by Relation (37.4).

Let us assume that pressure oscillations take place in the combustion chamber. It is then natural to introduce in lieu of (37.4) an expression analogous but written in the form of an integral

$$\int_{t_{11}}^t p' dt' = \text{const}. \quad (37.5)$$

It is easy to see that if $p = \text{const}$ then (37.4) and (37.5) coincide, but if $p = p(t')$ the phenomenon becomes more complicated. Assume, as was already mentioned, that the nozzles supply a constant amount of fuel. Pressure oscillations give rise to oscillations in the reduction period. A reduction in this period causes the combustion of the particles that enter into the combustion chamber during a definite instant to coincide in time with the combustion of particles which were

previously supplied. This increases the heat released compared with the value characteristic of the steady-state process. When the induction period increases, the opposite is observed. Thus, in the presence of pressure oscillations, the dependence of the induction period on the pressure will cause the perturbations of the heat supply to differ from zero, making self-excitation of the system possible. (For this purpose it is necessary, of course, to have not only $\bar{Q}^* \neq 0$, but a definite relation between the phase of the pressure perturbation and the phase of \bar{Q}^* .)

The example presented shows that the dependence of the induction period on the pressure can lead to realization of a feedback mechanism capable of exciting the oscillating system under consideration.

In §35 above we considered an example in which the pressure oscillations in the combustion chamber give rise to oscillations in the flow of fuel. It was indicated there that in this case the oscillations can be excited only when a delay in the ignition of the mixture is present in the system, i.e., the necessary feedback is obtained only under the simultaneous action of two causes, based on mixture production and combustion, respectively. It is easy to note that in this case the self-excitation of oscillations does not require the assumption of a pressure dependence of the induction period, since a nonzero value of \bar{Q}^* is obtained as a result of the variable fuel flow. Setting $t_{11} = 0$ in Formula (37.3) we obtain $t_1 = t_{10} = \text{const}$. The entire remainder of the analysis will be similar to the example considered in §26.

Everything stated here concerning the induction period and its influence on the excitation of acoustic oscillations holds true also with respect to other constructions, for example pulverized-coal furnaces. As was already indicated above, it is necessary to assume here,

too, the existence of a certain induction period in order to obtain the necessary phase relations between the oscillating component of the supply of pulverized coal to the combustion zone and the oscillating component of the heat release.

d) Instability of the flame front. This instability, and particularly its dependence on the accelerations, can lead to vibration combustion. In 1944, Landau showed* that a plane flame front is always unstable and that this instability depends on the accelerations acting on the flame front. Inasmuch as the flame front in vibration combustion can oscillate together with the oscillating medium, it will experience accelerations which reverse sign periodically. The periodically varying acceleration leads to a periodically arising instability of the flame front, capable of exciting acoustic oscillations. This is a rather complicated problem and it is best to devote a separate section to it.

§38. Stability of Plane Flame Front

Assume that a plane flame front normal to the stream velocity is located in a one-dimensional stream of combustible mixture. This plane flame front will be regarded as a strong-discontinuity surface, on which the velocity, pressure, and density of the stream vary abruptly. We raise the question of the stability of such a plane flame front. To obtain the connection between the stream parameters before and behind the heat-supply surface in the stationary process we use the continuity and momentum equations

$$\begin{aligned} \rho_1 v_1 &= \rho_2 v_2, \\ p_1 + \rho_1 v_1^2 &= p_2 + \rho_2 v_2^2. \end{aligned} \quad (38.1)$$

If we assume in addition that we are considering the flow of an incompressible liquid** (inasmuch as the velocities v_1 and v_2 are small compared with the velocities of sound a_1 and a_2) then, in exactly the

same manner as in §10 when we analyzed the question of thermal resistance, we can assume that the gas density is inversely proportional to its temperature

$$\rho_1/\rho_2 = T_2/T_1. \quad (38.2)$$

These equations define completely the stream parameters to the left and to the right of the heat-supply plane.

Let the stationary flow experience small velocity and pressure perturbations. We assume the density perturbations equal to zero, since the density depends in the assumed model of the phenomenon only on the temperature, and the latter depends in turn on the calorific value of the mixture. Assuming that the combustion in the flame front is complete both in the stationary and in the perturbed combustion modes, we obtain the conditions $\rho = \text{const}$ for the streams on both sides of the flame front.

Considering the stability of the flame front itself (which for the time being is not related at all with the possible acoustic oscillations), we introduce a plane y, z which we align with the plane of the flame front in the unperturbed process. We retain the direction of the x axis the same as before, along the stream velocity. Let the small velocity and pressure perturbations δv and δp be periodic in time and in the coordinate y , i.e., proportional to a factor $\exp(iky - i\Omega t)$, and independent of z .

To determine these perturbations we write down the linearized Euler equations and the continuity equation

$$\left. \begin{aligned} \frac{\partial \delta v_x}{\partial t} + v \frac{\partial \delta v_x}{\partial x} &= -\frac{1}{\rho} \frac{\partial \delta p}{\partial x}, \\ \frac{\partial \delta v_y}{\partial t} + v \frac{\partial \delta v_y}{\partial x} &= -\frac{1}{\rho} \frac{\partial \delta p}{\partial y}, \\ \frac{\partial \delta v_x}{\partial x} + \frac{\partial \delta v_y}{\partial y} &= 0. \end{aligned} \right\} \quad (38.3)$$

The system (38.3) should be written out separately for the cold

mixture and for the combustion products. The subscripts x and y designating the δv indicate the axis on which the velocity perturbation is projected. No indices are used for the y, since the stationary flow is one-dimensional (directed along the x axis).

Differentiating the first equation of (38.3) with respect to x and the second with respect to y, adding the two and taking into account the third equation of (38.3), we readily find that δp satisfies the Laplace equation

$$\frac{\partial^2 \delta p}{\partial x^2} + \frac{\partial^2 \delta p}{\partial y^2} = 0. \quad (38.4)$$

In a small area about the discontinuity surface (i.e., when $x \approx 0$), certain conditions should be satisfied. Let us consider them in greater detail.

First, the tangential velocity component must be continuous. Let $\delta x(y; t)$ be a small displacement of the points of the discontinuity surface in the x direction, which arises when the stationary process becomes perturbed. Then the derivative $\partial \delta x / \partial y$ is the tangent of the angle of inclination of the flame front to the y axis at the point under consideration. If we denote this angle by α , then we can easily see that the tangential component of the total velocity is expressed in the following fashion:

$$(v + \delta v_x) \sin \alpha + \delta v_y \cos \alpha.$$

Assuming the angle α to be small (the order of its smallness is determined by the perturbation δx), we retain, as is customary, only the first-order terms with allowance for the fact that for small angles we have $\sin \alpha = \tan \alpha = \partial \delta x / \partial y$, and then write the corresponding expression for the tangential component of the velocity, an expression which holds true in the linear approximation:

$$\delta v_y + v \frac{\partial \delta x}{\partial y}.$$

Then the condition that the tangential velocities be equal on both sides of the flame front will have the following form:

$$\delta v_{y1} + v_1 \frac{\partial \delta x}{\partial y} = \delta v_{y2} + v_2 \frac{\partial \delta x}{\partial y}. \quad (38.5)$$

Second, it is necessary to make some assumption regarding the dependence of the flame propagation velocity on the flame-front perturbations. Landau proposed that there is no such dependence, i.e., that the rate of propagation of the discontinuity must not experience a change when the front is disturbed. This means that the flame front will be displaced only by the velocity perturbations, i.e.,

$$\delta v_x = \partial \delta x / \partial t$$

or

$$\delta v_{1x} = \delta v_{2x} = \frac{\partial \delta x}{\partial t}. \quad (38.6)$$

Later on, Markstein* appreciably supplemented the Landau theory, assuming that the combustion velocity depends on the curvature of the flame front, i.e., that it can be related with the quantity $\partial^2 \delta x / \partial y^2$.

Further refinements were introduced in later papers, but these will not be considered here.

For the purposes of the present section, it is sufficient to use only the simple assumption of Landau. Whatever new factors are introduced by Markstein's refinement will be considered briefly below.

Conditions (38.5) and (38.6) relate the velocity perturbations on both sides of the flame. In order to relate also the pressure perturbations, it is necessary to introduce a third condition. Assume that a certain acceleration \underline{b} acts on the flame surface. We can then write for δp_1 and δp_2 , taken in a small vicinity of the separation surface, the following equation:

$$\delta p_1 - \delta p_2 = b (q_1 - q_2) \delta x. \quad (38.7)$$

As was already mentioned above, a solution of (38.3) and (38.4)

is sought in the form of exponential functions proportional to $\exp(iky - i\Omega t)$. Consequently, let

$$\left. \begin{aligned} \delta p &= c_1 \exp(iky + ax - i\Omega t), \\ \delta v_x &= c_2 \exp(iky + ax - i\Omega t), \\ \delta v_y &= c_3 \exp(iky + ax - i\Omega t), \end{aligned} \right\} \quad (38.8)$$

where a is a still undetermined factor. Substituting the expression for δp obtained here into the Laplace equation (38.4) we obtain immediately

$$a^2 - k^2 = 0 \quad (k > 0)$$

or $a = \pm k$. A suitable value of a can be chosen from the condition that the pressure perturbations, which are connected with the flame-front perturbation, have no effect at an infinite distance from the front, i.e., as $x \rightarrow \pm\infty$. But then, obviously, it is necessary to choose for $x < 0$ (cold gas) $a_1 = k$, and for $x > 0$ (hot gas) $a_2 = -k$.

In addition to the solution obtained, there can exist still another one. Indeed, the Laplace equation is satisfied, in particular, when $\delta p = 0$. Let us consider this case in greater detail. If we let $\delta p = 0$, then the right halves of the first two equations in (38.3) vanish. Substituting in them δv_x and δv_y in accordance with (38.8), we find that for this case $a = i\Omega/v$. However, to prevent the existence at an infinite distance from the flame surface (at $x \rightarrow \pm\infty$) of nonzero velocity perturbations δv_x and δv_y , we shall consider the solution obtained only for the hot gas ($x > 0$). This can be explained in the following fashion. The factor Ω , which is for the time being undetermined and which can be determined later on from the characteristic equation, will, in general, be complex. In this case, if Ω has a positive imaginary part, all the perturbations will tend to infinity with time, as can be seen from (38.8). For these values of Ω the perturbations will attenuate with increasing distance from the flame front only if $x > 0$. The case when the imaginary part of Ω is negative is of no interest,

since this represents stationary oscillations, whereas the purpose of the present analysis is to determine the unstable states of the flame front.

Substituting (38.8) in (38.3) and assuming that these equations are written for the cold gas, we take $a = k$ and choose such values of the constant coefficients c_1 , c_2 , and c_3 , as satisfy the system (38.3). From the third equation of this system we obtain immediately that $c_3 = ic_2$, and from any of the first two equations we get $c_1 = \rho_1(i\Omega/k - v_1)c_2$. Consequently, the coefficients c_1 , c_2 , and c_3 are determined apart from the indeterminate factor A_1 which, without loss of generality, can be set equal to c_2 . Thus, for the cold gas the solutions of (38.3) will have the form

$$\left. \begin{aligned} \delta p_1 &= A_1 \rho_1 \left(\frac{i\Omega}{k} - v_1 \right) \exp(iky + kx - i\Omega t), \\ \delta v_{1x} &= A_1 \exp(iky + kx - i\Omega t), \\ \delta v_{1y} &= iA_1 \exp(iky + kx - i\Omega t). \end{aligned} \right\} \quad (38.9)$$

Analogously, for the hot gas (taking into account the fact that there are two values of \underline{a}), we obtain the following expressions:

$$\left. \begin{aligned} \delta p_2 &= -A_2 \rho_2 \left(v_2 + \frac{i\Omega}{k} \right) \exp(iky - kx - i\Omega t), \\ \delta v_{2x} &= A_2 \exp(iky - kx - i\Omega t) + \\ &\quad + A_2 \exp\left(iky + \frac{i\Omega}{v_2} x - i\Omega t\right), \\ \delta v_{2y} &= -iA_2 \exp(iky - kx - i\Omega t) - \\ &\quad - \frac{\Omega}{kv_2} A_2 \exp\left(iky + \frac{i\Omega}{v_2} x - i\Omega t\right). \end{aligned} \right\} \quad (38.10)$$

We supplement (38.9) and (38.10) with still another equation

$$\delta x = A_1 \exp(iky - i\Omega t). \quad (38.11)$$

The last equation states that waves traveling in the direction of the y axis were produced on the flame front. In the case of harmonic oscillations these waves are characterized by a frequency Ω or by an oscillation period $T = 2\pi/\Omega$, and a wavelength $\lambda = 2\pi/k$. Equation (38.11) is an analytic way of writing down the assumption, which was made at the very outset, that a perturbation periodic in time and

in the coordinate y has been superimposed on a stationary plane flame front.

Substituting the values of the variables written in the form of Eqs. (38.9), (38.10), and (38.11) for $x = 0$ into the conditions that relate the solutions for the cold and the hot gases (38.5), (38.6), and (38.7) we obtain a system of four linear homogeneous equations, containing four indeterminate coefficients A_1 , A_2 , A_3 , and A_4 . The system will have a nontrivial solution when the following determinant vanishes:

$$\begin{vmatrix} i & i & \frac{\Omega}{kv_2} & ik(v_1 - v_2) \\ 1 & -1 & -1 & 0 \\ 1 & 0 & 0 & i\Omega \\ q_1\left(\frac{i\Omega}{k} - v_1\right) & q_2\left(\frac{i\Omega}{k} + v_2\right) & 0 & b(q_2 - q_1) \end{vmatrix} = 0.$$

This determinant can be transformed in the following manner. Multiplying its second row by Ω/kv_2 and adding it to the first, we obtain a third-order determinant, the central column of which contains the common factor $1 - \Omega/kv_2$. Taking this factor outside the determinant sign, we obtain

$$\left(i - \frac{\Omega}{kv_2}\right) \begin{vmatrix} i + \frac{\Omega}{kv_2} & 1 & ik(v_1 - v_2) \\ 1 & 0 & i\Omega \\ q_1\left(\frac{i\Omega}{k} - v_1\right) & -iq_2v_2 & b(q_2 - q_1) \end{vmatrix} = 0.$$

After simple calculations we obtain from this equation the characteristic equation of the system:

$$\left(i - \frac{\Omega}{kv_2}\right) [\Omega^2(q_1 + q_2) + 2i\Omega k q_1 v_1 + b k (q_2 - q_1) - k^2 q_1 v_1 (v_1 - v_2)] = 0. \quad (38.12)$$

It is obvious first of all that the characteristic equation has a root $\Omega = ikv_2$. However, this root must be discarded since in this case the terms with the coefficient A_3 vanish, the indicated terms become exactly the same as the terms with A_2 , and consequently the essential

properties of the phenomenon are lost. Consequently, the subsequent analysis of the stability of the discontinuity surface (of the flame front) will be carried out under the condition $1 - \Omega/kv_2 \neq 0$. From (38.12) we obtain

$$\Omega^2(q_1 + q_2) + 2i\Omega k q_1 v_1 + bk(q_2 - q_1) - k^2 q_1 v_1 (v_1 - v_2) = 0. \quad (38.13)$$

We introduce for the sake of convenience $\Omega_1 = -i\Omega$. Then we can write in place of (38.13)

$$\Omega_1^2(q_1 + q_2) + 2\Omega_1 k q_1 v_1 - bk(q_2 - q_1) + k^2 q_1 v_1 (v_1 - v_2) = 0. \quad (38.14)$$

Let us analyze the expression obtained in greater detail. Let $b = 0$ (i.e., no acceleration acting on the flame front). Then, by virtue of the fact that $v_2 > v_1$ (the rate of flow of the combustion products exceeds the rate of influx of the fresh mixture), the free term of the quadratic equation (relative to Ω_1) is negative, and consequently both roots are real and have opposite signs. Consequently, changing over to Ω , we can state that the motion of the discontinuity surface is characterized by two imaginary "frequencies" Ω , having opposite signs, i.e., the motion will have an unstable component. Thus, if we make Landau's assumptions, we conclude that any plane flame front is unstable.

As was already noted above, Markstein refined Landau's theory, introducing in place of the condition (38.6) a second condition, which takes into account the dependence of the combustion velocity on the curvature of the flame front. As a result, the equation for the determination of Ω becomes somewhat more complicated than (38.13), and its analysis shows that the instability becomes a function of the number \underline{k} , which is uniquely related with the wavelength of the perturbation on the flame front, $\lambda = 2\pi/k$. It is possible to show in this case that if the local rate of combustion increases with decreasing positive local

radius of the flame-front curvature,* then for sufficiently small λ the process will always be stable, at sufficiently large λ it is unstable, and when $\lambda = \infty$ it is neutral. It follows from the foregoing that there exists a certain value $\lambda = \lambda_{\max}$, at which the process has maximum instability.

If we consider that it is precisely this type of instability that manifests itself in the experiment, then we can expect the appearance of waves with length corresponding to λ_{\max} on the plane flame front.

Markstein carried out a series of precise experiments, in which he showed that such waves were actually formed and led to the so-called cellular structure of the flame front. High-speed motion picture photography has shown that the flame front breaks up, as it were, into a series of cells which are convex toward the side of the fresh mixture. The cells are in random motion at all times and the larger cells increase at the expense of the smaller ones and split up upon reaching excessive magnitude. As a result, there is a certain leveling out of the cell dimensions, and one can speak of their average size. An estimate made by Markstein has shown that the dimension of this cell does not contradict the assumption that their characteristic size is connected with the wavelength λ_{\max} .

Everything said so far pertained to the case when $b = 0$, i.e., no acceleration acts on the flame front.

It is sufficient to look at Eq. (38.14) to become convinced that, depending on the sign of \underline{b} , the acceleration can exert a stabilizing or an unstabilizing influence on the process. If $b < 0$ then the next to the last term in (38.14) will be negative (since heating causes $\rho_2 < \rho_1$), and consequently, the absolute value of the negative free term of the quadratic equation (38.14) increases, and this leads to an increase in the absolute value of the negative root Ω_1 , which gives

rise to the instability. The opposite tendency will be observed when $b > 0$.

In Markstein's experiments the tube in which the previously prepared mixture of air with various hydrocarbons was consumed was positioned vertically, in such a way that the cold gas (fresh mixture) was located at the bottom and the combustion products were in the upper part of the tube. Consequently, the flame front was acted upon by the acceleration due to gravity $b = g$. By virtue of the action of this acceleration, corresponding to $b > 0$, the process should become more stable than in the case of horizontal placement of the tube.

It must be stated that both the flame front instability in the sense of Landau and the similar structure of this front associated with this instability have no direct bearing on vibration combustion, i.e., on the excitation of acoustic oscillations in tubes. To observe such effects there is no need at all for acoustic oscillations of the medium. However, if acoustic oscillations did arise, they would exert a powerful influence on this type of instability of the flame front itself. Indeed, in acoustic oscillations, so long as the flame front is not located in a velocity node, the oscillating medium will "drag" the flame behind it. This unavoidably leads to accelerations acting on the flame front, these being nonzero even when it is not acted upon by gravitation (vertical position of the flame front). To the extent that the acceleration connected with the medium oscillations will reverse sign periodically, the instability of the flame front will become periodically intensified or weakened.

Markstein observed this phenomenon experimentally. In those cases when the flame front in his experiments started to oscillate as a unit, the high-speed motion picture photographs showed that the cellular structure of the flame had a tendency toward periodic intensification

and attenuation — the cells appeared and vanished in rhythm with the vibration motion of the flame front. Thus, it can be said that the acoustic oscillations influence the stability of the flame front, and consequently its structure.

The latter suggests the possibility of occurrence of the feedback necessary for the excitation of the acoustic oscillations. Indeed, if a change in the structure of the flame occurs in rhythm with the acoustic oscillations, then this can lead to a change in the effective rate of combustion, with the same rhythm, and this in turn can in principle be sufficient to maintain acoustic oscillations. This thought is advanced in a paper by Markstein and Squire.*

It must be stated that the phenomena connected with the cellular structure of the flame front can hardly play an important role in the excitation of acoustic oscillations in commercial devices. These effects were observed only at sufficiently small stream velocities. In the above-mentioned experiments of Markstein, the Reynolds number for the stream in the tube ranged between 400 and 600, i.e., it corresponded to laminar flow. Apparently a more important role is played by a somewhat different effect, which we now proceed to consider.

If we turn to Eq. (38.14), we can easily see that the occurrence of instability on the flame front is connected with two different effects. First, it may arise in the case when the flow of gas mass per second through the discontinuity surface differs from zero ($\rho_1 v_1 \neq 0$). Second, it can arise also if $\rho_1 v_1 = 0$, but only if a negative acceleration \underline{b} occurs. The first case was considered above with sufficient detail. The analysis of the second is quite elementary. If $\rho_1 v_1 = 0$, then we obtain from (38.13)

$$\Omega = \pm \sqrt{bk \frac{q_1 - q_2}{q_1 + q_2}}, \quad (38.15)$$

which is the well-known formula for the oscillation of two heavy liquids situated one on top of the other. In the latter case one sets $b = g$ and real values of Ω (stability) are obtained when $\rho_2 < \rho_1$, i.e., the upper liquid is lighter than the lower one.

The indicated two types of instability manifest themselves in different fashions. The first, connected with the passage of a gas mass through the flame front ($\rho_1 v_1 \neq 0$), imparts to the flame a cellular structure, as was considered in detail by Markstein. As was already mentioned earlier, this type of instability arises also in the absence of accelerations ($b = 0$). As regards the second type of instability, connected with the fact that \underline{b} differs from zero, its occurrence does not necessitate the assumption that the mass stream crosses the separation boundary between media having different temperatures, and can occur also on a surface which separates gases that are stationary on the average, provided the acceleration is directed from the cold gas to the hot one. The fact that the gases are stationary on the average means that combustion does not take place, since combustion is always connected with the passage of cold gases through the flame front, behind which they become hot. Consequently, the second type of instability can manifest itself in pure form on the boundary separating gases having different density (temperature) and subjected to an acceleration normal to the separation boundary. A typical form of such an instability is formation of waves on the surface of a heavy liquid under the action of acceleration.

The periodically sign-reversing accelerations which can act on the flame front in the case of acoustic oscillations unavoidably cause wave production on the separation surface (on the flame front). This wave formation will interact with the phenomena which occur in the cellular structure of the flame, but if we attempt to estimate these

two types of instability from the point of view of their reaction on the acoustic oscillations, the wave formation must be recognized to be more important. The latter is principally connected with the fact that the periodically increasing and decreasing wave formation leads to a periodic change in the integral separation surface (the area of the flame front), and consequently, to a periodic change in the effective velocity of combustion.

In order to trace this phenomenon in pure form and to obtain simple formulas, let us analyze the stability of the separation boundary when $v_1 = v_2 = 0$. Qualitatively the picture will not change if we take v_1 and v_2 different from zero, but this makes the analysis unnecessarily complicated. In order to consider the stability of the separation surface under the influence of an acceleration \underline{b} which has a periodic component, we can no longer use Formula (38.15), which was obtained under the assumption that \underline{b} is constant, and the derivation must be repeated here anew. Inasmuch as the conditions on the separation surface are now functions of the time, the solution of the system (38.3) must be sought not in the form (38.8), but in more general form, in the form of the product of as yet undetermined functions of the time $F(t)$ by a factor $\exp(iky + ax)$.

Thus, let

$$\left. \begin{aligned} \delta p &= F_1(t) \exp(iky + ax), \\ \delta v_x &= F_2(t) \exp(iky + ax), \\ \delta v_y &= F_3(t) \exp(iky + ax). \end{aligned} \right\} \quad (38.16)$$

Substituting δp in Eq. (38.4) we obtain, as before, $a = \pm k$, and the choice of the signs of \underline{k} remains the same: $a_1 = k$ for $x < 0$ and $a_2 = -k$ for $x > 0$.

For the cold portion of the gas ($x < 0$) the substitution of the values of the variables (38.16) into the system (38.3), taking into

account the fact that $v = 0$, yields the following relations between $F_1(t)$, $F_2(t)$, and $F_3(t)$:

$$\left. \begin{aligned} F_1 &= -\frac{q}{k} F_2' \\ F_3 &= i F_2 \end{aligned} \right\} \quad (38.17)$$

Setting $F_2(t) = A_1(t)$, we can write: when $x < 0$

$$\left. \begin{aligned} \delta p_1 &= -\frac{q_1}{k} A_1'(t) \exp(iky + kx), \\ \delta v_{1x} &= A_1(t) \exp(iky + kx), \\ \delta v_{1y} &= i A_1(t) \exp(iky + kx). \end{aligned} \right\} \quad (38.18)$$

For hot gas ($x > 0$) we obtain from perfectly analogous considerations:

$$\left. \begin{aligned} \delta p_2 &= \frac{q_2}{k} A_2'(t) \exp(iky - kx), \\ \delta v_{2x} &= A_2(t) \exp(iky - kx), \\ \delta v_{2y} &= -i A_2(t) \exp(iky - kx). \end{aligned} \right\} \quad (38.19)$$

Relations (38.18) and (38.19) are a more general form of writing down Relations (38.9) and (38.10), although, to be sure, it is for the case when $v_1 = v_2 = 0$.

In comparing Expressions (38.10) and (38.19), there is a striking absence of terms with coefficient A_3 in the second group of expressions. This is connected with the fact that when $v_1 = v_2 = 0$ we have $A_3 = 0$. Indeed, the solution with A_3 was obtained above as a solution satisfying the first two equations of (38.3) when $\delta p = 0$. Here, by virtue of the fact that $v = 0$, we get $\partial \delta v_x / \partial t = 0$ and $\partial \delta v_y / \partial t = 0$, and consequently the functions $F_2(t)$ and $F_3(t)$ in Formulas (38.16) are constant. If they differ from zero, then there should exist a certain non-zero time-invariant perturbation δv_x and δv_y along the coordinate x , which does not exist in the present problem. Consequently, the constants F_2 and F_3 are equal to zero and the terms with A_3 different from zero cannot appear in the solution. Let us supplement, as above, the equations (38.18) and (38.19) with still another equation

$$\delta x = A_4(t) \exp iky, \quad (38.20)$$

which is a more general form of writing down (38.11).

Let us turn now to the formulation of the conditions which must be satisfied on the separation boundary (at $x = 0$). Inasmuch as it is now necessary to relate only three functions, namely $A_1(t)$, $A_2(t)$, and $A_4(t)$, one of the four conditions (38.5), (38.6), and (38.7) is superfluous. It is easy to see that this is the condition that the tangential velocities be equal, (38.5), inasmuch as when $v_1 = v_2 = 0$, i.e., when the medium does not cross the separation surface, this condition loses its physical meaning.

Substituting the values of the variables (38.18), (38.19), and (38.20) into the conditions (38.6) and (38.7), we obtain immediately

$$\left. \begin{aligned} A_1(t) &= A'_1(t), \\ A_2(t) &= A'_2(t), \\ -\frac{1}{\lambda}(q_1 A'_1 + q_2 A'_2) - b(q_1 - q_2) A_4 &= 0, \end{aligned} \right\} \quad (38.21)$$

from which follows a differential equation for the determination of A_4 :

$$A''_4 + kb \frac{q_1 - q_2}{q_1 + q_2} A_4 = 0. \quad (38.22)$$

Setting $k = 2\pi/\lambda$, where λ is the wavelength on the separation surface, and assuming that in the case of acoustic oscillations the separation surface is shifted as a unit along the \underline{x} axis together with the oscillating medium, in accordance with the sinusoidal law

$$h = h_0 \cos \omega t \quad (38.23)$$

(\underline{h} is the displacement of the medium, ω is the dimensional frequency of the acoustic oscillations [1/sec]), we obtain Eq. (38.22) in the following form:

$$A''(t) + \frac{2\pi}{\lambda} \frac{q_1 - q_2}{q_1 + q_2} (g_x - \omega^2 h_0 \cos \omega t) A = 0. \quad (38.24)$$

Here $A = A_4$, $b = g_x - \omega^2 h_0 \cos \omega t$, and g_x denotes the projection of the acceleration due to gravity on the \underline{x} axis, taken with the opposite sign.

For a vertical tube, g_x corresponds with the total acceleration g due to the gravity, while for a tube with horizontal direction of the axis we have $g_x = 0$. The second term of \underline{b} is obtained by differentiating the expression for \underline{h} twice.

If we introduce as an independent variable $z = \omega t/2$, then Eq. (38.24) reduces to the well-known form of the Mathieu equation

$$A''(z) + (a - 2q \cos 2z) A(z) = 0, \quad (38.25)$$

where

$$a = \frac{8\pi g_x (\varrho_1 - \varrho_2)}{\lambda \omega^2 (\varrho_1 + \varrho_2)},$$

$$q = 4\pi \frac{h_0 (\varrho_1 - \varrho_2)}{\lambda (\varrho_1 + \varrho_2)}.$$

As is well known from mathematical analysis, the solution of a linear differential equation of this type has the form

$$A(z) = C_1 e^{sz}/f(z) + C_2 e^{-sz}/(-z), \quad (38.26)$$

where \underline{s} is a certain constant and $f(z)$ is a periodic function with period π or 2π .

From the solution (38.26) we see that any real value of \underline{s} different from zero corresponds to instability, since, independently of the sign of \underline{s} , the exponential function in one of the terms of (38.26) will have a positive exponent proportional to the time (proportional to \underline{z}). Stability corresponds only to imaginary values of \underline{s} .

We shall further consider a horizontal tube, i.e., we shall set $g_x = 0$, and consequently $a = 0$. If we vary the parameter \underline{q} in such a way that it runs through positive values starting from zero, then the so-called characteristic exponent \underline{s} , which is equal to zero when $q = 0$, becomes first imaginary with increasing \underline{q} , and then at $q = 0.91$ it becomes real and different from zero, while at $q = 7.5$ it again becomes imaginary, and then almost immediately real up to $q \cong 21$, etc. Consequently, with increasing \underline{q} , regions of stability and instability will

alternate, with the stability regions characterized by extremely small segments on the g axis, whereas the instability regions are quite extensive. Thus, the instability will be observed almost everywhere.

We shall not analyze here in detail the questions that call for the use of the theory of Mathieu equations. In §49 we shall give a solution of this problem in a somewhat simplified formulation, in which the solution can be obtained in terms of elementary functions.

For the derivations that follow it is also necessary to point out that the first of the mentioned instability regions, $0.91 < q < 7.5$, is characterized by a period of 2π for the function $f(z)$ found in the solution of (38.26). In the next instability region $7.5 < q < 21$ the functions $f(z)$ will have a period π , and then when $21 < q < 42$ the function $f(z)$ will have again a period 2π , etc. (the inequalities written out are approximate, and in addition they disregard the fact that narrow intervals of the values of g at which the separation surface is stable are situated between the instability regions).

Since the solution to Eq. (38.26) can have two-fold instability and in order that the instability of the separation surface (the flame front) may be able to play the role of a feedback mechanism, it is necessary that this periodicity be in suitable correspondence with the period of the acoustic oscillations; we therefore consider the question of the relationships between the periods.

The period of the acoustic oscillations of the gas column is $T_{ak} = 2\pi/\omega$. If we change over to the independent variable $z = \omega t/2$, then the period of the acoustic oscillations is $z_{ak} = \pi$. Thus the solutions for (38.26) in those regions of the values of g where the period of $f(z)$ is π will correspond to oscillations of the separation surface (flame front) with the frequency of the acoustic oscillations, whereas in the other regions of the values of g , where the period of the function

tions $f(z)$ is 2π , the period of the oscillations of the separation surface will be twice the period of the acoustic oscillations.

It is easy to visualize that in order for a feedback mechanism based on the oscillations of the separation surface (flame front) to become feasible under the action of the acoustic oscillations, it is necessary that the period of the oscillations of the separation surface be twice the acoustic period. Indeed, this can be seen from the following simple considerations. The increase that wave formation introduces in the total area of the separation surface leads, as is well known, to an increase in the effective flame propagation velocity. In order for the effective flame propagation velocity to change in rhythm with the acoustic oscillations (and this is necessary if feedback is to be produced) it is necessary that the period of the oscillations of the flame surface be twice the period of the acoustic oscillations, inasmuch as the area of the separation surface (of the flame front) will increase both when it bends in the positive direction and when it bends in the negative direction of the x axis. For greater clarity, the corresponding diagrams are shown in Fig. 75. On the left is shown the case when the periods of the acoustic oscillations (the variable δp) and of the separation-surface oscillations (the variable δx) coincide. Then the period of variation of the separation surface δs turns out to be half the acoustic one. On the right, in the same figure, is shown the case when the period of the oscillations of the separation surface exceeds the period of the acoustic oscillations by a factor of two; the change in δs occurs in this case in the same rhythm as the change in δp , and this in turn makes it possible for a feedback mechanism to occur.

Thus, not all the instability regions obtained in the analysis of Eq. (38.25) are of interest from the point of view of interaction with

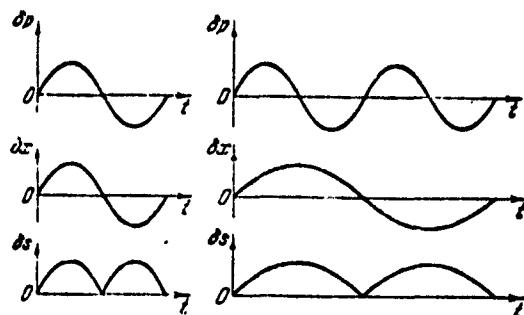


Fig. 75. Connection between the periods of the oscillations of the pressure δp , the displacement δx , and the perturbation of the flame surface δs .

the acoustic oscillations; it is necessary to regard as significant in this sense the region of values of q defined by the inequalities $0.91 < q < 7.5$ and then the region $21 < q < 42$, etc., i.e., the regions for which the period of the function $f(z)$ is equal to 2π .

If we compare the intervals of the values of q for which the period of the function $f(z)$ is equal to 2π , then the greatest practical interest attaches to the interval $0.91 < q < 7.5$, which is characterized by the smallest values of q . This follows from the following considerations. The quantity

$$q = 4\pi \frac{q_1 - q_2 h_0}{q_1 + q_2 \lambda} \quad (38.27)$$

is proportional to the ratio h_0/λ . The wavelength λ of the perturbation of the separation surface is connected with the dimensions of the tube cross section in which the oscillations take place, and if we disregard very high harmonics, it has the order of the characteristic linear dimension of this section. If we assume that the order of magnitude of λ is known, then the first region of values of q will correspond to the smallest amplitudes h_0 . Let us estimate the order of magnitude of these amplitudes. When $0.91 < q < 7.5$ and when the heating is characterized by $\rho_1/\rho_2 = 6$, we obtain for h_0/λ the following in-

equalities:

$$0,1 < \frac{h_2}{\lambda} < 0,83,$$

whereas for the nearest suitable region of values q , lying in the interval $21 < q < 42$, we have

$$2,3 < \frac{h_0}{\lambda} < 4,7.$$

The numbers presented are sufficiently convincing in themselves. To realize the instability corresponding to the second interval of the values of q , the displacement of the medium in the case of acoustic oscillations should exceed by a factor of 2-5 the wavelengths produced at the separation surface.

It is quite obvious that the realization of oscillations with smaller amplitude h_0 , corresponding to the first interval of the values of q , is much more probable. In addition, it is possible to advance also the following argument. If we consider growth of the oscillations when mentally increasing h_0 from zero, then the first suitable region of the values of q which is encountered is the interval $0.91 < q < 7.5$. At the same time, the changeover to the second region will be difficult, since the interval contains the region $7.5 < q < 21$, in which the maintenance of the acoustic oscillations by the considered feedback mechanism is impossible.

We have already mentioned above that the results obtained are approximately correct also for the case of combustion, i.e., for modes characterized by values of v_1 and v_2 different from zero. We therefore connect the oscillations of the separation surface with the perturbations of the effective flame propagation velocity. As can be seen from (16.5) and (16.7), the perturbation δU of the flame propagation velocity is determined by the equation

$$\delta U = -\frac{1}{F} \frac{\partial}{\partial t} V_r(t) - \delta v. \quad (38.28)$$

The change in the volume of the hot gases $V_g(t)$ consists of a displacement of the flame front by the stream velocity \underline{v} , this amounting to $Fvdt$ over a time dt if the transverse cross section of the tube is equal to F , and displacements of the flame front over the gas particles (as a result of combustion) by an amount $SU_n dt$, where S is the total area of the flame front (which generally speaking is curved), and U_n is the propagation velocity of an element of the flame front in a direction normal to its surface.

In the steady state, when the flame front is stationary relative to the walls, $Fv + SU_n = 0$. Consequently, in perturbed motion $V_g(t)$ changes within a time dt by an amount

$$(F\delta v + U_n \delta S + S\delta U_n) dt.$$

If we regard U_n as a constant quantity, then the last term in the sum written out above vanishes. In many cases this assumption can be regarded as correct in the first approximation, so that we can set

$$-\frac{\partial V_g(t)}{\partial t} = F\delta v + U_n \delta S.$$

Substitution of this equation in (38.28) yields the following expression for the perturbation of the effective combustion velocity:

$$\delta U = U_n \frac{\delta S}{F}. \quad (38.29)$$

We recall that an increase in the absolute value of the effective combustion speed corresponds to a displacement of the flame front toward the cold mixture, i.e., in a negative direction of the \underline{x} axis.

If we continue to consider the planar problem of the flame-front perturbation, then the area of the flame-front surface (for unit length in the direction of the \underline{z} axis) will be directly proportional to the height of the waves formed on the separation surface, i.e., proportional to the absolute value of δx , which is given by Formula (38.20). As was shown somewhat earlier, A_4 can under certain conditions fluctuate.

ate with a period equal to double the acoustic-oscillation period, and then the absolute value of A_4 will change in time with the same period as the acoustic oscillations. Expanding in this case the difference $|\delta x| - |\delta x|_{sr}$ in a Fourier series and discarding the higher harmonics of the expansion, we can write

$$|\delta x| - |\delta x|_{cp} = B_1 \sin(\omega t + \varphi), \quad (38.30)$$

where $|\delta x|_{sr}$ is the average absolute value of δx for a specified position of the point under consideration on the y axis.*

But then δS will oscillate about a certain average value in accordance with an analogous law:

$$\delta S = B_2 \sin(\omega t + \varphi). \quad (38.31)$$

Thus, the perturbation of the effective flame propagation velocity δU (38.29) will also change at the same frequency as the acoustic oscillations. This indicates that the feedback loop has been closed: the acoustic oscillations of the medium (more accurately, the accelerations connected with them) have led to a periodic wave production on the surface of the flame. This wave production has led to a pulsating change in the effective combustion speed, having the same frequency as the acoustic oscillations, and this, as is known from Chapter 4, will again give rise to acoustic oscillations if the amplitude-phase relationships are suitable.

In the present chapter, devoted to searches for possible feedback mechanisms, there is no need for making more precise the phase φ in Formula (38.31). It is sufficient to demonstrate the fundamental possibility of self-excitation of acoustic oscillations as a result of deformation of the flame front when the medium oscillates. The problem of the realization of such a form of self-excitation will be solved in greater detail, as was already mentioned, in §49.

In conclusion, attention should be paid to one singularity of the

considered feedback mechanism. Wave production on the flame surface is a typical parametric-resonance process: as a result of the periodicity of an essential parameter of the system (in this case acceleration), oscillations are excited on the surface of the flame front. The excitation of such oscillations can lead to an increase in the amplitudes of the wave formation on the front of the flame without an increase in the amplitude of the acoustic oscillations. Thus, feedback of the type considered is more complicated in a certain sense than the feedbacks described in the preceding sections. This raises certain difficulties in a rigorous analysis of the problem as a whole. A more complete study of this question is beyond the scope of the present book.

- 297 The symbol \bar{Q}^* is used below as shorthand notation for the effective perturbation of the heat supply \bar{Q}_e^* (16.14).
- 309 Strelkov, S.P., Bendrikov, G.A., and Smirnov, N.A., Pul'satsii v aerodinamicheskikh trubakh i sposoby dempfirovaniya ikh [Pulsations in aerodynamic tubes and methods of damping them], Trudy TsAGI [Transactions of the Central Aerohydrodynamical Institute], No. 593, 1946.
- 329 Crocco, L., Journal of the Amer. Rocket Society 21, No. 6., 163-178, 1951; 22, No. 1, 7-16, 1952. Russian translation: Problems of Rocket Technology, No. 3 (9), 1952, pp. 9-31.
- 333 L.D. Landau and Ye.M. Lifshits, Mekhanika sploshnykh sred [The Mechanics of Solid Media], Gostekhizdat [State Publishing House for Theoretical and Technical Literature], 1953.
- 333 This limitation can be readily lifted.
- 336 Markstein, G., Journ. of the Aeronautical Sciences, No. 3, 1951. There is a Russian translation: Markshteyn, Eksperimental'noye i teoreticheskoye izucheniye ustoychivosti fronta plameni [Experimental and theoretical study of the stability of a flame front], Voprosy raketnoy tekhniki [Problems of Rocket Technology], 1951, No. 4.
- 341 Curvature is assumed positive when the flame front is convex in the direction of the hot gas, $\partial^2 \delta x / \partial y^2 < 0$.
- 343 Markstein, G.H., Squire, W., On the Stability of a Plane Flame Front in Oscillating Flow, Journ. Acoust. Soc. Amer., 1955, Vol. 27, No. 3.
- 354 In actual fact the phenomenon is somewhat more complicated, since A_4 includes an exponential function of the time as a factor.

Manu-
script
Page
No.

[List of Transliterated Symbols]

295	г = g = goryucheye = fuel
296	ф = f = forsunky = nozzles
303	сг = sg = sgoraniye = combustion
316	хол = khol = kholodnyy = cold
316	гор = gor = goryachiy = hot
331	и = i = induktsiya = induction
349	ак = ak = akusticheskiy = acoustic
353	н = n = normal'nyy = normal
354	ср = sr = sredniy = average
356	э = eff = effektivnyy = effective

Chapter 8

CALCULATION OF SELF-OSCILLATIONS TAKING INTO ACCOUNT THE NONLINEAR PROPERTIES OF THE HEAT-SUPPLY ZONE

§39. General Characteristics of Self-Oscillations

It was already mentioned many times earlier that vibration combustion and other analogous processes are typical examples of self-oscillations. This manifests itself, in particular, in the fact that vibration combustion occurs suddenly, apparently without any visible cause. At the instant when the necessary conditions have arisen the amplitudes of the oscillations execute a sharp and almost instantaneous jump. The latter can be seen well, for example, from Fig. 76, which shows the average values of the pressure-oscillation amplitudes in a subsonic stream of air in which oscillations were excited by combustion. The plot in the indicated drawing is in the form of the dependence of the ratio of the pressure-oscillation amplitude δp in a certain section of the stream to the oscillation amplitude that is characteristic for normal (quiet) combustion δp_n in the same section on the excess-air coefficient α . The experiment whose result is plotted in Fig. 76 reduced to gradually enriching the mixture (decreasing α) after igniting the combustible mixture, and as the mixture became enriched the pressure-oscillation amplitudes were recorded for some section of the tube. It is seen from this experimental plot that, in a certain range of variation of α (from $\alpha = 2$ to $\alpha = 1.38$), no change takes place in the pressure-oscillation amplitude. Then, following the almost insignificant change in α from 1.38 to 1.34, a sudden jumpwise

five-fold increase in amplitude is observed. With further decrease in α , this amplitude remains practically constant. In addition to the jumpwise change in amplitude, the transition through $\alpha = 1.38-1.34$ is accompanied also by a change in the character of the oscillations themselves: whereas for $\alpha > 1.38$ the oscillations were indeterminate and variable, and had components with a large variety of frequencies, for $\alpha < 1.34$ clear-cut oscillations were observed comprising one or sometimes two harmonics characteristic of the acoustic properties of the tube as a whole. Both types of oscillogram are shown in Fig. 68.

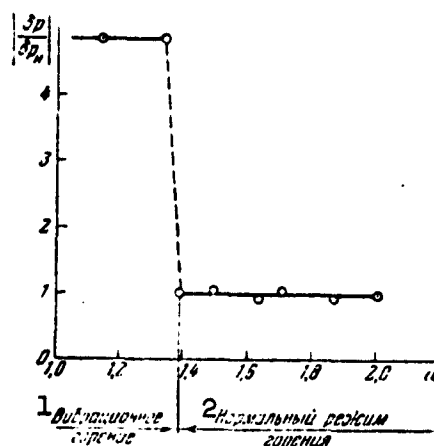


Fig. 76. Change in relative amplitude of the pressure oscillations on going over to vibration combustion. 1) Vibration combustion; 2) normal combustion mode.

Such a behavior of the oscillating system can be explained in the following manner. When $\alpha > 1.38$ the system is stable and the observed pressure oscillations are the consequences of the turbulence of the flow, pressure perturbations connected with combustion, etc. Somewhere between $\alpha = 1.38$ and $\alpha = 1.34$ the system becomes oscillatory-unstable with respect to small perturbations; the amplitudes of the harmonic that has become unstable begin to increase rapidly, and this harmonic soon becomes dominating. The growth of the amplitudes of the harmonic

that has become unstable is stopped by phenomena connected with the nonlinear properties of the system, which will be discussed below.

Inasmuch as the rate of growth of the oscillation amplitude of the unstable harmonic is sufficiently large (it usually reaches a steady-state value after 2-3 oscillations, i.e., within small fractions of a second), the changeover from the normal combustion to the vibration combustion occurs practically instantaneously.

As is well known, linear theory is capable of answering the question of system stability, but an actual calculation of the self-oscillation amplitudes is impossible within the framework of linear theory. Very frequently the amplitudes of self-oscillations are of no interest and their calculation is superfluous. In such cases it is possible to confine oneself to linear theory. Such requirements are imposed, in particular, on the theory whenever self-oscillations cannot be tolerated. Indeed, if vibration combustion must not occur (since it threatens to destroy the furnace or the engine), then it is sufficient to solve the problem of the stability of the process, and then see to it that the parameters of the system do not go beyond the stability limits. The situation is different if self-oscillations are the working mode, as is the case for example in furnaces with vibration ignition of the fuel. Then the calculation of the amplitudes is essential. Of course, this is not the only case when it is necessary to know the amplitudes of the self-oscillations; it may also be useful when it is necessary to estimate beforehand the magnitude of the amplitudes so as to solve the question of whether self-oscillating operating modes of the apparatus are permissible. In brief, cases may arise when calculation of the self-oscillation amplitudes is essential, i.e., it is necessary to take into account those properties of the oscillating system which cannot be described by linear relationships; these properties

will for brevity be called henceforth the essential nonlinearities.

From among the many nonlinear processes that accompany vibration combustion, one must separate the most important ones, leaving out the others so as not to make the solution of the problem excessively difficult. Losses with nonlinear characteristics can be localized in three ways. First, they can be distributed along the flow axis (friction and losses connected with the nonlinearity of the hydromechanics equations). Second, they can be connected with the radiation of energy from the ends of the tube; the corresponding condition can be given in the form of the dependence of the acoustic impedances on the ends of the tube on the oscillation amplitude. Finally, it is possible to assume that the heat-release process (combustion) differs appreciably in the case of sufficiently large amplitudes from that represented by the linear relations.

Attentive analysis of the experimental data shows that in a tremendous majority of cases it is possible to speak with full certainty of the dominating significance of the nonlinearities inherent in the combustion process. We shall therefore consider only this case in the present chapter. At the same time, the method employed below can be readily extended to include also a wider circle of problems.

In the preceding chapter we have given numerous examples of feedback mechanisms capable of leading to self-excitation of the oscillating system. The specific course of the solution of the problem depends, of course, on which of these feedback mechanisms is considered in the problem; however, the general solution procedure will not be noticeably modified on going over to a different mechanism. Therefore, although the solution given below does make use of one specific feedback mechanism, it must be regarded as an illustration of the application of the general method. The choice of feedback mechanism for the prob-

lem given below was made in such a way as to enable us to compare the calculated results with the experimental data.

§40. Essential Nonlinearities in the Combustion Zone

The considerations presented in the preceding chapter indicate that in order to describe the oscillations of the gas columns lying to the left and to the right of the combustion zone we can use, as before, the linear equations of §4, whereas for the combustion zone σ it is necessary to take into account the essential nonlinearities. The first of these statements is well confirmed by experiment: the pressure standing-wave patterns calculated from the linear theory are in good agreement with the experimental ones plotted during self-oscillations (Fig. 53). The correctness of the second statement will be demonstrated below.

We shall assume that the heat-supply process in the combustion zone depends on the oscillations of the gas stream. Let this dependence manifest itself in two ways: the flame front will be mobile and, in addition, the amount of heat released per unit mass will not be constant, i.e., we assume that $\bar{Q}^* \neq 0$. With respect to the mobility of the flame front we shall assume the following. Let the effective velocity of flame propagation relative to the tube walls N , defined by Formula (16.5), coincide with the instantaneous value of the oscillating component of the velocity δv_1 . Physically this means that the oscillating stream will "drag" the flame front behind it. Such an assumption makes it easily possible to find the quantities \bar{J}_1 , \bar{J}_2 , and \bar{J}_3 , which enter into the system (15.7) that describes the properties of the surface Σ (the region σ), with the aid of Relations (16.2), (16.3), and (16.4). The quantity $\bar{\eta}_{sg} + \bar{q}_1$, which figures in the last equation of the system (15.7), will be determined somewhat later.

It must be noted here that the use of the system (15.7) is per-

missile, strictly speaking, only for a problem defined by linear relations. Retaining the assumption of the possibility of describing by means of linear relations the processes at the ends of the tube and inside it, outside the heat-supply region σ , let us assume also that inside the heat-supply region all the quantities will continue to be related by linear equations, with the exception of the term $\bar{\eta}_{sg} + \bar{q}_1$, i.e., with the exception of the perturbation of the heat supply itself. As will be clear from what follows, the last limitation is not a principal one and can be readily lifted. This possibility is not used here in order not to make the solutions of the problem too cumbersome.

Let us use the system (15.7) and Relations (16.2), (16.3), (16.4), and (16.5), and let us also recognize that on the basis of the kinetic condition (16.6) we have

$$\delta v_1 + \delta U_1 = \delta v_2 + \delta U_2 = \delta N.$$

Then, on the basis of the assumption made at the beginning of the present section, namely that $\delta v_1 = \delta N$ (the value of N must obviously be zero in a stationary flow), and changing over to dimensional variables, we recast the system (15.7) in the form

$$\left. \begin{aligned} q_2 \delta v_1 + v_1 \delta q_1 &= q_2 \delta v_2 + v_2 \delta q_2, \\ v_1^2 \delta q_1 + 2q_1 v_1 \delta v_1 + \delta p_1 &= v_2^2 \delta q_2 + 2q_2 v_2 \delta v_2 + \delta p_2, \\ \left(\frac{v_1^2}{2} + q_1 \right) v_1 \delta q_1 + \left[q_1 v_1 \left(v_1 + \frac{v_1^2}{2} \right) + p_1 + \frac{1}{\kappa-1} p_2 \right] \delta v_1 + \\ &\quad + \frac{\kappa}{\kappa-1} v_1 \delta p_1 + q_1 v_1 \delta q = \\ &= \frac{v_2^2}{2} \delta q_2 + \left(\frac{3}{2} q_2 v_2^2 + \frac{\kappa}{\kappa-1} p_2 \right) \delta v_2 + \frac{\kappa}{\kappa-1} v_2 \delta p_2. \end{aligned} \right\} \quad (40.1)$$

We recall that q_1 is the latent chemical energy per unit mass of combustible mixture. The absence of the term q_2 indicates that total combustion is assumed in the stationary process ($\eta_{sg} = 1$). From a comparison of Eqs. (40.1), (15.2), (15.4), and (15.7) we can readily see that

$$\delta q = F(q_1; \eta_{sg}). \quad (40.2)$$

i.e., account is taken of the change in heat supply both due to the change in the latent chemical energy per unit mass of the combustible mixture and due to the change in the completeness of combustion. In the linear problem it would be necessary to write $\delta q = \eta_{sg} \delta q_1 + q_1 \delta \eta_{sg}$, but assuming that the most essential nonlinearity is connected with δq , we have introduced here a more general notation.

We shall seek the form of the nonlinear function δq . To this end it is first necessary to make more precise the character of the physical process under consideration. We choose a certain idealized scheme which is most readily realizable under laboratory conditions. The region of heat supply σ of the laboratory installations mentioned above is characterized by two singularities: the poorly streamlined bodies which stabilize the combustion process are small in dimension, are sufficiently densely placed, and all lie in one section, so that the length of the region of intense combustion behind the stabilizers can be assumed to be small compared with the length of the hot part of the tube (the length of the backwash zone behind the stabilizers is approximately proportional to their diameter); a second feature is that the nozzles which supply the fuel are located in the immediate vicinity of the stabilizers (ξ_f on Fig. 67 is close to zero).

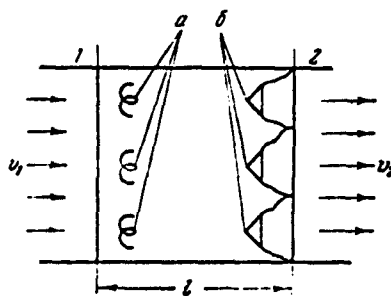


Fig. 77. Diagram of the combustion zone assumed in the calculation.

Let us represent these singularities by means of the diagram shown in Fig. 77. Let the sections 1 and 2 represent the boundaries of the zone where the mixture is prepared and where the combustion takes place, and let the distance \underline{l} between them be small. We assume that all the fuel injected by the nozzles \underline{a}

spreads instantaneously over the entire volume between sections 1 and

2 and is combusted in section 2 behind the stabilizers b. We shall take into account the time required for this purpose later on by introducing a delay time. If we assume that the fuel is fed by the nozzles at a constant rate of flow, $\dot{G}_g = \text{const}$, independently of the oscillations of the gas medium, then the change in the content of fuel mass in the volume of the region σ , a volume equal to $V = \underline{l}F$ (where F is the cross section of the stream), will be

$$\frac{1}{\rho_g} \dot{G}_g dt - \rho_g v F dt,$$

where ρ_g is the average density of the fuel in the volume $\underline{l}F$ and v is the stream velocity.

Dividing the expression obtained by $\underline{l}F$ we obtain the change in the fuel density in the volume $\underline{l}F$:

$$d\rho_g = \frac{\frac{1}{\rho_g} \dot{G}_g - \rho_g v F}{\underline{l}F} dt. \quad (40.3)$$

This equation describes the change in the fuel density also in section 2, in which the combustion takes place.

In order to integrate Eq. (40.3) it is necessary to specify $v = v(t)$. We shall consider steady-state oscillations, i.e., we set

$$v = v_0 + A_v \sin \omega t. \quad (40.4)$$

After substituting Expressions (40.4) into (40.3), it assumes the form

$$\frac{d\rho_g}{dt} = A - B\rho_g - C\rho_g \sin \omega t. \quad (40.5)$$

The solution of Eq. (40.5) cannot be represented in terms of elementary functions. The solid lines in Fig. 78 show the numerical solution of this problem under the condition that $\rho_g = 0$ at the instant $t = 0$. The example presented has been taken for flow parameters in that laboratory setup in which the experiments were carried out for the comparison of the theoretical calculations with the experimental

data. It was assumed in the calculations that $v_0 = 50$ m/sec, $A_v = 50$ m/sec, $l = 0.2$ m, and the fuel flow \dot{G}_g is such that in the absence of oscillations ($A_v = 0$) it yields $\rho_g = 0.008$ (this corresponds approximately to an excess-air coefficient $\alpha = 1$). It is necessary to explain here why the amplitude of the velocity oscillations A_v was taken in this example to be equal to the average stream velocity v_0 . The point is that in this case the singularities which can lead to the occurrence of nonlinear relationships between the velocity oscillation and the heat release become most clearly pronounced in this case. Indeed, as can be seen from Fig. 78, in the case under consideration σ_g fluctuates between 0.004 and 0.0225 for $\Omega = 32$ cps, which corresponds to fluctuations of the excess-air coefficient from $\alpha = 2$ to $\alpha = 0.35$. For $\Omega = 16$ cps, this range is even wider. It is quite clear that with such fluctuations of the composition of the combustible mixture, the completeness of the combustion will change in the strongest fashion and will undoubtedly be nonlinear. This question will be considered in greater detail below.

It is easy to see from Fig. 78 that the oscillations of ρ_g set in very rapidly, and the curve $\rho_g = \rho_g(t)$, once the oscillations have settled, is quite close in form to the sum of two sine waves with a frequency ratio equal to 2. We shall therefore seek an approximate solution of Eq. (40.5) in the following manner.

We assume that the approximate relation $\rho_g = \rho_g(t)$ can be written in the form

$$\rho_g = \rho_{g0} + D \sin(\omega t + \varphi) + E \sin(2\omega t + \alpha). \quad (40.6)$$

Substitution of this equation into (40.5) enables us to determine the constants contained in (40.6):

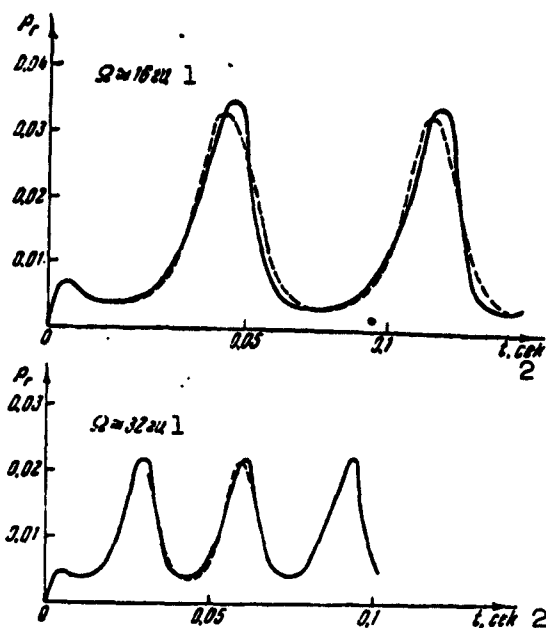


Fig. 78. Theoretical variation of the amount of fuel in the combustion zone in the case of oscillation of the air flow in the plane where the fuel nozzles are located. 1) cps; 2) sec.

$$\left. \begin{aligned}
 \beta &= \arctg \frac{\omega}{B}, \quad \gamma = \arctg \frac{2\omega}{B}, \quad \alpha = \frac{\pi}{4} - \gamma, \\
 \varphi &= \arctg \frac{\sin \beta + \frac{C^2}{4\sqrt{\omega^2 + B^2}} \cos \alpha}{\frac{C^2}{4\sqrt{\omega^2 + B^2}} \sin \alpha - \cos \beta}, \\
 Q_{r0} &= \frac{A}{B} - \frac{CD}{2B} \cos \varphi, \\
 D &= -\frac{\frac{A}{B}}{\frac{\sqrt{\omega^2 + B^2}}{C} \cos(\varphi + \beta) - \frac{C}{4\sqrt{4\omega^2 + B^2}} \sin(\varphi + \alpha) - \frac{C}{2B} \cos \varphi}, \\
 E &= \frac{CD}{2\sqrt{4\omega^2 + B^2}}.
 \end{aligned} \right\} (40.7)$$

In order to illustrate the accuracy of the approximate solution obtained, Fig. 78 shows dashed curves calculated by Formulas (40.6) and (40.7). Inasmuch as the agreement with the exact solution is quite satisfactory (this is confirmed also by other calculations), we shall employ henceforth the approximate procedure.

The functions $\rho_g = \rho_g(t)$ were obtained for different frequencies

Ω and different amplitudes of the oscillating component of the velocity A_v . Figure 79 shows by way of an example such curves for $\Omega = 48$ cps and for different values of A_v . Analogous relationships were constructed also for $\Omega = 16, 32$, and 100 cps (this range covers the frequencies observed in the experimental setup).

Unlike the preceding example, it is assumed here and below that in the absence of oscillations the combustion chamber operates with $\alpha \approx 1.5$. On the basis of the $\rho_g = \rho_g(t, \Omega, A_v)$ curves, heat-release curves were plotted as a function of the time. For this purpose an arbitrary plot of the dependence of the completeness of combustion on the excess-air coefficient was used (Fig. 80). The function $\eta_{sg} = \eta_{sg}(\alpha)$ (which has purposely been simplified) expresses the principal properties of such a dependence: in a certain range of α (here $1 \leq \alpha \leq 2$) the completeness of combustion is practically constant and close to unity. To the left and to the right of this region the completeness of combustion decreases sharply, becoming equal to zero in the case of a very rich and a very lean mixture (in the case under consideration, when $\alpha = 0.4$ and $\alpha = 4$). It must be noted that a refinement of this dependence would not be meaningful. On the one hand, this would change only slightly the quantitative but not the qualitative results of the calculation, and on the other hand, a relation which is made more precise in accordance with the results of experiments set up at stationary modes could be used for calculations of nonstationary (vibration) combustion only by stretching the point considerably.

The quantities ρ_g and α are obviously inversely proportional to each other, if we disregard oscillations of the density of the air connected with the oscillations of pressure. Inasmuch as the relative oscillation of the pressure is much less than the relative oscillation of the velocity, this dependence was not taken into account. Therefore

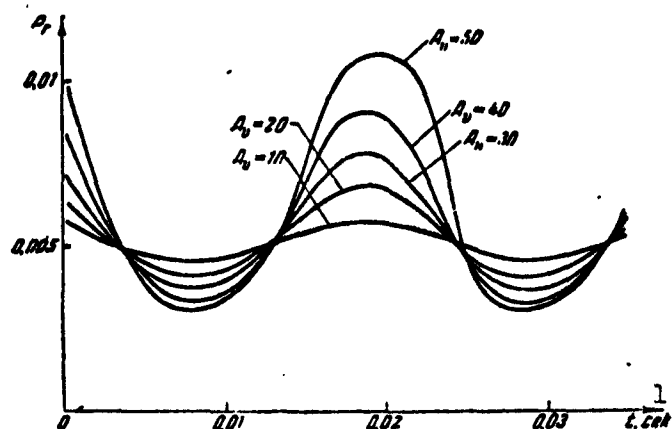


Fig. 79. Change in the amount of fuel in the combustion zone at different amplitudes of velocity oscillations in the plane containing the fuel nozzles.
1) sec.

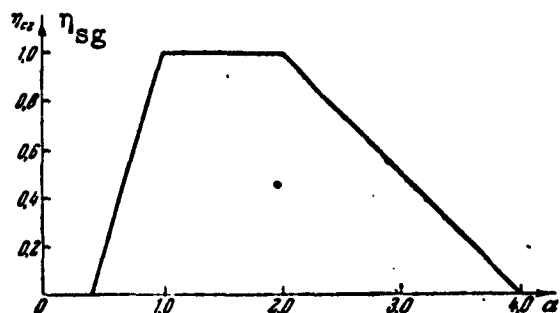


Fig. 80. The dependence of the instantaneous completeness of combustion on the excess-air coefficient α used in the calculations.

the connection between ρ_g and α was assumed to be as follows: $\alpha = 0.0078/\rho_g$. Using this connection between ρ_g and α and the plot of $\eta_{sg} = \eta_{sg}(\alpha)$, we plotted curves of $\rho_g \eta_{sg} = f(t)$. Such curves express, on a certain scale, the dependence of the heat release on the time. These graphical dependences were expanded further in Fourier series, and for each curve the first harmonic of the series, corresponding to the frequency ω of the velocity oscillations, was separated. The separation of this harmonic is physically justified, for acoustic oscillations with frequency ω will be maintained by heat-release oscillations

which occur at the same frequency.

As a result of such a calculation we obtained the amplitude of the sought harmonic of the Fourier series, A_1 , and its phase shift relative to the velocity oscillation, φ_1 :

$$\delta q = \text{const } A_1 \sin(\omega t + \varphi_1) \quad (40.8)$$

(the chemical energy per unit mass of combustible mixture is assumed invariant; it is characterized by the dimensional constant introduced here). Here

$$A_1 = A_1(A_v; \omega), \quad \varphi_1 = \varphi_1(A_v; \omega).$$

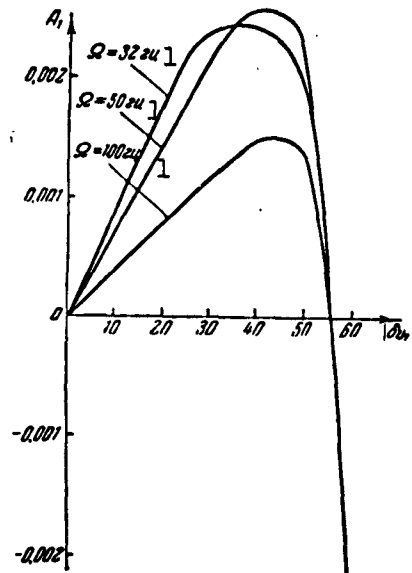


Fig. 81. Variation of the amplitude A_1 as a function of the absolute value of the velocity perturbation ahead of the combustion zone. 1) cps.

Calculations made for the frequencies indicated above and for $A_v = 10, 20, 30, 40, 50, 60$ m/sec have shown that the value of φ_1 fluctuates about π and deviates only slightly from this value. It was therefore possible to assume $\varphi_1 = \pi$. The dependence $A_1 = A_1(A_v; \omega)$ is shown in Fig. 81 for the three frequencies of greatest interest. The

curves calculated for the other frequencies are similar. The most important properties common to all the curves are the following: the curves start from the origin, reach a maximum, and then again cross the abscissa axis somewhere between $|\delta v_1| = A_v = 50$ m/sec and $|\delta v_1| = A_v = 60$ m/sec. To facilitate further calculations, it was decided to neglect the dependence of A_1 on the frequency. This neglect is not too crude, for it can lead only to an insignificant quantitative change in the results and does not change their nature at all. The form of the curve $A_1 = A_1(A_v)$ was approximately represented by the quadratic parabola

$$A_1 = 0.00000293(56 - A_v)A_v. \quad (40.9)$$

Before we proceed to further exposition of the solution of the problem, it is necessary to indicate the reason why in the example under consideration all the $A_1 = A_1(A_v)$ curves cross the abscissa axis at $50 \text{ m/sec} < A_v < 60 \text{ m/sec}$. For small frequencies this effect is natural, for at sufficiently large A_v the mixture becomes periodically excessively rich and excessively lean, which affects the combustion process adversely. For high frequencies such processes of excessive enrichment and excessive leanness do not have a chance to develop, but on the other hand a different process continues to act, being connected with the disruption of combustion when $A_v > v_0$. When the oscillating component of the velocity $|\delta v_1| = A_v$ becomes larger than the average stream velocity v_0 , the flow begins to move in the opposite direction, and the combustion at the stabilizers (which are located near the section 2) ceases, since the fresh mixture no longer reaches them (the combustion that continues on the free surface separating the cold and hot gases plays a relatively small role). This state continues not only during the time of motion of the combustion products in the negative x-axis direction, but also when the flow resumes its positive

direction, until a new mixture begins to flow into the stabilizer zone. After this, the combustion proceeds very poorly for a certain time, inasmuch as the fresh mixture is strongly overenriched, since it crossed the region where the nozzles are located three times (forward crossing, then return of the mixture when the gases flowed in the opposite direction, and finally again crossing during the motion in the positive direction). These circumstances are manifest in the plotting of the curves $\rho_g \eta_{sg} = f(t)$, on the basis of which the values of A_1 were determined. It is precisely these phenomena, which are connected with the jumping of the flame into the region ahead of the stabilizers, which lead to a sharp decrease in A_1 when $A_v > v_0$.

§41. Oscillations in the Absence of Losses at the Ends of the Tube

In the preceding section we obtained nonlinear relations describing the process of vibration combustion in the region σ . Many simplifications have made it possible to reduce the nonlinearity to a single quadratic dependence. The method developed below is suitable also for more complicated dependences, but it is hardly advantageous to make these nonlinearities more precise here, since the process of vibration combustion at large amplitudes of the stream velocity oscillations has still not been well studied. Under these conditions, any kind of refinement which can be introduced at the present time would be unavoidably offset by crude assumptions concerning the character of the combustion process. Therefore the idealization assumed in the preceding section describes only the fundamental and decisive aspects of the investigated phenomenon.

Unlike the preceding chapters, we shall solve the problem in the variables (u, w) in place of $(\delta p, \delta v)$. (The connection between them is given by Formulas (4.5).) The changeover to the variables (u, w) is due to the following considerations. The excitation of the oscillations

is connected, as is well known from the preceding, with the amplitude and the phase of δq relative to the phase of the oscillation of the air masses. In order to follow these parameters in terms of the variables (δp , δv) it would be necessary to follow simultaneously both the phases of δp and δv and their amplitudes, inasmuch as the latter vary with the oscillation frequency (for a specified position of the heat-supply region σ along the tube), in view of the variation of the standing waves of δp and δv . The variables (u , w), independently of the oscillation frequency, have amplitudes that are constant along the flow axis, so that it is possible to trace only the variation of the phase relationships in solving the problem.

In the present section we consider a case where there are no losses at the ends of the tube. As was already mentioned, this corresponds to boundary conditions in the form of nodes of δp or δv . Let us assume, for the sake of being definite, that the system has pressure nodes $\delta p = 0$ on both ends. In the new variable this condition assumes the form

$$u = w. \quad (41.1)$$

Actually, according to (4.5) we have

$$\delta p = \frac{1}{2}(u - w); \quad \delta v = \frac{1}{2} \frac{u + w}{\rho a}, \quad (41.2)$$

from which Condition (41.1) follows immediately.

Let the origin be located on the plane Σ (Fig. 22), and let the introduced variables have values u_0 and w_0 on this plane. If the coordinate of the end of the tube is ξ , then, on the basis of the expressions (4.12) for \underline{u} and \underline{w} and using the condition (41.1), we can write the following equation

$$u_0 \exp\left(-i\omega \frac{\xi}{M+1}\right) = w_0 \exp\left(-i\omega \frac{\xi}{M-1}\right).$$

It is assumed in this equation that $\beta = i\omega$, i.e., that the oscillations have already been established. If we denote the phase shift

between u_0 and w_0 by γ , then the last equation makes it possible to obtain its value

$$\gamma = \frac{2}{M^2 - 1} \omega \xi. \quad (41.3)$$

It is obvious that in the problem under consideration it will be necessary to distinguish between two angles γ , one corresponding to the left side of the discontinuity surface Σ and the other to the

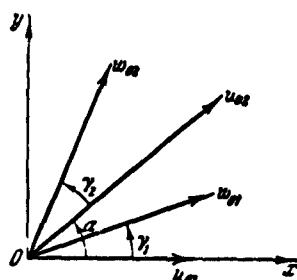


Fig. 82. Diagram showing the angles on the vector diagram of the quantities \vec{u} and \vec{w} .

right side. They will differ in the fact that for the left side this angle will depend on the values of M_1 , ω_1 , and ξ_1 , while for the right side it will depend on M_2 , ω_2 , and ξ_2 .

In order to establish the relative phase shifts between u_0 and w_0 on the left and on the right of Σ it is necessary to introduce still another angle, for example between u_0 for the left side and u_0 for the right side.

We denote this angle by α . Then, aligning u_0 for the left (cold) side of Σ with the abscissa axis, we can draw the vector diagram for u_0 and w_0 as shown in Fig. 82.

The angle α is determined by the properties of the surface Σ , which are expressed by the system (40.1). Using the first equation of this system and the condition that the flow is isentropic in the cold side, $\delta p_1 = \delta p_1 / a_1^2$, we eliminate δp_1 and δp_2 from the two last equations of the system. With the aid of Formulas (41.2) we transform further to the system of variables \underline{u} and \underline{w} . Let the numerical example under consideration be characterized by the following data:

$$\rho_1 = 0.125 \text{ kg} \cdot \text{sec}^2 / \text{m}^4; \quad v_1 = 50 \text{ m/sec}; \quad p_1 = 10,000 \text{ kg/m}^2; \\ T_1 = 300^\circ \text{K}; \quad T_2 = 1800^\circ \text{K}.$$

Then, after carrying out the calculations, the system (40.1) as-

sumes the following form (the subscripts 01 correspond here to the left side of the plane Σ , and 02 corresponds to the right side):

$$\left. \begin{aligned} u_{02} &= 0,583 u_{01} - 0,175 u_{01} + 0,00289 \delta q, \\ u_{02} &= -0,385 u_{01} + 0,792 u_{01} + 0,00603 \delta q. \end{aligned} \right\} \quad (41.4)$$

The system (41.4) relates vector quantities. To change over to scalar relations we project these vector equations on the \underline{x} and \underline{y} axes (Fig. 82). From the four equations obtained by projection we eliminate $\cos \alpha$ and $\sin \alpha$. We recognize further that in accordance with (41.2) in the case of steady-state oscillations the amplitudes \underline{u} and \underline{w} are independent of ξ , i.e., on the basis of the assumed boundary conditions we have $|u_{01}| = |w_{01}|$ and $|u_{02}| = |w_{02}|$. We then obtain after suitable transformations the following scalar relations:

$$\left. \begin{aligned} u_{01} (0,583 \cos \gamma_2 - 0,175 \cos \gamma_1 \cos \gamma_2 + \\ + 0,175 \sin \gamma_1 \sin \gamma_2 + 0,792 \cos \gamma_1 + 0,385) = \\ = (0,00603 - 0,00289 \cos \gamma_2) \delta q_x + 0,00289 \sin \gamma_2 \delta q_y, \\ u_{01} (0,583 \sin \gamma_2 - 0,175 \cos \gamma_1 \sin \gamma_2 - \\ - 0,175 \sin \gamma_1 \cos \gamma_2 - 0,792 \sin \gamma_1) = \\ = (0,00603 - 0,00289 \cos \gamma_2) \delta q_y - 0,00289 \sin \gamma_2 \delta q_x. \end{aligned} \right\} \quad (41.5)$$

We have omitted the absolute-value sign of u_{01} in the last equations, since we have previously introduced the condition that the vector \vec{u}_{01} is always directed along the positive abscissa axis. The quantities δq_x and δq_y occurring in the right halves are projections of δq on the \underline{x} and \underline{y} axes.

Let us now find the values of δq_x and δq_y . In the numerical example considered, the constant appearing in Formula (40.8) is equal to $2.27 \cdot 10^8 \text{ m}^6/\text{kg} \cdot \text{sec}^4$. It was already indicated above that in the calculations it is necessary to include only the first harmonic of the expansion of the function δq in a Fourier series, as given by (40.9). Using Formula (41.2) for δv we can readily obtain the value of $|\delta v_{01}|$, which coincides by definition with A_v of (40.9):

$$|\delta v_{01}| = \frac{1}{2\pi \Omega_1} |u_{01} + w_{01}| = \frac{u_{01}}{2\pi \Omega_1} \left| 1 + \exp i\omega_1 \frac{2\pi \Omega_1}{M} \right|.$$

Using (41.3), we can recast the formula obtained in the form

$$A_v = |\delta v_{01}| = \frac{u_{01}}{2\sigma_1 Q_1} \sqrt{2(1 + \cos \gamma_1)}. \quad (41.6)$$

Including only the first harmonic of the Fourier expansion we rewrite (41.6) on the basis of (40.8) and (40.9), in the form

$$\delta q = 665 \left(56 - \frac{u_{01}}{87} \sqrt{2(1 + \cos \gamma_1)} \right) \frac{u_{01}}{87} \sqrt{2(1 + \cos \gamma_1)}.$$

Here δq is numerically equal to the absolute value of $|\delta \vec{q}|$, but when $A_v > 56$ it can assume negative values. Therefore the absolute-value sign has been left out in the left side of the equation.

The phase of $\delta \vec{q}$ was already determined above (with respect to δv_1), and its value is $\varphi_1 \approx \pi$, i.e., we can assume that the heat supply $\delta \vec{q}$ oscillates in phase opposition with the velocity δv_1 . As follows from the second equation of (41.2), by virtue of the condition $|w| = |u|$ the vector $\delta \vec{v}$ will be directed along the bisector of the angle between \vec{u} and \vec{w} , i.e., in accordance with Fig. 83, it will make an angle $\gamma'_1/2$ with the abscissa axis for the left side of the plane Σ , the abscissa coinciding with the direction of u_{01} . The angle γ'_1 must be distinguished from the angle γ_1 . The latter can have any value, whereas the former does not exceed π in absolute value, since it is used to construct the bisector. The connection between γ_1 and γ'_1 is given by the obvious equation

$$\gamma'_1 = \gamma_1 - 2k\pi,$$

where the integer k is chosen such that

$$-\pi < \gamma'_1 < \pi.$$

Taking the foregoing into account, it is easy to see that the phase angle of $\delta \vec{q}$ with respect to \vec{u}_{01} will be equal to $\gamma'_1/2 + \pi$. Introducing the notation

$$\beta = \pi + \frac{\gamma'_1}{2}, \quad (41.7)$$

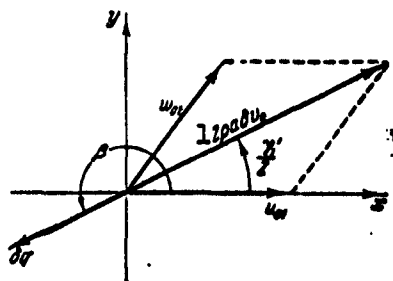


Fig. 83. Determination of the direction of the vector $\vec{\delta q}$ in the absence of losses or delay. 1) Grad v_0 .

we obtain the following obvious equations for the projections of the vector $\vec{\delta q}$ on the coordinate axes:

$$\left. \begin{aligned} \delta q_x &= \delta q \cos \beta, \\ \delta q_y &= \delta q \sin \beta. \end{aligned} \right\} \quad (41.8)$$

In the case under consideration

this yields:

$$\left. \begin{aligned} \delta q_x &= 665 \left(56 - \frac{u_{01}}{87} \sqrt{2(1 + \cos \gamma_1)} \right) \times \\ &\quad \times \frac{u_{01}}{87} \sqrt{2(1 + \cos \gamma_1)} \cos \beta, \\ \delta q_y &= 665 \left(56 - \frac{u_{01}}{87} \sqrt{2(1 + \cos \gamma_1)} \right) \times \\ &\quad \times \frac{u_{01}}{87} \sqrt{2(1 + \cos \gamma_1)} \sin \beta. \end{aligned} \right\} \quad (41.9)$$

Substitution of the obtained values of δq_x and δq_y into the system (41.5) enables us to find the two sought-for quantities, namely the circular oscillation frequency ω_1 and the amplitude u_{01} . These quantities determine completely all the parameters of the oscillating system.

It must be pointed out first of all that a solution of the system will be $u_{01} = 0$, independently of the frequency ω_1 . However, this solution (absence of oscillations) is of no interest.

Assuming that $u_{01} \neq 0$, we divide the left and right halves of both equations in (41.5), taking account of (41.9), by u_{01} . Then the system (41.5) becomes linear and inhomogeneous with respect to the variable u_{01} . The quantity u_{01} is readily separated in each of the two equations of the system. Taking ω_1 as a parameter, we plot curves of u_{01} as a function of ω_1 in accordance with both equations. The points of intersection of these curves yield the sought-for solutions.

We have assumed so far that there is no delay whatever in the combustion zone. Such an assumption is patently unfounded. Indeed, both

the atomization of the fuel by the nozzles and the mixing, evaporation, and ignition require a certain amount of time. This delay causes the phase of the heat supply to be shifted relative to u_{01} not by an angle β , but by a certain angle $\beta + \vartheta$. Inasmuch as the possible values of the delay are unknown, we shall vary ϑ in order to estimate the influence of this factor on the steady-state self-oscillation mode.

Figure 84 shows a diagram of the stability boundaries, constructed on the basis of Eqs. (40.1) by the method described in §19 (the region corresponding to instability is shaded). The diagram shown in Fig. 83 indicates that the angle ϑ which is added to β to take into account the delay must be reckoned from a direction opposing the direction of the vector $\delta\vec{v}$. In constructing the stability boundaries shown in Fig. 84, $\delta\vec{v}$ was directed along the positive ordinate direction, so that the angle ϑ is reckoned from the negative direction of the ordinate axis. Let us denote by ϑ' the angle between the vector $\delta\vec{q}$ and the direction opposite to $\delta\vec{v}$, assuming that the vector $\delta\vec{p}$ has a perfectly defined orientation (to the right). For a specified angle γ_1 we can always readily establish the mutual placement of $\delta\vec{v}$ and $\delta\vec{p}$ and measure the angle ϑ' , which will either coincide with ϑ , or differ from it in sign. On going over from $|\delta v_{01}| < 56$ m/sec to $|\delta v_{01}| > 56$ m/sec, the quantity δq reverses sign, as can be readily seen from (40.8) and (40.9). Inasmuch as in the procedure for calculating the stability boundaries δq can reverse sign only by rotation, it is necessary to add π to the phase of δq in order to obtain the angle ϑ' for $|\delta v_{01}| > 56$ m/sec. Thus, the transition from ϑ to ϑ' , depending on the mutual orientation of $\delta\vec{v}$ and $\delta\vec{p}$, must be carried out in accordance with the following formulas

$$\begin{aligned} \vartheta' &= \vartheta \quad \text{or} \quad \vartheta' = -\vartheta \quad \text{for } |\delta v_{01}| < 56 \text{ m/sec,} \\ \vartheta' &= \pi + \vartheta \quad \text{or} \quad \vartheta' = \pi - \vartheta \quad \text{for } |\delta v_{01}| > 56 \text{ m/sec.} \end{aligned}$$

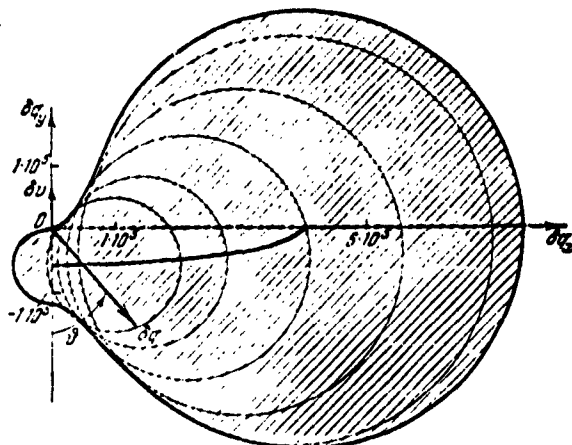


Fig. 84. Stability diagram for the computed example.

For such a rule for measuring the angles ϑ' , the presented diagram of the stability boundaries leads us to expect that the oscillating system will become excited at approximately $-90^\circ < \vartheta' < 140^\circ$.

Similar calculations, carried out in accordance with the procedure described above, confirm this statement. We present below results of such calculations. The table listing the characteristics of the self-oscillations contains, in addition to the frequencies ω_1 and the amplitudes of the oscillations of the velocity $|\delta v_{01}|$ satisfying the system (41.5), also the angles ϑ . All three quantities are plotted as functions of the angle ϑ . The cases for which there exist no solutions of the system (41.5), if we confine ourselves to the first three harmonics, are stricken from the table. All the calculations have been made, for the sake of being specific, for a central position of the plane Σ along the tube: $\xi_1 = -0.5$; $\xi_2 = 0.5$. This position of the heat-supply zone corresponds to the experimental data used below.

One remark must be made with respect to the solutions of the system (41.5) listed in the table. The solutions obtained here should have been analyzed from the point of view of the stability of these periodic solutions, in analogy with the theory of self-oscillating sys-

Characteristics of Self-Oscillations

ϕ	1-я гармоника			2-я гармоника			3-я гармоника		
	ϕ'	ω_1	$ \delta v_{01} $	ϕ'	ω_1	$ \delta v_{01} $	ϕ'	ω_1	$ \delta v_{01} $
0°	—	—	—	—	—	—	0°	12,5	54,7
30°	—	—	—	30°	7,5	51,7	30°	12,5	55,8
60°	*120°	*4,5	*58,5	60°	7,9	49,7	60°	12,5	55,2
90°	*90°	*4,7	*56,8	90°	8,1	52,0	90°	12,4	55,7
120°	*60°	*4,7	*57,0	120°	8,2	47,2	—	—	—
150°	*30°	*5,1	*58,0	—	—	—	*330°	*12,5	*56,2
180°	—	—	—	—	—	—	*0°	*12,5	*56,2
210°	—	—	—	*30°	*7,1	*51,2	*30°	*12,5	*56,2
240°	120°	4,5	51,5	*60°	*7,9	*58,2	*60°	*12,5	*57,0
270°	90°	4,7	53,7	*90°	*8,0	*60,8	*90°	*12,6	*57,0
300°	60°	4,7	53,3	*120°	*8,1	*66,8	—	—	—
330°	30°	5,1	52,0	—	—	—	330°	12,5	54,8

- 1) First harmonic; 2) second harmonic;
3) third harmonic.

tems for which stable and unstable limit cycles are known. However, such an analysis will not be carried out here. In its place we shall present approximate qualitative considerations, which enable us to break down all the solutions into two types. The first type includes the solutions which yield $|\delta v_{01}| < 56$ m/sec, while the second contains those yielding $|\delta v_{01}| > 56$ m/sec.

For the solutions of the first type, as the oscillations develop (as $|\delta v_{01}|$ increases) the vector $\delta \vec{q}$ will at first be directed into the shaded region of the diagram shown in Fig. 84 (this is seen from the values of the angles ψ'), and the system will be unstable (the amplitudes of the oscillations will increase). After going through the value $|\delta v_{01}|_I$, corresponding to the solution, the system becomes stable; this can be seen from the fact that further increase in $|\delta v_{01}|$ will lead more readily to a change in the sign of A_1 , i.e., to a rotation of the vector $\delta \vec{q}$ by π , after which it will be directed toward the unshaded region of Fig. 84. Thus, the solutions of the first type give stable oscillations: when $|\delta v_{01}| < |\delta v_{01}|_I$ the oscillations will increase in amplitude, and when $|\delta v_{01}| > |\delta v_{01}|_I$ they will decrease.

As regards the solutions of the second type, we can advance anal-

ogous considerations, which indicate that in this case stable stationary oscillations are impossible. Indeed, denoting the amplitude of the velocity oscillations for the solution of the second type by $|\delta v_{01}|_{II}$, we can readily visualize that if the angle ϑ when $|\delta v_{01}| = |\delta v_{01}|_{II}$ is such that the vector $\delta \vec{q}$ is directed toward the shaded region on Fig. 84, then when $|\delta v_{01}| < 56 \text{ m/sec} < |\delta v_{01}|_{II}$ it will certainly be directed toward the unshaded part of the diagram. This means that the amplitudes of δv_{01} will consequently decrease with time and the self-oscillations will stop. Therefore solutions of the second type are designated in the table by asterisks and will be disregarded in the analysis that follows.

The table, like the stability-boundary diagram, shows clearly that the value of the angle ϑ (i.e., the delay) can play an important role. Depending on ϑ , some particular harmonic will become excited, or else excitation becomes impossible. Incidentally, this result was obvious. The most interesting circumstance is that independently of the value of the angle ϑ , the amplitude of the oscillations can be regarded as practically constant in those cases when self-excitation sets in. At the same time, the amplitude of the velocity oscillation exceeds somewhat the average stream velocity $v_0 = 50 \text{ m/sec}$. Consequently, in steady-state self-oscillations a periodic jumping of the flame into the region ahead of the stabilizer should be observed.

This effect was observed many times in the experiments. In particular, in special experiments, by installing quartz windows in the tube walls and taking high-speed motion pictures of the vibration combustion, it was possible to register the jump of the flame upstream. Under normal combustion modes, the lateral surface of the stabilizer appeared to be dark on the photographs. In the case of developing self-oscillations, it was covered periodically (at the same frequency as

the observed oscillations) by the flame that had jumped into the zone ahead of the stabilizers.

It is even more interesting to compare the amplitudes of the pressure oscillations obtained by calculation with those observed in experiment, inasmuch as pressure oscillations are easy to measure. Let us estimate the theoretical value of the pressure oscillation amplitude at the section where a pressure antinode is located:

$$|\delta p|_{\max} = \left| \frac{u - w}{2} \right|_{\max}.$$

Taking into account the boundary condition $|\vec{u}| = |\vec{w}|$, this yields $|\delta p|_{\max} = |\vec{u}|$. The values of $u_{01} = |\vec{u}| = |\delta p|_{\max}$ for the solutions of the first type, corresponding to the first, second, and third harmonics of the oscillating system, are listed in the following table:

Table of Values of $|\delta p|_{\max}$ kg/m²

ϕ	0°	30°	60°	90°	120°	150°	180°	210°	240°	270°	300°	330°
1-я гарм.	—	—	—	—	—	—	—	—	3350	3150	3180	2650
2-я гарм.	—	2950	3550	3950	4250	—	—	—	—	—	—	—
3-я гарм.	2400	2450	2420	2445	—	—	—	—	—	—	—	2400

- 1) First harmonic; 2) second harmonic;
3) third harmonic.

In the experiments set up in order to compare the theoretically obtained values with those recorded experimentally, the values of p_1 , v_0 , etc. assumed in the calculations were obtained. In numerous experiments, which differed in the organization of the combustion process, the pressure-oscillation amplitudes ahead of the combustion zone were registered. As the self-oscillations developed, these amplitudes had values ranging between 2200 and 3500 kg/m². The slight reduction in the values of $|\delta p|$ compared with the theoretical calculations are due, in particular, to the fact that the pressure transducers were not al-

ways located in the pressure antinode, and of course, to the crude idealization of the process in the theoretical scheme.

However, the agreement between the calculated and experimental data must be recognized as being quite satisfactory. It offers evidence that in the assumed crude scheme of the phenomenon account was taken of the most essential nonlinear properties of the heat-supply zone.

§42. Self-Oscillations in the Presence of Losses at the Ends of the Tube

Unlike the problem considered in the preceding section, the flux of acoustic energy radiated by the heat-supply region σ will not be equal to the flux of energy of the same type returning into the region σ after reflection of the acoustic waves from the ends of the tube. Therefore, when averaged over the oscillation cycle, a flow of acoustic energy will be observed from the region σ to the ends of the tube. Analytically this is expressed by the fact that the amplitudes \underline{u} and \underline{w} cease to be equal to each other.

In §30 formulas were given for an account of the losses connected with the radiation of acoustic energy from the open ends of the tube. We introduced there, in particular, a coefficient ζ (defined by the equation $w = \zeta u$), the use of which in place of the impedance \underline{z} is advantageous when solving problems in the coordinates (u, w) . When acoustic energy is radiated into the external space, its average flux is directed toward the positive \underline{x} axis in the hot portion of the tube and in the opposite direction in the cold portion of the tube. Therefore, recalling the expression for the acoustic energy flux (30.7), we have $|\zeta_1| > 1$ and $|\zeta_2| < 1$.

Having made these introductory remarks, we can easily construct a calculation procedure for the case considered in the present section. The course of the problem solution differs little from that described in detail in the preceding section. All the differences that must be

borne in mind are the consequences of the new boundary conditions.

When determining the angles γ_1 and γ_2 between the vectors u_{01} and w_{01} and u_{02} and w_{02} one cannot use Formula (41.3), which is obtained under the assumption that \underline{u} and \underline{w} coincide at the ends of the tube. The equation

$$w = \zeta u \quad (42.1)$$

shows that they are, generally speaking, shifted by a certain angle θ , which can be determined from the relation (30.5):

$$\theta = \text{arctg} \left(-\frac{2x}{1-r^2-x^2} \right),$$

where \underline{r} and \underline{x} are the real and imaginary parts of the impedance $z = r + ix$. It must be borne in mind here that the sign of the numerator of the expression on the right side, proportional to $\sin \theta$, determines the quadrant in which the angle θ is located.

Thus, in place of the formula (41.3), it is necessary to use the formula

$$\gamma = \frac{2}{M^2 - 1} \omega \xi + \theta. \quad (42.2)$$

In precisely the same manner, on going over to the equations that do not contain the angle α and the quantities w_{01} , u_{02} , w_{02} , it is necessary to use in place of the conditions $|u_{01}| = |w_{01}|$ and $|u_{02}| = |w_{02}|$ the consequences of the new boundary conditions of the type (42.1):

$$\left. \begin{aligned} |w_{01}| &= |\zeta_1| |u_{01}|, \\ |w_{02}| &= |\zeta_2| |u_{02}|, \end{aligned} \right\} \quad (42.3)$$

with the quantity $|\zeta|$ readily obtained from Formula (30.6).

In addition, the phase angle δq relative to u_{01} in the absence of delay ($\vartheta = 0$), which was denoted above by β , will no longer be equal to $\pi + \gamma'_1/2$, inasmuch as the vector $\delta \vec{v}$ will not lie on the bisector of the angle γ'_1 . It is seen from Fig. 85 that now $\beta = \pi + \gamma''_1$, where

$$\gamma'_1 = \text{arctg} \frac{|\zeta_1| \sin \gamma_1}{1 + |\zeta_1| \cos \gamma_1}.$$

When $|\zeta_1| = 1$ (absence of losses at the ends) the angle γ''_1 coincides, as expected, with $\gamma'_1/2$.

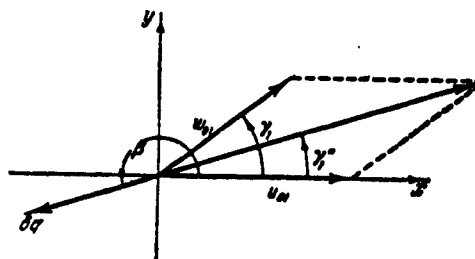


Fig. 85. Determination of the direction of the vector $\delta \vec{q}$ in the presence of losses.

Leaving out the cumbersome manipulations, we write out the final system of equations corresponding to the system (41.5) and considering Eqs. (41.6), (42.2), and (41.9) for the numerical example under consideration:

$$\left. \begin{aligned} u_{01} [0,000508 |\zeta_2| (1 + \cos \gamma_1) \cos (\gamma_2 + \gamma'_1) - \\ - 0,00106 (1 + \cos \gamma_1) \cos \gamma'_1] = -0,385 + \\ + 0,792 |\zeta_1| \cos \gamma_1 - 2,58 \sqrt{2(1 + \cos \gamma_1)} \cos \gamma'_1 - \\ - 0,583 |\zeta_2| \cos \gamma_2 + 0,175 |\zeta_1| |\zeta_2| \cos (\gamma_1 + \gamma_2) + \\ + 1,24 |\zeta_2| \sqrt{2(1 + \cos \gamma_1)} \cos (\gamma_2 + \gamma'_1), \\ u_{01} [0,000508 |\zeta_2| (1 + \cos \gamma_1) \sin (\gamma_2 + \gamma'_1) - \\ - 0,00106 (1 + \cos \gamma_1) \sin \gamma'_1] = 0,792 |\zeta_1| \sin \gamma_1 - \\ - 2,58 \sqrt{2(1 + \cos \gamma_1)} \sin \gamma'_1 - 0,583 |\zeta_2| \sin \gamma_2 + \\ + 0,175 |\zeta_1| |\zeta_2| \sin (\gamma_1 + \gamma_2) + \\ + 1,24 |\zeta_2| \sqrt{2(1 + \cos \gamma_1)} \sin (\gamma_2 + \gamma'_1). \end{aligned} \right\} \quad (42.4)$$

The system presented here was solved graphically by plotting the curves $u_{01} = f_1(\omega_1)$ and $u_{01} = f_2(\omega_1)$ in analogy with what was done in the preceding section. The calculations were carried out for different ratios d/L (d is the tube diameter and L its length) which, as can be seen from Formula (30.8), determine the losses to radiation.

The results of the calculations for the first three harmonics are

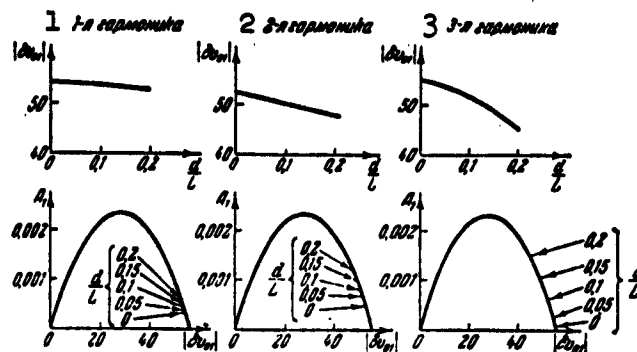


Fig. 86. Amplitudes of self-oscillations $|\delta v_{01}|$ for different losses of energy to radiation (parameter d/L). 1) First harmonic; 2) second harmonic; 3) third harmonic.

shown in Fig. 86. The influence of the losses on the characteristics of the self-oscillations is seen most clearly with the third harmonic as an example, inasmuch as the losses increase in proportion to ω^2 . The values of the angles ϑ for which the calculation was carried out were as follows: for the first harmonic $\vartheta = 270^\circ$, for the second $\vartheta = 90^\circ$, and for the third $\vartheta = 0^\circ$. These angles correspond to the self-excitation regions obtained in the preceding section. The oscillation frequencies are not presented here. They hardly change after the losses at the ends are taken into account; only a slight decrease in the self-oscillation frequencies is observed.

In the upper part of Fig. 86 is shown the variation of the velocity-oscillation amplitudes $|\delta v_{01}| = A_v$ as a function of d/L . As can be seen from the course of the curves, an increase in d/L (an increase in the losses) is accompanied by a certain decrease in the amplitudes of the stationary velocity oscillations.

In the lower part of Fig. 86 are shown plots of the dependence $A_1 = f(A_v)$ assumed in the calculations, on which are marked curves corresponding to the obtained velocity-oscillation amplitudes. These plots show that whereas in the absence of losses ($d/L = 0$) the value of A_1 ,

and consequently also of the oscillating component of the heat release δq , is close to zero, in the presence of losses ($d/L \neq 0$) it increases rapidly, particularly for the third harmonic. This result is perfectly natural, since for the scheme assumed for the process in the region σ only a sufficiently large oscillating component of the heat supply is capable of replenishing the losses of the acoustic energy at the ends of the tube.

It is interesting to note that at sufficiently large losses the amplitude of the oscillating component of the velocity $|\delta v_{01}|$ becomes smaller than $v_0 = 50$ m/sec, i.e., the jumping of the flame upstream, referred to above, may not be observed. To be sure, in order for this to occur, the tube must be sufficiently "short."

It follows therefore that in certain special cases it is possible to obtain vibration combustion without jumping of the flame, by increasing the losses.

At sufficiently high losses, excitation of a certain specified harmonic may turn out to be totally impossible. In the numerical example under consideration this corresponds to the fact that the range of values of ϑ for which excitation of self-oscillation with increasing parameter d/L is possible becomes narrower. Thus, for the third harmonic of the system, excitation was possible for $d/L = 0$ (at the values of ϑ assumed in the calculation) for $\vartheta = 330^\circ, 0^\circ, 30^\circ, 60^\circ$, and 90° . For $d/L = 0.2$, self-oscillation becomes possible only for $\vartheta = 0^\circ$ and 30° , while for $\vartheta = 330^\circ, 60^\circ$, and 90° the system (42.4) has no solutions.

§43. Applicability of the Methods Developed to Other Cases

The results of the theoretical calculations given in the present chapter are in good agreement with the experimental data. In particular, the expected orders of magnitudes of the pressure and velocity

oscillation amplitudes are well confirmed. However, inasmuch as we have considered only an example of the calculations, it remains unclear whether an analogous method can be used also in other cases.

Let us consider therefore the general scheme of the calculation method used in the preceding sections. It reduces, briefly, to the following:

1. It is assumed that the essential nonlinearity in the self-oscillations of the type under consideration is some regularity in the combustion process.

2. On the basis of the assumption made, the oscillations on the left and on the right of the heat-supply zone are described by linear equations. This finds its expression in the fact that to connect the oscillations on the left and on the right of the surface Σ with the oscillations at the end of the tubes one makes use of the formulas obtained in the second chapter.

3. In the idealization of the nonstationary-combustion process, the properties of the surface Σ are also written in the form of linear relations, in which is included as small a number as possible of the simpler nonlinear expressions which represent the principal nonlinear property of the heat-supply zone.

4. An isolated analysis is made of the idealized heat-supply zone. This analysis reduces to the fact that one assumes the oscillations ahead of the heat-supply zone to be specified, and the frequency and amplitude of the oscillations are varied. One determines by calculation the properties of the heat-supply zones (the quantities on which \bar{Q}^* , \bar{U}_1 , and \bar{P}_x depend) as functions of the frequency and amplitude of the oscillations. The regularities obtained are plotted as functions of the time, are expanded in a Fourier series, and then only the first harmonic (which coincides with the specified oscillation frequency) is

retained.

5. Using the obtained connection between the process in the heat-supply zone and the oscillations of the medium in the vicinity of this zone, on the one hand, and the formulas of Chapter 2 and the boundary conditions on the other, one seeks the frequencies and amplitudes of the oscillations simultaneously satisfying all these relations.

The solutions obtained are analyzed from the point of view of the stability of the obtained periodic modes.

From the brief computation scheme given here it is seen that all its items are suitable for any process in the heat-supply zone and are not connected at all with the specific type of combustion considered above.

If instead of investigating a process in which the main mechanism of excitation and maintenance of the oscillations is the connection between the mixture production and combustion we consider a different type of combustion, then all that changes is the actual content of item 3 of the foregoing computation scheme. In all other respects the entire course of the calculations can be retained. It is merely necessary to add that, depending on how complicated the introduced nonlinear relation may be, the volume of the computational work may vary. Therefore, as already mentioned, the nonlinear relation chosen should be as simple as possible.

In simplifying the nonlinear properties of the plane Σ , it is necessary to take account of the fact that the basic factor is not a detailed representation of the nonlinear dependence of the essential property of Σ (in the preceding example, δq) on the oscillation amplitude (in the preceding example, on A_v), but the retention of the characteristic points corresponding to the passage of this nonlinear quantity (for example, δq) through the zeros. In this case all the prin-

cipal features of the stationary self-oscillations are retained, and the distortions are introduced by relatively minor regularities of the transient modes from the small oscillations to the steady-state self-oscillations. These transient modes are not considered here at all. It is precisely these considerations that enabled us to replace the relatively complicated curves shown in Fig. 81 by a quadratic parabola which is common to all the curves and passes through the points $\delta v_1 = 0$ and $\delta v_1 = 56$ m/sec on the abscissa.

To confirm the foregoing, we could consider here also other cases of vibration combustion, for example the excitation of oscillations in a stream of a previously prepared combustible mixture ignited by some igniting device — even a gas burner (see §37). In this case, in the case of small amplitudes of the stream-velocity oscillations, the flame surface will also oscillate without detaching itself from the igniting source. These oscillations of the flame front can lead to instability, owing to the periodic variation of the volume $V_g(t)$ and the associated occurrence of a nonvanishing perturbation of the propagation velocity of the effective plane flame front δU . In this case the connection between the δv and δU oscillations will be linear. An increase in the amplitude of the velocity oscillation δv causes in final analysis the volumes of the hot gases to start to break away periodically from the igniting source and these breakaways make it necessary to change the mathematical description of the combustion process. The perturbation δU ceases to be a linear function of δv , for after detachment of the hot region from the ignition source the combustion process in it ceases to depend on δv . Later on, under even stronger velocity oscillations, the jumping of the flame into the region lying ahead of the burner sets in, and this complicates the picture still further. Thus, in the example considered, the essential nonlinearities will be the

properties of the combustion zone connected with the detachment of the hot regions from the ignition source and the jumping of the flame upstream. Mathematical formulation of these nonlinear properties entails no difficulty, once a particular theoretical scheme of the phenomenon is constructed.

As a result of the large number of actually existing feedback mechanisms, a detailed analysis of the example considered here is meaningless, since in final analysis this would be merely one more particular case, which would add little that is essential to the results obtained in the present chapter.

Manu-
script
Page
No.

[List of Transliterated Symbols]

357	n = n = normal'nyy = normal
361	cr = sg = sgoraniye = combustion
364	r = g = goryucheye = fuel

Chapter 9

VIBRATION COMBUSTION

§44. Stages of Development of the Vibration Combustion Process

It was already indicated above that vibration combustion is a typical self-oscillating process. At the instant when the necessary conditions have arisen, the amplitudes of the oscillations execute a sharp and practically instantaneous jump. The rapid onset of vibration combustion (it usually reaches its amplitude within a time equal to two or three oscillation cycles) greatly hinders the study of the stages of development of this process. In some cases, however, in experiments on special setups of the laboratory type, it is possible to trace how by gradual variation of the experimental conditions (the excess-air coefficient, the position of a movable stabilizer along the stream axis, etc.) one form of steady-state self-oscillations is replaced by a different form. It is usually possible to notice at the same time that different forms of self-oscillations correspond to different amplitudes.

It is frequently possible to observe how the initially random fluctuations of pressure, after a barely noticeable change in the experimental conditions, acquire clearly pronounced properties of self-oscillations (a clear-cut and constant frequency with constant amplitude), although the amplitude of the oscillations does not increase noticeably. With further (also barely noticeable) change in the experimental conditions, very powerful self-oscillations arise. This indicates that small and continuous changes in the experimental conditions frequently correspond not merely to a transition from quiet combustion

to powerful self-oscillations, as is illustrated in Fig. 76, but a gradual transition from quiet (more accurately, random) combustion to self-oscillations of one type, and then from these self-oscillations to others.

On the basis of the foregoing we can consider these steps as stages in the development of the vibration combustion process. Of course, the question of whether these stages (which are connected with the changes in the experimental conditions) coincide with the development of the vibration combustion process in time (without a change in the experimental conditions during that time) still remains open. That these two phenomena are to a certain degree similar is indicated by the following experimental fact. By producing self-oscillations of small amplitude, the experimenter can sometimes observe a spontaneous transition of the system to the next stage, i.e., to powerful self-oscillations.

A typical pattern of the succession of the three foregoing combustion stages can be readily traced by using as an example the development in vibration combustion of a previously prepared homogeneous mixture behind a conical stabilizer mounted in a tube.

First stage. The peculiarities of this type of combustion can be seen in high-speed motion-picture photographs. Although the surface of the flame behind the stabilizer has a configuration that varies from frame to frame, on the average it gives the usual approximately conical combustion surface characteristic of a point source of ignition. The variation of the flame-front configuration from frame to frame indicates that instability can set in as a result of the mobility of the flame front. No definite regularity is observed in this form of combustion. The amplitude of the pressure fluctuations is insignificant.

Second stage. This is the transition stage toward the powerful

self-oscillations. It is characterized by a clearly pronounced periodicity of the combustion and sufficiently large oscillation amplitudes. The transition from the first stage to the second stage occurs practically instantaneously.

Depending on the experimental conditions (in particular, on the type of ignition source), the second stage can have its own peculiarities, even to the extent of having different feedback mechanisms. In the case under consideration the principal mechanism whereby the oscillations are maintained is the periodic detachment of the hot regions from the stabilizer, similar to the detachment of vortices behind a poorly streamlined body. This phenomenon was already described above (see §36, Fig. 72).

Third stage. Unlike the second stage, which has some form of dependence on the specific experimental conditions, the third stage usually manifests itself outwardly in identical fashion — the jumping of the flame upstream into regions lying ahead of the stabilizer (in those cases when the combustion occurs in the trail behind the igniting source).

In Chapter 8 it was shown by means of a particular example that as the oscillations develop they can grow to the stage of the jumping of the flame upstream, and this jump causes the changes in the combustion process, which can be regarded as the cause of appearance of essential nonlinearities limiting the oscillation amplitudes in the equations describing the vibration combustion.

It was indicated in the same chapter that this conclusion can be extended also to include other cases of excitation of the oscillating system under consideration, and along with the jumping of the flame upstream it was disclosed that the periodic detachment of the flame from the ignition sources that maintain it is of great significance.

The fact that periodic jumping of the flame upstream and the usually corresponding detachment of the flame from the ignition source (which occurs a half cycle later) leads to a sharp change in the character of the combustion, causing a limitation of the oscillation amplitude, explains why the third stage of the vibration combustion has one and the same character regardless of the prior "history" of development of the oscillation process.

Oscillations of this type are maintained by a mechanism which differs from those described above. Here one can no longer speak of vortex formation behind the stabilizer or of oscillations of the flame front as being the principal causes whereby the vibration character of the combustion is maintained. It is probable that the very concept of "flame front" which is understood as a certain surface of sufficiently small thickness is not accurate here. The combustion has here more likely a volumetric nature owing to the strong turbulization.

Combustion of this type, recorded by high-speed motion picture photography, is shown in Fig. 87. It can be described schematically in the following fashion. A particle of hot gas, which previously has jumped upstream, acquires during its reverse motion a high velocity, and the zone separating the consumed and the unconsumed mixture is carried past the stabilizer, sometimes not leaving a visible hot trail behind it. But soon a flame is produced behind the stabilizer; the flame sometimes develops in the form of a string, which begins to glow in the region of the aerodynamic shadow (wake) behind the stabilizer. The strongly elongated and relatively thin region of the resultant flame begins to propagate in radial directions and, by the instant when the flame fills the entire cross section of the tube, a jump of the flame occurs again.

The jump of the flame is of course not an obligatory form of the

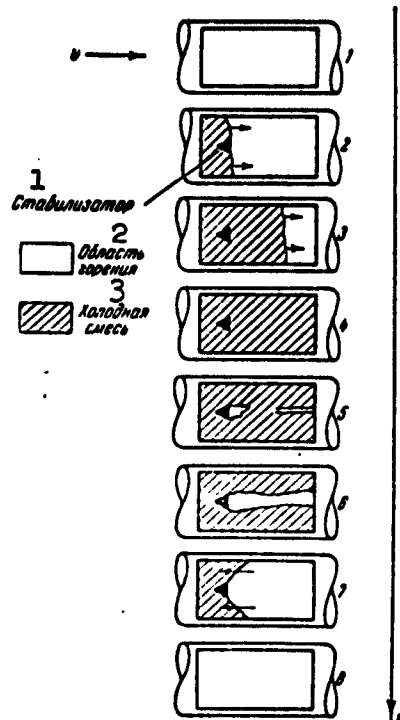


Fig. 87. Diagram of the combustion process in the case of intense "jumping" of the flame into the region lying ahead of the stabilizer. 1) Stabilizer; 2) combustion region; 3) cold mixture.

most developed self-oscillations. In many cases it simply cannot occur: for example, in the combustion of pulverized coal in a precombustion chamber, the flame has nowhere to "jump," since the combustion occurs in the immediate vicinity of the closed end of the precombustion chamber. The statement made above had a bearing only on combustion in tubes with stabilizers. However, the particular case described is important in the respect that it indicates the possibility of existence of stages of development of vibration combustion, each of which can have its own special mechanism for the excitation and maintenance of the oscillations. This indicates that it is completely hopeless to

try and find some one mechanism or one cause of occurrence of vibration combustion. Not only different laboratory installations, engines, or furnaces, but even one and the same simplest laboratory setup is capable, during a single startup, to permit different mechanisms of vibration combustion to manifest themselves.

In conclusion, a few words must be said concerning a question which is frequently raised by persons who are not sufficiently well acquainted with oscillation theory. We are speaking here of the so-called "first cause" of the occurrence of self-oscillations. If we consider modes of soft excitation of self-oscillations (i.e., self-oscillations that arise because the initial stationary mode is unstable

with respect to infinitesimally small excitations), then the very formulation of the question of the "first cause" or "first jolt" is absurd. The point is that in the case of instability of a stationary mode with respect to small perturbations, any perturbation, no matter how small, of this stationary mode resulting from any cause (and in a real stream there is a tremendous number of such causes) will lead to the development of instability and to a changeover to self-oscillations whose character does not depend in any way on the type of the initial perturbation. To raise the question of the "first cause" is in this case just as absurd as to seek the main reason why a pencil, when stood on its sharp point, immediately falls down.

However, the searches for the "first cause" are not so absurd if they are given a different meaning. Let us raise the question of feedback mechanisms that can manifest themselves even in the case of infinitesimally small perturbations of the stream. Apparently not all the feedback mechanisms considered in Chapter 7 have this property. It is not clear, for example, whether vortex formation behind a stabilizer or in the cold part of the stream will extend to acoustic frequencies at acoustic-oscillation amplitudes that are arbitrarily small. It is more likely that this is not the case, or else the detachment of the vortices behind the stabilizer would retune themselves to the acoustic frequencies even without combustion. One can therefore speak of feedback mechanisms that are effective from the very beginning (these include, for example, the mechanism connected with wave formation on the flame front), and of mechanisms which can manifest themselves only after the acoustic oscillations have reached a certain magnitude. If we define thus the "first cause" not as the first jolt, but as an aggregate of feedback mechanisms capable of acting during the initial stages of the development of the vibration combustion, then this

question becomes a valid one. This consideration illustrates also that the question concerning the stages of development of vibration combustion is not far-fetched.

§45. Hypothesis Concerning the Maximum Acoustic Energy Radiated by the Heat-Supply Region

The large number of feedback mechanisms described in Chapter 7 and the possibility of transition from one excitation mechanism to another in a single experiment, to which we referred in the preceding section, raise the question of the laws that govern the mechanism of excitation and maintenance of oscillations in each specific case.

It is quite clear that the experimental conditions define a certain set of probable feedback mechanisms. Thus, if combustion takes place in a homogeneous and previously prepared mixture, then the mechanisms connected with mixture production cannot occur. However, such limitations (if they do exist) nevertheless leave a sufficiently large number of probable feedback mechanisms.

Moreover, even if the expected excitation mechanism is known, then the question of what the amplitude and phase relations between the oscillations of the gas masses and the combustion process will be remains open almost always. As a rule, these relations are not amenable to calculation. Indeed, it is very difficult, for example, to calculate the phase of the detachment of a vortex in the supply channel or its dimensions. Whereas it may be possible, for example, to calculate the phase of the oscillation of a mixture composition at the instant when the mixture arrives at the stabilizers, an evaluation of all the numerous factors on which the ignition of this mixture depends is then impossible. It is impossible to calculate all the induction periods, to predict all the modifications in the flame-surface configurations, etc. Thus, there are serious difficulties encountered on the way to

predicting the probability of the vibration modes of engine or combustion-chamber operation.

On the other hand, however, the multiplicity of probable feedback mechanisms and the large number of "degrees of freedom" of the combustion process (including the possibility of excitation of oscillations with different frequencies), making feasible the realization of a great variety of ratios of standing-wave amplitudes and phase shifts between the gas-oscillation process and the combustion, may facilitate the problem of forecasting the vibration modes and may point to effective measures toward their suppression. The point is that both indicated circumstances (the large number of possible feedback mechanisms and the great freedom in the realization of the amplitude and phase relationships) allow the oscillating system to choose, as it were, the self-excitation mechanism and the amplitude-phase relationships.

In this connection we can advance the following hypothesis: during the process of development of vibration combustion, the oscillating system strives to realize such an excitation mechanism and such amplitude and phase relationships as would yield in specific experimental conditions a maximum value of acoustic energy \bar{A}_Σ radiated from the combustion region.

The hypothesis formulated here can be explained in the following manner. Assume that there exists simultaneously a set of various possible excitation mechanisms and each of them has a certain freedom in the realization of the amplitude-phase relationships. Then the mechanism which under the specific experimental conditions gives the largest work \bar{A}_Σ per second will overtake during its development the remaining ones and will ultimately become the decisive excitation mechanism for a given specific case.

The foregoing explanation makes it possible to point to one essen-

tial detail: it is obvious that we are dealing here with the selection of excitation mechanisms in accordance with the attribute $\bar{A}_\Sigma = \bar{A}_{\max}$ during the course of buildup of the oscillations. When the oscillations settle down, the flux of acoustic energy \bar{A}_Σ is determined by the losses. It is assumed here that by the instant when the oscillating process which yields under the experimental conditions $\bar{A}_\Sigma = \bar{A}_{\max}$ has already become established, it has also succeeded in overtaking in development the other possible processes.

It must be noted that the hypothesis presupposes the absence (or smallness) of acoustic-energy losses. If the losses cannot be neglected, then the formulation presented above must be refined. In the presence of losses we cannot merely speak of the largest energy flux \bar{A}_Σ generated in the heat-supply region, and it is necessary to subtract from this flux the indicated losses. In this connection we obtain the following refined formulation of the hypothesis concerning the maximum acoustic energy: the oscillating system strives to realize that process which, under specific experimental conditions, yields a maximum value of acoustic energy radiated by the combustion region minus the losses.

The foregoing refinement is absolutely necessary, for otherwise it would follow from the assumption that the oscillating system strives to realize the condition $\bar{A}_\Sigma = \bar{A}_{\max}$ that the system should strive toward a process with maximum losses, inasmuch as the maximum losses correspond to the largest value of \bar{A}_Σ in the steady-state oscillation mode. Below, in the consideration of certain theoretical premises and in the analysis of the experimental data, the foregoing refinement will not be used, since it is assumed everywhere that the losses are relatively small.

Let us consider certain consequences of the hypothesis of maximum

energy \bar{A}_2 . Let the characteristic of the combustion process (the values of δE and δX) be a function of one and the same variable, capable of varying in phase and in amplitude, for example the heat supply \bar{Q}^* or the effective flame propagation velocity \bar{U}_1 , or some other quantity. We can then, in order not to be tied down to a specific dependence of δE and δX on one of these quantities, introduce, as in §19, the variable \bar{Y} , writing down the conditions relating the oscillations to the left and to the right of the heat-supply zone in the form of Eqs. (19.6):

$$\left. \begin{aligned} \bar{v}_2 &= a_{11}\bar{v}_1 + a_{12}\bar{p}_1 + a_{13}\bar{Y}, \\ \bar{p}_2 &= a_{21}\bar{v}_1 + a_{22}\bar{p}_1 + a_{23}\bar{Y}. \end{aligned} \right\} \quad (45.1)$$

If we reduce these relationships to the canonical form (17.1), then they can be written in the following fashion:

$$\left. \begin{aligned} \delta E &= a_{11}\bar{v}_1 + a_{12}\bar{p}_1 + a_{13}\bar{Y}, \\ \delta X &= a_{21}\bar{v}_1 + a_{22}\bar{p}_1 + a_{23}\bar{Y}. \end{aligned} \right\} \quad (45.2)$$

In this notation, a transition was made from complex variables to vector variables, and the similarly designated real coefficients of the transformations (45.1) and (45.2) are, of course, different from one another.

The connection between the coefficients of the transformations (45.1) and (45.2) is quite simple and is determined during the process of numerical reduction of Eqs. (45.1) to canonical form. In the present section we shall use henceforth the transformation coefficients (45.2).

Let the phase shift between \vec{v}_1 and \vec{p}_1 be $\pi/2$, i.e., $\vec{v}_1 \vec{p}_1 = 0$. This assumption corresponds to the case when the average flux of acoustic energy in the cold part of the flow is equal to zero (for example, when the scheme of the process is as shown in Fig. 31).

Let us determine for this case, using Formulas (19.2) and (45.2), the flux of acoustic energy radiated by the heat-supply zone:

$$\bar{A}_2 = \frac{1}{2} (\bar{p}_1 \delta E + \bar{v}_1 \delta X + \delta E \delta X) = \frac{1}{2} (a_{11}(1 + a_{22})\bar{p}_1^2 +$$

$$+a_{11}(1+a_{11})\bar{v}_1^2 + [a_{12}(1+a_{22})+a_{12}a_{22}]\bar{p}_1\bar{Y} + \\ + [a_{22}(1+a_{11})+a_{22}a_{12}]\bar{v}_1\bar{Y} + a_{12}a_{22}\bar{Y}^2). \quad (45.3)$$

Inasmuch as the phase shift between \bar{p}_1 and \bar{v}_1 is equal to $\pi/2$, it is convenient to change over to a diagram of the same type as in Fig.

26. For the case under consideration it is shown in Fig. 88. If we denote the projections of the vector \vec{Y} on the \underline{x} and \underline{y} axes by \bar{Y}_x and \bar{Y}_y , then the expression for \bar{A}_Σ (45.3) assumes the following form:

$$\bar{A}_\Sigma = \frac{1}{2} \{ a_{12}(1+a_{22})\bar{p}_1^2 + a_{11}(1+a_{11})\bar{v}_1^2 + \\ + [a_{12}(1+a_{22})+a_{12}a_{22}]\bar{p}_1\bar{Y}_x + [a_{22}(1+a_{11})+a_{22}a_{12}]\bar{v}_1\bar{Y}_y + \\ + a_{12}a_{22}(\bar{Y}_x^2 + \bar{Y}_y^2) \}. \quad (45.4)$$

Here \bar{p}_1 , \bar{v}_1 , \bar{Y}_x , and \bar{Y}_y are scalar (real) quantities; the first two are the absolute values of the vectors \vec{p}_1 and \vec{v}_1 , inasmuch as these vectors are by definition always aligned with the \underline{x} and \underline{y} axes.

We now make the simplest assumption that \vec{Y}^2 is completely independent of \vec{p}_1 and \vec{v}_1 , and find the values of \vec{Y} that correspond to the maximum of \bar{A}_Σ . For this purpose we equate to zero the derivatives $\partial\bar{A}_\Sigma/\partial\bar{Y}_x$ and $\partial\bar{A}_\Sigma/\partial\bar{Y}_y$.

Simple calculations yield the sought-for values $\bar{Y}_x = \bar{Y}_{x0}$, $\bar{Y}_y = \bar{Y}_{y0}$ corresponding to $\bar{A}_\Sigma = \bar{A}_{\max}$:

$$\left. \begin{aligned} \bar{Y}_{x0} &= -\frac{a_{12}(1+a_{22})+a_{12}a_{22}}{2a_{12}a_{22}}\bar{p}_1, \\ \bar{Y}_{y0} &= -\frac{a_{22}(1+a_{11})+a_{22}a_{12}}{2a_{12}a_{22}}\bar{v}_1. \end{aligned} \right\} \quad (45.5)$$

Formulas (45.5) indicate that if the assumption that $\bar{A}_\Sigma = \bar{A}_{\max}$ is valid, then the oscillating system will always strive to have \vec{Y} in one quadrant of the diagram shown in Fig. 88. Indeed, inasmuch as \bar{p}_1 and \bar{v}_1 are by definition always positive, then independently of their value the signs of \bar{Y}_{x0} and \bar{Y}_{y0} are completely determined by the expressions preceding \bar{p}_1 and \bar{v}_1 , and consequently this determines the quadrant in which the vector \vec{Y} is located. The numerical calculations show that for $\vec{Y} = \vec{Q}^*$ and $\vec{Y} = \vec{U}_{\text{sgor}}$ (where \vec{U}_{sgor} is the dimensionless variation

$$+a_{21}(1+a_{11})\bar{v}_1^2 + [a_{12}(1+a_{22})+a_{12}a_{22}]\bar{p}_1\bar{Y} + \\ + [a_{22}(1+a_{11})+a_{21}a_{12}]\bar{v}_1\bar{Y} + a_{12}a_{22}\bar{Y}^2. \quad (45.3)$$

Inasmuch as the phase shift between \bar{p}_1 and \bar{v}_1 is equal to $\pi/2$, it is convenient to change over to a diagram of the same type as in Fig. 26. For the case under consideration it is shown in Fig. 88. If we denote the projections of the vector \bar{Y} on the \underline{x} and \underline{y} axes by \bar{Y}_x and \bar{Y}_y , then the expression for \bar{A}_Σ (45.3) assumes the following form:

$$\bar{A}_\Sigma = \frac{1}{2} \{ a_{12}(1+a_{22})\bar{p}_1^2 + a_{21}(1+a_{11})\bar{v}_1^2 + \\ + [a_{12}(1+a_{22})+a_{12}a_{22}]\bar{p}_1\bar{Y}_x + [a_{22}(1+a_{11})+a_{21}a_{12}]\bar{v}_1\bar{Y}_y + \\ + a_{12}a_{22}(\bar{Y}_x^2 + \bar{Y}_y^2) \}. \quad (45.4)$$

Here \bar{p}_1 , \bar{v}_1 , \bar{Y}_x , and \bar{Y}_y are scalar (real) quantities; the first two are the absolute values of the vectors \vec{p}_1 and \vec{v}_1 , inasmuch as these vectors are by definition always aligned with the \underline{x} and \underline{y} axes.

We now make the simplest assumption that \vec{Y}^2 is completely independent of \vec{p}_1 and \vec{v}_1 , and find the values of \vec{Y} that correspond to the maximum of \bar{A}_Σ . For this purpose we equate to zero the derivatives $\partial\bar{A}_\Sigma/\partial\bar{Y}_x$ and $\partial\bar{A}_\Sigma/\partial\bar{Y}_y$.

Simple calculations yield the sought-for values $\bar{Y}_x = \bar{Y}_{x0}$, $\bar{Y}_y = \bar{Y}_{y0}$ corresponding to $\bar{A}_\Sigma = \bar{A}_{\max}$:

$$\left. \begin{aligned} \bar{Y}_{x0} &= -\frac{a_{12}(1+a_{22})+a_{12}a_{22}}{2a_{12}a_{22}}\bar{p}_1, \\ \bar{Y}_{y0} &= -\frac{a_{22}(1+a_{11})+a_{21}a_{12}}{2a_{12}a_{22}}\bar{v}_1. \end{aligned} \right\} \quad (45.5)$$

Formulas (45.5) indicate that if the assumption that $\bar{A}_\Sigma = \bar{A}_{\max}$ is valid, then the oscillating system will always strive to have \vec{Y} in one quadrant of the diagram shown in Fig. 88. Indeed, inasmuch as \bar{p}_1 and \bar{v}_1 are by definition always positive, then independently of their value the signs of \bar{Y}_{x0} and \bar{Y}_{y0} are completely determined by the expressions preceding \bar{p}_1 and \bar{v}_1 , and consequently this determines the quadrant in which the vector \vec{Y} is located. The numerical calculations show that for $\vec{Y} = \vec{Q}^*$ and $\vec{Y} = \vec{U}_{\text{sgor}}$ (where \vec{U}_{sgor} is the dimensionless variation

of the flame-front propagation velocity, which differs in sign from \vec{U}_1), this quadrant is the fourth.

Consequently, although the diagrams of the stability boundaries (Fig. 27) indicate that oscillations can be excited when \vec{Y} lies in the first, third, and fourth quadrants if the foregoing hypothesis is valid, the oscillating system will tend to realize only the latter case.

Formulas (45.5) obtained for \bar{Y}_{x0} and \bar{Y}_{y0} necessitate knowledge of \bar{p}_1 and \bar{v}_1 . However, even these quantities, perhaps even with greater justification than \bar{Y}_x and \bar{Y}_y , can be "chosen" by the system in accordance with the excitation conditions. Indeed, the relationship between \bar{p}_1 and \bar{v}_1 is determined by the position of the heat-supply section Σ relative to the standing wave formed in the cold part of the stream. The latter is determined in turn not so much by the geometrical position of Σ along the tube axis (this is usually specified), as it is by the number of the excited harmonic. Let us therefore determine the relation between \bar{p}_1 and \bar{v}_1 which corresponds to $\bar{A}_\Sigma = \bar{A}_{\max}$ and which presupposes that the extremum conditions (45.5) have already been satisfied.

In the case under consideration \bar{p}_1 and \bar{v}_1 are connected by Condition (19.12). The constant contained in this relation determines the oscillation amplitudes; let us denote it by c^2 , i.e., we set

$$\bar{v}_1^2 + \bar{p}_1^2 = c^2. \quad (45.6)$$

Formulas (45.6) and (6.3) show that it is possible to write the following expressions for \bar{v}_1 and \bar{p}_1 :

$$\left. \begin{aligned} |\bar{v}_1| &= c \sin \varphi, \\ |\bar{p}_1| &= c \cos \varphi, \end{aligned} \right\} \quad (c > 0), \quad (45.7)$$

where φ is a certain free parameter. Let us find the value of φ for which \bar{A}_Σ assumes its extremal value. Physically this means that we are seeking a definite ratio between \bar{p}_1 and \bar{v}_1 in the section where the

heat-supply plane Σ is located. Realization of this ratio is possible only if the suitable harmonic is excited; thus, we are seeking essentially the harmonic whose excitation maximizes the energy flux \bar{A}_Σ .

It must be noted here that specification of φ (i.e., specification of \bar{p}_1 and \bar{v}_1) determines the number of the harmonics only when the boundary condition on the left end of the tube is simultaneously specified. But it must not be forgotten that it is necessary, in addition, to satisfy also the boundary condition on the right end. For specified properties of the heat-supply surface Σ , and for a limited number of harmonics which can actually be realized, there may not be among the obtained harmonics the one which simultaneously satisfies exactly the boundary condition on the right end. Therefore all the arguments that follow are valid for real systems only in first approximation. They indicate the tendency of the behavior of the oscillating system, but not the exact solution of the boundary-value problem. This remark must be constantly kept in mind when reading the present chapter.

If we substitute the values of \bar{Y}_{x0} and \bar{Y}_{y0} (45.5) into the expression (45.4), we immediately obtain the following formula for \bar{A}_Σ :

$$\bar{A}_\Sigma = c_1 \bar{p}_1^2 + c_2 \bar{v}_1^2,$$

where c_1 and c_2 are certain real coefficients. Taking into account Expressions (45.7), the last equation can be written in the form

$$\bar{A}_\Sigma = c^2 (c_1 \cos^2 \varphi + c_2 \sin^2 \varphi). \quad (45.8)$$

Taking the derivative $d\bar{A}_\Sigma/d\varphi$ and equating it to zero, we obtain the values of φ corresponding to the extrema of \bar{A}_Σ . It is easy to see that if $c_1 \neq c_2$, then these values will be $\varphi = 0, \pi/2, \pi, 3\pi/2$. Inasmuch as by definition \bar{v}_1 and \bar{p}_1 cannot be negative, the angle φ should satisfy the relation $0 \leq \varphi \leq \pi/2$, from which it follows that the energy flux \bar{A}_Σ reaches the extremal values only when $\varphi = 0$ and $\varphi = \pi/2$.

A numerical analysis carried out for typical values of the con-

version coefficients (45.2) has shown that the maximum of \bar{I}_2 corresponds to $\varphi = 0$. Thus, if the oscillating system has the possibility of free choice of both the magnitude and the phase of \vec{Y} , and also the number of the excited harmonic, then the system will strive to realize a process in which the phases of \vec{Y} and \vec{p}_1 will coincide.* This result is somewhat reminiscent of the Rayleigh hypothesis, although essentially its content is entirely different.

It must be stated that the possibility of free choice of the magnitude and phase of \vec{Y} and also of the number of the excited harmonic is inherent in far from all real combustion processes. This must be regarded more as an exceptional and limiting case. In real processes the amplitude of \vec{Y} can be limited by the physical properties of the phenomenon, which do not make it possible for the theoretically "optimal" value of $|\vec{Y}|$ to be attained, and the phase of \vec{Y} can turn out to be connected, say, with the velocity oscillations. This can be traced most clearly in the case of the Rijke tube, in which the heat transfer from the heated grid to the air is determined uniquely by the frequency and the amplitude of the velocity oscillations of the air flowing over the elements of the grid, and cannot be "chosen" by the system in some other manner.

Combustion processes have, of course, many more "degrees of freedom" than heat transfer from a grid, inasmuch as combustion depends on

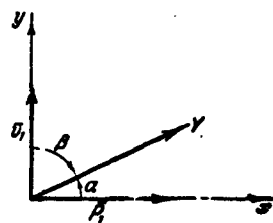


Fig. 88. Vector diagram for the calculated example.

the stream velocity, on the different induction periods, on the vortex formation process, and on many other mutually independent parameters. But even here \vec{Y} may not be completely independent of the oscillation process.

In order to show how the oscillating system will behave in such a case, let us consider the

following example. Let the excitation be the result of the mobility of the flame front, which is assumed to depend on the oscillations of the stream velocity. Let us assume, for simplicity, that this dependence can be expressed by the linear relation $|\vec{Y}| = b|\vec{V}|_1$. In order to take into account the possible delay, we introduce a phase shift between \vec{Y} and \vec{V}_1 , equal to an angle β (Fig. 88). Then obviously

$$\bar{Y}_x = b \sin \beta \bar{v}_1; \quad \bar{Y}_y = b \cos \beta \bar{v}_1, \quad (45.9)$$

$$\bar{A}_z = a_1 \bar{p}_1^2 + a_2 \bar{v}_1^2 + a_3 \bar{p}_1 \bar{Y}_x + a_4 \bar{v}_1 \bar{Y}_y + a_5 (\bar{Y}_x^2 + \bar{Y}_y^2), \quad (45.10)$$

where the coefficients a_1, a_2, \dots, a_5 are determined from a comparison of the equation written out with (45.4). Using (45.7) and (45.9) we rewrite (45.10) in the form

$$\frac{\bar{A}_z}{c^2} = a_1 \cos^2 \varphi + a_2 b \sin \beta \sin \varphi \cos \varphi + (a_3 + a_4 b \cos \beta + a_5 b^2) \sin^2 \varphi. \quad (45.11)$$

If we assume that the dependence of \vec{Y} on the process of acoustic oscillations is specified, i.e., b and β are specified, then the oscillating system retains its ability to choose the numbers of the harmonics, which in the present case are determined by the angle φ . Let us determine the value of φ satisfying the condition $\bar{A}_z = \bar{A}_{\max}$ for different fixed values of b and β . Inasmuch as the scale factor c cannot influence the sought result, we set it equal to unity. Equating to zero the derivative $d\bar{A}_z/d\varphi$, we obtain the relations which determine the values of φ corresponding to the extremum of \bar{A}_z :

$$\operatorname{tg} 2\varphi = - \frac{a_2 b \sin \beta}{a_3 - a_1 + a_4 b \cos \beta + a_5 b^2}. \quad (45.12)$$

The condition for a maximum, $d^2\bar{A}_z/d\varphi^2 < 0$, yields the inequality

$$(a_3 - a_1 + a_4 b \cos \beta + a_5 b^2) \cos 2\varphi - a_2 b \sin \beta \sin 2\varphi < 0, \quad (45.13)$$

which enables us to distinguish between the φ corresponding to the maximum of \bar{A}_z and the values corresponding to the minimum of this quantity.

We shall use the formulas obtained to calculate a typical case characterized by $M_1 = 0.1$; $M_2 = 0.25$. Let the excitation of the oscillating system be due to the mobility of the flame front, which we shall express in terms of \bar{U}_{sgor} . Then the dependence of φ on β , for different values of \underline{b} satisfying the condition $\bar{A}_\Sigma = \bar{A}_{max}$, can be represented by a family of curves as shown in Fig. 89. This family has been plotted for practically all interesting values of β , which range from 0 to π . The limits of variation of the values of \underline{b} are taken from 0.1 to 10. In order to estimate the probable numerical values of the coefficient \underline{b} , we argue as follows. In the example under consideration we have $\vec{Y} = \vec{U}_{sgor}$, and consequently $|\vec{U}_{sgor}| = b\bar{v}_1$. In the steady combustion mode $U_{sgor} = v_1$, i.e., the effective stationary flame propagation velocity is numerically equal to the steady-state value of the stream velocity. If we assume that the variations of these quantities also are of the same order, then the probable value of the coefficient \underline{b} should be close to unity. The range of variation of \underline{b} from 0.1 to 10 apparently covers, with margin, the probable values of this coefficient.

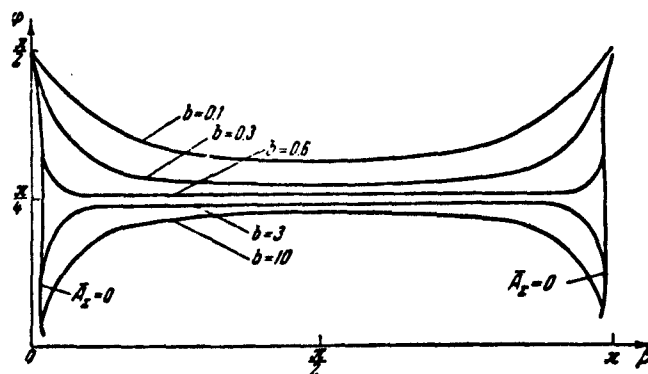


Fig. 89. Diagram showing the probable self-excitation modes obtained from the condition $\bar{A} = \bar{A}_{max}$.

Figure 89 shows not only the aforementioned curves of $\varphi = \varphi(\beta; b)$, but also the lines $\bar{A}_\Sigma = 0$ which limit them. Indeed, the presence of a

maximum of \bar{A}_Σ does not denote at all that the value of \bar{A}_Σ is in itself positive then, whereas it is quite clear that excitation of the oscillating system is possible only when $\bar{A}_\Sigma > 0$. Therefore the lines $\bar{A}_\Sigma = 0$ which separate the values of (β, φ, b) corresponding to $\bar{A}_\Sigma > 0$ from the regions for which $\bar{A}_\Sigma < 0$ are of undoubted interest. Figure 89 shows only those portions of the curves $\varphi = \varphi(\beta, b)$ corresponding to $\bar{A}_\Sigma = \bar{A}_{\max}$ for which $\bar{A}_\Sigma > 0$.

An examination of the curves shown in Fig. 89 enables us to draw the following conclusions. It is seen first of all that if we disregard the small portion corresponding to small values of b , at values of β somewhat larger than π , then the diagram covers the entire region corresponding to the self-excitation of the system, $\bar{A}_\Sigma > 0$. It is easy to visualize here that the curves obtained correspond fully to the stability-boundary diagrams, examples of which were given in Chapter 4 (see, for example, Fig. 27). Variation of β from 0 to π signifies that the vector \vec{Y} lies in the first and fourth quadrants, i.e., precisely in those in which the main instability regions lie.

The principal feature of the curves corresponding to the modes $\bar{A}_\Sigma = \bar{A}_{\max}$ and shown in Fig. 89 is as follows. If we eliminate the relatively narrow regions close to $\beta = 0$ and $\beta = \pi$ (they are of limited interest if for no other reason than that they correspond to small values of \bar{A}_Σ , inasmuch as they are adjacent to the lines $\bar{A}_\Sigma = 0$), then one observes for all β and b the tendency of the curves to approach the line $\varphi = \pi/4$. Thus, in first approximation we can say that independently of the delay in the combustion zone (β) and the quantitative dependence of the flame-propagation velocity perturbations on the stream-velocity perturbation (b), the oscillating system will strive to excite a harmonic corresponding to $\varphi = \pi/4$.

The value $\varphi = \pi/4$ corresponds to oscillation amplitudes \bar{p}_1 and \bar{v}_1

corresponding, as can be seen from (45.7), to the condition $\bar{p}_1 = \bar{v}_1$. This means that the cross section Σ should lie approximately halfway between the pressure and velocity nodes.

The physical meaning of the result obtained is sufficiently clear. It was already shown above that when \vec{Y} is completely independent of the amplitude and phase of the gas oscillation in the sections ahead of Σ , the optimum value of φ which the oscillating system will "choose" will be $\varphi = 0$. This corresponds to a velocity node $\bar{v}_1 = 0$ or, what is the same, to a pressure antinode. If we assume \vec{Y} differs from zero because of the existence of a nonvanishing perturbation velocity $\bar{v}_1 \neq 0$ ($|\vec{Y}| = b\bar{v}_1$), then it becomes immediately clear that the previous result no longer applies in the present case. We have here a struggle between two tendencies, on the one hand the just-mentioned tendency of bringing the heat-supply plane Σ close to the pressure antinode, and on the other hand a new tendency of shifting Σ to the velocity antinode so as to increase (for a given value of b) the amplitude of \vec{Y} . Calculation shows that this brings the plane Σ approximately halfway between the indicated antinodes (or, what is the same, nodes). From the point of view of this argument the distribution of the curves corresponding to different b , shown in Fig. 89, is quite regular. The larger b , the lower the curves, i.e., the closer the plane Σ to the pressure antinode ($\varphi = 0$), for with increasing b the same values of \vec{Y} can be obtained for smaller absolute values of the perturbations in the velocity v_1 .

A perfectly analogous analysis applies also to the case when the amplitude \vec{Y} depends not on \bar{v}_1 but on \bar{p}_1 . This can occur, for example, when the fuel is supplied by low-pressure devices, which change the amount of the fuel introduced into the combustion zone in accordance with the back pressure of the surrounding medium. Without describing

this process in specific detail, we assume that $|\vec{Y}| = \bar{b}p_1$ and that the delay is characterized by an angle α (Fig. 88). Then the mode corresponding to the maximum positive values of \bar{A}_Σ is determined by the following conditions:

$$\left. \begin{aligned} \lg 2\varphi &= \frac{a_2 b \sin \alpha}{a_1 - a_2 + a_2 b \cos \alpha + a_2 b^2}, \\ (a_2 - a_1 - a_2 b \cos \alpha - a_2 b^2) \cos 2\varphi - a_2 b \sin \alpha \sin 2\varphi &< 0, \\ \bar{A}_\Sigma &> 0. \end{aligned} \right\} \quad (45.14)$$

An analysis of the conditions (45.14), which are analogous to the corresponding conditions considered somewhat earlier, is also best carried out on the basis of numerical calculations. For the same example ($M_1 = 0.1$; $M_2 = 0.25$) the relationships obtained are so simple that it is not necessary to plot curves similar to those shown in Fig. 89. Irrespective of whether $\vec{Y} = \vec{U}_{sgor}$ or $\vec{Y} = \vec{Q}^*$ is assumed, and irrespective of α , the numerator of the first relation in (45.14) turns out to have an absolute value much smaller than that of the denominator and if the second relation of (45.14) is taken into account, the angle φ turns out to be very close to zero. This indicates that the oscillating system tends in such cases to excite harmonics at which the heat-supply plane will be situated in a pressure antinode.

Thus, if the essential parameter \vec{Y} which characterizes the combustion is perturbed by velocity oscillations, then the plane Σ tends as it were to lie between pressure and velocity antinodes, but if it is perturbed by pressure, then the plane Σ tends as it were to be situated in a pressure antinode. These general results can be traced sufficiently readily by comparing the experimentally obtained pressure standing-wave patterns with the position of the heat-supply region relative to these patterns.

§46. Experimental Verification of the Hypothesis Concerning the Maximum Acoustic Energy

Although the consequences obtained in the preceding section from

the hypothesis of the maximum acoustic energy radiated by the heat-supply region can indeed be confirmed by many qualitative considerations, it is desirable to have a more clear-cut confirmation of this assumption.

With an aim toward such an experimental verification it is possible, for example, to delay the vibration-combustion process during the second stage (inasmuch as oscillations with limited amplitudes are easier to investigate experimentally), and then register the amplitudes and phases of the oscillations and compare them with those predicted by the hypothesis advanced.

If an experiment is carried out in accordance with the scheme proposed here, then even an affirmative result will not yield, of course, full confirmation of the hypothesis advanced above. This follows already from the fact that, as indicated in §45, the hypothesis concerning the maximum acoustic energy points to a selection of the excitation mechanisms in accordance with the attribute $\bar{A}_\Sigma = \bar{A}_{\max}$ in the course of the buildup of the oscillations. At the same time an experiment based on the proposed scheme will give all the relations for steady-state oscillations. It is therefore necessary to assume an additional hypothesis, that in the steady-state oscillations, when the flux of acoustic energy is determined by the losses, the mechanism retaining its dominating significance is the one corresponding to the condition $\bar{A}_\Sigma = \bar{A}_{\max}$. In steady-state oscillations this will mean that the oscillating system will strive to realize under the specific experimental conditions a process which results in maximum oscillation amplitudes.

It is quite obvious that by measuring experimentally the amplitudes of the oscillations of the pressure, velocity, and other parameters when necessary, it is impossible to state that they are the

largest of all the possible ones under the specific experimental conditions. Therefore the hypothesis can apparently be verified in a somewhat less general formulation.

After first observing vibration combustion with a fully defined feedback mechanism and carrying out the required measurements, it is then possible to establish by theoretical calculations whether the oscillations observed were such that the amplitude-phase relationships satisfied the condition $\bar{A}_\Sigma = \bar{A}_{\max}$. Thus, in this formulation of the problem it is possible to establish only the extent to which the amplitude-phase relations of the vibration-combustion type that has occurred correspond to the hypothesis concerning the maximum of \bar{A}_Σ , but it is impossible to establish whether the oscillating system has "chosen" the very type of vibration combustion (the type of feedback mechanism) corresponding to the indicated hypothesis.

Consequently, the hypothesis advanced above concerning the maximum of \bar{A}_Σ , as applied to the proposed experiments, must be replaced by its corollary: the magnitude and phase of the perturbation of the essential heat-supply parameter \vec{V} which is realized in the experiment is such that for the perturbations \vec{p}_1 and \vec{v}_1 registered in the experiment it yields a maximum value of \bar{A}_Σ .

In order to verify this theoretical assumption, special experiments were set up. The experimental installation usually consisted of a tube 8 meters in length and 100 mm in diameter. Preheated air, in which a required amount of gasoline was evaporated beforehand, was fed into this tube. The combustion took place at relatively short lengths of the combustion chamber, amounting to about 800-900 mm. The flame was maintained by a stabilizer in the form of an angle element with the vertex facing the stream.

As can be seen from this short description, no feedback mechanisms

due to mixture production could occur in a setup of this type. One could expect the principal feedback mechanism to be the one brought about by periodic vortex production behind the stabilizer, and consequently the essential parameter of the heat-supply, the perturbations of which by the acoustic oscillations close the feedback loop, will be the effective flame propagation velocity \bar{U}_1 .

In order to verify this, the walls of the combustion chamber were made of quartz glass, and high-speed motion picture photography of the vibration combustion yielded the typical patterns of periodic powerful vortex formation behind the stabilizer. A colored flame, which was photographed with a motion picture camera, made it possible to record the integral luminosity of the nearest vicinity of the stabilizer on a loop oscillograph, on which the pressure oscillations were simultaneously recorded. The oscillograms obtained showed that the luminosity oscillations had a frequency coinciding with the pressure oscillations. The high-speed motion picture photography has verified that the aforementioned luminosity oscillations are connected with the change in the volume occupied by the hot (glowing) gases, which, as is well known from Chapter 4, can be reduced to a change in the effective flame propagation velocity \bar{U}_1 .

To calculate \bar{A}_2 from the experimental data it would be necessary to determine first of all the phase and the amplitude of $\vec{Y} = \vec{U}_1$ and the other quantities necessary for the calculation of the flux of acoustic energy.

As can be seen from (45.1), the conditions relating the oscillations on the left and on the right of the heat-supply zone contain six coefficients and five variables. All six coefficients are obtained in final analysis if M_1 and M_2 are specified. The first of these quantities can be readily measured directly, and the second is just as easy

to determine, provided the gas temperature behind the heat-supply zone is measured. Thus, the determination of the coefficients a_{11} , a_{12} , ..., a_{23} from the experimental data entails no difficulty. Measurement of the pressure oscillations directly ahead of the combustion zone and immediately behind it (\bar{p}_1 and \bar{p}_2) also entails no difficulty. Of the remaining three quantities, namely \bar{v}_1 , \bar{v}_2 and $\bar{Y} = \bar{U}_1$, only the former can be measured with the aid of a thermoanemometer. But as soon as \bar{p}_1 , \bar{p}_2 , and \bar{v}_1 are measured, the other two quantities, \bar{v}_2 and \bar{U}_1 can be calculated, inasmuch as only two unknowns remain in the system of two equations (45.1). The calculation of \bar{A}_Σ is best carried out then in accordance with Formula (19.7)

$$\bar{A}_\Sigma = \frac{1}{2} (nm\bar{p}_2\bar{v}_2 - \bar{p}_1\bar{v}_1).$$

Thus, measurement of the corresponding quantities makes it possible to determine the energy flux \bar{A}_Σ observed in the experiment. In order to decide whether this energy flux \bar{A}_Σ satisfies the condition $\bar{A}_\Sigma = \bar{A}_{\max}$, it is possible to carry out the following supplementary calculations. Inasmuch as during the course of determining the experimental value of \bar{A}_Σ we determine also the experimental value of \bar{U}_1 , we can analyze how \bar{A}_Σ would change were \bar{U}_1 to be characterized by other amplitudes and phases at the same values of \bar{p}_1 and \bar{v}_1 . In this case the variation of \bar{U}_1 must be carried out in the vicinity of values of \bar{U}_1 obtained from the processing of the experimental data.

The results of the corresponding calculations are shown in Figs. 90 and 91. These plots show the variation of \bar{A}_Σ for different experimentally observed frequencies, as functions of H or β (the amplitudes and phases of the flame propagation velocity perturbation relative to the tube walls, \vec{N}). The quantity $\vec{N} = \vec{v}_1 + \vec{U}_1$ determines uniquely (for specified values of \vec{v}_1) the perturbation of the flame propagation velocity \vec{U}_1 . The connection given above between \vec{N} and \vec{U}_1 shows that,

for the purposes of the present section, the transition from \vec{U}_1 to \vec{N} does not change anything: it is necessary to verify whether the experimentally recorded mode corresponds to the equality $\bar{A}_\Sigma = \bar{A}_{\max}$, i.e., whether \bar{A}_Σ obtained for \vec{N} other than those calculated from the experimental data is lower than A_Σ registered in the experiment.

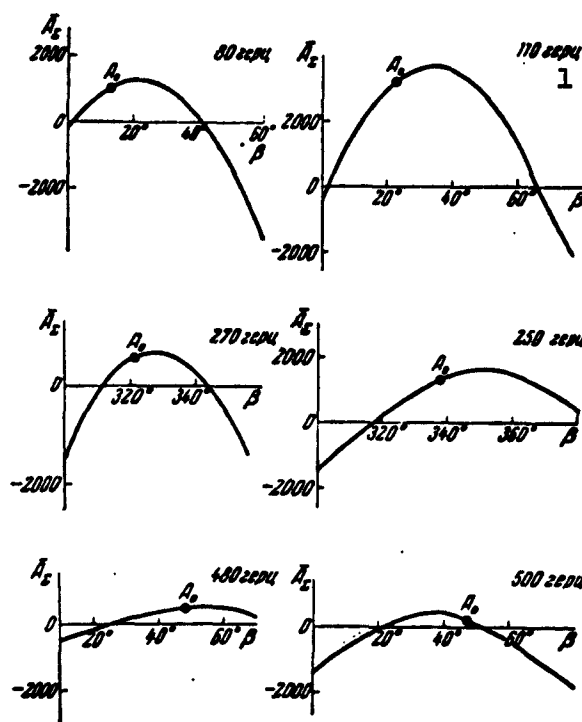


Fig. 90. Position of experimental points (A_0) on the curves $\bar{A}_\Sigma = \bar{A}_\Sigma(\beta)$. 1) cps.

Figures 90 and 91 show curves showing the variation of A_Σ as functions of $H = |\vec{N}|$ and of the phase of \vec{N} , denoted by β ; these curves show the points A_0 corresponding to the experiment. An estimate of the accuracy of the experiment has shown that the phases were registered by the oscillograph with an accuracy $\pm 15^\circ$, while the accuracy with H was calculated, determined by the accuracy of the measurements of \bar{p}_1 , \bar{v}_1 , and \bar{p}_2 , is of the order of ± 3 of the arbitrary units with which the abscissas of Fig. 91 are graduated.

If we take into account the accuracy with which β and H are de-

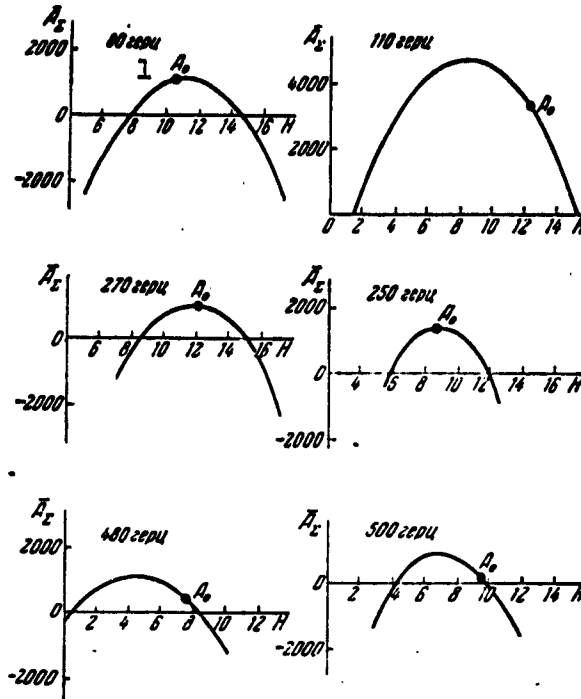


Fig. 91. Position of experimental points (A_0) on the curves $\bar{A}_\Sigma = \bar{A}_\Sigma(H)$. 1) cps.

terminated in the experiments, we can state that for all the frequencies observed and actually realized by the oscillating system, the vibration-combustion modes lie in the vicinity of the maxima of the $\bar{A}_\Sigma = \bar{A}_\Sigma(\beta)$ and $\bar{A}_\Sigma = \bar{A}_\Sigma(H)$ curves, something that can be regarded as a confirmation of one of the corollaries of the hypothesis that the oscillating system strives toward realization of a mode corresponding to the maximum of acoustic energy radiated by the heat-supply region.

In order to estimate the degree of reliability of the diagrams shown in Figs. 90 and 91, let us present some additional data. The curves on these diagrams were plotted in the following fashion. From the experimentally measured \bar{p}_1 , \bar{v}_1 , and \bar{p}_2 , the values of \bar{v}_2 , $\bar{Y} = \bar{N}$ and of the energy flux \bar{A}_Σ were obtained with the aid of equations of the type (45.1). Then the amplitude of \bar{N} (designated H) and the phase of \bar{N} (designated β) were varied for constant values of \bar{p}_1 , \bar{v}_1 , and the

energy flux \bar{A}_Σ was again determined for these modified values of \bar{N} , and this, as already mentioned, turned out to be less than for the actually realized mode. Consequently, the essential parameter \bar{Y} , characterizing the combustion zone, turns out to be realized every time in such a way that all other values of \bar{Y} (for the same values of \bar{p}_1, \bar{v}_1) yielded smaller values of \bar{A}_Σ . It is perfectly clear that the results of these calculations could be influenced both by the accuracy of the measurements of \bar{p}_1, \bar{v}_1 , and \bar{p}_2 and by the accuracy with which the coefficients $a_{11}, a_{12}, \dots, a_{23}$ in Eqs. (45.1) were determined. As regards the first source of errors, the lowest accuracy was for the measurements of \bar{v}_1 ; the measurements of \bar{p}_1 and \bar{p}_2 were practically perfectly accurate. The coefficients of Eqs. (45.1) could be determined from the formulas of Chapter 4 from the known values of M_1 and M_2 and by assuming that there occur in the combustion zone oscillations of a plane flame front behind which the temperature reaches the theoretical value instantaneously. One could, on the other hand, refine both the flame configuration in the combustion zone (from the motion picture photography data) and take into account the gradual nature of the temperature buildup in the flame. This approach would yield, of course, somewhat different numerical values of $a_{11}, a_{12}, \dots, a_{23}$ than the simple method mentioned above.

Numerical analysis has shown that although the error in the measurement of \bar{v}_1 and the possible differences in the coefficients of Eqs. (45.1) greatly influence the calculated value of \bar{A}_Σ , it cannot change the conclusions drawn. Although the numerical values of \bar{A}_Σ did change, the $\bar{A}_\Sigma = \bar{A}_\Sigma(H)$ and $\bar{A}_\Sigma = \bar{A}_\Sigma(\beta)$ curves retained their form and, in essence, the points A_0 hardly shifted on these curves relative to their maxima. Consequently, the conclusion that the oscillating system strives toward realization of the mode $\bar{A}_\Sigma = \bar{A}_{\max}$ would not be changed

by more careful measurements and by more precise processing of the experimental data.

With respect to the calculations performed, we must make still another remark. As can be seen from the procedure used to plot the curves in Figs. 90 and 91, in the variation of $\bar{Y} = \bar{N}$ it was not required that the boundary condition be satisfied at the outlet end of the tube. The calculations performed must be regarded as a disclosure of a tendency rather than exact computations.

The experiments considered here should be viewed as an experimental illustration of the hypothesis concerning the maximum of \bar{A}_Σ , and their scope is clearly insufficient to be able to speak with full assurance of a confirmation of the hypothesis. Therefore any new experiments in this direction are of undoubted interest.

It must be stated that many phenomena observed in vibration combustion can probably be treated from the point of view of the tendency of the oscillating system toward realization of modes characterized by $\bar{A}_\Sigma = \bar{A}_{\max}$.

In particular, the jump-like change in the oscillation frequency with displacement of the combustion zone along the tube, described in the preceding chapters, can be explained also from the point of view of the hypothesis advanced. The experimental data do not contradict the assumption that transition from one frequency to another is connected with the fact that at the new frequency the amount of acoustic energy generated in the heat-supply zone exceeds the amount generated at the old oscillation frequency.

§47. Excitation and Suppression of Vibration Combustion

We have already mentioned earlier that vibration combustion (the excitation of acoustic oscillations by heat supply in general) can, depending on the specific circumstances, be a process it is desir-

able to produce or else an undesirable phenomenon which must be combated. Therefore both formulations of the problem can be of practical interest, either a purposeful excitation of vibration combustion or a decisive struggle against it.

A detailed examination of vibration combustion from these opposing points of view would hardly be meaningful, since the solution of one of these problems determines to some degree also the opposite problem: all the measures which are useful for the suppression of oscillations will be harmful for their excitation, and vice versa.

As regards measures which contribute to the excitation of oscillations we can, starting from the results given in the preceding chapter, present the following general recommendations.

The tube in which it is proposed to excite the oscillations must not permit large losses of acoustic energy. In particular, if this tube is open on one or both ends, it must be made sufficiently "long," i.e., it is necessary to choose a sufficiently large ratio of the length to the tube diameter. This ratio is desirably of the order $L/d = 30-50$, although vibration combustion can be observed also in "shorter" tubes. In addition to the L/d ratio, a very important factor is the construction of the tube itself. One must avoid in any way all gaps (for example in the junctions between the elements comprising the tube), holes in the body of the tube, etc. If the gas in the tube is capable of interacting with the surrounding medium not only through the end sections but also through various holes and other faults in the body of the tube, this will lead to strong damping of the oscillations.

Depending on the character of the proposed heat-supply process (whether gas, pulverized coal, or some other fuel will be ignited; whether it is possible to install poorly streamlined bodies in the

stream, etc.), it is possible to produce conditions that favor to the greatest extent one of the feedback mechanisms listed in Chapter 7. If, for example, it is proposed to obtain vibration combustion in a stream of previously prepared gas-fuel mixture in a tube open on both ends, then it is most natural to generate the vibration combustion by producing conditions favoring the development of a combustion mechanism connected with periodic vortex formation. As is well known, this can be attained by organizing the combustion process behind a poorly streamlined body (stabilizer). It is merely necessary to recognize that the location of the stabilizer along the tube must be chosen in optimal fashion. This means that it is necessary to find that position of the stabilizer along the tube at which the largest amount of acoustic energy is generated in the combustion zone and the tube boundary conditions are simultaneously satisfied. It is best to seek this position by experiment. For this purpose it is possible to use a mobile stabilizer construction (for example, to displace the stabilizer with the aid of a rod which emerges through the "cold" end of the tube, but without any longitudinal slots in the body of the tube itself which would communicate with the external medium). If a movable stabilizer is available, it must be displaced in a way as not to interrupt the combustion process, and its position along the tube should be set such that the oscillations of the most desirable amplitude and frequency develop. If such a construction is impossible, then the stabilizer can be displaced during the intervals between startups of the installation. After choosing the stabilizer position along the tube it is necessary to secure the stabilizer finally in the chosen section of the tube.

In those cases when the vibration-combustion mechanism is different, the entire search for optimal excitation conditions must be reorganized in suitable manner, using as a guide the description of the

feedback mechanisms given in Chapter 7.

A more complicated process is to suppress vibration combustion once it has arisen. In some cases it is sufficient to break the feedback loop in the oscillating system. This break can be carried out in the case when the feedback mechanism which has given rise to the vibration combustion is known. In Chapter 7 above, in the description of the possible feedback mechanisms, examples of this type were already presented. In particular, if vibration combustion arises as a result of interaction between acoustic oscillations and the vortex production ahead of the combustion zone, then to suppress the vibration combustion it is sufficient to install rectifying grids between the place where the vortices are formed and the combustion zone (see §36). In other cases it is necessary to use certain other methods which make it possible to break the corresponding specific types of feedback loops.

The method indicated here for combating vibration combustion entails the overcoming of very great difficulties. The point is that the number of possible feedback mechanisms is quite large, and these can have entirely different physical natures (see Chapter 7). Therefore the desire to open the dangerous feedback loop may in practice impose the requirement that all possible feedback loops be open. If it is recognized that it is impossible to guess always the most dangerous feedback loops under given specific conditions, one is left only with advancing the most general requirement, namely attaining constancy of the fuel flow, seeing to it that all the passages in the tube are smooth in the inlet portion, etc. However, even the satisfaction of all these requirements makes it possible for processes to occur, connected with the action of variable accelerations on the flame front, etc.

In addition to the foregoing, it must also be remembered that in

feedback mechanisms given in Chapter 7.

A more complicated process is to suppress vibration combustion once it has arisen. In some cases it is sufficient to break the feedback loop in the oscillating system. This break can be carried out in the case when the feedback mechanism which has given rise to the vibration combustion is known. In Chapter 7 above, in the description of the possible feedback mechanisms, examples of this type were already presented. In particular, if vibration combustion arises as a result of interaction between acoustic oscillations and the vortex production ahead of the combustion zone, then to suppress the vibration combustion it is sufficient to install rectifying grids between the place where the vortices are formed and the combustion zone (see §36). In other cases it is necessary to use certain other methods which make it possible to break the corresponding specific types of feedback loops.

The method indicated here for combating vibration combustion entails the overcoming of very great difficulties. The point is that the number of possible feedback mechanisms is quite large, and these can have entirely different physical natures (see Chapter 7). Therefore the desire to open the dangerous feedback loop may in practice impose the requirement that all possible feedback loops be open. If it is recognized that it is impossible to guess always the most dangerous feedback loops under given specific conditions, one is left only with advancing the most general requirement, namely attaining constancy of the fuel flow, seeing to it that all the passages in the tube are smooth in the inlet portion, etc. However, even the satisfaction of all these requirements makes it possible for processes to occur, connected with the action of variable accelerations on the flame front, etc.

In addition to the foregoing, it must also be remembered that in

accordance with the hypothesis that the system strives to realize a process with maximum radiation of acoustic energy from the heat-supply region, a break in one or several feedback loops which assume the principal roles does not always lead to the suppression of vibration combustion. Some other feedback mechanism, which hitherto was perfectly insignificant, may become principal. In this case the oscillating system should "correct" in suitable manner the frequency and the phase of the oscillations in such a way that the new mechanism produces the amount of acoustic energy which is the maximum possible for it. This probably explains also the difficulty of combating vibration combustion by measures of this type. Effective suppression of vibration combustion is possible by using universal methods, which act in equal fashion on all or at least the majority of feedback mechanisms, or else on the oscillating system as a whole.

The most natural universal method of combating vibration combustion is to increase the losses of acoustic energy. Structurally this can be realized in the form of some devices placed at the end sections to absorb the acoustic impulses. Such a measure is not always realizable, since it can involve hydraulic losses or it can violate other requirements imposed on the construction. If it is not desirable to include absorbing devices in the construction of the end sections of the tube, it is possible to suggest, for example, such a radical measure as the introduction of a longitudinal cut in the body of the tube (or frequent holes on one of the generatrices), so as to allow the gases inside the tube to communicate with the space outside in addition to the end sections. To be sure, this measure is practically impossible if the pressure inside the tube exceeds greatly the pressure in the surrounding space.

In some cases it is possibly useful to equip the internal walls

of the tube with acoustic dampers similar to those used to improve the acoustics of buildings. It must be noted, to be sure, that whereas direct experimental data are available concerning the damping influence of acoustic-energy absorbers in the end sections and in holes in the body of the tubes, experiments using acoustic damping walls for the tube are still unknown.

The foregoing methods of directly damping the oscillations are on the whole quite effective and universal (they do not depend on the specific type of feedback mechanism). Among their shortcomings is their imposition of severe and sometimes impossible requirements on the construction of the tube and the devices associated with it, since they involve the introduction of additional hydraulic resistances, disturbing the sealing of the tube between its ends, deterioration of conditions under which the tube is cooled, etc. It is desirable therefore to develop where possible universal methods for suppressing vibration combustion by direct action on the combustion zone, without changing the construction of the tube and without devices associated with its ends.

A method of this type, which probably may prove useful in many cases, is to stretch out the combustion over the length of the tube. So far we have considered only those cases in which the extent of the heat-supply zone σ was small. To be sure, in Chapter 4 we gave a general method of reducing the process of nonstationary combustion in a certain extensive heat-supply zone σ to a process of heat supply on an effective strong-discontinuity plane Σ , but this method was not used from the point of view of finding such properties of the combustion process as would make impossible the self-excitation of the oscillating system.

Starting from the hypothesis that the oscillating system strives

to realize a process that yields a maximum flux of acoustic energy \bar{A}_Σ radiated by the heat-supply region, we can draw the following important conclusion. The excitation of oscillations is connected with a proper relationship between the amplitudes and phases of the perturbed heat supply \bar{Q}^* and the perturbations of the flame propagation velocity \bar{U}_1 on the one hand, and the acoustic oscillations on the other. Therefore in principle the struggle against vibration combustion can be carried on both by disturbing the phase relationships and by changing the relationships between the amplitudes of \bar{Q}^* and \bar{U}_1 and the amplitudes of the acoustic oscillations. However, the former of these ways can practically never attain the purpose. Indeed, assume that there exists in an excited self-oscillating system of this type a certain phase relationship which can be modified in the required direction. Then the excited oscillations will attenuate, but at the same time there are certain to be excited others which are characterized by a different frequency at which this change in parameter cannot interfere with the excitation of the oscillations. In addition, the combustion process has in real furnaces such a large number of "degrees of freedom" that a forced change in the phase of any one of the links of the complicated chain of causes and effects still leaves sufficiently many possibilities for the spontaneous change in phase of the other links in accordance with the hypothesis that the system strives to realize the mode $\bar{A}_\Sigma = \bar{A}_{\max}$.

The foregoing can be illustrated by means of the following simple example. In the excitation of vibration combustion in a stationary gas contained in a tube which has one end closed, the main feedback mechanism is the one connected with the action of the periodically varying accelerations on the flame front. It is quite obvious that as the flame front is slowly displaced along the combustible mixture, it will

gradually pass from a region where the phases of the acceleration are in suitable correspondence with the phases of the pressure oscillations into a region where this correspondence is violated (this is connected with the fact that on different sides of the pressure antinode the oscillating components of the velocity are directed in opposite directions). Were the assumption concerning the decisive role of the phase relationship to be correct, then the oscillations should stop. Actually, oscillations are excited at a different frequency.*

Consequently, even from general considerations it becomes clear that little promise is offered by fighting vibration combustion by disturbing the proper relationship between the phases of \bar{Q}^* and \bar{U}_1 and the phases of the acoustic oscillations.

Another possible way, as indicated above, is to violate the required amplitude relations. We can use here the following results, obtained in the preceding chapters. If the excitation of the system is connected only with \bar{Q}^* , then when $\bar{Q}^* = 0$ the oscillating system is stable; if the excitation is connected only with \bar{U}_1 , then when $\bar{U}_1 = 0$ the oscillating system is stable or neutral. Inasmuch as both results were obtained neglecting the energy lost to the surrounding medium, for real systems the following statement will hold true: when $\bar{Q}^* = 0$ and $\bar{U}_1 = 0$ the oscillating system is always stable. Thus, the principal factor in suppressing vibration combustion is the utmost reduction in the amplitudes \bar{Q}^* and \bar{U}_1 . One of the methods fulfilling this purpose is to stretch out the combustion. Let us illustrate this with two examples which have a qualitative character.

Assume that the combustion occurs in a mixture prepared directly ahead of the combustion zone. We suppose that the main feedback mechanism is one connected with the formation of a mixture of inhomogeneous composition as a result of oscillations in the flow of air

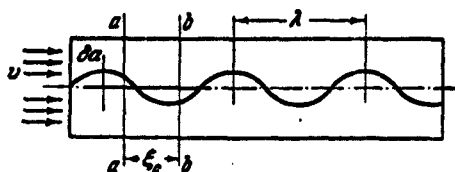


Fig. 92. Scheme for calculating a combustion process that occurs at two cross sections shifted by a distance ξ_s .

through the cross section in which the nozzles which inject the fuel into the flowing air medium are located. This mechanism was described in detail in §35. Formula (35.4) shows that when the combustible mixture moves along the tube the excess-air coefficient α does not remain constant. A periodic perturbation $\delta\alpha$ is superimposed on it. This perturbation is carried by the stream like any other inhomogeneity which is inherent in a medium that moves along a tube when the inhomogeneity is stationary relative to the gas particles. Therefore at one and the same instant of time α will be different at different sections of the tube. Figure 92 shows schematically the flow through a part of the tube. The wavy line oscillating relative to the tube axis shows arbitrarily the perturbation of the excess-air coefficient $\delta\alpha$. In section aa a certain part of the mixture is burned, and in section bb the remaining part of the mixture is burned. Between these sections, in the segment ab, no combustion of the mixture takes place. The distance between sections aa and bb is equal to ξ_s . The wavelength of the perturbation $\delta\alpha$ is denoted by λ . Let the section $\xi = 0$ coincide with the section aa. Then the oscillations $\delta\alpha$ in this section will occur in accordance with the law

$$\delta\alpha = \delta\alpha_0 e^{i\omega\tau}, \quad (47.1)$$

where $\delta\alpha_0$ is the value of $\delta\alpha$ determined by Formula (35.4) for the instant of time $\tau = 0$.

The oscillation $\delta\alpha$ in section bb can be determined by starting from the fact that it was observed in section aa during some preceding instant of time, differing from the present instant by an amount necessary for the portion of the mixture to move through a distance $ab = \xi_s$. This time is $\tau_s = \xi_s/M_s$, where M_s is the average value of the flow velocity between sections aa and bb referred to the velocity of sound in the cold stream. Consequently, in section bb the oscillation $\delta\alpha$ will be determined by the following formula:

$$\delta\alpha = \delta\alpha_0 e^{i\omega\left(\tau - \frac{\xi_s}{M_s}\right)}. \quad (47.2)$$

Assume that in each of the sections under consideration part of the mixture is burned, the fraction ζ in section aa (where $0 < \zeta < 1$) and the fraction $1 - \zeta$ in section bb. If we take the boundaries of the heat-supply region σ such that both these sections lie inside σ , then the total heat release in the region σ will be

$$\delta Q = \frac{\partial Q}{\partial \alpha} \delta\alpha_0 \left[\zeta + (1 - \zeta) e^{-i\omega \frac{\xi_s}{M_s}} \right] e^{i\omega\tau}. \quad (47.3)$$

Let us find the values of ξ_s and ζ such that $\delta Q = 0$ for a specified frequency ω . Writing (47.3) in trigonometric form and equating the real and imaginary parts to zero individually, we obtain

$$\left. \begin{aligned} \sin \omega \frac{\xi_s}{M_s} &= 0, \\ \zeta + (1 - \zeta) \cos \omega \frac{\xi_s}{M_s} &= 0. \end{aligned} \right\}$$

From this we obtain directly

$$\left. \begin{aligned} \omega \frac{\xi_s}{M_s} &= k\pi \quad (k = 1; 3; 5; \dots), \\ \zeta &= 0.5. \end{aligned} \right\} \quad (47.4)$$

The values of k in the first of these equations are chosen odd, since for even values of k we obtain $\zeta = \infty$, whereas by definition $0 < \zeta < 1$.

The perturbation wavelength $\delta\alpha$, like the entropy perturbation

wavelength, is (in dimensionless variables) $\lambda = 2\pi M_g/\omega$ and consequently we obtain from the first equation of (47.4)

$$\xi_c = k \frac{\lambda}{2}. \quad (47.5)$$

The smallest value of ξ_g is obtained when $k = 1$.

Thus, if it is desired to reduce the amplitude of the heat-release perturbation to zero, it is necessary to break the combustion process up in such a way that it occurs in two planes which are separated by half the wavelength of the entropy perturbation and, in addition, it is necessarily required that equal fractions of fuel be consumed in these sections. The result obtained is perfectly natural, for this is precisely the type of combustion process required in order that at each instant of time the excess heat (relative to the average value) released in the section where the mixture is rich be compensated by the deficit in the heat release in the section where a lean mixture crosses.

It must be stated that the foregoing calculation cannot pretend to be more than a crudely qualitative scheme. However, it does enable us to point to the principally new factor contained in the properties of a combustion chamber which is stretched out in length. Indeed, let the combustion occur in only one plane (and not in two). Then by displacing this plane along the tube axis, it is possible to change the relations between the phase of the heat-supply perturbation and the phase of the oscillation of the medium. It is then possible to obtain those positions of the heat-supply plane at which the self-excitation of the system becomes unavoidable. The situation is different if the combustion occurs in two planes corresponding to the conditions (47.4). Then excitation becomes impossible for any position of the heat-supply region along the tube axis, since the phase relations cease to play

any role whatever, inasmuch as the amplitude of the heat-supply perturbation vanishes. This indicates the great universality of the second method of suppressing vibration combustion (by reducing the relative amplitudes, and not by changing the phase relations). The reduction of the amplitude of the heat-release perturbation to zero is equivalent to breaking the feedback loop. In this case acoustic oscillations cannot cause oscillations of heat release, which are capable of maintaining the former.

Of course, exact satisfaction of Conditions (47.4) is difficult in practice. However, even a crudely approximate realization of these conditions is capable of yielding a noticeable effect. This can be verified by examining what results from a change in the entropy perturbation wavelength λ for a constant value of ξ_s . Variation of λ leads to a violation of the first equation in (47.4), written in the form of Relation (47.5). Let us find the absolute value of the heat-supply perturbation δQ , using the equation (47.3):

$$|\delta Q| = \text{mod } \frac{\partial Q}{\partial \alpha} \delta \alpha_0 \sqrt{\zeta^2 + 2\zeta(1-\zeta) \cos 2\pi \frac{\xi_s}{\lambda} + (1-\zeta)^2}. \quad (47.6)$$

Let the modulus of $(\partial Q / \partial \alpha) \delta \alpha_0$ be arbitrarily assumed equal to unity. Then the relative amplitude of the perturbation $|\delta Q|$ will depend on two parameters, ζ and ξ_s / λ . The character of this dependence for values of ζ equal to 0.25, 0.5, and 0.75 and also for the entire range of variation of ξ_s / λ ($0 < \xi_s / \lambda < 1$) is shown in Fig. 93. As can be seen from the curves, compared with combustion in one plane ($\xi_s = 0$) the amplitude of the heat-supply perturbation oscillations $|\delta Q|$ is reduced on the average to one half, and near the optimum value $\xi_s / \lambda = 0.5$ it amounts to 10-20% of the value characteristic of concentrated combustion. A plot made for $\zeta = 0.25$ and $\zeta = 0.75$ shows that even such appreciable deviations from the optimum value $\zeta = 0.5$ continue to re-

tain noticeable advantages for decentralized combustion. Thus, the distribution of the combustion between two centers may turn out to be useful when an attempt is made to suppress vibration combustion.

All the considerations advanced above remain valid also for other feedback mechanisms, for which the transport of some inhomogeneity by the stream is essential. In particular, the foregoing remains in force for the feedback mechanism due to periodic perturbation of the fuel supply (it was already stated earlier that this type of feedback is characteristic of low-pressure fuel-supply systems, for example the supply of coal in pulverized-coal furnaces). One can say literally the same for mechanisms connected with oscillations in the character of the atomization of the fuel by nozzles, resulting from the oscillations in the velocity head in the region where these nozzles are located, etc.

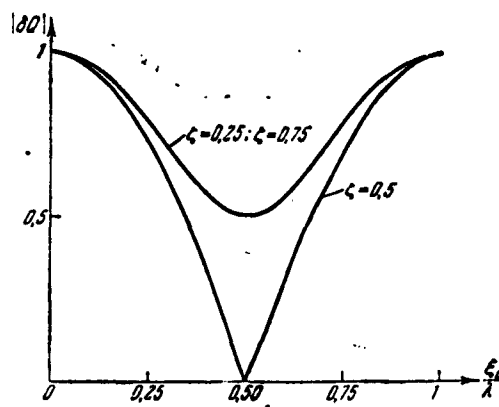


Fig. 93. Variation of the amplitude of the heat-supply perturbation as a function of the relative distance between the sections in which the combustion takes place, and as a function of the fraction of combustible mixture burned up in the first section.

One must not think that the distribution of combustion between two centers is useful only when the feedback mechanisms are included in the group which was characterized in Chapter 7 as being connected

with mixture production. One can assume that even such phenomena as vortices that advance on the combustion zone will perturb the combustion process to a lesser degree, inasmuch as they will not act simultaneously on the entire combustion zone, which in the case under consideration is greater in depth.

The foregoing analysis, as was already indicated, was more qualitative than quantitative in character. Essentially, the distribution of the combustion between two centers was merely a crude model of a combustion model which stretches out along the direction of the flow axis.

On the basis of the foregoing considerations we can state that the spreading out of the combustion influences favorably the reduction in the heat-supply perturbation amplitude. It is known, however (this

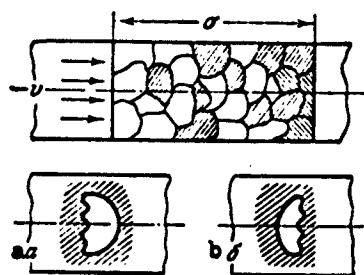


Fig. 94. Scheme showing the combustion of a homogeneous mixture (the batches of combustion products are shown as shaded).

can be seen at least from System (16.15), which describes the process in the heat-supply zone), that self-excitation of acoustic oscillations can occur both for nonzero perturbation of the heat supply, and for nonzero perturbation of the effective flame propagation velocity. The influence of the spreading of the combustion on the latter quantity must be considered separately.

If we speak of combustion that stretches out over a certain depth, we cannot confine ourselves to the notion of a thin flame front which separates the tube into two regions, namely the region of cold mixture and the region of the combustion products, in which the combustion process has terminated. Actually, in the case of extended combustion there will be located in the zone of the chemical reactions sufficiently large batches of cold mixture, in contact with batches of com-

bustion products; on the boundaries between them there will occur the combustion process. Schematically this is shown in the upper part of Fig. 94 (the batches of combustion products are shown shaded). At the end of Chapter 7 we presented a description of a rather effective feedback mechanism due to the influence of variable accelerations (connected with acoustic oscillations) on a thin flame front regarded as a surface separating two media of different density. It was shown there that this reduces in final analysis to a perturbation of the effective flame propagation velocity, due to wave formation on the surface of the front.

In the case of extended combustion, if the combustion zone has the structure shown in the upper portion of Fig. 94, the mechanism mentioned here for the perturbation of the effective flame propagation velocity, owing to wave formation on the separation surfaces, will be noticeably weakened. This can be verified by examining the two diagrams shown in the lower part of Fig. 94. In the left and the right halves of the figure is shown the behavior of one and the same batch of combustible mixture surrounded by combustion products. The boundary of the batch is the front of the flame. The instants a (left-hand diagram) and b (right-hand diagram) are shifted in time by one-half cycle of the acoustic oscillations, and therefore the directions of the accelerations acting on the batch during these instants are opposite. It is easy to visualize (this is clear from the general considerations given at the end of Chapter 7 and can be seen on the right half of Fig. 75) that if at the instant a the maximum wave production is observed on the left boundary of the batch, then on its right boundary there will be a minimum of wave production. This follows from the fact that on one of these boundaries the acceleration acts in the direction from the cold gas to the hot one, and on the other it acts in the di-

rection from the hot gas to the cold one. It is obvious further that half a cycle later, when the direction of the acceleration is reversed, the character of the wave formation will also change (instant b). The boundary on which there was a strong wave formation becomes unperturbed, and the previously unperturbed area is covered with waves. Let us now take into account the fact that the effective velocity of combustion is proportional to the overall surface of the flame. As a result of the fact that the left and right boundaries of the batch are covered with waves alternately, on the average the total area of the surface of separation remains constant for all instants of time. We do not take into account here, of course, the unavoidable reduction of this surface as a result of the combustion of the fresh mixture. An account of this phenomenon is inessential, since it has no periodic character. Inasmuch as the total area of the boundaries of the batch ceases to vary periodically, the effective velocity of flame propagation will not have a periodic component and this means that the perturbation of the effective flame propagation velocity is equal to zero. Consequently, self-excitation is excluded. Of course, these arguments are only a crude approximation to reality, but they do show that the structure of the combustion zone is capable of influencing appreciably the possibility of excitation of acoustic oscillations, and combustion that is stretched out along the tube axis should be characterized by a reduced tendency toward self-excitation of acoustic oscillations.

Summarizing the statements made concerning the properties of extended combustion, we can state that such a scheme of the combustion process has a tendency to reduce the amplitudes of the perturbations both in the heat supply and in the effective flame propagation velocity, and is in a certain sense a universal method of combating vibration combustion.

As will be shown in §52, excitation of acoustic oscillations in liquid-fuel jet engines is connected not with perturbations of the heat supply or the effective flame propagation velocity, but with a perturbation in the gas production in the combustion front. Nonetheless, the general conclusion that, in the case of extended organization of the combustion, the excitation of acoustic oscillations is less likely than in the case when the combustion is concentrated in one section is to a certain degree valid also for liquid-fuel jet engines. This was demonstrated by Crocco and Cheng,* who considered the stability of longitudinal acoustic oscillations in liquid-fuel jet engines under the assumption that the combustion is concentrated in two combustion fronts that are separated by a finite distance. In the case when the indicated two fronts were suitably placed (one at the head of the combustion chamber, i.e., in a pressure antinode, and the other in a pressure node), this has led in the calculations of these authors to a reduction in the probability of system excitation. Consequently, in liquid-fuel jet engines the extended combustion (combustion in two fronts) can also exert a damping influence on the self-excitation of longitudinal acoustic oscillations.

Extended combustion differs from ordinary combustion in that in place of one heat-supply plane there are produced two or more. This violates, as it were, the customary picture of heat supply in the longitudinal direction (along the x axis). An equally conceivable change in the organization of the combustion is one in the transverse direction, along axes normal to the x axis. One can, for example, arrange it so that only part of the gas crossing the heat-supply region is subjected to heat and the other remains cold. In this case there is formed behind the heat-supply zone a flow of parallel jets, some of which are heated and others are at the temperature of the gas ahead

of the heat-supply zone. If these jets do not mix in the direct vicinity of the heat source, then such a stratified construction of the stream behind the heat-supply zone can also contribute to the appearance of damping effects.

A detailed theoretical analysis of this problem cannot be carried out here, inasmuch as we have studied above only one-dimensional flow. However, general considerations show that in such a stratified construction of the stream the excitation of acoustic oscillations becomes less probable. It is known, for example, that when heat is supplied uniformly to all jets of the gas crossing the heat-supply plane, the thermal resistance becomes largest compared with cases when this entire amount of heat is imparted to only part of the jets that cross this plane. Consequently, the oscillation excitation mechanism connected with the perturbation of the thermal resistance cannot manifest itself here to its fullest extent.

Not being able to consider here the theoretical aspect of the problem, we shall refer to an experimental fact confirming the foregoing considerations. In Lehmann's* experiments on excitation of sound in a Rijke tube, which will be considered in detail in the next section, the air was heated by passing electric current through thin wires (0.2 mm in diameter) located at distances 2 mm apart in a certain section of the tube. The excitation of the acoustic oscillations occurred only when a dense wire net was placed at a distance of the order of 1 mm from these wires along the stream. This net was heated by the incandescent wires located nearby and transferred the heat to the flowing air. Removal of the net interrupted the sound even in the case when the total amount of heat supplied to the air stream remained the same as before. A possible explanation for this effect is that after removal of the dense net the stream behind the wires became stratified,

inasmuch as the heating wires were not sufficiently densely placed, and the distances between them exceeded their diameter by ten times.

Manu-
script
Page
No.

[Footnotes]

- 404 The latter follows, for example, from Eqs. (45.5). When $\varphi = 0$ we have $\bar{v}_1 = 0$ and consequently $\bar{Y}_{y0} = 0$, i.e., the direction of the vector \bar{Y} coincides with the direction of \bar{p}_1 .
- 424 See the experimental plots in Fig. 50. A more detailed discussion of this phenomenon will be given in the next chapter.
- 433 Crocco, L. and Cheng, S.I., High-Frequency Combustion Instability in Rocket Motor with Concentrated Combustion, Journ. of the Rocket Society 23; No. 5, 1953.
- 434 Lehmann, K.O. Über die Theorie der Netztöne [The theory of line hum], Annalen der Physik [Annals of Physics], 5, Series 29, 1937.

Manu-
script
Page
No.

[List of Transliterated Symbols]

- 401 crop = sgor = sgoraniye = combustion
- 425 c = s = sdvig = shift

Chapter 10

CERTAIN PARTICULAR CASES OF SELF-EXCITATION OF ACOUSTIC OSCILLATIONS

§48. Excitation of Sound in a Rijke Tube

While the vibration combustion processes considered in the preceding sections were connected to some degree or another with the mobility of the flame front, a classical example of a system in which the mobility of the surface of the heat conductor is completely excluded is the Rijke tube. In addition, the grid installed in such a tube is so thin, that its dimension in the direction of the tube axis can be neglected so that the volume V in Eqs. (15.5) can be equated to zero. This eliminates also the appearance of the mobility of a certain effective flame front, which is sometimes introduced to advantage out of formal considerations.

Consequently, the Rijke tube is the most outstanding example of the excitation of acoustic oscillations by the heat conductor. This circumstance makes it advantageous to consider the process of excitation of sound in such a tube, although it is not connected with any combustion process.

As already mentioned, a Rijke tube is a vertically mounted tube, in which a weak flow of air is produced. Usually this flow is connected with the fact that a heated grid placed in one of the cross sections of the tube heats the layers above it and thus produces a draft. A central factor in the analysis of the excitation of sound by a Rijke tube is the question of the transfer of heat from the heated grid to the

air flowing past it, and the connection between this heat transfer and the acoustic oscillations. Based on the results obtained in the preceding chapter, it is easy to carry out an analysis of these problems.

Let us consider the properties of the heat supply surface Σ . In the case described, the heated grid and the heat supply surface Σ , which is introduced in purely formal fashion, will coincide. This is perhaps the only case when the heat supply surface Σ has so clear-cut a physical meaning. Inasmuch as under ordinary conditions the grid can heat the air flowing past it only slightly, we shall assume that $M_1 = M_2$, $n = 1$, and therefore the equations for the connection between the parameters of the oscillations to the left and to the right of Σ assume in the simplest case the form (20.3):

$$\left. \begin{aligned} \bar{v}_2 &= \bar{v}_1 + \frac{\kappa-1}{2(1-M^2)} \bar{Q}, \\ \bar{p}_2 &= \bar{p}_1 - M \frac{\kappa-1}{2(1-M^2)} \bar{Q}. \end{aligned} \right\} \quad (48.1)$$

Attention should be called to the fact that the only parameter on which the self-excitation of the system can depend is the dimensionless perturbation of the heat supply \bar{Q} , which can be written [on the basis of Formulas (15.8) and (20.2)] in the form

$$\bar{Q} = 2M_1^2 \bar{Q}^* = \frac{2M_1^2}{Q^*} \delta Q^*. \quad (48.2)$$

Let us examine in greater detail the perturbation δQ^* of the heat supply. We shall assume that the wires making up the heated grid are sufficiently thin. In this case, to calculate the heat transferred per second from the grid to the air we can use one of the known formulas, for example, the King formula*:

$$\left. \begin{aligned} Q^* &= \frac{1}{\pi} \alpha (T_n - T) l, \\ \alpha &= \lambda \left(1 + \sqrt{\frac{2\pi Q^* D \nu}{\lambda}} \right), \end{aligned} \right\} \quad (48.3)$$

where λ is the heat conductivity of the air, D is the wire diameter, l

its total length, T_p the wire temperature, and T the temperature of the medium.

The factor $1/F$ is introduced in the first of these formulas to reduce the heat flow per second to a unit area of tube cross section.

If the oscillation frequency is low then, as can be seen from the second formula of (48.3) the perturbation of Q^* , i.e., the change δQ^* , will be in phase with the change in the stream velocity δv :

$$\delta Q^* = \frac{i\lambda(T_p - T)}{2F} \sqrt{\frac{2\pi\alpha c_p D}{\lambda_p}} \delta v. \quad (48.4)$$

At high oscillation frequencies, the picture is radically changed. The processes in the boundary layer become essentially nonstationary, and consequently the heat transfer also becomes nonstationary. A theoretical analysis of this phenomenon, and incidentally also its experimental investigation, entailed tremendous difficulties. Relatively recently, Lighthill obtained an approximate theoretical solution of such a problem for laminar flow past an infinitely long wire in a gas stream normal to the wire, the stream velocity in which had a small sinusoidal component.* The result obtained by him reduces, in short, to the following: if the oscillation frequency is quite large, then the phase of the perturbation in the heat transfer will start lagging the phase of the velocity perturbation by an angle $\pi/2$, independently of the frequency. The amplitude of the perturbation of the heat transfer decreases monotonically with increasing oscillation frequency. Figure 95, which is borrowed from the cited paper, shows two curves. One yields the value of ψ , which is the phase delay of δQ^* relative to the stationary value δQ^*_{st} (the value of δQ^* which would be obtained in the case of infinitesimally low oscillation frequency), while the second shows the ratio of the amplitudes $|\delta Q^*|/|\delta Q^*_{st}|$, equal to η . Both curves are plotted as functions of the parameter $2\pi\Omega D/v$, where Ω

is the frequency of the acoustic oscillations in cycles per second, while D is the diameter of the wire. The curves presented show that the attenuation η of the perturbation in the heat supply can become appreciable at sufficiently large values of Ω , while the phase delay increases with the frequency sufficiently rapidly and in practice reaches its limiting value, equal to $\pi/2$, at the instant when the attenuation of the amplitude of the heat supply perturbation is of the order of 0.15. If we estimate the order of magnitude of the parameter $2\pi\Omega D/v$, which can be observed in the Rijke tube, then we find it to be close to 30 when $D = 1$ mm, $\Omega = 500$ cps, and $v = 0.1$ m/sec. This indicates that one can expect in the Rijke tube an appreciable attenuation of the heat supply perturbation amplitude (by approximately a factor of ten compared with the corresponding value for the quasistationary process), and a limiting phase delay equal to $\pi/2$.

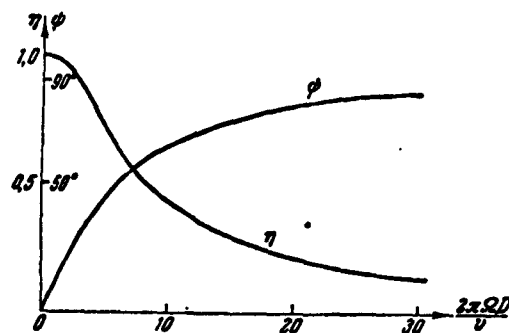


Fig. 95. Attenuation η of the amplitude and the phase delay ψ in the transfer of heat from a wire to a stream of air which has a harmonic component.

While the attenuation of the heat supply perturbation amplitude has only a quantitative influence on the excitation of sound in the Rijke tube, the phase delay is the most important factor in the present phenomenon. It is easy to verify that in the absence of a phase delay no sound would be ever excited in the Rijke tube. Indeed, when

the phase of \bar{Q} and the phase of \bar{v}_1 to coincide [Formula (48.4)], then on the basis of Formulas (17.1) and (48.1)

$$\left. \begin{aligned} \delta E = \bar{v}_2 - \bar{v}_1 &= \frac{\kappa-1}{2(1-M^2)} \bar{Q}, \\ \delta X = \bar{p}_2 - \bar{p}_1 &= -M \frac{\kappa-1}{2(1-M^2)} \bar{Q} \end{aligned} \right\} \quad (48.5)$$

δE would also have a phase that coincides with the phase of \bar{v}_1 , while δX would have an opposite phase. Assuming that there are no losses in the external medium, we could write the condition for the excitation of acoustic oscillations in the form of the inequality

$$\bar{A}_z > 0.$$

At the same time, according to Formula (19.2),

$$\bar{A}_z = \frac{1}{2} (\bar{p}_1 \delta E + \bar{v}_1 \delta X + \delta E \delta X).$$

Inasmuch as there are no external losses, $\bar{p}_1 \perp \bar{v}_1$ and consequently the first of the three components of A_z is equal to zero, while the two others are negative (δX is in phase opposition with \bar{v}_1 and δE). Consequently, $A_z < 0$, and excitation of sound is impossible. Thus, the delay in the phase of the velocity perturbation is a necessary condition for the self-excitation of acoustic oscillations in a Rijke tube.

One must not think that the use of Lighthill's theoretical curves always yields a limiting phase delay equal to $\pi/2$. The numerical example given above corresponded to some degree to the extreme case. A more real case would be the excitation of sound in a long Rijke tube with the aid of a grid consisting of relatively thin wires. If we put $\Omega = 100$ cps, $D = 0.3$ mm, and $v = 0.3$ m/sec, then $2\pi\Omega D/v \cong 0.6$, i.e., the phase delay ψ will be on the order of several degrees, and the attenuation in the amplitude of the heat supply perturbation will be practically nil in general ($\eta \cong 1$). Thus we can expect the parameter $2\pi\Omega D/v$ and the phenomena associated with it to have a rather wide range of variation in the Rijke tube.

It is appropriate to emphasize here that the use of Lighthill's theoretical results for the calculation of self-excitation of sound in a Rijke tube can hardly be recognized as a valid operation without a further investigation of this problem.

The wires making up the grid operate under entirely different conditions than those which Lighthill used as the basis of his calculation. He considered a single wire in infinite space, whereas in a grid the distances between the wires are of the same order of magnitude as their diameters, and the mutual influence of neighboring wires is undoubtedly appreciable. In addition, Lighthill assumed that the sinusoidal component of the stream velocity is small compared with its average velocity, whereas Lehmann's experiments have shown* that in a Rijke tube the amplitude of the velocity oscillation actually exceeds the average stream velocity by 2-6 times. It is quite clear that such a change in the conditions of flow past the wire should noticeably change the curves of Fig. 95.

Lehmann's experiments confirm the assumption advanced here indirectly. Were it possible to apply the Lighthill curves directly to grids in the Rijke tube, then the variation of the wire diameter would greatly influence the self-excitation of the sound. The aforementioned experiments show, however, that there is practically no such influence.

At the present time there are no data on the nonstationary heat transfer from heated grids, so that a quantitative analysis of the sound produced in a Rijke tube is factually impossible. In order to present a qualitative idea of this phenomenon, we can use Lighthill's curve, which makes it possible to take into account the most important factor, namely the presence of a phase delay between the perturbation of the heat supply and the perturbation of the velocity.

Before we proceed to a numerical analysis of the excitation of sound in a Rijke tube, we must make more precise the first-approximation formulas (48.1), which were used up to now as relations describing the process on the heat supply surface Σ . It is necessary to introduce refinements into these relations. First, they can be refined by taking into account the fact that the temperature of the air passing through the grid is higher than the temperature of the air approaching the grid. In the already-mentioned experiments by Lehmann it was shown that in normal conditions the air is heated by 100-150° past the grid, i.e., relatively little. Therefore an account of the heating (i.e., an account of the fact that $M_1 \neq M_2$; $n \neq 1$) cannot noticeably influence the results of the analysis.

More significant is an account of the hydraulic resistance of the grid. In considering the combustion process in furnaces or in combustion chambers it is usually possible to neglect hydraulic losses, since they are small. In describing the excitation of sound in a Rijke tube, it is always indicated that the grid must be dense, and this involves noticeable hydraulic resistances. The general equations obtained in Chapter 4 enable us to take this factor into account, too. If we start from the system of equations (20.1) and assume that all the terms connected with the perturbation of heat supply are equal to zero, with the exception of $\bar{Q} = 2M_1^3 Q^*$, then we can obtain in place of the relations (48.1) the following equations

$$\left. \begin{aligned} \bar{v}_2 &= \bar{v}_1 + \frac{\kappa-1}{2(1-M^2)} \bar{Q} - \frac{\kappa M^2}{1-M^2} \bar{P}_2, \\ \bar{P}_2 &= \bar{P}_1 - M \frac{\kappa-1}{2(1-M^2)} \bar{Q} + \frac{(\kappa-1)M^2 + M^2}{1-M^2} \bar{P}_2. \end{aligned} \right\} \quad (48.6)$$

Accordingly, in place of (48.5) we must write

$$\left. \begin{aligned} \delta E &= \frac{\kappa-1}{2(1-M^2)} \bar{Q} - \frac{\kappa M^2}{1-M^2} \bar{P}_2, \\ \delta X &= -M \frac{\kappa-1}{2(1-M^2)} \bar{Q} + \frac{(\kappa-1)M^2 + M^2}{1-M^2} \bar{P}_2. \end{aligned} \right\} \quad (48.7)$$

The quantity \bar{P}_x can be readily related with the hydraulic resistance coefficient ζ , if it is assumed that the steady-state hypothesis is applicable in this case. Indeed, denoting the pressure losses on the grid by p_ζ , let us write down the ordinary hydraulic equation

$$p_\zeta = \zeta \frac{\rho v^2}{2}.$$

The perturbation of this quantity will be

$$\delta p_\zeta = \zeta \rho v \delta v_1.$$

The quantity $\bar{P}_x = -\delta p_\zeta$ will characterize the force action of the grid on the stream. By changing to the dimensionless variables (15.8) we obtain

$$\bar{P}_x = -\frac{\delta p_\zeta}{\rho v^2} = -\frac{\zeta}{M} \bar{v}_1. \quad (48.8)$$

We determine the quantity \bar{Q} by starting from Eqs. (48.2) and (48.3). We assume that the root entering into the expression for α (48.3) is appreciably larger than unity*:

$$\sqrt{\frac{2\pi Q c_p D v}{\lambda}} \gg 1. \quad (48.9)$$

We can then write

$$Q^* = A \sqrt{v},$$

where A is a certain constant.

Accordingly

$$\delta Q_{cr}^* = \frac{A}{2\sqrt{v}} \delta v_1$$

or

$$\delta Q_{cr}^* = \frac{Q^*}{2v} \delta v_1. \quad (48.10)$$

Using Formula (48.2), we write

$$\bar{Q}_{cr} = \frac{Q^*}{\rho v^2} \bar{v}_1. \quad (48.11)$$

where Q^* corresponds to the heat supplied from the grid in the absence of flow perturbations.

Formulas (48.7), (48.8), and (48.11) define completely the process on the discontinuity surface Σ , if we regard as known the heat supply Q^* , the hydraulic resistance coefficient of the grid ζ , and the parameters η and ψ , which characterize the deviation of the process of heat transfer from the grid to the air from the steady state.

With all the foregoing data available, one could solve the corresponding boundary problem, similar to what was done in Chapters 5, 6, and elsewhere. However, it is simpler to obtain a sufficiently complete notion of the excitation of sound in a Rijke tube by using the energy method, developed in Chapters 3 and 4. In the case under consideration, the use of the energy method is suggested because the frequencies of the excited oscillations can be regarded as known. All the researchers who have investigated the sound produced by a Rijke tube always indicate that the oscillations excited have frequencies determined by the usual acoustic relations (i.e., they can be determined without account of the constant component of the stream velocity along the tube or an account of the properties of the heat supply zone). Inasmuch as the only important parameter of the oscillations, namely the frequency, the determination of which is impossible from energy considerations, is known, the use of the energy method is perfectly natural.

By way of typical numerical data we shall use those realized in Lehmann's experiments. This makes it possible to compare the calculation results with experiment. In the experiments cited, the bulk of the tests were made on a tube with diameter $d = 67$ mm and total length $L = 1140$ mm. Oscillations at the fundamental frequency were usually excited in the tube (165 cps), and sometimes also the second harmonic (frequency 330 cps). The flow velocity in the tube was varied at the experimenter's will, since it was produced not by draft but with a fan

which fed air to a large receiver, to which the tube was connected. A thin wire located at some cross section of the tube (diameter 0.2 mm, pitch 2 mm) was heated with electric current. A dense metallic grid was placed in the direct vicinity of the incandescent wire, received the heat from the latter, and transferred it to the air. As already indicated, the incandescent wire itself (without the dense grid) could not excite sound. The diameter of the wires of which the dense grid was made up exerted only a slight influence on the process of sound excitation (in Lehmann's experiments, the number of meshes per square centimeter was varied from 1115 to 46.8, which apparently corresponds to a variation in the diameters of the wires making up the grid from 0.1 mm to 0.5 mm). The average flow velocity in the tube changed from 0 to 0.7 m/sec. The strongest sound was obtained at velocities 0.3 to 0.45 m/sec. The amount of heat transferred from the grid to the air varied from 272 to 480 watts.

We shall assume for our calculations certain average values of the parameter, with which the Lehmann experiments were characterized. Let the stream velocity be $v = 0.35$ m/sec, the average heat supply $Q^* = 432$ watts, the average velocity of sound in the tube 376 m/sec (determined from the observed oscillation frequencies), and the diameter of the wire of which the grid is made up $D = 0.35$ mm. For the fundamental tone ($\Omega = 165$ cps) this yields $2\pi\Omega D/v \cong 1$ and accordingly $\eta \cong 1$ and a delay $\psi \cong 6^\circ$.

Although the latter quantities were obtained on the basis of Lighthill's plot (Fig. 95), the validity of which is subject to legitimate doubt, they will be used here as certain first-approximation parameters, which probably are of the correct order of magnitude, particularly since there are no other data at present. The principal factor introduced here is a certain delay in the perturbation of the heat

supply \bar{Q} relative to the perturbation of the velocity \bar{v} .

We now use the well-known energy condition (19.3) which is valid for the stability boundary

$$\bar{A}_z - \bar{R} = 0. \quad (48.12)$$

Let us calculate both quantities contained in this equation. As already mentioned in the present section

$$\bar{A}_z = \frac{1}{2} [\bar{p}_1 \delta E + \bar{v}_1 \delta X + \delta E \delta X].$$

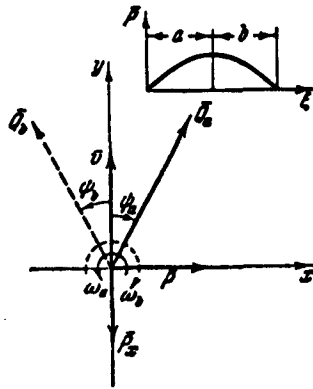


Fig. 96. Phase shift of the vector \bar{Q} resulting from the delay, as a function of the position of the heat supply section relative to the standing wave of the pressure oscillations.

Let us determine the phase shifts between the vectors contained in the equation written out. We first consider the position of the vectors in Fig. 96. The vectors \bar{p} and \bar{v} have the customary directions, the first along the positive x axis and the second along the y axis (it is assumed here that \bar{R} is small). The vector \bar{P}_x , as follows from Eq. (48.8) is always directed opposite to the vector \bar{v} . The vector \bar{Q} has at very low frequencies the same phase as \bar{v} , and in general its phase is shifted relative to \bar{v}_1 by an angle ψ , as a result of the delay. In order

to determine in which direction relative to the y axis to draw the angle ψ , it is necessary to take into consideration, in order to find the phases of \bar{Q} , the direction of rotation of the entire vector diagram with angular velocity ω . It is easy to visualize that this direction will be different for different portions of the standing pressure wave. In the upper part of Fig. 96 is shown a standing wave of the pressure oscillations, covering half of a complete wavelength. The half wave shown in this figure is broken up into sections a and b , lying on both sides of the pressure antinode. In

section a the perturbation of stream velocity reverses sign on going through the pressure maximum, and changes from positive (directed toward the pressure antinode) to negative. The reason for it is that upon gradual compression of the gas by the masses moving toward the pressure antinode, the pressure increases, reaches a maximum, after which the oscillatory component of the stream velocity reverses sign, since the gas acquires a component of motion to the left, toward the lower pressures. And exactly the same process in section b causes the oscillatory component of the stream velocity to reverse sign when the pressure perturbation goes through the maximum, and to change from negative to positive. This is why the direction of ω will be different in the vector diagram of Fig. 96 for sections a and b: for section a it will be counterclockwise and for section b clockwise. In general, for the assumed measurement directions, the portions of the standing wave lying between the node and the antinode of the pressure and those located to the left of the pressure antinode, will be characterized by the direction of the angular velocity ω_a , while the remaining sections will be characterized by angular velocity ω_b . Inasmuch as the phase shift ψ is due to delay, the position of the vector \vec{Q} will be different: for section a \vec{Q} will be shifted by an angle ψ to the right of \vec{v}_1 , while for section b it will be shifted to the left.

Let us consider now the expression for \bar{A}_Σ .

Using (48.7) and neglecting the small term $\kappa M^3 \bar{P}_x / (1 - M^2)$ and the quantity M^4 compared with M^2 , we can write for sections a

$$\begin{aligned} \bar{A}_i = \frac{1}{2} \left\{ \frac{\kappa - 1}{2(1 - M^2)} |\bar{P}_1| |\vec{Q}| \cos(90^\circ - \psi) + \right. \\ \left. + M \frac{\kappa - 1}{2(1 - M^2)} |\vec{v}_1| |\vec{Q}| \cos(180^\circ + \psi) - \right. \\ \left. - \frac{M^2}{1 - M^2} |\bar{P}_x| |\vec{v}_1| - \left[\frac{\kappa - 1}{2(1 - M^2)} \right]^2 M |\vec{Q}|^2 + \right. \\ \left. + \frac{(\kappa - 1) M^2}{2(1 - M^2)} |\vec{Q}| |\bar{P}_x| \cos(180^\circ - \psi) \right\}. \end{aligned}$$

For section b, the expression for \bar{A}_z will be exactly the same, except that the signs in front of ψ must be reversed.

Let us simplify the expression written out by putting $1 - M^2 = 1$, $(\kappa - 1)/2 = 0.2$, and assuming the angle ψ to be small in absolute value. We then have for sections a

$$\begin{aligned} \bar{A}_z \approx \frac{1}{2} [0.2|\bar{p}_1||\bar{Q}|\sin\psi - 0.2M|\bar{v}_1||\bar{Q}| - \\ - M^2|\bar{p}_x||\bar{v}_1| - 0.04M|\bar{Q}|^2 - 0.2M^2|\bar{Q}||\bar{p}_x|]. \end{aligned} \quad (48.13)$$

As follows from this equation, at small absolute values of ψ all the terms except the first yield negative quantities, i.e., they suppress the oscillations. Only the first term can be positive when $\psi > 0$, which is possible only for the sections a. For sections b we have $\psi < 0$ and consequently excitation is impossible, as follows from this formula. This result can be expected, since it was indicated above many times that when the vector of the perturbed heat supply is in the second quadrant, excitation is impossible (see, for example, the stability diagrams in Fig. 29).

Let us substitute the values of \bar{Q} and \bar{p}_x obtained a little while ago into Relation (48.13). For the chosen numerical quantities we get

$$|\bar{Q}| = \frac{0.7}{y} \bar{v}_1, \quad (48.14)$$

where y must be taken in m/sec. To determine the value of \bar{p}_x we specify $\zeta = 5$, which corresponds approximately (at small Reynolds numbers) to a wire grid with a ratio of live cross section to the tube cross section on the order of 0.4-0.5.* Carrying out the necessary calculations, we obtain the following expressions

$$\begin{aligned} \bar{A}_z = 0.02|\bar{v}_1||\bar{p}_1| - 0.0035|\bar{v}_1|^2 \text{ for section } \underline{a}, \\ \bar{A}_z = -0.02|\bar{v}_1||\bar{p}_1| - 0.0035|\bar{v}_1|^2 \text{ for section } \underline{b}. \end{aligned} \quad (48.15)$$

The variation of $|\bar{v}_1|$ and $|\bar{p}_1|$ as a function of the position of the grid along the length of the tube can be assumed to be

$$|\vec{v}_1| = c |\cos \varphi|, |\vec{p}_1| = c |\sin \varphi| (c > 0),$$

where $\varphi = k\pi\xi$, as follows from Formulas (6.3).

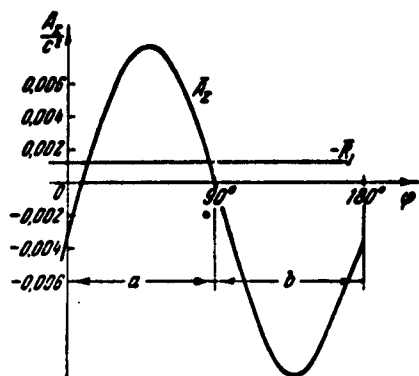


Fig. 97. Flux of acoustic energy as a function of the position of the heat supply plane along the length of the tube.

A plot of \bar{A}_Σ / c^2 as a function of the parameter φ is shown in Fig. 97. As can be seen from the plot, positive values of \bar{A}_Σ extend from $\varphi = 10^\circ$ to $\varphi = 90^\circ$. Equation (48.2) enables us to calculate the energy losses due to radiation from the open ends of the tube. In the presence of radiation losses, the vectors \vec{p}_1 and \vec{v}_1 cease to be mutually perpendicular and therefore Formula (48.13) should include in addition the rotation of \vec{v}_1

relative to \vec{p}_1 , but inasmuch as this rotation will be small for small losses, we shall not introduce here a corresponding correction, and assume that the expression for \bar{A}_Σ , given by Formulas (48.15), is correct.

For specified values of \underline{d} and L , the end impedance of the tube (30.8) will be equal to

$$z = 0,000216\omega^2 + 0,0187\omega i,$$

where the dimensionless frequency of the oscillations ω is $\omega = \pi$ for the first harmonic and $\omega = 2\pi$ for the second.

Using the obtained value of \underline{z} , let us determine the radiation losses from both ends of the tube. This can be done by doubling the flux of acoustic energy from one end cross section

$$\bar{R} = \bar{p} \bar{v}.$$

It must be taken into account here that $|\vec{v}| \cong c$ and the quantity $|\vec{p}|$ and the angle between \vec{p} and \vec{v} can be readily obtained from the equation

$$\vec{p} = z\vec{v}.$$

Calculations yield for the first harmonic

$$\frac{\bar{R}_I}{c^2} = 0,0014,$$

and for the second

$$\frac{\bar{R}_{II}}{c^2} = 0,0056.$$

The line \bar{R}_I/c^2 is drawn on the plot of Fig. 97. It makes it possible to separate the instability region, corresponding to $\bar{A}_\Sigma - \bar{R}_I > 0$, which extends from $\varphi \cong 14^\circ$ to $\varphi \cong 87^\circ$. A perfectly analogous construction can be made also for the second harmonic. If it is recognized here that doubling the parameter $2\pi\Omega D/v$ increases the delay by approximately the same factor, and that the losses are $\bar{R}_{II}/c^2 \cong 0.0056$, the instability region is found to extend from $\varphi = 13^\circ$ to $\varphi = 83^\circ$.

Using the relation $\varphi = k\pi\xi$ which was already given above ($k = 1$ for the first harmonic and $k = 2$ for the second), let us plot the instability regions for the first two harmonics as functions of the relative position of the grid along the length of the tube (Fig. 98). The diagram presented is in good agreement with the experimental data. First, we see that the fundamental tone of the tube can be excited only if the coordinate $\xi < 0.5$, i.e., if the grid is in the lower part of the tube. Moreover, if we turn to Fig. 97, we see immediately that the difference $\bar{A}_\Sigma - \bar{R}$ reaches a maximum value at approximately $\varphi = \pi/4$, i.e., when $\xi = 0.25$. This is in complete agreement with the indications made by the experimenters, that the strongest sound is produced when the heated grid is located at a distance equal to $1/4$ of the total length of the tube, measuring from the lower end. When $\xi < 0.25$ the second harmonic also becomes unstable. In Lehmann's experiments this circumstance was registered in the form of a superposition of the two harmonics at $\xi < 0.25$, and with decreasing ξ the second harmonic started to play an ever more noticeable role. The corresponding oscillograms are shown in Fig. 99.

An analysis of the diagrams constructed explains why, in the experiments of Bossch and Reiss, sound was excited only when $\xi > 0.5$, i.e., with the grid in the top of the tube. Inasmuch as the grid

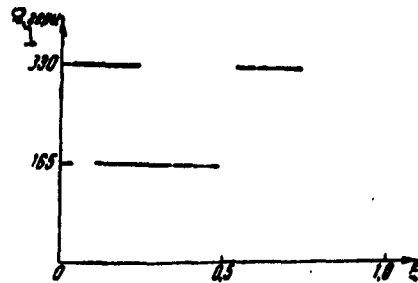


Fig. 98. Distribution of the instability regions along the tube for the first two harmonics. 1) Ω , cps.

produced cooling in these experiments, the phase of the heat supply, determined in accord with the steadystate hypothesis, differed by π from that in the case when the grid is heated. This is seen from Formula (48.4), inasmuch as the signs of the difference $T_p - T$ are different for the cooling and heating grids. Then, when the phase of the heat supply lags, the vector \bar{Q} falls in the fourth quadrant

if the grid is located in region b on Fig. 96, and this corresponds to the best excitation conditions. At the same time, the position of the grid in region a moves \bar{Q} to the third quadrant, in which there are practically no excitation regions at small values of M , inasmuch as the stability diagram approaches the form shown in Fig. 29c.

Summarizing, we can state that even the use of a scheme of non-steady-state heat transfer which is crude under the conditions considered, as is the scheme that follows from Lighthill's theoretical calculations, yields all the most essential properties of the Rijke tube.

In addition to the already known properties of the Rijke tube, Lehmann made use of the fact that he was able to regulate the average flow velocity at his convenience, detected a new property of this tube: with increasing average stream velocity and at a constant average heat supply, the sound produced by the Rijke tube first increases, reaches a maximum intensity, and then decreases and ceases completely after reaching a certain velocity, depending on the average heat supply.

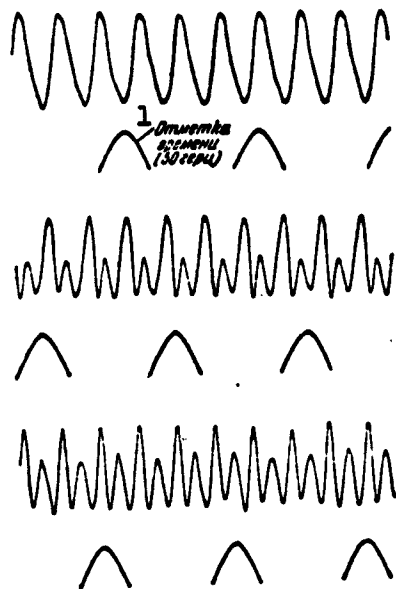


Fig. 99. Oscillogram of pressure oscillations in Rijke tube in accordance with Lehmann's experiments. The upper oscillogram corresponds to $\xi = 0.25$; the central one to $\xi = 0.125$; the lower one to $\xi = 0.0625$. 1) Time marker (50 cps).

The fact that the Rijke tube ceases to produce sound at a certain sufficiently large velocity can be understood from the formulas written out above. Indeed, let the average heat supply remain constant: $Q^* = \text{const.}$ Then, as follows from (48.11), $|\bar{Q}|$ will decrease and consequently the only term of the expression (48.13) which gives a positive flux of acoustic energy \bar{A}_Σ will also decrease. At the same time, the main term which produces a negative component of \bar{A}_Σ , namely $M^2 |P_x| |\bar{v}_1|$, will increase because, with account of (48.8), we have

$$M^2 |P_x| |\bar{v}_1| = \zeta M |\bar{v}_1|.$$

In the case considered above, at the optimum grid position ($\xi = 0.25$,

i.e., $|\bar{v}_1| = |\bar{p}_1| = 0.707c$), the indicated two terms in the sum (48.13) will yield

$$\frac{1}{2} 0.707^2 c^2 \left(0.2 \frac{0.7}{\sigma} \sin \psi - 5 \frac{\nu}{a} \right),$$

i.e., an expression that decreases monotonically with increasing ν . If a more accurate numerical analysis is made, then, without taking account of the possible change in ψ , \bar{A}_Σ / c^2 becomes equal to \bar{R} / c^2 at a velocity on the order of 0.75 m/sec. Experiment yielded for this quantity a value 0.6 m/sec. For so complicated a phenomenon, we must admit that such agreement between the theoretical calculation and the experimental data is good.

In addition to the cessation of the sound from the Rijke tube

when the average flow velocity is increased, we also observe the same effect when it is reduced to values of the order of 0.15 m/sec. This is in all probability linked with the fact that when the average flow velocities are reduced while maintaining the same heat-supply value, sharp heating of the air occurs in the neighborhood of the grid (including in advance of it) and preheating of the oncoming air is effected to a considerable degree by the natural turbulence of the flow, as a result of mixing of the moles of cold and hot air even before the former have crossed the first section in which grids are positioned. To the extent that turbulent mixing of the cold and hot moles takes place, in first approximation, independently of acoustic vibrations, this results in breaking off of the feedback in the oscillatory system. It must be noted that the assumption made here has not been subjected to quantitative verification and that it should therefore be regarded as only one of the possible explanations for cessation of sounding in the Rijke tube at low values of the average flow velocities.

§49. Vibrational Combustion in Propagation of Flame in Stationary Gas

One of the first carefully designed experiments with vibrational combustion was that of Coward, Hartwell and Georgson, who have already been mentioned in earlier Chapters. It will be recalled that this experiment studied the propagation of a flame front along a tube filled with a stationary combustible mixture, with one end of the tube closed and ignition supplied at the open end.

The basic feedback mechanism was determined almost unequivocally in this experiment, permitting quite complete analytical examination of the problem. Actually, since we deal with combustion in a prepared homogeneous mixture, all feedback mechanisms that are based on mixture formation are excluded at once, and mechanisms in which the basic role

is played by vortex formation and other hydromechanical factors are likewise eliminated. From among the phenomena connected with the combustion proper, we eliminate immediately the entire group of processes whose realization requires the presence of an igniting source (such as an acetylene torch, etc.). The dependence of the rate of flame propagation on the parameters of the stationary medium in which the front of the flame moves is more or less known. However, neither the pressure oscillations, nor the temperature oscillations in the stationary gas, which were observed in experiment, can cause so strong a change in the rate of propagation of the flame as to cause the system to become excited. For this reason, the inclusion of various types of considerations connected with the period of induction, due for example to oscillations of pressure, can likewise yield no convincing results. Apparently the principal feedback mechanism, which plays a decisive role in this experiment, is the mechanism connected with the periodic wave production on the surface of the flame, which was considered in the second half of §38.

Unlike the principal analysis of this problem, which we considered above, we shall give here a solution for several simplified conditions, but the solution will be carried through to conclusion.

As was indicated in §38, in the case of acoustic oscillations of the medium, the flame front situated in it experiences the action of periodically varying accelerations. In this case the deviation of the perturbed flame front from its steady-state position $x = 0$ in the \underline{x} direction (for a certain specified value of the coordinate \underline{y}) is described by the Mathieu equation (38.25) (here \underline{z} is a quantity proportional to the time \underline{t}):

$$A''(z) - 2q \cos 2z A(z) = 0. \quad (49.1)$$

Inasmuch as the tubes in which the experiments were made by Coward,

Hartwell, and Georgson were positioned horizontally, the coefficient a in Eq. (38.25) was assumed equal to zero. With this, in order to make a solution of this equation possible in terms of elementary functions, we introduce the following assumption. We replace the periodic function $\cos 2z$ by an approximate function made up of sections with constant values of the function, as shown in Fig. 100. In addition, we shift the origin of the argument z by $\pi/4$, introducing the variable $z_1 = z + \pi/4$. We can then write in place of (49.1)

$$A''(z_1) + \varphi(z_1) A(z_1) = 0, \quad (49.2)$$

where $\varphi(z_1) = +m^2$ for the intervals $0 < z_1 < \pi/2$, $\pi < z_1 < 3\pi/2$, etc., and $\varphi(z_1) = -m^2$ for the intervals $\pi/2 < z_1 < \pi$, $3\pi/2 < z_1 < 2\pi$, etc.

The value of m^2 is determined here by the formula

$$m^2 = 16 \frac{h_0(q_1 - q_2)}{\lambda(q_1 + q_2)}. \quad (49.3)$$

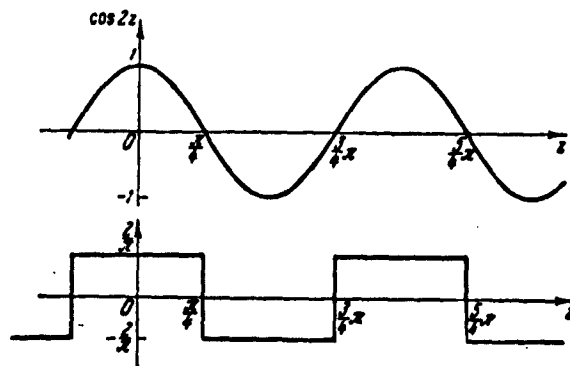


Fig. 100. Replacement of the cosine function by a discontinuous square-wave function.

The expression presented here for m^2 has been derived by comparing Eq. (38.25) with Eq. (49.2). It is taken into account here that the average value of $\cos 2z$ has an absolute value $2/\pi$ over the interval where this function does not reverse sign.

Equation (49.2), like the Mathieu equation, is an equation with periodic coefficient (the coefficient of $A(z_1)$ varies as a function of

z_1 in accordance with the law shown in the lower plot of Fig. 100). In the appropriate branches of mathematical analysis it is shown that an equation of this type has a solution in the form

$$A(z_1) = C_1 e^{s_1 z_1} f_1(z_1) + C_2 e^{s_2 z_1} f_2(z_1), \quad (49.4)$$

to which the solution (38.26) also belongs. Here the functions $f_1(z_1)$ and $f_2(z_1)$ are periodic and the characteristic exponents s_1 and s_2 are constant quantities.

On the basis of the foregoing we shall seek a solution of Eq. (49.2) in the form

$$A(z_1) = C e^{i z_1} f(z_1). \quad (49.5)$$

We break up the entire z_1 axis into segments of length $\pi/2$; we shall designate as segments of the first type those in which $\varphi(z_1) = m^2$ and of the second type those where $\varphi(z_1) = -m^2$. Let us consider an aggregate of two neighboring segments of the first and second types. Assume, for the sake of being definite, that these are the segments $0 \leq z_1 \leq \pi/2$ and $\pi/2 \leq z_1 \leq \pi$. Then the solution of the differential equation (49.2) will be, for the first segment,

$$A_1 = C_1 e^{i m z_1} + C_2 e^{-i m z_1} \quad (49.6)$$

and for the second segment,

$$A_2 = C_3 e^{m z_1} + C_4 e^{-m z_1}. \quad (49.7)$$

These solutions must be joined together in suitable fashion. For this purpose we must stipulate that on the boundaries between the segments the quantities A_1 and A_2 , as well as their derivatives dA_1/dz_1 and dA_2/dz_1 coincide. In addition, it is necessary to take into consideration the requirement which is the consequence of the periodicity of the function $f(z_1)$ in Eq. (49.5). We denote the period of this function by τ ; it is then natural to assume that this period will coincide with the period of the function $\varphi(z_1)$ which is contained in Eq. (49.2), or else be its multiple. The period of the function $\varphi(z_1)$ is, as fol-

lows from Fig. 100, $\tau = \pi$; we can therefore write two more conditions relating the start and the end of the interval corresponding to the aggregate of two neighboring segments of the first and second types: $\alpha A_1(0) = A_2(\pi)$; $\alpha(dA_1/dz_1)(0) = dA_2/dz_1(\pi)$, where $\alpha = e^{s\pi}$. We thus have the following four conditions:

$$\left. \begin{aligned} A_1\left(\frac{\pi}{2}\right) &= A_2\left(\frac{\pi}{2}\right); & \alpha A_1(0) &= A_2(\pi), \\ \frac{dA_1}{dz_1}\left(\frac{\pi}{2}\right) &= \frac{dA_2}{dz_1}\left(\frac{\pi}{2}\right); & \alpha \frac{dA_1}{dz_1}(0) &= \frac{dA_2}{dz_1}(\pi). \end{aligned} \right\} \quad (49.8)$$

Substitution of Solutions (49.6) and (49.7) into the conditions (49.8) yields the following system of equations:

$$\left. \begin{aligned} C_1 e^{im\frac{\pi}{2}} + C_2 e^{-im\frac{\pi}{2}} - C_3 e^{m\frac{\pi}{2}} + C_4 e^{-m\frac{\pi}{2}} &= 0, \\ iC_1 e^{im\frac{\pi}{2}} - iC_2 e^{-im\frac{\pi}{2}} - C_3 e^{m\frac{\pi}{2}} + C_4 e^{-m\frac{\pi}{2}} &= 0, \\ \alpha C_1 + \alpha C_2 - C_3 e^{m\pi} - C_4 e^{-m\pi} &= 0, \\ i\alpha C_1 - i\alpha C_2 - C_3 e^{m\pi} + C_4 e^{-m\pi} &= 0. \end{aligned} \right\} \quad (49.9)$$

The system (49.9) can have nontrivial solutions only if its determinant vanishes. If we write this condition, then after simple but rather cumbersome calculations we obtain the following equality:

$$\alpha^2 - 2 \left(\frac{e^{im\frac{\pi}{2}} + e^{-im\frac{\pi}{2}}}{2} \right) \left(\frac{e^{m\frac{\pi}{2}} + e^{-m\frac{\pi}{2}}}{2} \right) \alpha + 1 = 0$$

or

$$\alpha^2 - 2 \cos m \frac{\pi}{2} \operatorname{ch} m \frac{\pi}{2} \alpha + 1 = 0. \quad (49.10)$$

Using the equality written out here, we can find two values of α for which the system (49.9) has solutions that differ from zero. These two values (α_1 and α_2) determine two values of the characteristic exponents s_1 and s_2 , which enter into the general solution (49.4). Even without finding the numerical values of α_1 and α_2 , we can point to several properties of these quantities. From the form of the coefficients of the quadratic equation (49.10) it follows that $\alpha_1 \alpha_2 = 1$. Consequently, if the modulus of one of the numbers is larger than unity, then the modulus of the second is less than unity, and vice versa.

Thus, the difference between the modulus of one of the numbers α_1 or α_2 from unity is evidence that the wave motion on the flame surface is unstable, for then there must exist $|\alpha| > 1$ between α_1 and α_2 , which corresponds to $s > 0$, i.e., to an instability [one must not forget that the independent variable z_1 in the solution (49.4) is proportional to the time t]. Consequently, a stable process (without a growth in the oscillation amplitudes with time) is possible only when $\alpha_1 = \alpha_2 = 1$ or for complex values of α_1 and α_2 . Indeed

$$\alpha_{1,2} = \cos m \frac{\pi}{2} \operatorname{ch} m \frac{\pi}{2} \pm i \sqrt{1 - \cos^2 m \frac{\pi}{2} \operatorname{ch}^2 m \frac{\pi}{2}}. \quad (49.11)$$

When $\cos m\pi/2 \operatorname{ch} m\pi/2 < 1$, the modulus of the number α_1 or α_2 (the square of which is equal to the sum of the squares of the real and imaginary parts) is exactly equal to unity. This shows that the characteristic exponent s has a real part equal to zero, i.e., the amplitudes of the waves on the surface of the flame will not start to grow with time z_1 .

Formula (49.11) shows that the quantities $\alpha_{1,2}$ depend on the number m . Let us analyze this influence of the number m on stability in greater detail. Such an analysis will be analogous to the problem considered in §38, concerning the influence of the coefficient q on the character of the solution of the Mathieu equation. Comparing Eqs. (49.1) and (49.2) we can establish between these two parameters a numerical correspondence which approximately corresponds to the essence of the phenomenon:

$$m^2 = \frac{4}{\pi} q \quad (49.12)$$

(it is assumed here that the average absolute value of $\cos 2z$ is equal to $2/\pi$).

When the number m is varied continuously, the roots α_1 and α_2 likewise vary continuously. By virtue of the fact that $\alpha_1 \alpha_2 = 1$, it is

sufficient to follow the variation of only one of these roots. Before we proceed to the analysis of the dependence of α on \underline{m} , we recall that the function $\text{ch } x$ is even, always positive, monotonically increasing in $|x|$ and reaches its lowest value $\text{ch } x = 1$ when $x = 0$.

Let \underline{m} increase from zero to infinity. When $m = 0$ we have $\alpha_1 = 1$. With increasing \underline{m} , α_1 becomes a complex quantity until $\cos^2 m\pi/2 \text{ch}^2 m\pi/2$ begins to exceed unity (owing to the monotonic increase in $\text{ch}^2 m\pi/2$). At this instant, α_1 becomes a real root. Further, as a result of the approach of $\cos^2 m\pi/2$ to zero, α_1 again assumes a complex value, etc. Consequently, α_1 will alternately become real and complex, and as \underline{m} increases the intervals of the values of \underline{m} where α_1 is complex will become narrower and narrower owing to the rapid growth of $\text{ch}^2 m\pi/2$.

The alternation of the intervals of the values of \underline{m} where the root α_1 is real or complex, as described here, corresponds to an alternation of the regions of stability and instability of the wave formation on the flame front. A similar alternation of the stability and instability regions was described also above, in the analysis of the Mathieu equation (see §38).

Numerical analysis yields in this case the following results:

when	$0 < m^2 < 1.39$	α_1 is complex
when	$1.39 < m^2 < 9$	α_1 is negative real
when	$9 < m^2 < 25$	α_1 is positive real
when	$25 < m^2 < 49$	α_1 is negative real

.....

In writing out these inequalities we disregarded the narrow intervals of m^2 near $m^2 = 9$, $m^2 = 25$, $m^2 = 49$, ... in which α_1 is complex (the continuous transition from negative α_1 to positive α_1 and back occurs via complex values of α_1).

If we compare these intervals with the corresponding intervals of

the values of the coefficient g in the Mathieu equation (see §38) then, by using Formula (49.12), we can set up the following comparative table of the values of g :

Intervals of Values of g Corresponding to the Instability Regions

1 По уравнению Маттье (49.1)	2 По уравнению (49.2)
$0,91 < g < 7,5$ $7,5 < g < 21$ $21 < g < 42$	$1,09 < g < 7,05$ $7,05 < g < 19,6$ $19,6 < g < 38,4$

1) According to the Mathieu equation (49.1); 2) according to Eq. (49.2).

As can be seen from the foregoing table, the numerical correspondence between the two series of regions is much better than could be expected from so crude an idealization, namely replacement of a sine wave by a square wave. This circumstance gives grounds for hoping that other aspects of the investigated phenomenon will also be correctly represented by the approximate equation (49.2) not only qualitatively, but also with fully satisfactory quantitative correspondence.

As is known from §38, where the Mathieu equation is considered, the period of the functions $f(z_1)$ in the solution (49.4), of which the solution (38.26) is a particular case, is equal to 2π in the first and third intervals listed in the table, whereas in the second interval it is one half as large. The same property is also possessed by the functions $f(z_1)$, obtained by solving Eq. (49.2). In fact, for the first and third intervals α_1 is a negative quantity, while for the second interval it is positive. Consequently, in the latter case the function $f(z_1)$ returns to the same phase (more accurately, the phase changes by 2π) when z_1 changes by π , while in the first case ($\alpha_1 < 0$) the phase

of $f(z_1)$ will differ from the initial phase by π (since the amplitude of $f(z_1)$ reverses its sign). Therefore when $\alpha_1 < 0$ two steps are necessary in order to return to the initial phase, with each step changing the phase by π and both together changing it by 2π . This proves the foregoing statement.

At the end of §38 above we already mentioned that in order for the oscillations of the flame front surface to play the role of a feedback mechanism maintaining the acoustic oscillations of the medium the period of this wave production should be twice as large as the period of the acoustic oscillations (which is equal to π in terms of the variable z_1). Therefore, for an analysis of the interaction of the wave production on the flame surface and of the acoustic oscillations it is necessary to consider only those ranges of values of m^2 , for which α_1 is negative real. Of greatest interest here is the first of these intervals $1.39 < m^2 < 9$, which corresponds [as follows from Formula (49.3)] to the smallest amplitudes h_0 of the displacements of the medium during the acoustic oscillations.

In order to obtain a clear idea of the function $A(z_1)$, which is the solution of Eq. (49.2), we present here a numerical example. Let the initial perturbation on the surface of the flame be sufficiently small and assume that prior to the instant under consideration a sufficiently long time interval has lapsed, to permit one of the terms of the solution (49.4) to decrease to a negligibly small value. Inasmuch as we are considering here the case of instability, $|\alpha_1| > 1$, we find by virtue of the condition $\alpha_1 \alpha_2 = 1$ that $|\alpha_2| < 1$, i.e., the second term will decrease with time. We choose the value of m^2 near the boundary of the first interval characterized by $\alpha_1 < 0$. Let, for example, $m^2 = 1.46$. Then $\alpha_1 = -1.6$. We choose as the start of the time z_1 the instant when $A(z_1)$ is real and equal to unity. Then, putting $z_1 = 0$,

we obtain from (49.6) $C_1 + C_2 = 1$. The constants C_1 , C_2 , C_3 , and C_4 contained in the solutions (49.6) and (49.7) are generally speaking complex. Therefore, putting $C_k = B_k + iD_k$ ($k = 1, 2, 3, 4$), we can write

$$\left. \begin{aligned} B_1 + B_2 &= 1, \\ D_1 + D_2 &= 0. \end{aligned} \right\} \quad (49.13)$$

Let us introduce the notation

$$e^{im\frac{\pi}{2}} = a + bi; \quad e^{m\frac{\pi}{2}} = c. \quad (49.14)$$

Then

$$e^{-im\frac{\pi}{2}} = a - bi; \quad e^{-m\frac{\pi}{2}} = \frac{1}{c}.$$

At the end of the first interval the function $A_1(z_1)$ is equal to

$$A_1\left(\frac{\pi}{2}\right) = a(B_1 + B_2) - 2bD_1 + ib(B_1 - B_2).$$

It is easy to visualize that the imaginary part of $A_1(\pi/2)$ is equal to zero. Indeed, at the end of the second interval the function $A_2(z_1)$ should be real, since $A_1(0) = \alpha_1 A_2(\pi)$, and α_1 and $A_1(0)$ are real quantities. But the change in the function A_2 in the second interval is connected with factors e^{mz_1} and e^{-mz_1} , which are also real. Consequently, the function $A_2(z_1)$ is real on the entire interval, including the start of the interval. But then, by virtue of the continuity of the function A [the first "joining" condition (49.8)] we can state that $A_1(z_1)$ is also real at the end of its interval. The condition that $A_1(\pi/2)$ has no imaginary part leads to the equality

$$B_1 = B_2,$$

which in conjunction with (49.13) yields $B_1 = B_2 = 1/2$.

The just mentioned requirement that the function $A_2(z_1)$ be real everywhere enables us to find two more quantities, $D_3 = D_4 = 0$. Taking into account the obtained values of B_1 , B_2 , D_3 , and D_4 and also the condition $D_1 = -D_2$ (49.13), the equality of the quantities $A_1(z_1)$ and

$A_2(z_1)$ when $z_1 = \pi/2$ is expressed in the following fashion:

$$a - 2bD_1 = cB_1 + \frac{B_1}{c}.$$

The condition $A_2(\pi) = \alpha A_1(0)$ yields

$$B_1 c^2 + \frac{B_1}{c^2} = a_1,$$

while the condition for the equality of the derivatives [the last condition of (49.8)] yields

$$B_1 c^2 - \frac{B_1}{c^2} = -a_1 2D_1.$$

A system consisting of the last three equalities enables us to find D_1 , B_3 , and B_4 . Simple calculations yield the following (we give the values of all the B_k and D_k):

$$\begin{aligned} B_1 &= 0.5, & D_1 &= -0.6; & B_3 &= -0.0392, & D_3 &= 0, \\ B_2 &= 0.5, & D_2 &= 0.6; & B_4 &= 7.4, & D_4 &= 0. \end{aligned}$$

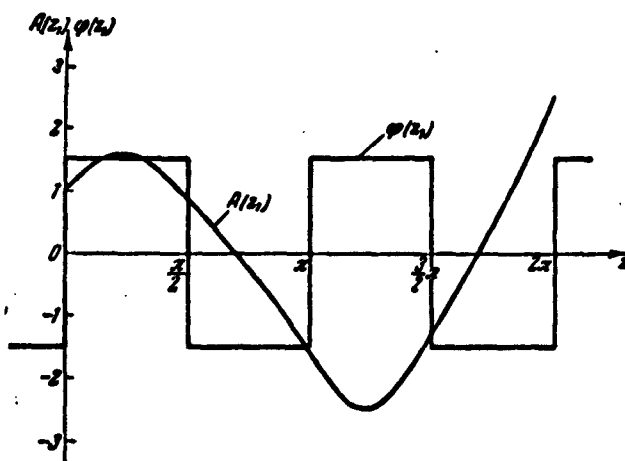


Fig. 101. Variation of the amplitude A of the flame-surface perturbation as a function of the dimensionless time z_1 .

Thus, the function $A(z_1)$ has been determined. The corresponding plot is shown in Fig. 101. The same figure shows the dependence $\varphi(z_1)$. If we disregard the increase of the average amplitude $A(z_1)$ with increasing time z_1 (the consequence of the instability), we can say that $A(z_1)$ is a periodic function of the time, and reaches absolute maximum

values at approximately the centers of the intervals characterized by the positive values of $\varphi(z_1) = m^2$. This means that the most positive perturbation of the summary flame surface will occur at these instants of time.

The perturbation of the effective flame propagation velocity δU_{sgor} (we recall that δU_{sgor} is positive when the absolute rate of combustion increases and differs in sign from δU_1) can be written on the basis of Formula (38.29) in the following manner:

$$\delta U_{\text{crop}} = U_{\text{n. cr}} \frac{\delta S}{S} \quad (U_{\text{n. cr}} = -U_{\text{n}} > 0). \quad (49.15)$$

Consequently [see (38.20), (38.24), (38.30), (38.31)], the maximum value of U_{sgor} , like that of $A(z_1)$, will be attained at instants corresponding to the centers of the sections $\varphi(z_1) = +m^2$.

The function $\varphi(z_1)$ is the result of a crude idealization of the function $2q \sin 2z_1 = 2q \sin \omega t$. We recall [this is easiest to see from the inequalities (38.22), (38.24), and (38.25)] that g is proportional to the accelerating acting on the flame surface. This enables us to relate the oscillations in the rate of combustion δU_{sgor} with the velocity oscillations. Indeed, let the velocity oscillations in the cold part of the stream ahead of the front of the flame be

$$\delta v_1 = -(\delta v_1)_0 \cos \omega t, \quad (49.16)$$

where $(\delta v_1)_0$ is the amplitude of the oscillations δv_1 . Then the perturbation of the acceleration acting on the flame front is written in the form

$$\delta b = \omega (\delta v_1)_0 \sin \omega t. \quad (49.17)$$

It can be assumed that in the schematization employed this law is represented, accurate to a scale factor, in the form of the function $\varphi(z_1)$ on Fig. 101, and with this the maxima of δb correspond to the centers of these sections $\varphi(z_1) = +m^2$. Inasmuch as the maxima of the

absolute values of $A(z_1)$, i.e., the maxima of the wave formations on the surface of the flame, and consequently also the maxima of the perturbations of the surface of the flame δS , also coincide with the centers of the sections $\varphi(z_1) = +m^2$ (with the maximum values of the acceleration perturbations δb), the phase shift between δS and δb is equal to zero and consequently

$$\delta S = (\delta S)_0 \sin \omega t. \quad (49.18)$$

Here $(\delta S)_0$ is the amplitude of the oscillations of the flame surface. We note that in accordance with the plot of the function $A(z_1)$ on Fig. 101, there exist instants when $A(z_1)$ becomes equal to zero, and the flame front ceases to be perturbed. Obviously, in this case S reaches a minimum, i.e., these instants correspond in the present notation to $\delta S = -(\delta S)_0$ (the minimum of δS). Consequently, the "natural" state of the flame front is regarded to be one with some average curvature, and the maximum perturbations [corresponding to $\delta S = +(\delta S)_0$ and $\delta S = -(\delta S)_0$] are such as to either double this average curvature, or reduce it to zero. In the former case the flame surface increases compared with the average value, and in the latter it decreases.

If we denote the value of the relative change in the flame surface contained in Formula (49.15) by $\overline{\delta S} = \delta S/F$, then, by using Eqs. (49.16) and (49.18), we can establish the phase relation between δU_{sgor} and δv_1 :

$$\left. \begin{aligned} \delta U_{crop} &= U_{n. cr} (\overline{\delta S})_0 \sin \omega t, \\ \delta v_1 &= (\delta v_1)_0 \sin \left(\omega t - \frac{\pi}{2} \right). \end{aligned} \right\} \quad (49.19)$$

As can be seen from the foregoing equations, the phase shift between δU_{sgor} and δv_1 is $\pi/2$.

Let us consider the question of the excitation of acoustic oscillations in a tube closed on one end, when the perturbed-combustion process is described by the first equation in (49.19). On the closed

end of the tube there can exist no average flux of acoustic energy other than zero. Therefore the oscillations of the velocity δv_1 and of the pressure δp_1 will be shifted in phase by $\pi/2$ in the case of steady-state oscillations. This means that the oscillations in the rate of combustion δU_{sgor} will be in phase or out of phase with the oscillations of the pressure. We have already mentioned above that the conditions under which excitation is produced by heat supply oscillations and by oscillations of δU_{sgor} are the same in their main outlines, and it was shown in §45 that the near equality of the phases of $Y = \delta U_{sgor}$ and δp_1 is the most favorable for the excitation of acoustic oscillations. In those cases when δp_1 and δU_{sgor} are in phase opposition, the excitation of acoustic oscillations is impossible. The foregoing follows, in particular, also from the form of the typical diagram for the stability boundaries, shown in Fig. 27.

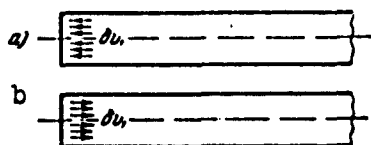


Fig. 102. Perturbations in the stream velocity in the vicinity of the closed end of the tube.

Let us consider in greater detail the question of when the phases of δU_{sgor} and δp_1 will coincide. Figure 102 shows the motion of the gas in the vicinity of the closed end of the tube at the instant when the pressure perturbation δp_1 goes through a maximum. At the instant directly preceded-

ing the maximum compression of the gas, the air masses still move toward the closed end (scheme a), while at the instant directly following the maximum compression of the gas at the closed end of the tube, the masses begin to move toward the open end of the tube (scheme b). This character of motion indicates that the gases are acted upon by an acceleration in the positive x direction. Inasmuch as the velocity perturbation δv_1 goes through zero at the instant of maximum compression, the acceleration δb reaches at that instant its maximum absolute value

[see (49.16) and (49.17)].

Thus, at the instant of maximum compression at the closed end, the gas located near this compression region is acted upon by maximum positive acceleration. Physically this result is almost self-evident. The maximum of positive acceleration corresponds to the center of the section $\varphi(z_1) = +m^2$, i.e., to instants when δS and consequently also δU_{sgor} reaches a maximum. Consequently, in the nearest vicinity of the closed end, an agreement between the phases of δp_1 and δU_{sgor} will always be observed, i.e., the excitation conditions will always be satisfied. As regards the other portions of the tube, the possibility of self-excitation of oscillations upon passage of the flame front through them depends essentially on the number of the excited harmonic. To consider this question in somewhat greater detail, let us turn to Fig. 103.

Figure 103 shows standing wave patterns for the oscillations of δp and δv for the first three harmonics, with the patterns of δp and δv arbitrarily drawn in one plane. As was indicated just now, at the closed end (when $x = 0$) the excitation conditions are satisfied always, i.e., for all harmonics. It is clear from the foregoing that in final analysis the question of the possibility of excitation reduces to the question of the relationship between the phases of the pressure and the acceleration; if positive δb corresponds to positive δp_1 , then the oscillating system is capable of excitation. Let us consider from this point of view the second harmonic (the middle diagram of Fig. 103). In the vicinity of $x = 0$ the excitation conditions are satisfied, and when the pattern of δp goes through zero they are violated. Indeed, in this case δp reverses sign, i.e., its phase changes by π , whereas the phase of δb remains the same [it is seen from Formula (49.17) that a change in the phase of δb is possible only when the phase of $(\delta v_1)_0$

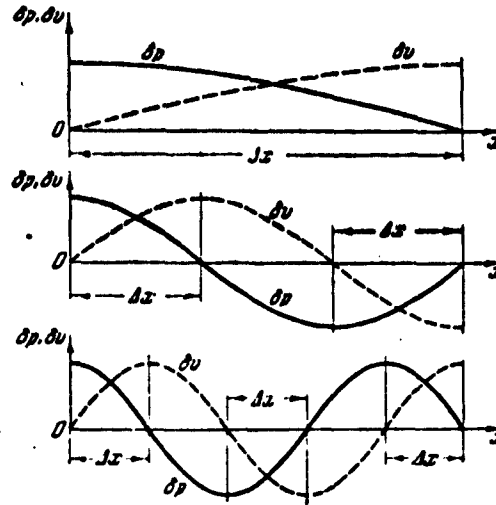


Fig. 103. Standing wave patterns for the first three harmonics (tubes with one closed end); Δx are the intervals inside which the flame front should be situated in order for excitation to be possible.

changes, while the pattern of δv in Fig. 103 indicates that upon going through the section corresponding to $\delta p = 0$ the phase of δv remains the same as before]. Consequently, whereas in the section adjacent to the closed end of the tube the phases of δp and δb were the same, in the vicinity lying to the right of the section where $\delta p = 0$ they turn out to be shifted by π . This means that δp and δU_{sgor} are in phase opposition and the acoustic oscillations will be damped out.

Further motion in the positive x direction leads to a section where the perturbation δv changes sign (i.e., changes the phase by π). As regards the phase δp , it remains the same as before. Thus, to the right of the node of δv , the phases of δp and δb will again be such that the excitation of acoustic oscillations becomes possible. Consequently, whereas the first harmonic shown in the upper part of Fig. 103 admitted of excitation of the system for any position of the flame front inside the tube, for the second harmonic there exist two regions

in which excitation is possible, one in the vicinity of the closed end and the other in the vicinity of the open end of the tube.

In the lower part of Fig. 103 are plotted the standing wave patterns of δp and δv for the third harmonic. We can apply precisely the same arguments to these patterns and show that for the third harmonic there exist three regions inside of which the excitation conditions are satisfied, and two regions where they are not. The intervals of the values of x within which the flame front should be located in order to permit excitation of acoustic oscillations are designated in Fig. 103 by Δx .

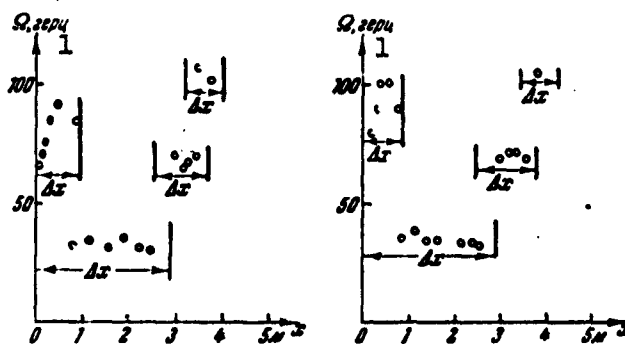


Fig. 104. Comparison with experiment of the obtained theoretical intervals Δx within which the flame front should be located to make self-excitation possible.
1) cps.

The result obtained here on the basis of a theoretical analysis is in good agreement with experiment. By way of an example, Fig. 104 shows the results of the experiments of Coward, Hartwell, and Georgson, which were already shown in Figs. 49 and 50. Along with the experimental points, the diagrams show the zones Δx , constructed in the following manner. Since the cold mixture used in the experiments under consideration was stationary, one quarter of the length of the standing wave of the pressure and velocity perturbations is equal to $a_1/4\Omega$ (a_1 is the velocity of sound in the cold gas and Ω is the oscillation fre-

quency in cycles per second). The first quarter wave, reckoned from the closed end (from the origin in the figure) was regarded as a zone in which excitation is possible, as was every second analogous region (Fig. 103). The oscillation frequency Ω , which was substituted in the expression derived somewhat earlier, was taken from experiment.

As can be seen from Fig. 104, the excitation of acoustic oscillations occurred only when the front of the flame was inside the zones Δx .* This is a good confirmation of the assumption made at the start of the present section, that the main mechanism for feedback is the interaction between the acoustic oscillations and the wave production on the flame front and the action of this wave production on the effective velocity of flame propagation.

Figure 104 gives grounds for making a few other remarks concerning the mechanism of oscillation excitation. It is first necessary to point out that the ends of the Δx zones correspond to the following: the left to a velocity node and the right to a pressure node. Therefore the system cannot be excited on the ends of the Δx zones. The fact that there is no excitation in the pressure node can be seen from the right-hand diagram on Fig. 30 (it is merely necessary to recall that in this diagram the amplitude of the perturbation δv_1 is directed upward, and consequently $\delta \vec{U}_{sgor}$ will be directed along the abscissa axis). When $\delta \vec{U}_{sgor}$ is turned through $\pi/2$ relative to δv_1 , the diagram of the stability boundaries does not show in this case that the end of the vector $\delta \vec{U}_{sgor}$ falls in the instability region. In the vicinity of the velocity node, the oscillation system is not excited because along with the decrease in the amplitude of the velocity oscillations the amplitude of the displacements of the medium, h_0 , which is contained in the expression for m^2 , also decreases (for a given frequency) [see Formula (49.3)]. If it is assumed that the wavelength λ on the flame

front retains the same order of magnitude, then $m^2 \approx 0$ near the velocity nodes. At the same time it was shown above that the excitation of the wave production on the flame front is possible only when $m^2 > 1.39$. Consequently, the oscillating system cannot be excited not only when the flame front is located in the direct vicinity of the velocity node, but also when the flame moves a certain distance away from this node.

The experimental points lie, in full accordance with the foregoing, inside the intervals Δx , and the tendency of the experimental points to shift toward the right ends of the intervals Δx indicates that the oscillation excitation is more influenced by the velocity perturbation than by the pressure perturbation. Particularly instructive in this sense are the experimental points corresponding to the position of the flame front directly at the closed end. At that instant the oscillations occur with the second-harmonic frequency, and as the front of the flame approaches the closed end of the tube the oscillation process clearly begins to break down. This is externally manifest in the disappearance of regularity and the rapid decrease of the oscillation frequency.

Were the feedback mechanism to be caused by some physical processes which depend on the pressure (for example, the variation of the period as a function of the pressure etc.), then as the flame approached the closed end there would be no breakdown observed in the oscillation process. The observed deviations from the expected character of the phenomenon become understandable if the feedback mechanism is based on the "dragging" of the flame front by the oscillating medium. Then the closeness of the closed end of the tube should greatly disturb the entire hydromechanics of such a "dragging" and cause deviations from the theoretical pattern.

In §§28 and 29 above, we considered the question of the jump-like

change in the oscillation frequencies for a continuous variation of the length of the hot part of the tube. The corresponding results were obtained there on the basis of formal considerations and were not connected at all with the concrete mechanism of oscillation excitation. The analysis given here of a concrete phenomenon leads to the same regularity, but we now understand the internal essence of this phenomenon. If we consider the gradual motion of the flame front from the open end of the tube (abscissa equal to 5 meters on Fig. 104) then initially (as follows from the scheme on Fig. 103) all the harmonics will be unstable (we disregard losses here). However, the oscillating system will start to be excited not by the first harmonic but by the highest possible one (with account of the losses). The reason for it is that for the higher frequencies the motion away from the node δp located at the open end of the tube will occur earlier than for the lower harmonics. As soon as the motion of the flame front toward the closed end of the tube causes the amplitude of the velocity oscillations δv to decrease (as a result of the approach of the flame front to the δv node) to a suitable value, a "jump" to the next harmonic occurs, for which the δv node is located farther away from the open end. From this point of view, the second transition to oscillations with the second-harmonic frequency at the closed end of the tube becomes understandable. It occurs when the transition to the second harmonic "removes" the flame front from the δv node (which coincides with the end of the tube), and this removal must be understood as a displacement relative to the standing wave pattern: whereas the extreme left experimental points, corresponding to the fundamental tone, lie at a distance of approximately $1/3$ of the quarter wave length of the standing wave from the velocity node, for the second harmonic the entire quarter wave length lies within the same distance from the closed end,

i.e., the front of the flame is situated at the δv node.

The concrete analysis of the experiment considered explains also why the experimental points on Fig. 50 agree better with the theoretical instability regions than the points on Fig. 49. In §29 we could state in this respect only that the characters of the perturbed combustion process during the instant of occurrence of the instability and during the instant of its vanishing were not completely the same. We can now make this general remark more specific: the occurrence of the instability is connected with the removal from the pressure node, whereas its vanishing is connected with an approach to the velocity node. These external causes have a very deep physical meaning. At the instant of occurrence of the instability, the wave production on the surface of the flame can gradually occur and the limiting factor is that as a result of the closeness of the flame front to the pressure node a nonvanishing δU_{sgor} cannot cause a positive influx of acoustic energy. At the instant of the disappearance of the instability, the flame front approaches the pressure node and the conditions for obtaining a positive influx of acoustic energy are quite favorable, but owing to the decrease in $|\delta v|$ the feedback mechanism ceases to function (wave production on the flame front stops). It becomes clear from the foregoing that the reason for the start and end of the instability is quite different; this is why no agreement between the theoretical and experimental boundaries of the disappearance of the instability should be obtained on Fig. 49.

The results obtained in §§28 and 29 have the advantage of greater generality, since they do not depend on the concrete type of vibration combustion. But being quite general, these results cannot explain many particulars of the observed phenomenon. One must not forget likewise that the deductions of §28 are based on the assumption that the insta-

bility region exists. The deductions of the present section are more complete in this respect and state that an instability region should exist for the combustion mode under consideration.

In conclusion it is useful to return again to an analysis of the experimental data, so as to analyze them from the point of view of generation of acoustic energy in the heat-supply zone.

Inasmuch as the principal role in vibration combustion of the type considered here is played by the perturbation of the effective rate of propagation of the flame, the condition on the discontinuity surface Σ , which represents the region of heat supply, must be written in the form of the system (16.12). Taking Eqs. (15.9) and (15.10) into account, and also assuming that the average rate of displacement of the flame front along the tube is quite small, and consequently M_1 and M_2 are close to zero, we can readily reduce the system of three equations (16.12) to the form

$$\left. \begin{aligned} \bar{v}_2 &= \frac{1}{n} \bar{v}_1 + \left(\frac{1}{n} - n \right) \bar{U}_1, \\ \bar{p}_2 &= \bar{p}_1. \end{aligned} \right\} \quad (49.20)$$

In place of the three equations (16.12) we have obtained the two equations (49.20), because the first and third equations of (16.12) become identical after the assumption $M_1 = M_2 = 0$ is introduced.

The summary flux of acoustic energy radiated by the heat supply zone can be determined from Eq. (19.7), putting in it $m = 1$. Then, taking Conditions (49.20) into account and noting that $\vec{p}_1 \vec{v}_1 = 0$, we obtain

$$\bar{A}_1 = \frac{1}{2} (1 - n^2) \bar{p}_1 \bar{U}_1. \quad (49.21)$$

As already indicated, $\delta \bar{U}_1$ and $\delta \bar{U}_{sgor}$ differ only in sign. Consequently, going over to dimensionless variables, we can write

$$\bar{U}_1 = - \frac{\delta U_{sgor}}{a_1}.$$

If we take the equations in (49.19) into account and assume that for the section of type b in Fig. 96, which corresponds to the flow adjacent to the closed end, we have

$$\delta p_1 = (\delta p_1)_0 \sin \omega t,$$

then we can state that

$$\bar{U}_1 = -\frac{U_{n,cr}(\delta \bar{S})_0}{a_1 |\bar{p}_1|} \bar{p}_1.$$

Let us substitute the obtained value of \bar{U}_1 in (49.21). Then

$$\bar{A}_\Sigma = \frac{1}{2}(n^2 - 1) \frac{U_{n,cr}}{a_1} (\delta \bar{S})_0 |\bar{p}_1|. \quad (49.22)$$

For sections of type a in Fig. 96, the sign of \bar{A}_Σ will be the opposite of that given by Formula (49.22). Inasmuch as $n > 1$, the system will be excited only on the sections of the type b.

Formula (49.22) obtained here is an analytic way of writing down the fact already discussed somewhat above, namely that the excitation of the vibration combustion (i.e., the attainment of positive work \bar{A}_Σ per second) is connected both with the presence of a nonvanishing perturbation of the pressure \bar{p}_1 , and with a nonvanishing wave production on the flame surface $(\delta \bar{S})_0$. Whereas this conclusion was based previously on purely qualitative considerations concerning typical configurations of the stability boundaries, it has now acquired a quantitative character, indicating that both these factors play an equally important role. It should be recalled that in the derivation of (49.22) the required phase relations were already assumed, so that they did not enter into the final expression for \bar{A}_Σ .

In order for wave production on the surface of the flame to become possible, as already mentioned, the parameter m^2 must exceed 1.4 but be smaller than 9. If we turn to the expression (49.3) for m^2 , we obtain after changing over from h_0 to $(\delta v_1)_0 = h_0 \omega$ the condition for the wave production in the form of the inequality

$$1.4 < 16 \frac{(c_1 - c_2)(\delta r_1)_0}{(c_1 - c_2)\omega\lambda} < 9.$$

(49.23)

from which it follows that the velocity oscillations δv should exceed a certain limit. Therefore $(\delta \bar{S})_0$ can be different from zero only at a certain distance away from the velocity node. It must be noted that a more accurate numerical estimate of this circumstance based on experimental results is difficult, since no data are obtained in this experiment concerning the wavelength λ on the flame surface.

A second difficulty in the analysis of (49.22) is the fact that the quantity $(\delta \bar{S})_0$ which is contained in it as a factor is not determined by the parameters of the acoustic oscillations. If Condition (49.23) is satisfied, then at constant oscillations of the medium [constant $(\delta v_1)_0$] the quantity $(\delta \bar{S})_0$ can vary with the time. In §38 this circumstance was already emphasized, and it was pointed out there that such a property of wave production is connected with the fact that the formation of waves on the boundary surface constitutes parametric resonance. Consequently, although the amplitude $(\delta v_1)_0$ will monotonically decrease as the flame front moves away from the pressure node (displacements from the right to the left inside the interval Δx on Fig. 104), the amplitude $(\delta \bar{S})_0$, which characterizes the wave production, can increase. Consequently, the product $(\delta \bar{S})_0 |\bar{p}_1|$, contained in Formula (49.22) can also increase not only because of the increase in $|\bar{p}_1|$, but also as a result of the increase in $(\delta \bar{S})_0$. The increase in \bar{A}_Σ with increasing distance from the flame front to the pressure node will cause the amplitudes of the acoustic oscillations to start increasing. This increase in the over-all level of oscillations will in turn act on the quantity m^2 , so that the change in the oscillation amplitude with motion of the flame front along the length of the tube will not be as regular as the change in the frequencies.

§50. Occurrence of Oscillations in Pulverized Coal Furnaces

As the rating of various types of commercial furnaces is increased, the excitation of oscillations connected with vibration combustion in such furnaces becomes more and more probable. As already mentioned in the introduction, in some cases these oscillations are useful and the designer attempts to produce them by suitable means. In other cases the occurrence of vibration combustion is extremely undesirable and the appearance of such modes in furnace operation causes damage to the structure, premature wear of individual units, etc.

Recently V.V. Solov'yev observed and described vibration combustion in a furnace operating on pulverized hard and soft coal,* with these oscillations localized in the preliminary chamber of the furnace, which we shall call henceforth the combustion chamber. V.V. Solov'yev pointed out that during the operation of highly loaded combustion chambers vibrations were produced, accompanied by strong noise and considerable pressure oscillations. The experiments described below were set up by the aforementioned author.

Figure 105 shows schematically one of the combustion chambers, in which the experiments described below were set up. The combustion chamber constituted a vertically placed cylinder 2 m in diameter with a 90° turn in the lower part. From the point of view of acoustics, such a combustion chamber can be regarded as a tube with one closed end (on top) and one open end (at the bottom), and the length of such a tube must be measured along the broken axis ABC. If we estimate the tube length in this fashion, we find it to equal 12.5 m. In the upper part of the combustion chamber is located a burner consisting of two pipes. The inner pipe, which is provided with blades at its outlet, serves to supply the pulverized coal and the primary air. In Fig. 105 the supply of air and pulverized coal is indicated by the arrow v_1 . The outer

pipe, which serves for the supply of the secondary air, is also provided with blades. In Fig. 105 the secondary air is indicated by the arrow v_2 . In addition, the air necessary for the combustion is supplied along the periphery, tangentially, through suitably installed nozzles (v_3 on Fig. 105). The interaction between all these devices results in twisting of the flame torch, and this contributes to better combustion. Although, as can be seen from the description, there are several openings in the upper part of the combustion chamber, this end can be regarded in first approximation as "closed" since the total area of these openings and the general character of the way they are obstructed makes them less effective by an order of magnitude than the opening in section C in the lower part of the combustion chamber. As regards the lower end of the chamber, an essential factor is that located to the left of section C is a large volume, which greatly exceeds the volume of the combustion chamber; this allows us to regard the section C as being an open end of the tube, communicating with an unbounded space.

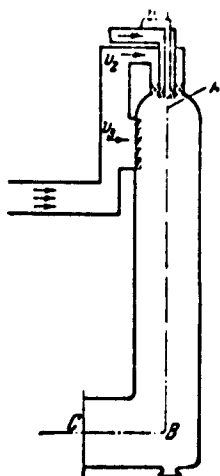


Fig. 105. Schematic representation of the combustion chamber.

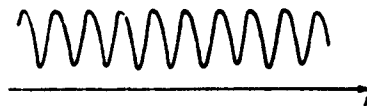


Fig. 106. Oscillogram of pressure at the burner (in the upper part of the combustion chamber).

The relatively small ratio of the tube length L to its diameter d ($L/d = 6.25$) indicates that the combustion chamber will be characterized by relatively large radiation losses (see Chapter 6), and consequently only the

excitation of fundamental (first-harmonic) oscillations is likely in it. In order to estimate these frequencies we assume the simplest formula, based on the fact that the first harmonic in a tube with one end closed and the other open corresponds to its supporting one quarter of the perturbation wavelength

$$\Omega = a/4L,$$

where Ω is the frequency in cycles per second and a is the velocity of sound.

At the average temperatures, and hence sound velocity, observed in the experiments the frequency calculated from the foregoing formula turns out to be 16.9 cps, whereas measurements made in the vibration combustion modes yielded values ranging from 16.1 to 17.2 cps.

In another furnace, which was similar in construction to that described above, and which was characterized by $L = 7$ m and $d = 1.4$ m, the calculated frequency turned out to be 28 cps, while the measured value was 25 cps. Oscillograms obtained in vibration combustion show that the pressure has an almost exactly sinusoidal variation at the closed end of the tube. An example of such an oscillogram is shown in Fig. 106. Although the agreement between the calculated and experimental frequencies gives rise to almost complete assurance that the observed oscillations had an acoustical nature, an additional experiment was set up, which finally confirmed this assumption. The experiment consisted of plotting the standing wave patterns of the oscillations produced in the combustion chamber. By aligning the origin with the closed end of the tube, we obtain as a boundary condition $\bar{v} = 0$ ($\xi = 0$). Another condition will obviously be $\bar{p} = 0$ ($\xi = 1$). Disregarding the combustion process for the time being, let us calculate the standing wave pattern for the pressure in such a tube.

From Eqs. (4.13) and (4.14), putting $A_p = \bar{p}_0$, we obtain

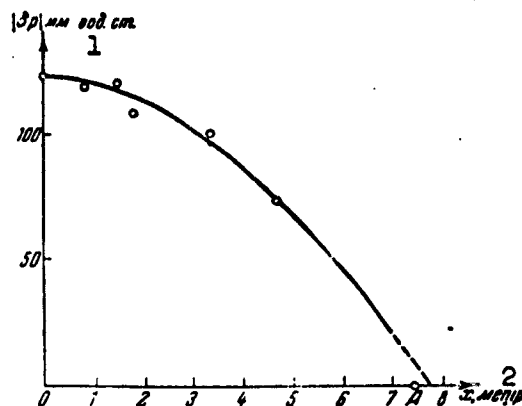


Fig. 107. Comparison of the theoretical curve (continuous line) and the experimental points of the oscillation amplitude distribution along the combustion chamber. 1) mm water pressure; 2) meters.

$$\bar{p} = \bar{p}_0 \frac{1}{2} \left[\exp \left(-\frac{i}{M+1} \omega x \right) + \exp \left(-\frac{i}{M-1} \omega x \right) \right].$$

Here we already put $\beta = i\omega$. The transition from dimensional to dimensionless variables is in the usual manner, using Formulas (4.8). If we make the suitable calculations and take the pressure oscillation amplitude at the closed end from experiment, and furthermore use the experimentally obtained oscillation frequency, we can compare the theoretical and actually observed configurations of the pressure pattern. Such a comparison is shown in Fig. 107. As can be seen from the figure, the experimental points fit the theoretical curve quite well. What attracts attention is only a slight disparity between the theoretical boundary condition at the open end ($\delta p = 0$) and the course of the curve. This is explained by the fact that the real oscillating system has without doubt radiated acoustic energy from the open end (and consequently could not have a pressure node), and is explained in addition by the "open-end effect" which was already mentioned at the end of §30. If we allow for this effect by adding to the open end of the

tube a length on the order of 0.3 diameters, this will yield on Fig. 107 the point A. Then continuation of the theoretical curve, determined from the measured frequency and amplitude of the pressure oscillations at the closed end, shown dashed in the figure, will pass quite close to the point A. Consequently, not only the value of the oscillation frequency, but also the existence and the configuration of the standing pressure wave confirm that the observed phenomenon has an acoustic nature.

In the analysis of the described process it is necessary to take it into account that the combustion occurs at the closed end, i.e., in sections where large pressure oscillation amplitudes and relatively low stream velocity oscillations are observed. If the acoustic oscillations lead, via some feedback mechanism, to oscillations in the heat release, then the diagram of the stability boundaries will have the character shown in the left part of Fig. 28. The vector \vec{Y} shown in this diagram will represent in this case the oscillating component of the heat release (we recall that on diagrams of this type the pressure oscillation vector is directed along the x axis while the velocity oscillation vector is directed along the y axis). If a feedback mechanism exists in the system, causing the appearance of an oscillating component in the heat release, then in order for such a perturbation in the heat release to be capable of exciting acoustic oscillations it is necessary that the relative magnitude of this perturbation exceed a certain minimum value (the circumference of the stability boundary does not touch the y axis) and, in addition, that it be approximately in phase with the pressure (the aforementioned circle lies in the region of positive values of x symmetrically about this axis).

The first of these conditions is realized relatively easily; the realization of the second is not so simple a matter. In order to con-

sider this problem in greater detail, let us turn to a study of the possible feedback mechanism. In §35 above we already mentioned that as a result of the relatively small pressure head under which the primary air with the pulverized coal and the secondary air are fed, the pressure oscillations in the upper part of the combustion chamber can cause periodic oscillations in the supply of fuel and air. This makes possible the realization of a feedback mechanism based on mixture formation.

The pulverized coal was fed to the combustion chamber by the primary air under a pressure of 200-250 mm water pressure, while the remaining air was fed at a pressure of 100-150 mm water. As can be seen from Fig. 107, the oscillations of pressure at the closed end of the tube (at the burner) were on the order of 125 mm water. Consequently, at the instant of maximum increase in pressure the supply of air should be almost completely stopped, and the supply of pulverized coal should be noticeably reduced. If it is assumed that the combustion of the fuel occurs instantaneously, immediately after it is fed to the combustion chamber, then the increase of pressure in the chamber will correspond to a reduction in the heat supply. Consequently, excitation of the oscillations is impossible. In the described scheme of the phenomenon one important circumstance was not taken into account: inasmuch as the fuel ignites not instantaneously, the phase relation between the pressure and heat release oscillations may change. Furthermore, a phase shift is possible between the perturbation of the pressure and the supply of the fuel, owing to the deviation of the oscillations in the fuel supply from the quasistationary scheme adopted in the preceding very simple analysis.

The delay in the ignition of the fuel-air mixture may be connected with a number of factors. First, it must be recognized that for coal

dust to ignite it must be heated to a suitable temperature. This heating is produced both by the heat radiated from the combustion zone (i.e., from the very instant of entry of the dust into the combustion chamber), and by contact with the combustion products (this necessitates a certain time, since the zone of intense combustion lies at a certain distance from the burner and the dust must take time to reach it). Second, the heating of the dust is in itself insufficient if the small dust particles are not surrounded with air, the bulk of which, as can be seen from the schematic diagram of the combustion chamber in Fig. 105, is supplied independently of the pulverized coal. Consequently, the combustion must be preceded by a mixing of the dust with the air, which also necessitates a certain time. The qualitative description of the ignition of the dust presented here shows that the delay in the ignition is quite unavoidable and that its magnitude cannot be negligibly small. This can lead, under certain conditions, to an agreement between the phases of the pressure and heat-release oscillations, i.e., to self-excitation of the system.

In the discussion presented at the end of Chapter 9 of the influence of the "stretching out" of the combustion zone on the probability of self-excitation of acoustic oscillations it was established that the more extensive the combustion zone (in the direction of the tube axis), the less likely is the excitation of the oscillations. Consequently, a factor contributing to the occurrence of acoustic oscillations is the relatively narrow localization of the intense-combustion zone: the combustion process must occur vigorously and in a sufficiently narrow combustion front. In the case considered here, the factor contributing to intense heat release at the top of the combustion chamber is, in particular, the excess of the pressure under which the coal dust is supplied over the pressure under which the remaining

air is supplied. Then after the pressure goes through the maximum the first to enter into the combustion chamber is the dust, which begins to be heated and to become gasified, and is mixed with the remaining air already prepared for the ignition. This should be accompanied by a vigorous reaction in a relatively narrow zone (along the length of the tube).

The zone of intense heat supply will be shortened also if fuels rich with "volatiles" are used, i.e., gaseous substances released during heating of the fuel and representing the easily ignited part of the fuel. The bulk of the "volatiles," and also the small fractions of the coal dust, should burn in a relatively short zone at a small distance from the burner. Therefore the use of rapidly igniting fuels should also contribute to the possibility of occurrence of vibration combustion.

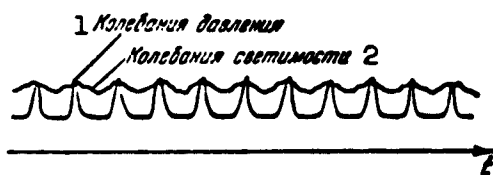


Fig. 108. Oscillogram showing simultaneous recording of pressure and luminance oscillations (the record of the pressure oscillation amplitude is distorted in the lower parts of the oscillogram because the pressure transducer operated beyond the linearity region).
1) Pressure oscillations; 2) luminance oscillations.

The delay in the ignition and the possibility of relatively narrow localization of the combustion process was actually observed in pulverized coal furnaces. V.V. Solov'yev set up a special experiment to determine the phase shift between the pressure and heat-release oscillations actually obtained in vibration combustion in a pulverized

coal furnace. For this purpose a photocell responding to the glow of the flame was installed in the upper part, in the burner zone (i.e., where the most intense combustion was localized). If it is assumed that the instants of most intense combustion (heat release) coincide with the instants of most intense glow, then the oscillations of the latter yield an idea of the variation of the heat release in the intense-combustion zone. In this case it is simplest to fix the phase relations. Figure 108 shows the result of such a recording. As can be seen from the presented oscillogram, the phases of the glow and of the pressure coincide, indicating the realization of a phase relation between these quantities that is most favorable for the excitation of the oscillating system.

The fact that the oscillating system realized the required phase relationships can be explained, as already indicated, only by the fact that the process of mixture production and ignition requires a certain time. Of particular interest, however, is the circumstance that the curves recorded by the oscilloscope indicate not merely the realization of one of the necessary phase relations, but the realization of the one and only relation which guarantees the most favorable excitation conditions. As was already shown in §45, the coincidence of the heat-release and pressure phases is optimal from this point of view. Thus, the presented experimental facts can be regarded as one of the confirmations of the hypothesis that the oscillating system has a tendency to realize that process, which is characterized by a maximal of radiation of acoustic energy from the heat-supply zone.

§51. Vibration Combustion in Ram-Jet Engines

Among the various types of jet engines used by modern technology, ram-jet engines have a certain range of application. Such an engine is shown schematically in Fig. 109. The distinguishing features of these

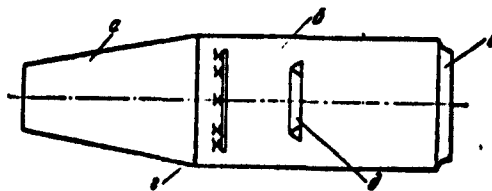


Fig. 109. Diagram of ram-jet engine.

engines are as follows: first, air is used to ignite the fuel and, second, the pressure of this air is not increased by some compressor that is mechanically driven. When the ram-jet engine moves in air (from right to left in Fig. 109), the opposing air enters an inlet nozzle a, where it is slowed down and consequently its pressure increased. Behind the inlet nozzle is located the combustion chamber b, which terminates in an exhaust nozzle c. Inside the combustion chamber is placed a set of fuel inlets d and a flame stabilizer e. As can be seen from this brief description, the idealized ram-jet engine scheme can be represented by a tube, inside of which, particularly in the stabilizer zone e, intense combustion takes place. A more detailed description of the construction, operating principle, and other characteristics of such engines can be found in special texts, for example the book by M.M. Bondaryuk and S.M. Il'yashenko.*

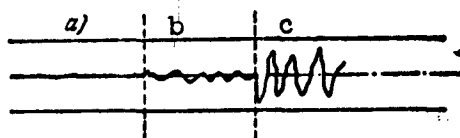


Fig. 110. Typical oscillograms of the pressure in a ram-jet engine (a — normal, b — hard, c — pulsating combustion).

These authors point out in their book that in tests of ram-jet engines oscillations are sometimes observed at the acoustic frequency that is characteristic of the engine as a whole.

The small and irregular pressure and velocity oscillations which are unavoidable in technical combustion are customarily not singled out and such a process is called quiet combustion. If the amplitudes of the pressure oscillations increase by a factor of several times but remain essentially smaller than the relative pressure in the chamber, while the frequency remains regular, the combustion is customarily called "hard." If the pressure oscillations reach the order of magnitude of the average relative pressure in the combustion chamber and these oscillations retain a regular character, the combustion is called pulsating. M.M. Bondaryuk and S.M. Il'yashenko present typical pressure oscillograms for these cases (a, b, and c in Fig. 110) and indicate that hard and pulsating pressure cannot be tolerated in engines, since they can cause failure of its structural elements.

It is obvious that in the case considered here one observed excitation of acoustic oscillations by the combustion. The zone of intense heat supply located in the stabilizer region can excite longitudinal acoustic oscillations of the gas column between the front section of the inlet nozzle and the rear section of the exhaust nozzle. As is well known from the preceding chapters, for this purpose it is necessary that the phase of the combustion (which now includes in its definition both the heat supply and the displacement of the flame front) be tied in a definite fashion with the phase of the oscillations of the gas column. In addition, a certain feedback mechanism must exist, capable of perturbing the combustion process at the same rhythm as the acoustic oscillations.

In experiments especially set up by Fenn, Forney, and Garmon using a model of the combustion chamber of a ram-jet engine, aimed at studying oscillatory processes in these experiments, several types of oscillations were recorded.* One of these types owes its existence to

longitudinal acoustic oscillations of the gas column inside the ram-jet engine. The authors of these experiments have shown that the frequency of the produced oscillations agrees in general with the frequency determined by the simplest formula of the type of (5.4), and they observed only excitation of the fundamental tone.

It must be stated that these experiments were of interest because the boundary conditions at the inlet to the combustion chamber and at the exhaust (the chamber included not only a combustion zone behind the stabilizer but also a large section for the flow from the fuel nozzles to the stabilizer) were typical of supersonic flight velocity. A special compressor raised the pressure of the air in the combustion chamber with a cylindrical mixture-preparation zone ahead of the flame stabilizer to 2.5 atm abs. As a result, critical velocity (i.e., the local velocity of sound) was reached in the exhaust nozzle. At the inlet to the tube, in the zone where the nozzles were located, the cross sections for the flow of air were so small, that from the acoustic point of view the inlet cross section of the tube should be regarded as "closed." As was already mentioned above (see, for example, §26), the existence of critical velocity at some section of the tube causes the velocity oscillations in this section to become impossible. Thus, the boundary conditions in both the inlet and outlet cross sections of the experimental setup had the form $v = 0$. These boundary conditions are in some sense the opposite of those realized in the experiments on vibration combustion described in Chapter 5. Inasmuch as the flow at the inlet and outlet of the tube was subsonic in the experiments previously described, the boundary conditions realized there were of the form $\bar{p} = 0$. Although changing from boundary conditions of the form $\bar{v} = 0$ to boundary conditions of the form $\bar{p} = 0$ barely produces any theoretical changes (except for the distribution of the in-

stability regions along the length of the tube), an experimental confirmation of this fact is of undoubted interest.

From the point of view of the previously obtained deductions we now understand why the fundamental tone was excited in the described experiments. The total length of the tube in which the experiments were made fluctuated between 1525 and 1780 mm, while the length of the hot portion had in this case an order of 350 mm, i.e., it was relatively short. It might appear that one of the higher harmonics should be excited in the system. Indeed, in the experiments reported on Figs. 50 and 51, at the same relative length of the hot portion, approximately equal to 0.2, the third and fourth harmonics were excited. However, in experiments with critical exhaust, the boundary condition at the outlet end of the tube has the form $\bar{v} = 0$ and not $\bar{p} = 0$, as was the case in the experiments whose results are shown in Figs. 50 and 51. Consequently, the vicinity of the open exhaust end was in that case the vicinity of an antinode and not of a node of pressure. But then the excited frequency should be those characterizing tubes in which the heat supply is effected near a pressure antinode. Under ordinary conditions, with both ends of the tube open, this corresponds to locating the heat supply zone in the central portion of the tube or, for a tube with one closed end, at the closed end. In both indicated cases, as follows in particular also from Figs. 50 and 51, the fundamental tone (the first harmonic) should be excited.

Unfortunately, the authors of the experiments described here did not consider the feedback mechanism, which causes the combustion process to become perturbed in rhythm with the acoustic oscillations. In order to present an example of one of the probable feedback mechanisms in ram-jet engines, we can refer to the opinion of Nicholson and Radcliffe, who investigated analogous processes in booster chambers of

turbojet engines.* They attribute the excitation of acoustic oscillations to the occurrence of alternating heat supply, resulting from the dependence of the completeness of combustion on the excess-air coefficient and on the stream velocity ahead of the combustion zone. If one agrees with that point of view, the entire analysis of vibration combustion can be built up in analogy with the problem considered in §§23-25. The only difference will be other boundary conditions, but this cannot justify the repetition of all the derivations of the present section.

§52. Longitudinal Oscillations in Liquid Fuel Jet Engines

During the course of operation of a liquid fuel jet engine, pressure oscillations are always observed in the combustion chamber, and the flow of fuel, etc. This leads to oscillations of thrust, which are transmitted to the structure on which the engine is mounted in the form of some mechanical vibration. It must be stated that this vibration presents no danger whatever to the structure, nor do they reduce the engine efficiency, so that they should be regarded as just a natural phenomenon as vibration and noise in an automobile engine. It was noted, however, that under certain conditions the irregular oscillations referred to here change their character sharply. They increase appreciably in amplitude, become strictly periodic, and by the same token become quite dangerous to the engine structure. Therefore the demands for successful advance in rocket technology have led to the necessity of investigating in detail the self-oscillations in combustion chambers of liquid fuel jet engines. It is not surprising that many articles were published in the periodic literature dealing with this problem, and recently a very valuable book was published by Crocco and Cheng.**

The authors of this book, in full agreement with many other re-

searchers who have published papers in the journals, distinguish between two types of self-oscillations in liquid fuel jet engines. One of these types is customarily called low-frequency self-oscillations (chugging) and the other high-frequency self-oscillations (screaming). The difference between them reduces to the following.

Low-frequency oscillations are caused by the fact that the system consisting of the combustion chamber and the heat supply devices becomes unstable with respect to small perturbations. In this case the mechanism whereby this instability is produced is due to the influence of periodic pressure oscillations in the combustion chamber on the supply of fuel and on the delay time of the ignition. A characteristic of this type of self-oscillations is that it is possible to neglect in their investigation the length of the combustion chamber, which can be regarded as a certain volume in which the pressure variation is the same at all the cross sections.

High-frequency oscillations are also brought about by the fact that the system becomes unstable with respect to small perturbations, and in this case the interaction between the pressure oscillations in the combustion chamber and the preparation and ignition of the combustible mixture also plays a definite role. However, unlike the preceding case, one can no longer neglect here the length of the combustion chamber and one cannot assume that the pressure and other parameters change in like fashion in all the cross sections of the combustion-chamber volume.

From the mechanical point of view, the former case is analogous in many respects to ordinary dynamic systems (described by means of ordinary differential equations), while the latter case is connected with the propagation of perturbations in a continuous medium, i.e., with phenomena of the acoustic type (described by partial differential

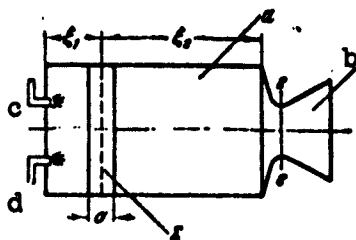


Fig. 111. Diagram of liquid fuel jet engine.

equation systems). Inasmuch as the present book is devoted to a study of the processes involved in the excitation of longitudinal acoustic oscillations, it is natural to consider here only the question of longitudinal high-frequency oscillations. Although the exposition of

the problem presented below differs somewhat from that given in the book of Crocco and Cheng (this being due to the desire to stay close to the content of the preceding chapters), the main ideas and results have been borrowed from the cited book. Those who wish to become acquainted in greater detail with low-frequency oscillations in liquid jet engines are advised to turn to the work of Crocco and Cheng.

Before we proceed to a discussion of this question, let us present a brief description of the liquid jet engine. As is well known, this type of engine comprises a cylindrical tube a, with a supersonic nozzle b installed in one end and a device for the injection of fuel into the combustion chamber installed on the other (Fig. 111). The latter includes, in particular, devices for the supply and atomization of the fuel (pipe d in the figure) and of the oxidant (pipe c in the figure). It is necessary to supply continuously to the closed volume of the combustion chamber, as is well known, the combustible matter (for example alcohol) and the oxidant (for example liquid oxygen). The combination of combustible matter and oxidant is customarily called the fuel. The fuel need not always consist of two components, as in the example just considered. There exist so-called single-component fuels, capable of self-ignition when entering the combustion chamber of the engine. In this case only one of the two pipes c and d in Fig. 111 is retained. The closed end of the combustion chamber, together

with the nozzles located there, used to atomize the fuel, is customarily called the head, while the opposite end is called the exhaust nozzle.

Combustion in the engine depends most strongly on those processes which occur at the engine head. Inasmuch as liquid components are injected into the combustion chamber, the mixture formation plays a very important role. The efficiency and speed of combustion of the injected liquid depend on the quality of the atomization and mixing of the components (if the fuel is not of the single-component type), on the speed of evaporation of the fuel droplets, and on the speed with which the combustible mixture is heated. The aggregate of all these processes calls for certain time for its completion, and only after this time has elapsed can the intense chemical reaction take place.

Being unable to present to some degree a clear-cut quantitative description of these processes, we introduce by way of a certain summary characteristic the delay time which we take to mean the time elapsed from the instant of injection of the fuel to the instantaneous conversion of the fuel into the combustion products.

We assume that the induction period t_1 satisfies Relation (37.5), which states that the induction period is connected only with the pressure. It was indicated in §37 that many aspects of the physical and chemical processes that are idealized by introducing the induction period t_1 are actually connected with the pressure. But Relation (37.5) can be ascribed a more general significance. If other factors (for example, the relative velocities of the fuel droplets and of the combustion products) also play an appreciable role but their variation is connected in regular fashion with the variation of the pressure, then the influence of these factors can, in final analysis, be expressed in terms of the pressure. On going over to dimensionless variables Rela-

tion (37.5) assumes the form

$$\int_{\tau-\tau_n}^{\tau} (1 + \bar{p})' d\tau' = \text{const.} \quad (52.1)$$

Let us use the formula obtained to write down the conditions on the heat supply surface (the cross section of the stream in which the fuel drops are instantaneously converted into combustion products).

We assume that the amount of fuel supplied to the combustion chamber is constant, i.e., entirely independent of possible pressure fluctuations inside the combustion chamber (this corresponds physically to the supply of fuel at very high pressures).

If the consumption of fuel mass per second is denoted by \underline{m} and the mass of fuel combusted per unit time is denoted by m_{cr} , then the relative perturbation in the mass combustion rate can be defined as

$$\bar{m} = \frac{m_{\text{cr}} - \underline{m}}{\underline{m}}. \quad (52.2)$$

If the combustion of the fuel is characterized by an induction period τ_1 , then the mass of fuel combusted within a time $d\tau$ should equal the mass of fuel injected during the time $d(\tau - \tau_1)$

$$m_{\text{cr}} d\tau = \underline{m} d(\tau - \tau_n)$$

or

$$m_{\text{cr}} = \underline{m} \left(1 - \frac{d\tau_n}{d\tau} \right). \quad (52.3)$$

Going over to the dimensionless perturbation \bar{m} , we can rewrite the last equation in the form

$$\bar{m} = -\frac{d\tau_n}{d\tau}. \quad (52.4)$$

Let us find an expression for the derivative $d\tau_1/d\tau$ in terms of known quantities. For this purpose we turn to Relation (52.1). Differentiating it with respect to τ and assuming that \bar{p} depends only on the integration variable τ' but is independent of the instantaneous

value of τ_1 , we obtain the sought-for quantity by using the rule for differentiating an integral with variable upper limit.

To make use of this rule, we break up the left half of (52.1) into two components

$$\int_{\tau-\tau_n}^{\tau} (1+\bar{p})' d\tau' = \int_a^{\tau} (1+\bar{p})' d\tau' - \int_a^{\tau-\tau_n} (1+\bar{p})' d\tau',$$

where a is a certain arbitrary constant. In differentiating with respect to τ we recognize that τ_1 is a function of τ so that the second component must be differentiated in accordance with the rule for differentiating a complicated function, multiplying the derivative of this integral with respect to the expression used as the upper limit of integration by the derivative of this expression with respect to τ . Thus

$$\frac{d}{d\tau} \int_{\tau-\tau_n}^{\tau} (1+\bar{p})' d\tau' = [1+\bar{p}(\tau)]' - [1+\bar{p}(\tau-\tau_n)]' \left(1 - \frac{d\tau_n}{d\tau}\right).$$

Inasmuch as Eq. (52.1) has a constant in its right half, the expression obtained is equal to zero. From this we readily obtain $d\tau_1/d\tau$

$$\frac{d\tau_n}{d\tau} = 1 - \left[\frac{1+\bar{p}(\tau)}{1+\bar{p}(\tau-\tau_n)} \right]'$$

The second component of the equation obtained can be simplified, since $\bar{p} \ll 1$, and consequently the deviations of the induction period from a certain value $\tilde{\tau}_1$ averaged over the cycle, resulting from the pressure oscillations, are relatively small. This enables us to write

$$\left[\frac{1+\bar{p}(\tau)}{1+\bar{p}(\tau-\tau_n)} \right]' \approx 1 + r[\bar{p} - \bar{p}(\tilde{\tau}_n)].$$

We have left out here the symbol for the dependence of \bar{p} on τ , and the expression $\bar{p}(\tilde{\tau}_1)$ indicates only that the quantity \bar{p} is taken only at a certain instant preceding the present instant by an amount equal to the average induction period $\tilde{\tau}_1$. Thus,

$$\frac{d\tau_n}{d\tau} = -r[\bar{p} - \bar{p}(\tilde{\tau}_n)]. \quad (52.5)$$

By combining the equation obtained with the previously derived expression (52.4) we obtain a relation capable of serving as the basis for the formulation of the heat supply region properties

$$\bar{m} = r[\bar{p} - \bar{p}(\bar{\tau}_u)]. \quad (52.6)$$

The relation obtained should be used in writing down the equations connecting the perturbed flow parameters on the left and on the right of the discontinuity surface Σ , which, as is well known, is the idealized immobile heat supply plane. In order to write down the properties of the surface Σ , we make use of the relationships given in Chapter 4. It is clear from the foregoing that in equations describing the combustion process in liquid fuel jet engines one must not neglect the fluctuations in the supply of the gaseous mass to the combustion chamber, for even if the supply of the liquid fuel is at a constant rate the combustion (i.e., the conversion into gas) can occur at a variable rate. Neglecting the volume occupied by the fuel drops, we can assume that the instant when the mass enters the combustion chamber is the instant when the fuel goes over into the gaseous state. We therefore write down the equations for the combustion region σ in the form (15.5), without neglecting the term δM^* .

In the case under consideration we can make the following simplifications in the equations (15.5). We shall assume that in the steady-state process the gas temperature is the same on the right and on the left of the region σ (Fig. 111), i.e., $a_1 = a_2$. This is connected with the fact that on the left and on the right of σ the volume of the combustion chamber is filled with the combustion products. In addition, to the left of σ the gas can be regarded in the mean (in the steady state) as immobile and isentropic, i.e., we can put $v_1 = 0$ and $\delta s_1 = 0$. If we take this into consideration, then by dividing the first equation of (15.5) by $\rho_2 v_2$, the second by $\rho_2 v_2^2$, and the third by $\rho_2 v_2^3$, and

recognizing that $\rho_2 v_2 = M^*$, we can obtain the following system of equations, written out in the dimensionless variables employed in the present book

$$\left. \begin{aligned} \frac{1}{M} \bar{v}_1 + \bar{p}_1 - \bar{s}_1 &= \frac{1}{M} \bar{v}_1 + \bar{m}, \\ 2v_1 + \left(M + \frac{1}{M}\right) \bar{p}_1 - M \bar{s}_1 &= \frac{1}{M} \bar{p}_1 + M J'_1, \\ \left(3M + \frac{2}{M(\kappa-1)}\right) \bar{v}_1 + \left(M^2 + \frac{2\kappa}{\kappa-1}\right) \bar{p}_1 - M^2 \bar{s}_1 &= \\ &= \frac{2}{M(\kappa-1)} \bar{v}_1 + 2M^2 J'_1 + 2M^2 \bar{Q}^*. \end{aligned} \right\} \quad (52.7)$$

Here

$$\left. \begin{aligned} J'_1 &= -\frac{1}{\rho_0 v_1} \frac{\partial}{\partial t} \int_V q v_x dV, \\ J'_2 &= \frac{1}{\rho_0 v_1} \frac{\partial}{\partial t} \int_V q \frac{v^2}{2} dV, \\ \bar{Q}^* &= \frac{\delta Q^*}{\rho_0 v_1}, \\ \bar{m} &= \frac{\delta M^*}{M^*}, \\ M &= \frac{v_1}{a_1}. \end{aligned} \right\} \quad (52.8)$$

Comparing the system (52.7) with the previously obtained system (15.7) we can see that the relations on Σ for a liquid fuel jet engine are appreciably simpler than the relations valid for the combustion of moving gases. Some of the simplifications are connected with the fact that $v_1 = 0$ and others are connected with the constancy of the gas parameters in the steady state for the entire combustion chamber. The latter, in particular, lead to $a_1 \cong a_2$, $\rho_1 \cong \rho_2$, and $T_1 \cong T_2$, which in turn yields $\frac{\partial}{\partial t} \int_V q dV \cong 0$ and $\frac{\partial}{\partial t} \int_V q (c_p T + q) dV = 0$. The value of q can be set equal to zero, since the entire gas medium in the chamber consists of the combustion products (we disregard in this idealization the presence of gaseous fuel components in the combustion chamber).

Let us introduce another simplifying assumption. We assume that the spatial distribution of the combustion does not change under acoustic oscillations. Then $J'_2 = 0$ and $J'_3 = 0$. In addition, we take account of the fact that the heat supplied directly to the zone σ is

uniquely related with the mass supply

$$Q^* = Q_M M^*$$

or

$$\bar{Q}^* = Q_V \bar{m}; \quad \left(Q_V = \frac{Q_M}{s_1} \right). \quad (52.9)$$

Then, eliminating \bar{s}_2 from the system (52.7), we can obtain the properties of the plane Σ in the form of the following two equations:

$$\left. \begin{aligned} \bar{v}_1 + \frac{1}{M} \bar{p}_1 &= -\bar{v}_1 + \frac{1}{M} \bar{p}_1 - M \bar{m}, \\ \left[M + \frac{1}{M(x-1)} \right] \bar{v}_1 + \frac{x}{x-1} \bar{p}_1 &= \\ &= \left[\frac{1}{M(x-1)} - \frac{M}{2} \right] \bar{v}_1 + M \frac{2Q_V - 1}{2} \bar{m}. \end{aligned} \right\} \quad (52.10)$$

If we add to these the relation (52.6) and assume further that the value of \bar{p} contained in it coincides with \bar{p}_1 (this is natural, since the induction period should depend on the parameters of the medium through which the fuel drops move toward the combustion zone σ), then the number of variables in the system (52.10) can be reduced to four. The difference $\bar{p} - \bar{p}(\tilde{\tau}_1)$ in the right half of (52.6) can be expressed [see (4.13)] in the following fashion:

$$\bar{p} - \bar{p}(\tilde{\tau}_1) = \bar{p}(1 - e^{-\tilde{\tau}_1}).$$

Finally, the expression for the properties of the surface Σ in the case under consideration will assume the appearance

$$\left. \begin{aligned} \bar{v}_1 + \frac{1}{M} \bar{p}_1 &= -\bar{v}_1 + \left[\frac{1}{M} - M r (1 - e^{-\tilde{\tau}_1}) \right] \bar{p}_1, \\ \left[M + \frac{1}{M(x-1)} \right] \bar{v}_1 + \frac{x}{x-1} \bar{p}_1 &= \\ &= \left[\frac{1}{M(x-1)} - \frac{M}{2} \right] \bar{v}_1 + M \frac{2Q_V - 1}{2} r (1 - e^{-\tilde{\tau}_1}) \bar{p}_1. \end{aligned} \right\} \quad (52.11)$$

It is now necessary to specify two boundary conditions.

One of the boundary conditions is obtained immediately: there can be no velocity oscillations at the head, i.e. (taking the origin of ξ on the plane Σ),

$$\bar{v}_1 = 0 \text{ when } \xi = \xi_1. \quad (52.12)$$

In order to formulate the second boundary condition, let us turn to examine the character of the flow at the exhaust nozzle. If we assume that the engine has a "short" nozzle, i.e., the distance from the cross section corresponding to $\xi = \xi_2$ in Fig. 111 to the critical section of the nozzle (section ee) is small compared with the length of the combustion chamber $|\xi_1| + \xi_2$ (more accurately, compared with the length of the standing wave of the oscillations excited in the combustion chamber), then in accordance with the arguments presented above for an analogous case (page 214) we have

$$\bar{v}_2 = 0 \text{ when } \xi = \xi_2. \quad (52.13)$$

Let now $\xi_1 = 0$ and $\xi_2 = 1$, i.e., we shall consider the combustion occurring in the direct vicinity of the head. We can then put $v_1 = 0$ in the equations of (52.11) and reduce them by simple transformation to the form

$$\left. \begin{aligned} \bar{v}_{20} &= (a_{10} + a_{12}r + a_{14}r^2 e^{-\beta \tilde{\tau}_2}) p_{10}, \\ \bar{p}_{20} &= (a_{20} + a_{22}r + a_{24}r^2 e^{-\beta \tilde{\tau}_2}) \bar{p}_{10}. \end{aligned} \right\} \quad (52.14)$$

Here a_{1k} are certain constants which are determined during the course of transforming Eqs. (52.11) to the form (52.14). The variables are marked with a zero subscript to emphasize that they correspond to $\xi = 0$.

The relations obtained coincide almost literally with Eqs. (26.4) which were considered above. Recognizing that the boundary condition (52.13) coincides with the boundary condition used in §26, we can immediately, in analogy with (26.5), write down the following expression, which is the characteristic equation of the problem under consideration

$$\begin{aligned} &(a_{10} + a_{12}r + a_{14}r^2 e^{-\beta \tilde{\tau}_2}) \left(1 + \exp \frac{2}{1-M^2} \beta\right) + \\ &+ (a_{20} + a_{22}r + a_{24}r^2 e^{-\beta \tilde{\tau}_2}) \left(1 - \exp \frac{2}{1-M^2} \beta\right) = 0. \end{aligned} \quad (52.15)$$

Hence

$$re^{-\beta\tilde{\tau}_n} = \frac{(a_{11}+a_{12}r)\left(1+\exp\frac{2}{1-M^2}\beta\right)+(a_{21}+a_{22}r)\left(1-\exp\frac{2}{1-M^2}\beta\right)}{a_{11}\left(1+\exp\frac{2}{1-M^2}\beta\right)+a_{21}\left(1-\exp\frac{2}{1-M^2}\beta\right)} = A(r, \beta) + iB(r, \beta). \quad (52.16)$$

Here A and B are the real and imaginary parts of the fraction in the central part of the equation.

We shall seek the stability boundary. As is well known, on the stability boundary $\beta = i\omega$, and consequently

$$\left. \begin{aligned} r \cos \omega\tilde{\tau}_n &= A(r, \omega), \\ r \sin \omega\tilde{\tau}_n &= -B(r, \omega), \end{aligned} \right\} \quad (52.17)$$

from which we get

$$r^2 = A^2(r, \omega) + B^2(r, \omega). \quad (52.18)$$

By specifying different values of ω we obtain \underline{r} from Eq. (52.18), and then $\tilde{\tau}_1$ from (52.17).

The actual satisfaction of these operations is simplified by the fact that, as can be seen from the system (52.11), the numerical coefficients of \underline{r} and of $re^{-\beta\tilde{\tau}_1}$ differ only in sign. Therefore, we can state the same with respect to the coefficients of the corresponding terms in (52.14):

$$a_{14} = -a_{13}, \quad a_{24} = -a_{23}.$$

But then we can rewrite (52.16) (with $\beta = i\omega$) in the form

$$r \exp(-i\omega\tilde{\tau}_n) = r + b + ic, \quad (52.19)$$

where

$$\begin{aligned} b &= \frac{a_1 a_3 - a_2 a_4}{a_1^2 + a_2^2}, \quad c = \frac{a_2 a_3 - a_1 a_4}{a_1^2 + a_2^2}, \\ a_1 &= (a_{11} + a_{22}) + (a_{11} - a_{22}) \cos \frac{2}{1-M^2} \omega, \\ a_2 &= (a_{12} + a_{21}) + (a_{12} - a_{21}) \cos \frac{2}{1-M^2} \omega, \\ a_3 &= (a_{11} - a_{22}) \sin \frac{2}{1-M^2} \omega, \\ a_4 &= (a_{12} - a_{21}) \sin \frac{2}{1-M^2} \omega. \end{aligned}$$

Changing over then to the equation of the type (52.18) we obtain a relation that is linear with respect to \underline{r}

$$r = -\frac{b^2 + c^2}{2b}. \quad (52.20)$$

After determining r from (52.20), we obtain immediately $\tilde{\tau}_1$. From a comparison of the imaginary and real parts of (52.19) it follows that

$$\sin \omega \tilde{\tau}_n = -\frac{c}{r}, \quad \cos \omega \tilde{\tau}_n = 1 + \frac{b}{r}. \quad (52.21)$$

For a theoretical analysis of the high-frequency oscillations in liquid fuel jets the system of equations (52.7), which describes the properties of the heat supply region, is usually replaced by an approximate system. Writing down only the first equation, which is a consequence of the law of the conservation of mass flow, one supplements it with the two equations $\bar{p}_1 = \bar{p}_2$ and $\bar{s}_1 = \bar{s}_2 = 0$, which are used in lieu of the second and third equations of (52.7).

Physically this is connected with the fact that the combustion products in a liquid fuel jet engine chamber have essentially the same temperature on both sides of the combustion front. This essentially distinguishes the process in engines of the type under consideration from processes in furnaces and other devices, in which the heat is supplied to a stream of cold gas which crosses the flame front usually without a noticeable increase in the mass of the flowing gas.

If we make this assumption, we can write in place of the system (52.7) the following:

$$\left. \begin{aligned} \frac{1}{M} \bar{v}_2 + \bar{p}_2 &= \frac{1}{M} \bar{v}_1 + r(1 - e^{-\beta \tilde{\tau}_n}) \bar{p}_1, \\ \bar{p}_2 &= \bar{p}_1. \end{aligned} \right\} \quad (52.22)$$

Equations (52.14) assume the very simple form

$$\left. \begin{aligned} \bar{v}_{20} &= \bar{v}_{10} + M[r(1 - e^{-\beta \tilde{\tau}_n}) - 1] \bar{p}_{10}, \\ \bar{p}_{20} &= \bar{p}_{10}. \end{aligned} \right\} \quad (52.23)$$

and the coefficients of Eq. (52.19) can be written directly in explicit form

$$b = -1; \quad c = -\frac{\sin \frac{2}{1-M^2} \omega}{M \left(1 + \cos \frac{2}{1-M^2} \omega \right)}. \quad (52.24)$$

Before proceeding further, let us estimate the validity of the simplification introduced here. To this end we construct the instability region for the fundamental tone of the tube using both methods, the exact and the approximate. For this purpose we take the following numerical example: $\kappa = 1.2$, $M = 0.213$, and the calorific value of the fuel is assumed to be 2000 kcal/kg. It must be noted that there is no need for knowing the calorific value of the fuel if the approximate procedure is used.

A pair of values of \underline{r} and $\tilde{\tau}_1$ is obtained from (52.20) and (52.21) and are marked on the plot shown in Fig. 112. Curve 1 corresponds to the exact calculation and curve 2 to the approximate one. As can be seen from the plot, both stability boundaries (the instability region is shown shaded) are quite close to each other and therefore the usually employed approximation can be regarded as fully justified. We shall henceforth obtain all the results by the approximate procedure.

If we turn to the diagram of Fig. 112, for purposes of understanding the main properties of a liquid fuel jet engine as an oscillating system in which longitudinal acoustic oscillations can develop, we can state that at small \underline{r} ($r < 0.5$) the self-excitation of acoustic oscillations is impossible at all. This is connected with the fact that at small values of \underline{r} the induction period depends little on the pressure. The smallest value of \underline{r} , at which self-excitation is still possible, is $r = 0.5$. This can be verified most simply in the following fashion. Using (52.23), we obtain an expression for the flux of acoustic energy radiated by the heat supply region. We take account here of the fact that $\bar{v}_{10} = 0$ in accordance with the boundary condition, and that the

temperatures and pressures of the gases on both sides of the combustion front are the same. Then, following Formula (19.7), we can write

$$\bar{A}_\Sigma = \frac{1}{2} \bar{p}_{20} \bar{v}_{20} = M [(r-1) - r \cos \omega \tilde{\tau}_1] \bar{p}_{10}. \quad (52.25)$$

Inasmuch as we are considering the self-excitation of a system that loses no acoustic energy at the ends of the tube, the stability boundary will correspond to $\bar{A}_\Sigma = 0$, self-excitation will correspond to $\bar{A}_\Sigma > 0$, and the damping of the oscillations to $\bar{A}_\Sigma < 0$.

It is easy to see that the expression in the square brackets is negative when \underline{r} is small. To make this expression a maximum for a specified value of \underline{r} , we must choose $\tilde{\tau}_1$ such that $\cos \omega \tilde{\tau}_1 = -1$. We then obtain $2r - 1$ in the square brackets. This expression vanishes when $r = 0.5$. Thus, the smallest value of \underline{r} at which the condition $\bar{A}_\Sigma = 0$ can be satisfied is $r = 0.5$, and when $r < 0.5$ we get $\bar{A}_\Sigma < 0$, i.e., self-excitation is impossible.

This result was obtained in this case not on the basis of a numerical example, so that the statement that when $r < 0.5$ the oscillating system cannot be excited under any conditions, assumes the character of a general law.

When $r > 0.5$ a region of values $(r, \tilde{\tau}_1)$ appears, at which the oscillating system becomes excited. The interval of values of $\tilde{\tau}_1$ which admit of self-excitation increases with increasing \underline{r} . These are the general laws which follow from Expression (52.25) and which are represented in Fig. 112.

In order to make this diagram even clearer, let us give the order of magnitude of the experimentally observed values of \underline{r} and $\tilde{\tau}_1$. According to data obtained in the experiment of Crocco, Grey, and Harrije,* \underline{r} has an order of magnitude 1.3-1.7 (depending on the relation between the amounts of the oxidant and combustible matter supplied to the chamber).

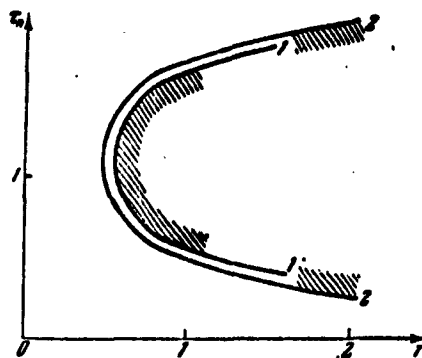


Fig. 112. Instability regions obtained by the exact (1) and approximate (2) methods.

ber), while the measured value of the induction period lies in the interval 0.15-0.22 milliseconds. Consequently, the actually observed values of \underline{r} make the excitation of longitudinal acoustic oscillations quite probable.

The type of acoustic oscillations considered here differs principally in some aspects from the excitation of oscillations by the heat supply, which was investigated in the preceding chapters, and it is therefore advantageous to plot for this case the stability boundaries similar to those plotted in Chapters 3 and 4. Let us write down (52.23) in the form

$$\left. \begin{aligned} \bar{v}_{10} &= \bar{v}_{10} - M\bar{p}_{10} + M\bar{m}, \\ \bar{p}_{10} &= \bar{p}_{10}. \end{aligned} \right\}$$

With this notation, the perturbation of \bar{m} can depend not only on \bar{p}_{10} but also on \bar{v}_{10} .

Let us take the scalar product of these equations and recognize that $\bar{v}_{20}\bar{p}_{20} = 0$, $\bar{v}_{10}\bar{p}_{10} = 0$ because there are no losses of acoustic energy in the system. Then the quantities \bar{p}_{10} and \bar{m} will be related by

$$\bar{p}_{10}\bar{m} = \bar{p}_{10}^2,$$

which is represented graphically in Fig. 113 for $|\bar{p}_{10}| = 1$ in the form of the vertical line $x = 1$. As can be seen from this diagram, the ex-

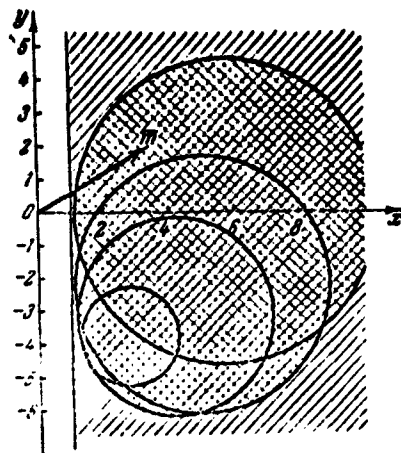


Fig. 113. Diagram of stability regions in the self-excitation resulting from perturbation of gas formation.

citation of the system becomes possible only when the projection of the dimensionless perturbation of gas production \vec{m} on the x axis (on the \vec{p}_{10} direction) exceeds the absolute value of \vec{p}_{10} . Since under the assumptions made above the absolute value of \vec{m} is directly proportional to the absolute value of \vec{p}_{10}

$$\bar{m} = r(1 - e^{-\tilde{\tau}_1}) \bar{p}_{10}, \quad (52.26)$$

the conditions for excitation depend on their relative magnitude and on the phase shift, i.e., in final analysis, on r and $\tilde{\tau}_1$.

The principal difference between the case considered here and those previously investigated lies in the fact that in place of the perturbation of heat supply or of the rate of flame propagation we deal here with a perturbation of gas production. Inasmuch as the gas production must generally speaking not necessarily be connected with the heat supply (combustion), this type of excitation of acoustic oscillations is conceivable in devices in which combustion or heat supply are completely excluded, but in which gas production takes place (for example, evaporation of strongly heated liquid, which is injected into a chamber with reduced pressure) if, of course, this gas production will depend in one manner or another on the oscillations of the pressure or velocity.

It must be pointed out that in place of constructing the approximate stability boundary shown in Fig. 113 in the form of a vertical line, we can construct also the exact boundary, making use of (52.10) and not (52.22). In this case, as in Chapters 3 and 4, we can obtain a

family of circles, the centers of which move [depending on the variation of the quantities \bar{p}_{10} and \bar{v}_{10} which are mutually interrelated by (19.12)] along part of an elliptical arc. The corresponding construction is shown in Fig. 113 for the already mentioned numerical example. All the plotted circles lie to the right of the approximate stability boundary and are sufficiently close to it. Thus, the line $x = 1$ on the diagram of Fig. 113 can be regarded as an approximate configuration of the stability boundary for arbitrary position of the combustion zone along the axis of the combustion chamber of the engine. The distance between the stability boundary and the x axis is equal in this case to the square root of the constant in the right half of (19.12), which coincides with $|\bar{p}_{10}|$ in the pressure antinode (in the example constructed here this constant was taken equal to unity).

From an examination of the stability diagrams it becomes obvious that the system cannot become excited if the combustion front lies in a pressure node even in the case if (for example, under the influence of velocity oscillations) the gas production has a nonvanishing oscillatory component. This is seen from the fact that the instability region does not encompass even one part of the y axis; a more detailed analysis shows that, for example when $\bar{p}_{10} = 0$; $\bar{v}_{10} = 1$, the circle corresponding to that shown in the right half of Fig. 28 has an imaginary radius.

Having made these remarks, let us turn to a discussion of the diagram shown in Fig. 112. This diagram shows not all the instability regions, but only one of them, corresponding to oscillations of the fundamental tone and characterized by the smallest values of $\tilde{\tau}_1$ for this harmonic. To be sure, we must mention that the very concept of a harmonic can be applied to a system in which the properties of Σ are viable only under certain stipulations (see §27 for more details on this

subject). If we agree to define the natural frequencies of the system as those which would be obtained in the case of acoustic oscillations in the same combustion chamber and at the same gas flow, but without interaction with the combustion zone, then these frequencies are defined by Formula (5.4)

$$\omega = (1 - M^2) K \pi \quad (K = 1; 2; 3; \dots). \quad (52.27)$$

In the case under consideration, such frequencies occur when $r = 0.5$ and

$$\omega \tau_1 = N \pi \quad (N = 1, 3, 5, \dots). \quad (52.28)$$

It is simplest to verify this by using the first equation of (52.23). Recalling that $\beta = i\omega$ on the stability boundary, we can easily see that when $r = 0.5$ and $\omega \tau_1$ are defined by Relation (52.28), we get $\bar{v}_{20} = 0$, since the boundary condition yields $\bar{v}_{10} = 0$. Consequently, in this case the boundary conditions can be written in the form $\bar{v}_2 = 0$ when $\xi = 0$ and $\bar{v}_2 = 0$ when $\xi = 1$, i.e., they can be formulated for the ends of the tube in such a way that there is no combustion front between the end sections (when $\xi = 0$ the boundary condition is now expressed in terms of \bar{v}_2 and not \bar{v}_1). Formula (52.27) which was obtained in §5 was derived under precisely this approximation, namely that on the ends of the tubes we have identical nodes (either both pressure or both velocity), and there are no discontinuity surfaces between them. Incidentally, the frequencies given by Formula (52.27) can be obtained also directly from the relations obtained in the present section. When $\omega \tau_1$ are determined by Formula (52.28) (which can be regarded as a consequence of Eq. (52.21) for $b = -1$ and $r = 0.5$), the value of the imaginary part of (52.19) should be equal to zero. This corresponds to $c = 0$ or, in accordance with (52.24), to $\sin 2\omega/(1 - M^2) = 0$, which yields $2\omega/(1 - M^2) = 2K\pi$, i.e., Formula (52.27) [$2\omega/(1 - M^2) = K\pi$ is not a solution for odd k , for in this case the denominator in the ex-

pression (52.24) for c vanishes and $c = \infty$].

Consequently, those frequencies which are customarily called the natural frequencies, are excited only under definite values of r and $\tilde{\tau}_1$. In Fig. 112 this corresponds to only one point on the stability boundary, namely the one for which $r = 0.5$. It is easy to verify that this point is obtained when $K = 1$ and $N = 1$ in Formulas (52.27) and (52.28).

For other points lying on the stability boundary, the frequencies ω differ from those defined by Expression (52.27). If we stay within the limits of the values of r shown in Fig. 112, then these frequencies for the extreme points will differ from the frequency corresponding to $r = 0.5$ by $\pm 10\%$ (for the upper branch of the stability boundary they will be smaller and for the lower branch they will be larger). Inasmuch as the excited frequencies, as can be seen from the foregoing example, are close over a sufficiently wide range of variation of r to the values given by Formula (52.27), the latter expression can be used for an approximate estimate of the oscillation frequencies.

The curve shown in Fig. 112 is not the only stability boundary in the plane of the parameters $(r; \tilde{\tau}_1)$. Indeed, if we turn to Expression (52.19), we see immediately that if there exists for it at least one solution $\tilde{\tau}_1^*; \omega^*$, then it is possible to construct on its basis an infinite set of solutions using the following two methods.

First, without changing r and making no changes whatever in the right half of the equation (including ω^*), we can immediately state that if a solution exists for a certain $\tilde{\tau}_1^*$, then it will exist for all

$$\tilde{\tau}_n = \tilde{\tau}_1^* + \frac{2(N-1)\pi}{\omega^*} \quad (N = 1, 2, 3, \dots) \quad (52.29)$$

Second, we can proceed as follows. Putting $N = \text{const}$ and retaining r , we change the arguments of the trigonometric functions contained

in the coefficients b and c in the following manner:

$$\left. \begin{aligned} \omega \tilde{\tau}_n &= \omega^* \tilde{\tau}_n^*, \\ \frac{2}{1-M^2} \omega &= \frac{2}{1-M^2} \omega^* + 2(K-1)\pi \\ (K &= 1, 2, 3, \dots). \end{aligned} \right\} \quad (52.30)$$

Here, as in the preceding case, ω^* is the frequency corresponding to $K = 1$ (the first harmonic) and ω are the frequencies for all the harmonics.

The arguments presented here can be applied to each point of the stability boundary shown in Fig. 112. Consequently, we can reconstruct the entire boundary and obtain an infinite set of instability regions for all the combinations of K and N .

The corresponding construction for several combinations of the values of K and N is shown in Fig. 114. As can be seen from the presented diagram, an increase in K lowers the stability region, whereas an increase in N raises it. If we take all the possible combinations of the values of K and N , then practically the entire region lying to the right of the cross-hatched line $r = 0.5$ will be filled with instability regions. Consequently, when $r > 0.5$ and for arbitrary $\tilde{\tau}_1$ (except, of course, when $\tilde{\tau}_1 = 0$) the oscillating system is capable of excitation. Depending on $\tilde{\tau}_1$ and r , this will concern some particular harmonic or several harmonics simultaneously.

So far we have considered almost exclusively the case when the combustion front is located in the direct vicinity of the engine head. The only exception was the construction of the stability diagram on Fig. 113, which remains valid for an arbitrary location of the combustion front along the length of the combustion chamber.

In discussing the foregoing diagram we stated, in particular, that no excitation of the system is possible in a pressure node. It is therefore necessary to analyze in greater detail the question of the

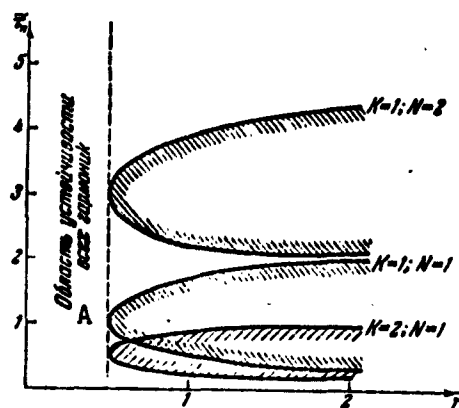


Fig. 114. Instability regions for two harmonics of the system. A) Region of stability of all harmonics.

tendency of the oscillating system under consideration toward self-excitation as a function of the position of the combustion front along the combustion chamber of the engine.

In order to make such an analysis, we must use the exact relations (52.11) for the combustion front, and not the approximate ones (52.22). The reason for it is that as one moves toward the pressure node (i.e., with decreasing absolute values of \bar{p}_1 and \bar{p}_2 and with increasing \bar{v}_1 and \bar{v}_2) it is not legitimate to neglect the term which contains \bar{v}_2 as a factor in the second equation of (52.7). Indeed, the condition $\bar{p}_1 = \bar{p}_2$, which replaces the second equation of (52.7) in the relations (52.22) (in which, in addition, we put $\bar{s}_1 = \bar{s}_2 = 0$) can be regarded as an approximate notation for the second equation of (52.7) when $\bar{s}_2 = 0$, inasmuch as $1/M \gg 1$. However, when $\bar{p}_2 \rightarrow 0$ and $\bar{p}_1 \rightarrow 0$ such a statement becomes erroneous.*

It was shown above that the excitation of longitudinal acoustic oscillations in liquid fuel jet engines is essentially related with two parameters, \underline{r} and $\tilde{\tau}_1$. Proceeding to the analysis of the influence of the relative distance from the combustion front to the engine head,

ξ_r , on the self-excitation of the oscillations, we must agree on the assumptions that will be made relative to \underline{r} and $\tilde{\tau}_1$. The value of \underline{r} will be specified and maintained constant. The parameter $\tilde{\tau}_1$ will be assumed variable and chosen such as to make $\cos \omega \tilde{\tau}_1 = -1$. If we choose $\tilde{\tau}_1$ on the basis of the foregoing condition, this will ensure the best conditions for the excitation of the oscillations. This is seen, for example, from the fact that when $\cos \omega \tilde{\tau}_1 = -1$ the vector \bar{m} on the diagram of Fig. 113 is horizontal (the phases of \bar{m} and \bar{p} will coincide), so that excitation of the system is possible at a minimum absolute value of \bar{m} . If the foregoing condition is satisfied and $r = 0.5$, then the oscillation frequencies are given by Formula (52.27), i.e., they coincide with the "natural" acoustic frequencies. Since we shall consider henceforth values of \underline{r} that are relatively close to 0.5, the oscillation frequencies should also be close to the frequencies (52.27).

Thus, we shall consider below oscillations with frequencies close to the ordinary acoustic frequencies, and for such values of $\tilde{\tau}_1$ as will contribute the most, to a certain degree, to the occurrence of self-oscillations.

Let $r > 0.5$. Then when the combustion front is located at the head, the oscillating system will become excited (this is seen from Fig. 114). We start displacing the combustion front away from the head and find a position at which self-excitation becomes impossible. We write out the expression for the flux of acoustic energy radiated by the combustion zone and set it equal to zero. Under the assumptions made it will be equal to

$$\bar{A}_1 = \frac{1}{2}(\bar{p}_0 \bar{v}_0 - \bar{p}_0 \bar{v}_0) = \frac{1}{2}(a_1 \bar{p}_0^2 + a_2 \bar{v}_0^2) = 0, \quad (52.31)$$

where a_1 and a_2 are numerical coefficients that are readily obtained by taking a term by term scalar product of Eqs. (52.11), after first

reducing them to the form (52.14), with account of the fact that when the values of $\beta\tilde{\tau}_1 = i\omega\tilde{\tau}_1$ are taken in accordance with the condition mentioned above, we get $1 - e^{-\beta\tilde{\tau}_1} = 2$.

The quantities \vec{p}_{10}^2 and \vec{v}_{10}^2 are related by Eq. (45.6) and therefore the absolute values of \vec{p}_{10} and \vec{v}_{10} can be written with the aid of Formulas (45.7). Then Eq. (52.31) reduces to the following equation in the parameter φ which determines the position of the cross section Σ along the standing wave of the acoustic oscillations:

$$a_1 \cos^2 \varphi + a_2 \sin^2 \varphi = 0$$

or

$$a_1 + (a_2 - a_1) \sin^2 \varphi = 0,$$

hence

$$\sin \varphi = \sqrt{\frac{a_1}{a_1 - a_2}}. \quad (52.32)$$

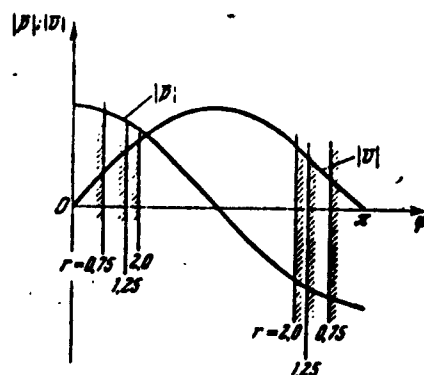


Fig. 115. Pressure and velocity standing wave patterns in the instability region for different values of \underline{r} .

Let us construct for the numerical example mentioned above the dependence of φ on \underline{r} (the coefficient a_1 is a function of \underline{r}). The results of the calculations can be represented by the following table:

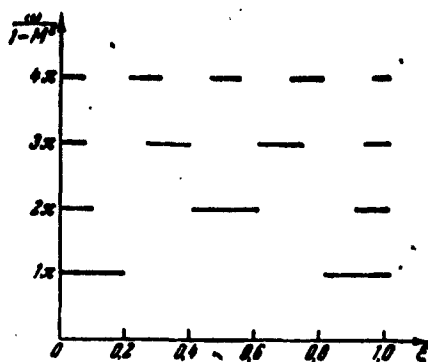


Fig. 116. Diagram showing the distribution of the instability regions for the first four harmonics as a function of the position of the combustion plane along the combustion chamber.

r	0.50	0.75	1.25	2.00
φ	0	0.35	0.59	0.71
	π	2.79	2.55	2.43
	0	-0.35	-0.59	-0.71
	$-\pi$	-2.79	-2.53	-2.43

In order to clarify this calculation, Fig. 115 shows a pressure and velocity standing wave pattern as φ varies from 0 to π , and of the position of the determined sections on the pattern. As can be seen from the diagram, with increasing r the instability regions in the vicinities of $\varphi = 0$ and $\varphi = \pi$ increase. For the first harmonic this means that the instability will occur in two cases: when the combustion front is at the head and when it is at the exhaust nozzle. Using the obtained values, we can plot the distribution of the stability zones and the distribution of the unstable process, as a function of the position of the combustion front along the tube, similar to the diagrams of Fig. 48. Inasmuch as the gas temperature is the same on the left and on the right of the combustion zone, the frequency of the harmonic will not change when the combustion plane is displaced along

the engine chamber. On each standing wave we can note the points corresponding to the values of the parameter ϕ given in the table. In this case, denoting as in the preceding chapters the instability regions by means of straight lines, we can readily construct the diagram shown in Fig. 116 for any fixed value of \underline{r} .

It is seen from the diagram on Fig. 116 that if the process in the combustion chamber has a tendency toward vibration combustion, then it should occur independently of the position of the combustion zone along the combustion chamber. The only difference will be that, depending on the coordinate of the combustion front $0 < \xi_f < 1$, a particular harmonic will become excited.

To clarify this question still further, we recall that we consider in the present section a lossless system. If we write down the boundary condition at the exhaust nozzle more rigorously, with account of the velocity gradient in it, then, as shown in the book of Crocco and Cheng, the damping influence of the exhaust nozzle will increase with increasing oscillation frequency. Consequently, the excitation of higher harmonics becomes a little probable, something characteristic of vibration combustion of gas combustible mixtures in tubes (see Chapter 6).

The diagram shown in Fig. 116 recalls analogous diagrams in Figs. 48, 49, etc. In both cases one considers the change in the number of the excited harmonic as a function of the position of the combustion zone along the tube. At the end of Chapter 5 the inverse problem was considered, that of tracing the influence of a change in the total length of the tube on the character of the oscillations for a fixed length of the hot portion and for fixed properties of the combustion zone. It was shown there that a general lengthening of the tube while maintaining the hot portion constant causes the system to go over to

higher harmonics, with the dimensional oscillation frequency remaining approximately constant.

An analogous conclusion should hold true also for liquid fuel jet engines. This phenomenon was actually observed by Crocco, Grey, and Harrije.* By gradually lengthening the combustion chamber, they registered a transition of the oscillations from the fundamental tone to the second harmonic, and from the second to the third, in full agreement with the point of view developed at the end of Chapter 5.

In the present section we have presented only an elementary discussion of the theory of high-frequency longitudinal acoustic oscillations in liquid fuel jet engines. Those interested in a more complete exposition of the problem are advised to turn to the already mentioned book by Crocco and Cheng and to the corresponding articles in the periodic literature.

To conclude the present section we make one more remark. In all the preceding sections it was emphasized many times that in final analysis the reason for the excitation of vibration combustion is the perturbation in the heat supply or in the effective flame propagation velocity. In the case of excitation of acoustic oscillations in liquid fuel jet engines, the main perturbation is that of gas production (the perturbation in the consumption from a certain source of mass located in the combustion zone). Consequently, vibration combustion can have a highly varied nature. In the general case its excitation may be due to any term contained in the system (15.5) and describing the process within the zone σ . This may be δM^* (the case just considered), δQ^* (Rijke tube), the mobility of the flame front, i.e., the nonvanishing of the partial derivatives of the integrals over the volume V in all three equations (the case considered in §49), perturbation of the calorific value of the mixture δq_1 or of the completeness of combustion

$\delta q_1 - \delta q_2$ (example given in §25). Finally, the excitation of acoustic oscillations may turn out to be connected with the nonvanishing of the term δP_x . This process is realized, for example, in those cases when a periodic cessation of the vortices (without combustion) occurs in the zone σ . Then the interaction between the vortex formation and the acoustic oscillations can lead to self-excitation of the oscillating system. Inasmuch as this case is not at all related with the combustion process, it is not considered in this book.

Such a variety of causes for the excitation of longitudinal acoustic oscillations calls for a most careful analysis of all the variables contained in the system (15.5) prior to adopting a particular scheme for the idealization of the process of perturbed combustion.

Manu-
script
Page
No.

[Footnotes]

- 437 Popov, S.G., Izmereniye vozdushnykh potokov [Measurement of Air Flows], Gostekhizdat [State Unified Scientific and Technical Publishers], 1947.
- 438 Lighthill M.I., The Response of Laminar Skin Friction and Heat Transfer to Fluctuations in the Stream Velocity. Proceedings of the Royal Society, Ser. A, Vol. 224, No. 1156, 1954.
- 441 Lehmann K.O., Ueber die Theorie der Netztoene [On the Theory of Alternating-Current Hum], Annalen der Physik, [Annals of Physics], 5th Series, 29, 1937.
- 443 If this condition is not satisfied, Formula (48.10) becomes somewhat more complex and is readily derived from (48.3) and (48.4). Conditions (48.9) are usually satisfied.
- 448 Idel'chik, I.Ye., Spravochnik po gidravlicheskomu soprotivleniyu fazonnykh i pryamykh chastey truboprovodov [Handbook on the Hydraulic Resistance of Shaped and Straight Parts of Pipelines], Izdaniye Tsentral'nogo aerogidrodinamicheskogo instituta im. N.Ye. Zhukovskogo [Publishing House of the Central Aerohydrodynamic Institute imeni N. Ye. Zhukovskiy], 1950.
- 470 The fact that the interval Δx does not extend to the open end of the tube may give rise to objections. However, this

is quite in order. In constructing the regions of Δx in Fig. 104, the calculation was made for assigned experimental frequencies through the cold gas, since there is no need to know the nature of the oscillations in the hot part of the tube in order to evaluate the oscillations δp and δv in advance of the flame front. For this reason, the right end of the region Δx for the first harmonic is where the pressure node would be in the event that the entire tube was filled with cold gas and the oscillations were taking place at the observed frequency. Actually, the nature of the hot-gas vibrations to the right of the experimental point (which is of no interest here) is quite different, since there is hot gas here; moreover, on passage through the flame front the parameters of the vibrations also change, so that actually the pressure node is, of course, situated at the open end of the tube.

- 477 Solov'yev, V.V., K voprosu vibratsionnogo goreniya v vysokonapryazhennykh topochnykh kamerakh [On the Problem of Vibrational Combustion in Severely Stressed Boiler Chambers], Inzherno-fizicheskiy zhurnal [Engineering-Physical Journal], No. 1, 1959.
- 486 Bondaryuk, M.M. and Il'yashenko, S.M., Pryamotochnyye voz-dushno-reaktovnyye dvigateli [Ramjet Engines], Oborongiz [State Scientific and Technical Publishing House for the Defense Industry], Moscow, 1958.
- 487 Fenn Y.B., Forney H., Garmon R., Industrial and Engineering Chemistry 43 No. 7, 1951. Russian translation in collection entitled Voprosy raketnoy tekhniki [Problems of Rocket Engineering], No. 4 (10), 1952.
- 490 Nicholson H.M., Radcliffe A., Pressure Fluctuations in a Jet Engine. Brit. Journ. Appl. Phys., v. 4, N 12, 1953.
- 490 Luigi Crocco and Sin-J Cheng, Theory of Combustion Instability in Liquid Propellant Rocket Motors. Butterworth Scientific Publications, 1956. Russian translation: Luidzhi Krokko i Chzhen sin'-i, Teoriya neustoychivosti goreniya v zhidkostnykh reaktivnykh dvigatelyakh, Izd-vo inostr. literatury [Foreign Literature Press], Moscow, 1958.
- 505 Crocco L., Grey J., Harrije D.T., Jet Propulsion, 1958, No. 12.
- 510 An error crept into the above-mentioned book of Crocco and Cheng (and into articles published by these authors in the periodical literature) in connection with this point. They employ an approximate relationship of the type of (52.28) for an arbitrary combustion-front position and make a number of simplifying assumptions the justification for which is not quite clear. As a result, the stability be-

that they obtained (Fig. 29 in the book cited and at a number of other places) would seem doubtful. This is evident, for example, from the following example. Consider the stability of the basic tone with the combustion front in the middle of the combustion chamber, i.e., at the pressure node. If we use a relationship of the type of (52.22), this will give $\bar{p}_1 = \bar{p}_2 = 0$ and $\bar{v}_1 = \bar{v}_2$ or (taking into account that $n = 1$ and $m = 1$) $\delta E = 0$ and $\delta X = 0$ (see Formulas (17.1)). Then in a loss-free system of the type considered in the present section, we have neutral oscillations. This was demonstrated in detail in §22 in the discussion of Equality (22.6.). Consequently, the system will be at the stability boundary when the combustion front is in the center of the combustion chamber. In the book of Crocco and Cheng, however, stability corresponds to this position of the combustion front. It should be noted that the possible improvements could change only the quantitative aspect of Crocco and Cheng's conclusions but not their qualitative aspect.

515 Crocco L., Grey J., Harrije D.T., Jet Propulsion, 1958, No. 12.

[List of Transliterated Symbols]

437	$\pi = p = \text{provolochnka} = \text{wire}$
438	$\text{CT} = \text{st} = \text{statsionarnyy} = \text{stationary}$
464	$\text{COP} = \text{sgor} = \text{sgoraniye} = \text{combustion}$
464	$\text{CT} = \text{sg} = \text{sgoraniye} = \text{combustion}$
464	$n = n = \text{normal'nyy} = \text{normal}$
493	$i = i = \text{induktsiya} = \text{induction}$

DISTRIBUTION LIST

DEPARTMENT OF DEFENSE

Nr. Copies

MAJOR AIR COMMANDS

Nr. Copies

HEADQUARTERS USAF

AFCIN-3D2
ARL (ARB)

1
1

OTHER AGENCIES

CIA
NSA
DIA
AID
OTS
AEC
PWS
NASA
ARMY (FSTC)
NAVY
NAFPC
RAND
SPECTRUM
PGE

1
6
9
2
2
2
1
1
3
3
1
1
1
12

AFSC

SCFED
DDC
TDBIL
TDBEL
TDBEL (Parkins)
AEL (AEY)
SSD (SEF)
RSD (ESF)
AFPC (FTY)
AFWC (SIF)
ASD (ALY M)
ESD (SIL)

1
25
5
5
1
1
2
1
1
1
1
1